

Prepared for:

Rijkswaterstaat/RIKZ

# Calibration of SWAN 40.20 for field cases Petten, Slotermeer, and Westerschelde

A1168

December 2003

Client

**Rijkswaterstaat/RIKZ**

Title

**Calibration of SWAN 40.20 for field cases Petten,  
Slotermeer and Westerschelde**

Abstract

The SWAN model version 40.20 has been calibrated against wave observations carried out in the storm of 26-27 October 2002 for the coastal area near Petten, the Slotermeer and the Westerschelde. Relevant parameters for the calibration have been determined on the basis of a sensitivity study of SWAN 40.20 with respect to numerical and physical settings for these field cases, for a wave flume situation and academic fetch-limited wave growth. In addition, the cumulative wave steepness method for the computation of whitecapping has been tested for these situations. A technique for the automatic calibration of SWAN against measured wave data has been developed and applied to a number of situations in the 26-27 October 2002 storm. The newly obtained settings have been verified against different field measured data in the same storm. In addition a number of suggestions for improving SWAN 40.20 have been formulated.

References

Requests for proposal RIKZ/2003/05621, 20 June 2003 and  
RIKZ/2003/05673 of June 25 2003  
Proposal A1168LE01, July 8, 2003  
Contract RKZ 1318

Rev.	Originator	Date	Remarks	Checked by	Approved by
0	G.Ph. van Vledder	14 Oct. 2003	Draft	D.P. Hurdle	G.Ph. van Vledder
1	G.Ph. van Vledder	2 Nov. 2003	Revised draft	D.P. Hurdle	G.Ph. van Vledder
2	G.Ph. van Vledder	18 Nov. 2003	Revised draft	D.P. Hurdle	G.Ph. van Vledder
3	G.Ph. van Vledder	26 Nov. 2003	Draft final	D.P. Hurdle	G.Ph. van Vledder
4	G.Ph. van Vledder	3 Dec. 2003	Final	D.P. Hurdle	G.Ph. van Vledder

Document Control	Contents	Status
Report number: A1168R1r4 Keywords: SWAN , calibration, sensitivity Westerschelde, Slotermeer, Petten Project number: A1168 File location: a1168r1r4	text pages : 46 tables : 14 figures : 183 appendices: 2	<input type="checkbox"/> preliminary <input type="checkbox"/> draft <input checked="" type="checkbox"/> final



## Samenvatting

Het SWAN model versie 40.20 is gecalibreerd op basis van golfmetingen in de storm van 26-27 oktober 2002 voor het kustgebied bij Petten, het Slotermeer en de Westerschelde. De relevante parameters voor de calibratie zijn gekozen op basis van een gevoeligheids-onderzoek van SWAN met betrekking tot numerieke en fysische instellingen. Deze gevoeligheidsstudie is uitgevoerd voor deze drie veldsituaties, een 1D golfgoot situatie en een academische strijklengtebeperkte groei situatie. De resultaten van de gevoeligheidsanalyse geven aan dat numerieke instellingen weinig invloed hebben op de berekeningsresultaten, terwijl de fysische instellingen voor white-capping (CDS2), vier-golf wisselwerkingen (LAMBDA en CNL4) en diepte geïnduceerd breken (GAMMA) een beduidend effect hebben op de resultaten. Tevens is de recent ontwikkelde cumulatieve golfsteilheidsmethode voor de berekening van whitecapping toegepast voor deze gevallen. Deze methode blijkt echter nog te leiden tot spectra met onrealistisch hoge waarden voor de golfrichtingspreiding. Er is een methode ontwikkeld en toegepast om SWAN automatisch te calibreren op basis van deels andere veldmetingen uit de oktober 2002 storm. Op grond van de calibratie zijn de volgende waarden bepaald:  $CDS2=1.36E-5$ ,  $LAMBDA=0.28$ ,  $CNL4=4.0E7$  en  $GAMMA=0.90$ . Alle andere SWAN parameters behouden hun standaardinstelling. De verkregen nieuwe instellingen zijn geverifieerd tegen waarnemingen bij Petten, in het Slotermeer en in de Westerschelde, eveneens uit deze storm. De verificatie geeft aan dat de nieuw verkregen set instellingen bevredigende resultaten geeft. Tevens zijn aanbevelingen geformuleerd voor verdere verbeteringen aan SWAN 40.20.



# Contents

1	Introduction .....	1
2	Methodology.....	3
2.1	Introduction	3
2.2	Areas of interest	4
2.3	Generation of input files	5
2.4	Presentation of results	5
3	Description of cases .....	7
3.1	Introduction	7
3.2	Slotermeer	7
3.3	Petten field case	8
3.4	Westerschelde	8
3.5	Petten wave flume	9
3.6	Fetch-limited case	9
4	Sensitivity of SWAN 40.20 to numerical parameters.....	10
4.1	Introduction	10
4.2	Spectral resolution	11
4.2.1	Introduction	11
4.2.2	Frequency resolution	12
4.2.3	Directional resolution	12
4.3	Percentage of Phillips' limiter	13
4.4	Under-relaxation	13
4.5	Simultaneous activation of triads and quadruplets	13
4.6	No limiter in case of strong decreasing wave action due to wave breaking	14
4.7	Convergence criteria	14
4.8	Results of the numerical sensitivity study	15
4.8.1	Slotermeer	15
4.8.2	Westerschelde	17
4.8.3	Petten	17
4.8.4	Petten wave flume	18
4.8.5	Fetch-limited wave growth	19
4.9	Conclusions	19
4.10	Recommendations	21



5	Sensitivity of SWAN 40.20 to physical settings .....	23
5.1	Introduction	23
5.2	Depth limited wave breaking	23
5.3	Bottom friction	24
5.4	Whitecapping dissipation	24
5.5	Quadruplet interactions	24
5.6	Triad interactions	25
5.7	Results of the physical sensitivity study	25
5.7.1	Slotermeer	25
5.7.2	Westerschelde	26
5.7.3	Petten	27
5.7.4	Petten wave flume	27
5.7.5	Fetch-limited wave growth	28
5.8	Conclusions	28
5.9	Recommendations	30
6	Calibration .....	31
6.1	Introduction	31
6.2	Method of calibration	32
6.3	Results of the calibration	34
6.4	Discussion	34
7	Verification .....	36
7.1	Introduction	36
7.2	Slotermeer	36
7.3	Westerschelde	37
7.4	Petten	37
7.5	Conclusions	38
8	Conclusions .....	39
8.1	Sensitivity of numerical settings	39
8.2	Sensitivity of physical settings	40
8.3	Calibration and verification	40
9	Recommendations .....	42

References

Tables

Figures

Appendices

A Coding conventions

B Example of master SWAN input file



## List of tables

- 3.1 Wind, water level and wave conditions in the Sloterneer for the selected moments in the storm of 27 October 2002.
- 3.2 Date and time of the Petten cases of the storm of 26/27 October 2002.
- 3.3 Integral wave parameters for imposed spectra in the Petten flume.
- 3.4 Wind speed and water depth for the fetch-limited growth cases.
  
- 4.1 Overview of numerical settings
- 4.2 Summary of parameter settings for numerical sensitivity study for the Sloterneer.
- 4.3 Summary of parameter settings for numerical sensitivity study for the Westerschelde, Petten, Petten flume and fetch-limited situations.
- 4.4 Impact of a certain numerical parameters on the integral wave parameters  $H_s$  and  $T_m-10$ .
  
- 5.1 Overview of physical settings for all areas.
- 5.2 Summary of parameter settings for physical sensitivity study
- 5.3 Impact of a certain physical parameters on the integral wave parameters  $H_s$  and  $T_m-10$ .
  
- 7.1 Optimal settings for the physical parameters of SWAN 40.20.
  
- 8.1 Recommended settings for the physical parameters of SWAN 40.20 per area and for all areas together.
- 8.2 Summary of effect of new calibration on computational results for Sloterneer, Petten and Westerschelde



## List of figures

- 3.1 Bottom topography of Sloterneer, location of measurement station F29 and location of test points.
- 3.2 Variation in time of wind, wave and water level parameters in the Sloterneer during the storm of 27 October 2002.
- 3.3 Location of SWAN computational grids at Petten and offshore stations ELD and YMW.
- 3.4 Bottom topography and location of measurement points in computational grid E24.
- 3.5 Location of SWAN computational grids for Westerschelde and location of station EUR.
- 3.6 Location of measurement locations in the Westerschelde and detailed computational grids.
- 3.7 Bottom profile and location of output points in Petten wave flume.
  
- 4.1.2-4.1.19 Iteration behaviour of  $H_s$ ,  $Tm-1,0$ ,  $Tm01$  and total integral of source function in the Sloterneer for case SL\_C03, output location 4 (Figure 4.1.1 does not exist).
- 4.2.2-4.2.19 Scatter diagrams of  $H_s$ ,  $Tm-10$ ,  $Tm01$ ,  $Tm02$ , mean direction  $\theta$  and directional spreading  $\sigma$  for grid W01 in the Westerschelde showing the sensitivity of numerical settings compared to the base case (Figure 4.2.1 does not exist).
- 4.3.2-4.3.19 Iteration behaviour of  $H_s$ ,  $Tm-1,0$ ,  $Tm01$  and total integral of source function in the Sloterneer for case SL\_C03, output location 4, station F29 (Figure 4.3.1 does not exist).
- 4.4.2-4.4.19 Scatter diagrams of  $H_s$ ,  $Tm-10$ ,  $Tm01$ ,  $Tm02$ , mean direction  $\theta$  and directional spreading  $\sigma$  for grid W01 in the Westerschelde showing the sensitivity of numerical settings compared to the base case (Figure 4.4.1 does not exist).
  
- 4.5.1-4.5.8 Spatial variation of  $H_s$ ,  $Tm-10$ ,  $\sigma$ ,  $\kappa$  and  $Qb$  in the Petten Flume for case B12 showing the sensitivity of SWAN to numerical settings.
- 4.6.1-4.6.8 Spatial variation of  $H_s$ ,  $Tm-10$ ,  $\sigma$ ,  $\kappa$  for the fetch-limited case C08 (depth 10 m and a wind speed of 30 m/s) showing the sensitivity of SWAN to numerical settings.
  
- 5.1.2-5.1.19 Scatter diagrams of  $H_s$ ,  $Tm-10$ ,  $Tm01$ ,  $Tm02$ , mean direction  $\theta$  and directional spreading  $\sigma$  showing the sensitivity of physical settings compared to the base case (Figure 5.1.1 does not exist).
- 5.2.2-5.2.16 Scatter diagrams of  $H_s$ ,  $Tm-10$ ,  $Tm01$ ,  $Tm02$ , mean direction  $\theta$  and directional spreading  $\sigma$  showing the sensitivity of physical settings compared to the base case (Figure 5.2.1 does not exist).
- 5.3.1-5.3.8 Spatial variation of  $H_s$ ,  $Tm-10$ ,  $\sigma$ ,  $\kappa$  and  $Qb$  in the Petten Flume for case B12 showing the sensitivity of SWAN to physical settings.
- 5.4.1-5.4.8 Spatial variation of  $H_s$ ,  $Tm-10$ ,  $\sigma$ ,  $\kappa$  for the fetch-limited case C08 (depth 10 m and a wind speed of 30 m/s) showing the sensitivity of SWAN to physical settings.
  
- 5.5.1 One dimensional spectrum and source functions for run SL\_C03\_P10.
- 5.5.2 One dimensional spectrum and source functions for run SL\_C03\_P11.
- 5.6.1 One dimensional spectrum and source functions for run SL\_C03\_P14, iteration 5.
- 5.6.2 One dimensional spectrum and source functions for run SL\_C03\_P14, iteration 20.
- 5.7 Two-dimensional spectrum and source functions for run SL\_C03\_P14, iteration 5
- 5.8 Two-dimensional spectrum and source functions for run SL\_C03\_P14, iteration 10
- 5.9 Two-dimensional spectrum and source functions for run SL\_C03\_P14, iteration 20



- 5.10 Spatial variation of Ursell number in the Sloterveer for run SL\_C03.
- 5.11 Spatial variation of Ursell number in grid E24 in the Petten coastal area for run PT\_C05.
- 5.12 Spatial variation of Ursell number in grid W01 in the Westerschelde for run WS\_C03.
- 5.13 Spatial variation of the  $H_s/d$  ratio in the Sloterveer for run SL\_C03.
- 5.14 Spatial variation of the  $H_s/d$  ratio in grid E24 in the Petten coastal area for run PT\_C05.
- 5.15 Spatial variation of the  $H_s/d$  ratio in grid W01 in the Westerschelde for run WS\_C03.
  
- 6.1 Illustration of the transfer function used in the optimisation of SWAN input parameters (in main text).
  
- 7.2.1 Verification of integral wave parameters for station F29 in the Sloterveer. Comparison of default settings against measurements (Set N01).
- 7.2.2 Verification of integral wave parameters for station F29 in the Sloterveer. Comparison of calibration settings against measurements for set SL.
- 7.2.3 Verification of integral wave parameters for station F29 in the Sloterveer. Comparison of calibration settings against measurements for set ALL.
- 7.2.4 Verification of wave spectra for station F29 in the Sloterveer. Comparison of default settings against measurements for set N01.
- 7.2.5 Verification of wave spectra for station F29 in the Sloterveer. Comparison of calibration settings against measurements for set SL.
- 7.2.6 Verification of wave spectra for station F29 in the Sloterveer. Comparison of calibration settings against measurements for set ALL.
  
- 7.3.1 Verification of integral wave parameters for station CDD in the Westerschelde. Comparison of default settings N01 against measurements.
- 7.3.2 Verification of integral wave parameters for station CDD in the Westerschelde. Comparison of calibration set "WS" against measurements.
- 7.3.3 Verification of integral wave parameters for station HFP in the Westerschelde. Comparison of default settings N01 against measurements.
- 7.3.4 Verification of integral wave parameters for station HFP in the Westerschelde. Comparison of calibration set "WS" against measurements.
- 7.3.5 Verification of integral wave parameters for station BAT in the Westerschelde. Comparison of default settings N01 against measurements.
- 7.3.6 Verification of integral wave parameters for station BAT in the Westerschelde. Comparison of calibration set "WS" against measurements.
- 7.3.7 Verification of integral wave parameters for station WIE in the Westerschelde. Comparison of default settings N01 against measurements.
- 7.3.8 Verification of integral wave parameters for station WIE in the Westerschelde. Comparison of calibration set "WS" against measurements.
- 7.3.9 Verification of integral wave parameters for station SCW in the Westerschelde. Comparison of default settings N01 against measurements.
- 7.3.10 Verification of integral wave parameters for station SCW in the Westerschelde. Comparison of calibration set "WS" against measurements.
  
- 7.4.1 Verification of integral wave parameters for station 062 at Petten. Comparison of default settings N01 against measurements.
- 7.4.2 Verification of integral wave parameters for station 062 at Petten. Comparison of calibration set "ALL" against measurements.
- 7.4.3 Verification of integral wave parameters for station 062 at Petten. Comparison of calibration set "PT" against measurements.





- 7.4.4 Verification of integral wave parameters for station 021 at Petten. Comparison of default settings N01 against measurements.
- 7.4.5 Verification of integral wave parameters for station 021 at Petten. Comparison of calibration set "ALL" against measurements.
- 7.4.6 Verification of integral wave parameters for station 021 at Petten. Comparison of calibration set "PT" against measurements.
- 7.4.7 Verification of integral wave parameters for station 175 at Petten. Comparison of default settings N01 against measurements.
- 7.4.8 Verification of integral wave parameters for station 175 at Petten. Comparison of calibration set "ALL" against measurements.
- 7.4.9 Verification of integral wave parameters for station 175 at Petten. Comparison of calibration set "PT" against measurements.

# 1 Introduction

An important task of the Institute of Marine and Coastal Management of the Rijkswaterstaat is to ensure the safety of the Dutch sea dikes. To that end every 5 years normative conditions (NC) have to be determined to check the safety of existing dikes and for the design of new dikes. Presently RIKZ is making preparations for the determination of new NC in the framework of the so-named HR-2006 project.

One of the important tools is the wave model SWAN, which is used to transform offshore wave conditions to wave conditions at the toe of the sea dikes. The wave model SWAN is being developed at Delft University of Technology and regularly new versions are being released. In May 2003, version 40.20 has been released, and RIKZ is considering to apply this model version for the determination of the HR-2006. At present, detailed information is lacking about the performance of this model version with respect to the Dutch water systems. Therefore this wave model version needs to be tested for its applicability for typical Dutch coastal and inland waters and optimal model settings for its application need to be determined.

The SWAN 40.20 model has several new features in comparison with earlier model versions. It has different numerical techniques for the solution of the systems of equations, such as the option of under-relaxation. It also has new model physics such as a new method for computing the whitecapping dissipation by means of the cumulative wave steepness method.

The purpose of this study is twofold. Firstly determine the relevant numerical and physical settings that can be used for the HR 2006. These settings must be chosen on the basis of a sensitive study and relevant parameters need to be used in a calibration of SWAN. The chosen parameter settings must be determined in such a way that they produce reliable and plausible results.

In this study the SWAN model has been applied to three field situations and two 1D situations. The field situations comprise the Slotermeer, the coastal area near Petten and the Westerschelde. The 1D-situations comprise a wave flume experiment of the Petten ray and an idealised fetch-limited wave growth in deep and shallow water.

In the present study the emphasis is on the integral wave parameters for the significant wave height  $H_s$  and the mean wave period  $T_{m-10}$ . These two parameters are used in the calibration of SWAN. The mean period measures  $T_{m01}$  and  $T_{m02}$ , the mean wave direction  $\theta$  and the directional spreading  $\sigma$  are used in the sensitivity analyses. The frequently used peak period measures  $T_p$ ,  $T_{pb}$  and  $T_{pm}$  are not used because they are either not part of the SWAN output ( $T_{pb}$  and  $T_{pm}$ ) and because they are not robust enough when the spectra have multiple peaks ( $T_p$  and  $T_{pm}$ ). For the 1D cases also the spectral narrowness  $\kappa$  (denoted as FSPR in SWAN) and the fraction of breaking waves ( $Q_b$ ) are shown.

The results of this study will be used in subsequent model computations with SWAN 40.20. One of these studies concerns the correction of wave periods as predicted by SWAN. For the short term a parametric correction is foreseen. A definite solution of the period under-prediction by SWAN requires long-term scientific investigations.



In this study a huge amount of computational results and plots has been produced. To keep the report manageable, only a selection of all generated plots is included in this report. All computational results and plots are available on the CD-ROM accompanying this report.

This study has been carried out by Gerbrant van Vledder of Alkyon in co-operation with Marcel Zijlema and André van der Westhuyzen of the SWAN development team at Delft University of Technology. David Hurdle of Alkyon was quality manager. Marcel Bottema of RIZA provided the SWAN schematisation for the Sloterveer and he provided wind, water level and wave measurements in the Sloterveer. Project co-ordination at RIKZ was carried out by Annette Kieftenburg and Marcel Zijlema. Their help with the execution of this study and preparation of this report is greatly appreciated.

Chapter 2 describes the methodology to obtain reliable settings for the SWAN model. The areas of interest are described in Chapter 3. The investigations to the numerical settings are described in Chapter 4. The results of the analyses of the physical processes for wave dissipation in shallow water and the applicability of an alternative way for white-capping dissipation is described in Chapter 5. The calibration of SWAN 40.20 is described in Chapter 6 and the results of the verification are given in Chapter 7. Conclusions are formulated in Chapter 8. Finally, recommendations for further work are given in Chapter 9.

## 2 Methodology

### 2.1 Introduction

To obtain reliable numerical and physical settings for SWAN 40.20, the following activities have been carried out:

1. A sensitivity study to identify relevant numerical settings.
2. A sensitivity study to identify relevant physical settings.
3. Calibration of SWAN 40.20 against field measurements.
4. Verification of the new numerical and physical settings against field measurements.

In the numerical study attention is given to the following parameters:

- Lower and upper limit of frequency range;
- Frequency resolution;
- Directional resolution;
- Percentage of the Phillips' limiter;
- Under-relaxation in combination with Phillips' limiter;
- Combined activation of source terms for triads and quadruplets;
- Limiter on decreasing wave action;
- Convergence criteria and number of iterations.

In the physical study attention is given to the following processes:

- Depth limited wave breaking;
- Bottom friction;
- Whitecapping dissipation;
- Non-linear triad interactions;
- Non-linear quadruplet interactions;
- The combination of triad and quadruplet interactions;
- Cumulative wave steepness method for computing whitecapping dissipation.

In the sensitivity analysis of the numerical settings the required number of iterations was set at a high value, whereas in the sensitivity analysis of the physical settings standard convergence criteria were used. Details are given in Chapter 4.

The numerical and physical settings have been tested against a number of field situations of October 26-27, 2002 storm for the coastal area near Petten, the Westerschelde and the Slotermeer. In addition, three cases of a wave-flume experiment and twelve cases of an academic fetch-limited situation have been considered.

The October 2002 has been the subject in recent hindcast studies with SWAN 40.16 for the Westerschelde (Gautier, 2003) and the coastal area near Petten (WL & Alkyon, 2003). Measured wave, wind and water level data for the Slotermeer for 27 October 2002 have been provided by Marcel Bottema of RIZA. The October 2002 storm was one of the severest storms in the last 10 years. During this storm the wind speed peaked at about 23 m/s and the wind direction turned from 250° to 290°.

The relevance of these settings was studied in a systematic way. For all five cases, a number of base cases were considered using the existing (default) settings of the SWAN 40.20 model. For Petten, the Westerschelde, the wave flume and academic situation, the chosen settings are based on the defaults of the WAM model (WAMDI, 1988), and experience with SWAN 40.11. For the Slotermeer, however, a different (with respect to

the SWAN 40.20 manual) default setting is used as based on recent studies by RIZA in this lake (Bottema, 2001). For this situation triads and quadruplets may be active at the same time and the limiter is always active in case of decreasing wave action due wave breaking (the so-called Qb-limiter).

The motivation to study the numerical settings is based on the fact that that SWAN 40.20 has an option to obtain a more stable solution by frequency dependent under-relaxation. Moreover, effects of both the Phillips' limiter and convergence criteria on numerical errors need to be considered.

The motivation to study the physical settings is twofold. In the coastal zone SWAN generally under-predict period measures, which is of prime interest for RIKZ. In the shallow inland lakes (e.g. IJsselmeer and Slotermeer) SWAN under-predicts both the significant wave height and mean wave periods, especially in areas with flat bottoms. In Alkyon (2001) and Bottema (2001) it was found that the source terms for triad and quadruplet interactions need to be activated simultaneously in these shallow areas. These applications are of specific interest for RIZA. Another motivation to study the physical settings is to test the applicability of the newly developed cumulative wave steepness methods in field cases.

The results of the sensitivity studies have been be used to determine the best numerical settings for SWAN 40.20 that produce reliable and plausible results that are free from numerical errors. They have also been used to select parameters for the calibration of SWAN 40.20.

In the third part of this study SWAN 40.20 will be calibrated against a number of field observations in the 27 October 2002 storm.

In the fourth part of this study the new model settings are verified against additional field data of the October storm that have not been used in the calibration.

## 2.2 Areas of interest

The sensitivity study with respect to numerical and physical settings has been carried out for 5 cases, 3 typical Dutch water systems, a wave flume experiment of a schematised Petten situation and an academic fetch limited situation. The field cases are coded with a 2-letter acronym:

- Sloterneer (SL)
- Coastal area near Petten (PT)
- Westerschelde (WS)
- Petten wave flume (FP)
- Fetch-limited situation (FL).

This coding appears in all SWAN input and output files, as well as in the figures showing results of this study.

For each field case five basic configurations have been considered. These configurations refer to a certain moment of time in the October 2002 storm with corresponding boundary conditions for wind, waves, currents and water levels.

For the Petten wave flume these configurations refer to the wave boundary conditions. For the fetch-limited situation the configurations refer to the wind speed and water depth.

Each of these areas and the characteristics of their configurations are described in detail in Chapter 3. In the SWAN input and output files as well as in the plots different configurations are coded with the acronym Cnm, where nm refers to the digits of the sequence number of the configuration.

## 2.3 Generation of input files

For each area of interest a series of SWAN input files was made. To distinguish between all resulting SWAN input and output files a special coding is introduced. File names generally consist of 4 parts.

- The first part refers to the area of interest (SL, PT, WS, FP or FL).
- The second part refers to the general situation, generally a moment of time with corresponding wind and flow conditions for the field cases, or to the wind speed in the academic case. It is coded as Cnm, where nm are the digits of the sequence number.
- The third part refers to the specific numerical or physical setting that has been used. Numerical settings are coded as Nnm, physical settings as Pnm and verification runs are coded as Vnm.
- The last part of the file name refers to the type or contents of the specific file. More details of the coding conventions are given in Appendix A of this report. For example, the file name SL\_C03\_P03.SWN refers to the Sloterveer, the third selected moment of time, the third physical setting and the extension SWN indicates that this file is a SWAN input file.

The input files are generated using a master input file for each computational grid. This master file contains the relevant keywords between brackets. An example of such a master file is given in Appendix B. The keywords in each master file refer to all numerical and physical settings used in this study. Lists of general, numerical and physical settings are specified in configuration files (\*.cfg). A special program has been applied to combine the information from the general configurations, numerical and physical settings into SWAN input files. At the same time a batch script is generated to start a sequence of SWAN computations. In this script a test is carried out to check if a certain computation has already been done. In this way a sequence of runs can be interrupted and restarted easily without redoing previously performed computations.

The first setting of a series of sensitivity runs corresponds to a base case, in which the currently used standard settings of SWAN 40.20 are used. The origin of these settings is described in Komen et al. (1994) and Booij et al. (1999). In the following settings, variations in each of the chosen parameters are included.

To study the sensitivity of SWAN 40.20 for different numerical and physical settings, special test output points are defined for each area of interest. For each test point SWAN produces so-called test output files containing the iteration behaviour of integral wave parameters and wave spectra.

## 2.4 Presentation of results

The sensitivity study regarding the numerical and physical settings of SWAN 40.20 produced a large amount of data. In this report only a selection is presented. To study the relevance of the numerical settings three main types of plots are made.

The first type of plots presents the iteration behaviour of the integral wave parameters  $H_s$ ,  $Tm-10$ ,  $Tm01$ , the mean direction  $\theta$ , the directional spreading  $\sigma$  and the magnitude of the source terms.

The second type of plot contains scatter diagrams showing the parameter values from the last iteration of the significant wave height  $H_s$ , the mean period measures  $Tm-10$ ,  $Tm01$ ,  $Tm02$ , the mean wave direction  $\theta$  and the directional spreading  $\sigma$ .

The third type of plot contains the spatial variation of integral wave parameters along the 1D-transect of the 1D computations for the Petten Flume (FP) and the fetch limited (FL) cases. For the Petten Flume the following parameters are shown: the significant wave height  $H_s$ , the mean wave period  $Tm-10$ , the directional spreading  $\sigma$  (DSPR), the spectral narrowness  $\kappa$  (denoted as frequency spreading FSPR in SWAN), and the fraction of breaking waves ( $Qb$ ). For the fetch-limited growth cases the significant wave height  $H_s$ , the mean wave period  $Tm-10$ , the directional spreading  $\sigma$  (DSPR), and the spectral narrowness  $\kappa$  (FSPR) are shown. In each of these plots the spatial variation of the selected parameters of the base case is shown, together with the results of related numerical or physical cases.

The iteration behaviour of integral wave parameters was initially obtained from SWAN PAR test files. They contain the values of the significant wave height  $H_s$ , the mean wave period  $Tm01$  and the total integral of the absolute values of the source terms as a function of iteration number. A disadvantage of the PAR files is that they lack information on other relevant integral wave parameters such as  $Tm-10$ ,  $Tm02$ , the mean direction  $\theta$  and the directional spreading  $\sigma$ . Another disadvantage of the PAR test files is that the integral wave parameters are only based on the finite frequency range of SWAN spectra. They do not contain the contribution of the spectral tail.

Full spectral information is available in the so-called S2D test files, but these are often too large for efficient post-processing. Therefore, a program was applied to convert the S2D test files in extended PAR test files. These extended PAR test files are referred to as S2P test files. They contain the following integral wave parameters:  $H_s$ ,  $Tm-10$ ,  $Tm01$ ,  $Tm02$ ,  $\theta$  and  $\sigma$ , all including the contribution of the spectral tail. In addition they contain the total integral (integrated over all frequencies and directions) of the source terms  $Swind$ ,  $Swcap$ ,  $Ssurf$ ,  $Sfric$ ,  $Snl3$  and  $Snl4$ . For  $Snl3$  and  $Snl4$  also the sum of the positive and negative parts has been computed.

In the plots showing the iteration behaviour of the integral wave parameters, the results for  $H_s$  and  $Tm-10$  and  $Tm01$ , are normalised with respect to the final (last iteration) values of the base case. In this way the relative importance of the effect of each numerical settings on the iteration behaviour of these integral parameters can be inspected.

The scatter plots are made for all test output points per computational grid and for all conditions. The x-axis relates to the base case, and the y-axis relates to a specific numerical or physical setting. These figures also contain a 1:1 line to find any deviations from the base case.

In addition, some plots have been made of the different 1D and 2D spectra and source terms for a specific area, output point, general condition, numerical or physical setting, and iteration number. These spectra are taken from the SWAN S1D and S2D test files generated with the SWAN TEST option.

## 3 Description of cases

### 3.1 Introduction

In this study five different geometry's have been considered: three field cases, one wave flume and one academic situation. The field cases are for the Slotermeer, the coastal area near Petten and the Westerschelde. These cases are considered to be representative for the Dutch coastal and inland waters. The wave flume case is based on a schematised Petten situation. The academic case was added to study fetch-limited wave growth at various wind speeds and water depths.

### 3.2 Slotermeer

The Slotermeer is a shallow inland lake in the province of Friesland in the north of the Netherlands. The size of the lake is approximately 4.5 km by 2.5 km. The main axis of the lake is from south-west to north-east. Most of the strong wind conditions are from the south-west. The average depth is about 1.8 m.

In the north-eastern part of this lake a capacitance-wire wave measuring device is placed with co-ordinates  $x=172,496$  (m),  $y=548,506$  (m) in the Paris co-ordinate system. The bottom topography of this lake is shown in Figure 3.1 together with the location of the measurement point F29. M. Bottema of RIZA provided a SWAN schematisation of the Slotermeer. The resolution of the computational grid is 40 m in x- and y-direction, with the origin at location  $x_0=168,800$  (m),  $y_0=545,600$  (m).

The variation of wind and wave parameters on the 27<sup>th</sup> of October 2002 is shown in Figure 3.2. For the sensitivity study of the numerical settings the moment of maximum wind speed has been taken. This occurred at 15:00 hours. The corresponding conditions are:

$$U_{10}=21.4 \text{ m/s}$$

$$\theta_w = 251^\circ$$

$$\text{water level} = \text{NAP} - 0.43 \text{ m}$$

At this time the measured significant wave height was 0.71 m and the mean period  $T_{m-10}$  was 2.95 s. Computations by Bottema with SWAN version 40.16 give an under-prediction of both the significant wave height (0.56 m) and the mean period  $T_{m-10}$  (2.35 s).

For the sensitivity study and calibration of SWAN 40.20 the following moments of time were selected to include the build-up, the peak and the decay phase of this storm. In this way a range of wind speeds and wind directions are included.

Case	Time (hours)	$U_{10}$ (m/s)	$\theta_w$ (°)	$H_s$ (m)	$T_{m-10}$ (s)	$h$ NAP (m)
C01	04:00	10.6	168	0.25	1.72	-0.57
C02	07:00	13.5	195	0.37	2.03	-0.56
C03	15:00	21.3	257	0.71	2.96	-0.45
C04	18:00	20.0	285	0.63	2.76	-0.51
C05	21:00	18.0	300	0.56	2.46	-0.53

Table 3.1: Wind, water level and wave conditions in the Slotermeer for the selected moments in the storm of 27 October 2002.



### 3.3 Petten field case

The Petten field case was investigated by WL|Delft Hydraulics & Alkyon (2003) to investigate the reliability of the RAND2001 database and the SWAN model. In that study two versions of the wave model SWAN were used, viz. 30.62 and 40.16. A detailed description of this situation can be found in WL&Alkyon (2003). For the present study the schematisation for the advanced case were used. This comprises the computational grids N02, K12 and E24, with spatial resolution of 500 m, 100 m and 20 m respectively. In addition the 'best' wind fields, current and water level fields were used. The location of the SWAN computational grids is shown in Figure 3.3 together with the measurement station ELD and YMW. These stations provided the wave boundary conditions for the SWAN computations. Closer to the coast a number of measurement stations are location along a ray. The bottom topography and the locations of the measurement points are shown in Figure 3.4.

For the present study the storm of 27 October 2002 was used. In this storm 5 moments of time were hindcast. The dates and time of this storm are shown in Table 3.2.

Case	Date and time
C01	26 October 2002, 7:00 hours
C02	27 October 2002, 6:00 hours
C03	27 October 2002, 11:00 hours
C04	27 October 2002, 14:20 hours
C05	27 October 2002, 17:00 hours

Table 3.2: Date and time of the Petten cases of the storm of 26/27 October 2002.

### 3.4 Westerschelde

The Westerschelde case is taken from Gautier (2003). For this study the same model schematisation has been used, no modifications were made to the boundary conditions driving the wave model. In that study 3 types of rectangular computational grids were used. A course North Sea grid N01 with a spatial resolution of about 500 m, three nested grids in the Westerschelde (W01, W02 and W03) with a resolution of 100 m, and 9 detailed computational grids (D01 through D09) located around the measurement locations. The location of these grids is shown in Figure 3.5. The names of the measurement stations and their position in the detailed grids are shown in Figure 3.6.

Following Gautier (2003) the following 5 instants in the storm of 27 October 2003 are considered:

1. 8:20 hours (C01)
2. 12:00 hours (C02)
3. 14:40 hours (C03)
4. 17:20 hours (C04)
5. 19:40 hours (C05)

In the present study only the computational grids N01, W01, W02, W03 and D01 through D04, and D06 through D09 have been used.



### 3.5 Petten wave flume

In 1999 the Petten topography was rebuild in a wave flume. A detailed description thereof can be found in WL|Delft Hydraulics (1999). In 2000 numerical model investigations with SWAN 30.75 were performed (WL|Delft Hydraulics, 2000). For this study, 3 cases were considered for the numerical analysis, viz. 2.11, 2.13 and 2.51. These cases were also considered in the SWAN physics + project (WL&Alkyon, 2002). These cases correspond to the following boundary conditions:

Test	$H_{m0}$ (m)	$T_{m0.1}$ (s)	$T_p$ (s)	Water level (m)
2.11 (C01)	2.06	7.15	8.36	2.1
2.13 (C02)	3.81	10.11	11.53	2.1
2.51 (C03)	5.64	7.88	8.79	4.7

Table 3.3: Integral wave parameters for imposed spectra in the Petten wave flume.

The bottom profile of the Petten flume and the location of the output points is shown in Figure 3.7. The locations of the output points are: 0 m, 670 m, 830 m, 910 m, 1000 m, 1170 m and 1240 m.

### 3.6 Fetch-limited case

The fetch-limited case is taken from Alkyon (1999) "Investigation of the iteration behaviour of SWAN". It consists of a uniform fetch with a length of 25 km. Output points were defined at the locations: x=5 km, 10 km, 15 km, 20 km and 25 km. The spatial resolution in x-direction was 100 m.

Three wind speeds and 3 water depths were considered. These are summarised in Table 3.4.

Case	Wind speed (m/s)	Water depth (m)
C01	10	1000
C02	10	10
C03	10	5
C04	20	1000
C05	20	10
C06	20	5
C07	30	1000
C08	30	10
C09	30	5
C10	40	1000
C11	40	10
C12	40	5

Table 3.4: Wind speed and water depth for the fetch-limited wave growth cases.

## 4 Sensitivity of SWAN 40.20 to numerical parameters

### 4.1 Introduction

Prior to the calibration of the SWAN model, the sensitivity of its computational results to numerical settings has been determined. Since SWAN uses an iterative procedure to obtain the solution of its systems of equations, sufficient iterations should be carried out to ensure that the final solution is obtained.

To determine the sensitivity of the numerical settings, a reference run has been carried out for each situation (viz. for each computational grid and case). The numerical and physical settings for this reference run are based on the default settings that are now being used in SWAN (Holthuijsen et al. 2003). This reference run is coded as [N01]. Next, 15 variations of numerical settings have been imposed, these settings are coded as [N02] through [N16]. In view of known deficiencies of the currently implemented convergence criteria of SWAN, 3 additional sensitivity cases have been added to investigate the effect of various settings for these criteria. These settings are coded as [N17] through [N19].

The list of settings considered in the sensitivity analysis is given in Table 4.1. The codes in the first column are also used in the names of the corresponding files and plots. The second column gives the description of the variation. In the following sections each of these variations is explained in more detail. The precise numerical values are given in the Table 4.2 for the Slotermeer and in Table 4.3 for the other areas (Petten, Westerschelde, Petten flume and fetch-limited case). The Tables 4.2 and 4.3 are given after the main text of this report. The chosen variations in numerical settings are based on expert judgement, in order to see some effect of variations. No systematic study was performed to investigate other values.



Code of	Description
N01	Base case, different for each area of interest
N02	Lower lower frequency
N03	Higher upper frequency
N04	Increased number of frequency intervals
N05	Decreased number of frequency intervals
N06	Increased directional resolution
N07	Decreased directional resolution
N08	Double value for fraction of Phillips' limiter
N09	Triple value for fraction of Phillips' limiter
N10	Small amount of under-relaxation
N11	Small amount of under-relaxation and increased fraction of Phillips' limiter
N12	Large amount of under-relaxation
N13	Large amount of under-relaxation and increased fraction of Phillips' limiter
N14	Combined (de)activation of triads and quadruplets
N15	No (de)activation of limiter with decreasing wave action
N16	No (de)activation of limiter with decreasing wave action and combined (de)activation of triads and quadruplets
N17	Convergence criteria based on 2% level and in 98% of the grid points
N18	Convergence criteria based on 1% level and in 99% of the grid points
N19	Convergence criteria based on 3% level and in 97% of the grid points

Table 4.1: Summary of numerical variations.

In the first 16 cases, [N01] through [N016], the number of iterations is set to a high value. The required number of iterations was set to 100 for the Sloterneer, Petten wave flume and the fetch-limited wave growth tests. For the Westerschelde and Petten cases a value of 25 for most numerical tests. It was set to 50 for the tests with under-relaxation [N10, N11, N12 and N13]. The values of 25 and 50 were chosen to keep the computational times acceptable.

The required number of iterations in these SWAN computations was specified using the command NUMERIC ACCURACY in which the parameter NPNTS was set to 101, and the parameter MXITST to the required number of iterations.

## 4.2 Spectral resolution

### 4.2.1 Introduction

The spectral resolution of SWAN 40.20 (and previous versions) is specified by the command:

CGRID CIRCLE [MDC] [FLOW] [FHIGH] [MSC]

with

[FLOW]      the lowest discrete model frequency.  
[FHIGH]     the highest discrete model frequency.  
[MSC]       number of discrete model frequencies intervals.

[MDC]        number of discrete model directions, distributed over the full circle.

The default spectral resolution of SWAN 40.20 is based on previous experience. The SWAN manual recommends the frequency range [0.03 Hz – 0.8 Hz] with 30 frequency bands. This range was used in the SWAN computations for the Westerschelde, Petten, Petten flume and fetch-limited wave growth. For the Sloterveer another distribution of frequencies was used (Bottema, 2001). The frequency range was from 0.08 to 1.7 Hz with MSC=32. Bottema (2003) suggests varying the frequency range with wind speed, but this was not done in this study.

The discrete frequencies are distributed geometrically according to:

$$f_i = f_1 (1 + x)^{i-1} \quad \text{for } i = 1, \text{MSC} + 1 \quad (4.1)$$

with  $x$  the frequency resolution, and  $f_1 = \text{FLOW}$ .

In the SWAN manual it is recommended to choose a frequency resolution of 10%. This corresponds  $x=0.1$ . This recommended value seems to originate from experience with the Discrete Interaction Approximation (Hasselmann, et al. 1985), although systematic study is known supporting this value. Van Vledder et al. (2000) performed a numerical experiment with SWAN and a frequency resolution 3.4% causing undesired instabilities, which could be traced to limitations of the DIA.

The default setting of SWAN for the frequency range and number of frequency intervals is 0.03 Hz – 0.8 Hz, and MSC=30. Using (4.1) this leads to a resolution of  $x=0.1157$ , which is slightly higher than the recommended 10%. In fact, a resolution of 10% would lead to MSC=34.

For the Sloterveer, the default settings have been modified by Bottema (2003), who uses a frequency range of 0.08 Hz – 1.7 Hz and MSC=32, corresponding to a frequency resolution of  $x=0.1002$ .

#### 4.2.2 Frequency resolution

To test the frequency range four settings are modified:

- [N02]: The lower minimum frequency is reduced by 25%, while the number of frequencies (MSC) is increased to keep the same frequency resolution. The variation by 25 % was selected after some trial and error in order to see some effect.
- [N03]: The maximum discrete model frequency is increased by 25%, while the number of frequencies (MSC) is increased to keep the same frequency resolution..
- [N04]: The frequency resolution is reduced by 20%, by choosing more frequency intervals.
- [N05]: The frequency resolution is increased by 20% by choosing less frequency intervals.

#### 4.2.3 Directional resolution

The default directional resolution is 10°. To test the sensitivity of SWAN results regarding other resolution two settings are modified:

- [N06]: The directional resolution is increased from 10° to 7.5° (MDC=48).
- [N07]: The directional resolution is decreased from 10° to 15° (MDC=24).

### 4.3 Percentage of Phillips' limiter

The default value of the fraction of the Phillips' limiter is now 10%. This value is based on experience with the WAM model and the WAVEWATCH model. To investigate if this value is not too stringent, two larger values are tested. Therefore the following settings were modified using the command NUMERICS LIMITER=[limiter]:

- [N08]: Limiter=0.2, corresponding to a level of 20%, and
- [N09]: Limiter=0.3, corresponding to a level of 30% code.

The chosen values of 20% and 30% were chosen on the basis of expert judgement.

### 4.4 Under-relaxation

A frequency-dependent under-relaxation as described in Zijlema and Westhuyzen (2003) has been introduced in SWAN 40.20 to stabilise the iteration process. In the SWAN 40.20 model under-relaxation is controlled by the parameter [ALFA] in the NUMERICS command. It is noted that in SWAN 40.20 the under-relaxation is not active by default (ALFA=0). On page 24 of the User manual a value of ALFA=0.05 is recommended if the user is intended to use under-relaxation.

Under-relaxation is considered to be a promising approach to limit the influence of limiters and to avoid that limiter may become part of the solution.

To test the performance of under-relaxation four settings are considered. In these settings two values are distinguished, with ALFA=0.025 and 0.05 in combination with the LIMITER=0.1 and 0.5. Test cases are coded as [N10, N11, N12 and N13].

It is expected that the use of under-relaxation reduces the effect of the Phillips' limiter. Also, under-relaxation is expected to give slower, but more robust, convergence behaviour.

### 4.5 Simultaneous activation of triads and quadruplets

In previous versions of SWAN (version 40.11 and lower) the source terms for triads and quadruplets were not allowed to be active at the same time. In general the source term for the quadruplets is always active. The activation and deactivation of these source terms is controlled by the Ursell number, defined as:

$$U_r = \frac{g}{8\sqrt{2}\pi^2} \frac{H_s T_{m01}^2}{d^2} \quad (4.2)$$

In the case the Ursell number exceeds a pre-set threshold the quadruplet source term was deactivated and the triad source term becomes activated. Initially, this was imposed per sweep sector. For the Dutch coastal waters this approach seemed to work satisfactory, since it was based on the reasonable assumption that in shallow water triads are dominant over quadruplets. However, experience with SWAN 40.11 in the Markermeer (Alkyon, 2001) indicated clearly that this approach was not valid. This could result in a strange behaviour strongly affecting the convergence behaviour of SWAN, as was shown in Alkyon (2001) and Bottema (2001). Here it was shown that for some sweep sectors the triads were activated and the quadruplets for the other sectors.

In 2001 slight improvements were implemented in SWAN version 40.11 by letting the triads or quadruplets be active or de-active for all sweep sectors per iteration. With the release of beta-version SWAN 40.16 and the official release SWAN 40.20, triads and quadruplets can be active simultaneously. This approach was followed in the hindcast studies for the Westerschelde (Gautier, 2002) and Petten (WL & Alkyon, 2002).

In view of continuing investigations to the optimal limiter an option was introduced to deactivate the quadruplets and the limiter when the Ursell number exceeds (another) threshold value. This option is build in the LIMITER command.

The Ursell number is used to control the activation and deactivation of the triads and quadruplets. Triads are active when  $U_r > URSLIM$ , and quadruplets are deactivated when  $U_r > URSELL$ . Furthermore,  $URSLIM < URSELL$ . These commands are described under the items LIMITER and TRIAD.

The default settings in SWAN 40.20 are such that quadruplets are deactivated when triads become active. The default threshold values for the Ursell number are  $URSELL=0.1$  and  $URSLIM=0.1$ . For the sensitivity study, these settings were used in the base case for the Westerschelde and Petten, whereas for the Sloternmeer the following parameter settings were used in the base case:  $URSELL=10$  and  $URSLIM=0.01$ .

In this study the effect of allowing the simultaneous activation of triads and quadruplets was analysed in test [N14]. For the Westerschelde, Petten, Petten flume and fetch-limited wave growth, triads and quadruplets are set both active, whereas for the Sloternmeer triads and quadruplets are set mutually exclusive.

## 4.6 No limiter in case of strong decreasing wave action due to wave breaking

The limiter on decreasing action is turned off when the fraction of breaking waves (as computed by SWAN) exceeds a certain threshold  $Q_b$ . The default value is  $Q_b=0.00001$ . Several studies have indicated that this might lead to instabilities (Bottema, 2001). Therefore, two tests are performed to see investigate if this limiter may be turned off, optionally in combination with the combined computation of triads and quadruplets. In this study the  $Q_b$ -limiter was set to 1 to ensure that this limiter is always active. This relatively high setting was taken from Bottema (2001). No systematic study was carried out if intermediate values of the  $Q_b$ -limiter are possible.

In this study a distinction is made between the Sloternmeer area and the other cases. For the Sloternmeer case the first test [N15] the limiter is switched off and in the second test [N16] also the combined computation of triads and quadruplets is disabled. For the other cases the opposite choices are made.

## 4.7 Convergence criteria

In all previous cases [N01] through [N016], section 4.2.1 through 4.2.7 the number of iterations is set to a high value and  $NPNTS=101\%$  thus forcing SWAN to make the maximum number of iterations. For the Westerschelde and Petten cases a value of 25 was used, except for the tests with under-relaxation [N10, N11, N12 and N13] in which 50 iterations were used. For the Sloternmeer and the Petten Flume experiments 100 iterations were imposed and for the Fetch Limited growth cases 50 iterations were imposed.



The convergence criteria are specified with the command:

```
NUM ACCUR [DREL] [DHOVAL] [DTOVAL] [NPNTS] STAT mxitst= [MXITST] alfa=[ALFA]  
limiter=[LIMITER]
```

In the default settings of SWAN 40.20 the values for the parameters [DREL], [DHOVAL] and [DTOVAL] are equal. This equivalence was also used in this study; therefore they are coded here with the (same) keyword [DFRAC]. In the master input file, the NUM command is specified by:

```
NUM ACCUR [DFRAC] [DFRAC] [DFRAC] [NPNTS] STAT mxitst= [MXITST] alfa=[ALFA]  
limiter=[LIMITER]
```

By default the tolerances are 2% and the number of points that should satisfy this condition if NPNTS=98%. In this study, also two other settings are tested, a stricter criterion and a less stricter. Therefore the following convergence criteria have been tested:

- [N17]: 2% level, [dfrac]=0.02 and [npnts]=98.
- [N18]: 1% level, [dfrac]=0.01 and [npnts]=99.
- [N19]: 3% level, [dfrac]=0.03 and [npnts]=97.

## 4.8 Results of the numerical sensitivity study

### 4.8.1 Sloterneer

The iteration behaviour of SWAN for all numerical settings at location F29 at the peak of the storm (case C03) is shown in the Figures 4.1.2 through 4.1.19. (Figure 4.1.1 is intentionally left out). In addition scatter diagrams for all situations (C01 through C05) and all test output points in the Sloterneer (see Figure 3.1) are shown in the Figures 4.2.2 through 4.2.19 for all numerical settings (Figure 4.2.1 is intentionally left out).

Inspection of these results leads to the following findings:

Based on the results the following results are relevant.

N02: A lower minimum frequency has little effect on the final, but the convergence behaviour is smoother.

N03: A higher maximum frequency has a small effect on the  $H_s$  and  $T_{m-10}$ , and it decreases the mean period measures  $T_{m01}$  and  $T_{m02}$ ;

N04: A higher frequency resolution does not significantly affect the results;

N05: A lower frequency resolution does not significantly affect the results;

N06: A higher directional resolution does not significantly affect the results;

N07: A lower directional resolution does not significantly affect the results;

N08: A higher fraction of the Phillips' limiter (20%) does not affect the final (last iteration) results but it affects the convergence behaviour of  $H_s$  during the first 40 iterations in negative sense;



N09: A even higher value of the fraction of the Phillips' limiter (30%) does not affect the final results but it leads to more wiggles in the convergence behaviour of the  $H_s$  and the quadruplet source term. It is also found that the level of the quadruplet source term is about 40% higher.

N10: A small amount of under-relaxation ( $\alpha=0.025$ ) leads to stable convergence behaviour since there are less wiggles. More iterations are needed to reach full convergence. The level of quadruplet magnitude is lower than in the base case.

N11: A small amount of under-relaxation ( $\alpha=0.025$ ) with a more flexible Phillips' limiter (50%) gives a similar behaviour as case N10; the level of the magnitude of the quadruplet source term is lower.

N12: A large amount of under-relaxation ( $\alpha=0.05$ ) gives robust convergence behaviour but it takes longer to reach convergence; even after 100 iterations no convergence has been obtained.

N13: A large amount of under-relaxation ( $\alpha=0.05$ ) and a high value of the Phillips' limiter (50%) produce similar results as the previous case. This shows that  $\alpha$  is dominant over the the value of the Phillips' limit becomes less important.

N14: Switching off the combined computation of triads and quadruplets has hardly any effect on the results;

N15: Resetting the Qb-limiter to its default produces erratic oscillating convergence behaviour. Also the scatter diagram shows that this setting affects the final results, yielding more scatter. Clearly no convergence is obtained.

N16: Resetting the Qb-limiter to its default and allowing the combined combination of triads and quadruplets produces similar results as case N15.

N17: Using the 0.02% and 98% convergence criteria yields results that did not converge. There is no systematic effect on the final results;

N18: Using the 0.01% and 99% convergence criteria yields slightly better results than case N17, but still the model has not fully converged;

N19: Using the 0.03% and 97% convergence criteria of SWAN 30.62 produces unconverged results. The results in Figure 4.2.19 show that small values of  $H_s$  and  $Tm01$  (corresponding to low wind speeds) tend to be lower, whereas high values of  $H_s$  and  $Tm01$  tend to be higher (corresponding to the high wind speed cases).

## Conclusions

Based on these finding the following conclusions can be drawn for the Slotermeer.

- Variations in spectral resolution hardly affect the convergence behaviour and final results. Although the choice of the highest model frequency influences the period measures for  $Tm01$  and  $Tm02$ .
- Allowing a higher value for the Phillips' limiter produces less stable convergence behaviour than the present setting of 10%. Although it does not affect the final results, it may affect the convergence criteria in an unexpected way.
- The combined activation or deactivation of triad and quadruplets gives similar results. It is therefore not necessary to treat them exclusively in SWAN.

- Using a low value of the Qb limiter produces erratic behaviour. It is therefore better to activate this limiter always.
- Under-relaxation generally leads to more stable convergence behaviour, but it takes more iterations to reach full convergence. The smooth behaviour of integral wave parameters has the risk that the present method to treat the convergence criteria may stop the iteration process before full convergence is reached.
- The present convergence criteria, when using the 1%, 2% and 3% accuracy's lead to unconverged results. This implies that the present implementation of the convergence criteria needs to be revisited.

#### 4.8.2 Westerschelde

The results of the Westerschelde are made for the computational grids W01, W02 and W03, and they are available in the form of line plots of the convergence behaviour and scatter diagrams.

For grid W01 results of the iteration behaviour for all numerical settings for situation C03 and the measurement location (station CDD) are shown in the Figures 4.3.2 through 4.3.19. (Figure 4.3.1 is intentionally left out). In addition scatter diagrams for all situations (C01 through C05) and all output points in computational grid W01 are shown in the Figures 4.4.2 through 4.4.19 for all numerical settings.

Inspection of the results for grid W01 leads to the following findings:

- Lowering the minimum model frequency does not affect the results, but increasing the upper model frequency slightly affects the results for the significant wave height and  $Tm-10$  and more for the  $Tm01$  and  $Tm02$ .
- Changing the frequency resolution does not significantly affect the results.
- Increasing the directional resolution gives slightly smaller directional spreading, whereas a lower directional resolution gives slightly higher directional spreading.
- Relaxing the Phillips' limiter produces less stable convergence behaviour. It hardly affects the final results.
- Under-relaxation leads to smoother but slower convergence behaviour. The convergence behaviour for the mean wave period  $Tm01$  is more slowly than for the significant wave height  $Hs$ . Comparison with the base case also shows that the base case has not fully converged for the period measures.
- Combined computation of triads and quadruplets give very similar results.
- Keeping the Qb-limiter active with decreasing wave action affects gives slightly lower wave heights and lower wave periods in the order of 1%.
- Use of the convergence criteria with 1%, 2% or 3% limits leads to unconverged results and non-systematic effects on the results.

For the W02 grid very similar results are obtained, except for the fact that the differences with the base case show less scatter.

For the W03 grid it is found that choosing a higher model frequency leads to lower results for the period measures. This is due to the fact local wave growth (at high frequencies) is dominant in this part of the Westerschelde.

#### 4.8.3 Petten

For the coastal area near Petten a deep water test point (MP2/021) in computational grid E24 and a shallow point (062) in computational grid E24 are considered. The results of the computations for Petten are visualised in the same way as for the Slotermeer and

Westerschelde. These plots are not included in this report because they show very similar results as for the Slotermeer and Petten. However, the plots are available on the CD-ROM accompanying this report.

Inspection of the results generally leads to the same conclusions as for the Westerschelde. For the deep water point (MP3) in the E24 grid the following observations are made:

- Changing the spectral range does not significantly affect the results for the  $H_s$ , but it does affect the period measures. The runs for case N02, corresponding to a lower minimum frequency lead to significantly higher values for the  $Tm-10$ . This is a direct effect of the fact that the boundary spectra have a relatively large amount of energy at lower frequencies, and the energy in these low frequency bands affects the computed values of  $Tm-10$  the most.
- Changing the frequency and directional resolution does not affect the results in a significant way.
- Relaxing the Phillips' limiter to 20% or 30% leads to relatively large wiggles.
- Under-relaxation leads to very slow convergence behaviour, and it tends to an under-prediction of measured period measures.
- The combined computation of triads and quadruplets gives very similar results, although the period measures are slightly lower.
- Changing the Qb-limiter on decreasing wave action hardly affects the results
- The convergence criteria based on the 1% and 2% give converged results for the significant wave height but not for the mean wave period.

For the shallow water point (171) in the E24 grid the following extra (deviating from those for the deep water point in K12) observations were made.

- Relaxing the Phillips' limiter to 20% and 30% gives slightly less stable iteration behaviour.
- Under-relaxation gives stable, but still rather slow convergence. Compared to the deep water point, convergence is much better.
- The convergence criteria based on the 1% and 2% lead to better converged results than for the deep water point. The 3% criterion leads to unconverged results for  $H_s$  and  $Tm01$  that deviate a few percent from those with a large number of iterations.

#### 4.8.4 Petten wave flume

The results for the Petten wave flume are similar to the results for the Petten field case. Only for case [N16] the results produce much higher wave height and wave periods. In this case triads and quadruplets are both active and the Qb-limiter is always activated.

An overview of the spatial variation of integral wave parameters along the 1D-transect for case B12 is shown in the Figures 4.5.1 through 4.5.8. Figure 4.5.1 shows the effect of a lower model frequency (case N02). Figure 4.5.2 shows the effect of a higher upper model frequency (case N03). Figure 4.5.3 shows the effect of different frequency resolutions (cases N04 and N05). Figure 4.5.4 shows the effect of different directional resolutions (cases N06 and N07). Figure 4.5.5 shows the effect of various values of the Phillips' limiter (cases N08 and N09). Figure 4.5.6 shows the effect of various settings for under-relaxation (cases N10, N11, N12 and N13). Figure 4.5.7 shows the effect of various combinations of the Ursell limits and the Qb limiter (cases N14, N15 and N16). Figure 4.5.8 shows the effect of various threshold values for the convergence criteria (cases N18, N18 and N19).

The similar figures for the other cases, the plots showing the iteration behaviour and the scatter plots are available on the CD-ROM accompanying this report.

#### 4.8.5 Fetch-limited wave growth

The results for the fetch-limited situation are in general not sensitive for variations in numerical settings. This is probably due to the fact that wave growth is not affected by variations in bottom topography. Only for the shallow water runs some effects are visible in the results. For deep water, variation in the numerical settings have no effect on the results.

An overview of the spatial variation of integral wave parameters along the 1D-transect for case C08 is shown in the Figures 4.6.1 through 4.6.8. This case corresponds to fetch-limited wave growth in water with of depth of 10 m and a wind speed of 30 m/s. The description of these plots is similar to those of the Figures 4.5.1 through 4.5.8.

The similar figures for the other cases, the plots showing the iteration behaviour and the scatter plots are available on the CD-ROM accompanying this report.

### 4.9 Conclusions

Based on the results of the sensitivity study of numerical settings for SWAN 40.20 for all computational areas the following conclusions can be formulated.

- Changing the upper and lower model frequency has a small effect on the convergence behaviour and final results. For Petten a smaller value for the lower frequency affects the predicted period measure  $Tm-10$ . This is a direct effect of low frequency in the wave boundary conditions. Increasing the highest model frequency generally affects the prediction of the period measures  $Tm01$  and  $Tm02$  especially in areas with local wave growth. The sensitivity of  $Tm-10$  with respect to the choice of flow is not considered to be a problem of SWAN, but more a problem in the handling of SWAN model results and the comparison of measured wave data.
- Changing the frequency resolution has little effect on the results. Increasing this resolution would yield increased computational time and is therefore not recommended. Also because a too high resolution will generate undesirable results with the DIA.
- Modifying the directional resolution is not recommended. A higher resolution does not yield different results and would lead to increase computational times. Lowering the directional resolution is not recommended because it leads to some random scatter compared to the base case. For wind-driven seas the current resolution of  $10^\circ$  is deemed sufficient. For the prediction of swell, probably a finer resolution is needed, say  $5^\circ$ .
- Relaxing the Phillips' limiter from 10% to 20% or 30% has a small effect on the computational results. Its main effect, however, is to produces more unstable convergence behaviour of integral wave parameters. It is therefore not recommended to use a less stricter criterion.
- The combined computation of triads and quadruplets gives similar results compared to the situation that either one of them may be active per iteration. From a theoretical point of view it is better to keep them both active.
- Keeping the Qb-limiter active with decreasing wave action is necessary for the Sloterneer case, but not for the other field cases. Since it hardly affects the results for these other areas, it is recommended to keep this limiter active by setting Qb=10 in the LIMITER command.



- Under-relaxation generally leads to robust, but slower, convergence behaviour. In the interplay with the Phillips' limiter it was found that a high amount of under-relaxation make the Phillips' limiter obsolete. It was also found that under-relaxation works better in the detail computational grid E24 for Petten.
- The current method to end the iteration process based on the default convergence criteria using 0.02% fractions and 98% of the number of grid point is too loose in many cases. Even using 0.01% and 99% values does not improve the situation (forcing more iterations). For future production runs an even stricter convergence criterion must be found.

The results of the sensitivity analysis can be summarised in the following table. This shows the impact of changing a certain numerical setting on the prediction of the significant wave height  $H_s$  and mean wave period  $Tm-10$ .



	SL		WS		PT		FP		FL	
	<i>H</i>	<i>T</i>	<i>H</i>	<i>T</i>	<i>H</i>	<i>T</i>	<i>H</i>	<i>T</i>	<i>H</i>	<i>T</i>
Fmin ↓	0	0	0	+	0	+	0	0*	0	0
Fmax ↑↓	0	0	0	0	0*	+	0	0*	0	0
MSC↑	0	0	0	0	0	0*	0*	-	0	0
MSC↓	0	+	0	0	0	-	0	0*	0	0
MDC↑	0	0	0*	0*	0	0*	0	-	0	0
MDC↓	0	0	-	-	0	0*	-	-	0	0
Phillips. 20%	0	0	0*	0*	0*	0*	0*	-	0	0
Phillips 30%	0	0	0*	-	0	-	0*	-	0*	0*
UR [N10]	0	0	0*	-	0*	-*	0	0*	0*	-
UR [N11]	0	0	+	--	0*	--	0*	0*	0*	0*
UR [N12]	0	+/-	-	0*	0*	-	0*	0*	0*	-
UR [N13]	0*	-	-	-	0*	--	0*	0*	0*	0*
SnI3 & SnI4 [N14]	0	0	0*	+	0	+	-	+	0	0
SnI3 & SnI4 [N15]	0	++	-	-	+	--	+	-	0	0
SnI3 & SnI4 [N16]	0	++	0*	0*	+	0*	++	++	0	0
Convergence 0.02% & 98%	--	++	0	0	0	+	0*	-	0*	0*
Convergence 0.01% & 99%	-	+	0	0	0	00	-	0*	+	
Convergence 0.03% & 97%	--	++	0	0	+	0*	0*	-	-	0*

Table 4.3: Impact of a certain physical parameter on the integral wave parameters *Hs* and *Tm-10*.

In Table 4.3 the meaning of the symbols is as follows:

Strong decrease	(--)
Small decrease	(-)
No effect	(0)
No mean effect	(0)
Small increase	(+)
Strong increase	(++)
Additional scatter	(*)

## 4.10 Recommendations

Based on the results of the sensitivity study of the numerical settings, the following recommendations are made:

- The frequency range and resolution are sufficient.
- The directional resolution of 10° is sufficient.
- Under-relaxation is promising development to obtain stable convergence behaviour, but the amount of iterations needed to reach full convergence is still too large for practical (operational) computations.



- Triads and quadruplets must be activated simultaneously, this can be obtained by choosing  $URSLIM=0.01$  and  $URSELL=10$ .
- The Qb-limiter in the case of strong wave breaking must remain activated. This can be obtained by choosing  $Qb=1$ .
- The convergence criteria need to set to strict values. Choosing the fraction equal to 0.01 and the number of required points to 99%, may provide results that are closer to full convergence.

## 5 Sensitivity of SWAN 40.20 to physical settings

### 5.1 Introduction

In this Chapter the results are presented of the sensitivity of the physical settings of the SWAN 40.20 model. The reference case uses the recommended default setting as described in the SWAN manual. This includes the following settings:

The source terms for deep water wave growth are based on WAM 3 physics as specified by the command GEN KOMEN. For shallow water the source terms for depth limited wave breaking, bottom friction and triad wave-wave interactions given by their default values. The base case is coded as P01.

In the SWAN input file the default physical settings for these source terms are given as:

GEN KOMEN CDS2=2.32e-5  
QUAD LAMBDA=0.25 CNL4=3e7  
BREAK ALPHA=1.0 GAMMA=0.73  
FRIC CFJON=0.067  
TRIAD TRFAC=0.1 URSLIM=0.1

In this study 18 variations have been imposed on the physical settings of the magnitude and other parameters of the source terms for surf breaking (ALPHA and GAMMA), bottom friction (CFJON), white-capping dissipation (CDS2), quadruplets (CNL4 and LAMBDA) and triads (TRFAC). In addition, some settings of the cumulative wave steepness method for the computation of white-capping dissipation have been investigated. A list of the actual values of the physical settings is given in Table 5.1.

It is noted that the CSM settings for the cases [P17], [P18] and [P19] have only be applied to the Slotermeer, the Petten Flume and the Fetch Limited wave growth situations. So, these settings have not been used for the Westerschelde and the Petten field situations.

The size of the variations imposed on the physical settings is 10% in most cases. In some other cases, the variations are larger in order to see some effect on the computational results. For LAMBDA the variation is 20%, for CNL4 it is 16.7%, for TRFAC the variation is a factor 2 and for CST a variation of 30% is imposed.

In contrast to the sensitivity study of numerical settings, the number of required iterations is not pre-set at a (high) fixed value. Instead, relatively strict convergence criteria are used. These criteria correspond to case [N18] in which DREL=DHOVAL=DTOVAL=0.01 and NPTNS=99%.

### 5.2 Depth limited wave breaking

Depth limited wave breaking is influenced by the parameters  $\alpha$  and  $\gamma$  of the modified Battjes-Janssen (1978) source term. These parameters can be specified by the command BREAK alpha=[ALPHA] gamma=[GAMMA]. In the present study four different settings have been used:

- [P02]: A higher value of [ALPHA]=1.10,
- [P03]: A lower value of [ALPHA]=0.90,
- [P04]: A higher value of [GAMMA]=0.80,
- [P05]: A lower value of [GAMMA]=0.67.





### 5.3 Bottom friction

Bottom friction is computed using the JONSWAP formulation for bottom friction. In this study two settings have been used:

- [P06]: A higher value of [CFJON]=0.075,
- [P07]: A lower value of [CFJON]= 0.060.

### 5.4 Whitecapping dissipation

The default method for whitecapping dissipation is based on the Hasselmann formulation as modified by Komen for application in the WAM model. This method is activated by means of the command GEN KOMEN.

The strength of the whitecapping formulation is given by the parameter CDS2. In this study 2 different settings have been used for this parameter.

- [P08]: A higher value of [CDS2]=2.60e-5,
- [P09]: A lower value of [CDS2]= 2.13e-5.

In addition, some sensitivity tests have been carried out with the cumulative wave steepness method as described in the SWAN physics + project (WL & Alkyon, 2002). To activate this setting the following command with default settings should be added; WCAP CSM [CST]=1.8 [POW]=0. This case is coded as [P14]. In addition to settings, three other values for the parameters CST and POW have been tested.

- [P17]: Inclusion of directional effects [POW]=1,
- [P18]: A higher value of [CST]=2.5.
- [P19]: A lower value of [CST]=1.0.

### 5.5 Quadruplet interactions

The quadruplet wave-wave interactions are computed according to the Discrete Interaction Approximation (DIA). In SWAN 40.20 the DIA source term has two relevant parameters that can be varied. The first is the shape parameter LAMBDA, which is related to the shape of the interacting wave number configuration. The second parameter is the strength of the quadruplet interactions given by the parameter [CNL4].

These parameters are specified with the command QUAD lambda=[LAMBDA] and cnl4=[cnl4]. In this study these parameters have been varied as follows:

- [P10]: Higher lambda value, LAMBDA=0.30
- [P11]: Lower lambda value, LAMBDA=0.20,
- [P12]: Stronger quadruplet interaction, CNL4=3.5e7
- [P13]: Weaker quadruplet interactions, CNL4=2.5e7.

The relatively high variation of the LAMBDA parameter is based on findings of Hashimoto and Kawaguchi (2001) who found a value of LAMBDA=0.19 as recommended value to approximate the non-linear transfer rate for JONSWAP shaped wave spectra.

The source term for quadruplet interactions theoretically conserves wave energy, wave action and wave momentum. To first order, it does not affect the total wave energy or the significant wave height. It does however affect the transfer of energy between different wave components and will affect the period measures.

## 5.6 Triad interactions

In the sensitivity study regarding the physical parameters, the setting determining the strength of the triads interaction have been varied as follows:

[P15]: Stronger triads, TRFAC=0.2

[P16]: Weaker triads, TRFAC=0.05.

## 5.7 Results of the physical sensitivity study

### 5.7.1 Sloterneer

The results of the sensitivity study of the physical settings for the Sloterneer are presented in the form of scatter diagrams in the Figures 5.1.2 through 5.1.19 (Figure 5.1.1 has intentionally been left out). Inspection of the results in these figures leads to the following observations:

[P02] and [P03]: Changing the parameter  $\alpha$  of the modified Battjes-Janssen surf breaking source term hardly affects the results.

[P04] and [P05]: Changing the parameter GAMMA of the modified Battjes-Janssen surf breaking source slightly affect the results. A higher value of GAMMA leads to slightly higher values of  $H_s$  and the period measures at least for the higher wind speeds. This is consistent with the results of choosing a lower value of GAMMA, which leads to lower values for  $H_s$  and period measures.

[P06] and [P07]: bottom friction does not play a role in the Sloterneer.

[P08] and [P09]: increasing or decreasing the strength of the (standard) whitecapping dissipation slightly influences the results of the significant wave height  $H_s$  and the mean wave period  $Tm-10$ .

[P10] and [P11]: changing the value of the  $\lambda$  parameter in the DIA for computing the quadruplet source term has a significant effect on the results. Choosing a higher value for  $\lambda$  leads to increased value for the significant wave height as well as the period measures. Choosing a lower value results in opposite behaviour. The effect on the one-dimensional spectrum and source functions is shown in the Figure 5.5.1 and 5.5.2 for case SL\_C03, station F29.

[P12] and [P13]: Modifying the strength of the quadruplet source term slightly affects the period measures in a systematic way. There are hardly any affects on the significant wave height.

[P14], [P17], [P18] and [P19]: Applying the cumulative wave steepness method for computing the whitecapping dissipation gives considerably higher results for the significant wave height and period measures. The settings of the CSM method have been determined in the SWAN physics + project (WL& Alkyon, 2002). The effect on the one-dimensional wave spectrum and source functions is shown in the Figures 5.6.1 and 5.6.2 for case SL\_C03 output point 4 (station F29) and after 5 and 20 iterations. However, inspection of the 2-dimensional spectra shows that the directional spreading is much too large. The development of the 2D spectrum and 2D source functions with iteration number is illustrated in the Figures 5.7, 5.8 and 5.9 for case SL\_C03, output station F29 and for the iterations 5, 10 and 20. In the runs [P17], [P18] and [P19] additional parameters of the CSM method have been tested. They all lead to unrealistic broad

directional wave spectra. Comparison of the corresponding plots show only minor differences, indicating that the various settings for the CSM hardly affect the results.

[P15] and [P16]: triad wave-wave interactions do not play a role in the Slotermeer, at least during this storm.

Based on the findings for the Slotermeer the following conclusions can be drawn:

- The parameter GAMMA of the modified Battjes-Janssen surf breaking source slightly affects the results for the higher waves.
- Bottom friction has a very small effect on the wave evolution.
- Changing the strength of the white-capping dissipation slightly affects the results.
- Changing the shape of the interaction wave number configuration in the DIA has a significant and systematic effect on the results for the significant wave height as well as the period measures.
- Changing the strength of the quadruplet source term slightly affects the period measures but not the significant wave height.
- Triad interactions do not play a role in the Slotermeer.
- The various settings for the CSM all have a similar significant effect on the computational results. They all lead to an increase in significant wave height and mean period measures and an unrealistically large directional spreading.

### 5.7.2 Westerschelde

For the Westerschelde results are available in the form of scatter plots for the computational grids W01, W02 and W03. For grid W01, the results for all output points are given in the Figures 5.2.2 through 5.2.16. Since the CSM method has not been applied to the Westerschelde for the cases [P17], [P18] and [P19] no results and figures are available for these cases.

Inspection of the results for W01 leads to the following observations:

- Variations in the parameter  $\alpha$  give basically the same results
- Increasing the parameter  $\gamma$  gives higher significant wave heights, and reducing this parameter gives lower wave heights. For the period measures slightly different results are found. A higher  $\gamma$  gives slightly higher wave periods, but a lower  $\gamma$  gives lower periods when the periods are lower than 6 s and higher wave periods when they are higher than 6 s.
- Bottom friction does not play a role.
- Changing the strength of white-capping dissipation slightly affects the results on the significant wave height, but less on the period measures.
- Modifying the  $\lambda$  parameter in the DIA source term affects the period measures, but not the significant wave height. Higher values of  $\lambda$  yield higher period measures, and vice versa.
- Changing the strength of the quadruplets gives minor changes in the results
- Applying the cumulative wave steepness method (case P14 only) gives higher wave periods and lower wave heights. This is different compared to the Slotermeer, where applying the CSM yields both higher wave heights and wave periods.
- Modifying the strength of the triads does not really affect the results for the significant wave height and the period measures.

For grid W02 the following observations are made:

- In general the results are very similar to those of grid W01, but with less scatter.

For grid W03 the following observations are made:

- The cumulative wave steepness method produces similar results as the modified Komen method.

### 5.7.3 Petten

The results of the computations for Petten are visualised in the same way as for the Sloterneer and Westerschelde. These plots are not included in this report because they show very similar results as for the Sloterneer and Petten. However, the plots are available on the CD-ROM accompanying this report.

Similar to the results of the numerical study a distinction is made between the coarser computational grid K12 and the finer more near-shore computational grid E24. The plots contain information of all output points in the grids K12 and E24 are considered as well as all 5 moments of time in the storm of 27 October 2002. Inspection of the results leads to the following observations:

- The  $\alpha$  parameter of the modified Battjes-Janssen model has almost no effect on the results.
- The  $\gamma$  parameter of the modified Battjes-Janssen model affects the results in a systematic and significant way. Choosing a higher value leads to higher significant wave heights and more or less the same periods. This effect is more pronounced for the near-shore grid E24.
- Bottom friction plays a minor but detectable role in the outer K12 grid. But the deviations are not systematic. In the inner E24 grid bottom friction has a marginal effect on the significant wave height and period measures.
- Changing the strength of the white-capping dissipation has a very small effect on the results.
- Changing the  $\lambda$  parameter in the DIA does not affect the significant wave height but it has effect on the period measures in a systematic way. Increasing  $\lambda$  leads to higher period measures.
- Changing the strength of the quadruplets affects the results slightly.
- Applying the cumulative wave steepness method for whitecapping dissipation (only case P14) increases the predicted period measures, but not the significant wave height.
- Changing the strength of the triads affects the period measures in the shallower points near Petten. Stronger triads lead to lower period measures and vice-versa.

### 5.7.4 Petten wave flume

The results for the Petten wave flume are hardly affected by variations in the strength of surf breaking, bottom friction, white-capping and quadruplet interactions. Only variations in the GAMMA parameter and the strength of the triads affect the results.

The spatial variation of integral wave parameters along the 1D-transect for case B12 for various physical settings is shown in the Figures 5.3.1 through 5.3.8. Figure 5.3.1 shows the effect of different values of the parameter ALPHA in the surf breaking source term (cases P02 and P03). Figure 5.3.2 shows the effect of different values of the GAMMA parameter in the surf breaking source term (cases P04 and P05). Figure 5.3.3 shows the effect of various settings for the strength of the bottom friction (cases P06 and P07). Figure 5.3.4 shows the effect of various settings for the strength of the white-capping dissipation (cases P08 and P09). Figure 5.3.5 shows the effect of other values of the shape parameter LAMBDA in the DIA (cases P10 and P11). Figure 5.3.6 shows the results of various settings for the strength of the DIA (cases P12 and P13). The effect of various

settings for the CSM method for white-capping is shown in Figure 5.3.7. The effect of various values for the strength of the triad source term is shown in Figure 5.3.8.

The similar plots for the other cases, the plots showing the iteration behaviour and the scatter diagrams are available on the CD-ROM accompanying this report.

### 5.7.5 Fetch-limited wave growth

The results for fetch-limited wave growth are very similar to the results of the Sloterneer. This holds especially for the deep water cases. For shallow water the effects of the Qb-limiter affect the results considerably. See also the results in Table 5.3.

For case C08 (depth 10 m and a wind speed of 30 m/s) the spatial variation of four integral wave parameters is shown in the Figure 5.4.1 through 5.4.8. The description of these figures is similar to those of the figure 5.3.1 through 5.3.8.

The similar plots for the other cases, the plots showing the iteration behaviour and the scatter diagrams are available on the CD-ROM accompanying this report.

## 5.8 Conclusions

Based on the results of the sensitivity study with respect to the physical settings of SWAN the following conclusion are formulated:

- Depth-limited wave breaking according to the modified Battjes-Janssen method plays an important role in the shallow areas. The parameter  $\alpha$  in the Battjes-Janssen plays a minor role, whereas the parameter  $\gamma$  significantly affects the results in the shallow areas. In the Sloterneer surf breaking only plays a role in high wind speed situations.
- Bottom friction can practically be neglected. It only plays a minor role when waves propagate over a large area.
- Whitecapping dissipation parameter  $C_{ds2}$  of the Komen method has a small effect on the wave model results.
- The cumulative white-capping dissipation in standard mode (case P14) produces higher significant wave heights and period measures for the Sloterneer, whereas for Petten and the Westerschelde the significant wave height decreases. The one-dimensional spectra are realistic. However, the directional spreading is unrealistically large. This is probably due to an imbalance in the source term balance. With the iteration number more and more energy is accumulating in opposing wind directions. This energy is pumped in those direction sectors by the non-linear quadruplet wave-wave interactions. The accumulation occurs probably due to a slightly too low dissipation.  
The other settings for the CSM method, cases [P17], [P18] and [P19], have only been applied to the Sloterneer, Petten Flume and Fetch Limited cases. The results of these other settings are very similar to those obtained for case [P14].
- Modifying the interacting wave number configuration has a significant effect on the evolution of the wave field. Increasing the  $\lambda$  parameter increases both the significant wave heights and wave periods in the Sloterneer, but it only increases period measures in the coastal area near Petten and the Westerschelde. Increasing the strength of the quadruplet interactions has a noticeable effect on the results.
- In general triad interactions do not play a role in the Sloterneer and the coastal areas near Petten and the Westerschelde. They only play a role in the very shallow points.



The fact that triads (at least as modelled in SWAN) only play a minor role is illustrated by means of contour plots of the Ursell number for the Sloterveer (Figure 5.10), grid E24 for Petten (Figure 5.11) and grid W01 for the Westerschelde (Figure 5.12). The moments of time correspond to the peak of the storm. For the Sloterveer, triads only seem to become at the end of the fetch where the water becomes shallower. Near Petten, triads only become in the shallow areas close to the coast. In the Westerschelde triads are only active in some shallow areas located around shallow banks.

In addition results are shown for the  $H_s/d$  ratio are shown in the Figures 5.13 through 5.15 for the Sloterveer, grid E24 near Petten and grid W01, respectively. The Sloterveer becomes rather shallow near the measurement location F29, but not enough to impose a limit to wave growth. Near Petten, the water remains relatively deep for almost the whole area. Only close to the coast the water becomes shallow. The same findings hold for the Westerschelde.

The results of the sensitivity analysis can be summarised in the following table. This shows the impact of changing a certain physical settings on the prediction of the significant wave height  $H_s$  and mean wave period  $T_{m-10}$ .



	SL		WS		PT		FP		FL	
	<i>H</i>	<i>T</i>	<i>H</i>	<i>T</i>	<i>H</i>	<i>T</i>	<i>H</i>	<i>T</i>	<i>H</i>	<i>T</i>
$\alpha \uparrow$	0	0	0	0	0	0*	0*	0*	0	0
$\alpha \downarrow$	0	0	0	+	0	0*	0	-	0	0
$\gamma \uparrow$	+	+	+	+	++	--	++	-	0	0
$\gamma \downarrow$	-	-	-	-	--	++	--	+	0*	+
CFJON $\uparrow$	0	0	-	-	0	0*	0	0	0	0
CFJON $\downarrow$	0	0	0	+	0	+	0	0	0	0*
Cds2 $\uparrow$	-	-	-	-	-	0*	0	0	-	-
Cds2 $\downarrow$	+	+	+	+	0*	0*	0	0	+	+
$\lambda \uparrow$	++	++	-	++	+	++	0	0	++	++
$\lambda \downarrow$	--	--	-	--	-	--	0	0	--	--
Cnl4 $\uparrow$	+	+	-	+	0	+	0	0	+	+
Cnl4 $\downarrow$	-	-	0	-	0*	-	0	0	-	-
Cnl3 $\uparrow$	0	0	0	-	-	--	-	--	0	0
Cnl3 $\downarrow$	0	0	0	+	-	++	0	++	0	0
CSM	++	++	--	++	--	++	0	0	++	++
CSM POW=1	++	++	--	++	--	++	0	0	++	++
CSM CST $\uparrow$	++	++	--	++	--	++	0	0	++	++
CSM CST $\downarrow$	++	++	--	++	--	++	0	0	++	++

Table 5.3: Impact of a certain physical parameter on the integral wave parameters *H<sub>s</sub>* and *T<sub>m-10</sub>*.

In Table 5.3 the meaning of the symbols is as follows:

Strong decrease	(--)
Small decrease	(-)
No effect	(0)
No mean effect	(0)
Small increase	(+)
Strong increase	(++)
Additional scatter	(*)

## 5.9 Recommendations

Based on the findings of the sensitivity study with respect to the physical settings of SWAN it is recommended to use the following parameters for the calibration of SWAN:

- The  $\gamma$  parameter of the source term for depth-limited wave breaking.
- The magnitude of white-capping dissipation CDS2.
- The shape parameter  $\lambda$  of the Discrete Interaction Approximation (DIA) for the computation of non-linear quadruplet interactions.
- The magnitude CNL4 of the DIA source term for non-linear quadruplet interactions.

Although Table 5.3 suggests that the CSM parameter has a significant effect on the model results, it is recommended not to employ this parameter in the calibration, because it produces an unrealistic large directional spreading.

## 6 Calibration

### 6.1 Introduction

The calibration of SWAN is posed as a mathematical multi-variable unconstrained minimisation problem. The basic problem is to find a combination of a set of SWAN parameters that yields the smallest error in terms of a set of predicted and observed integral wave parameters.

The aim of the calibration of SWAN is to find settings that may remedy the observed under-prediction of wave heights and wave periods in the areas of interest. It is therefore important to choose calibration parameters that significantly affect the prediction of these parameters. It is also important to have calibration parameters that affect the significant wave height differently than period measures. It is therefore expected that inclusion of parameters of the quadruplets (viz. CNL4 and LAMBDA) have more effect on period measures than the significant wave height.

In view of the NC, the most important wave parameters for the NC are the significant wave height  $H_s$  and the mean wave period  $T_{m-10}$ . Other parameters may be included, such as the mean periods  $T_{m01}$  and  $T_{m02}$  or directional parameters like the mean wave direction  $\theta$  and directional spreading  $\sigma$ . The mean periods  $T_{m01}$  and  $T_{m02}$  are not used because they are less robust than the  $T_{m-10}$ . Moreover, the frequently used peak period measures  $T_p$ ,  $T_{pb}$  and  $T_{pm}$  are not used because they are either not part of the SWAN output ( $T_{pb}$  and  $T_{pm}$ ) and because they are not robust enough when the spectra have multiple peaks ( $T_p$  and  $T_{pm}$ ). Directional parameters are also not used because no directional wave information is available.

The risk of using a mathematical procedure for the calibration is that some parameters may obtain unrealistic values (as imposed by the numerical minimisation procedure). This may happen when parameters are used that hardly influence the results, like the bottom friction, as is the case in the cases considered. To avoid such problems insignificant parameters are excluded and constraints are imposed on the selected parameters to keep them within physically acceptable limits.

Based on the results of the sensitivity study of numerical (Chapter 4) no changes were deemed necessary on the spectral discretisation. In addition, triads and quadruplets are allowed to be both active, and the Qb-limiter in the case of strong decreasing wave action by wave breaking is always active. Further, the following convergence criteria are recommended: the fractions [DREL], [DHOVAL] and [DTOVAL] are equal to 0.01%, which should be satisfied in 99% of the grid points. Spatially varying currents and water levels are imposed were applicable.

Based on the results of the sensitivity study of physical settings (Chapter 5), the following four physical parameters are used in the calibration of SWAN 40.20.

- The  $\gamma$  of the Battjes-Janssen depth limited wave breaking.
- The  $\lambda$  and  $Cn/4$  parameter of the DIA for the computation of the quadruplet wave-wave interactions.
- The strength of the white-capping dissipation  $C_{ds2}$ .



The choice of the calibration points is also important. Wave observations must be available and they should be representative for the area of interest, in view of future wave model computations for HR2006. For Petten the calibration point(s) should be close to the coast and not too far offshore. For the Westerschelde the calibration points should also be close to the coast and not too far inside the Westerschelde estuary.

So, for the Westerschelde, the stations Cadzand (CDD) and Hoofdplaat (HFP) were selected. The stations Hansweert (HSR/W) and Bath (BAT) were rejected, also because only a few wave observations are available. For Petten, the nearshore stations 062 and 175 in the Petten ray were used. For the Slotermeer only station F29 is available.

The calibration has been performed on 2 moments in the storm of the October 27, 2002 storm. For the Slotermeer, the cases C03 and C05 have been used, for the Westerschelde the cases C03 and C04 have been used and for Petten the cases C03 and C05 have been used.

## 6.2 Method of calibration

The aim of the calibration is to minimise the following error measure:

$$\varepsilon = \sqrt{\frac{1}{N} \left\{ \sum_{i=1}^N \left( H_{s,obs}^i - H_{s,comp}^i \right)^2 + \sum_{i=1}^N \left( T_{m-10,obs}^i - T_{m-10,comp}^i \right)^2 \right\}} \quad (6.1)$$

In which  $N$  is the number of calibration points, corresponding to a set of chosen output points and moments of time. A mix of Matlab 6.5 and SWAN 40.20 solves the multi-variable minimisation problem. To that end the Matlab function FMINSEARCH is used as the minimisation engine.

FMINSEARCH is a multidimensional unconstrained non-linear minimisation technique and is based on the Nelder-Mead method (Lagarias et al., 1998). FMINSEARCH needs a set of initial values. In the present calibration the default settings of SWAN are used (LAMBDA=0.25, CNL4=3.e7, CDS2=2.36e-5 and GAMMA=0.73). Other initial values are also possible, but have not been used here.

The purpose of routine FMINSEARCH is to find the minimum location in the multi-dimensional variable space. To that end the function FMINSEARCH makes small perturbations in each of the calibration parameters to determine the direction of the minimum. After some initial perturbations, the function FMINSEARCH uses all previous information to make educated guesses about the direction of the minimum. The function FMINSEARCH stops when the error can not be decreased any further.

To apply this minimisation technique to SWAN a mix of Matlab scripts, batch scripts and the SWAN program has been set up. A brief outline of the procedure is as follows. Based on a certain set of calibration parameters the function FMINSEARCH calls a Matlab script called ERRORSWAN.M that creates a set of SWAN input files with the chosen parameter values. Next, the batch-script is started that performs a number of SWAN computations. Each SWAN computation creates a TAB file with the computed integral wave parameters in the calibration points. Next, the results of the SWAN computation are compared with the measured values of the integral wave parameters in the calibration points for the chosen moments of time. On the basis of this comparison, the error measure  $\varepsilon$  is computed.

The calibration tool of SWAN is aimed to be generic. It is relatively simple to extend the list of parameters to be optimised, to extend the list of integral wave parameters and to extend the number of cases (= SWAN computations). The computational time of such a SWAN calibration might be a critical factor, since the amount of necessary CPU time increases with the number of variables to be optimised and the number of SWAN computations. The number  $N$  in expression (6.1) is usually larger than the number of SWAN computations because one computational grid may contain more than one output point for the calibration.

The function FMINSEARCH is formulated as an unconstrained minimisation problem. To avoid physically unrealistic outcomes a transformation is applied to treat the calibration of SWAN as a constrained minimisation problem. This is achieved by means of a transformation using the *tanh*-function.

Let  $p$  a physical parameter of the SWAN model, with the following limits ( $p_1$  and  $p_2$ ), and  $q$  the unconstrained mathematical parameter used by the function FMINSEARCH. Then the following equation maps the parameter  $q$  on the parameter  $p$ .

$$p = p_0 + \frac{1}{2}(p_2 - p_1) \tanh(q - 10) \quad (6.2)$$

in which  $p_0$  is the default value of the parameter  $p$ . The value of 10 is used to influence the rate of change of variation in the parameter  $q$  on the parameter  $p$ . Choosing  $q=10$  as initial value in the minimisation procedure gives  $p=p_0=2$ .

In this way the unconstrained parameter  $q$  is projected onto the constrained parameter  $p$  within the limits ( $p_1, p_2$ ). This is illustrated in Figure 6.1 for a hypothetical parameter  $p$  with default value 2 and which should have the limits (1,3).

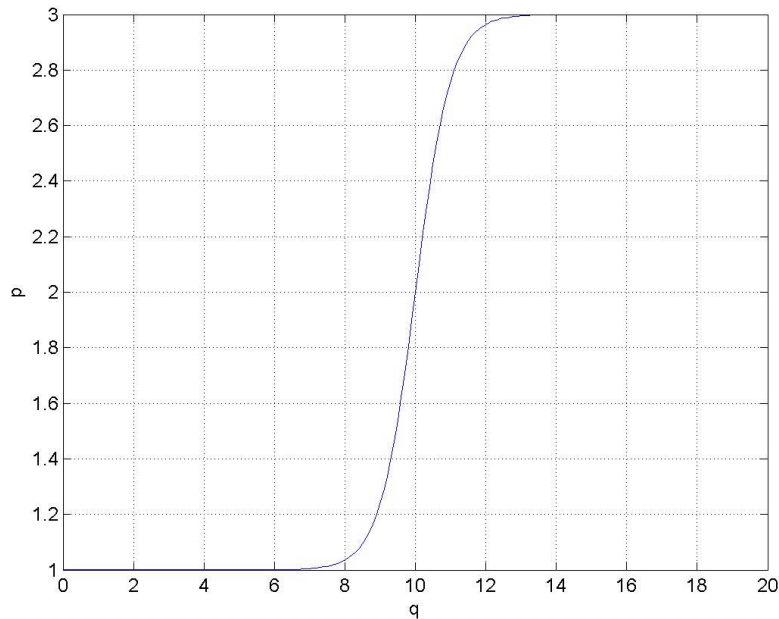


Figure 6.1: Illustration of the transfer function used in the optimisation of SWAN input parameters.

## 6.3 Results of the calibration

Initially, the calibration procedure has been applied to all three areas simultaneously. This did not result in applicable calibration settings in the sense that automatic minimisation procedure did not converge. This is due to the fact that areas have different characteristics. Further analysis showed that the Sloterveer should be treated separately. The wave growth characteristics in the Sloterveer correspond to initial wave growth, whereas those of Petten and the Westerschelde correspond to the propagation of storm waves in a shallow coastal area.

In a second set of calibrations, the Westerschelde and the Petten area were treated simultaneously. For the **Westerschelde and Petten** the following settings were obtained for the calibration stations 062 and 175 at Petten and Cadzand (CDD) and Hoofdplaat (HFP) in the Westerschelde:

$CDS2 = 1.36E-5$ ,  $LAMBDA=0.28$ ,  $CNL4=4.0E7$  and  $GAMMA=0.90$ .

Analysis of the results of this setting showed that the results for the Westerschelde improved but that they slightly worsened for Petten. This is due to the fact that in the Westerschelde the stations CDD and HFP show an under-estimation of both the significant wave height  $H_s$  and the mean period  $Tm-10$ , whereas for Petten, both the significant wave height  $H_s$  and the mean wave period  $Tm-10$ , show a rather good model behaviour, at least for the October 2002 storm.

Next, SWAN 40.20 was calibrated for each area individually.

For the **Sloterveer** the following settings were obtained for calibration station F29:

$CDS2 = 0.86E-5$ ,  $LAMBDA = 0.32$ ,  $CNL4=9E7$  and  $GAMMA=0.95$ .

For the **Westerschelde** the following settings were obtained using the stations CDD and HFP:

$CDS2 = 2.0E-5$ ,  $LAMBDA=0.28$ ,  $CNL4=4.4E7$  and  $GAMMA=0.90$ .

For **Petten**, using data from the stations 062 and 175, the following settings were obtained.

$CDS2 = 2.0E-5$ ,  $LAMBDA=0.28$ ,  $CNL4=4E7$  and  $GAMMA=0.70$ .

## 6.4 Discussion

The results of the automatic calibration are different for each area of interest. The most striking difference is between the Sloterveer and the other areas with respect to the parameters of the quadruplets ( $LAMBDA$  and especially  $CNL4$ ). The results for Petten and the Westerschelde are relatively similar, except for the value of gamma in the surf breaking source term. For the Westerschelde this value is rather high to compensate for the under-prediction of significant wave heights, whereas for Petten this value is lower than the default to compensate for the over-prediction of the significant wave heights at the stations 062 and especially 175. As noted in WL & Alkyon (2002) the wave



observations may be unreliable because of uncertainties in the actual depth as used in the SWAN computations.

A limitation of the present study is that the calibration of SWAN was limited to measured wave data of only one storm and only 2 moments of time in this storm per area. This is a small basis for the calibration of SWAN and the results should be treated accordingly.

An overall evaluation of these settings is presented in Chapter 7.

## 7 Verification

### 7.1 Introduction

The settings determined in the calibration of SWAN have been applied to the three areas of interest. Although the calibration has been performed for two moments of time in the October 2002 storm, results of the verification are given for **all** five selected moments of time per area. This implies that the data used for the calibration are included in the verification and that the verification is not fully independent. This approach was chosen to obtain sufficient data for the statistical analysis. Since it was found that the deviations between computational results and observations are rather systematic, it was deemed acceptable to include the results for all moments of time in the verification.

The results are presented as a scatter plot showing a comparison of the observed and predicted significant wave height  $H_s$  and the period measures  $Tm-10$ ,  $Tm01$  and  $Tm02$ . To assess the verification quantitatively, these plots also contain a set of computed statistical parameters. In addition, some observed and computed spectra are shown. In addition, each scatter plot contains three lines. A dashed line corresponding to a perfect fit, a linear regression line of the form  $y=a+bx$  and a linear regression line of the form  $y=b_x x$  which crosses the origin. The coefficients of the regression lines are obtained by a least squares analysis and they are also listed in the figures.

For all selected output point, results are presented based on the basis of the default settings as computed with the numerics run, code N01, and with the verification run, code Vnm, where nm are the digits of the sequence number.

Based on the results of the calibration of SWAN 40.20 for each area and for combinations of areas, a set of physical settings has been obtained. This set is given in Table 7.1. In view of the objective to have one set applicable for all three typical Dutch water systems (shallow lakes, closed coast and an estuary) a compound setting has been defined. This compound setting is also listed in Table 7.1 and referred to as "ALL", it is based on the calibration of both the Westerschelde and Petten. The headers of the columns in Table 7.1 are used to identify the verification runs. This name also appears in the plots presented in the following sections.

The optimal settings for the physical parameters are summarised in Table 7.1.

	PT	SL	WS	ALL
CDS2	2.0E-5	0.86E-5	2.0E-5	1.36E-5
CNL4	4.0E7	9.0E7	4.4E7	4.0E7
$\lambda$	0.28	0.32	0.28	0.28
$\gamma$	0.70	0.95	0.90	0.90

Table 7.1 Optimal settings for the physical parameters of SWAN 40.20.

### 7.2 Slotermeer

The results of the verification for station F29 in the Slotermeer for the base case N01 are shown in Figure 7.2.1. As can be seen, both the significant wave height  $H_s$  and the period measures are systematically under-predicted. The results of the calibration are

shown in Figure 7.2.2 for the optimal set of the Sloterveer. It is evident that the results are significantly improved. Not only in terms of bias and error measures, but also in terms of the slope of the regression lines. In addition the compound settings have been applied to the Sloterveer. The results of the verification for this set are shown in Figure 7.2.3. Compared to the base case (N01), it can be seen that the results are sufficiently improved.

A comparison of the computed and observed spectra is shown in the Figures 7.2.4 and 7.2.6. It is again evident that for both calibration sets the spectral shape improves, except for the spectral width, which seems too wide.

## 7.3 Westerschelde

The results of the verification for the Westerschelde are shown in the Figure 7.3.1 through and 7.3.4 for the stations CDD and HFP for the base case N01 and the verification set "WS", respectively. The locations of these stations are shown in Figure 3.6. The results indicate that the under-prediction of both the significant wave height  $H_s$  and the mean wave period  $Tm-10$  has been diminished considerably.

The results of the calibration have also been verified for a station at the end of the Westerschelde, viz. Station BAT and two further offshore stations, viz. WIE and SCW. See Figure 3.6 for their locations. The results thereof are given in the Figures 7.3.5 through 7.3.10. However, the numerical results indicate that the significant wave height is now over-predicted in comparison with the base case. This is probably a result of the relatively high value of gamma in the verification runs.

## 7.4 Petten

The results of the verification for Petten are shown in the Figures 7.4.1 through 7.4.9 for two points close to the dike (062 and 175) and one further offshore (021). The locations of these stations are shown in Figure 3.4. The verification results of for the base case N01 are shown in the Figures 7.4.1, 7.4.4 and 7.4.7. In general, the results agree rather well.

For Petten two calibration sets have been verified. The first set is based on the mutual calibration of Petten for the stations 062 and 175, and the Westerschelde for the stations CDD and HFP. This set is indicated as "ALL". The results of the verification are presented in the Figures 7.4.2, 7.4.5 and 7.4.8. Inspection of these results showed that the significant wave heights are generally over-predicted. This is direct consequence of the fact that the value of GAMMA is rather high. This over-prediction is also present in the other stations.

The second set is based on the calibration for Petten only. This set is indicated as "PT". The results of this calibration run, in which only the stations 062 and 175 were involved, are shown in the Figures 7.4.3, 7.4.6 and 7.4.9. The main difference with the previous run (set ALL) is that value of GAMMA is much lower. It is now set at 0.7 and the strength of the quadruplet interactions is also slightly lower and set at 4.0E7. Comparison with the results of the base case (N01) shows that the results are only slightly improved.

The results of the verification for station 175 raise doubts about the validity of the measured waves at this location. Especially the observed significant wave height is rather high. This behaviour might explain the lower GAMMA value when SWAN 40.20 is calibrated for Petten only.



## 7.5 Conclusions

The results of the calibration and verification show that no unified set of SWAN settings can be found that is applicable for all three areas considered. Instead different optimal settings have been obtained. The settings for the Sloterveer deviate the most from the default SWAN settings.

For the Sloterveer an almost perfect fit has been obtained for the new settings, although there are some doubts about the spectral width, which is considered too large.

The results for the Westerschelde improve, both for the significant wave height  $H_s$  and the mean wave period  $T_m-10$ . The initial under-prediction has been eliminated reduced by about 50%.

For Petten the results of the verification indicate a slight improvement, at least if GAMMA is set to 0.70.

## 8 Conclusions

### 8.1 Sensitivity of numerical settings

Based on the results of the sensitivity study of numerical settings for SWAN 40.20 for all computational areas the following conclusions can be formulated.

- Changing the upper and lower model frequency has a small effect on the convergence behaviour and final results. For Petten a smaller value for the lower frequency affects the predicted period measure  $Tm-10$ . This is a direct effect of low frequency energy in the wave boundary conditions. Increasing the highest model frequency generally affects the prediction of the period measures  $Tm01$  and  $Tm02$  especially in areas with local wave growth. The sensitivity of  $Tm-10$  with respect to the choice of lowest model frequency ( $flow$ ) is not considered to be a problem of SWAN, but more a problem in the handling of SWAN model results and the comparison of measured wave data.
- Changing the frequency resolution has little effect on the results. Increasing this resolution would yield increased computational times. Therefore increasing the frequency resolution is not recommended. (Further, a high frequency resolution will generate undesirable results with the DIA).
- Modifying the directional resolution is not recommended. A higher resolution does not yield different results and would lead to increased computational times. Lowering the directional resolution is not recommended because it leads to some random scatter compared to the base case. For wind-driven seas the current resolution of  $10^\circ$  is deemed sufficient.  
This conclusion holds for wind-driven seas. For the prediction of swell, a finer resolution is probably needed. Although not tested in this study, a directional resolution of, say  $2.5^\circ$ , is probably needed for accurate swell predictions. But this will lead to unacceptable long run times in case also wind sea situations are computed with such a fine resolution.
- Relaxing the Phillips' limiter from 10% to 20% or 30% has a small effect on the computational results. Its main effect, however, is to produce an unstable convergence behaviour of integral wave parameters. It is therefore not recommended to use a less strict criterion.
- The combined computation of triads and quadruplets gives similar results compared to the situation that either one of them may be active per iteration. From a theoretical point of view it is better to keep them both active. From a practical point of view it is difficult to determine the conditions when either of them is dominant over the other. We therefore recommend to allow them to be active at the same time.
- Keeping the  $Qb$ -limiter active in case of decreasing wave action is necessary for the Sloterneer case, but not for the other field cases. Since it hardly affects the results for the other areas, it is recommended to keep this limiter active by setting  $Qb=10$  in the LIMITER command. In this study no attempt was made to find lower values of the  $Qb$ -limiter, since this would require an extensive study to find conditions in which this limiter can be deactivated.
- Under-relaxation generally leads to robust, but slower, convergence behaviour. In the interplay with the Phillips' limiter it was found that a high amount of under-relaxation makes the Phillips' limiter obsolete. It was also found that under-relaxation works better in nested and finer computational grids.
- The current method to end the iteration process based on the default convergence criteria using 0.02% and 98% values is insufficiently stringent in many cases. Even



using 0.01% and 99% values does not improve the situation (forcing more iterations). For future production runs an even stricter convergence criterion must be found.

## 8.2 Sensitivity of physical settings

Based on the results of the sensitivity study with respect to the physical settings of SWAN the following conclusions are formulated:

- Depth-limited wave breaking according to the modified Battjes-Janssen method is important in the shallow areas. The parameter  $\alpha$  in the Battjes-Janssen plays a minor role. Instead the parameter  $\gamma$  significantly affects the results in the shallow areas. In the Sloterneer surf breaking only plays a role in high wind speed situations.
- Bottom friction can be neglected. It only plays a minor role when waves propagate over a large area.
- Whitecapping dissipation parameter  $Cds2$  of the Komen method has a small effect on the wave model results.
- The cumulative white-capping dissipation produces higher significant wave heights and period measures. Also the one-dimensional spectra are realistic. However, the directional spreading is unrealistically large. This is probably due to an imbalance in the source term balance. With the iteration number more and more energy is accumulating in opposing wind directions. This energy is pumped in those direction sectors by the non-linear quadruplet wave-wave interactions. The accumulation occurs probably due to a slightly too low dissipation. Sensitivity runs with other values of the magnitude and power in the CSM formulation produce very similar results, indicating that the CSM settings have little effect on the results.
- Modifying the shape interacting wave number configuration has a significant effect on the evolution of the wave field. This shape is controlled by the  $\lambda$  parameter and it affects the flow of energy within the wave spectrum. In this way it directly affects the growth rate of the waves and the directional spreading. The directional spreading in turn is important for the impact of the wind on the wave field. Increasing the  $\lambda$  parameter increases both the significant wave height and wave periods in the Sloterneer, but it only increases period measures in the coastal area near Petten and the Westerschelde. Increasing the strength of the quadruplet interactions has a lesser but still noticeable effect on the results.
- Triad interactions do not play a role in the Sloterneer and the coastal areas near Petten and the Westerschelde. They only play a role in the very shallow points.
- For the Sloterneer it is more important to keep the Qb-limiter always active, than to allow the simultaneous activation of triads and quadruplets, contrary to our perception before this study was carried out.
- It is noted that the Sloterneer measurements are ideal to calibrate SWAN for deep-water fetch-limited wave growth.

## 8.3 Calibration and verification

Based on the results of the calibration and verification the following conclusions are formulated.

- A new set of SWAN settings has been found that can be applied to all areas considered. This new set improves the results for the Westerschelde and Sloterneer, but not necessarily for the Petten situation.
- For the Sloterneer a separate calibration set has been found that further improves model behaviour.



- The results of the calibration for the coastal areas differ mainly in the value of the parameter gamma in source term for depth-limited wave breaking.
- The choice of calibration points, in space and time, can affect the results of the calibration.
- The automatic calibration works best, where significant differences exist between observations and predictions.
- In case small differences exist between observation and predictions, the automatic calibration is likely to generate unrealistic model settings. In such cases, the results of sensitivity analysis should be used to correct the results of the calibration process.
- The number of calibration points is probably too small to obtain generally applicable settings.
- The uncertainty of the observed integral wave parameters is a source of error in the settings obtained by calibration.

	PT	SL	WS	ALL
CDS2	2.0E-5	0.86E-5	2.0E-5	1.36E-5
CNL4	4.0E7	9.0E7	4.4E7	4.0E7
$\lambda$	0.28	0.32	0.28	0.28
$\gamma$	0.70	0.95	0.90	0.90

Table 8.1 Recommend settings for the physical parameters of SWAN 40.20 per area and for all areas together.

	<i>H<sub>s</sub></i>	<i>T<sub>m-10</sub></i>
Petten	+/-	+/--
Westerschelde	+	+
Slotermeer	++	++

Table 8.2 Summary of calibration results per field case.

## 9 Recommendations

Based on the experience and results of this project the following recommendations are made.

1. To further analyse the optimal convergence criteria, it would be meaningful if the development of the values of [DREL] [DHOVAL] [DTOVAL] and [NPTNS] were output as a function of iteration number, preferably to a certain test file.
2. Different settings for the convergence criteria [DREL], [DHOVAL] and [DTOVAL] should be considered.
3. The criteria for ending the iteration process should be modified to ensure that sufficient iterations are carried out. Suggestions for improvement are to include also the mean wave direction, and the rate of change of a certain parameters based on a moving average over a number of previous iterations.
4. The cumulative white capping dissipation shows promising results, but further research is needed to avoid the large amount of directional spreading due to the accumulation of wave energy in opposing wind directions. Possible methods to improve the situation are to increase the dissipation in opposing wind directions, or to introduce 'negative' wind input. In addition, further work is needed to investigate the effect of other physical settings of the CSM on the computational results.
5. A re-calibration of SWAN is recommended using the parameters of the CSM method and parameters of the quadruplets. It is noted that such a re-calibration can only be performed after the noted problems with the CSM method are solved.
6. Under-relaxation yields robust convergence behaviour and it avoids the growth of wiggles in the variation of integral wave parameters with iteration. However, it is still not fast enough to use it in production runs. Further research is advised to make it operationally feasible.
7. The PAR test output should be extended with more integral wave parameters, preferably  $Tm-10$ , the mean direction  $\theta$  and the directional spreading  $\sigma$ .
8. The settings for the Slottermeer should be analysed in more detail with respect to the inclusion of better parameterisations for the quadruplets.
9. The effect of different values of the shape parameters  $\lambda$  in the DIA on the flow of energy in the energy spectrum and its effects on the evolution of the wave field should be analysed in more detail.
10. The wind input source function, as generated by the TEST option, contains negative values for the first iteration. This is probably a bug in the present version of SWAN and it should be fixed.
11. The specification of the frequency range and frequency resolution should be modified such that a frequency resolution of 10% is generated for given frequency limits (suggested by M. Zijlema).
12. The recommended SWAN 40.20 settings are: GAMMA=0.90, CDS2=1.36E-5, CNL4=4.0E7 and LAMBDA=0.28.
13. The recommended set of new SWAN settings should be verified against a wider set of conditions. In this verification, special attention must be given to the prediction of correction of period measures.
14. Further analysis is recommended of results of the sensitivity analyses that have not been presented in this report.

## References

- Alkyon, 1999: Investigation of the iteration behaviour of the wave model SWAN, report A415, G.Ph. van Vledder.
- Alkyon, 2001: Iteration behaviour of SWAN 40.11 in the Markermeer. Report A637, October 2001, G.Ph. van Vledder.
- Alkyon & WL|Delft Hydraulics, 2002: Generieke methode hindcasten van gemeten stormen met SWAN, rapport A1002/H4149. G.Ph. van Vledder, D.P. Hurdle, J. Dekker, J. Groeneweg.
- Battjes, J.A., and J.P.F.M. Janssen, 1978: Energy loss and set-up due to breaking of random waves. Proc. 16th Int. Conf. on Coastal Engineering, 569-587.
- Booij, N., R.C. Ris, and L.H. Holthuijsen, 1999: A third-generation wave model for coastal regions, J. Geophys. Res., Vol. 104, C4, 7649-7666.
- Bottema, M., 2001: Nader onderzoek numeriek gedrag SWAN, RIZA-werkdocument 2001.101X.
- Bottema, M, 2003: personal communication.
- Gautier, C., 2003: Betrouwbaarheid SWAN in de Westerschelde: Vergelijking golfberekeningen en metingen, Royal Haskoning rapport 9M5697/R03035/CG/Rott2b, juni 2003.
- Hashimoto, N., and K. Kawaguchi, 2001: Extension and modification of discrete interaction approximation (DIA) for computing nonlinear energy transfer of gravity wave spectra. Proc. 4th Int. Symp. Waves, 2001: 530-539.
- Hasselmann, S., K. Hasselmann, J.A. Allender, and T.P. Barnett (1985): Computations and parameterizations of the non-linear energy transfer in a gravity-wave spectrum. Part 2: parameterizations of the non-linear transfer for application in wave models. J. Phys. Oceanogr., Vol. 15, 1378-1391.
- Holthuijsen, L.H., N. Booij, R.C. Ris, I.J.G. Haagsma, A.T.M.M. Kieftenburg, E.E. Kriezi, M. Zijlema, 2003: SWAN Cycle III version 40.20, User Manual (not the short version). Delft University of Technology.
- Komen, G.J., L. Cavaleri, M. Donelan, K. Hasselmann, S. Hasselmann, and P.A.E.M. Janssen, 1994: Dynamics and Modelling of Ocean Waves, Cambridge University Press. 532p.
- Lagarias, J.C., J. A. Reeds, M. H. Wright, and P. E. Wright, "Convergence Properties of the Nelder-Mead Simplex Method in Low Dimensions," SIAM Journal of Optimization, Vol. 9 Number 1, pp. 112-147, 1998.
- Van Vledder, G.Ph., T.H.C. Herbers, R.E. Jensen, D.T. Resio and B.A. Tracy (2000): Modelling of non-linear quadruplet wave-wave interactions in operational wave models. Proc. 27th Int. Conf. on Coastal Engineering, Sydney, Australia, 797-811.
- WAMDI group, 1988: The WAM model – a third generation ocean wave prediction model. J. Phys. Oceanography, Vol. 18, 1775-1810.
- WL|Delft Hydraulics, 1999: Physical model investigations on coastal structures with shallow foreshores, rapport H3129, Juli 1999.
- WL|Delft Hydraulics, 2000: Numerical model investigations on coastal structures with shallow foreshores, WL | Delft Hydraulics rapport H3351, May 2000.
- WL|Delft Hydraulics & Alkyon, 2002: SWAN fysica plus. WL | Delft Hydraulics / Alkyon report H3937/A832 (J. Groeneweg, J.G. Bonekamp, G.Ph. van Vledder, and D.P. Hurdle, September 2002).
- WL|Delft Hydraulics & Alkyon, 2003: Reliability of SWAN at the Petten Sea Defence, WL | Delft Hydraulics & Alkyon rapport H4197 (J. Groeneweg, G.Ph. van Vledder, D.P.Hurdle, N. Doorn, N. and C. Kuiper, June 2003).



Zijlema, M, and A.J. van der Westhuyzen, 2003: On convergence behaviour and numerical accuracy in stationary SWAN simulation of nearshore wind wave spectra. Submitted to Coastal Engineering.



case	flow	fhigh	msc	mdc	npnts	mxist	urslim	ursell	qb	alfa	limiter	dfrac
1	0.08	1.7	32	36	101	100	0.01	10	1	0	0.1	0.02
2	0.06	1.7	35	36	101	100	0.01	10	1	0	0.1	0.02
3	0.08	2	33	36	101	100	0.01	10	1	0	0.1	0.02
4	0.08	1.7	40	36	101	100	0.01	10	1	0	0.1	0.02
5	0.08	1.7	28	36	101	100	0.01	10	1	0	0.1	0.02
6	0.08	1.7	32	48	101	100	0.01	10	1	0	0.1	0.02
7	0.08	1.7	32	24	101	100	0.01	10	1	0	0.1	0.02
8	0.08	1.7	32	36	101	100	0.01	10	1	0	0.2	0.02
9	0.08	1.7	32	36	101	100	0.01	10	1	0	0.3	0.02
10	0.08	1.7	32	36	101	100	0.01	10	1	0.025	0.1	0.02
11	0.08	1.7	32	36	101	100	0.01	10	1	0.025	0.5	0.02
12	0.08	1.7	32	36	101	100	0.01	10	1	0.05	0.1	0.02
13	0.08	1.7	32	36	101	100	0.01	10	1	0.05	0.5	0.02
14	0.08	1.7	32	36	101	100	0.1	0.1	1	0	0.1	0.02
15	0.08	1.7	32	36	101	100	0.1	0.1	1E-05	0	0.1	0.02
16	0.08	1.7	32	36	101	100	0.01	10	1E-05	0	0.1	0.02
17	0.08	1.7	32	36	98	100	0.01	10	1	0	0.1	0.02
18	0.08	1.7	32	36	99	100	0.01	10	1	0	0.1	0.01
19	0.08	1.7	32	36	97	100	0.01	10	1	0	0.1	0.03

Table 4.2: Summary of parameter settings for numerical sensitivity study for the Sloterveer.

case	flow	fhigh	msc	mdc	npnts	mxist	urslim	ursell	qb	alfa	limiter	dfrac
1	0.03	0.8	30	36	101	50	0.1	0.1	1E-05	0	0.1	0.02
2	0.02	0.8	30	36	101	50	0.1	0.1	1E-05	0	0.1	0.02
3	0.03	1.2	38	36	101	50	0.1	0.1	1E-05	0	0.1	0.02
4	0.03	0.8	38	36	101	50	0.1	0.1	1E-05	0	0.1	0.02
5	0.03	0.8	25	36	101	50	0.1	0.1	1E-05	0	0.1	0.02
6	0.03	0.8	30	48	101	50	0.1	0.1	1E-05	0	0.1	0.02
7	0.03	0.8	30	24	101	50	0.1	0.1	1E-05	0	0.1	0.02
8	0.03	0.8	30	36	101	50	0.1	0.1	1E-05	0	0.2	0.02
9	0.03	0.8	30	36	101	50	0.1	0.1	1E-05	0	0.3	0.02
10	0.03	0.8	30	36	101	50	0.1	0.1	1E-05	0.025	0.1	0.02
11	0.03	0.8	30	36	101	50	0.1	0.1	1E-05	0.025	0.5	0.02
12	0.03	0.8	30	36	101	50	0.1	0.1	1E-05	0.05	0.1	0.02
13	0.03	0.8	30	36	101	50	0.1	0.1	1E-05	0.05	0.5	0.02
14	0.03	0.8	30	36	101	50	0.01	10	1E-05	0	0.1	0.02
15	0.03	0.8	30	36	101	50	0.1	0.1	1	0	0.1	0.02
16	0.03	0.8	30	36	101	50	0.01	10	1	0	0.1	0.02
17	0.03	0.8	30	36	98	50	0.1	0.1	1E-05	0	0.1	0.02
18	0.03	0.8	30	36	99	50	0.1	0.1	1E-05	0	0.1	0.01
19	0.03	0.8	30	36	97	50	0.1	0.1	1E-05	0	0.1	0.03

Table 4.3: Summary of parameter settings for numerical sensitivity study for the Westerschelde, Petten, Petten flume and fetch-limited situations.



case	alpha	gamma	cfjon	cds2	lambda	cnl4	csm	cst	pow	trfac
P01	1	0.73	0.067	2.36E-05	0.25	3.00E+07	off	1.8	0	0.1
P02	1.1	0.73	0.067	2.36E-05	0.25	3.00E+07	off	1.8	0	0.1
P03	0.9	0.73	0.067	2.36E-05	0.25	3.00E+07	off	1.8	0	0.1
P04	1	0.8	0.067	2.36E-05	0.25	3.00E+07	off	1.8	0	0.1
P05	1	0.64	0.067	2.36E-05	0.25	3.00E+07	off	1.8	0	0.1
P06	1	0.73	0.075	2.36E-05	0.25	3.00E+07	off	1.8	0	0.1
P07	1	0.73	0.06	2.36E-05	0.25	3.00E+07	off	1.8	0	0.1
P08	1	0.73	0.067	2.60E-05	0.25	3.00E+07	off	1.8	0	0.1
P09	1	0.73	0.067	2.13E-05	0.25	3.00E+07	off	1.8	0	0.1
P10	1	0.73	0.067	2.36E-05	0.30	3.00E+07	off	1.8	0	0.1
P11	1	0.73	0.067	2.36E-05	0.20	3.00E+07	off	1.8	0	0.1
P12	1	0.73	0.067	2.36E-05	0.25	3.50E+07	off	1.8	0	0.1
P13	1	0.73	0.067	2.36E-05	0.25	2.50E+07	off	1.8	0	0.1
P14	1	0.73	0.067	2.36E-05	0.25	3.00E+07	on	1.8	0	0.1
P15	1	0.73	0.067	2.36E-05	0.25	3.00E+07	off	1.8	0	0.2
P16	1	0.73	0.067	2.36E-05	0.25	3.00E+07	off	1.8	0	0.05
P17	1	0.73	0.067	2.36E-05	0.25	3.00E+07	on	1.8	1	0.1
P18	1	0.73	0.067	2.36E-05	0.25	3.00E+07	on	2.5	0	0.1
P19	1	0.73	0.067	2.36E-05	0.25	3.00E+07	on	1	0	0.1

Table 5.2: Summary of parameter settings for physical sensitivity study.



## Appendix A

### Coding conventions

#### Coding conventions

In this study a large number of computations are made which can be divided into a number of characteristics.

#### File name convention:

The following characteristics are distinguished:

- Computational area AA
- Date and time of field case DyyyymmddThhmm
- Selected case Cn
- Numerical settings Nnn
- Iteration number Snn
- Parameter of block file pp
- Extension xxx

Composite name: AA\_DyyyymmddThhmm\_Cn\_Nnn[-Snn][pp].xxx

The quantities between square brackets are needed for special file types or conditions.

The computational areas are coded as follows:

Petten	PT
Westerschelde	WS
Slotermeer	SL
Fetch limited growth	FL

Date and time are coded according to the following convention:

DyyyymmddThhmm

in which

yyyy year

mm month

dd day

hh hour on selected day

mm minutes

The date and time field is omitted for the fetch-limited computations

For the field cases various cases can be considered. For instance, in the Petten (Groeneweg et al. 2003) and Westerschelde (Gautier, 2003) hindcast studies 4 cases were distinguished. These are coded as Cn with n an integer (n=1-9).

In the calibration and sensitivity study various numerical settings are used. All settings are coded with three characters Snn with nn the number of setting (nn=01 – 99).

#### Extensions





The contents of each file is characterised by its extension. In this study the following extensions are used:

- BLK Block file
- BOT Bottom topography
- CFG Configuration file
- DAT Input or output data file
- EXE Executable
- HOT SWAN restart file
- INP Input file for program other than SWAN
- LOG Logging file
- MAS Master input file
- PAR Parameter file with SWAN test output
- PRT Print file
- SD1 1D spectral SWAN test output
- SD2 2D spectral SWAN test output
- SP1 1D spectrum file
- SP2 2D spectrum file
- SWN SWAN input file
- TAB SWAN table output file
- TST Test output file
- WND Wind file

As an example the file name PT\_D19950110T0700\_C4\_N12.SWN refers to a SWAN input file for Petten on January 10, 1995, 7 hours, case 4 and the 12<sup>th</sup> sensitivity run.

In addition, the SWAN block files have two extra characters pp indicating the parameter they contain. These two characters are placed at the end of the trunc name. The following quantities are distinguished:

- HS significant wave height
- TP peak wave period
- DE computation depth
- T0 mean wave period  $T_{m-10}$ , using the output parameter PER, in combination with the command QUANTITY
- T1 mean wave period  $T_{m01}$
- T2 mean wave period  $T_{m02}$
- DS directional spreading
- DI mean wave direction
- FS frequency spreading (spectral narrowness)
- ST mean wave steepness
- VE current velocity (both components in one file)
- WI wind direction (both components in one file)
- WL mean wave length
- DH difference in  $H_s$  between last two iterations
- DT difference in  $T_{m01}$  between last two iterations
  
- VD direction of current field (Cartesian convention, direction to)
- VM magnitude of current field
- WD direction of wind field (Cartesian convention, direction to)
- WM magnitude of wind field

The following quantities are computed on the basis of standard SWAN output block file

- HD ratio of  $H_s$  over  $d$  (computed outside SWAN)



- KD product of mean wave number time water depth (computed outside SWAN)
- UR Ursell number, based on the output data for HS, DE and T1.

In the analysis of the iteration behaviour some file are also distinguished by mean of their iteration number. These are coded with the characters Snn with nn the iteration number.

In this way the file name consists of

WS\_D19950110T0700\_C4\_N12[\_Snn][pp].BLK

In the case no iteration information is available the 4 characters “\_Snn” are omitted. In the case of a non-block file, the characters “pp” are also omitted. The use of the token \_S identifies directly if a file belongs to a iteration dependent file. In the case of a BLK file it is automatically assumed that the last two characters of the trunc part of the file name refer to the type of parameters in the file.



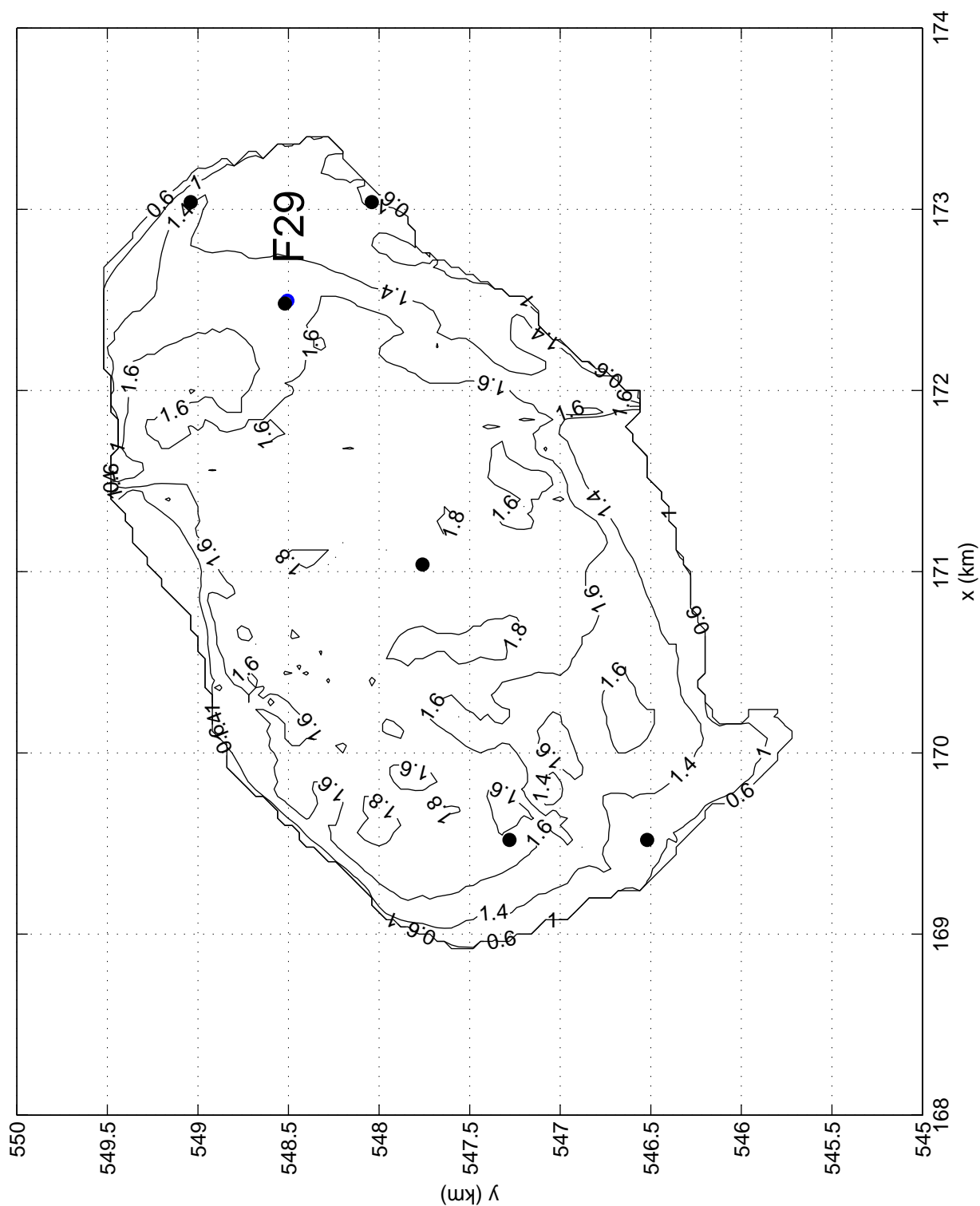
## Appendix B

### Example of master input file

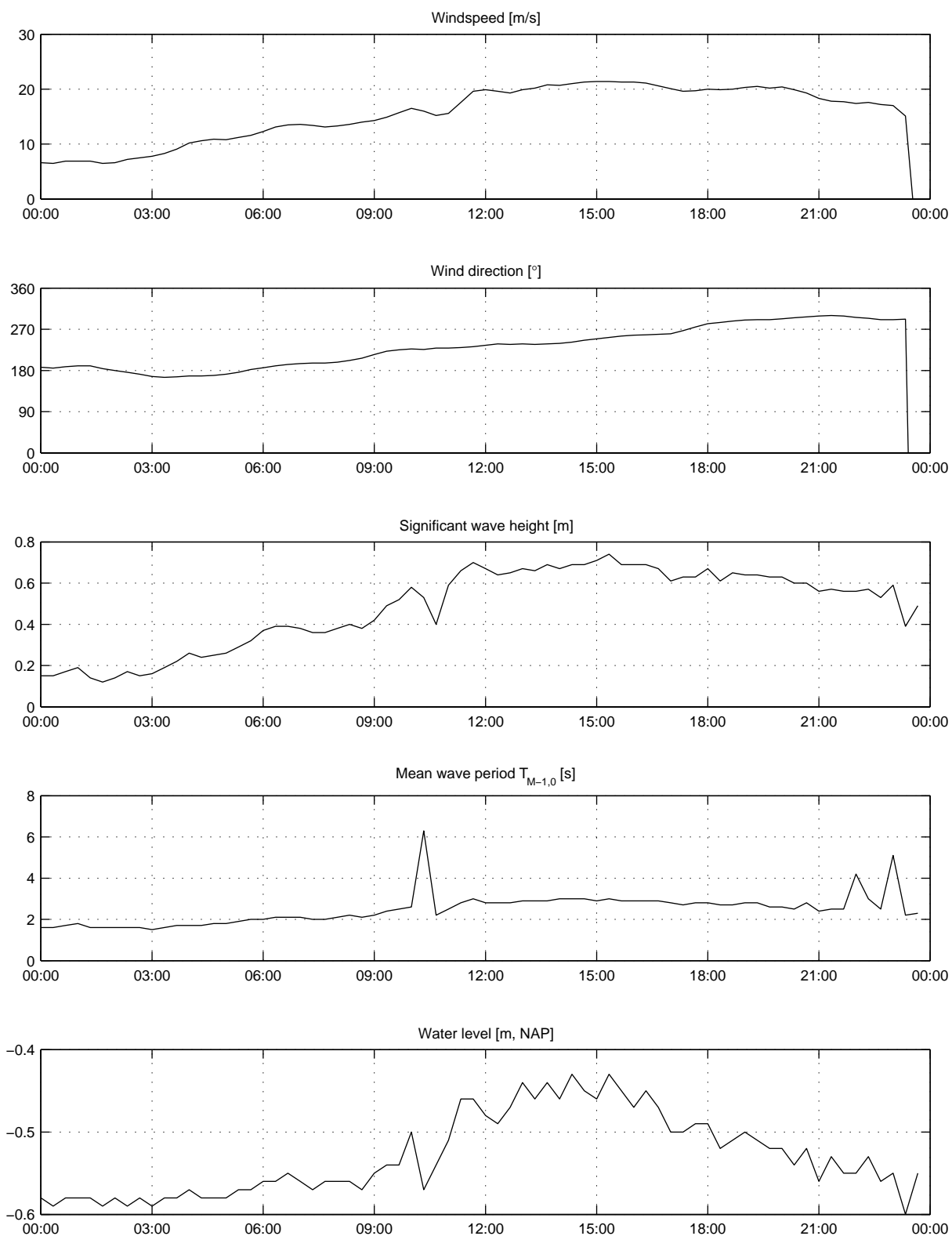
```
PROJECT 'Calibration ' '[nr]'      &
      'Fetch limited growth'
$
$*****
$
MODE  STATIONARY ONED
SET   LEVEL=0.0  DEPMIN=0.01  MAXMES=999  MAXERR=3  &
      pwtail=4
QUANTITY PER SHORT='Tm-1,0' POWER=0
$
CGRID REGULAR 0. 0. 0. [xlen]  0.  [mx]  0      &
      CIRCLE [mdc] flow=[flow]  fhigh=[fhigh] [msc]
INPGRID BOTTOM REGULAR 0. 0. 0. 1 0  [xlen]  1.
READ  BOTTOM [dep] 'depth.bot' 1 0  FREE
BOUN SHAPE JONSWAP 3.3 PEAK DSPR DEGREES
WIND   [u10]  0.

GEN3 KOMEN cds2=[cds2]
BREAK CON ALPHA=[alpha] GAMMA=[gamma]
FRIC JONSWAP CFJON=[cfjon]
TRIADS trfac=[trfac] URSLIM=[urslim]
[csn]WCAP CSM cst=[cst] pow=[pow]
QUAD lambda=[lambda]  cnl4=[cnl4]

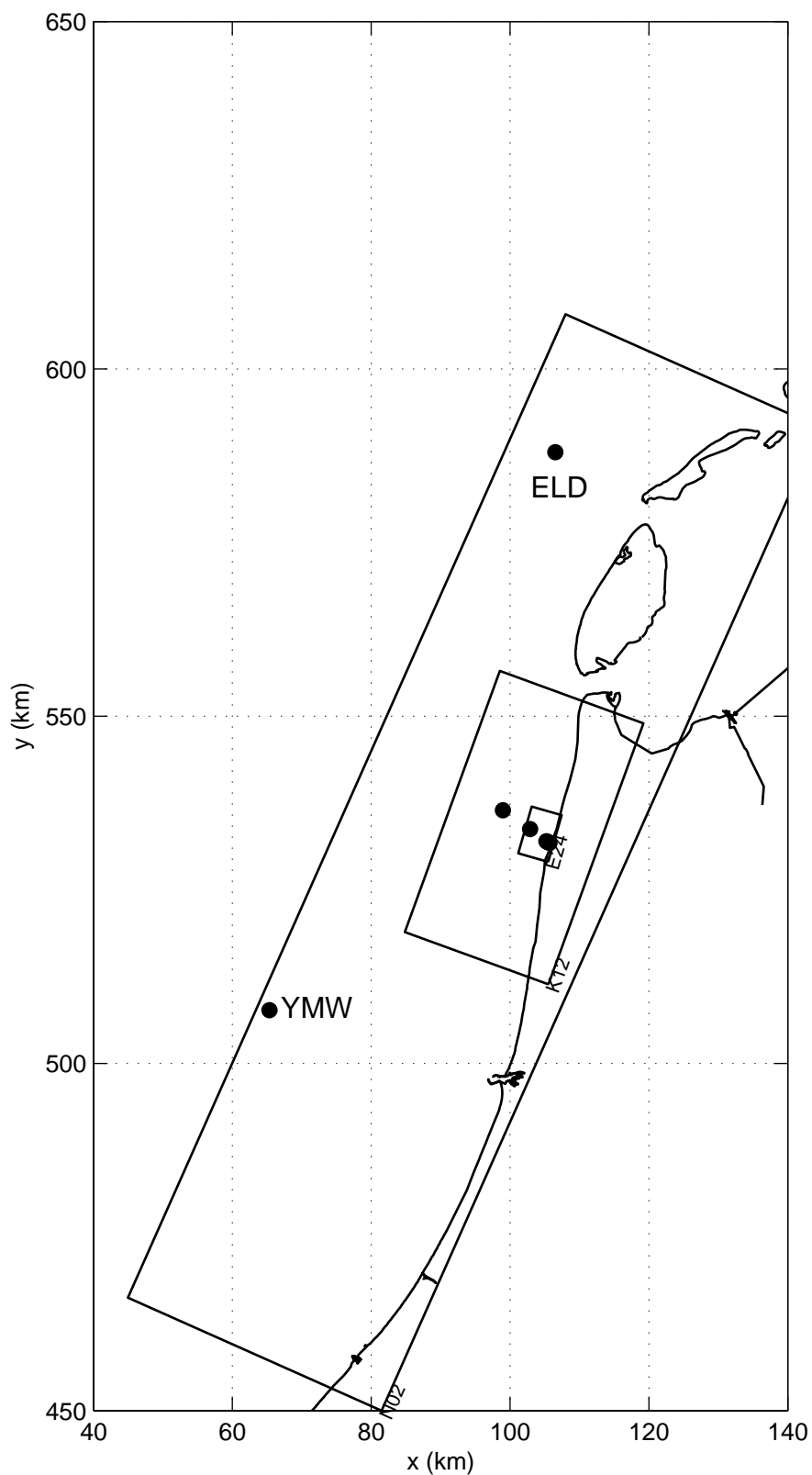
LIMITER ursell = [ursell]
NUM ACCUR [dfrac] [dfrac] [dfrac] [npnts] STAT mxitst=[mxitst] alfa=[alfa]
limiter=[limiter]
$
$*****OUTPUT*****
$
CURVE 'curve' 0. 0. 250  [xlen]  0.
CURVE 'spectra' 0. 0. 5  [xlen]  0.
TABLE 'curve' NOHEAD 'FL_[case].tab' &
      XP YP DEP HS TM01 RTP DIR DSPR FSPR TM02 PER WLEN STEEP QB &
      DHS DRTM01 WIND VEL
SPEC  'spectra' SPEC1D ABS 'FL_[case].sp1'
SPEC  'spectra' SPEC2D ABS 'FL_[case].sp2'
TEST  0 0  POINTS  0 0  50 0 100 0 150 0 200 0 250 0  &
PAR  'FL_[case].par' &
S1D  'FL_[case].s1d' &
S2D  'FL_[case].s2d'
POOL
COMPUTE
$HOTFILE {h_file}
STOP
```



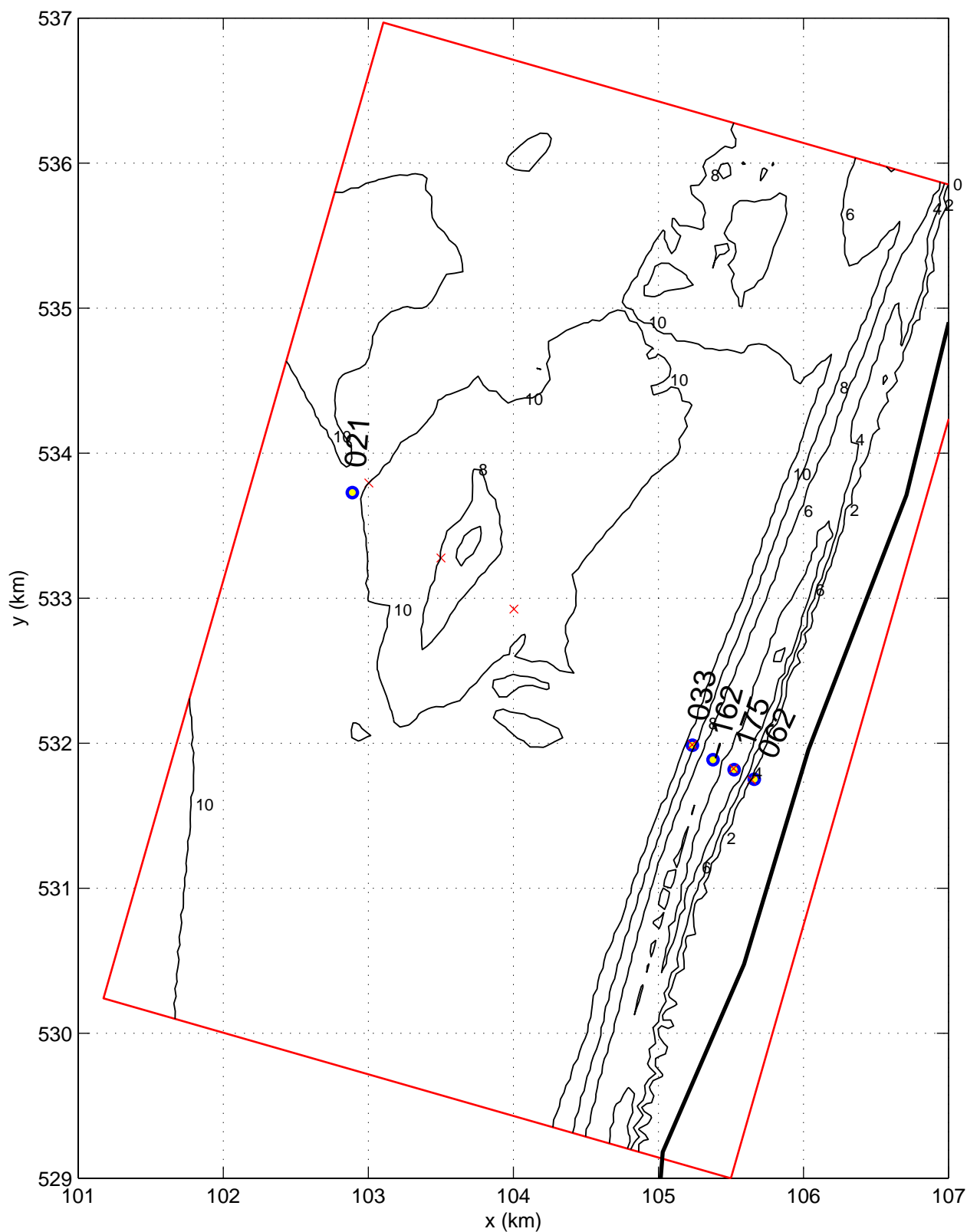
Bottom topography of Sloterveer (NAP)  
location of measurement station F29, and  
location of test points (black dots)



Variation in time of wind, wave and water level parameters  
in the Sloterveer during the storm of 27 October 2002

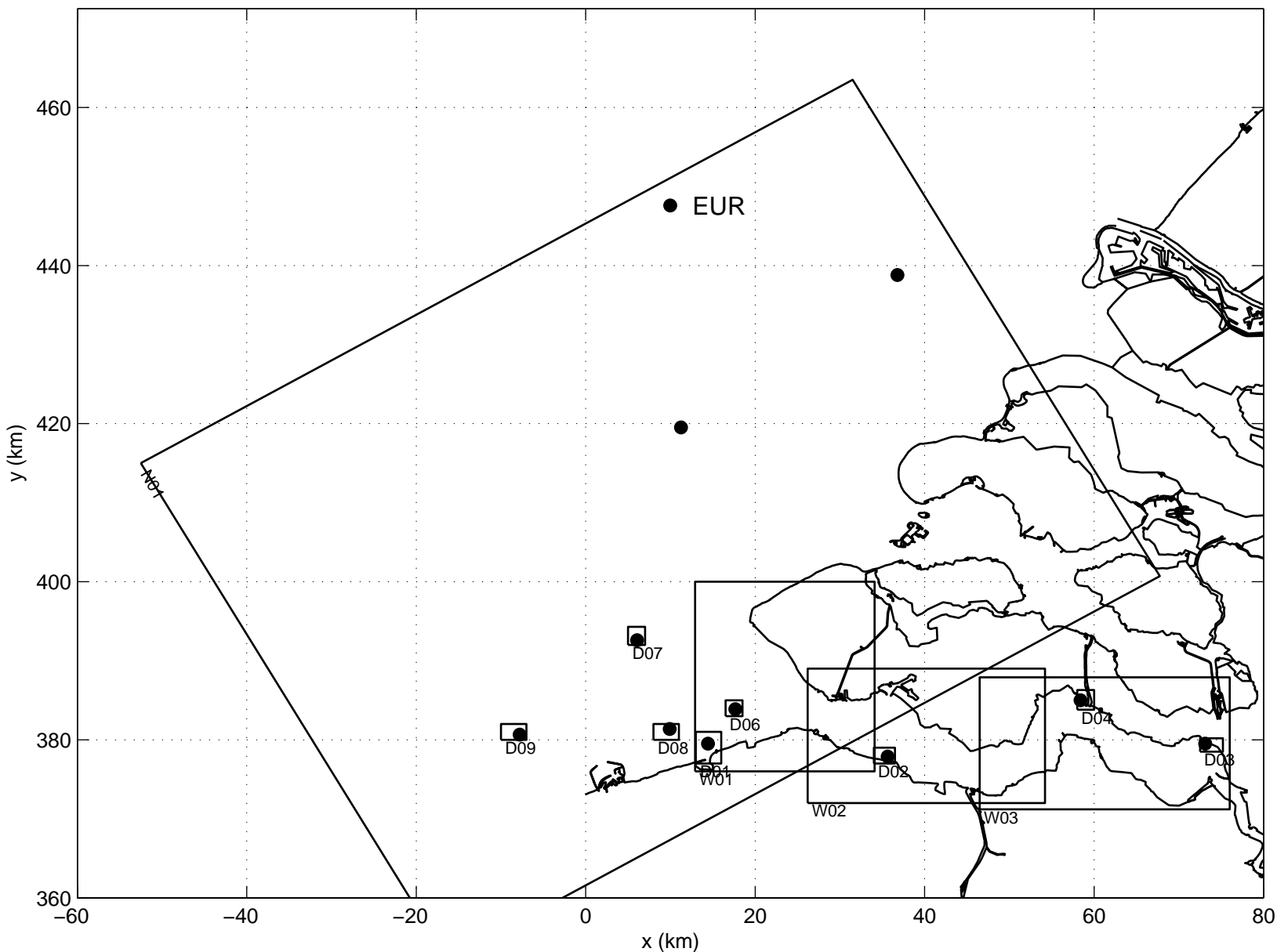


Location of SWAN computational grids at Petten  
and offshore stations ELD and YMW



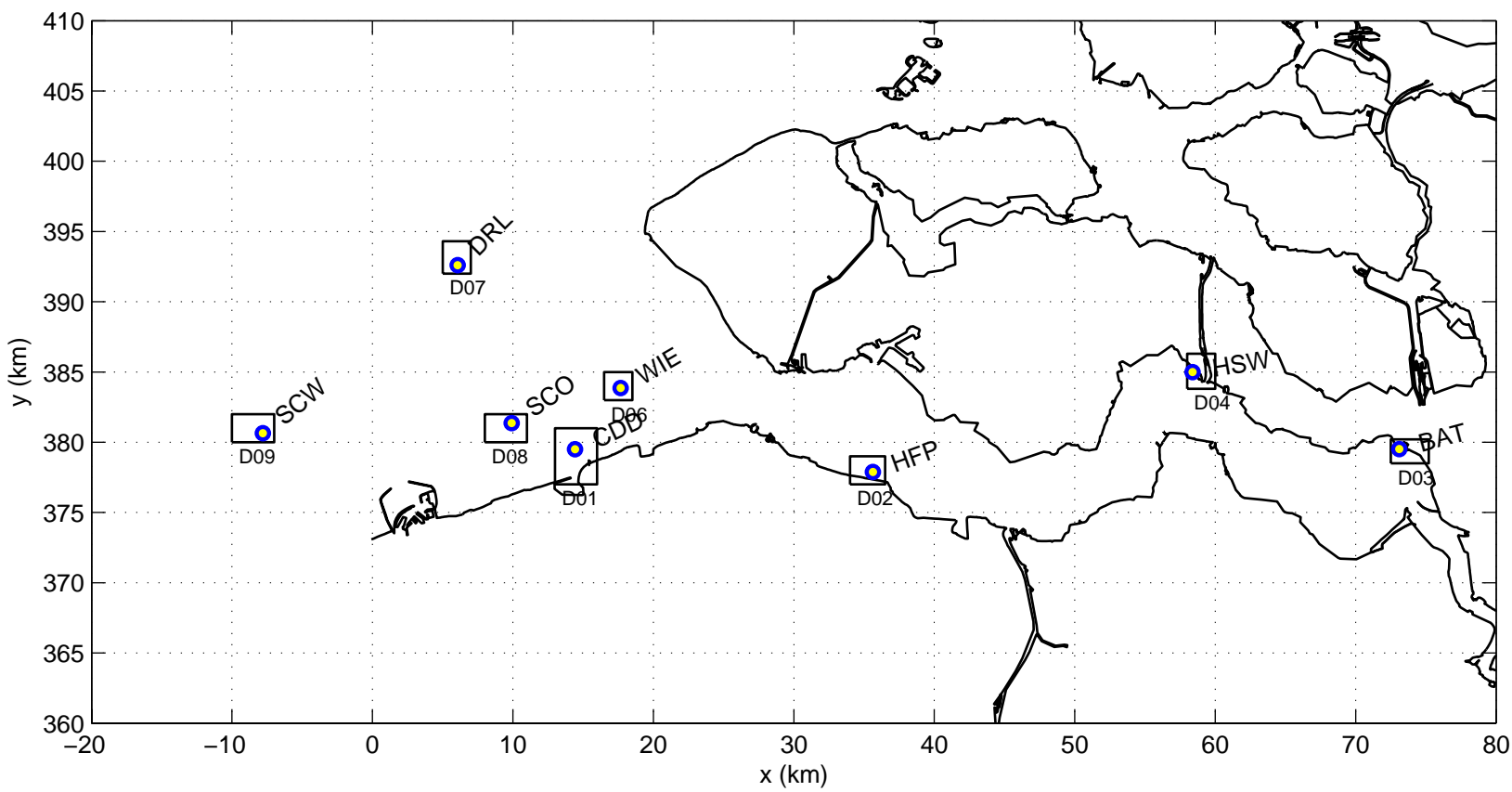
Bottom topography and location of measurement points in SWAN computational grid E24

E24



Location of SWAN computational grids for Westerschelde  
and location of station EUR





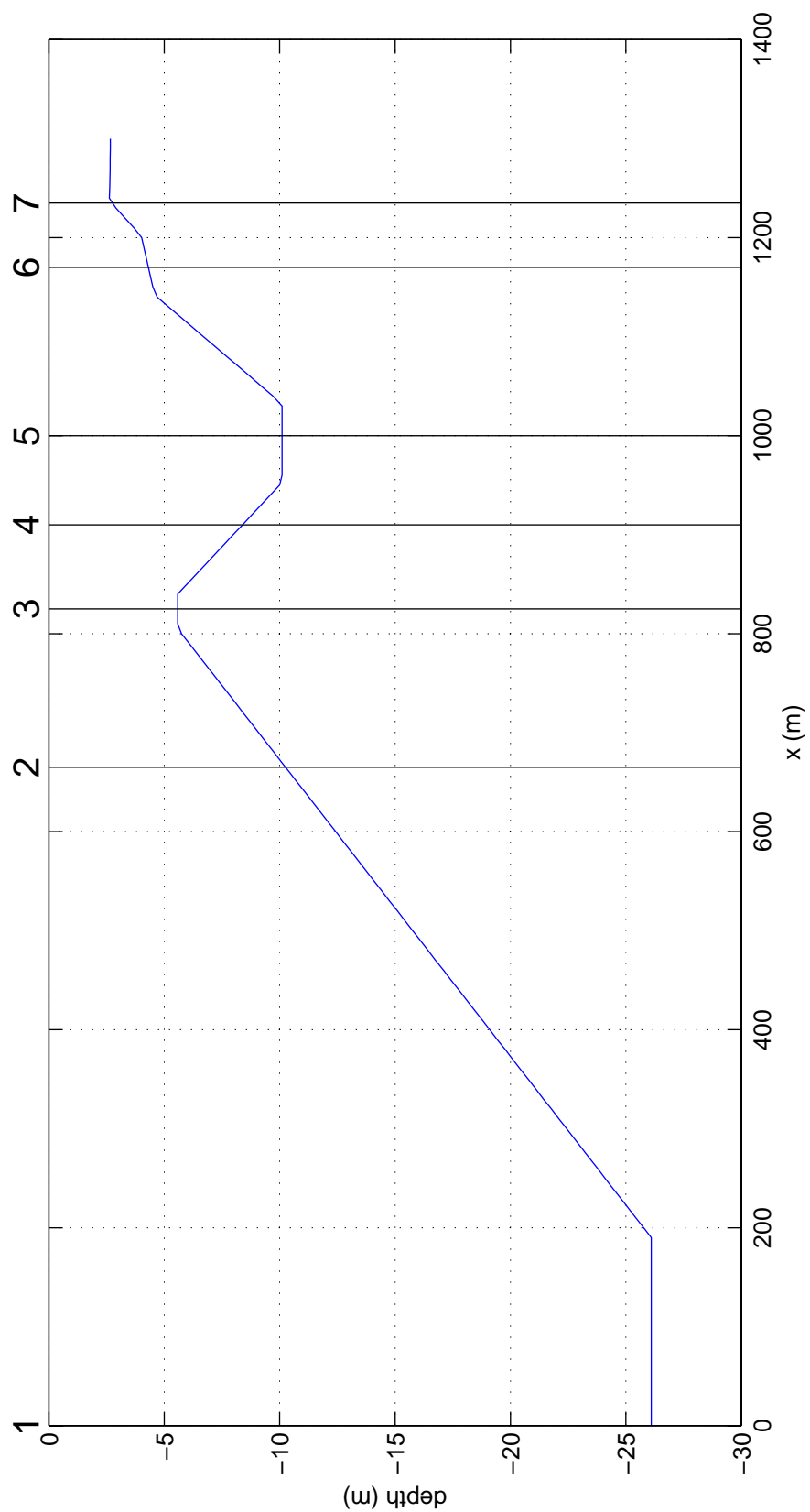
Location of measurement locations in the Westerschelde  
and detailed computational grids

Calibration SWAN 40.20

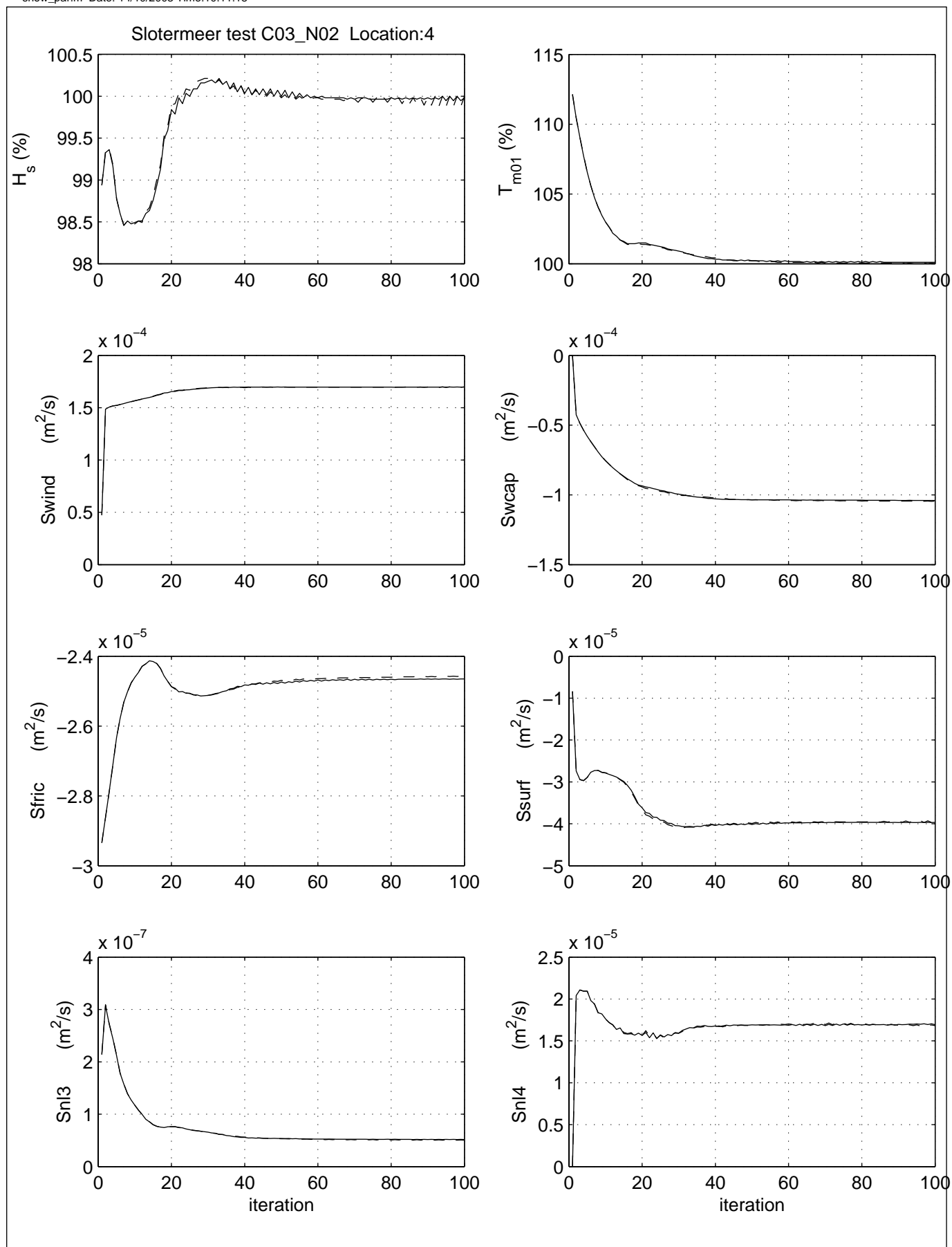
A1168



Fig. 3.6



### Bottom topography and location of output points in Petten wave flume



Iteration behaviour of integral wave parameters

Base case, inclusive triads and quadruplets,  $Q_b=1.0$  (dashed line)

Lower minimum frequency (solid line)

Area: SL

Grid: SL

C03\_N02

Loc:4

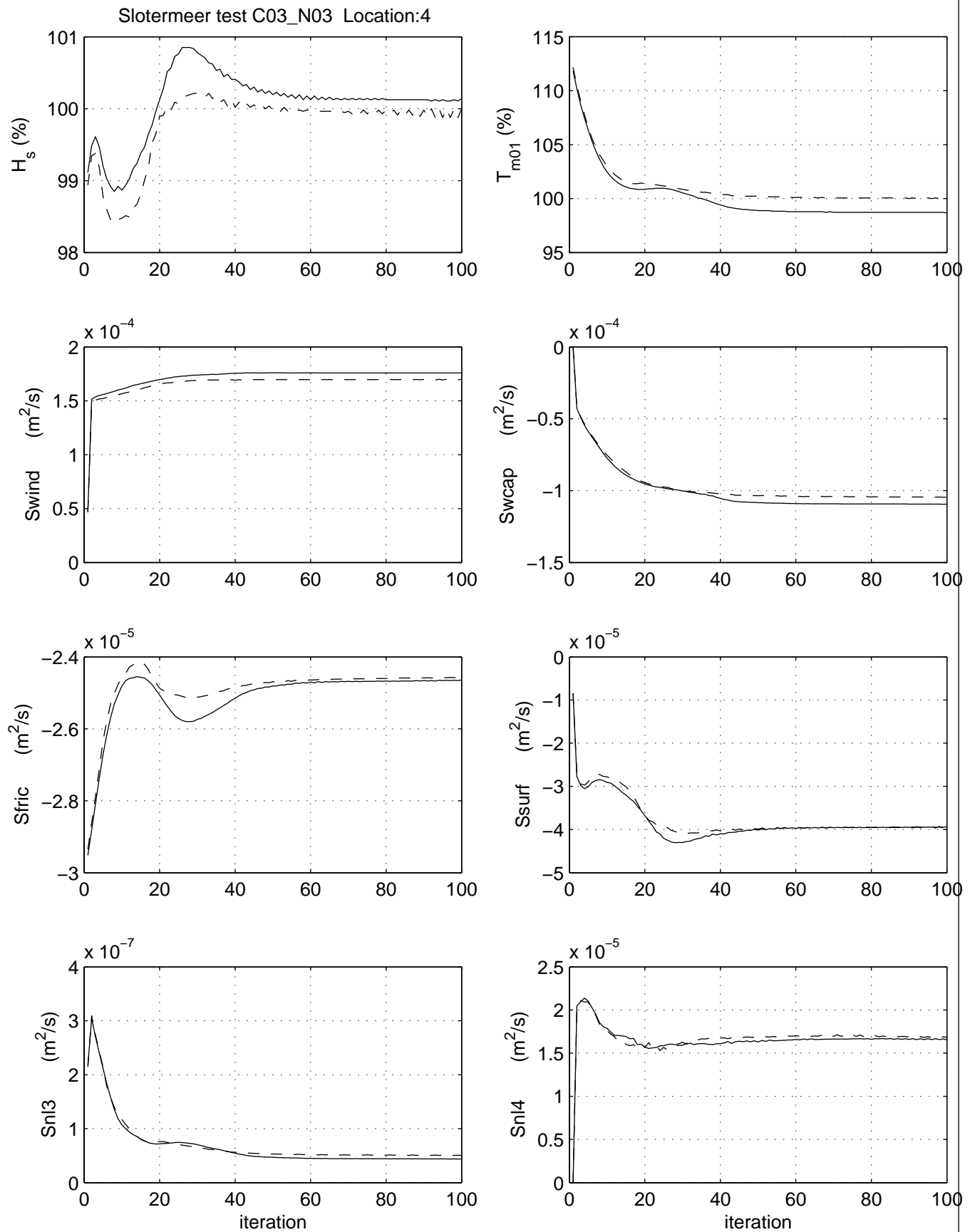
PAR\_SL\_SL\_C03\_N02\_L4

Calibration SWAN 40.20

A1168

 **Alkyon**

Fig. 4.1.2



Iteration behaviour of integral wave parameters

Base case, inclusive triads and quadruplets,  $Q_b=1.0$  (dashed line)

Higher maximum frequency (solid line)

Area: SL

Grid: SL

C03\_N03

Loc:4

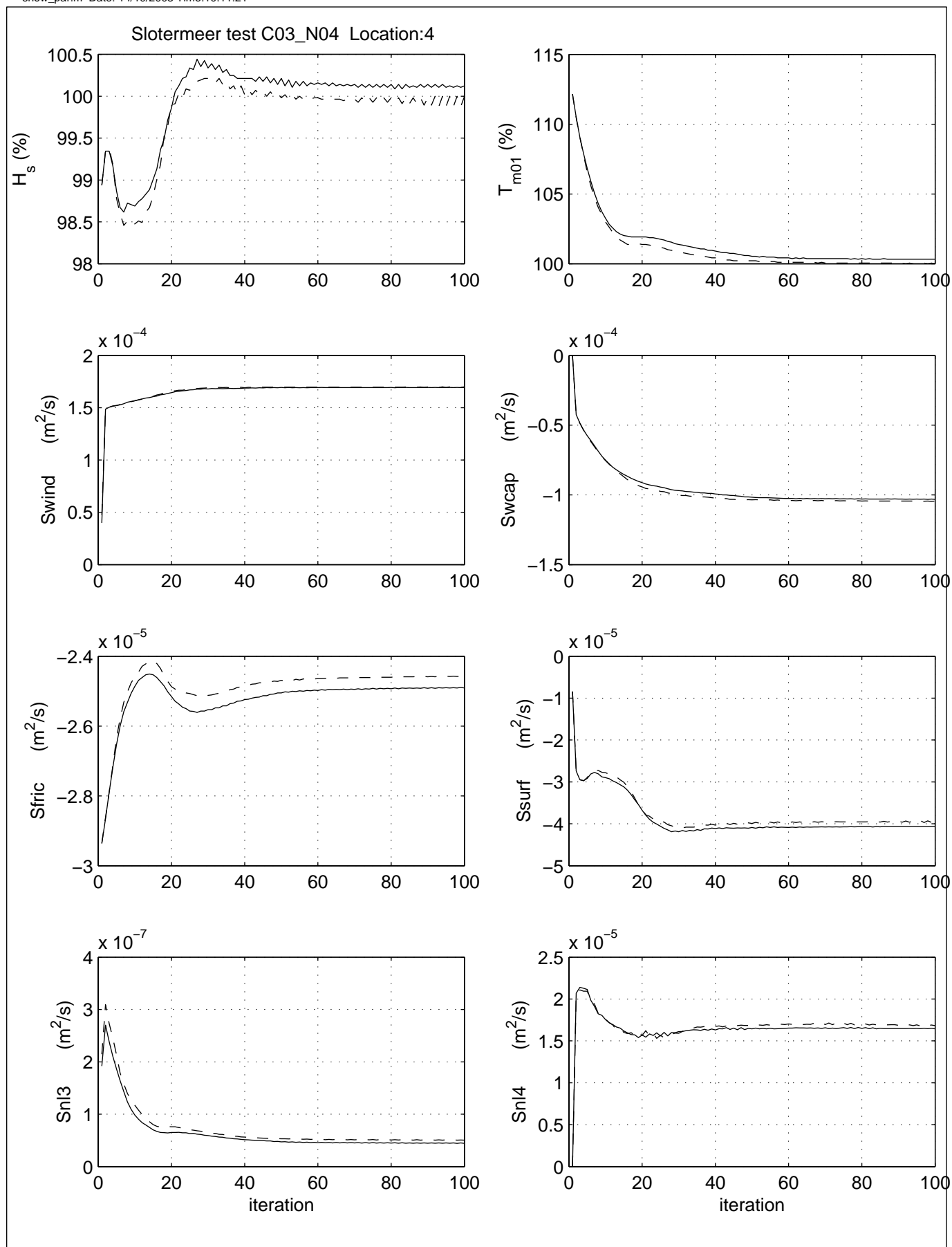
PAR\_SL\_SL\_C03\_N03\_L4

Calibration SWAN 40.20

A1168

 **Alkyon**

Fig. 4.1.3



Iteration behaviour of integral wave parameters

Base case, inclusive triads and quadruplets,  $Q_b=1.0$  (dashed line)

Higher frequency resolution (solid line)

Area: SL

Grid: SL

C03\_N04

Loc:4

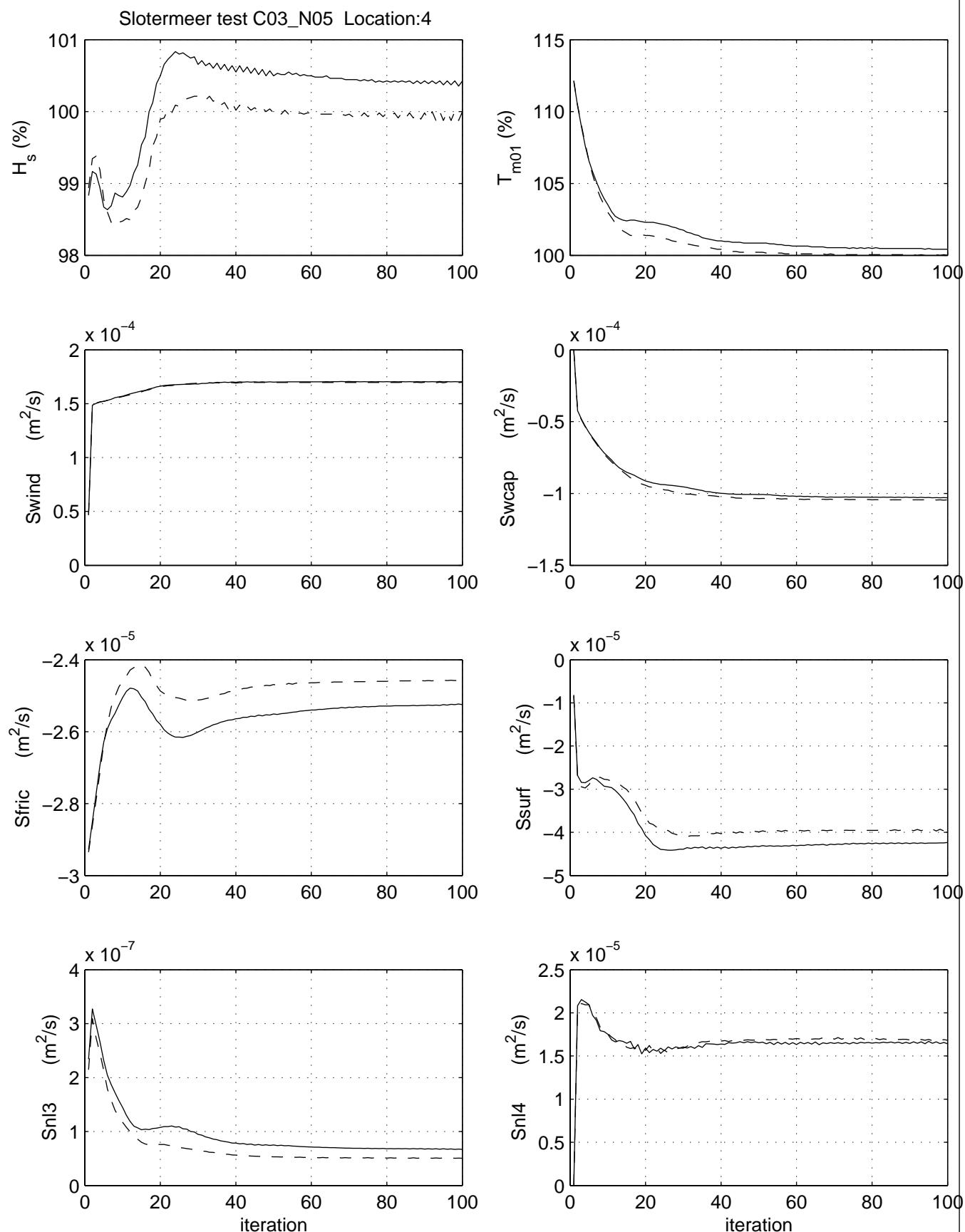
PAR\_SL\_SL\_C03\_N04\_L4

Calibration SWAN 40.20

A1168

 **Alkyon**

Fig. 4.1.4



Iteration behaviour of integral wave parameters

Base case, inclusive triads and quadruplets,  $Q_b=1.0$  (dashed line)

Lower frequency resolution (solid line)

Area: SL

Grid: SL

C03\_N05

Loc:4

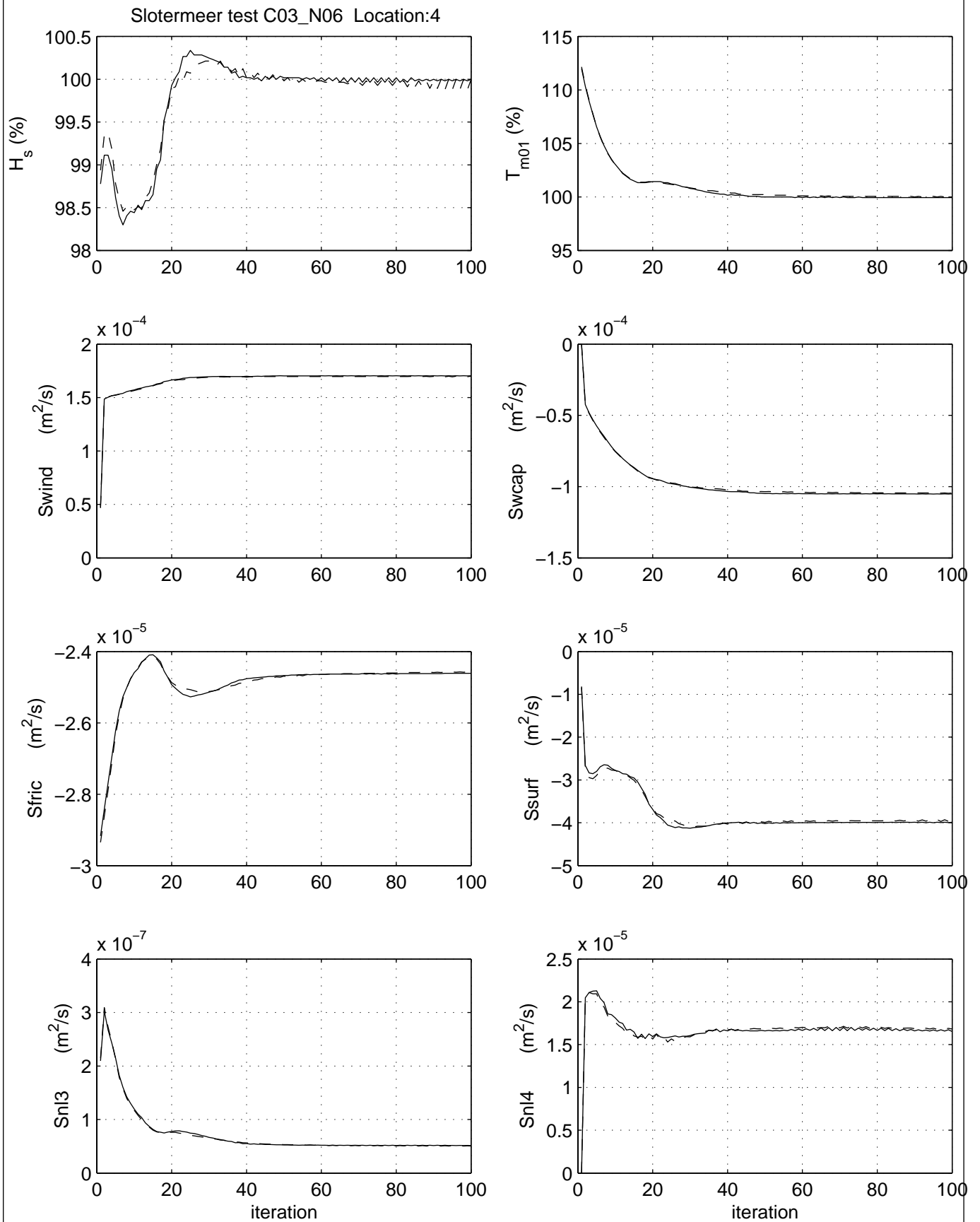
PAR\_SL\_SL\_C03\_N05\_L4

Calibration SWAN 40.20

A1168

 **Alkyon**

Fig. 4.1.5



Iteration behaviour of integral wave parameters

Base case, inclusive triads and quadruplets,  $Q_b=1.0$  (dashed line)

Higher directional resolution (solid line)

Area: SL

Grid: SL

C03\_N06

Loc:4

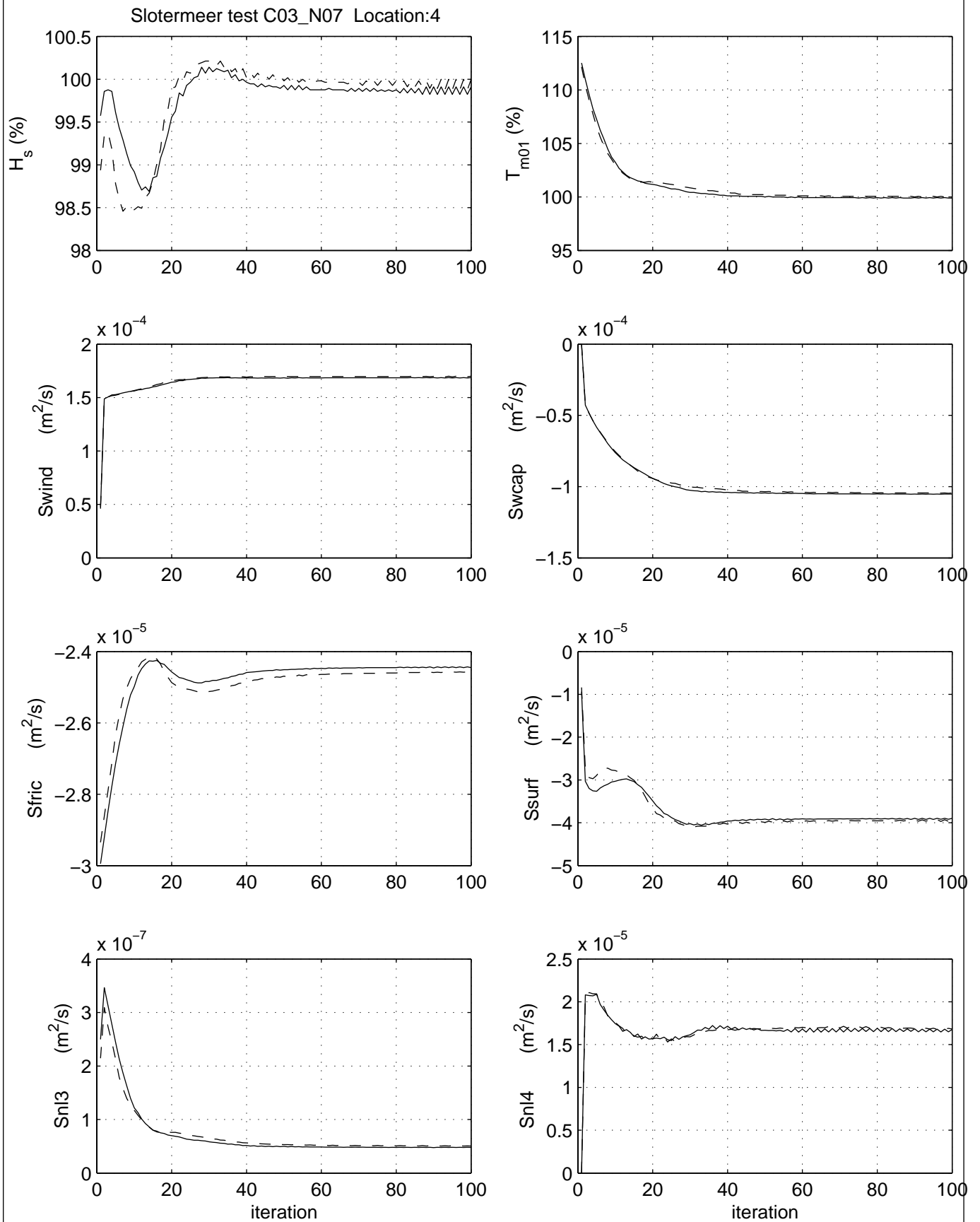
PAR\_SL\_SL\_C03\_N06\_L4

Calibration SWAN 40.20

A1168

 **Alkyon**

Fig. 4.1.6



Iteration behaviour of integral wave parameters

Base case, inclusive triads and quadruplets,  $Q_b=1.0$  (dashed line)

Lower directional resolution (solid line)

Area: SL

Grid: SL

C03\_N07

Loc:4

PAR\_SL\_SL\_C03\_N07\_L4

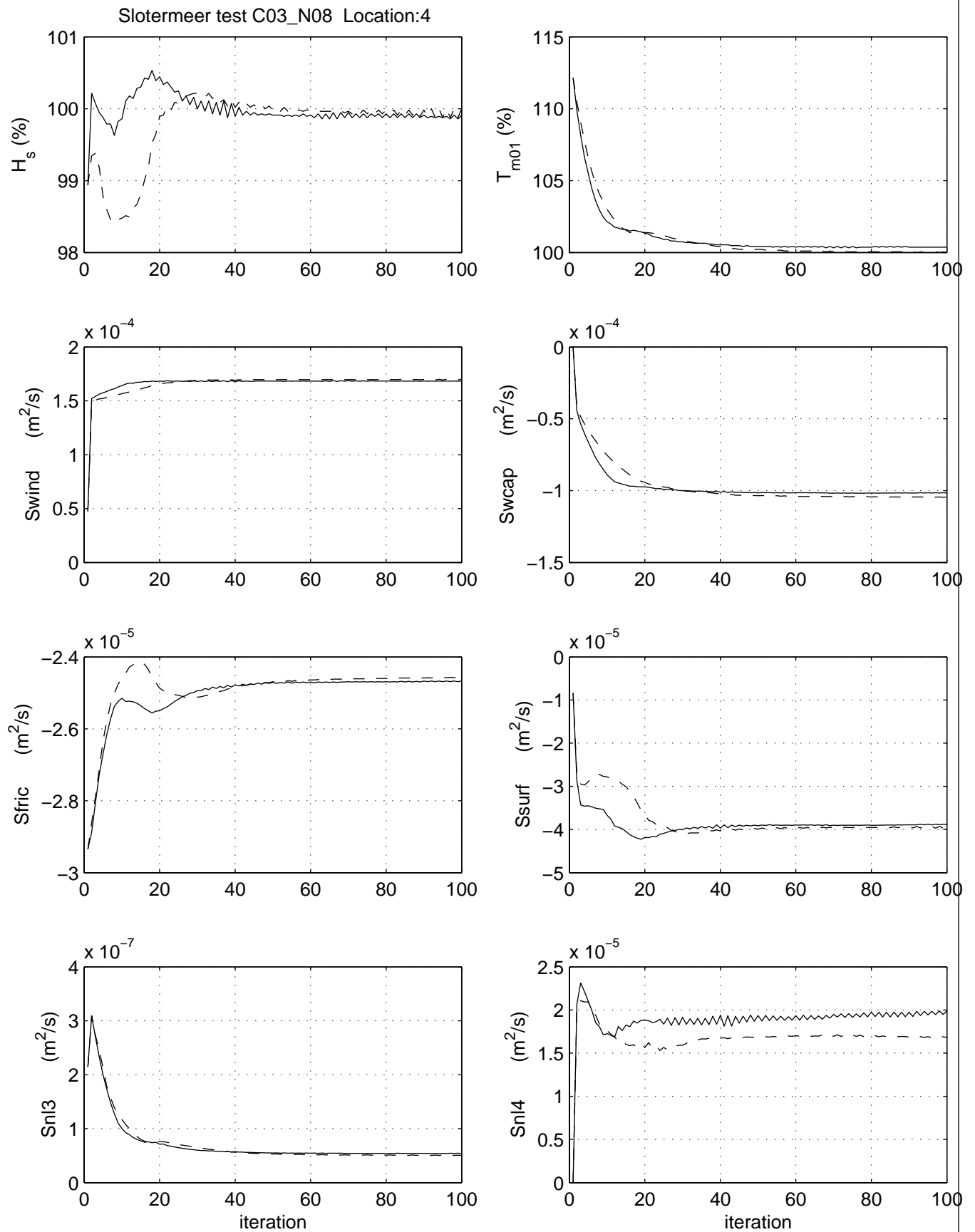
Calibration SWAN 40.20

A1168

 **Alkyon**

Fig. 4.1.7





Iteration behaviour of integral wave parameters

Base case, inclusive triads and quadruplets,  $Q_b=1.0$  (dashed line)

Phillips limit 20% (solid line)

Area: SL

Grid: SL

C03\_N08

Loc:4

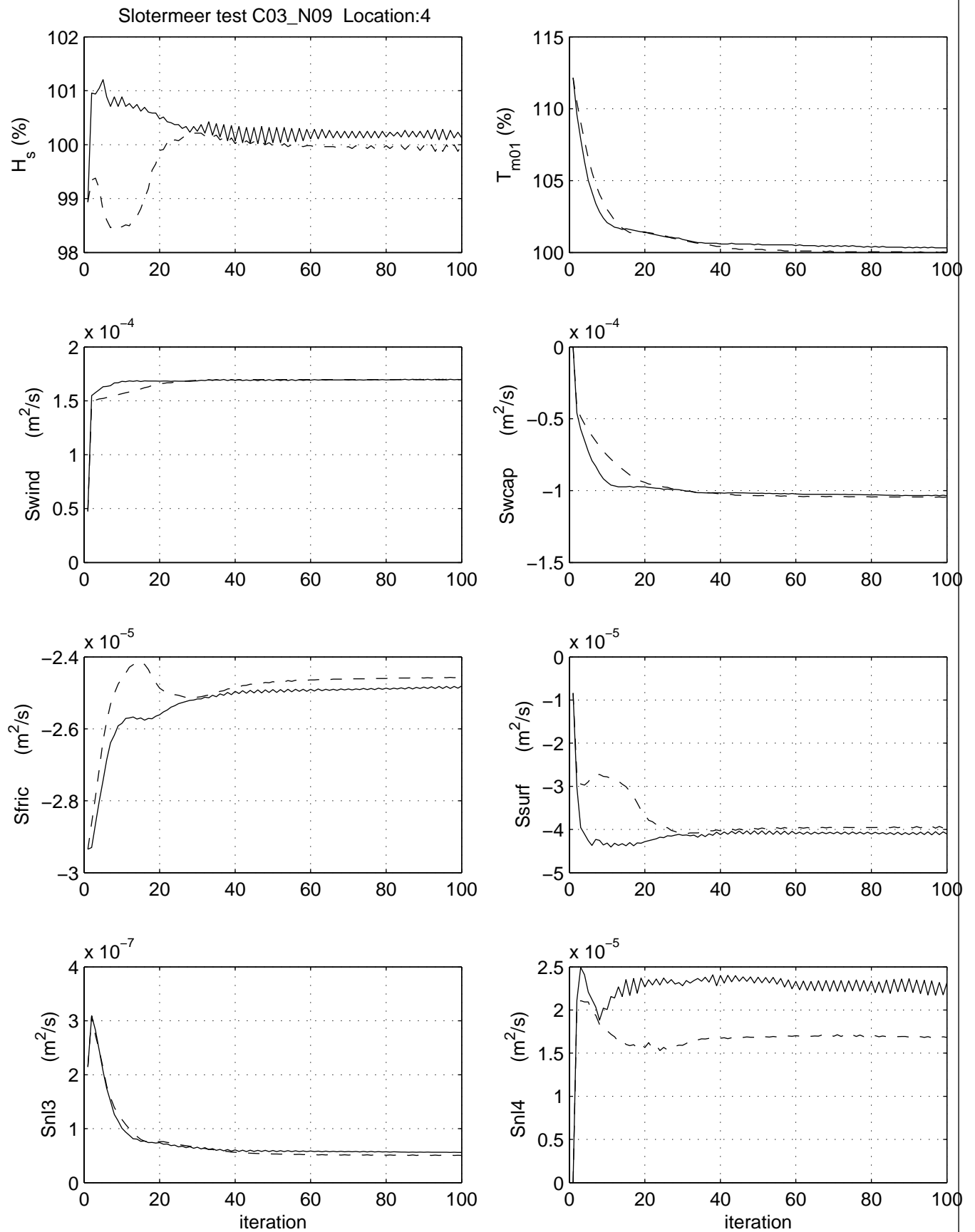
PAR\_SL\_SL\_C03\_N08\_L4

Calibration SWAN 40.20

A1168



Fig. 4.1.8



Iteration behaviour of integral wave parameters

Base case, inclusive triads and quadruplets,  $Qb=1.0$  (dashed line)

Phillips limit 30% (solid line)

Area: SL

Grid: SL

C03\_N09

Loc:4

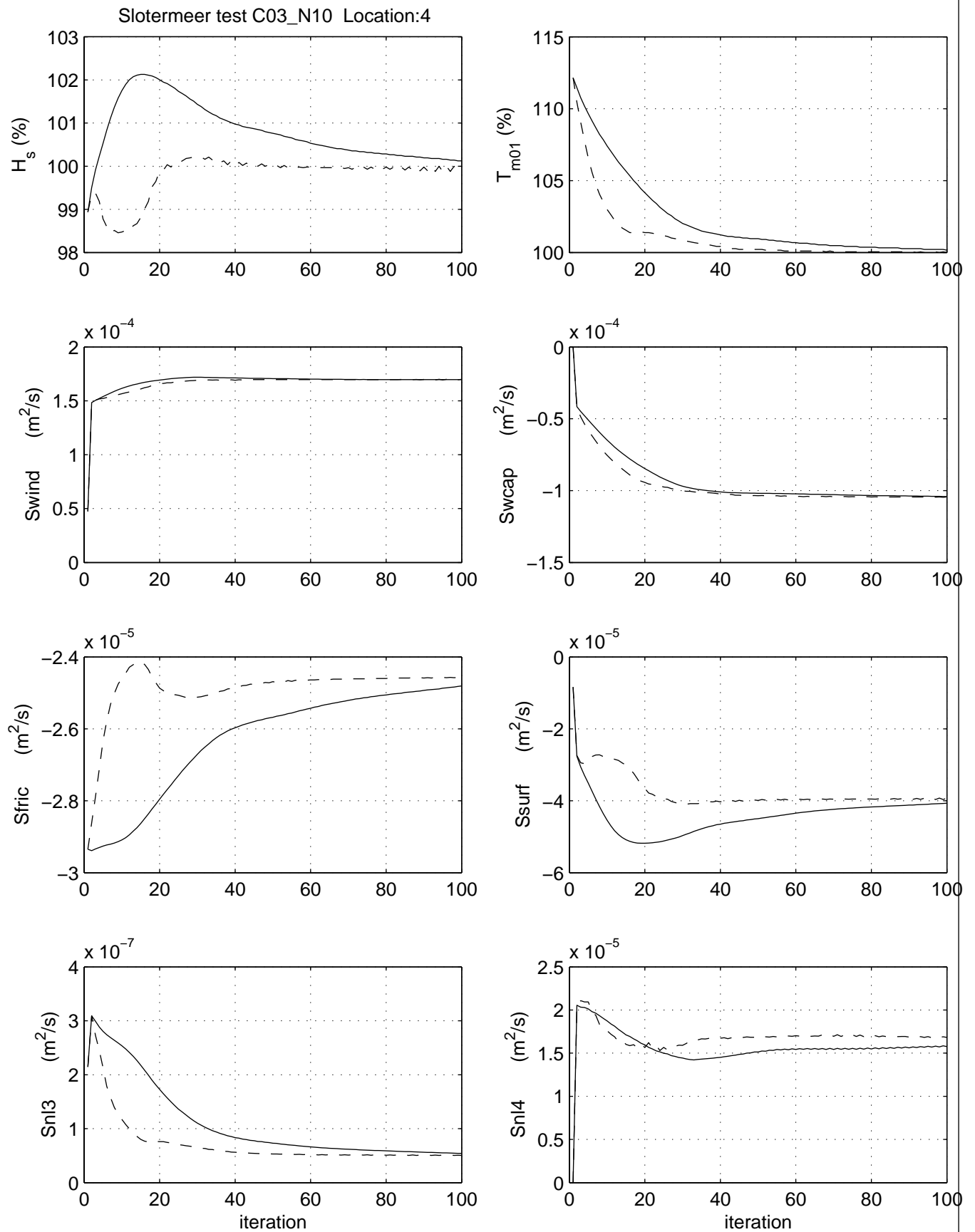
PAR\_SL\_SL\_C03\_N09\_L4

Calibration SWAN 40.20

A1168



Fig. 4.1.9



Iteration behaviour of integral wave parameters

Base case, inclusive triads and quadruplets,  $Q_b=1.0$  (dashed line)Under-relaxation  $\alpha=0.025$ , Phillips limit 10% (solid line)

Area: SL

Grid: SL

C03\_N10

Loc:4

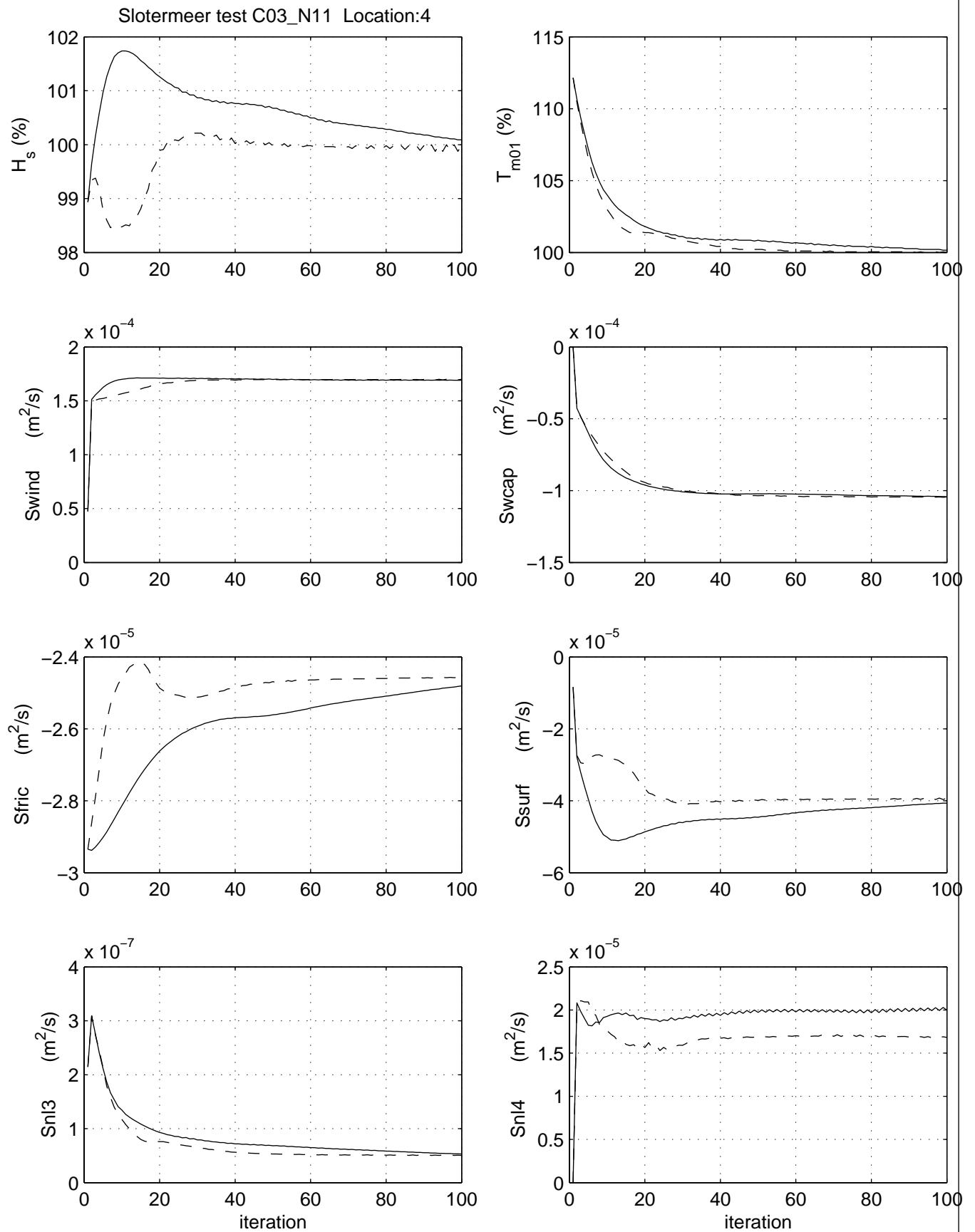
PAR\_SL\_SL\_C03\_N10\_L4

Calibration SWAN 40.20

A1168

 **Alkyon**

Fig. 4.1.10



Iteration behaviour of integral wave parameters

Base case, inclusive triads and quadruplets,  $Q_b=1.0$  (dashed line)Under-relaxation  $\alpha=0.025$ , Phillips limit 50% (solid line)

Area: SL

Grid: SL

C03\_N11

Loc:4

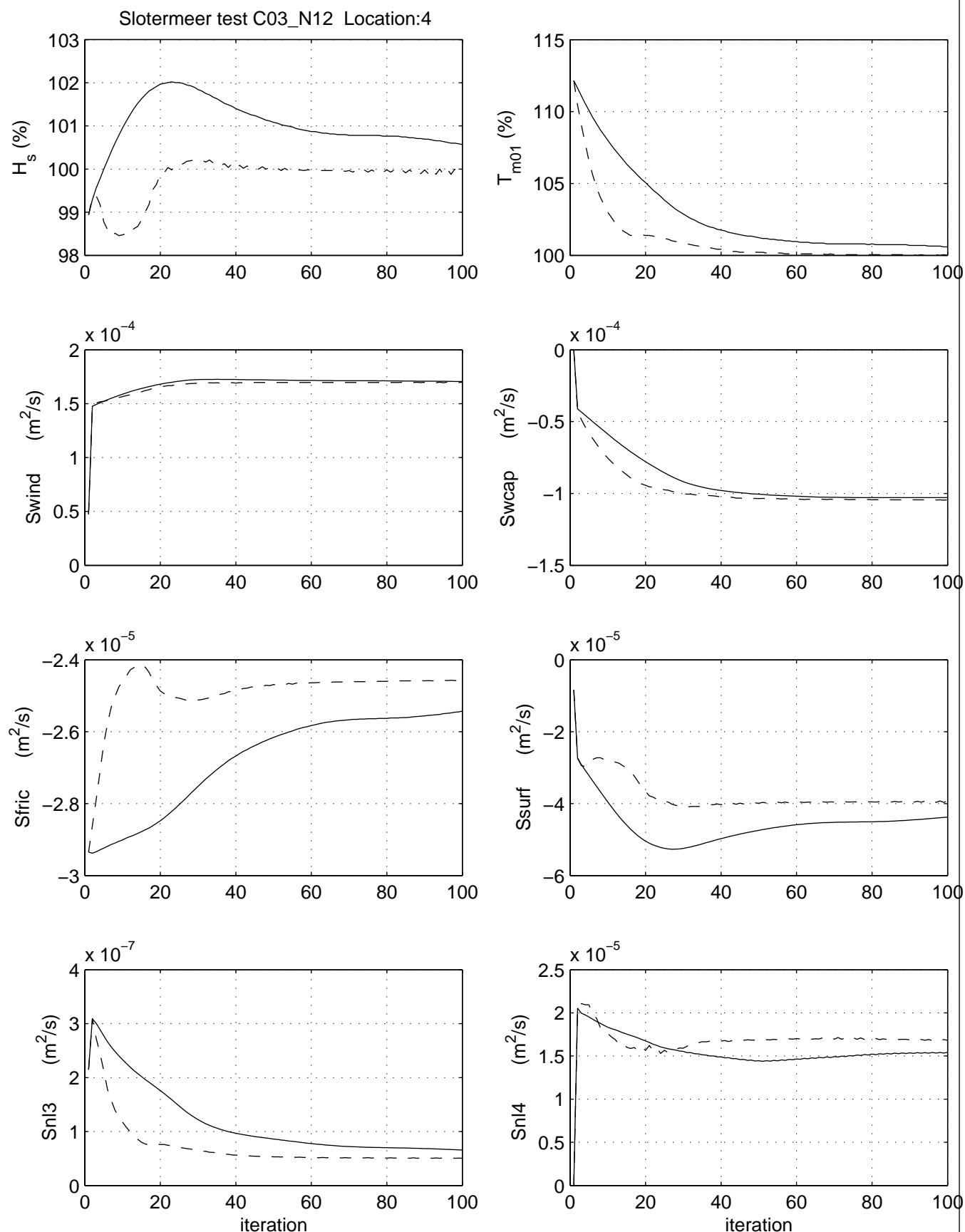
PAR\_SL\_SL\_C03\_N11\_L4

Calibration SWAN 40.20

A1168

 **Alkyon**

Fig. 4.1.11



Iteration behaviour of integral wave parameters

Base case, inclusive triads and quadruplets,  $Q_b=1.0$  (dashed line)Under-relaxation  $\alpha=0.05$ , Phillips limit 10% (solid line)

Area: SL

Grid: SL

C03\_N12

Loc:4

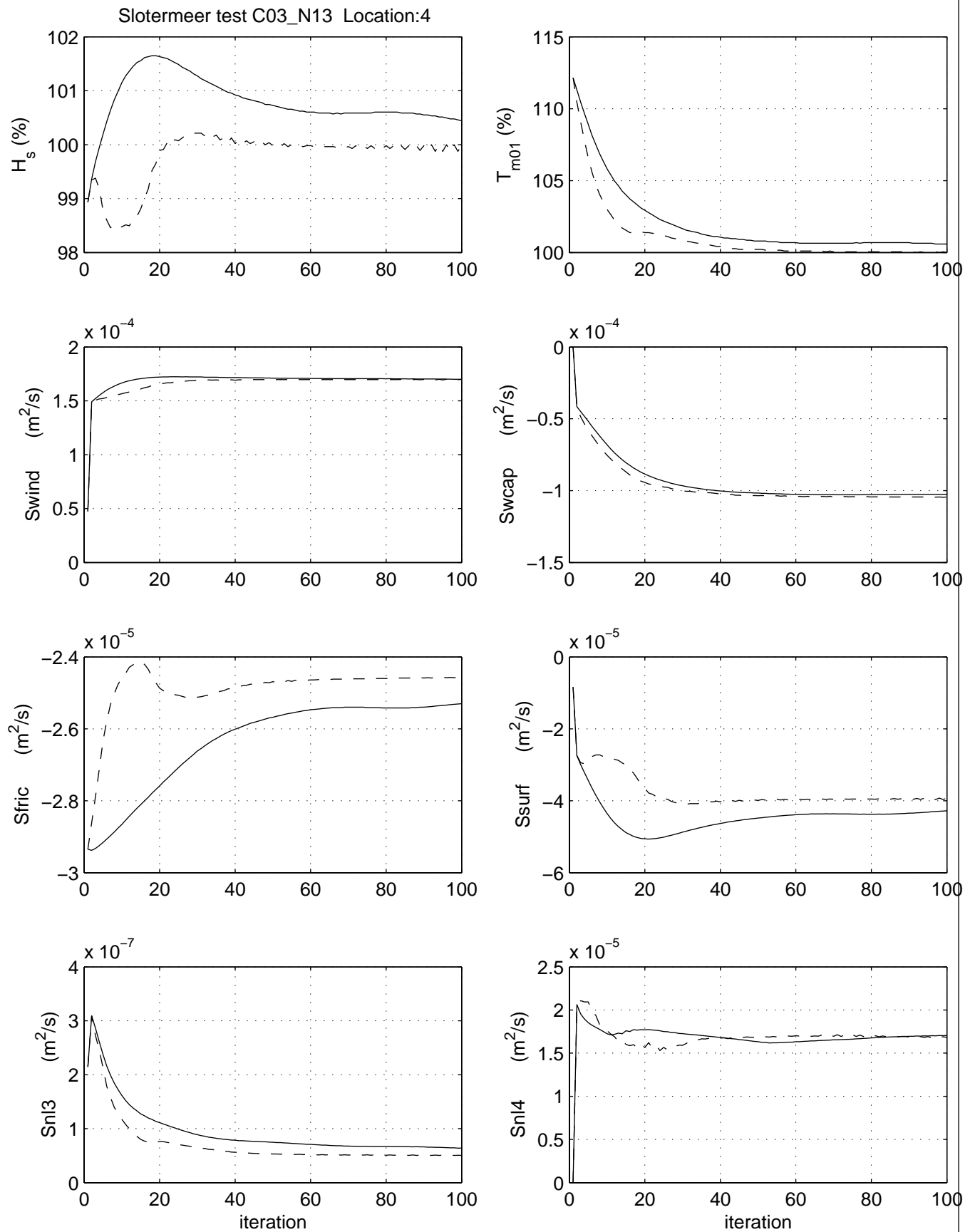
PAR\_SL\_SL\_C03\_N12\_L4

Calibration SWAN 40.20

A1168



Fig. 4.1.12



Iteration behaviour of integral wave parameters

Base case, inclusive triads and quadruplets,  $Q_b=1.0$  (dashed line)Under-relaxation  $\alpha=0.05$ , Phillips limit 50% (solid line)

Area: SL

Grid: SL

C03\_N13

Loc:4

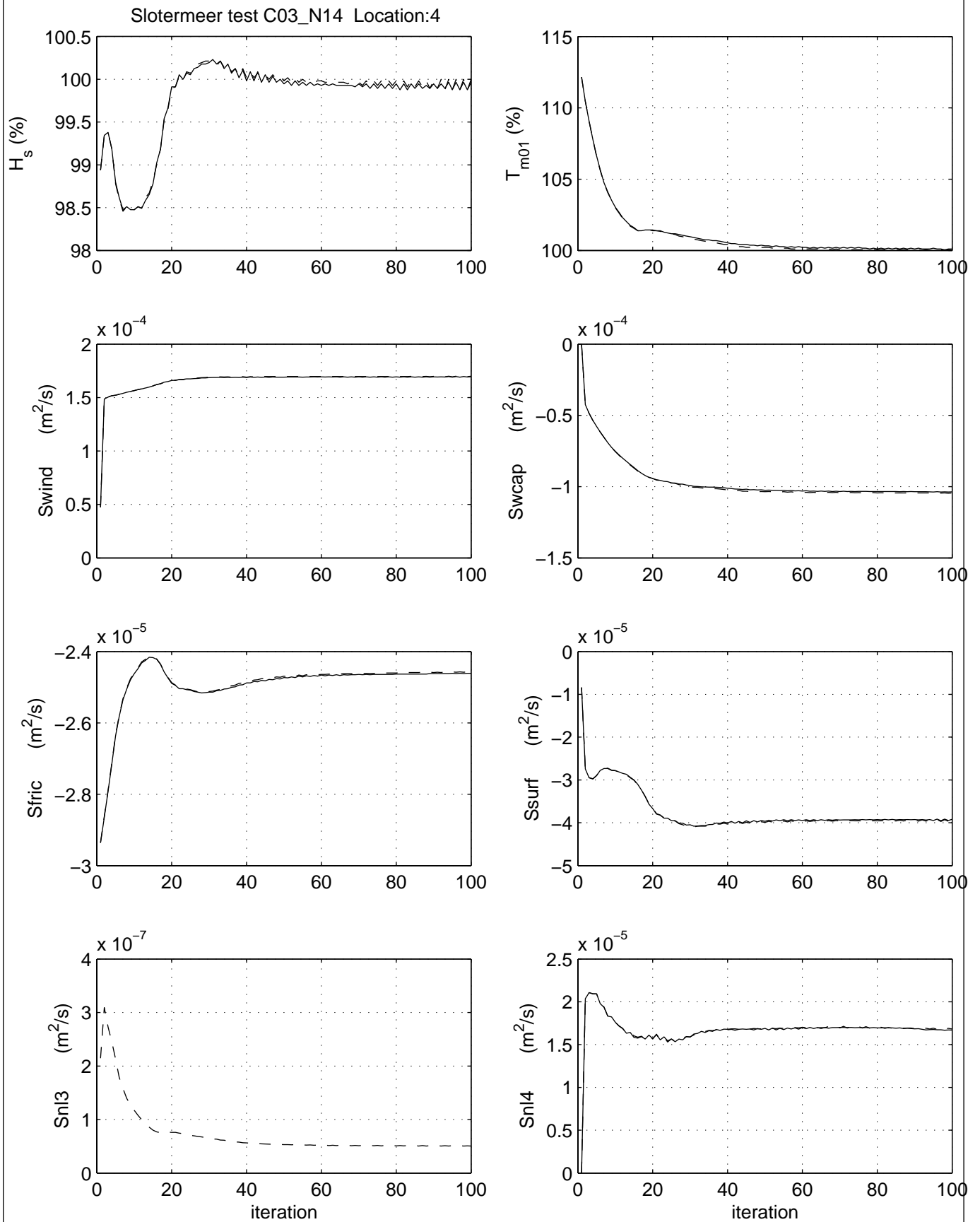
PAR\_SL\_SL\_C03\_N13\_L4

Calibration SWAN 40.20

A1168

 **Alkyon**

Fig. 4.1.13



Iteration behaviour of integral wave parameters

Base case, inclusive triads and quadruplets,  $Q_b=1.0$  (dashed line)Exclusive triads and quadruplets,  $Q_b = 1.0$  (solid line)

Area: SL

Grid: SL

C03\_N14

Loc:4

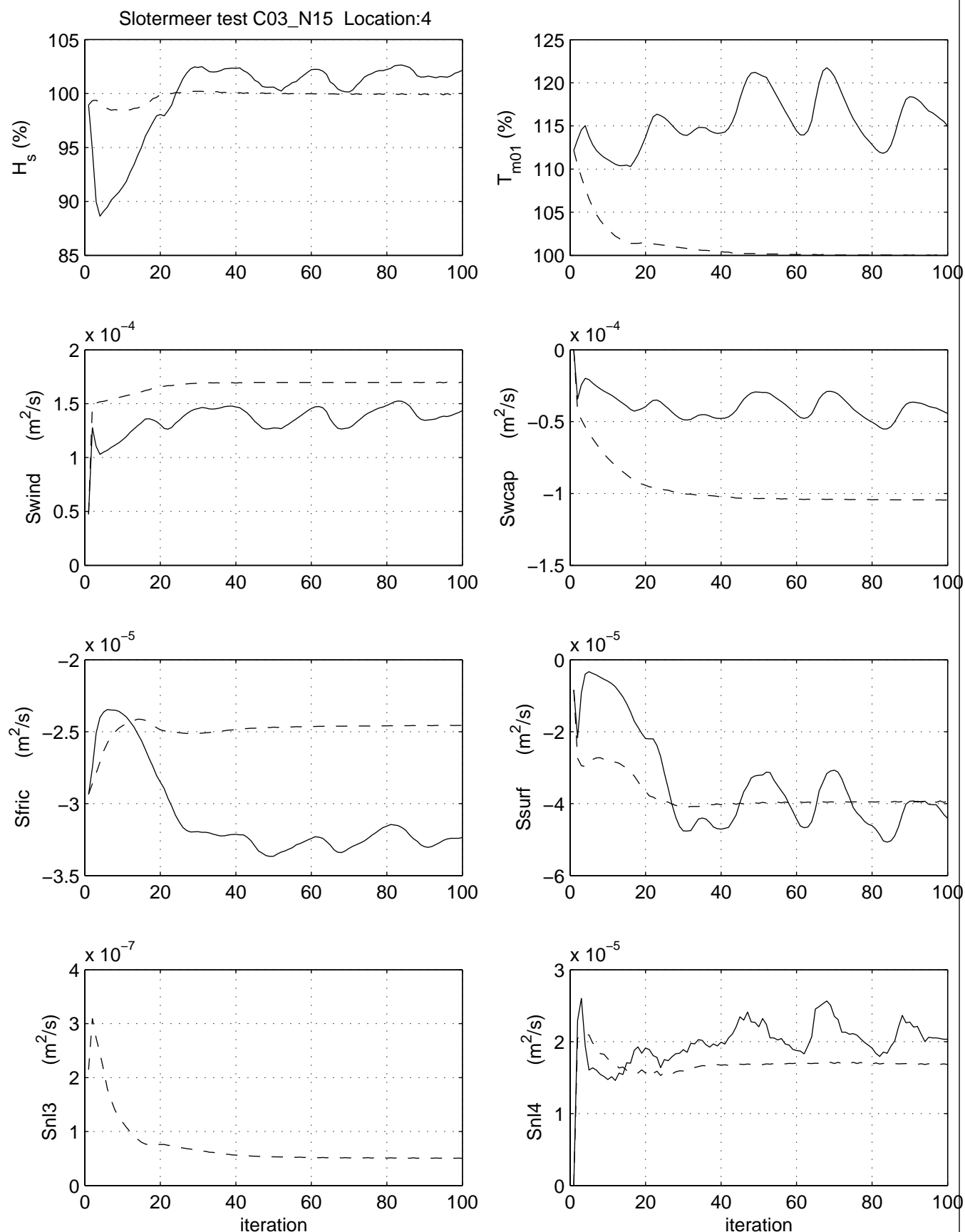
PAR\_SL\_SL\_C03\_N14\_L4

Calibration SWAN 40.20

A1168

 **Alkyon**

Fig. 4.1.14



Iteration behaviour of integral wave parameters

Base case, inclusive triads and quadruplets,  $Q_b=1.0$  (dashed line)Exclusive triads and quadruplets,  $Q_b = 0.00001$  (solid line)

Area: SL

Grid: SL

C03\_N15

Loc:4

PAR\_SL\_SL\_C03\_N15\_L4

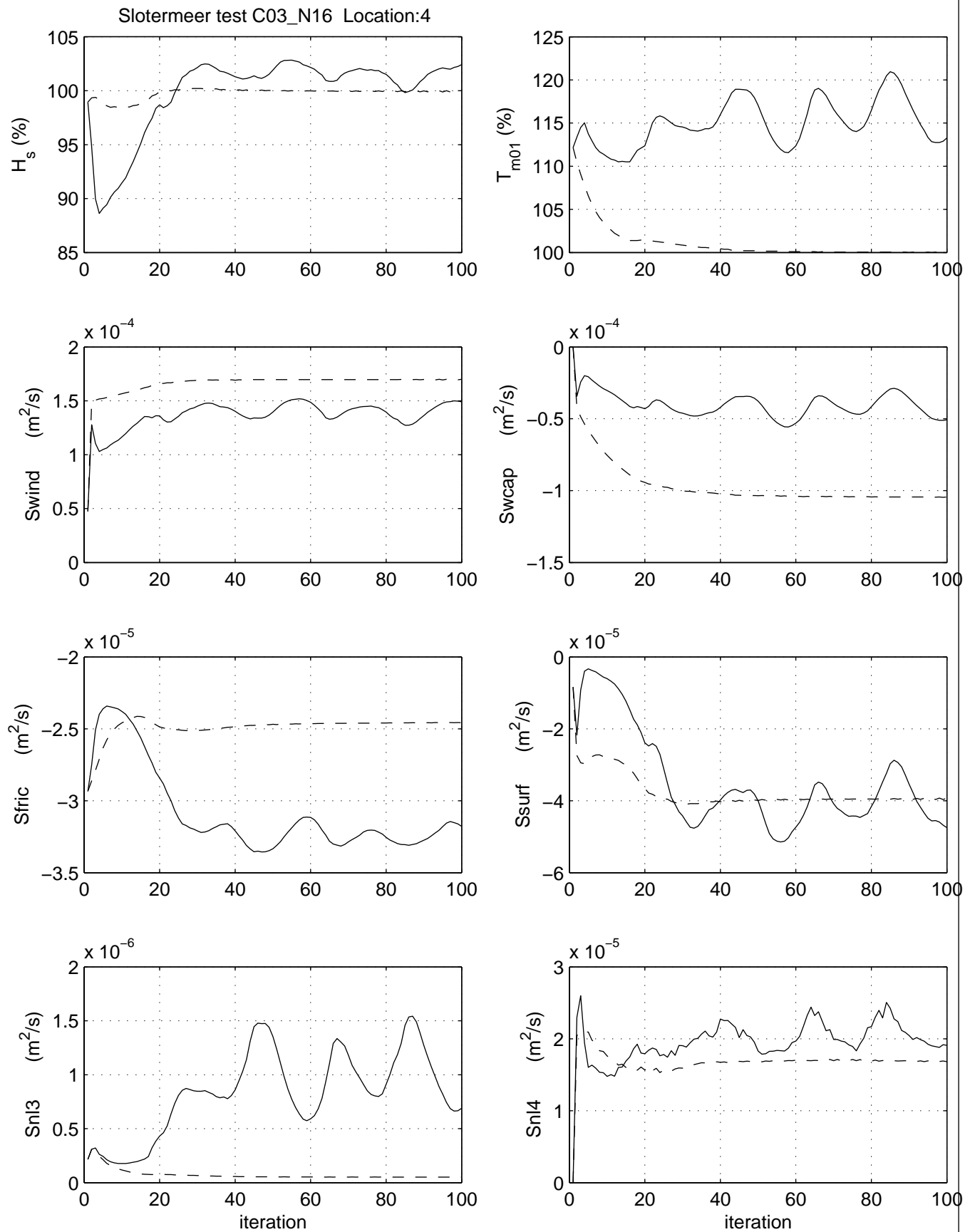
Calibration SWAN 40.20

A1168



Fig. 4.1.15





Iteration behaviour of integral wave parameters

Base case, inclusive triads and quadruplets,  $Q_b=1.0$  (dashed line)Inclusive triads and quadruplets,  $Q_b = 0.00001$  (solid line)

Area: SL

Grid: SL

C03\_N16

Loc:4

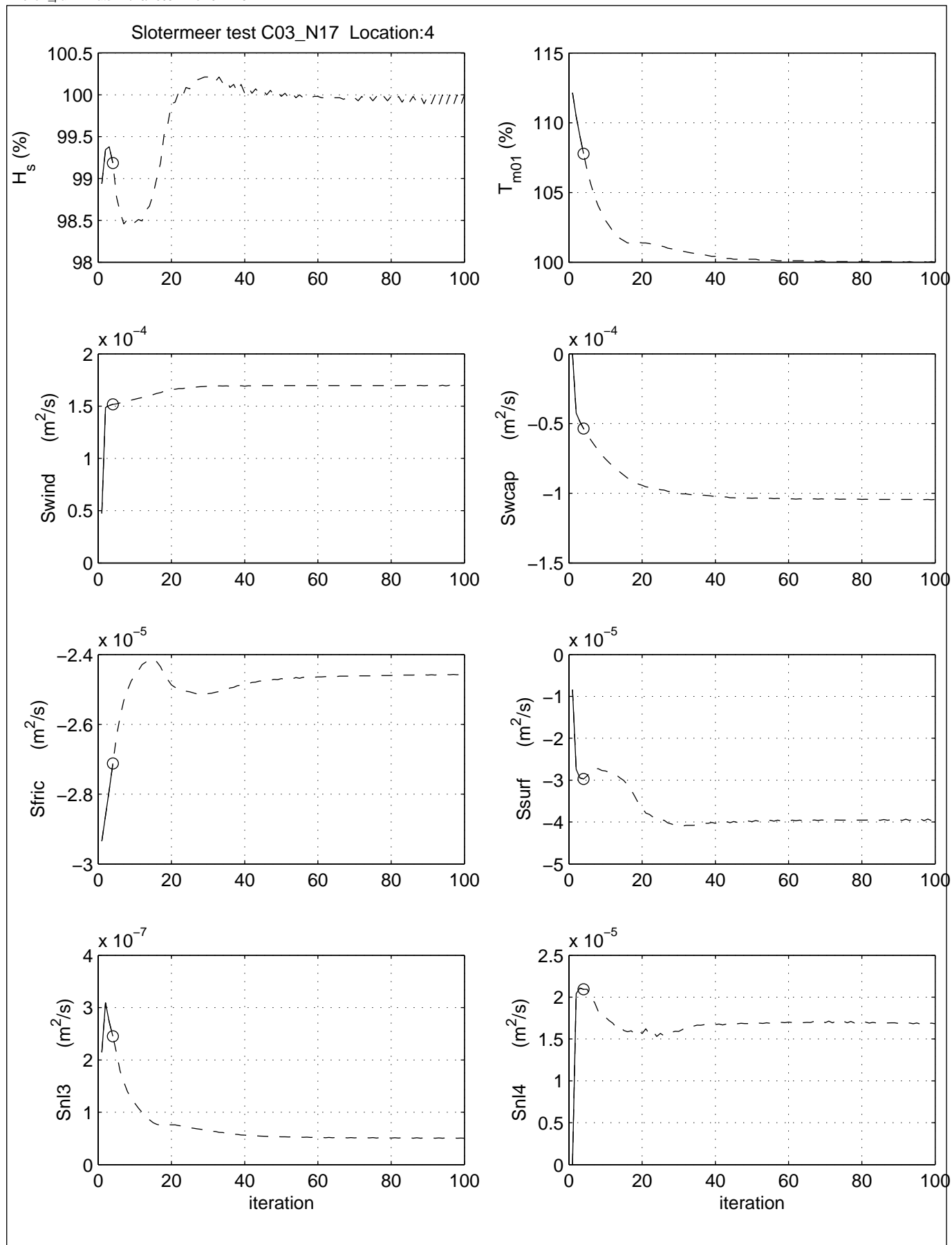
PAR\_SL\_SL\_C03\_N16\_L4

Calibration SWAN 40.20

A1168

 **Alkyon**

Fig. 4.1.16



Iteration behaviour of integral wave parameters

Base case, inclusive triads and quadruplets,  $Qb=1.0$  (dashed line)

Convergence criterion 0.02% &amp; 98% (solid line)

Area: SL

Grid: SL

C03\_N17

Loc:4

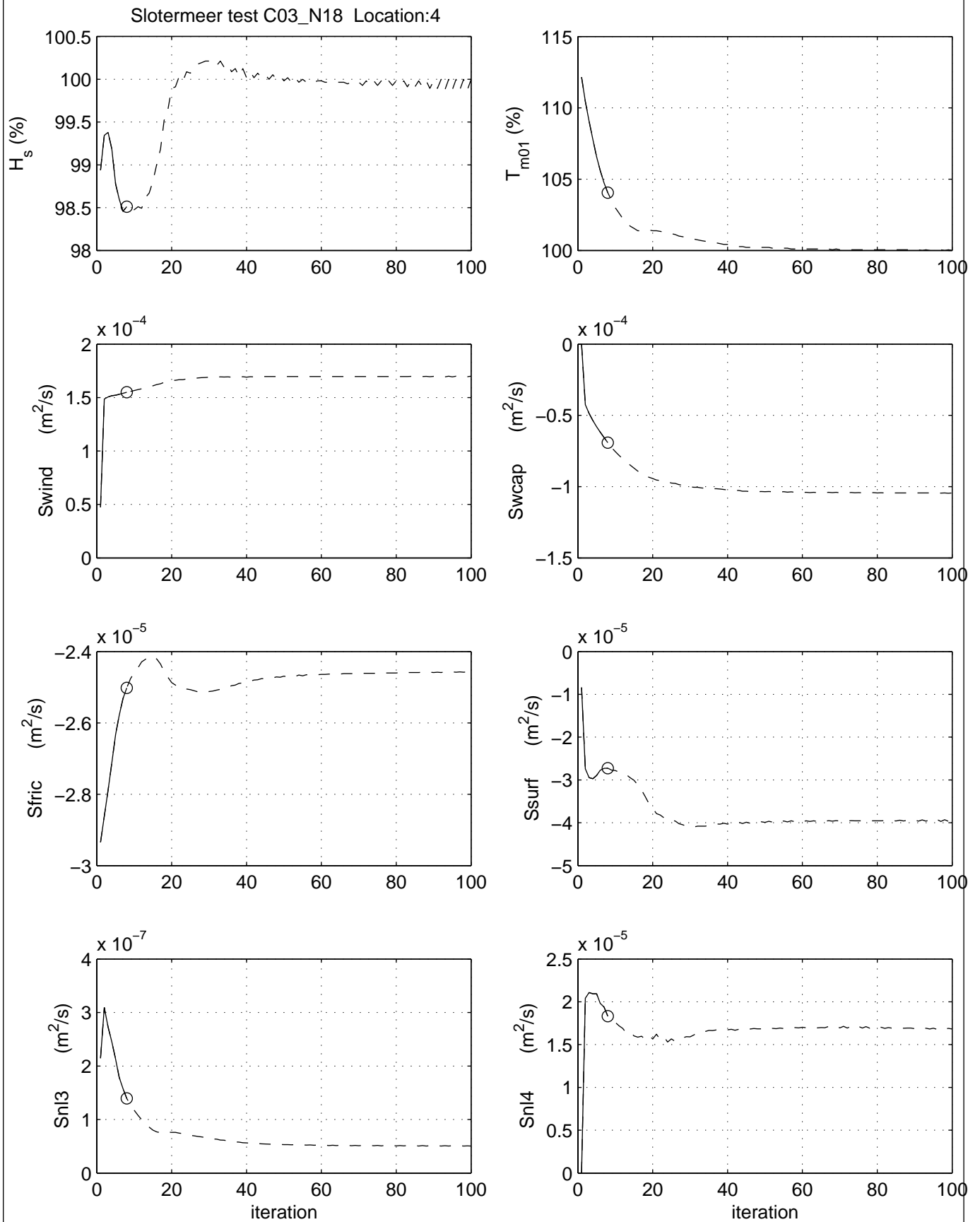
PAR\_SL\_SL\_C03\_N17\_L4

Calibration SWAN 40.20

A1168

 **Alkyon**

Fig. 4.1.17



Iteration behaviour of integral wave parameters  
 Base case, inclusive triads and quadruplets,  $Q_b=1.0$  (dashed line)  
 Convergence criterion 0.01% & 99% (solid line)

Area: SL

Grid: SL

C03\_N18

Loc:4

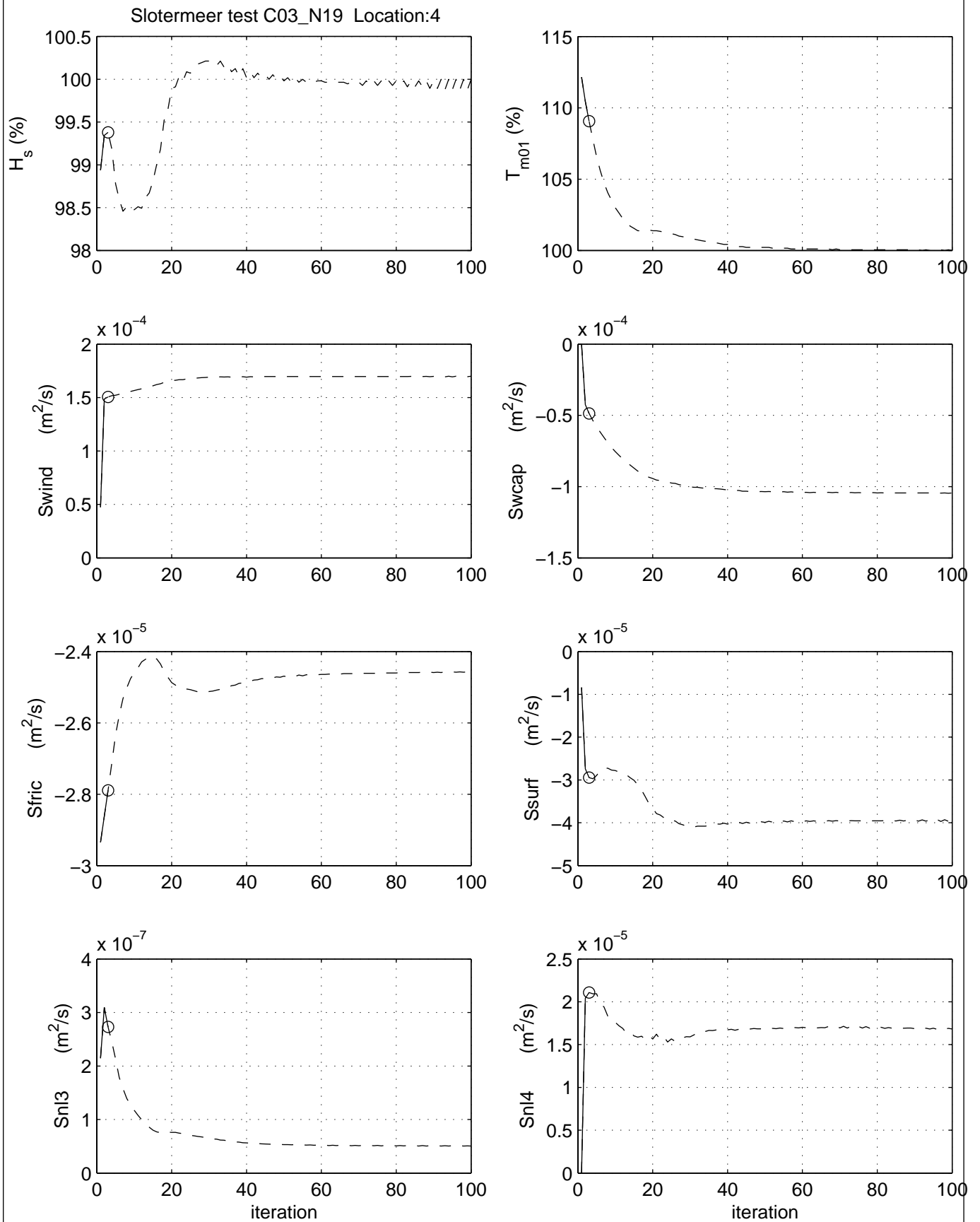
PAR\_SL\_SL\_C03\_N18\_L4

Calibration SWAN 40.20

A1168

 **Alkyon**

Fig. 4.1.18



Iteration behaviour of integral wave parameters  
 Base case, inclusive triads and quadruplets,  $Q_b=1.0$  (dashed line)  
 Convergence criterion 0.03% & 97% (solid line)

Area: SL

Grid: SL

C03\_N19

Loc:4

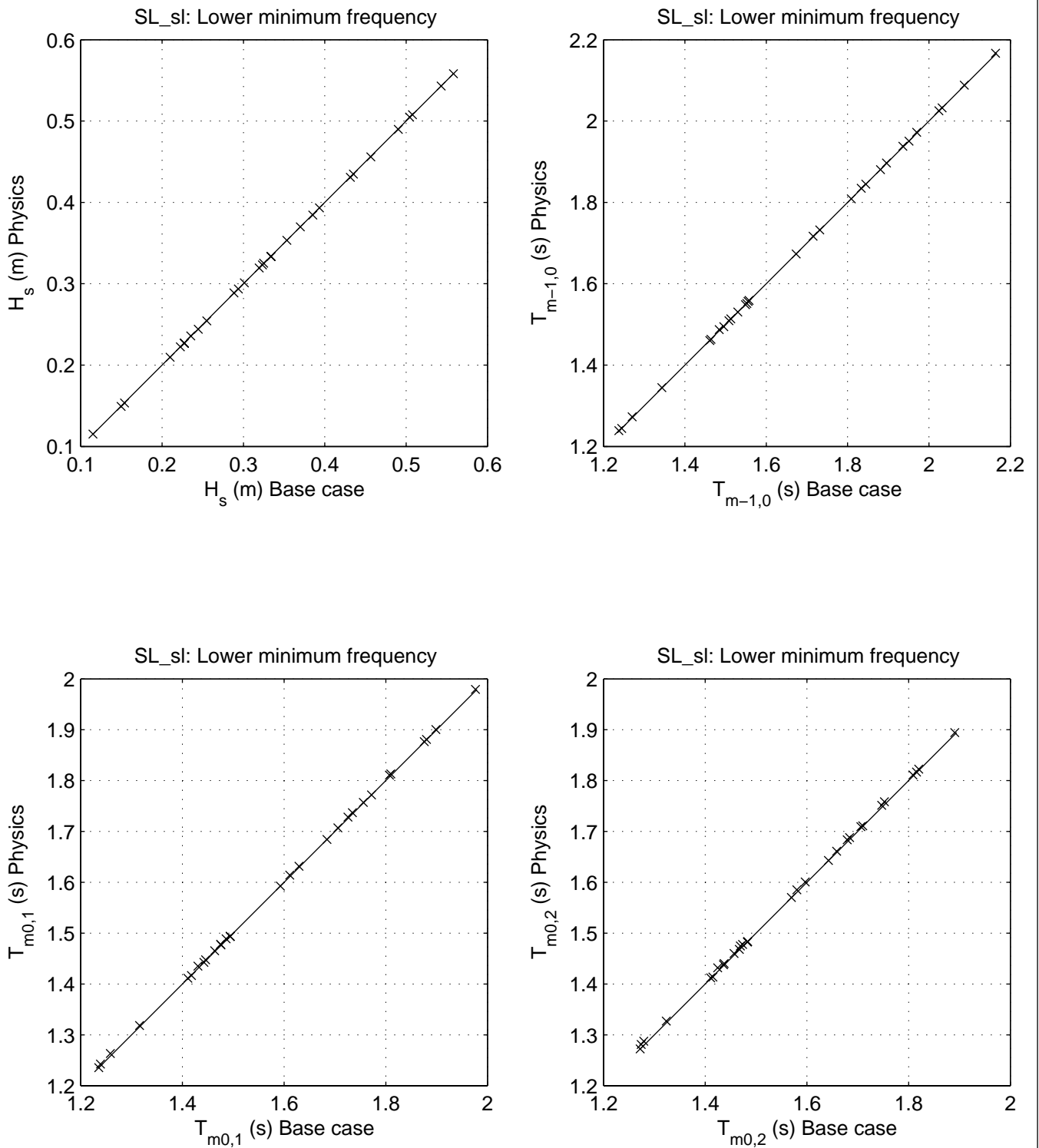
PAR\_SL\_SL\_C03\_N19\_L4

Calibration SWAN 40.20

A1168

 **Alkyon**

Fig. 4.1.19



Sensitivity of SWAN 40.20 to variation in numerical parameters  
Comparison of base case against:  
Lower minimum frequency

Area:SL

Grid:SL

N02

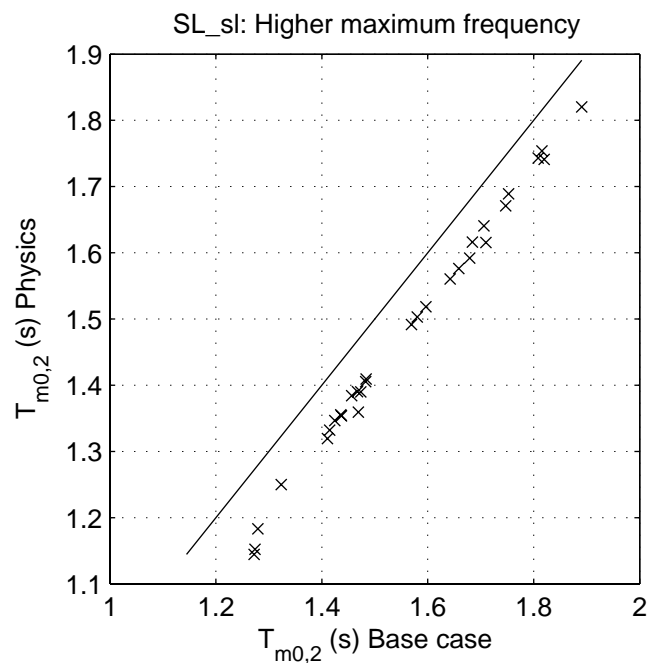
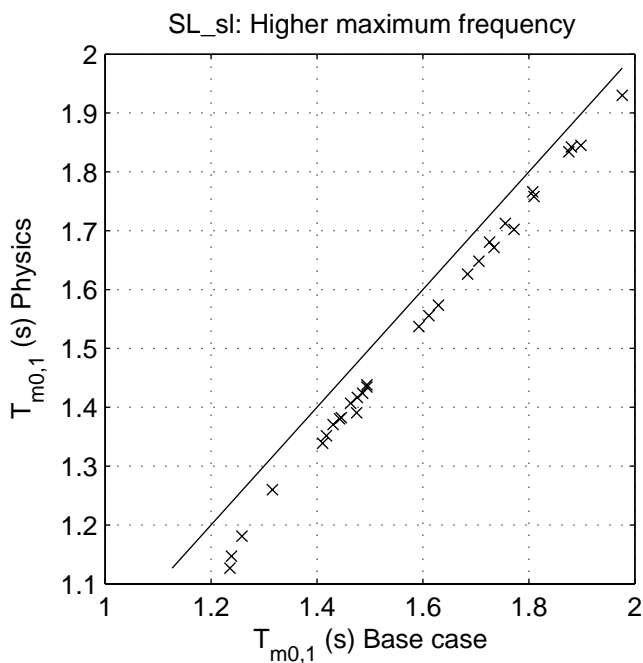
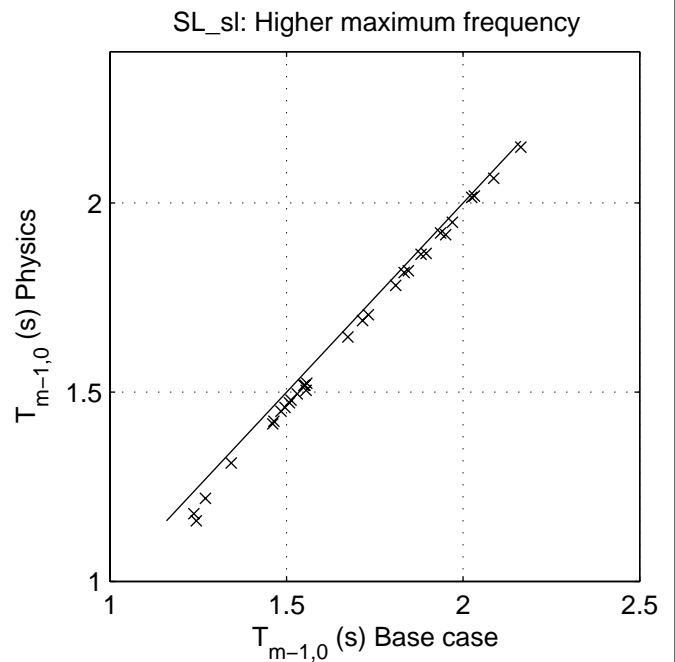
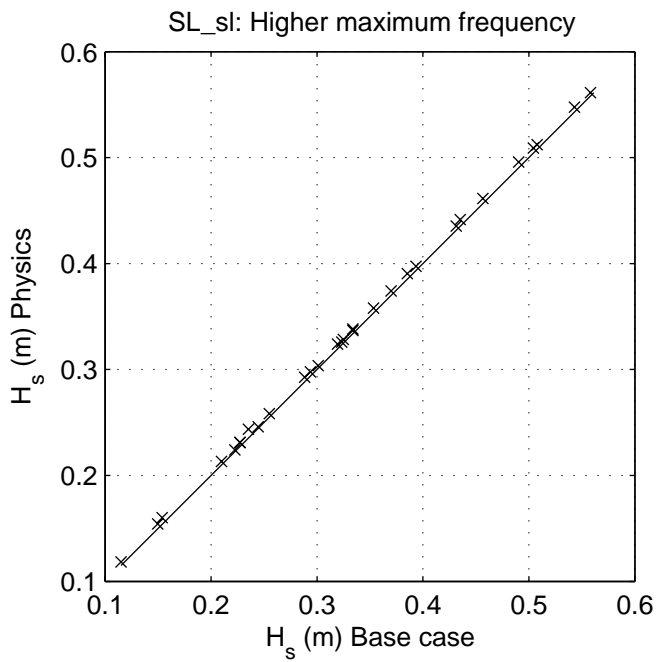
SCAT\_SL\_SL\_N2

Calibration SWAN 40.20

A1168

 **Alkyon**

Fig. 4.2.2



Sensitivity of SWAN 40.20 to variation in numerical parameters  
Comparison of base case against:  
Higher maximum frequency

Area:SL

Grid:SL

N03

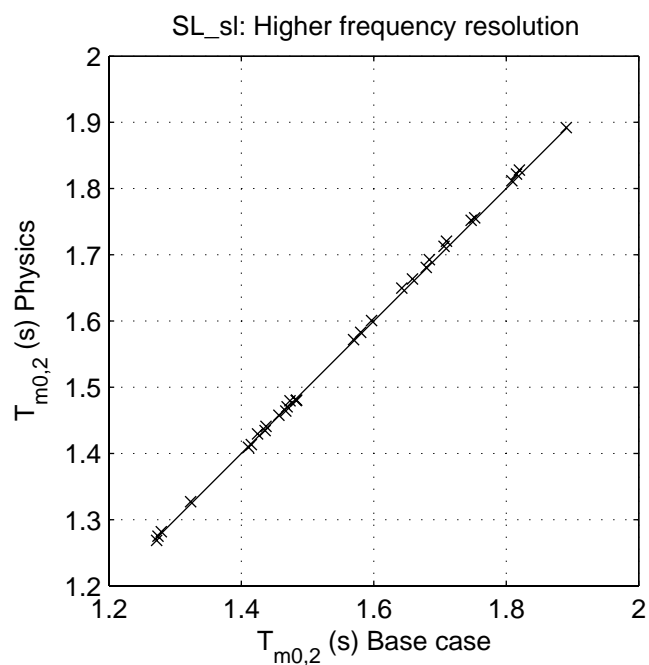
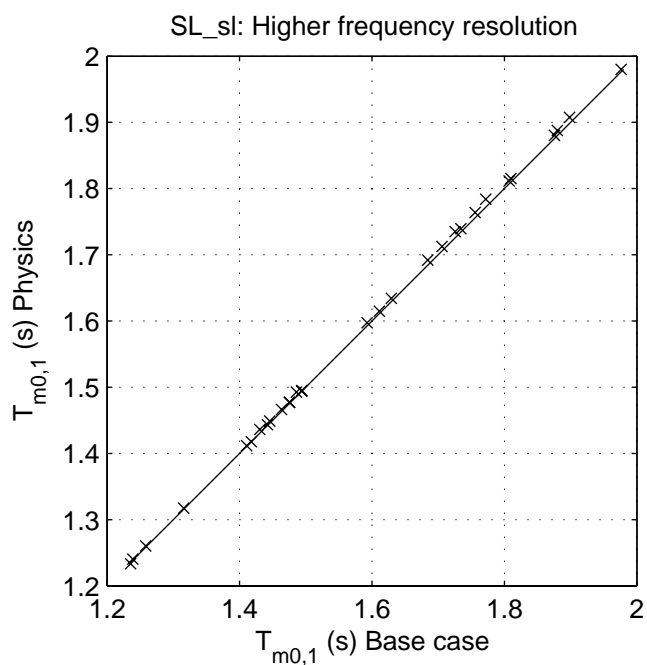
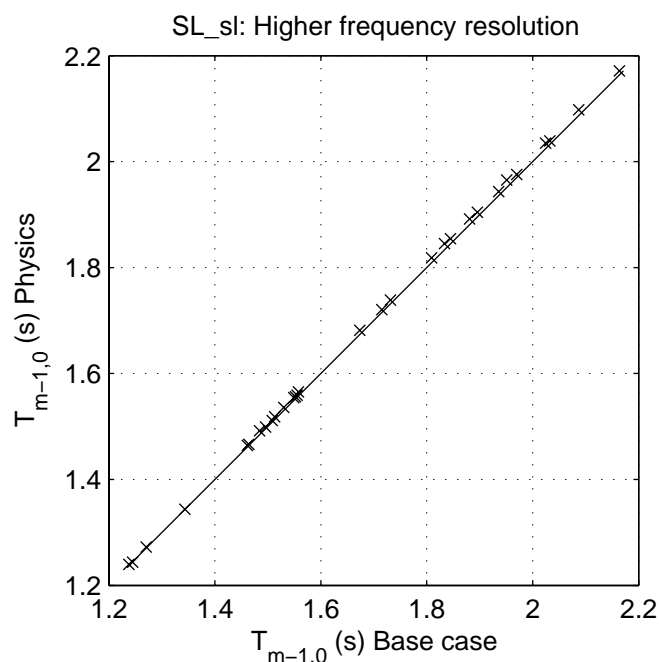
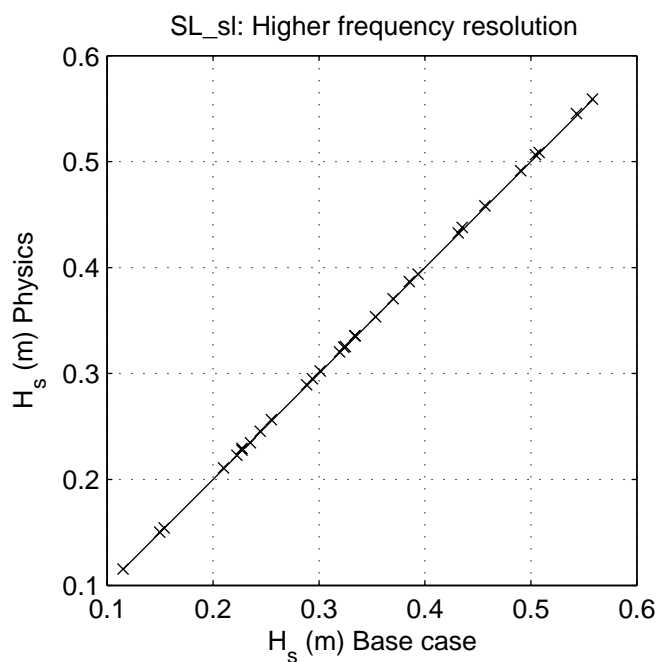
SCAT\_SL\_SL\_N3

Calibration SWAN 40.20

A1168

 **Alkyon**

Fig. 4.2.3



Sensitivity of SWAN 40.20 to variation in numerical parameters  
Comparison of base case against:  
Higher frequency resolution

Area:SL

Grid:SL

N04

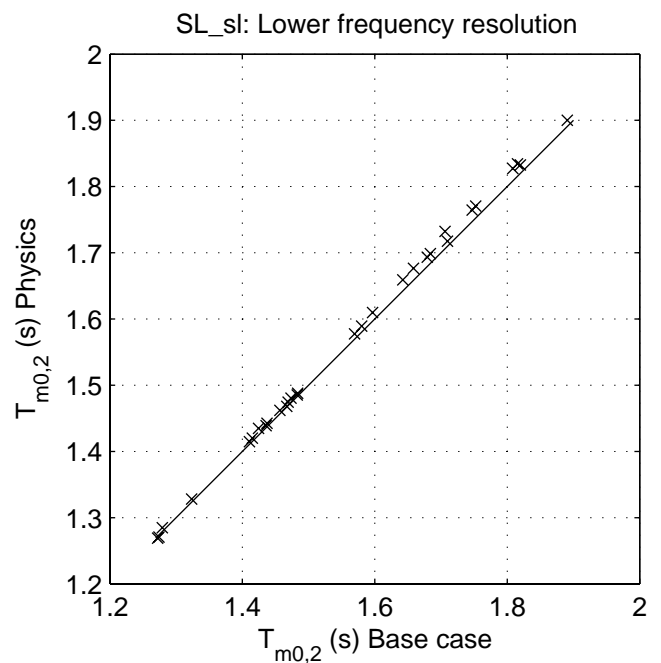
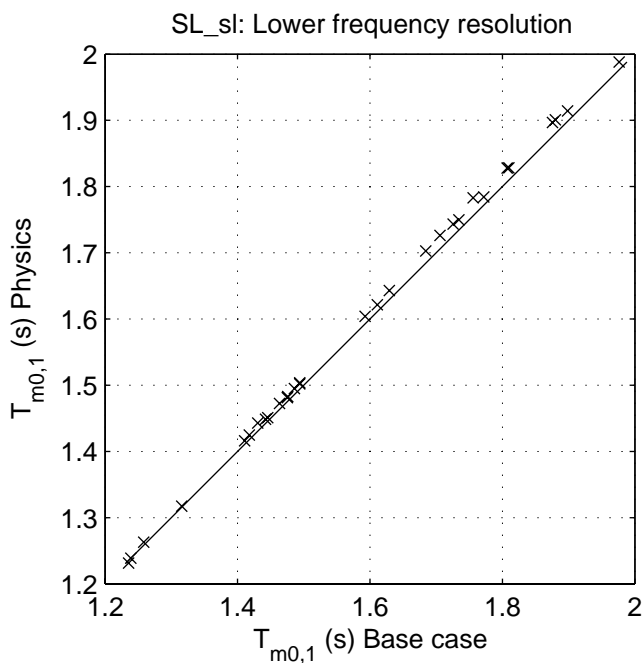
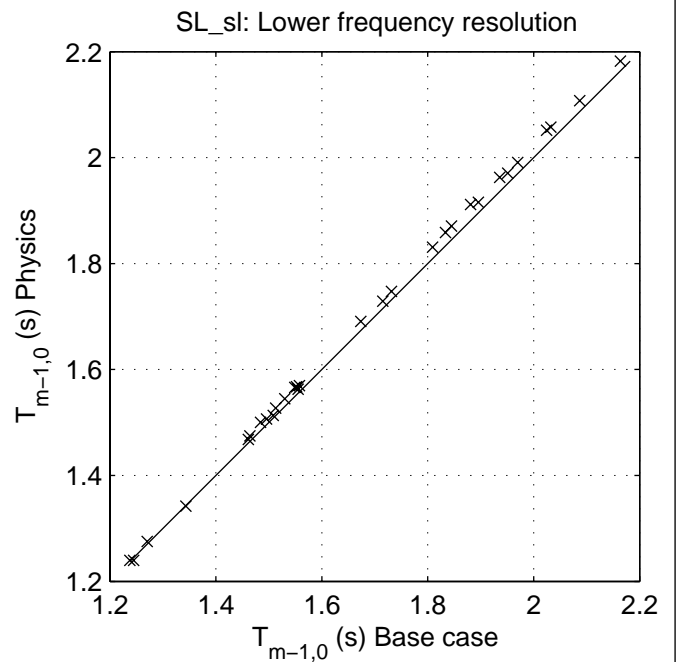
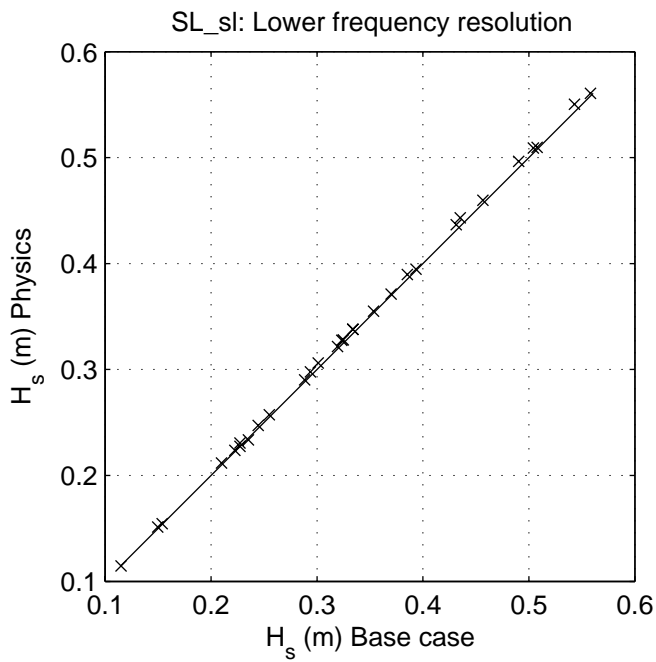
SCAT\_SL\_SL\_N4

Calibration SWAN 40.20

A1168

 **Alkyon**

Fig. 4.2.4



Sensitivity of SWAN 40.20 to variation in numerical parameters  
Comparison of base case against:  
Lower frequency resolution

Area:SL

Grid:SL

N05

SCAT\_SL\_SL\_N5

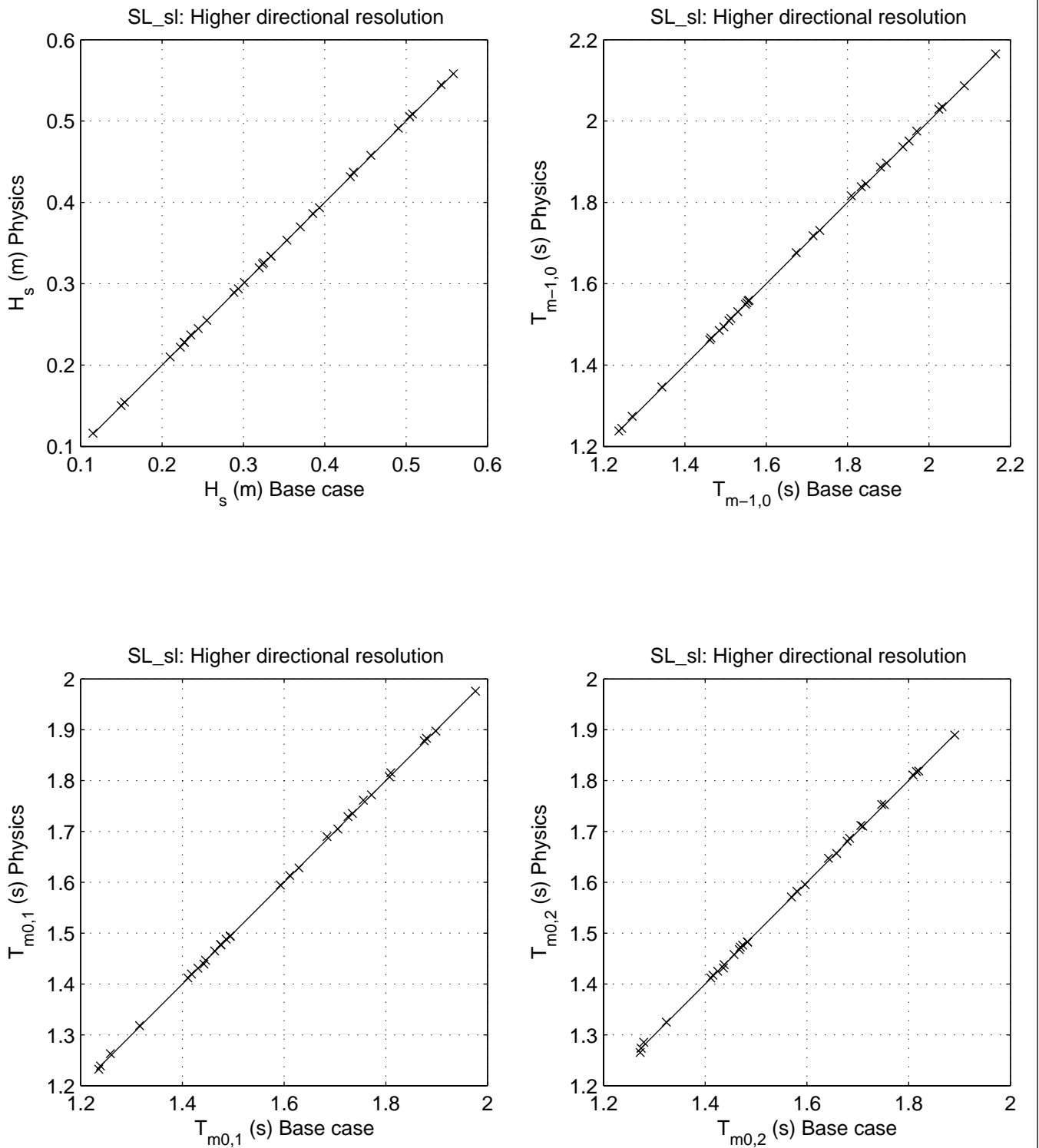
Calibration SWAN 40.20

A1168

 **Alkyon**

Fig. 4.2.5





Sensitivity of SWAN 40.20 to variation in numerical parameters  
Comparison of base case against:  
Higher directional resolution

Area:SL

Grid:SL

N06

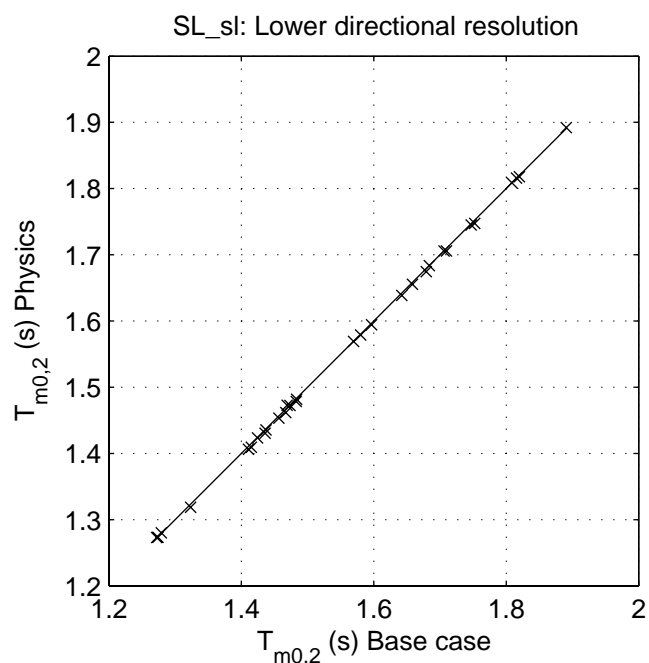
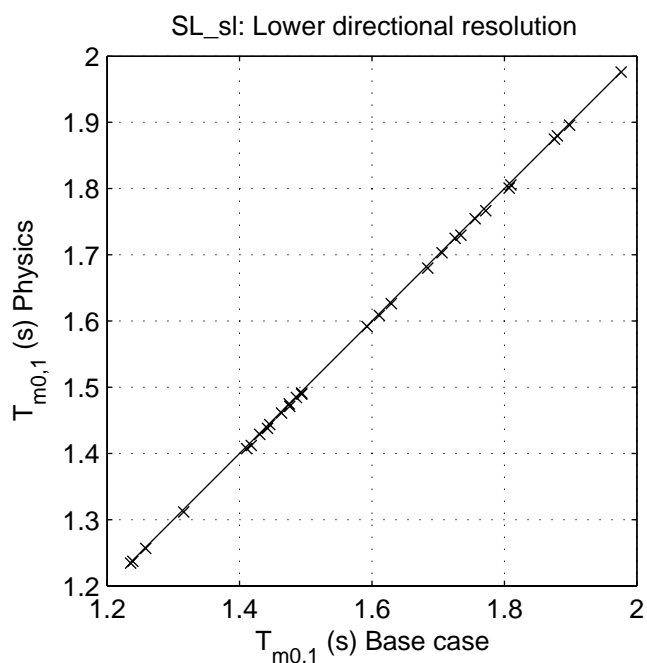
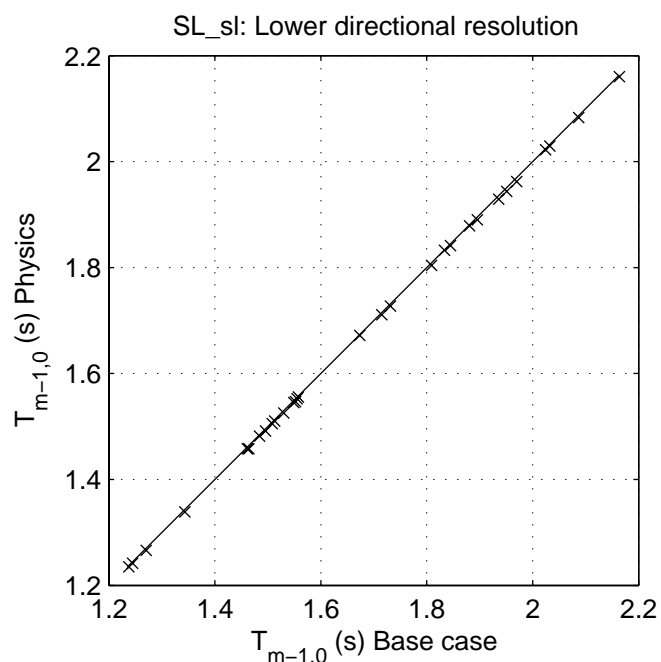
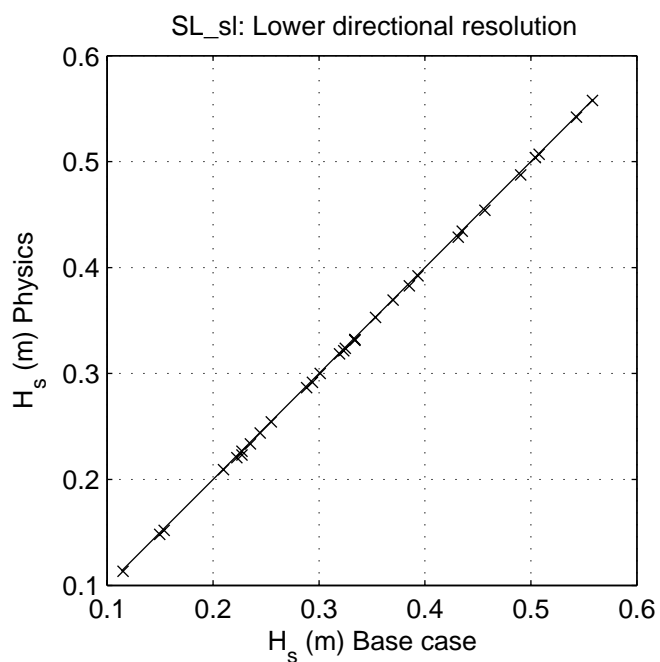
SCAT\_SL\_SL\_N6

Calibration SWAN 40.20

A1168

 **Alkyon**

Fig. 4.2.6



Sensitivity of SWAN 40.20 to variation in numerical parameters  
Comparison of base case against:  
Lower directional resolution

Area:SL

Grid:SL

N07

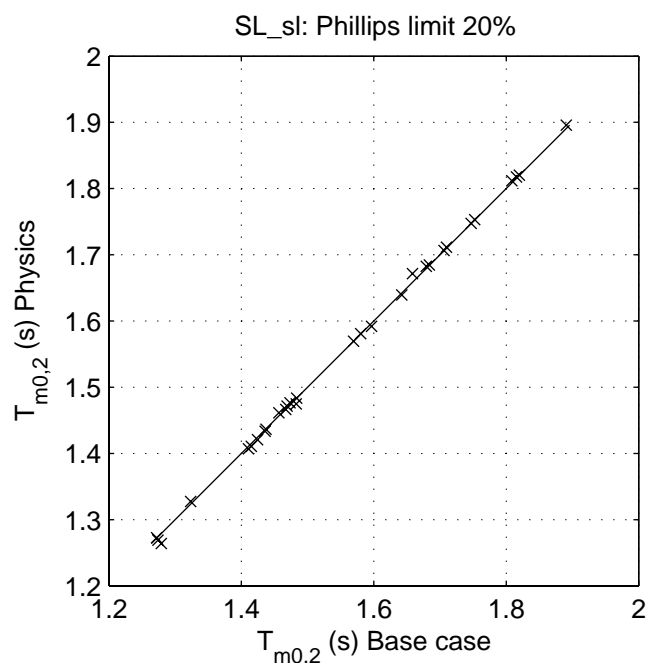
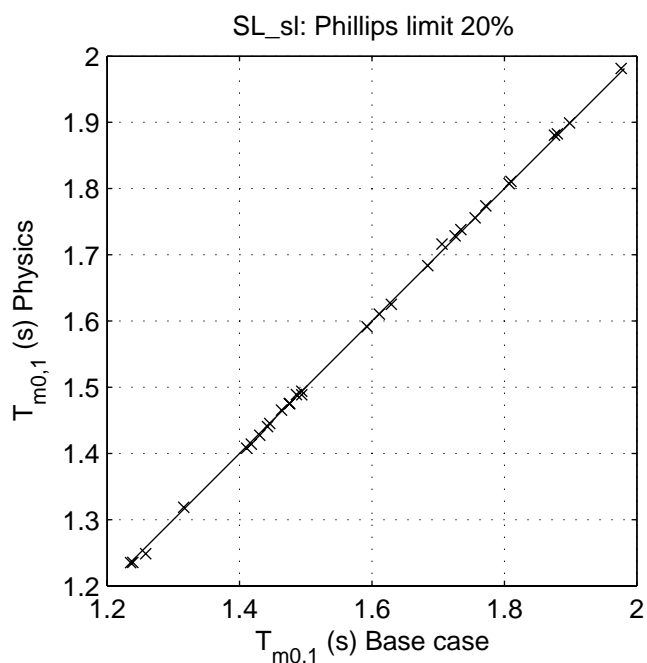
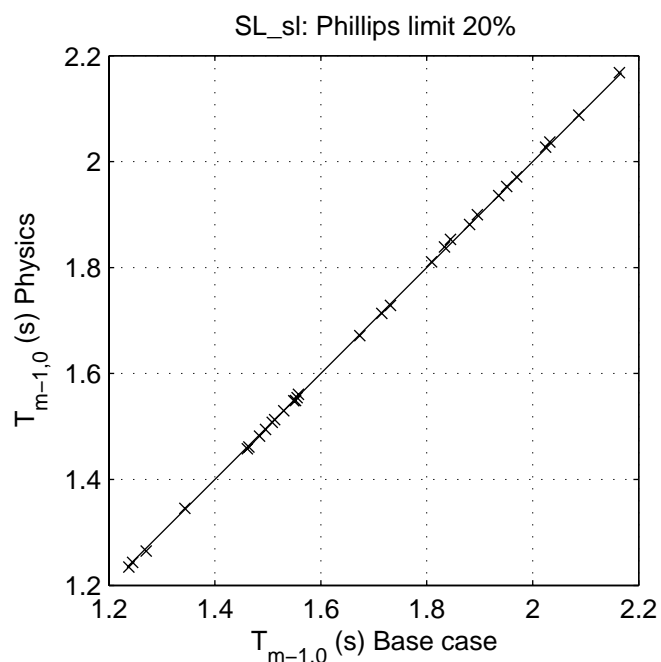
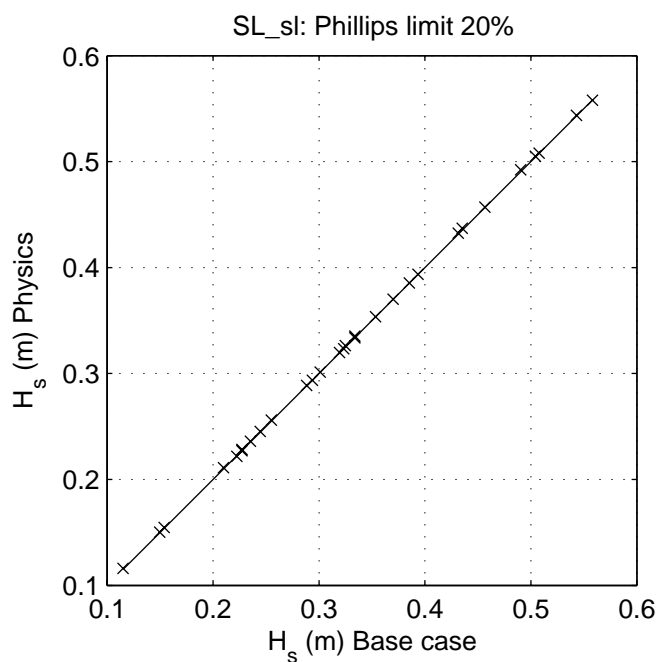
SCAT\_SL\_SL\_N7

Calibration SWAN 40.20

A1168

 **Alkyon**

Fig. 4.2.7



Sensitivity of SWAN 40.20 to variation in numerical parameters  
Comparison of base case against:  
Phillips limit 20%

Area:SL

Grid:SL

N08

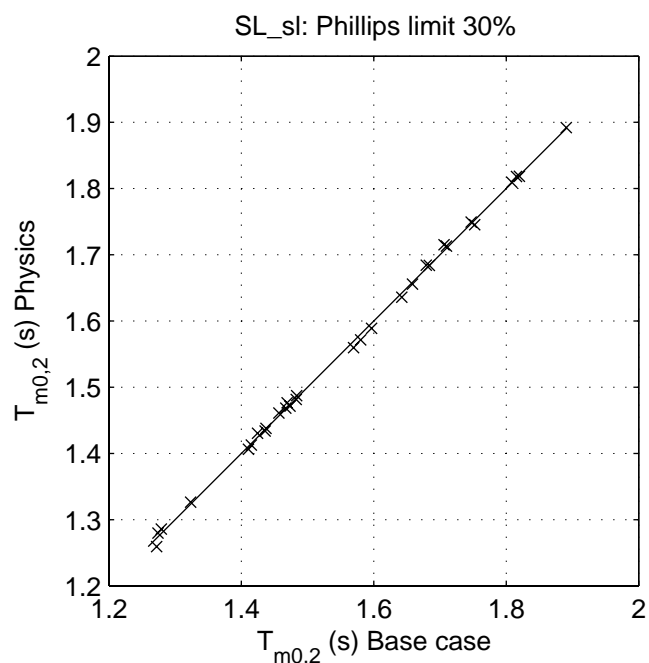
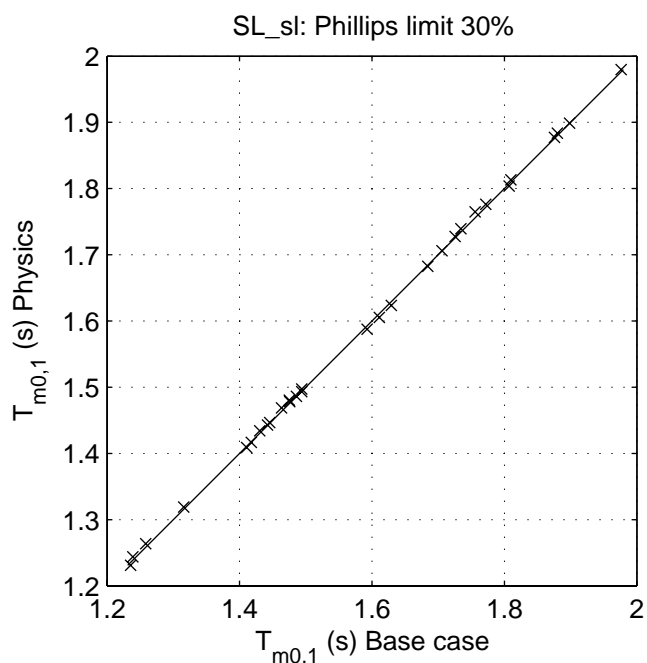
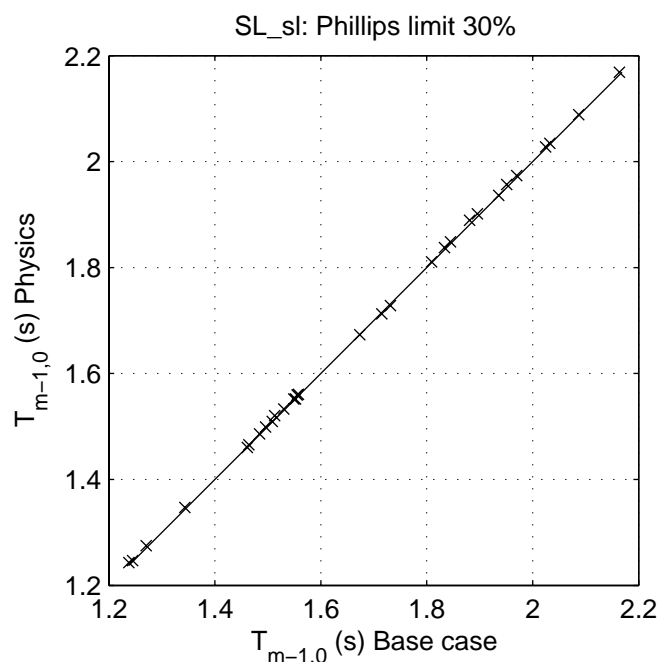
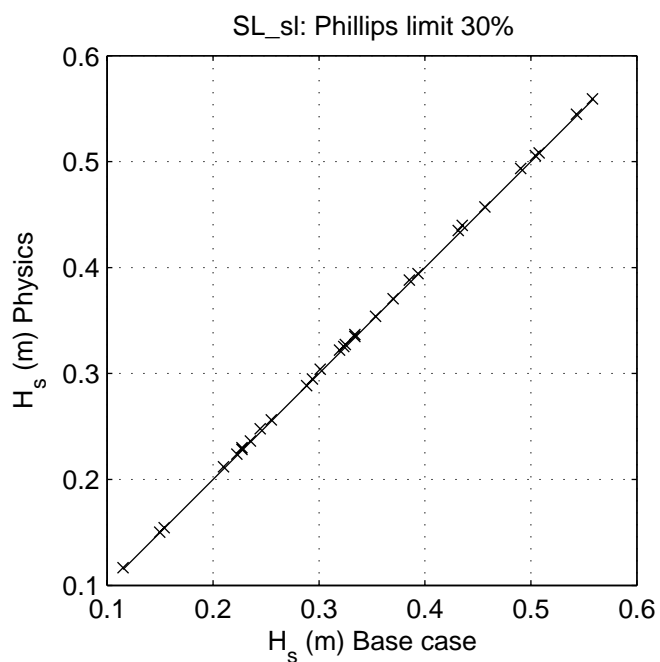
SCAT\_SL\_SL\_N8

Calibration SWAN 40.20

A1168

 **Alkyon**

Fig. 4.2.8



Sensitivity of SWAN 40.20 to variation in numerical parameters  
Comparison of base case against:  
Phillips limit 30%

Area:SL

Grid:SL

N09

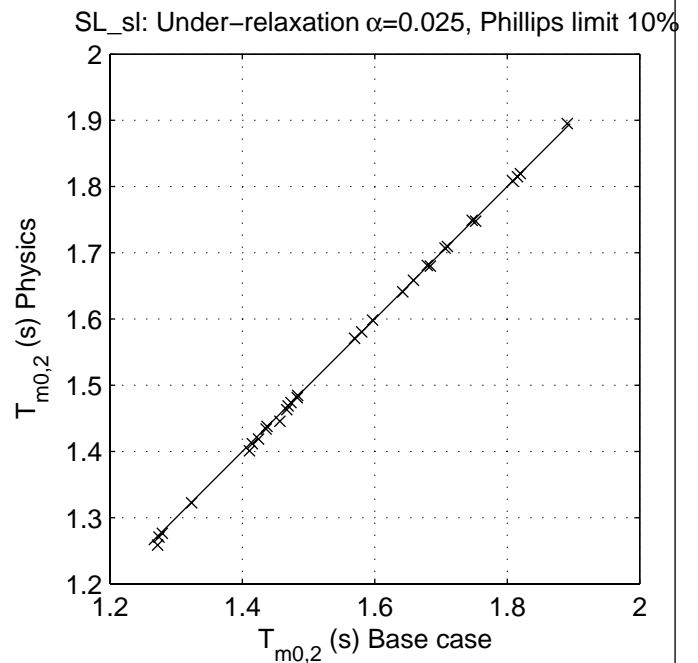
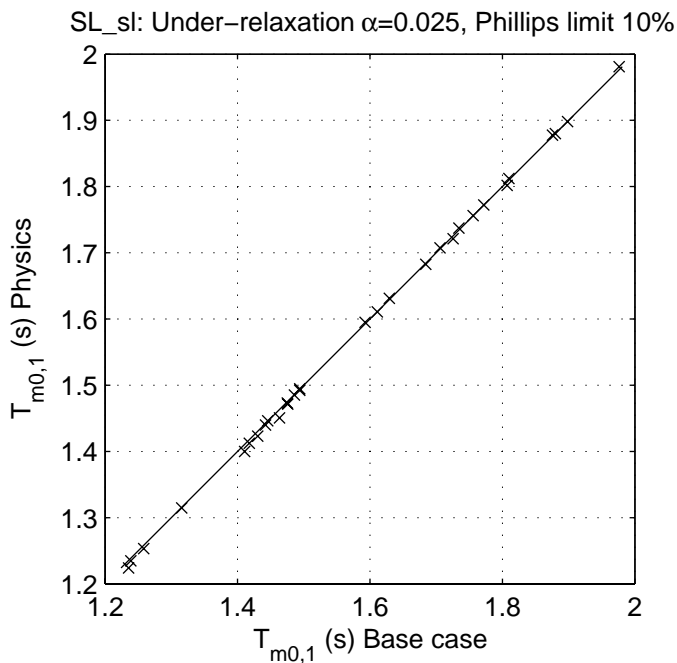
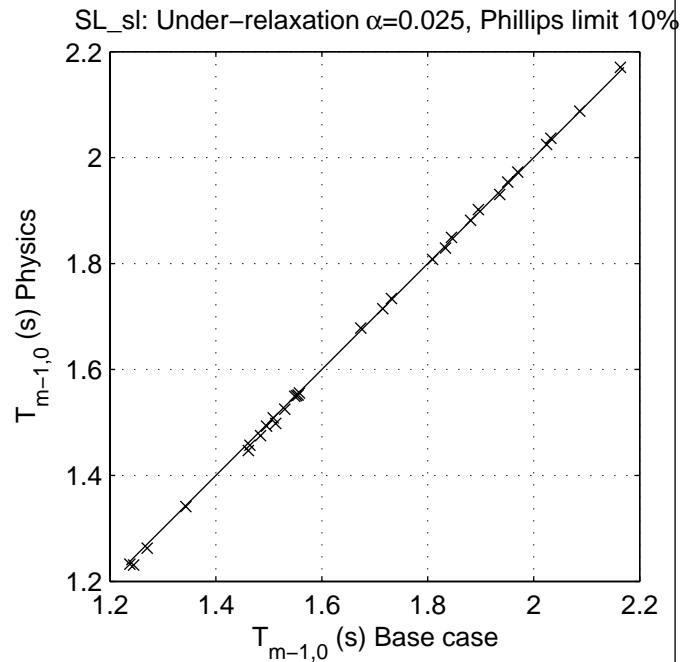
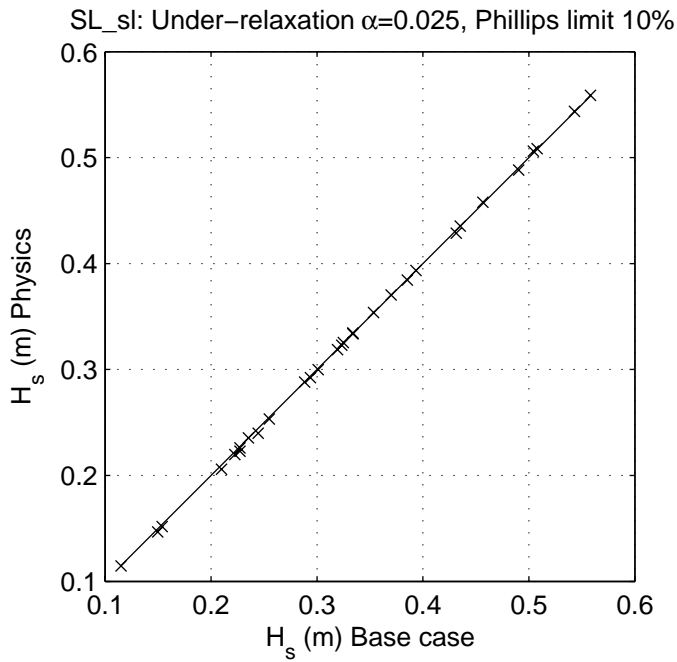
SCAT\_SL\_SL\_N9

Calibration SWAN 40.20

A1168

 **Alkyon**

Fig. 4.2.9



Sensitivity of SWAN 40.20 to variation in numerical parameters  
Comparison of base case against:  
Under-relaxation  $\alpha=0.025$ , Phillips limit 10%

Area:SL

Grid:SL

N10

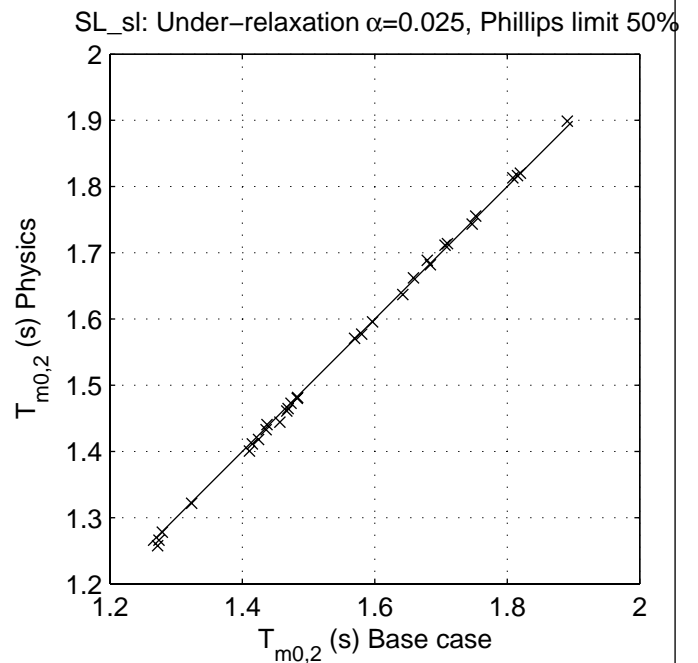
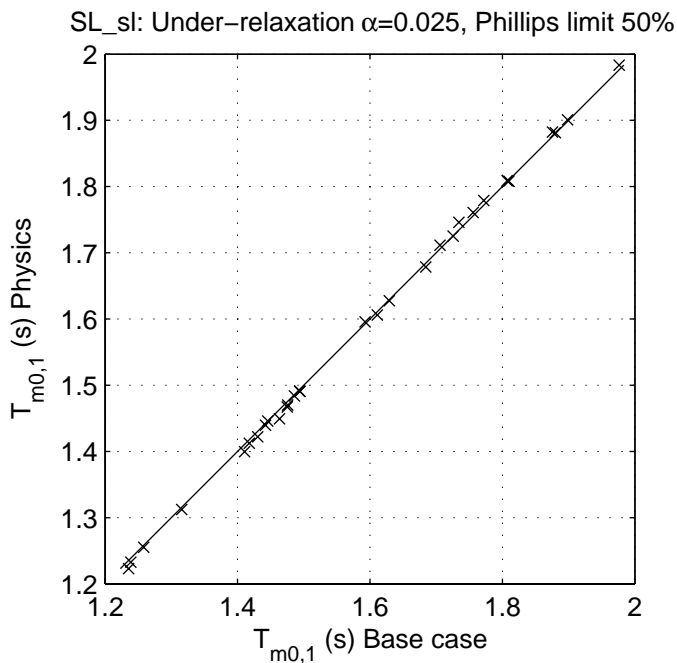
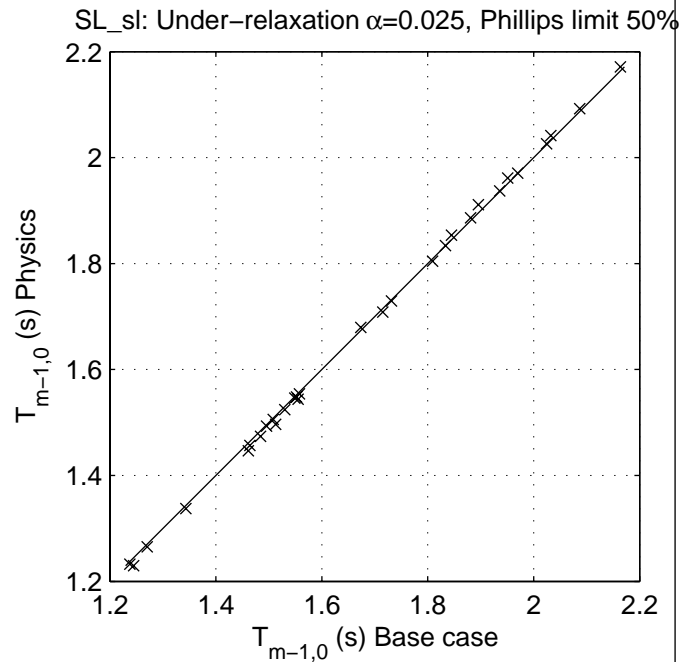
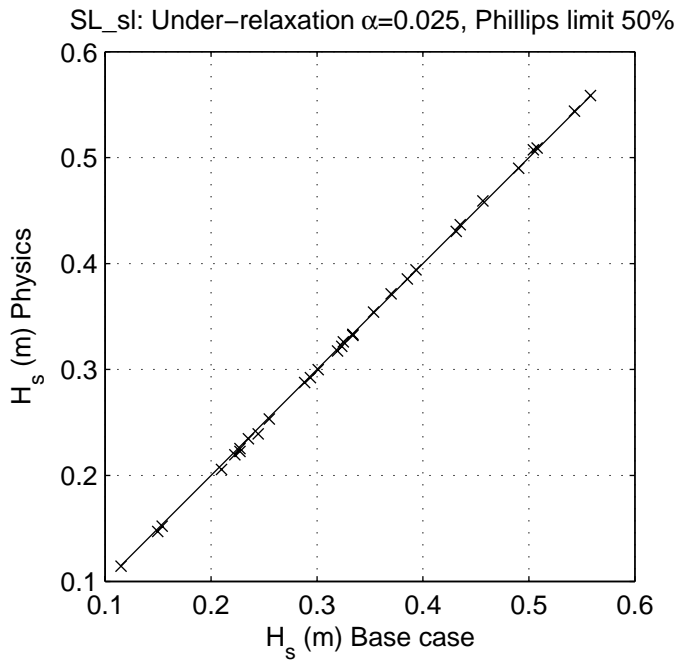
SCAT\_SL\_SL\_N10

Calibration SWAN 40.20

A1168

 **Alkyon**

Fig. 4.2.10



Sensitivity of SWAN 40.20 to variation in numerical parameters  
Comparison of base case against:  
Under-relaxation  $\alpha=0.025$ , Phillips limit 50%

Area:SL

Grid:SL

N11

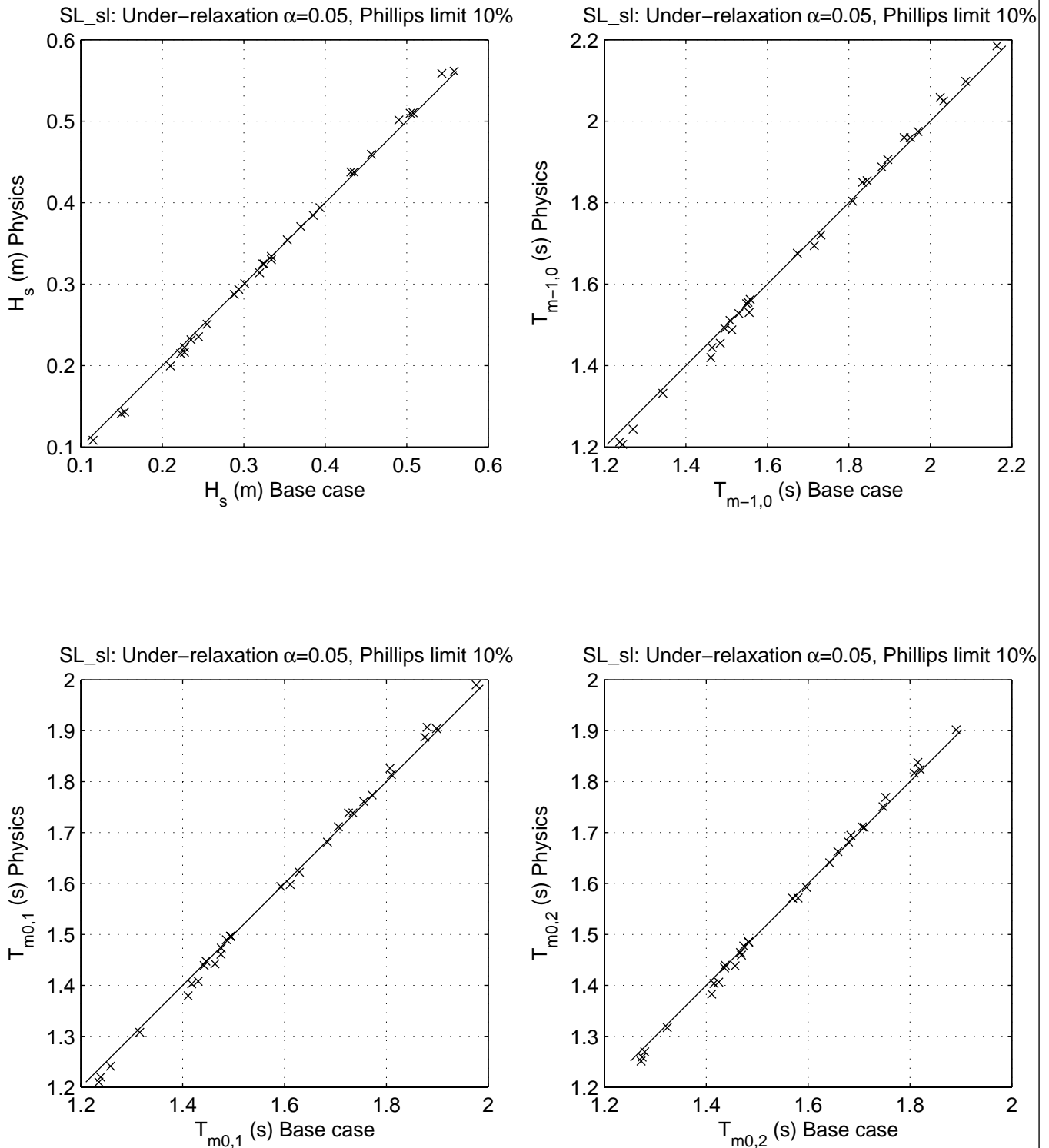
SCAT\_SL\_SL\_N11

Calibration SWAN 40.20

A1168

 **Alkyon**

Fig. 4.2.11



Sensitivity of SWAN 40.20 to variation in numerical parameters  
Comparison of base case against:  
Under-relaxation  $\alpha=0.05$ , Phillips limit 10%

Area:SL

Grid:SL

N12

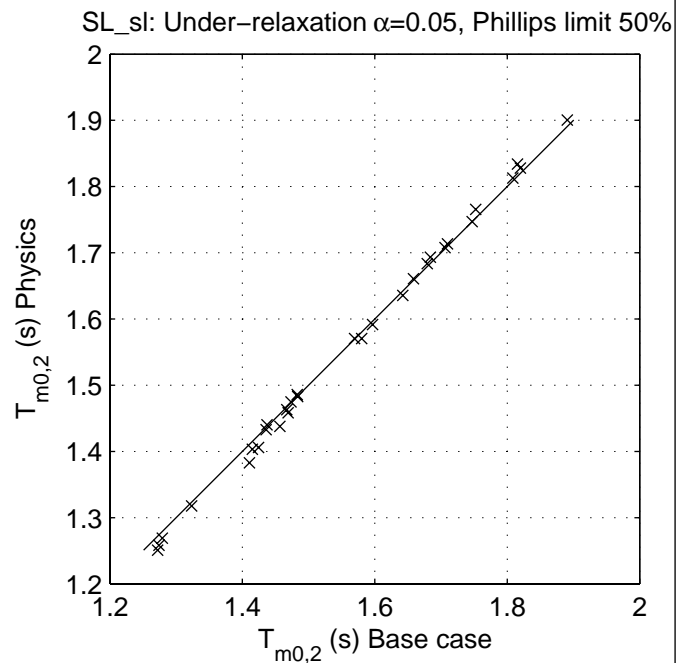
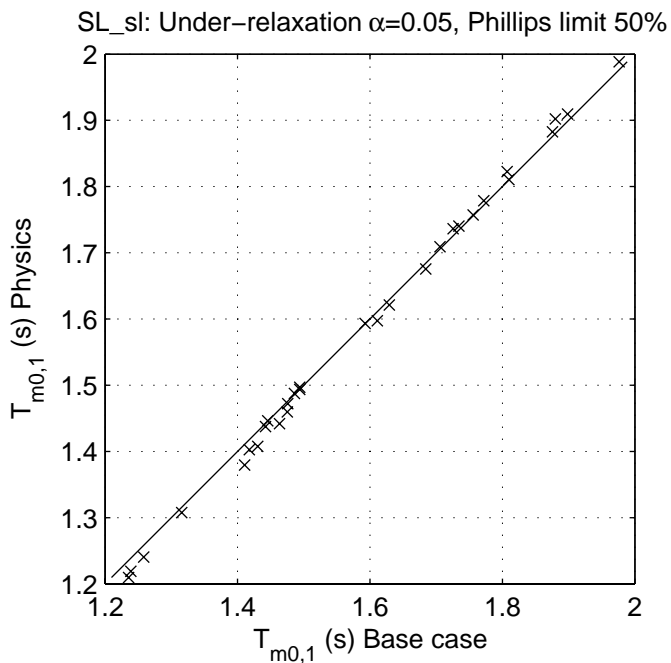
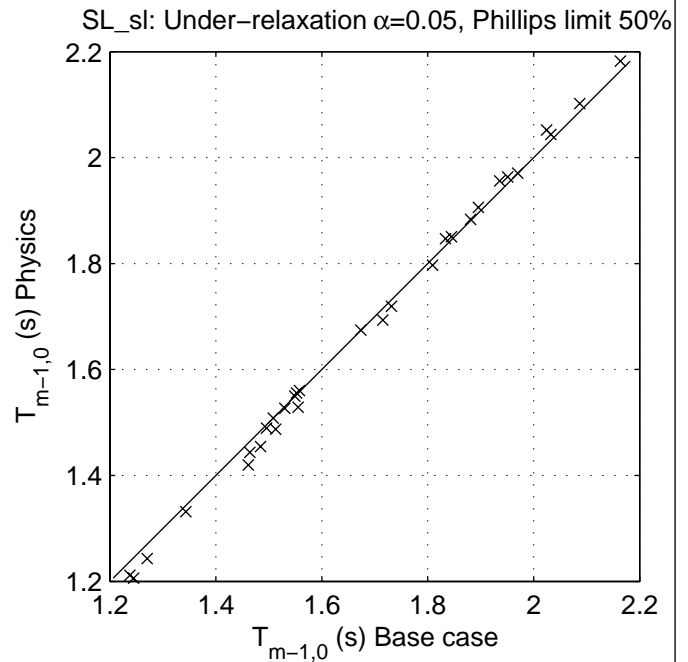
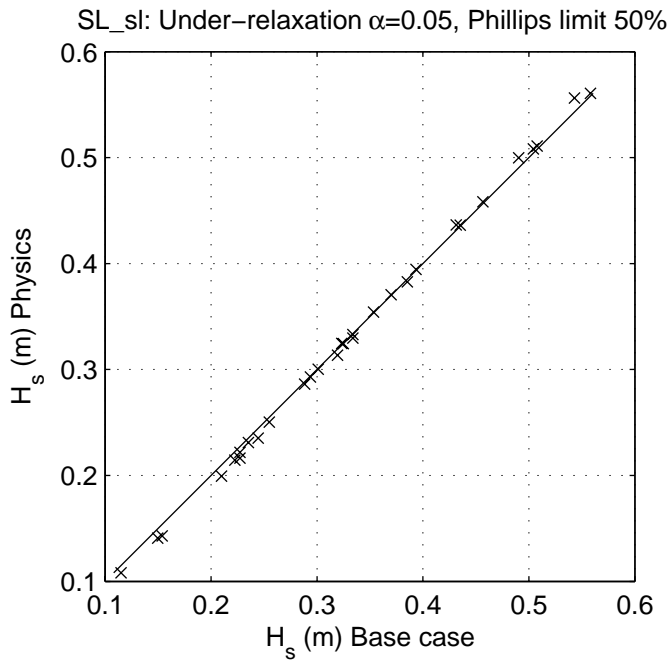
SCAT\_SL\_SL\_N12

Calibration SWAN 40.20

A1168

 **Alkyon**

Fig. 4.2.12



Sensitivity of SWAN 40.20 to variation in numerical parameters  
Comparison of base case against:  
Under-relaxation  $\alpha=0.05$ , Phillips limit 50%

Area:SL

Grid:SL

N13

SCAT\_SL\_SL\_N13

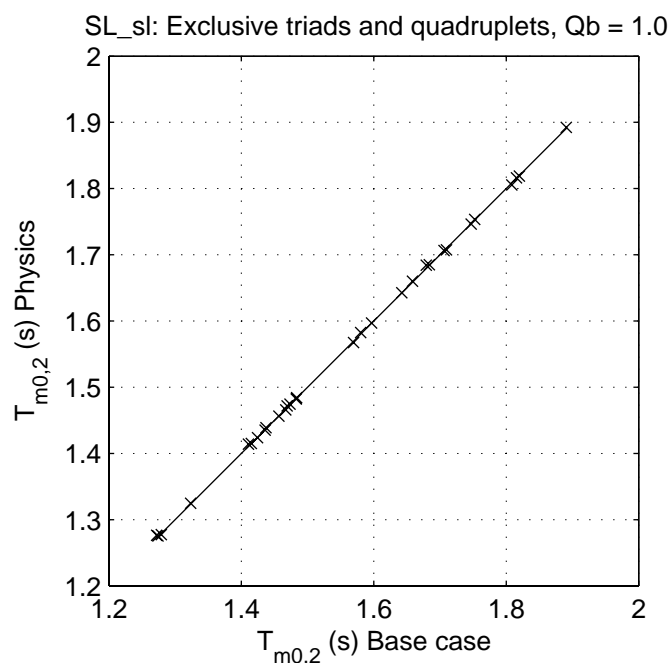
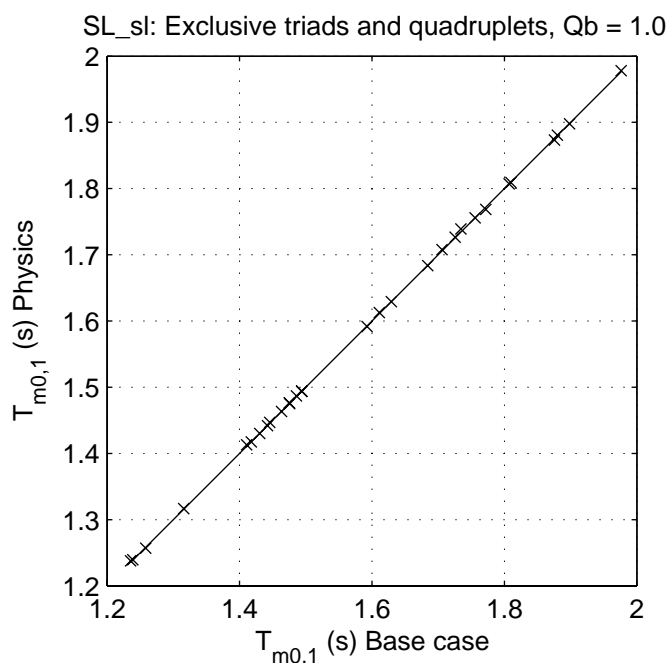
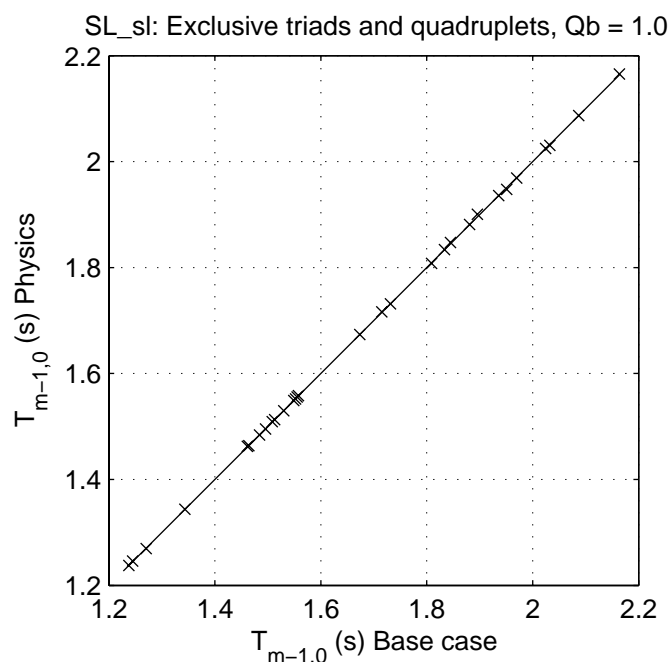
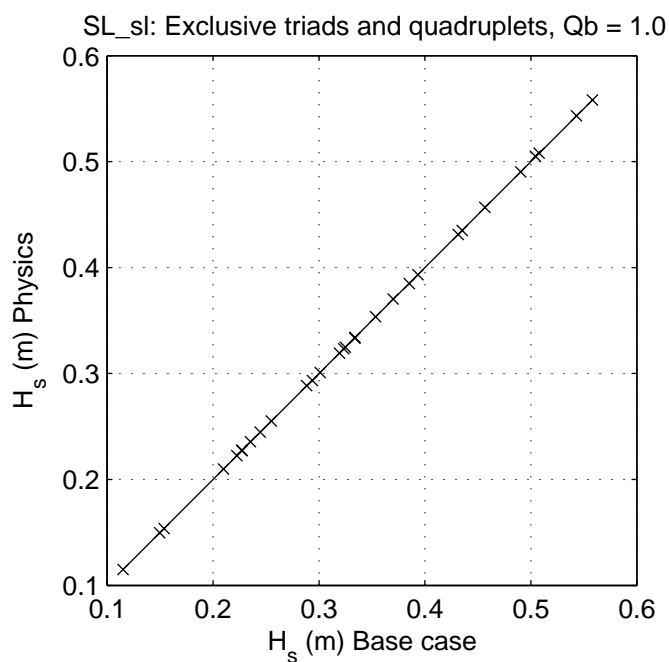
Calibration SWAN 40.20

A1168

 **Alkyon**

Fig. 4.2.13





Sensitivity of SWAN 40.20 to variation in numerical parameters  
Comparison of base case against:  
Exclusive triads and quadruplets, Qb = 1.0

Area:SL

Grid:SL

N14

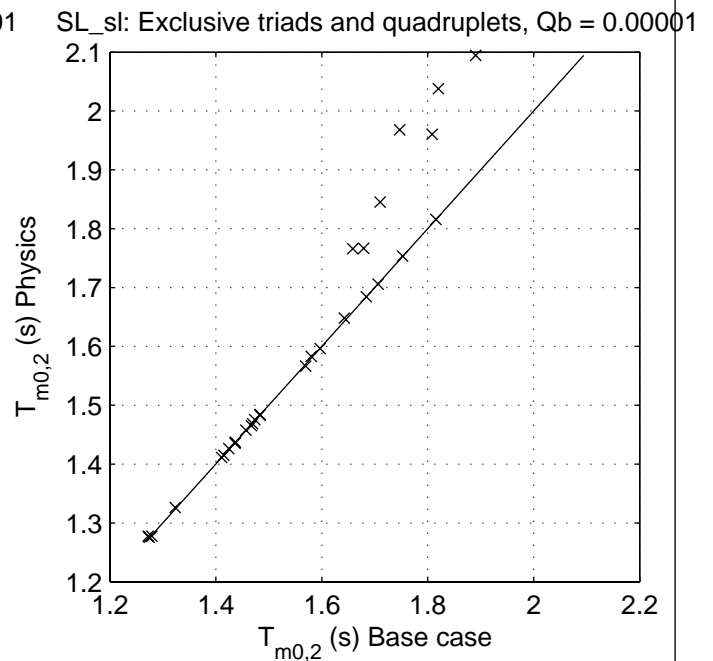
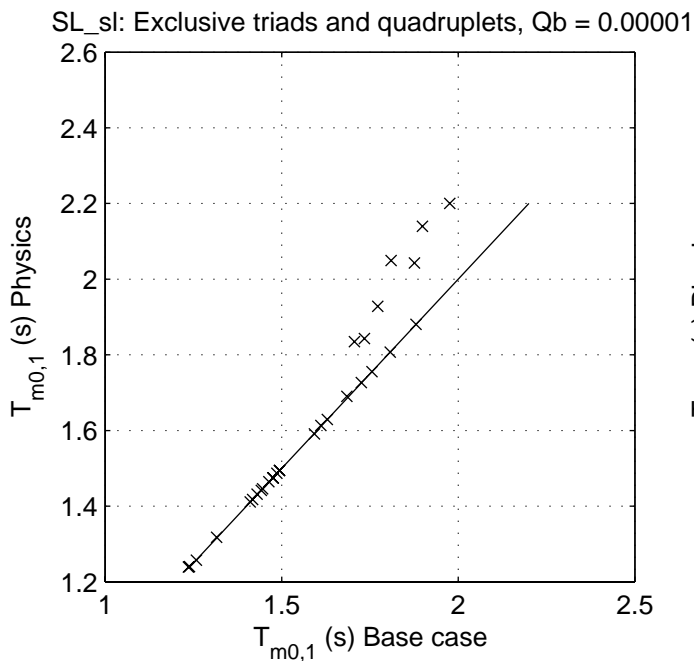
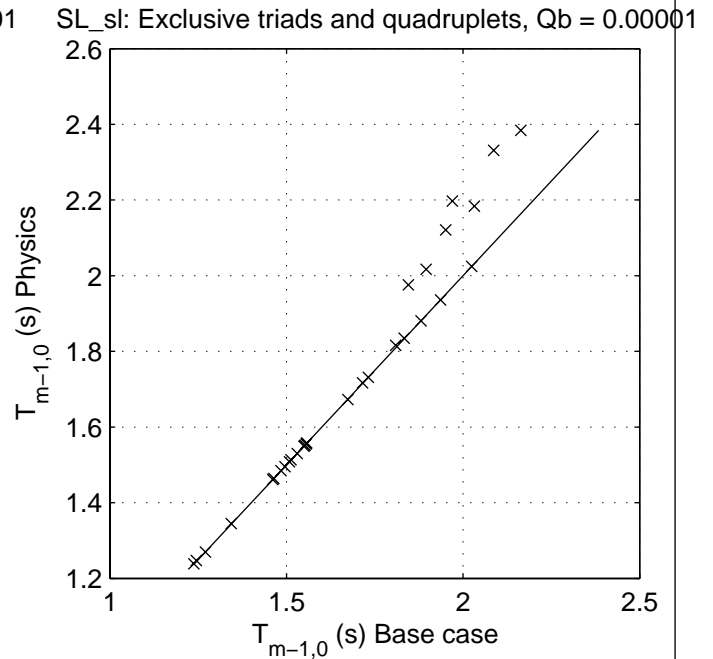
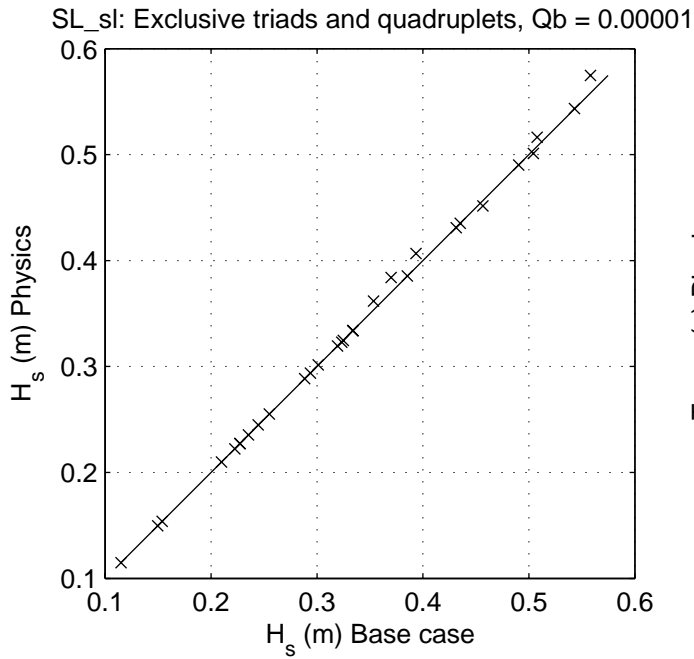
SCAT\_SL\_SL\_N14

Calibration SWAN 40.20

A1168

 **Alkyon**

Fig. 4.2.14



Sensitivity of SWAN 40.20 to variation in numerical parameters  
Comparison of base case against:  
Exclusive triads and quadruplets, Qb = 0.00001

Area:SL

Grid:SL

N15

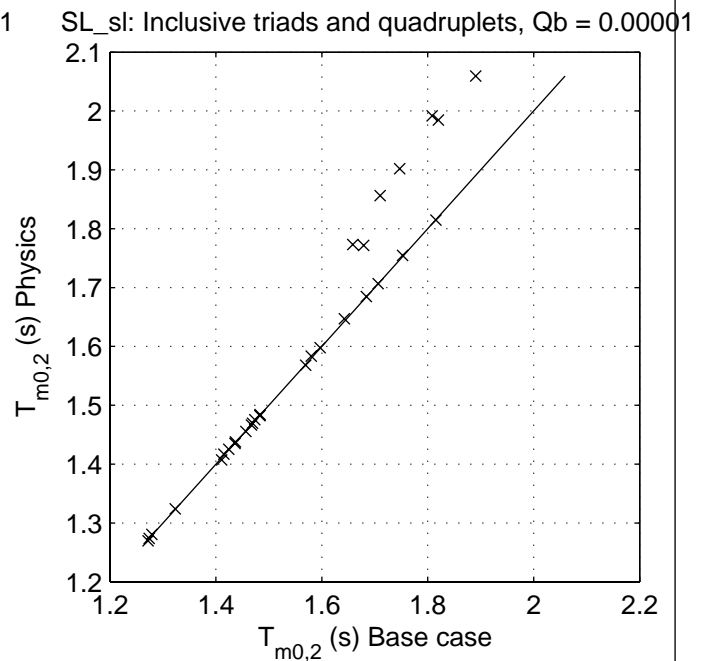
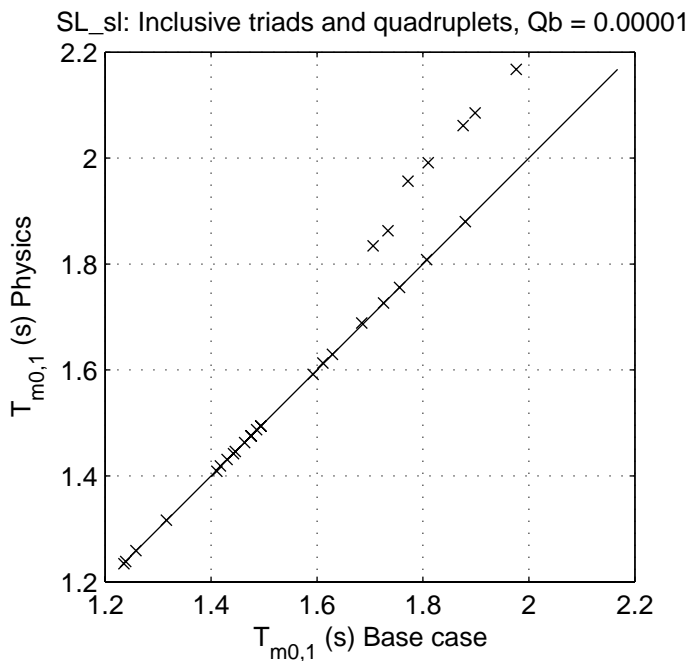
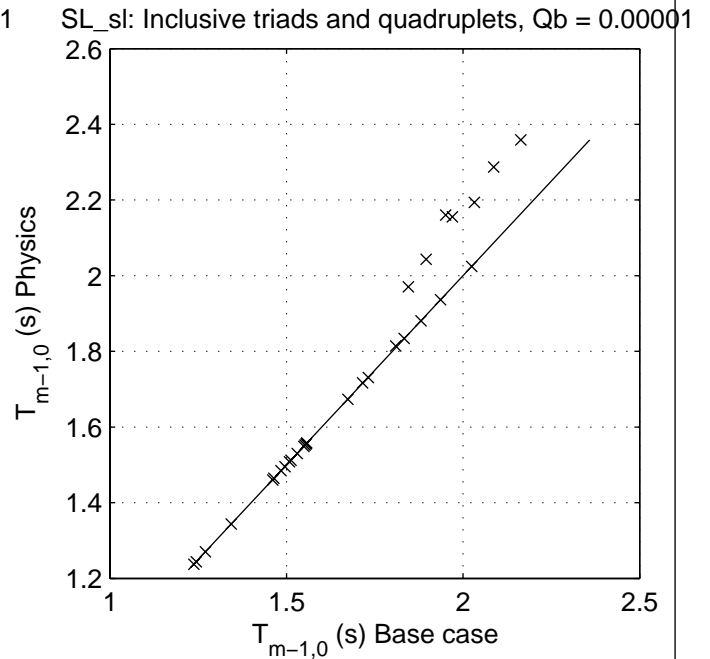
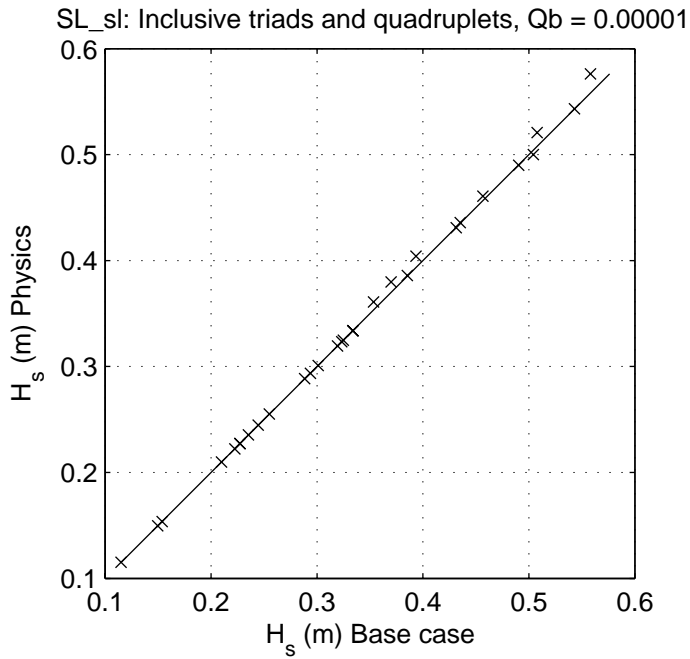
SCAT\_SL\_SL\_N15

Calibration SWAN 40.20

A1168

 **Alkyon**

Fig. 4.2.15



Sensitivity of SWAN 40.20 to variation in numerical parameters  
Comparison of base case against:  
Inclusive triads and quadruplets, Qb = 0.00001

Area:SL

Grid:SL

N16

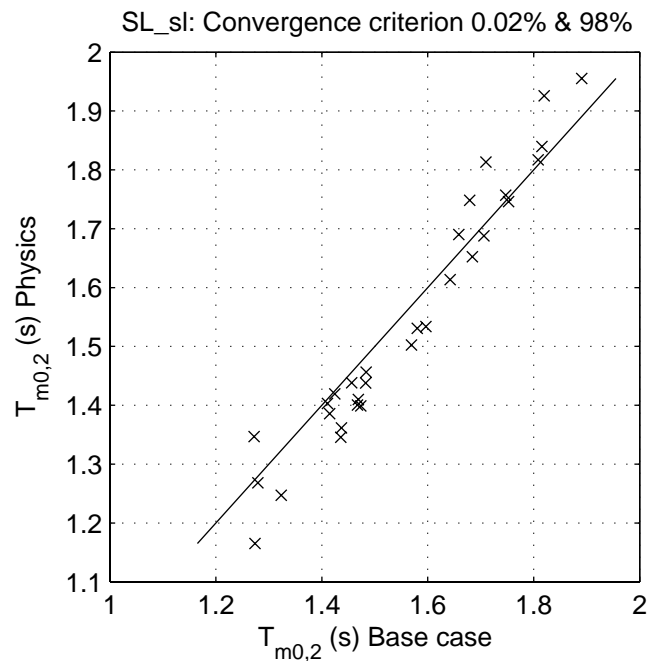
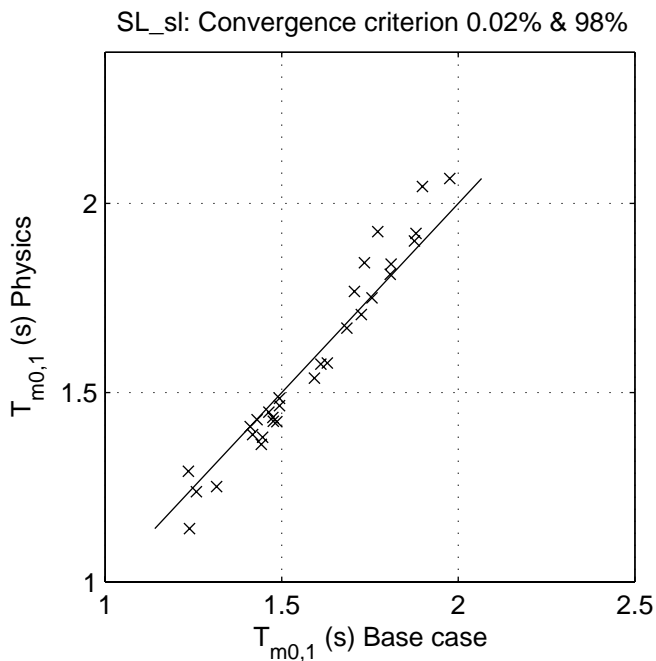
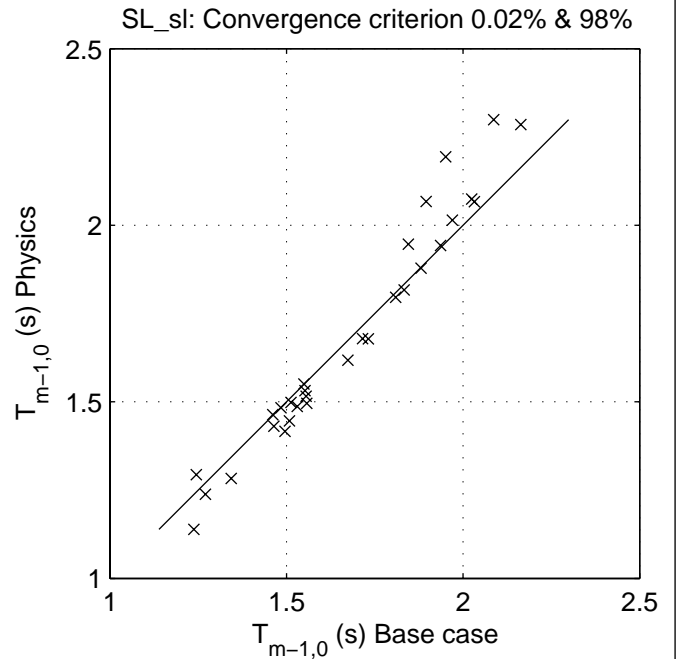
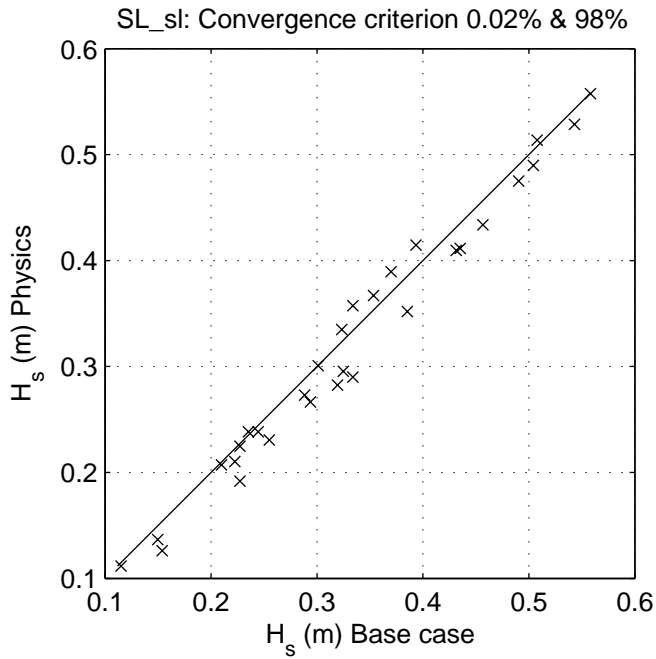
SCAT\_SL\_SL\_N16

Calibration SWAN 40.20

A1168

 **Alkyon**

Fig. 4.2.16



Sensitivity of SWAN 40.20 to variation in numerical parameters  
Comparison of base case against:  
Convergence criterion 0.02% & 98%

Area:SL

Grid:SL

N17

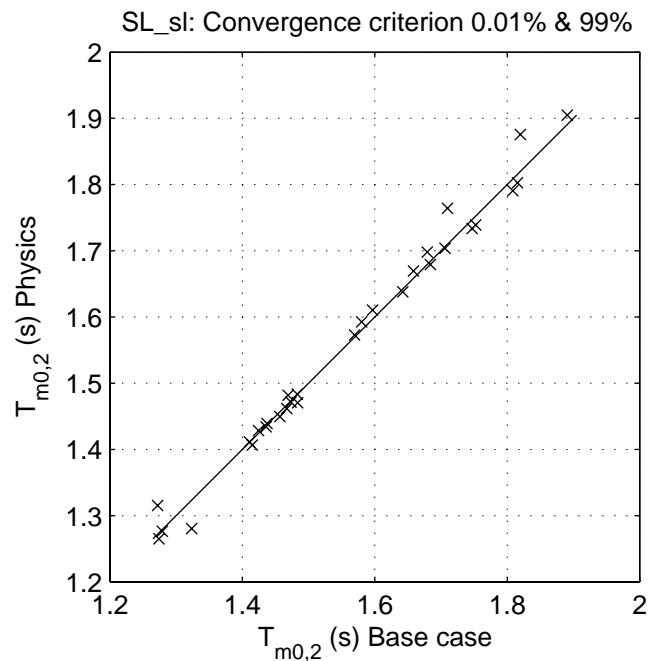
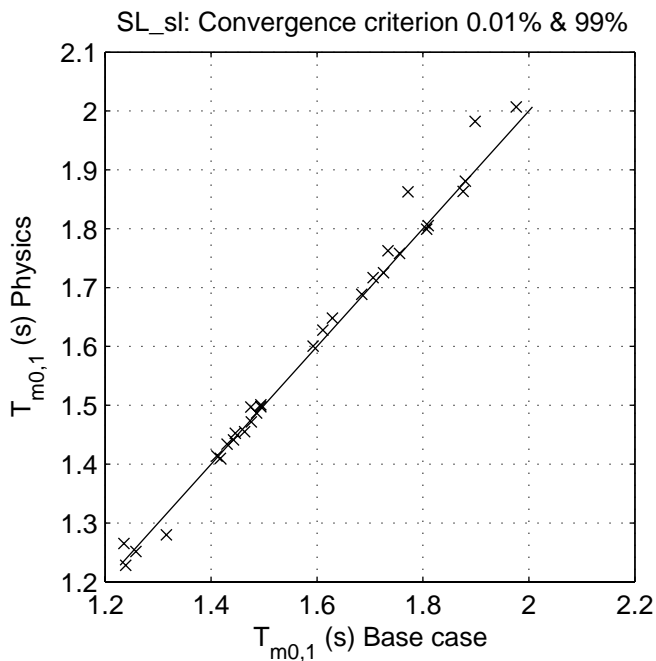
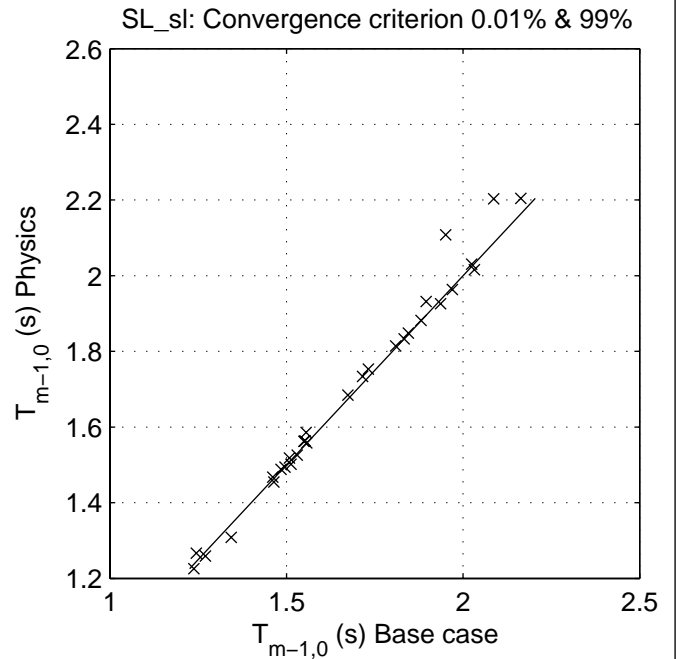
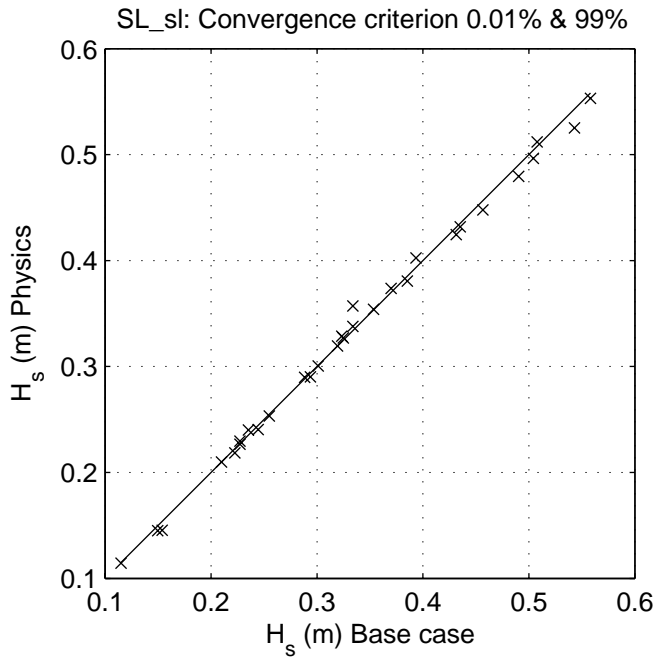
SCAT\_SL\_SL\_N17

Calibration SWAN 40.20

A1168

 **Alkyon**

Fig. 4.2.17



Sensitivity of SWAN 40.20 to variation in numerical parameters  
Comparison of base case against:  
Convergence criterion 0.01% & 99%

Area:SL

Grid:SL

N18

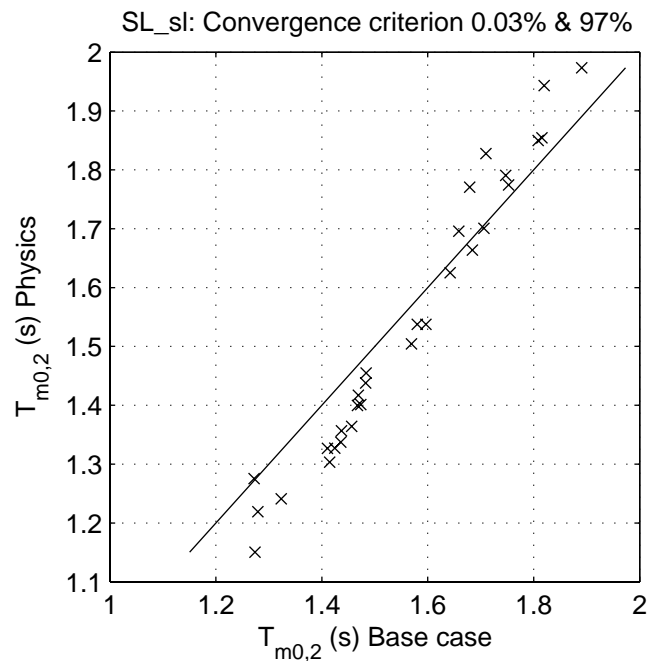
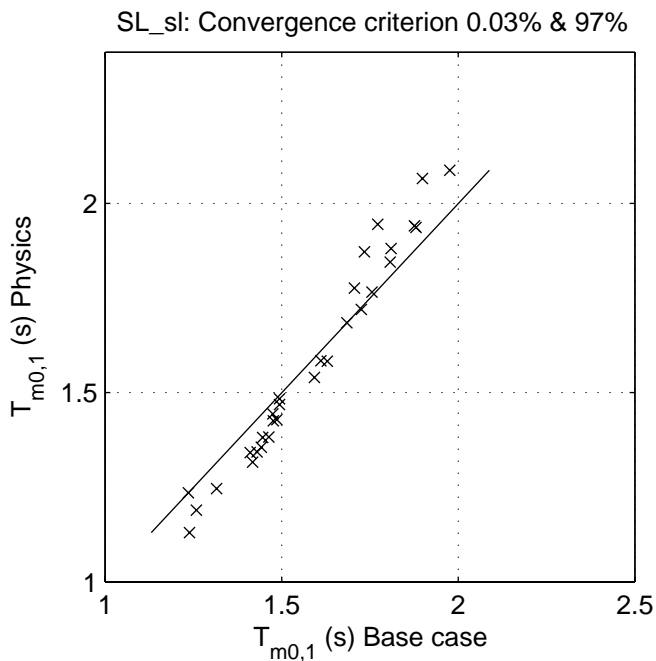
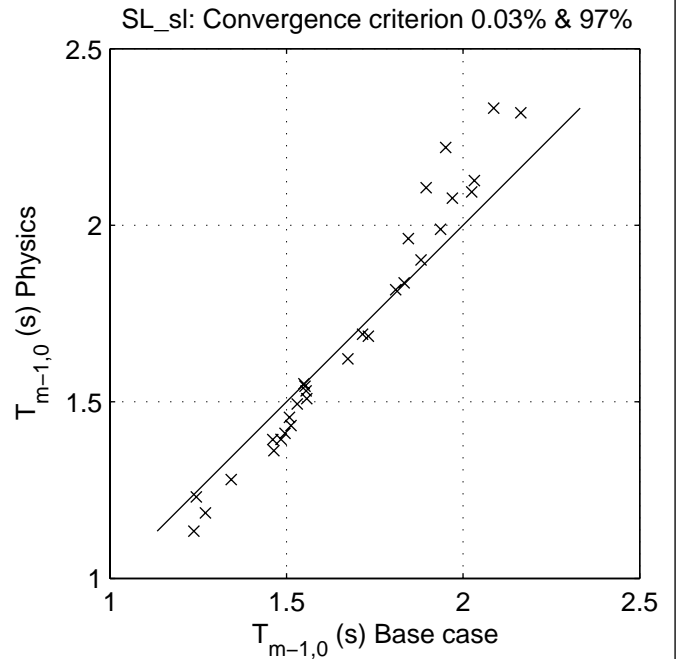
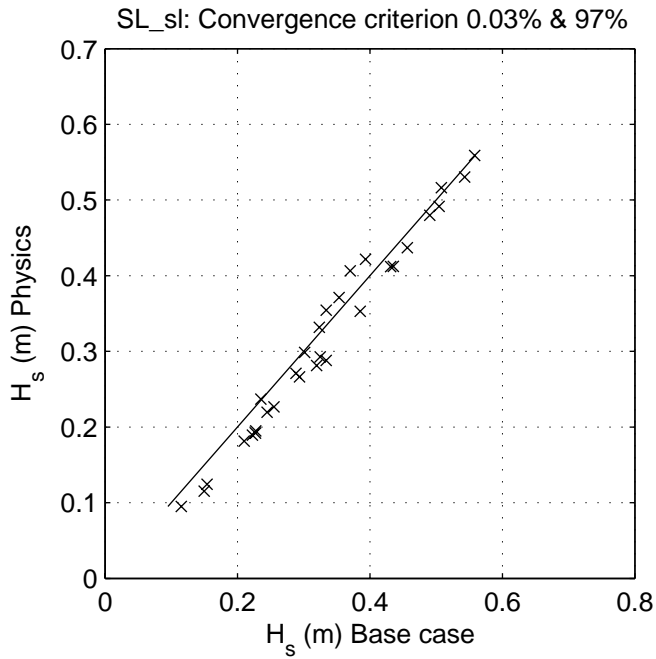
SCAT\_SL\_SL\_N18

Calibration SWAN 40.20

A1168

 **Alkyon**

Fig. 4.2.18



Sensitivity of SWAN 40.20 to variation in numerical parameters  
Comparison of base case against:  
Convergence criterion 0.03% & 97%

Area:SL

Grid:SL

N19

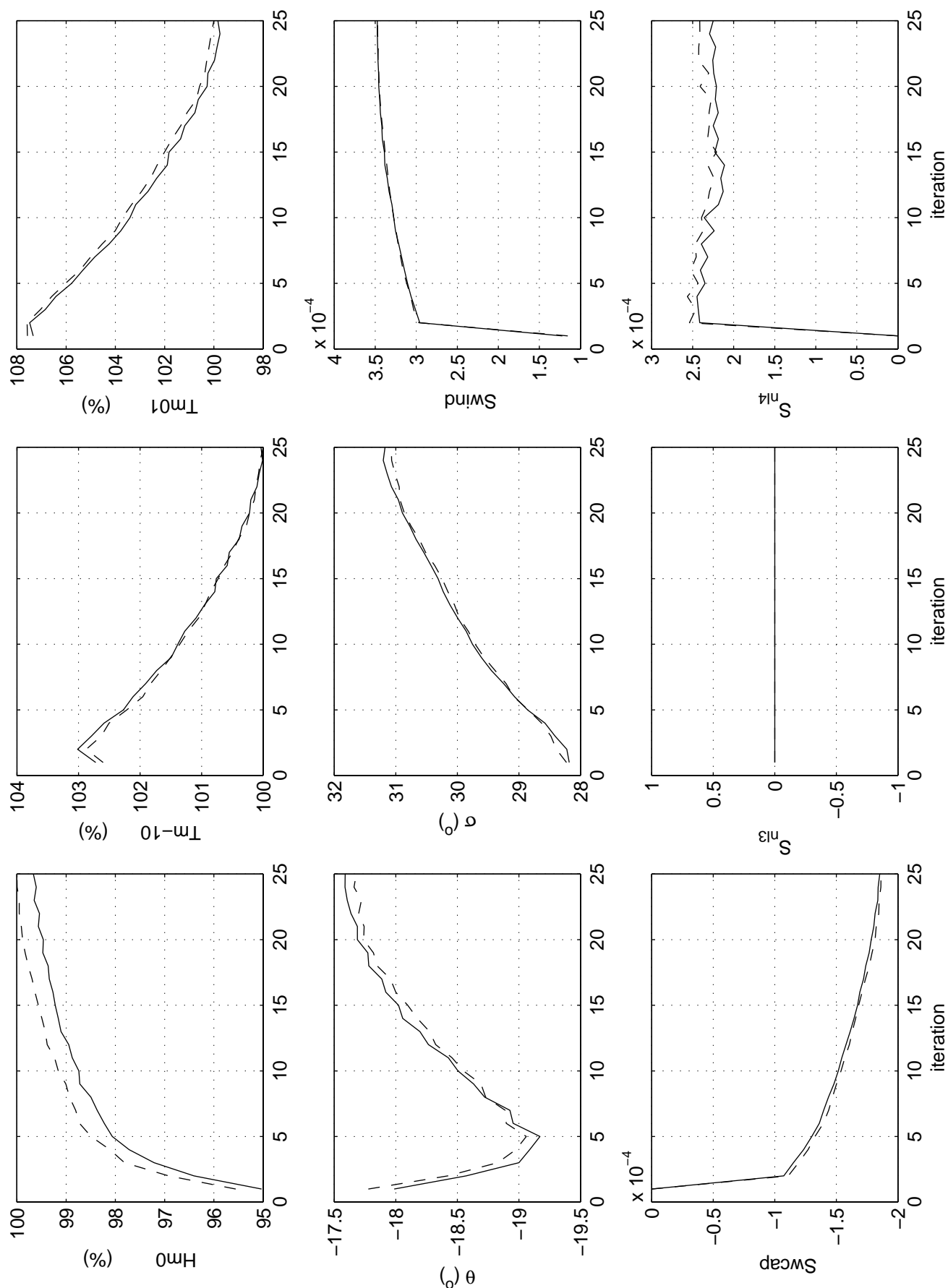
SCAT\_SL\_SL\_N19

Calibration SWAN 40.20

A1168

 **Alkyon**

Fig. 4.2.19



Iteration behaviour of integral wave parameters in Westerschelde  
 Base case (dashed line) Position: x=14400 y=379500  
 Lower minimum frequency (solid line)

Area: WS

Grid: w01

c03\_n02

CDD

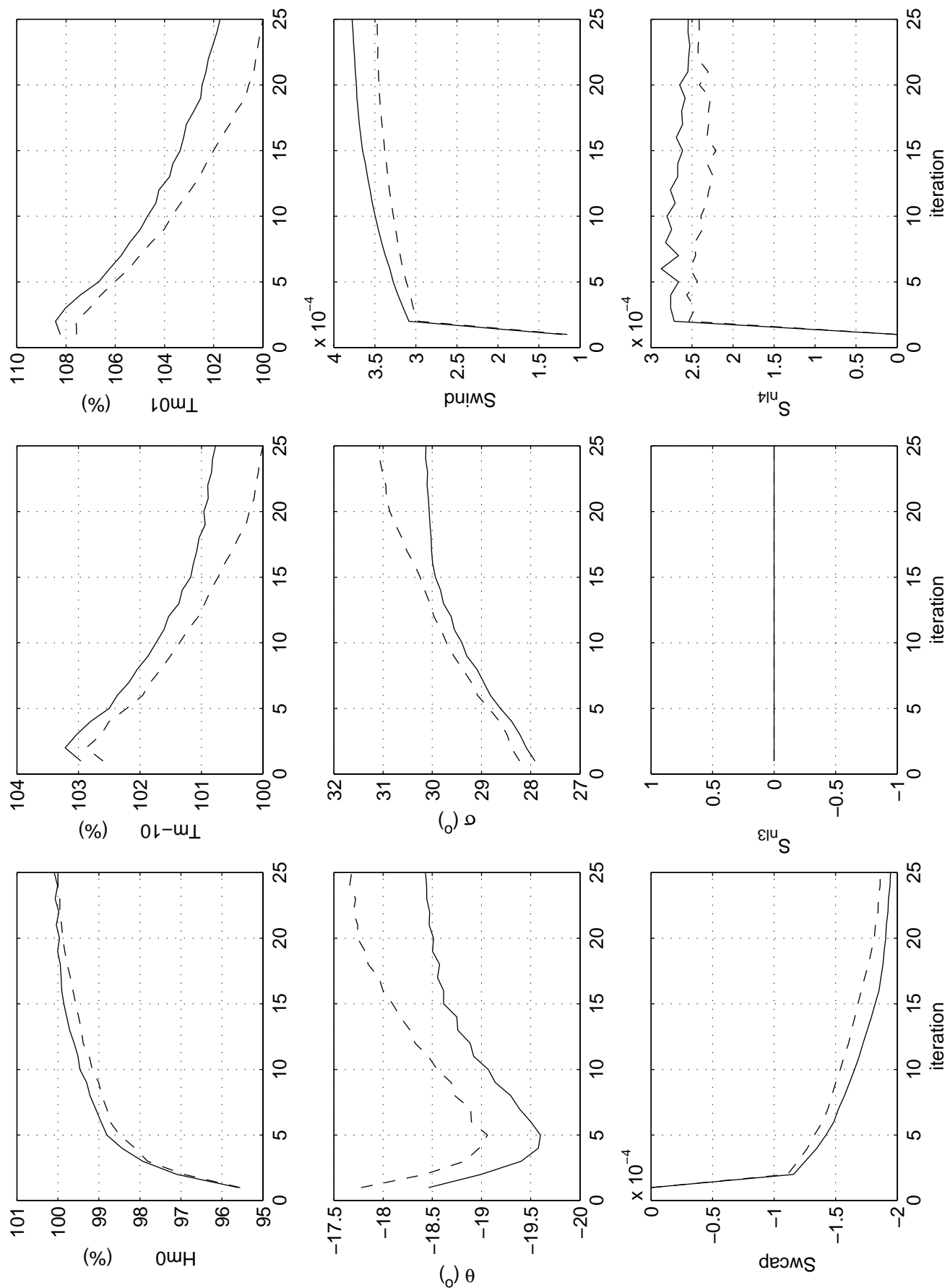
WS\_w01\_c03\_n02\_loc1\_s2p

Calibration SWAN 40.20

A1168

 **Alkyon**

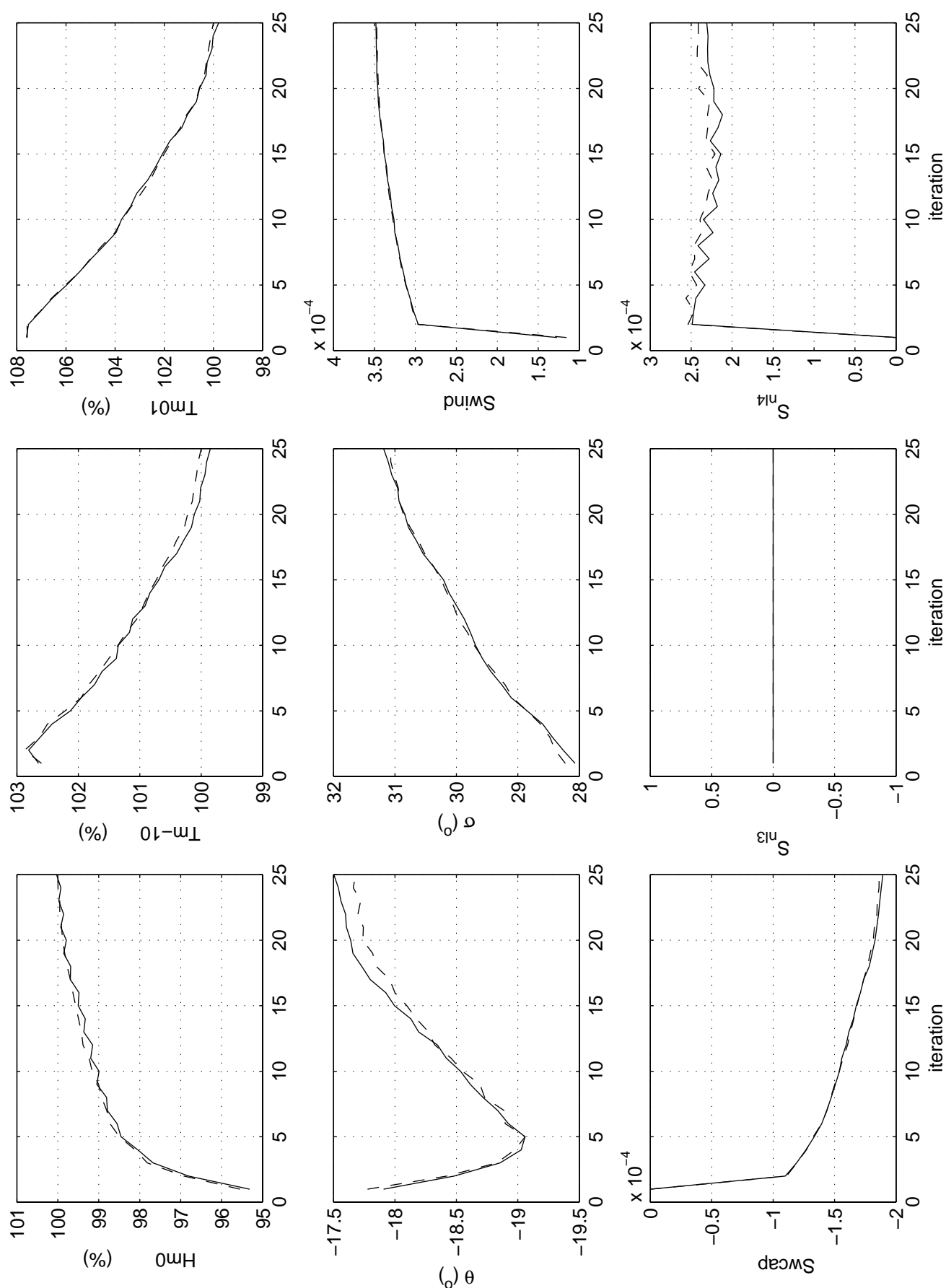
Fig. 4.3.2



Iteration behaviour of integral wave parameters in Westerschelde  
Base case (dashed line) Position: x=14400 y=379500  
Higher maximum frequency (solid line)

Area: WS	Grid: w01
c03_n03	CDD
WS_w01_c03_n03_loc1_s2p	





Iteration behaviour of integral wave parameters in Westerschelde  
 Base case (dashed line) Position: x=14400 y=379500  
 Higher frequency resolution (solid line)

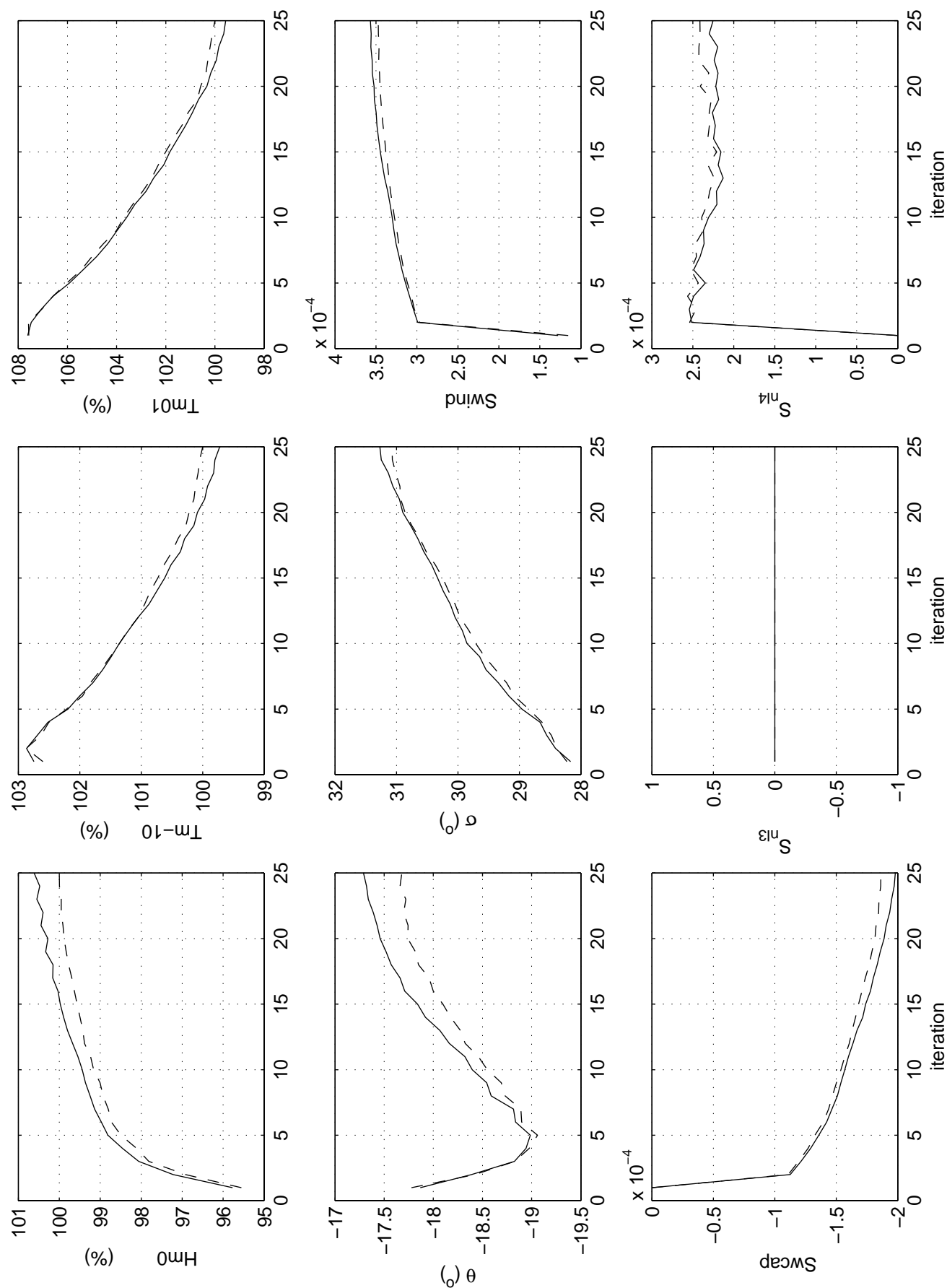
Area: WS

Grid: w01

c03\_n04

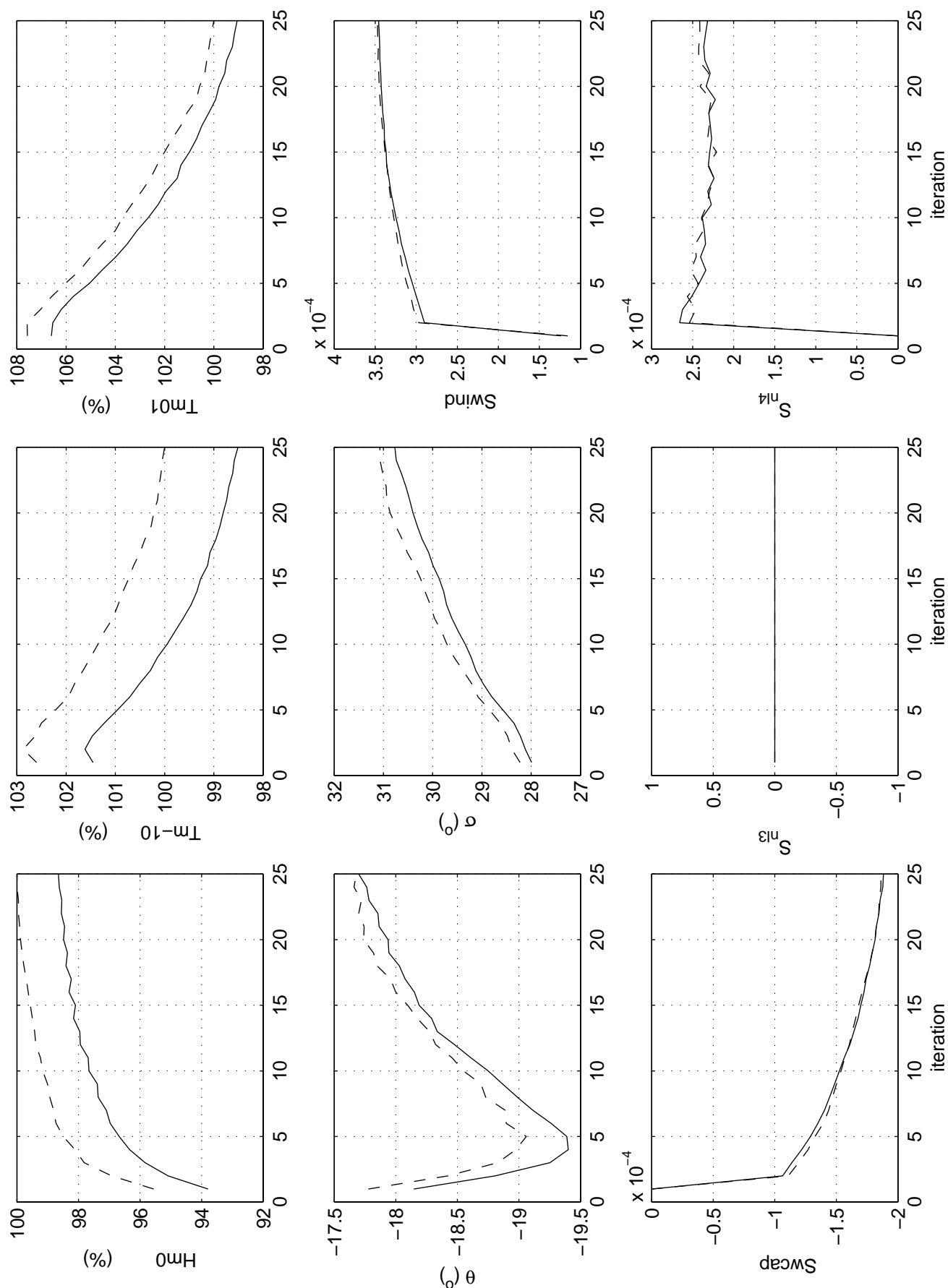
CDD

WS\_w01\_c03\_n04\_loc1\_s2p



Iteration behaviour of integral wave parameters in Westerschelde  
Base case (dashed line) Position: x=14400 y=379500  
Lower frequency resolution (solid line)

Area: WS	Grid: w01
c03_n05	CDD
WS_w01_c03_n05_loc1_s2p	



Iteration behaviour of integral wave parameters in Westerschelde  
 Base case (dashed line) Position: x=14400 y=379500  
 Higher directional resolution (solid line)

Area: WS

Grid: w01

c03\_n06

CDD

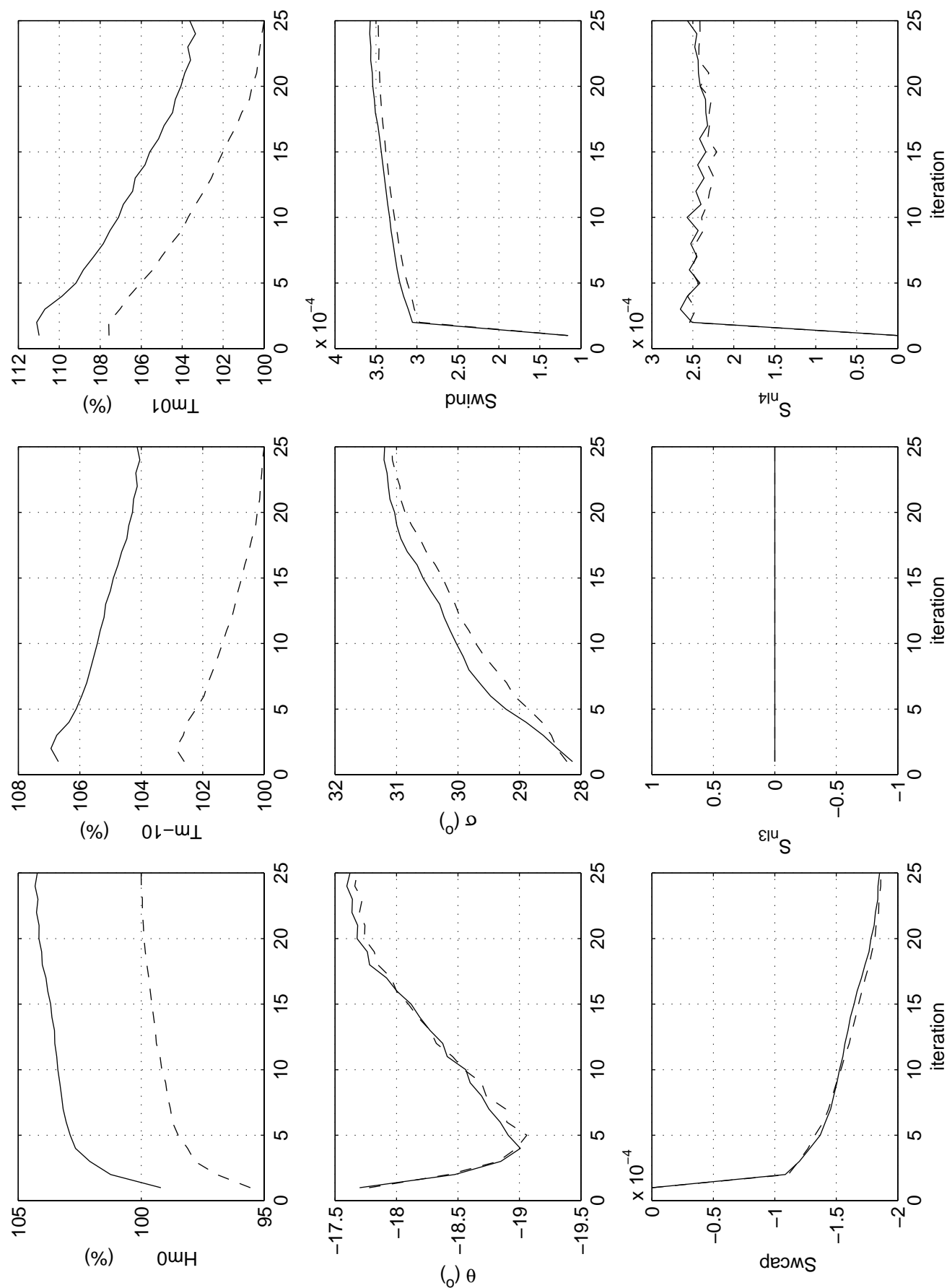
WS\_w01\_c03\_n06\_loc1\_s2p

Calibration SWAN 40.20

A1168

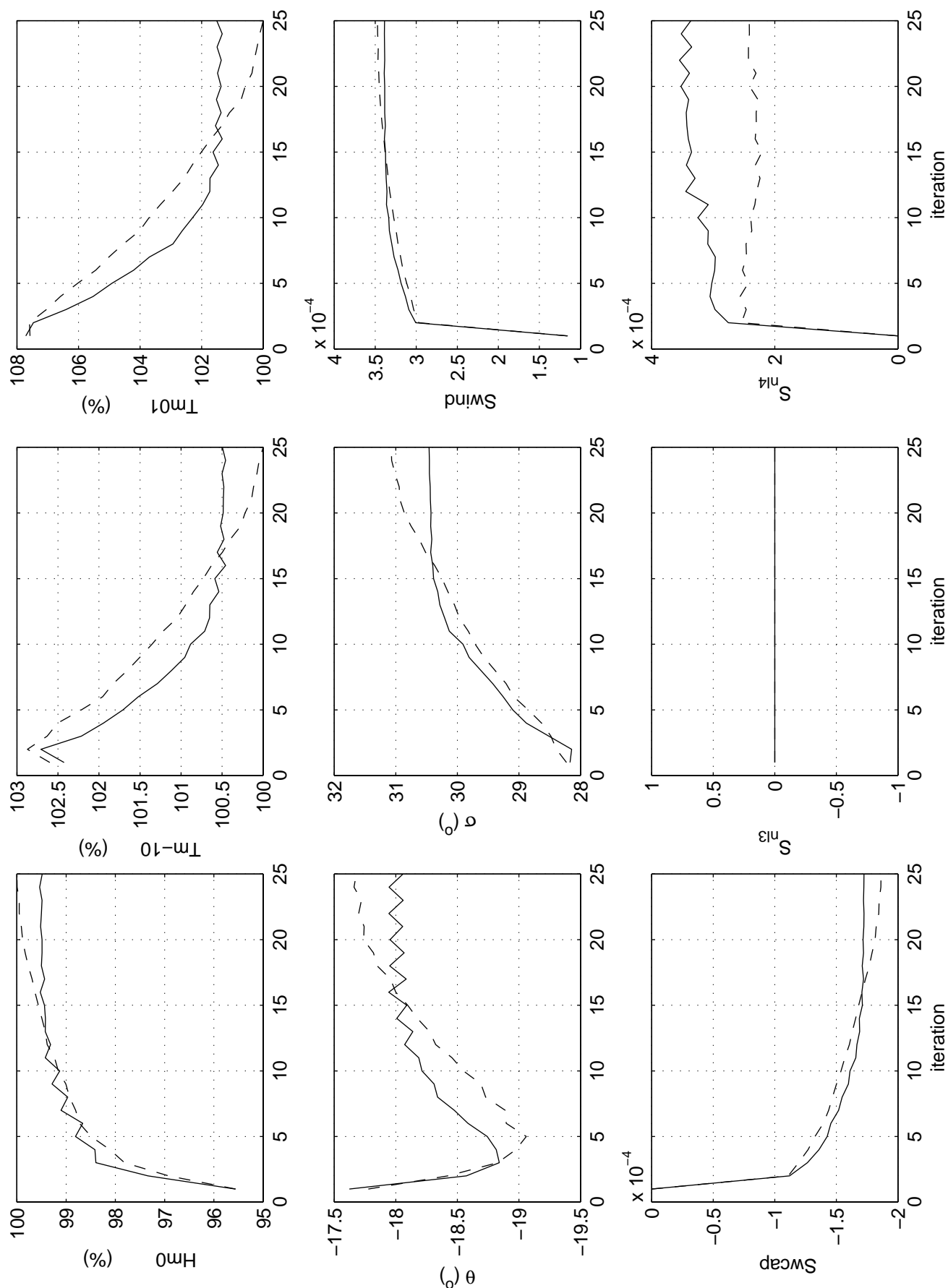
 **Alkyon**

Fig. 4.3.6



Iteration behaviour of integral wave parameters in Westerschelde  
Base case (dashed line) Position: x=14400 y=379500  
Lower directional resolution (solid line)

Area: WS	Grid: w01
c03_n07	CDD
WS_w01_c03_n07_loc1_s2p	



Iteration behaviour of integral wave parameters in Westerschelde  
 Base case (dashed line) Position: x=14400 y=379500  
 Phillips limit 20% (solid line)

Area: WS

Grid: w01

c03\_n08

CDD

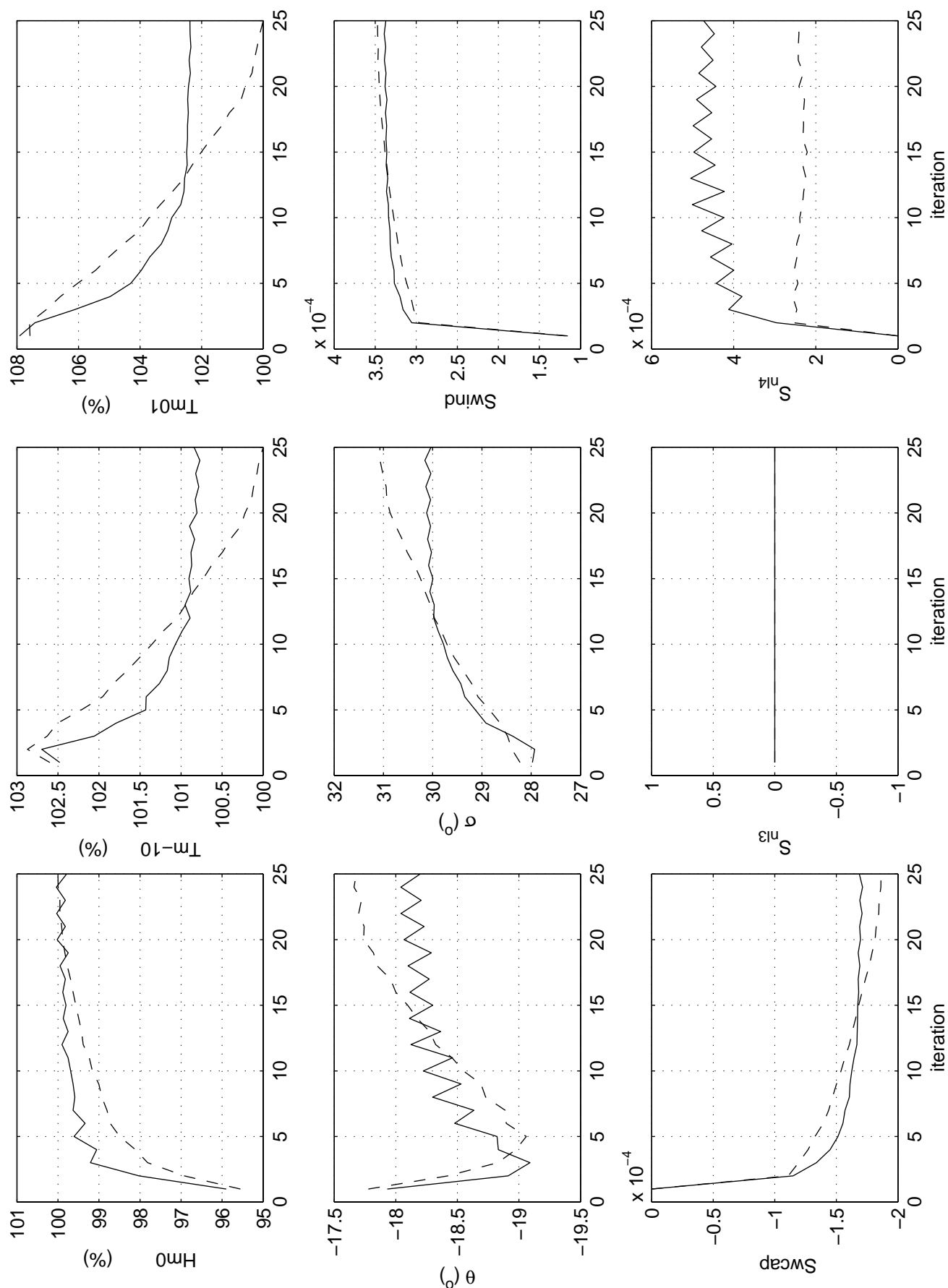
WS\_w01\_c03\_n08\_loc1\_s2p

Calibration SWAN 40.20

A1168

 **Alkyon**

Fig. 4.3.8



Iteration behaviour of integral wave parameters in Westerschelde  
 Base case (dashed line) Position: x=14400 y=379500  
 Phillips limit 30% (solid line)

Area: WS

Grid: w01

c03\_n09

CDD

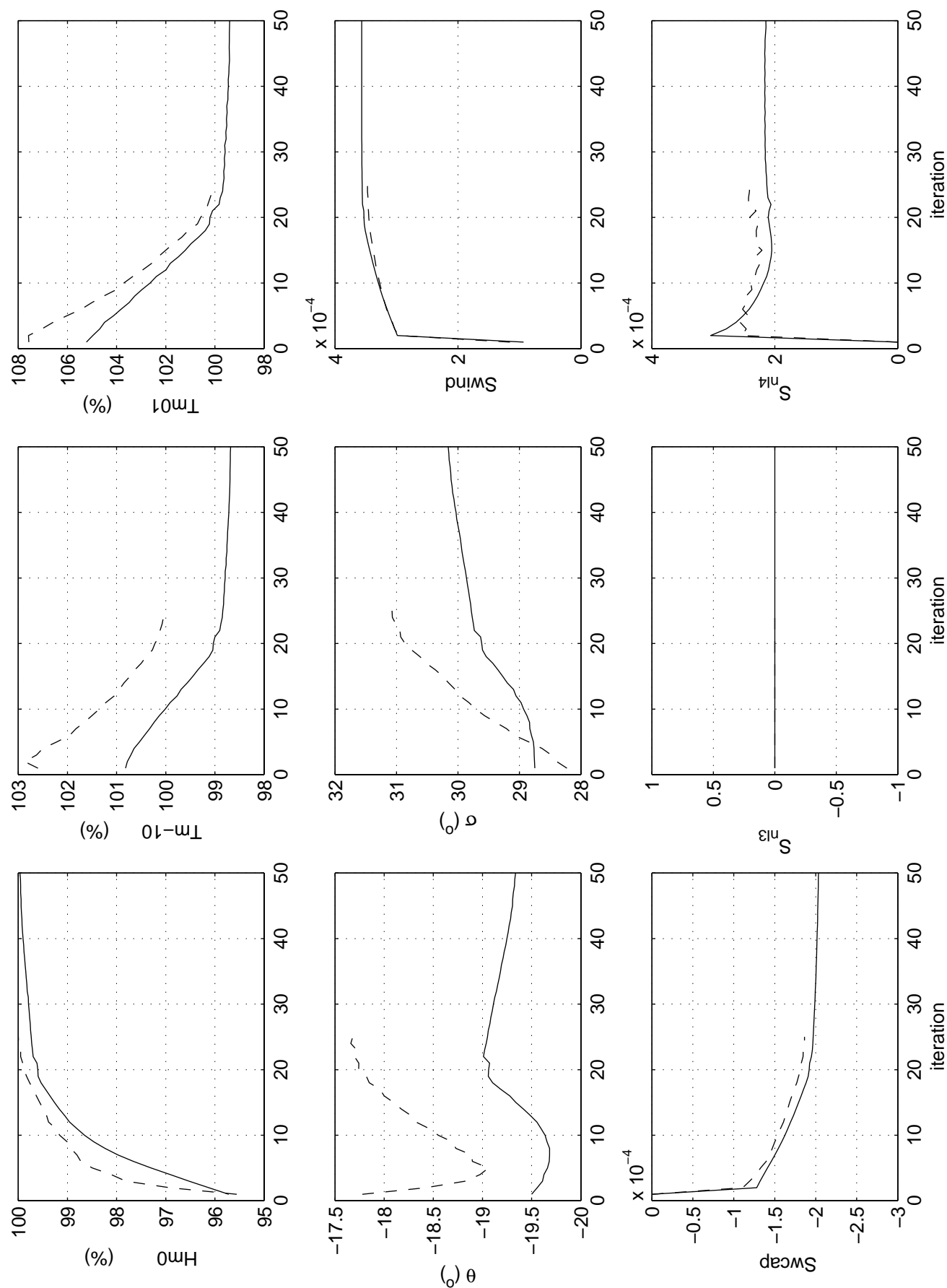
WS\_w01\_c03\_n09\_loc1\_s2p

Calibration SWAN 40.20

A1168

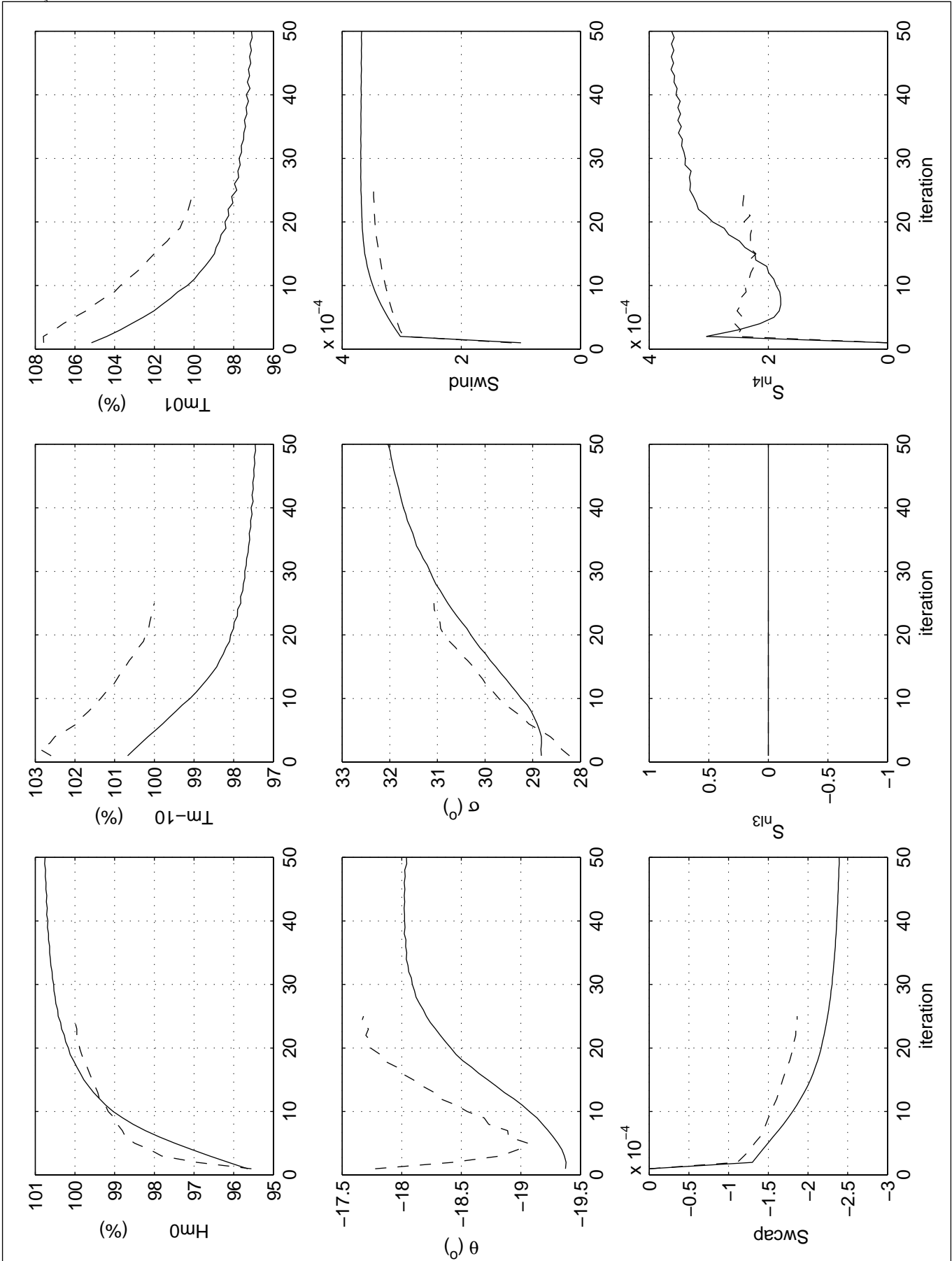
 **Alkyon**

Fig. 4.3.9



Iteration behaviour of integral wave parameters in Westerschelde  
Base case (dashed line) Position: x=14400 y=379500  
Under-relaxation  $\alpha=0.025$  Phillip limit 10% (solid line)

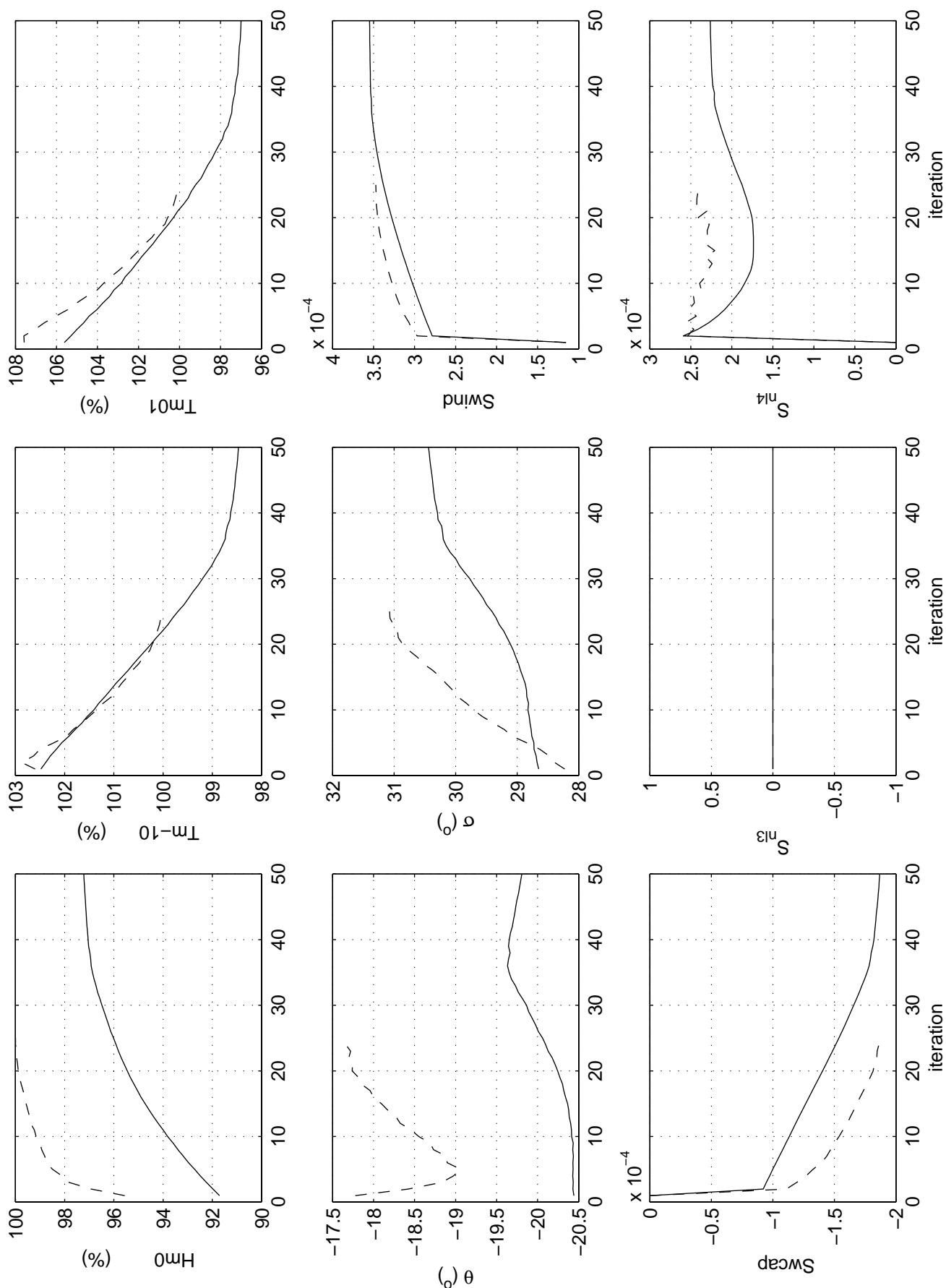
Area: WS	Grid: w01
c03_n10	CDD
WS_w01_c03_n10_loc1_s2p	



Iteration behaviour of integral wave parameters in Westerschelde  
Base case (dashed line) Position: x=14400 y=379500  
Under-relaxation  $\alpha=0.025$  Phillip limit 50% (solid line)

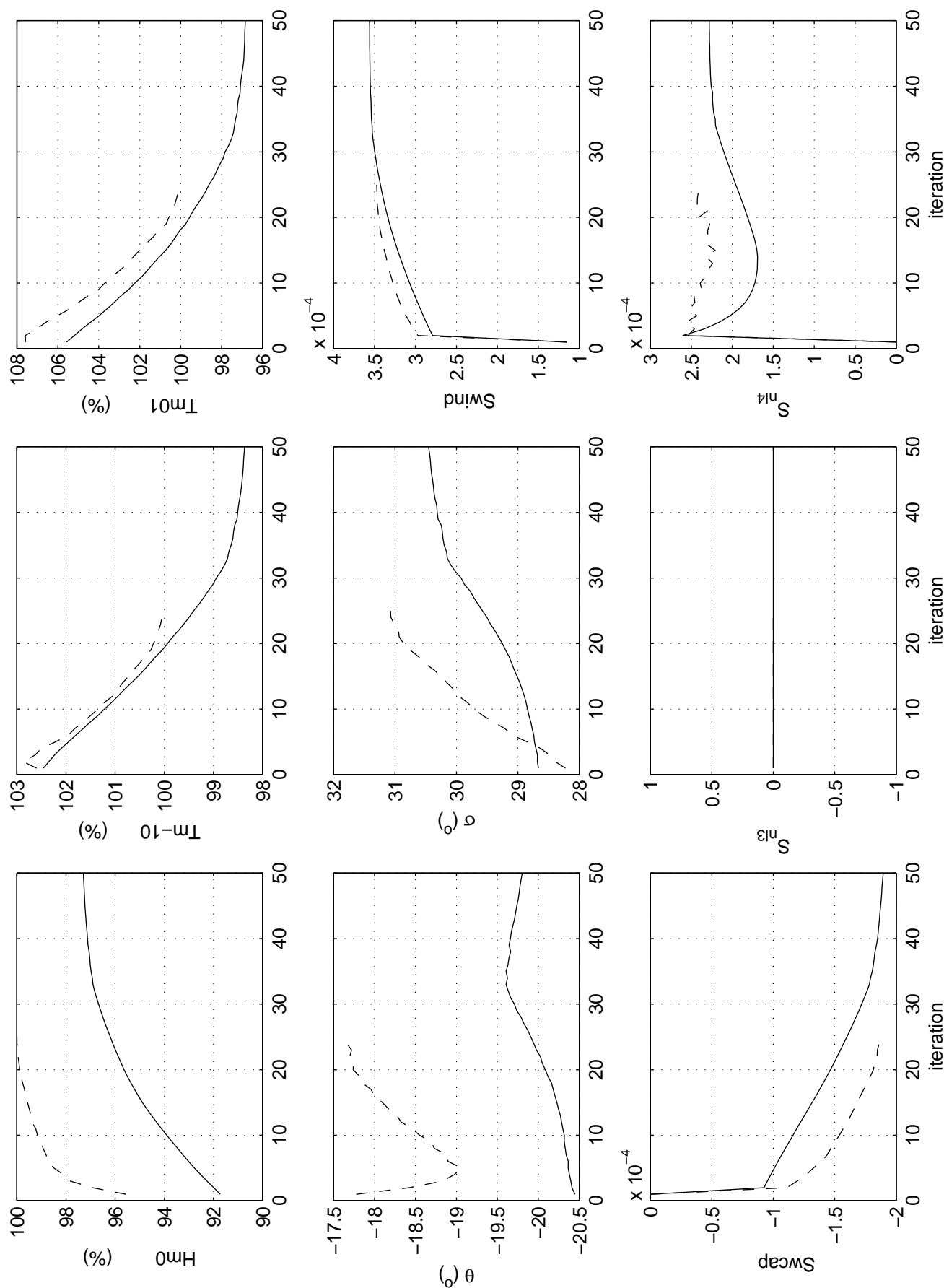
Area: WS	Grid: w01
c03_n11	CDD
WS_w01_c03_n11_loc1_s2p	





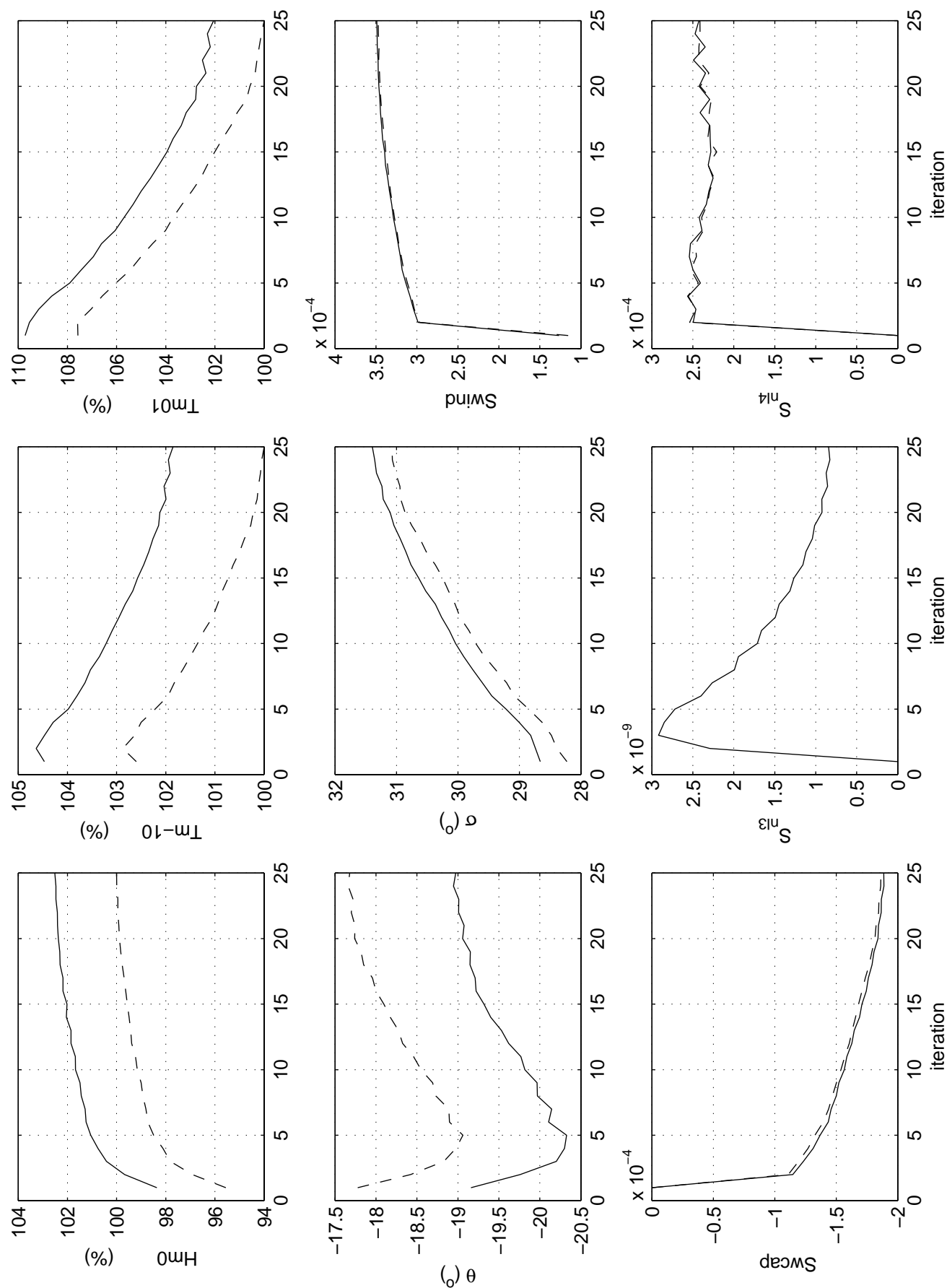
Iteration behaviour of integral wave parameters in Westerschelde  
Base case (dashed line) Position: x=14400 y=379500  
Under-relaxation  $\alpha=0.05$  Phillip limit 10% (solid line)

Area: WS	Grid: w01
c03_n12	CDD
WS_w01_c03_n12_loc1_s2p	



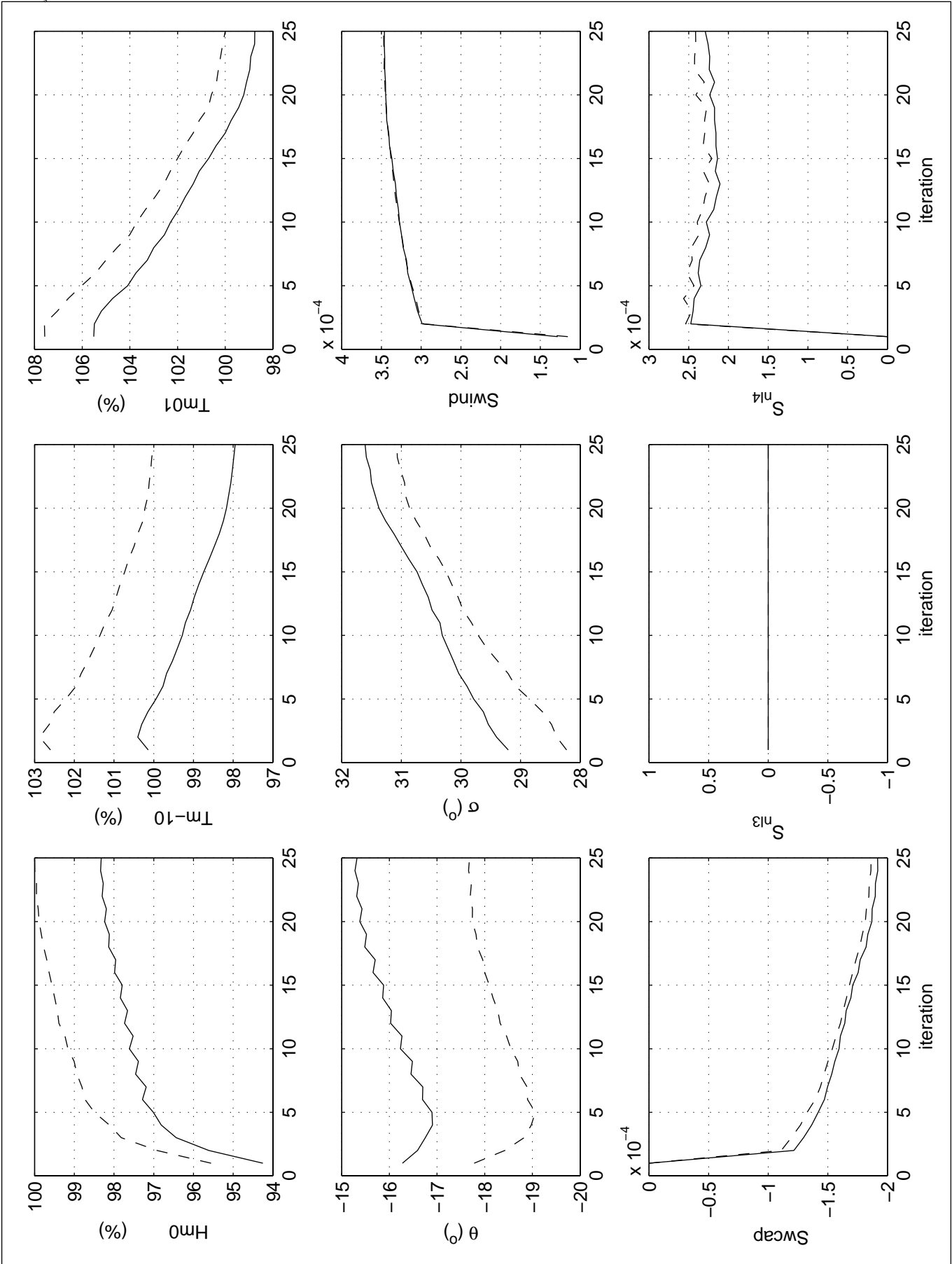
Iteration behaviour of integral wave parameters in Westerschelde  
Base case (dashed line) Position: x=14400 y=379500  
Under-relaxation  $\alpha=0.05$  Phillip limit 50% (solid line)

Area: WS	Grid: w01
c03_n13	CDD
WS_w01_c03_n13_loc1_s2p	



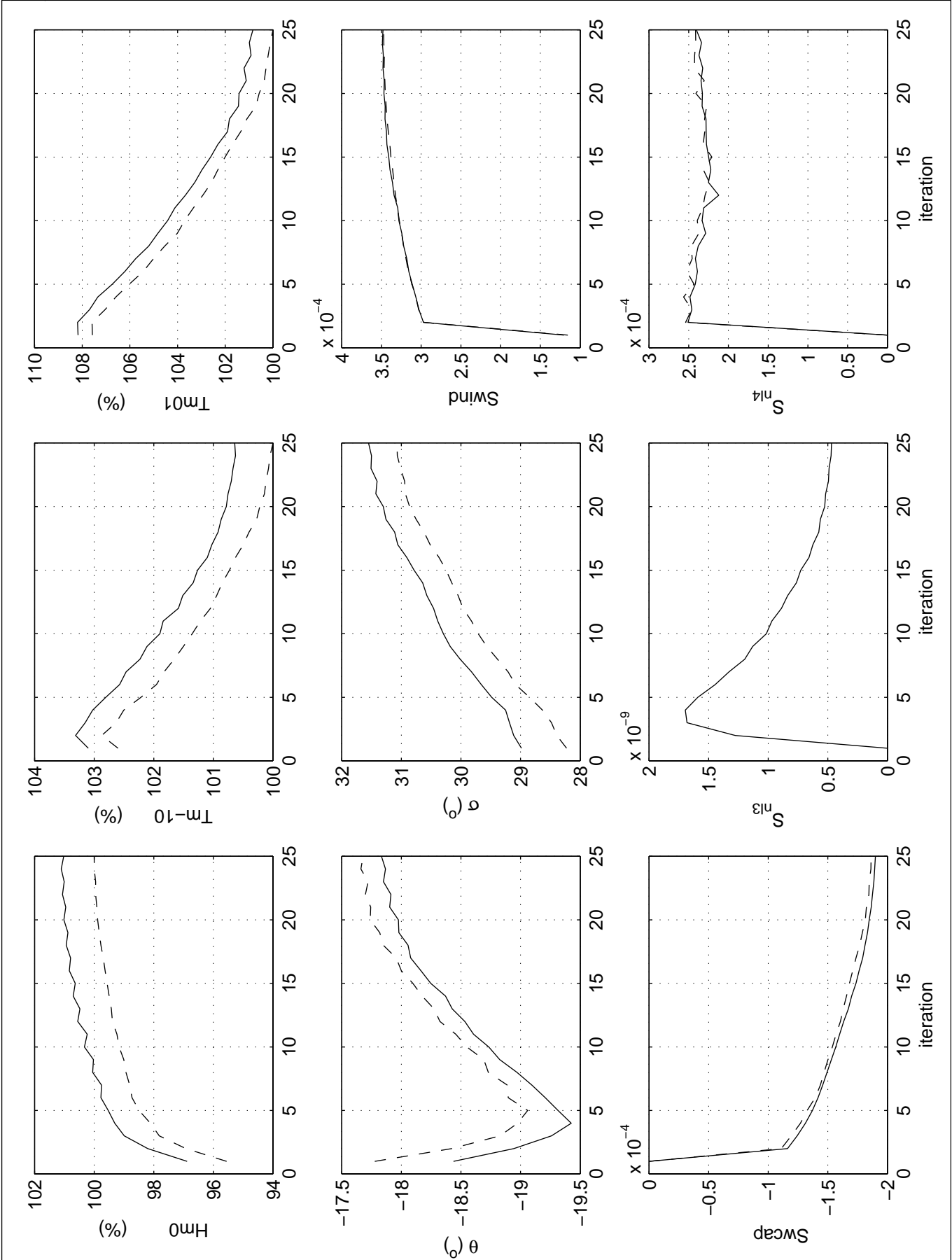
Iteration behaviour of integral wave parameters in Westerschelde  
Base case (dashed line) Position: x=14400 y=379500  
Inclusive triads and quadruplets, Qb = 0.00001 (solid line)

Area: WS	Grid: w01
c03_n14	CDD
WS_w01_c03_n14_loc1_s2p	



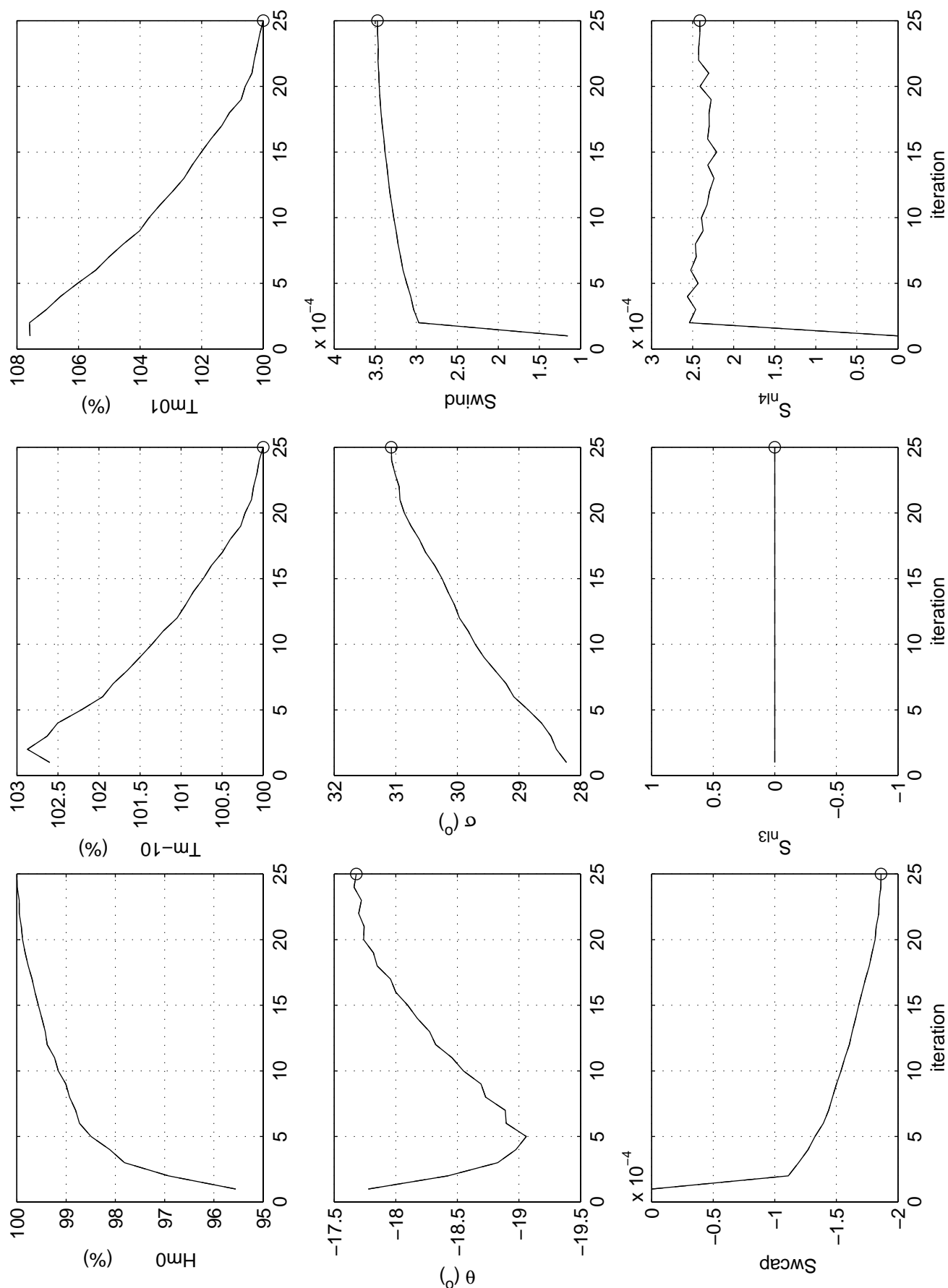
Iteration behaviour of integral wave parameters in Westerschelde  
Base case (dashed line) Position: x=14400 y=379500  
Exclusive triads and quadruplets,  $Q_b = 1.0$  (solid line)

Area: WS	Grid: w01
c03_n15	CDD
WS_w01_c03_n15_loc1_s2p	



Iteration behaviour of integral wave parameters in Westerschelde  
Base case (dashed line) Position: x=14400 y=379500  
Inclusive triads and quadruplets,  $Q_b = 1.0$  (solid line)

Area: WS	Grid: w01
c03_n16	CDD
WS_w01_c03_n16_loc1_s2p	



Iteration behaviour of integral wave parameters in Westerschelde  
 Base case (dashed line) Position:  $x=14400$   $y=379500$   
 Convergence criterion 0.02% & 98% (solid line)

Area: WS

Grid: w01

c03\_n17

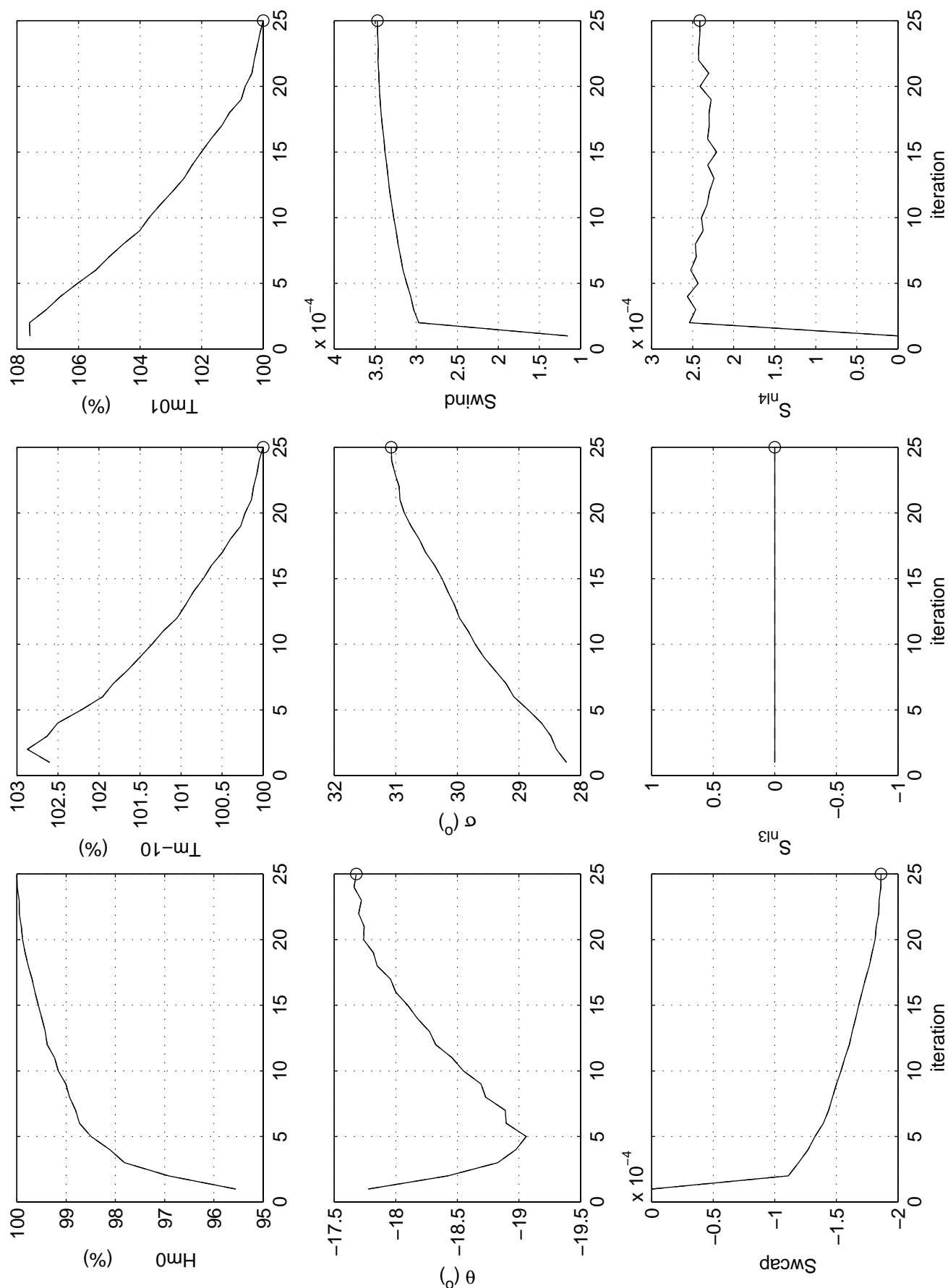
CDD

WS\_w01\_c03\_n17\_loc1\_s2p

Calibration SWAN 40.20

A1168

Fig. 4.3.17



Iteration behaviour of integral wave parameters in Westerschelde  
 Base case (dashed line) Position:  $x=14400$   $y=379500$   
 Convergence criterion 0.01% & 99% (solid line)

Area: WS

Grid: w01

c03\_n18

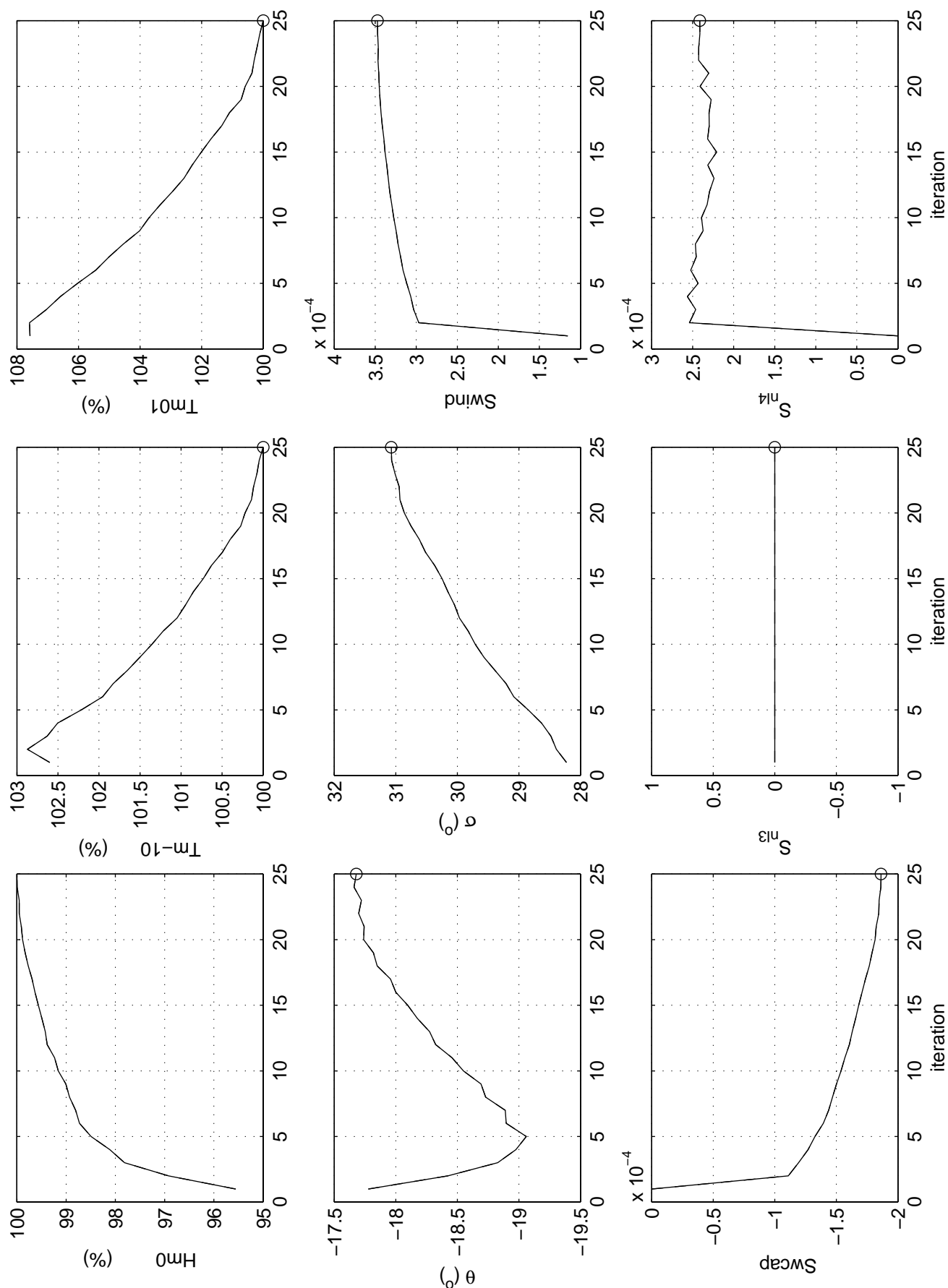
CDD

WS\_w01\_c03\_n18\_loc1\_s2p

Calibration SWAN 40.20

A1168

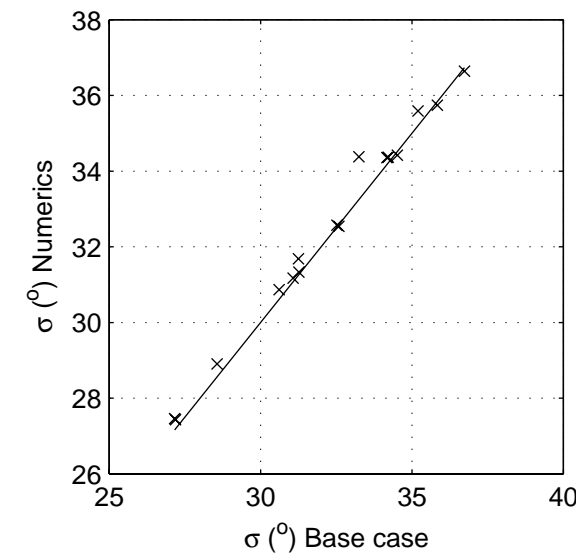
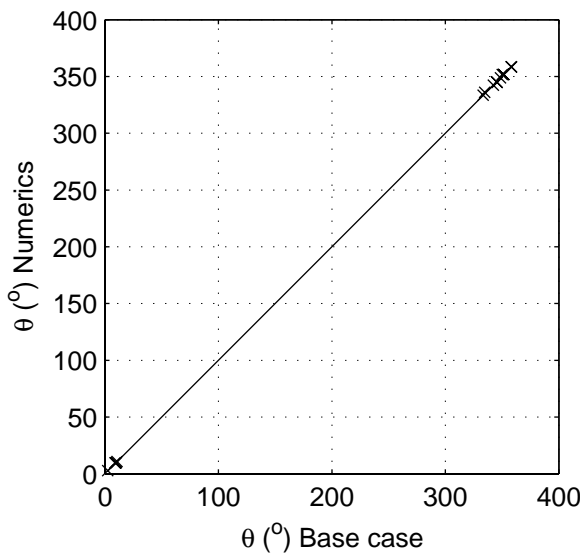
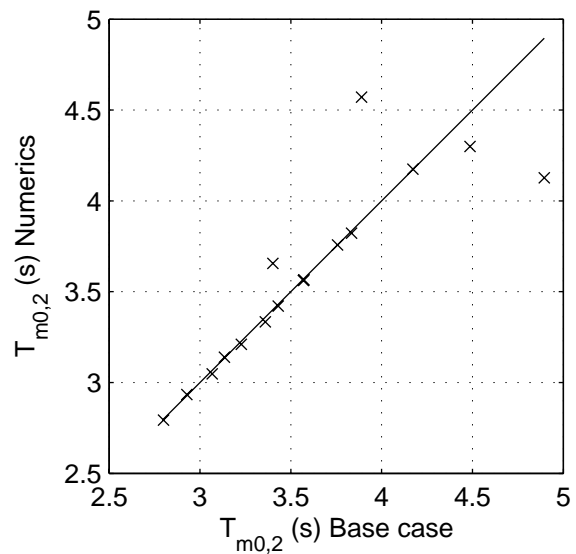
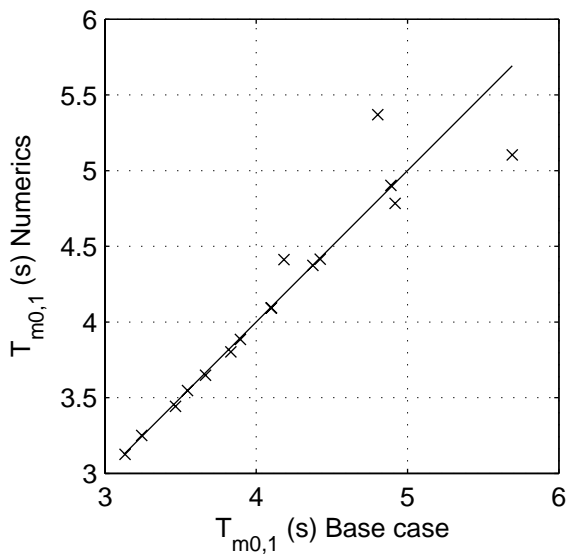
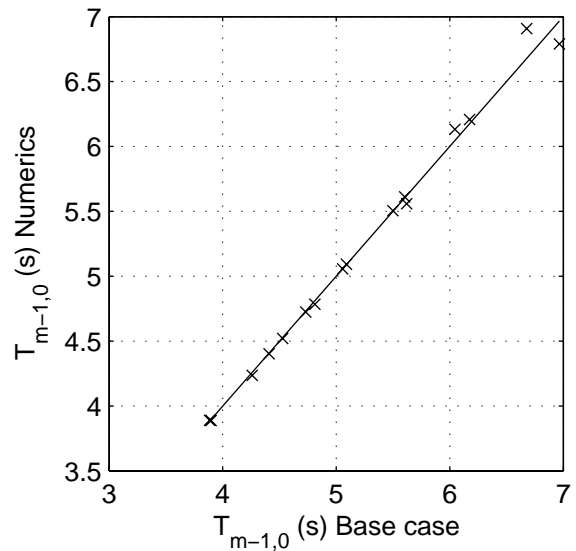
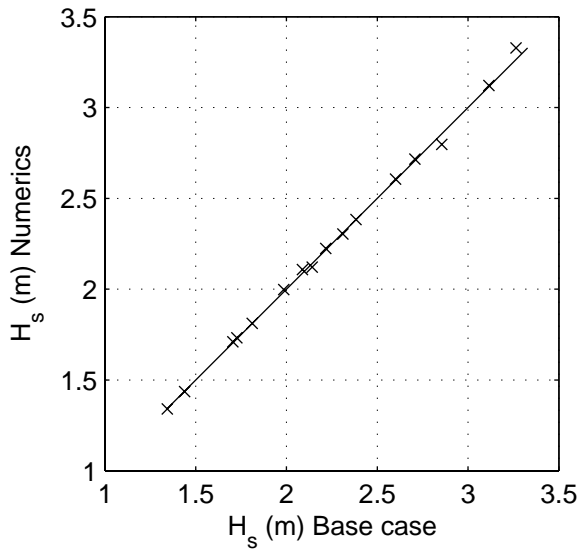
Fig. 4.3.18



Iteration behaviour of integral wave parameters in Westerschelde  
Base case (dashed line) Position: x=14400 y=379500  
Convergence criterion 0.03% & 97% (solid line)

Area: WS	Grid: w01
c03_n19	CDD
WS_w01_c03_n19_loc1_s2p	





Sensitivity of SWAN 40.20 to variation in numerical parameters  
Comparison of base case against:  
Lower minimum frequency

Area:WS

Grid:W01

N02

Numerics

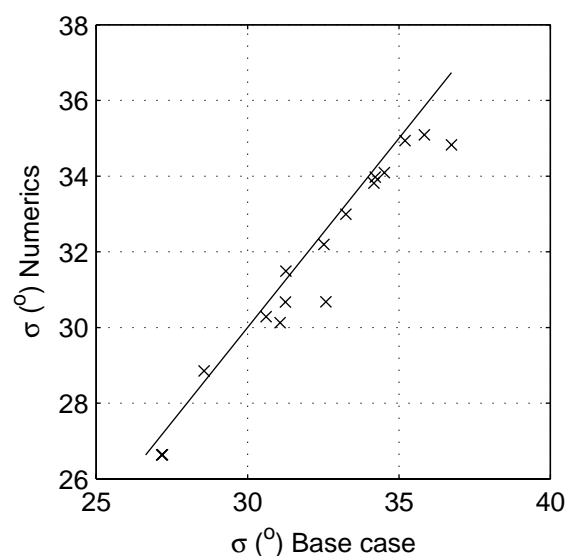
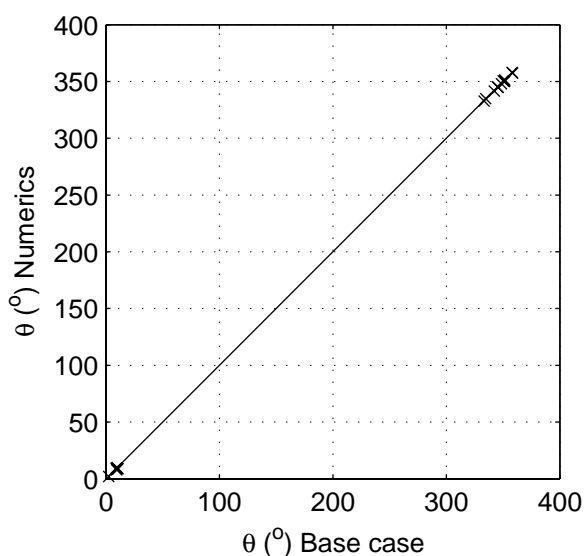
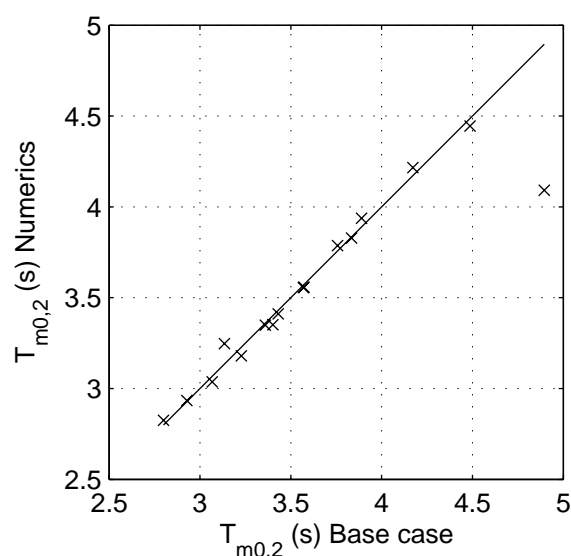
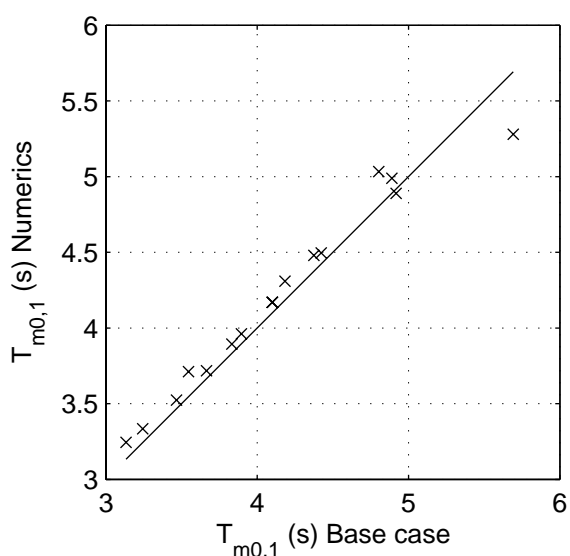
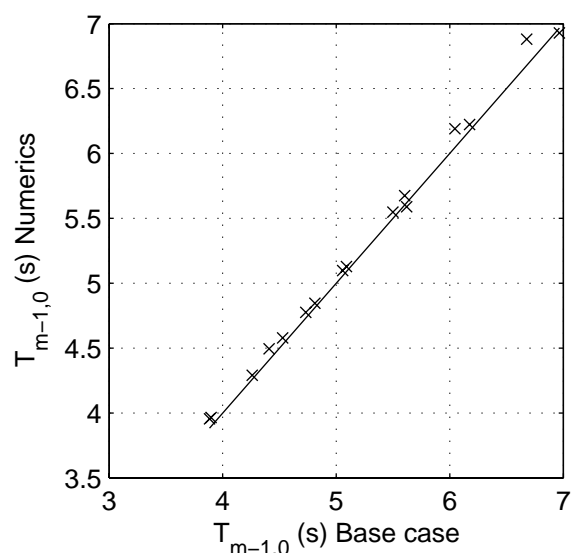
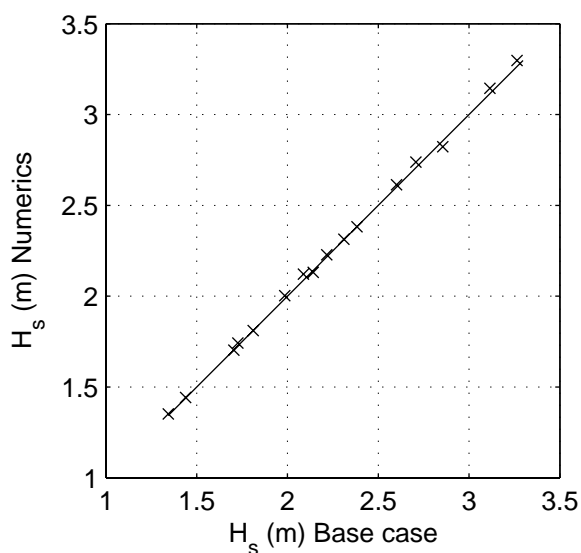
SCAT\_WS\_W01\_N2\_s2p

Calibration SWAN 40.20

A1168

 **Alkyon**

Fig. 4.4.2



Sensitivity of SWAN 40.20 to variation in numerical parameters  
Comparison of base case against:  
Higher maximum frequency

Area:WS

Grid:W01

N03

Numerics

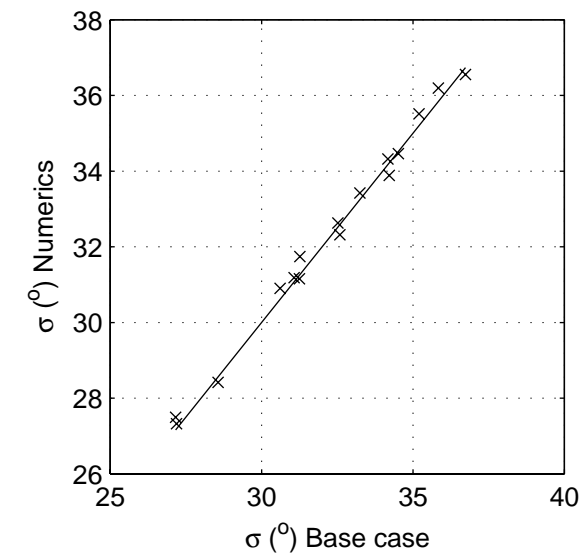
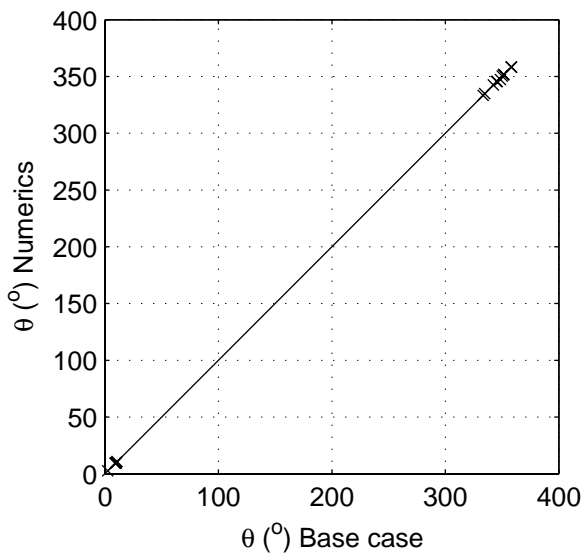
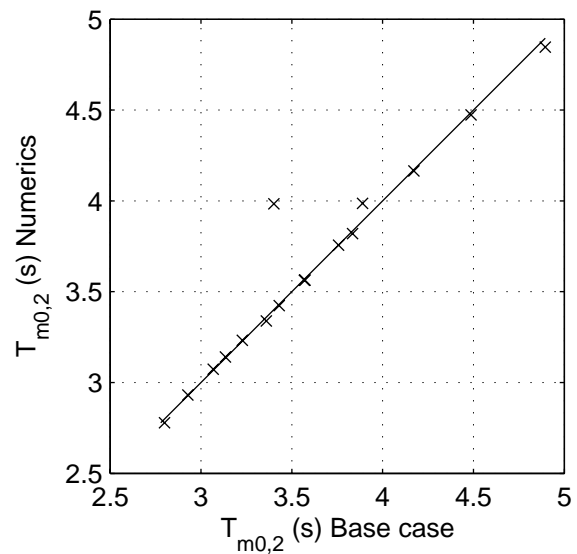
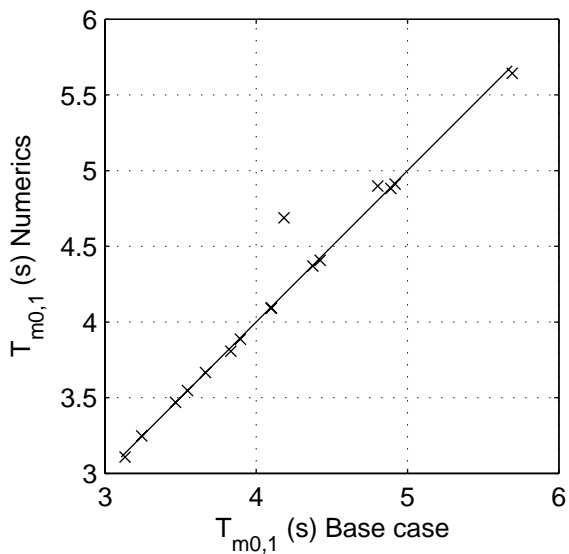
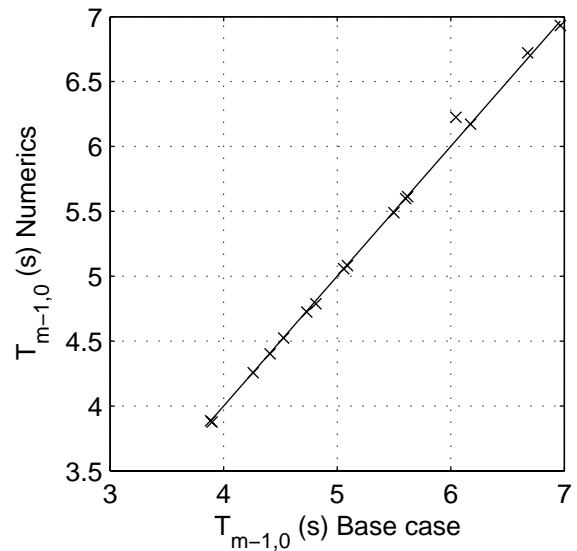
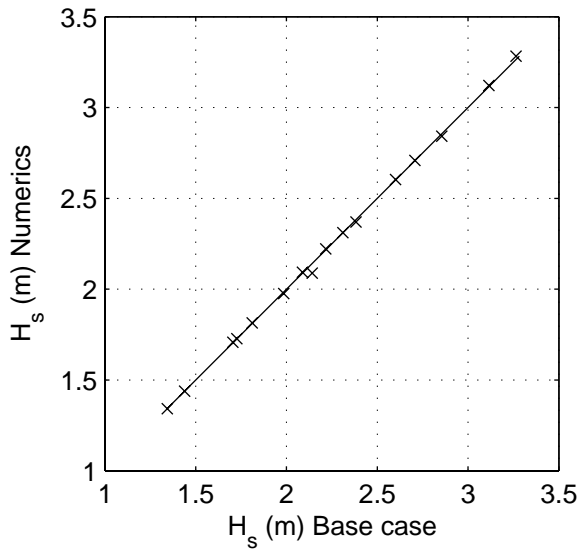
SCAT\_WS\_W01\_N3\_s2p

Calibration SWAN 40.20

A1168

 **Alkyon**

Fig. 4.4.3



Sensitivity of SWAN 40.20 to variation in numerical parameters  
Comparison of base case against:  
Higher frequency resolution

Area:WS

Grid:W01

N04

Numerics

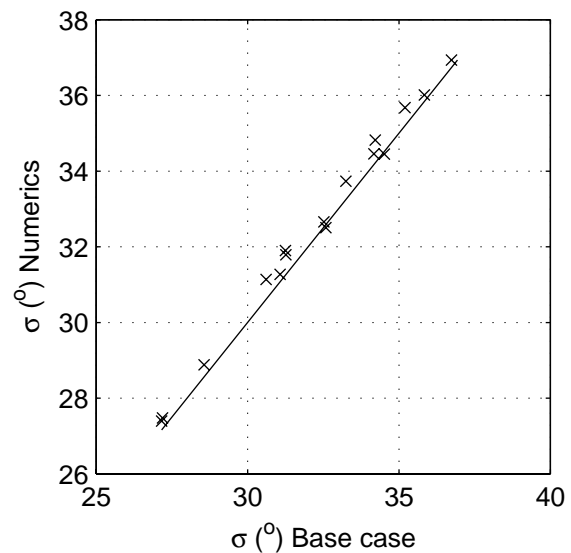
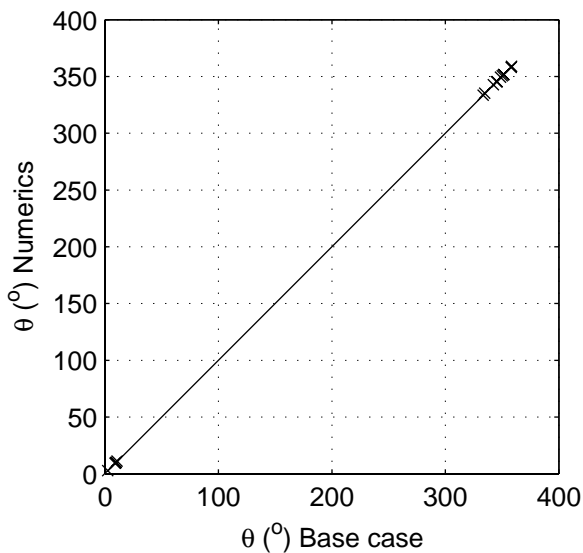
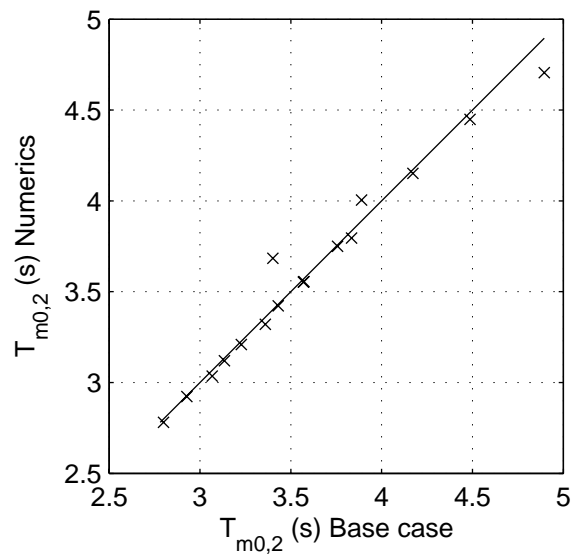
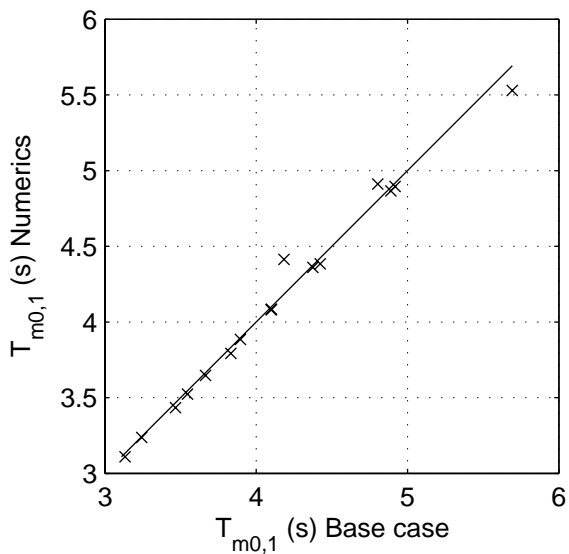
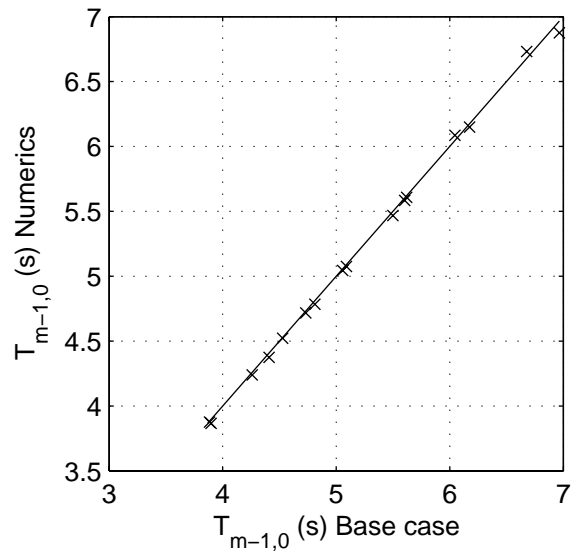
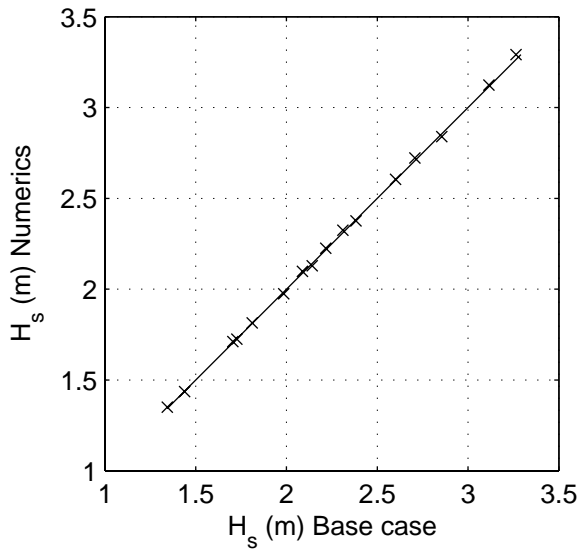
SCAT\_WS\_W01\_N4\_s2p

Calibration SWAN 40.20

A1168

 **Alkyon**

Fig. 4.4.4



Sensitivity of SWAN 40.20 to variation in numerical parameters  
Comparison of base case against:  
Lower frequency resolution

Area:WS

Grid:W01

N05

Numerics

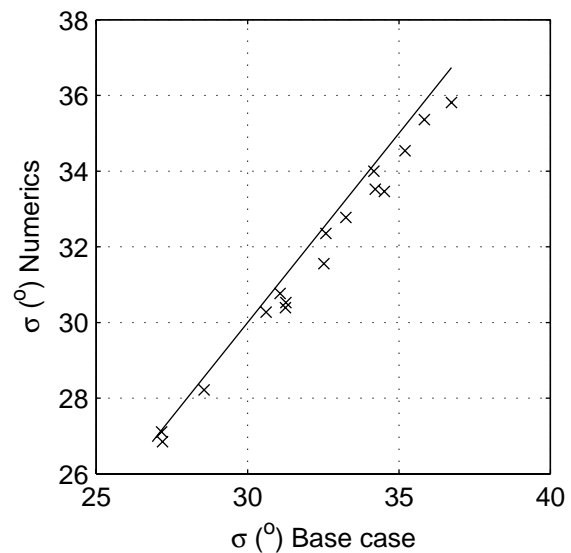
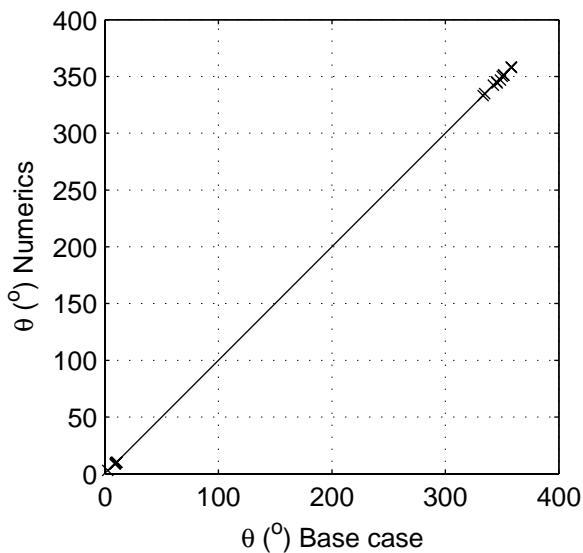
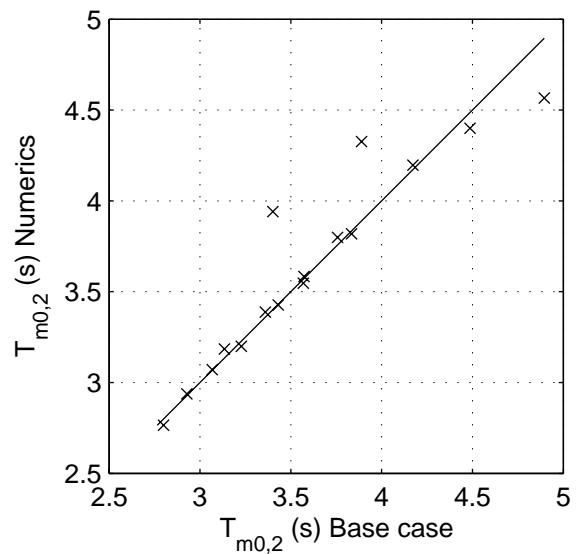
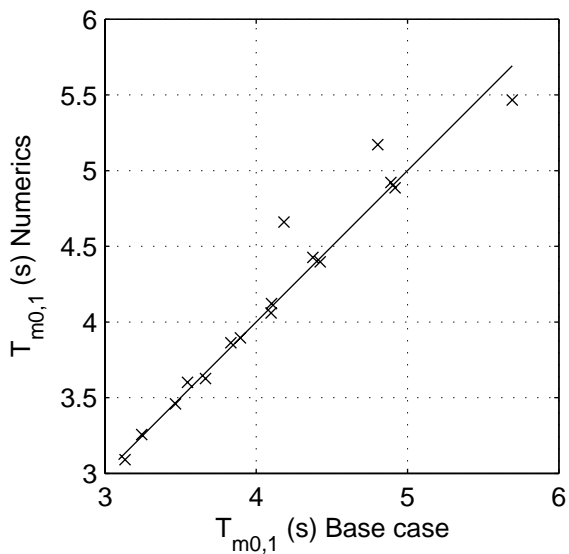
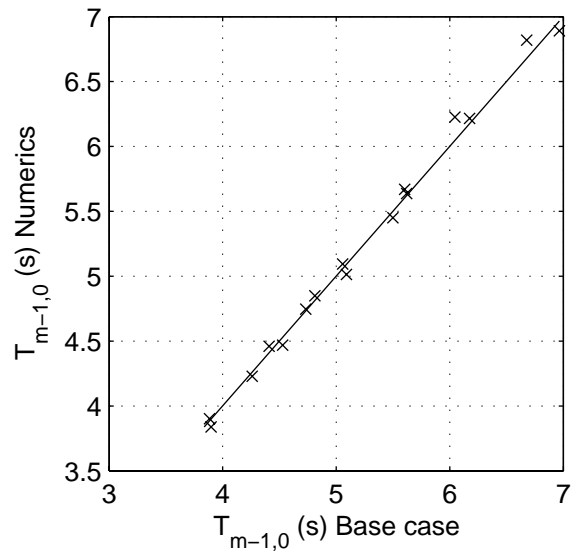
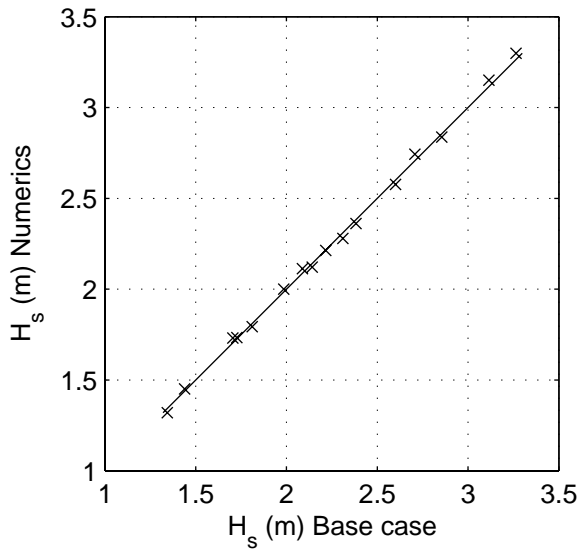
SCAT\_WS\_W01\_N5\_s2p

Calibration SWAN 40.20

A1168

 **Alkyon**

Fig. 4.4.5



Sensitivity of SWAN 40.20 to variation in numerical parameters  
Comparison of base case against:  
Higher directional resolution

Area:WS

Grid:W01

N06

Numerics

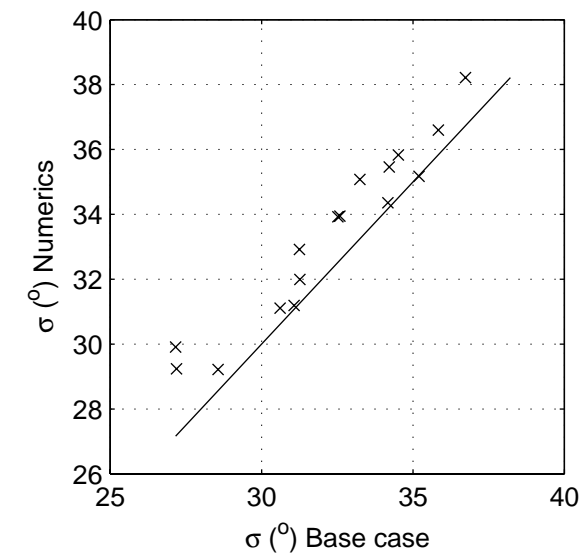
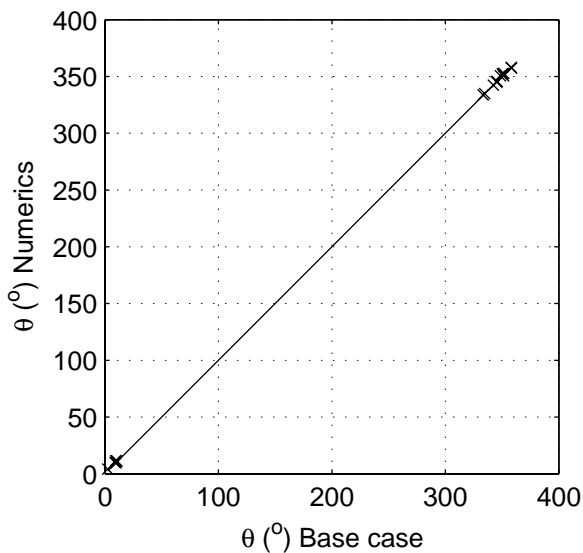
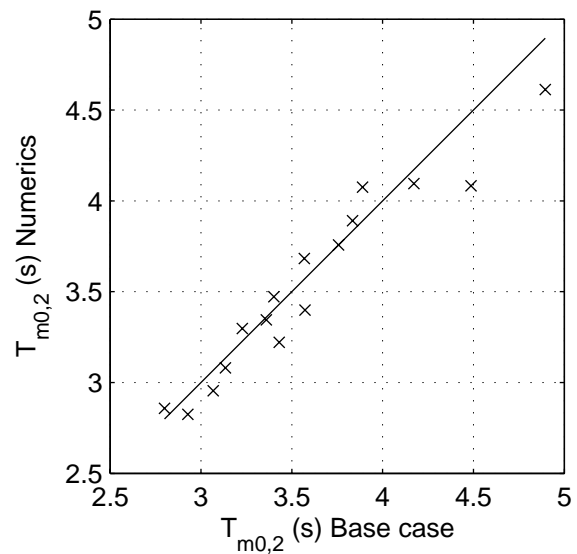
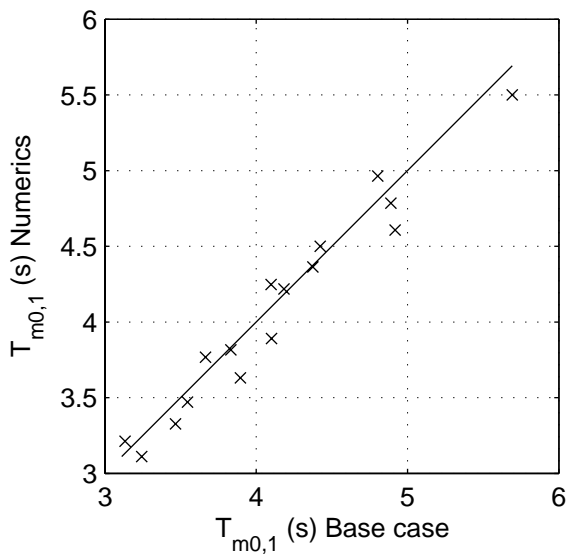
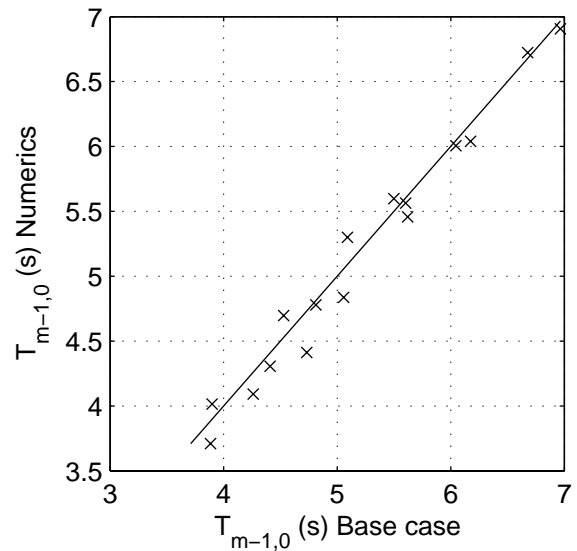
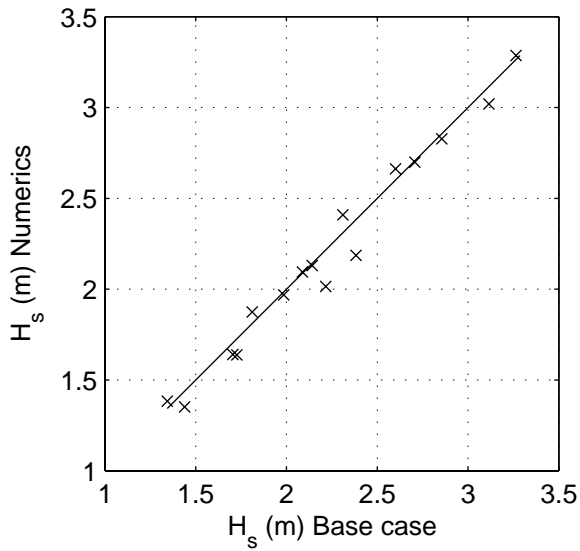
SCAT\_WS\_W01\_N6\_s2p

Calibration SWAN 40.20

A1168

 **Alkyon**

Fig. 4.4.6



Sensitivity of SWAN 40.20 to variation in numerical parameters  
Comparison of base case against:  
Lower directional resolution

Area:WS

Grid:W01

N07

Numerics

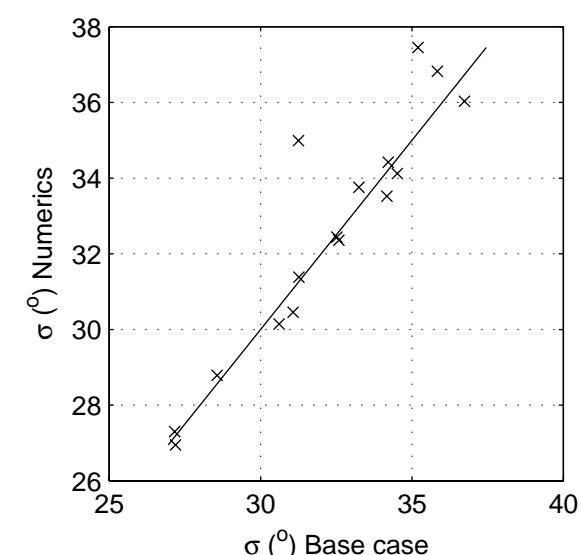
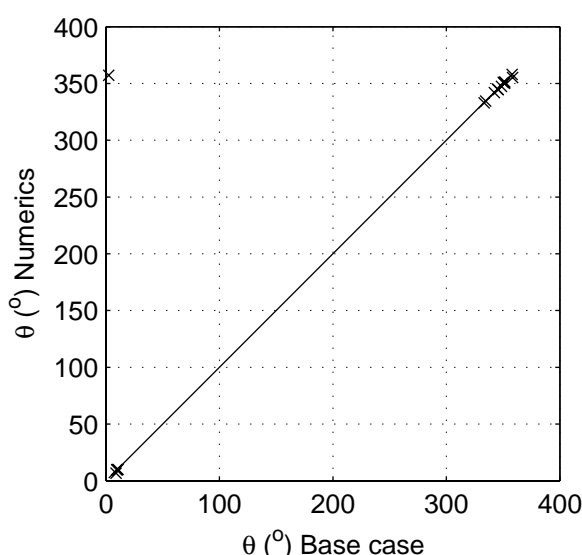
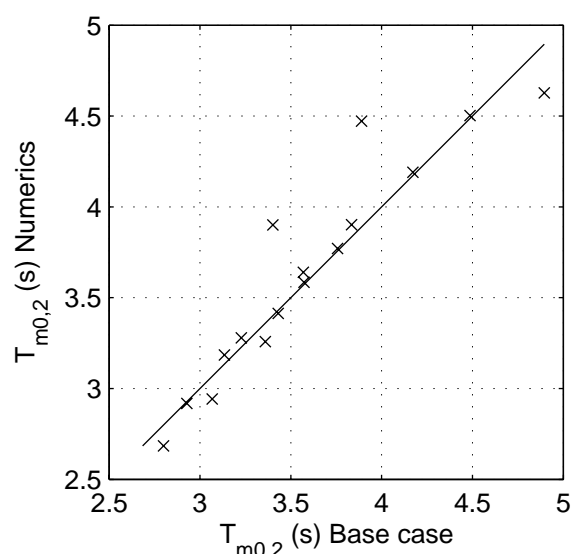
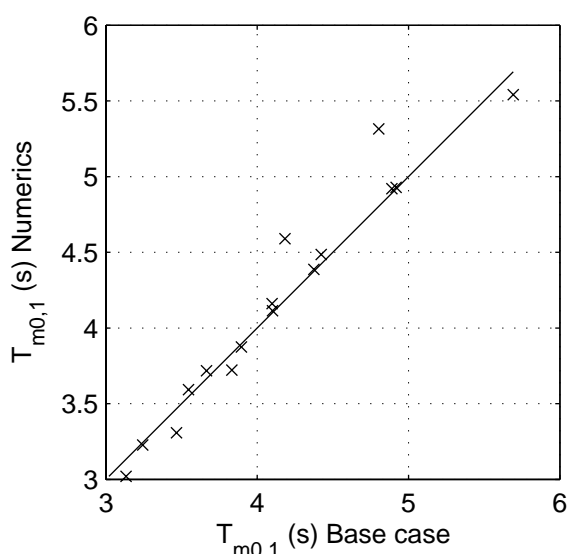
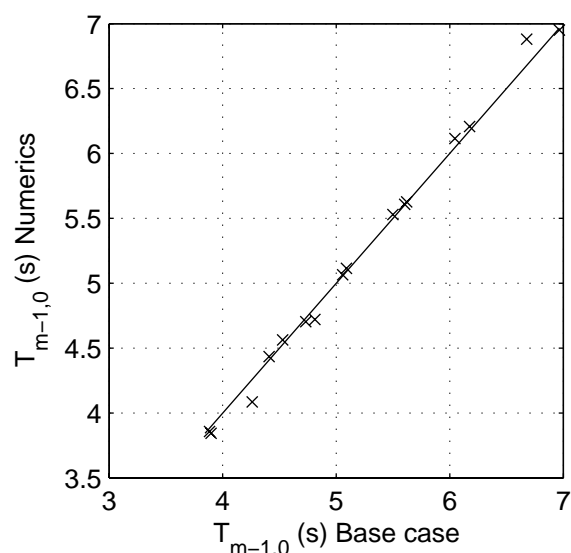
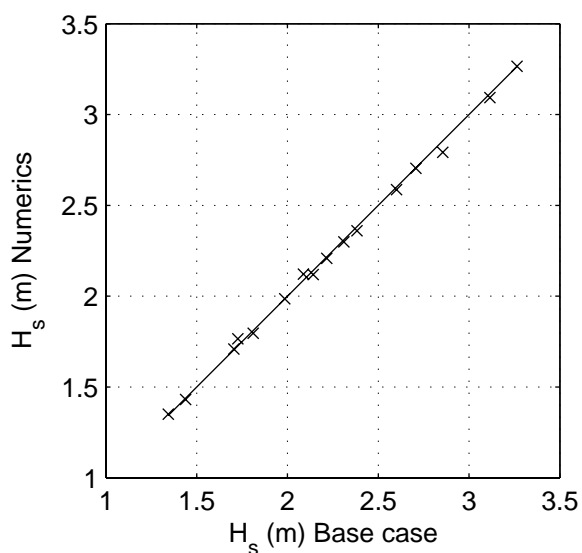
SCAT\_WS\_W01\_N7\_s2p

Calibration SWAN 40.20

A1168

 **Alkyon**

Fig. 4.4.7



Sensitivity of SWAN 40.20 to variation in numerical parameters  
Comparison of base case against:  
Phillips limit 20%

Area:WS

Grid:W01

N08

Numerics

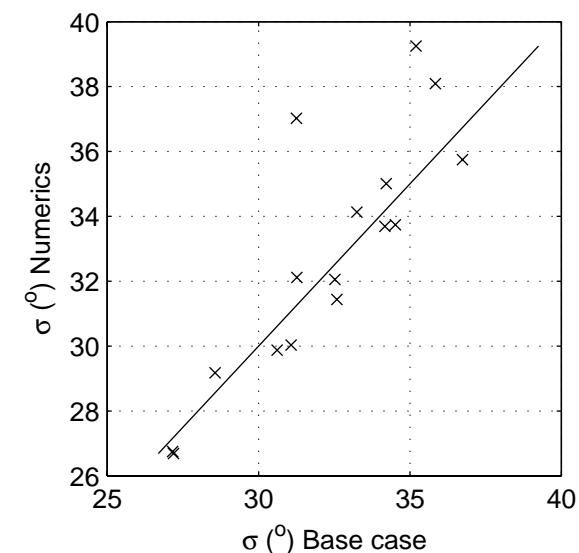
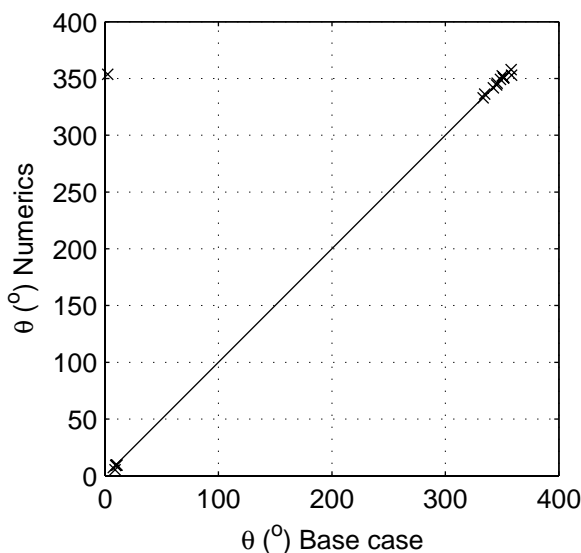
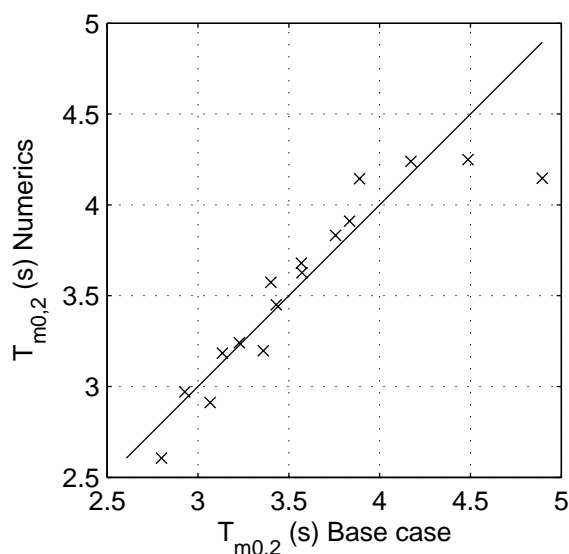
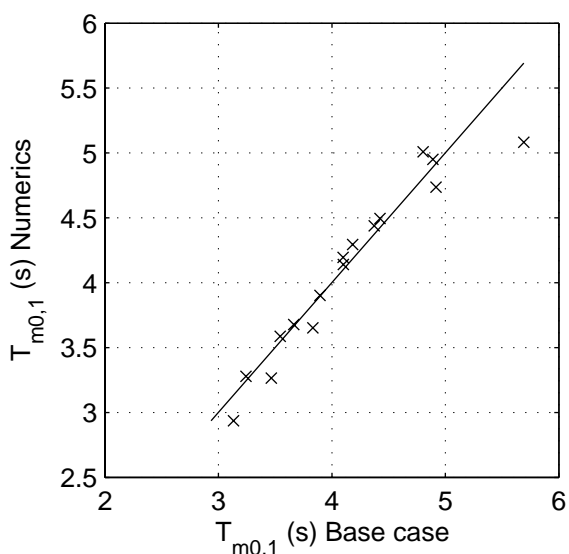
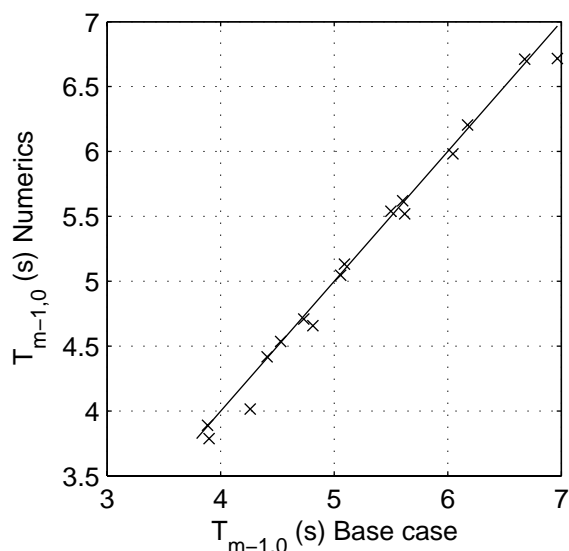
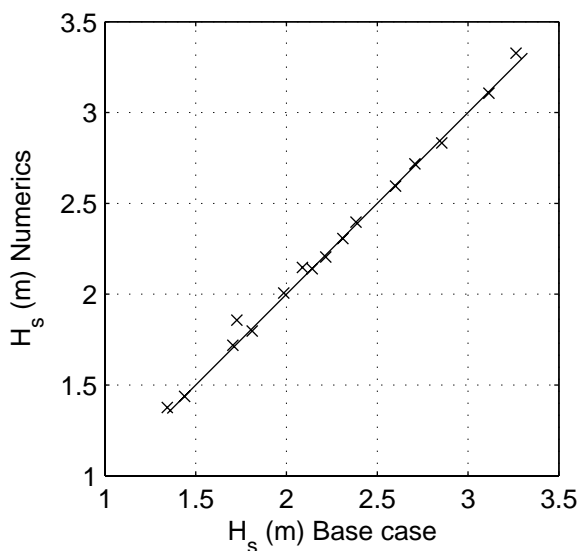
SCAT\_WS\_W01\_N8\_s2p

Calibration SWAN 40.20

A1168

 **Alkyon**

Fig. 4.4.8



Sensitivity of SWAN 40.20 to variation in numerical parameters  
Comparison of base case against:  
Phillips limit 30%

Area:WS

Grid:W01

N09

Numerics

SCAT\_WS\_W01\_N9\_s2p

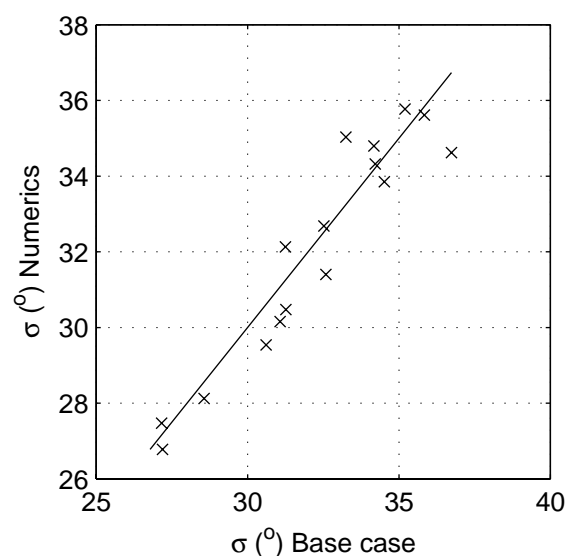
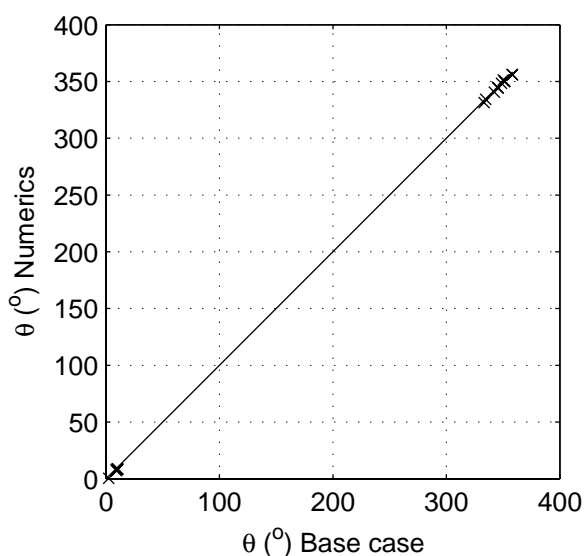
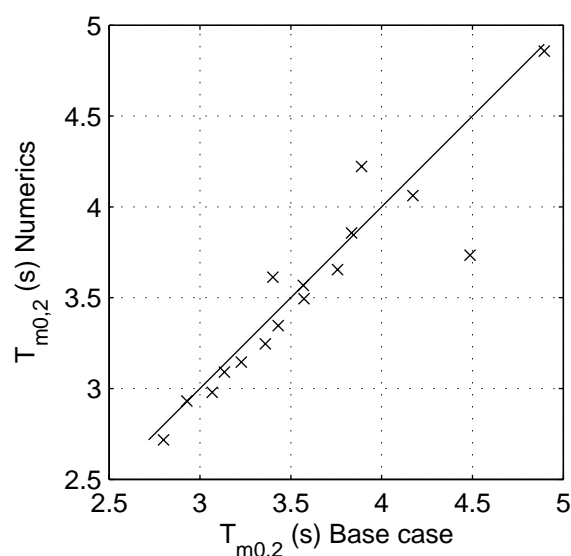
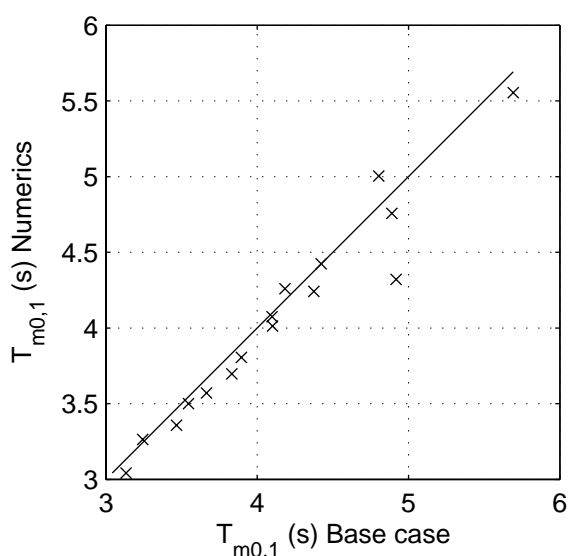
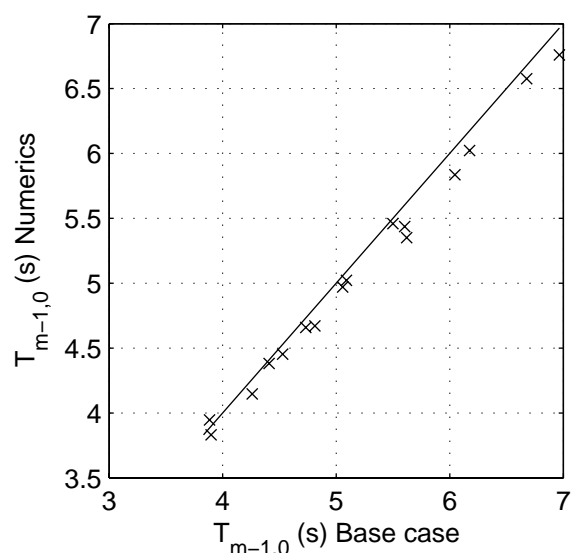
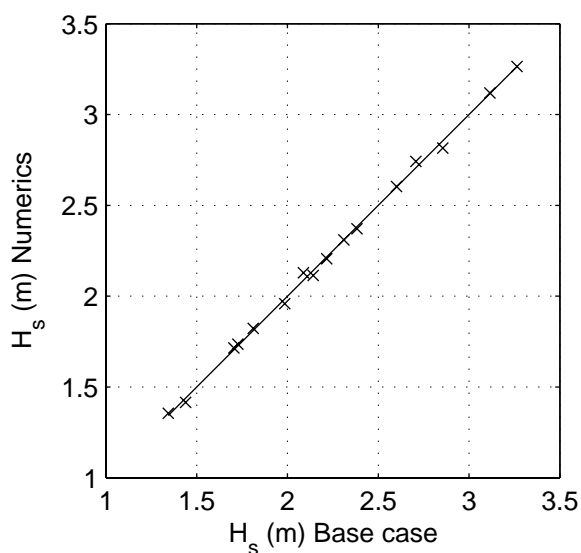
Calibration SWAN 40.20

A1168

 **Alkyon**

Fig. 4.4.9





Sensitivity of SWAN 40.20 to variation in numerical parameters  
Comparison of base case against:  
Under-relaxation  $\alpha=0.025$  Phillip limit 10%

Area:WS

Grid:W01

N10

Numerics

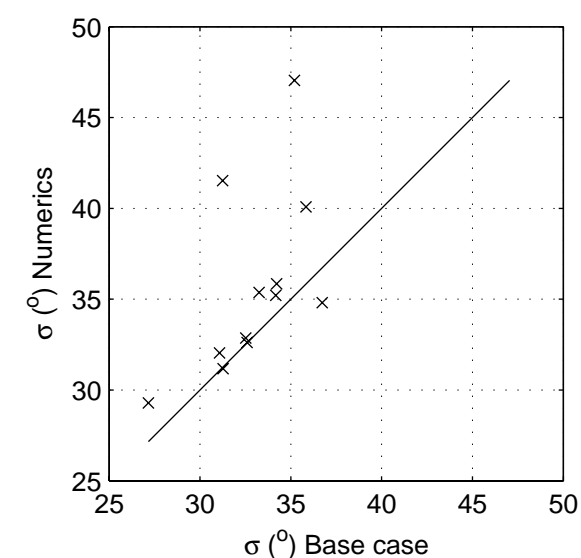
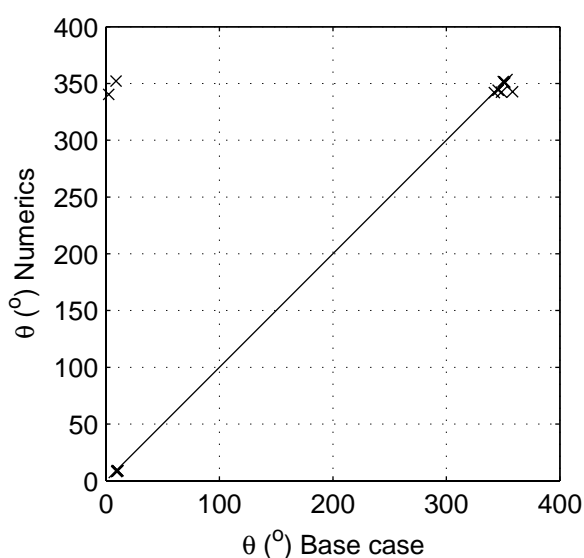
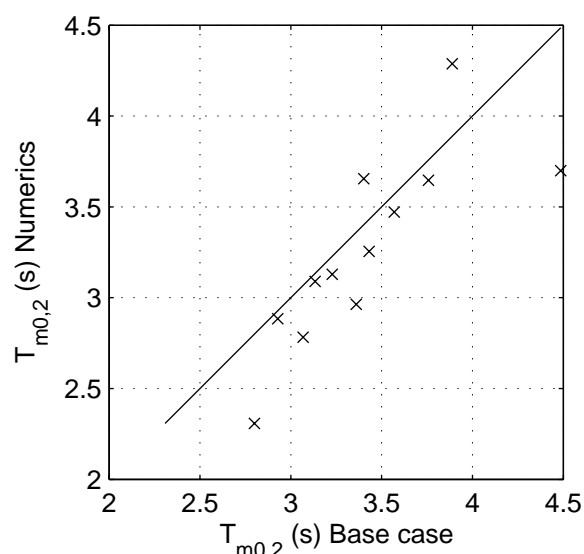
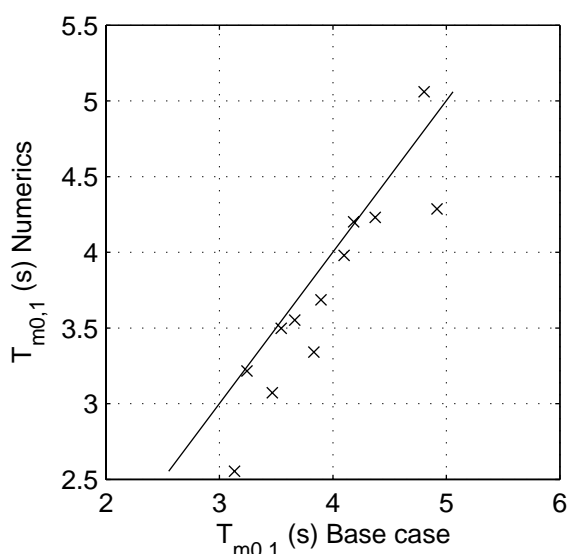
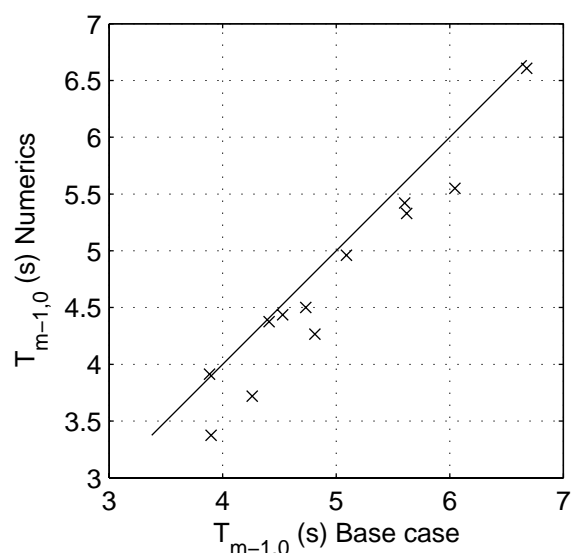
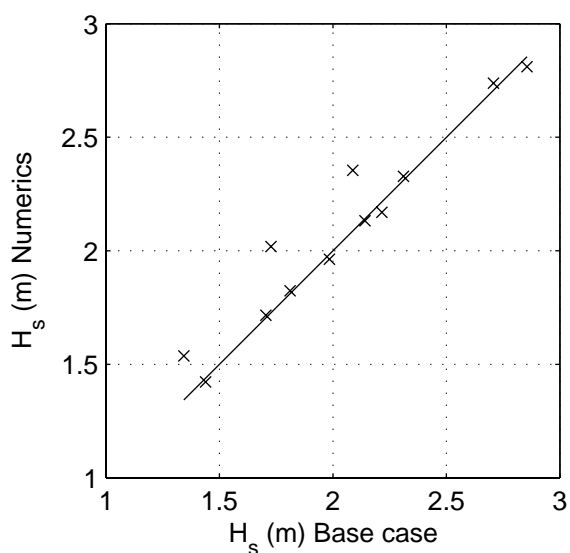
SCAT\_WS\_W01\_N10\_s2p

Calibration SWAN 40.20

A1168

 **Alkyon**

Fig. 4.4.10



Sensitivity of SWAN 40.20 to variation in numerical parameters  
Comparison of base case against:  
Under-relaxation  $\alpha=0.025$  Phillip limit 50%

Area:WS

Grid:W01

N11

Numerics

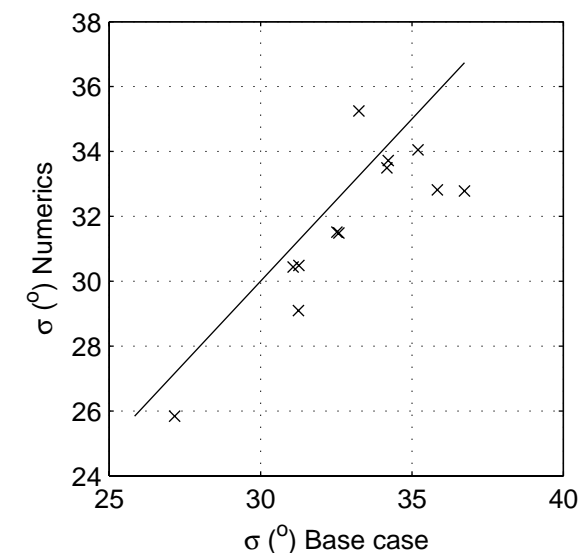
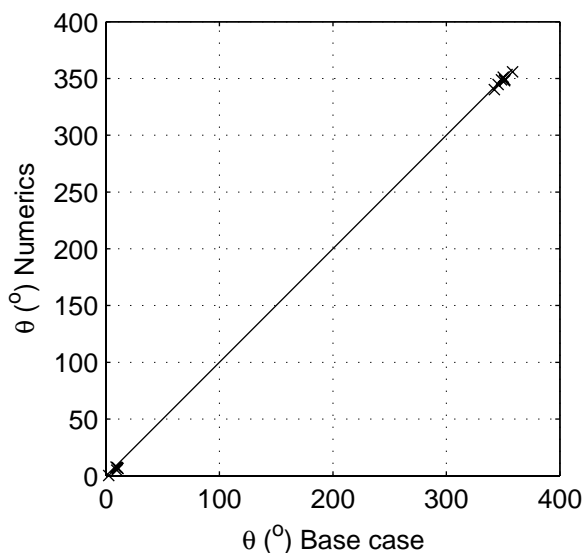
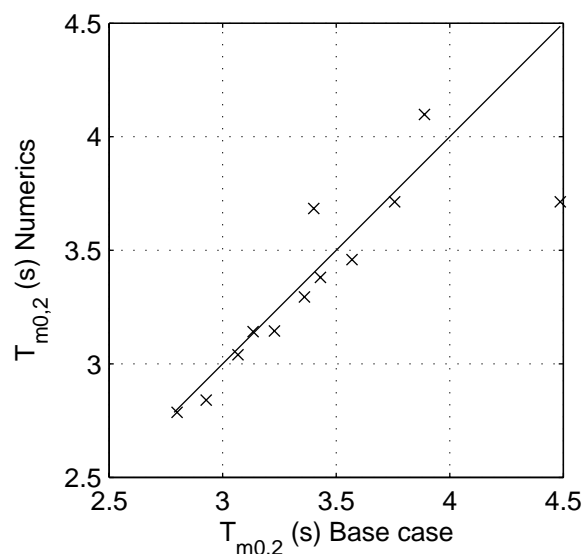
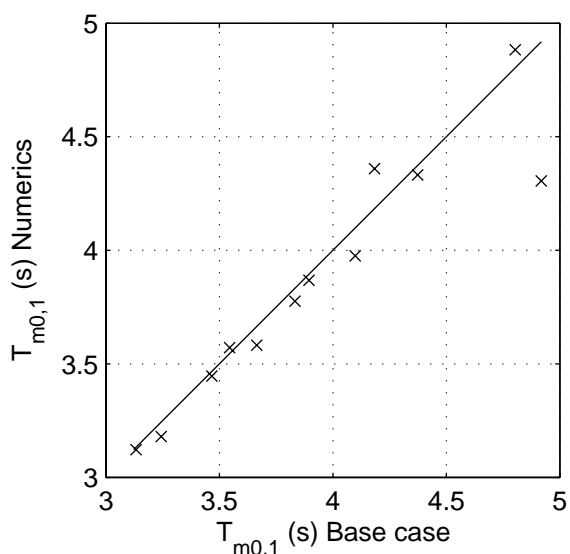
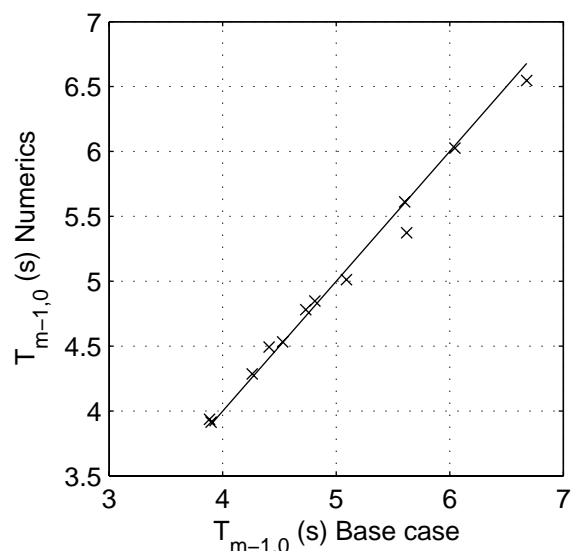
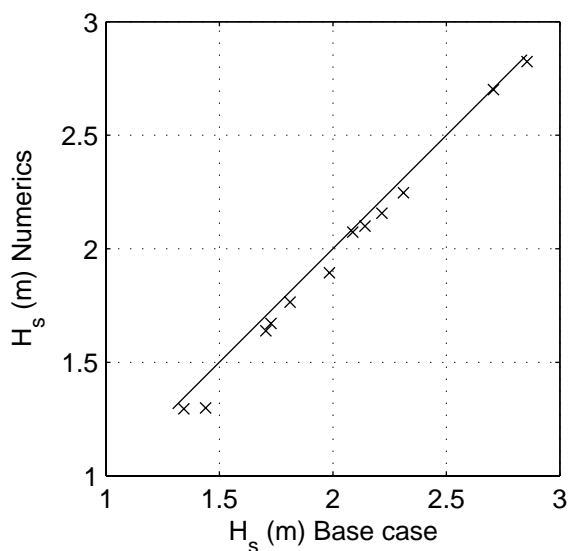
SCAT\_WS\_W01\_N11\_s2p

Calibration SWAN 40.20

A1168

 **Alkyon**

Fig. 4.4.11



Sensitivity of SWAN 40.20 to variation in numerical parameters  
Comparison of base case against:  
Under-relaxation  $\alpha=0.05$  Phillip limit 10%

Area:WS

Grid:W01

N12

Numerics

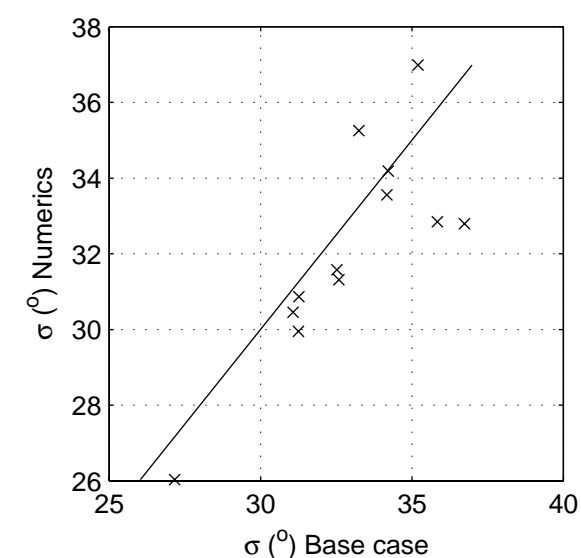
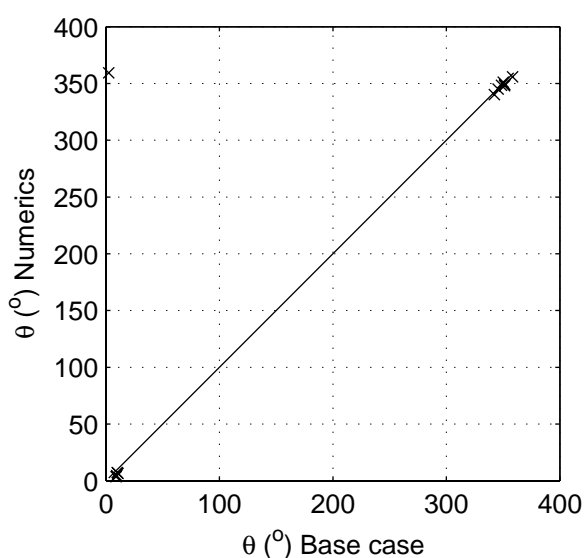
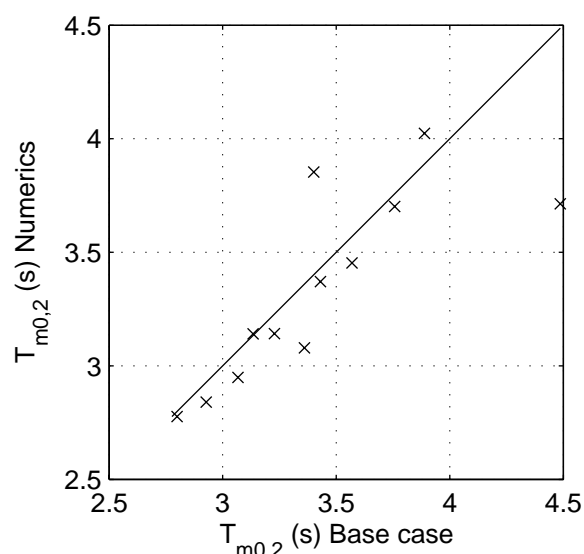
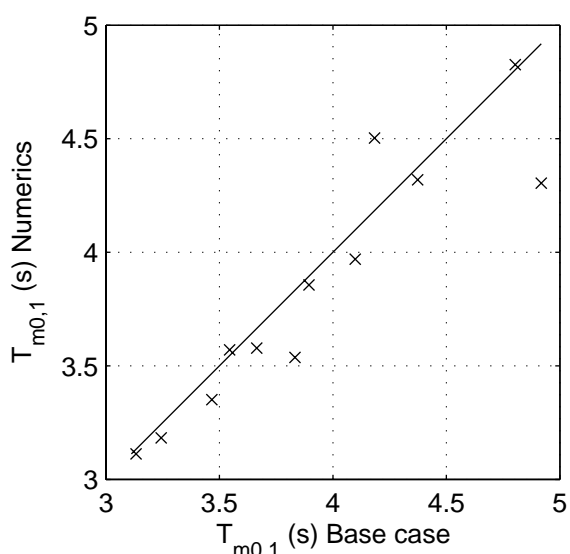
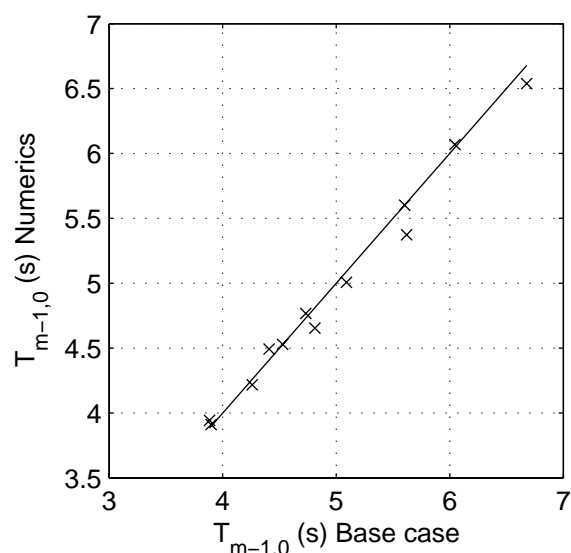
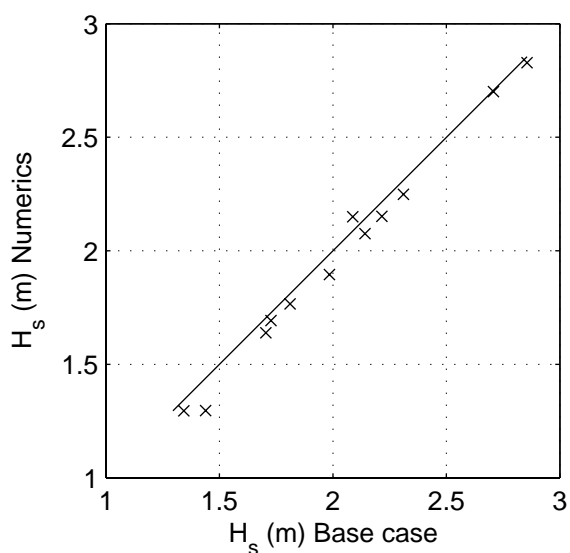
SCAT\_WS\_W01\_N12\_s2p

Calibration SWAN 40.20

A1168

 **Alkyon**

Fig. 4.4.12



Sensitivity of SWAN 40.20 to variation in numerical parameters  
Comparison of base case against:  
Under-relaxation  $\alpha=0.05$  Phillip limit 50%

Area:WS

Grid:W01

N13

Numerics

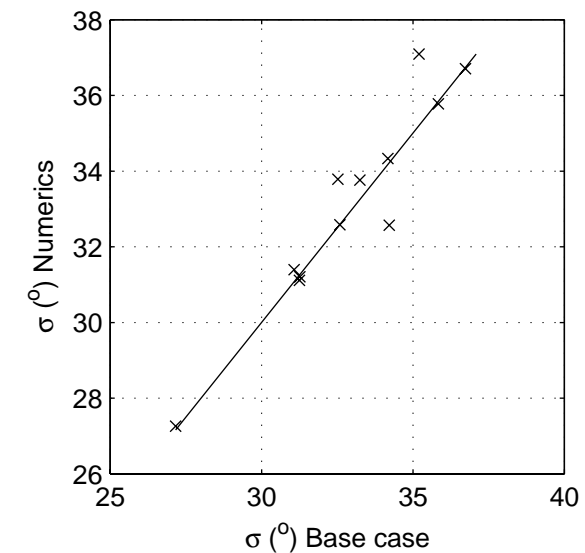
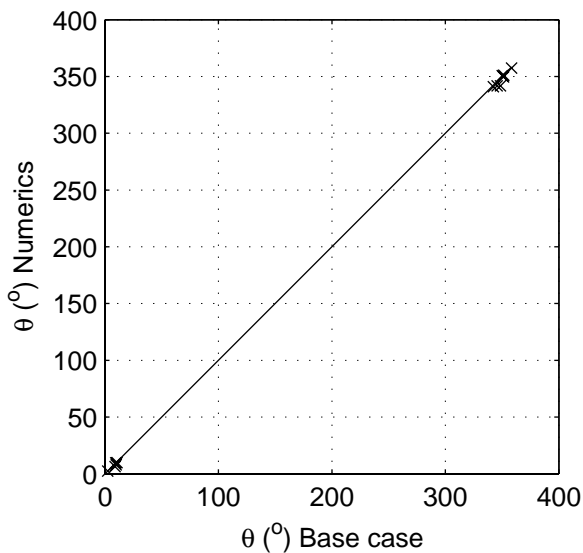
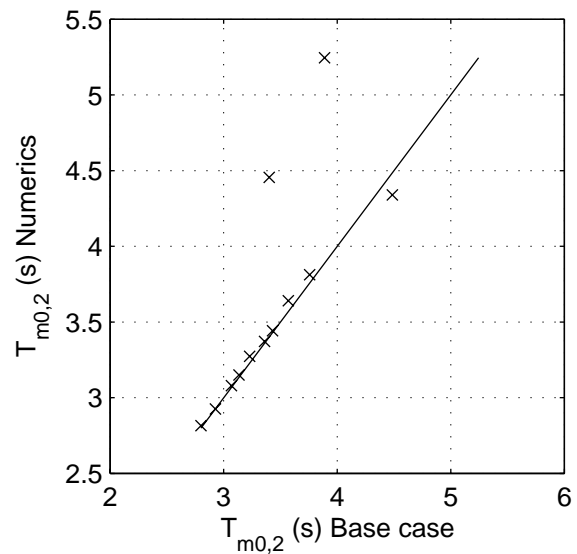
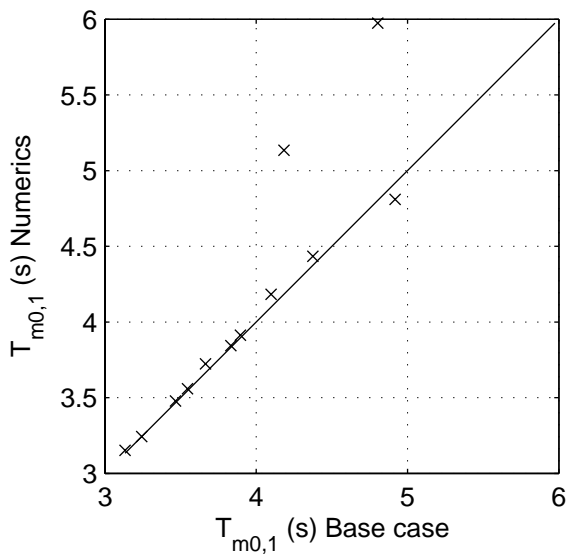
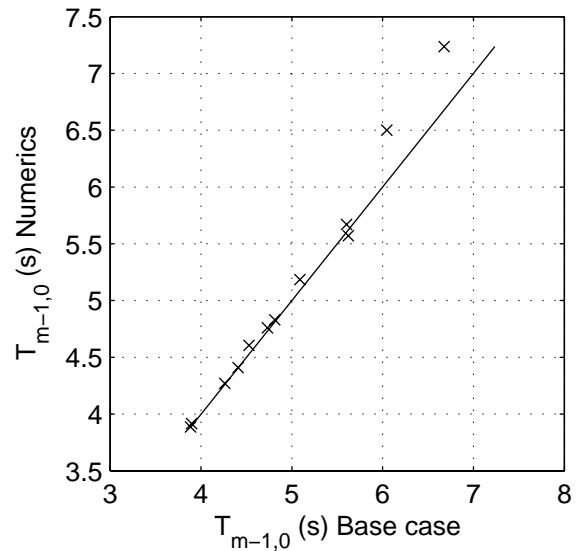
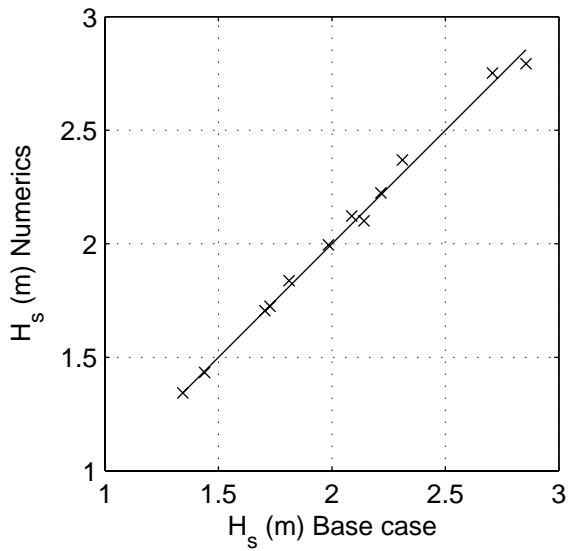
SCAT\_WS\_W01\_N13\_s2p

Calibration SWAN 40.20

A1168

 **Alkyon**

Fig. 4.4.13



Sensitivity of SWAN 40.20 to variation in numerical parameters  
Comparison of base case against:  
Inclusive triads and quadruplets,  $Q_b = 0.00001$

Area:WS

Grid:W01

N14

Numerics

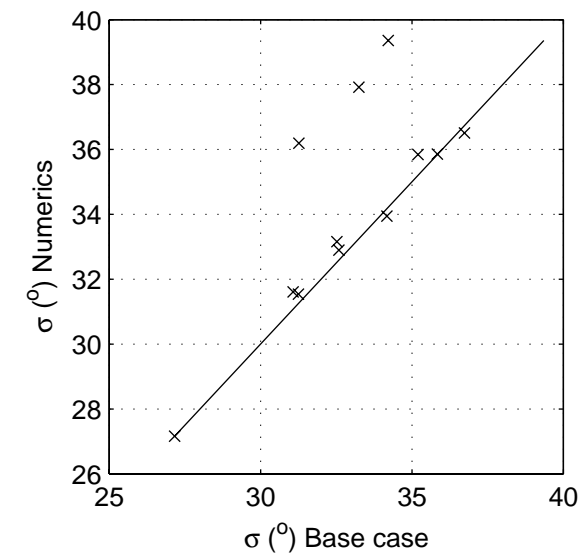
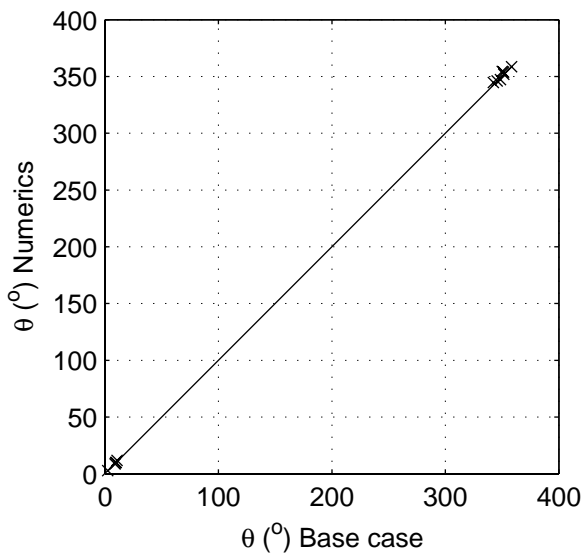
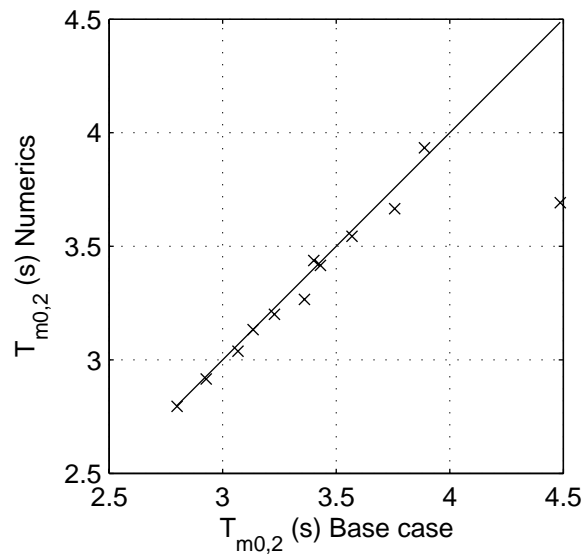
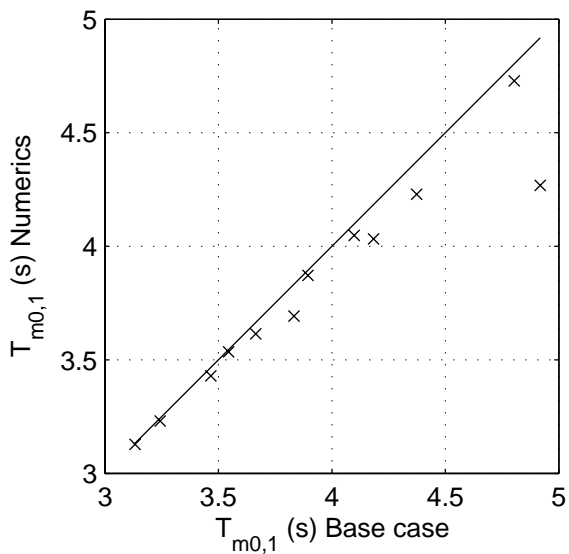
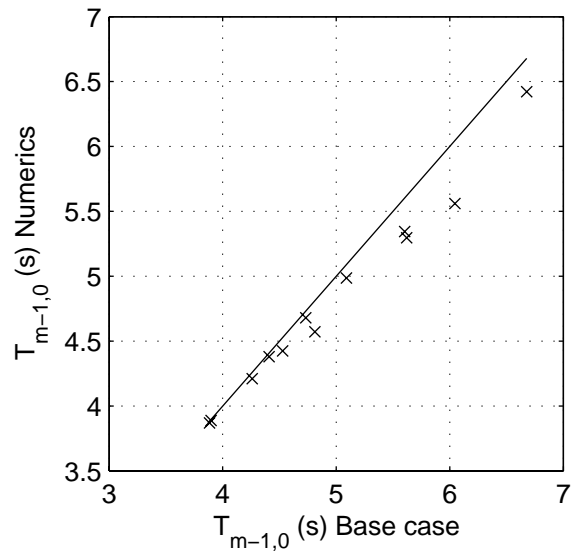
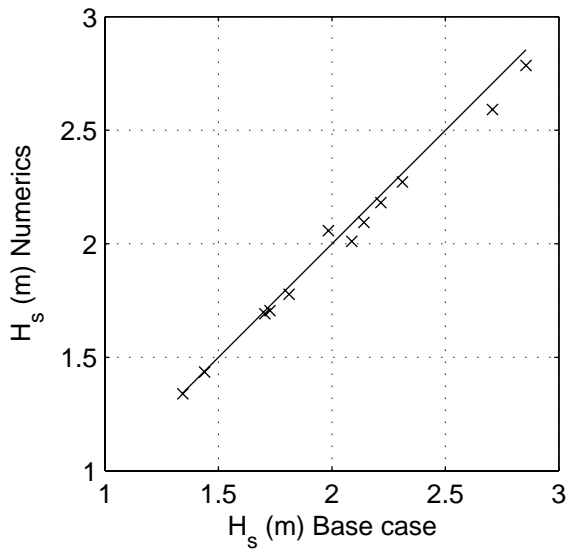
SCAT\_WS\_W01\_N14\_s2p

Calibration SWAN 40.20

A1168

 **Alkyon**

Fig. 4.4.14



Sensitivity of SWAN 40.20 to variation in numerical parameters  
Comparison of base case against:  
Exclusive triads and quadruplets,  $Q_b = 1.0$

Area:WS

Grid:W01

N15

Numerics

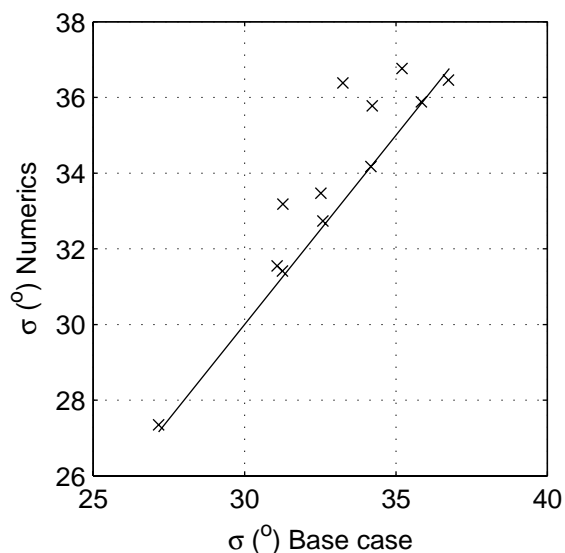
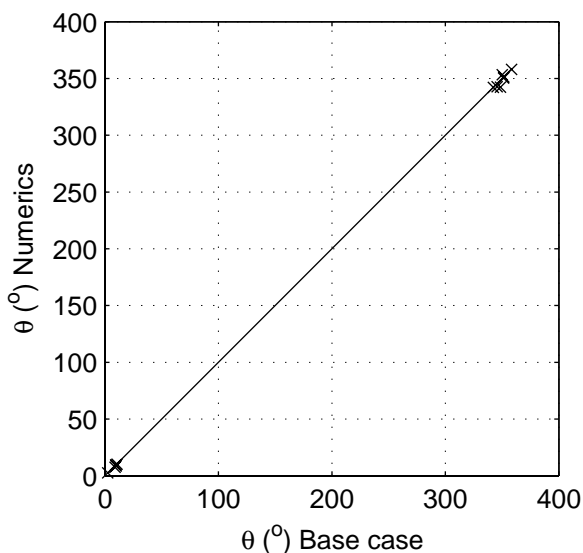
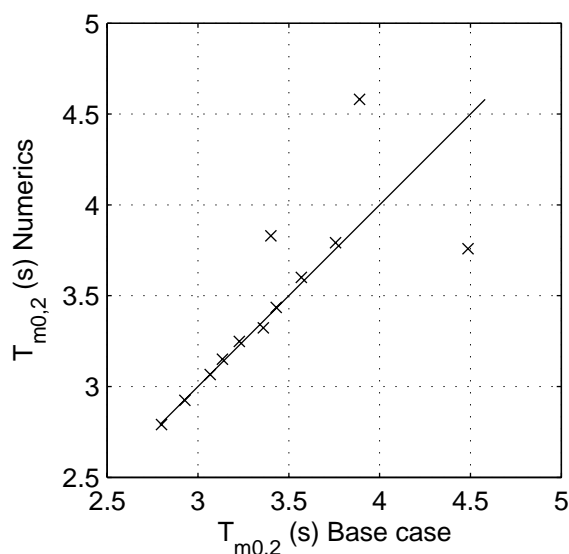
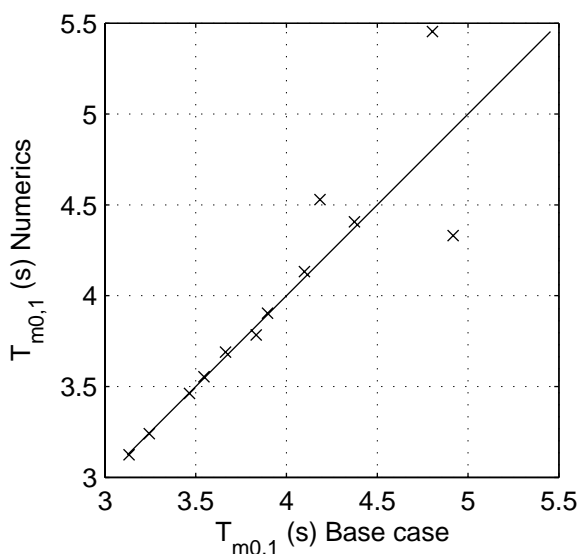
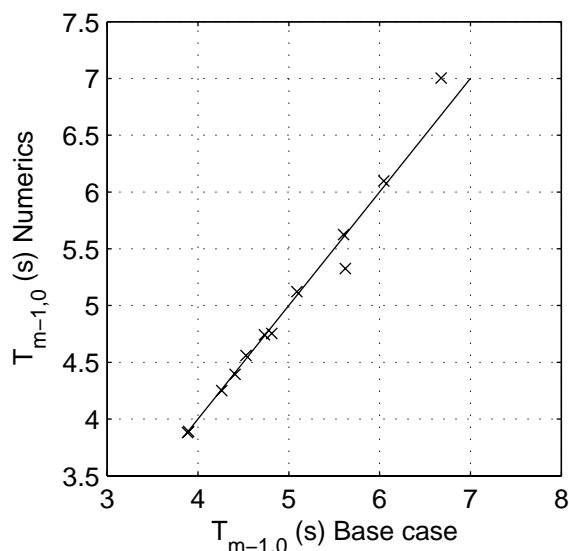
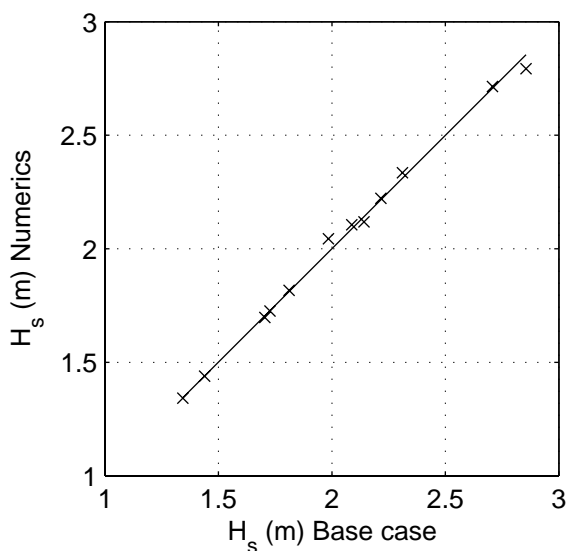
SCAT\_WS\_W01\_N15\_s2p

Calibration SWAN 40.20

A1168

 **Alkyon**

Fig. 4.4.15



Sensitivity of SWAN 40.20 to variation in numerical parameters  
Comparison of base case against:  
Inclusive triads and quadruplets,  $Q_b = 1.0$

Area:WS

Grid:W01

N16

Numerics

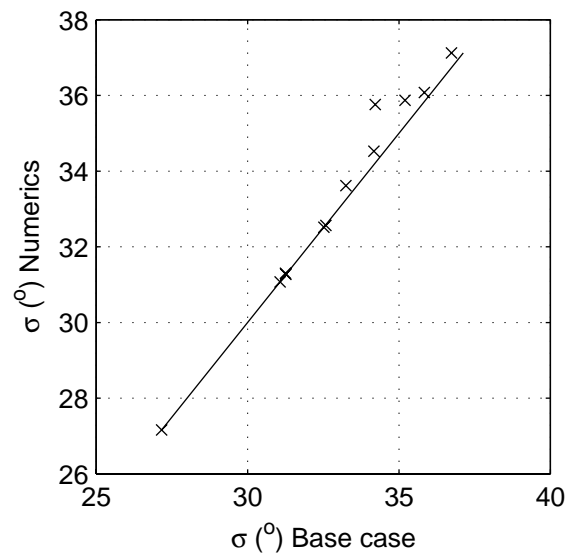
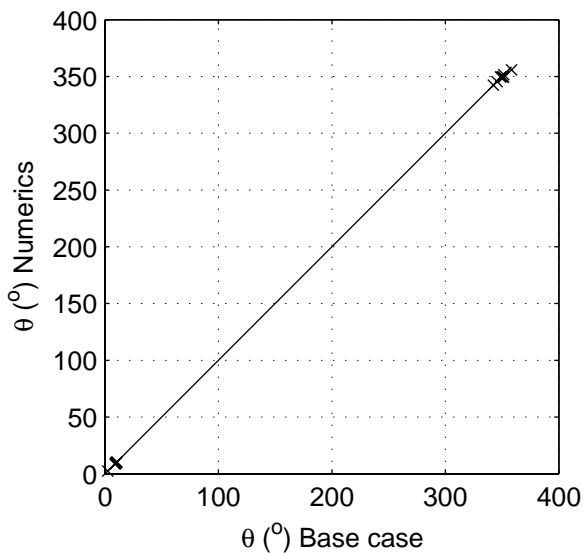
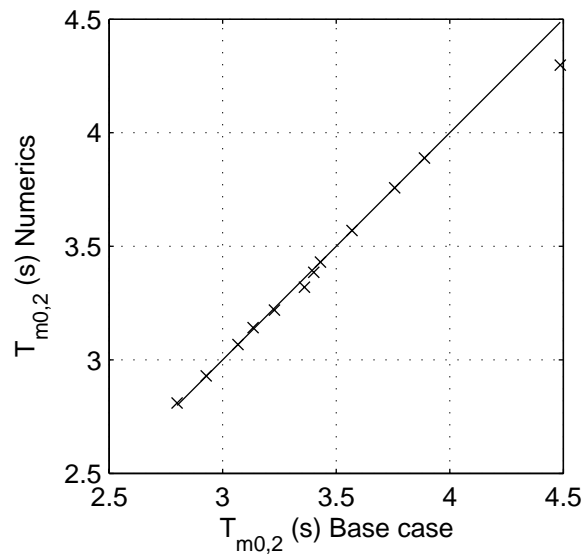
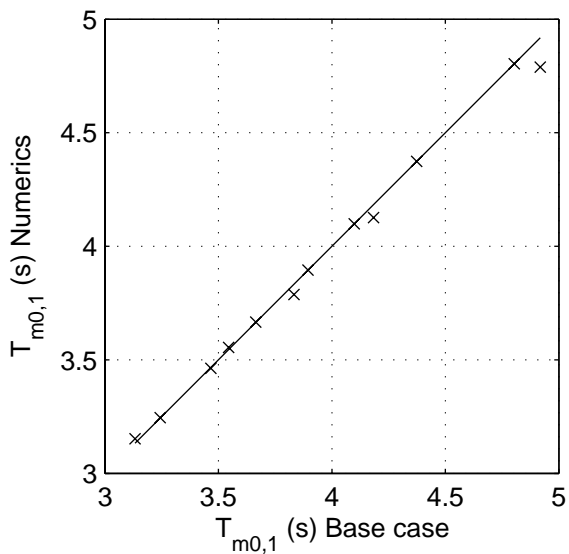
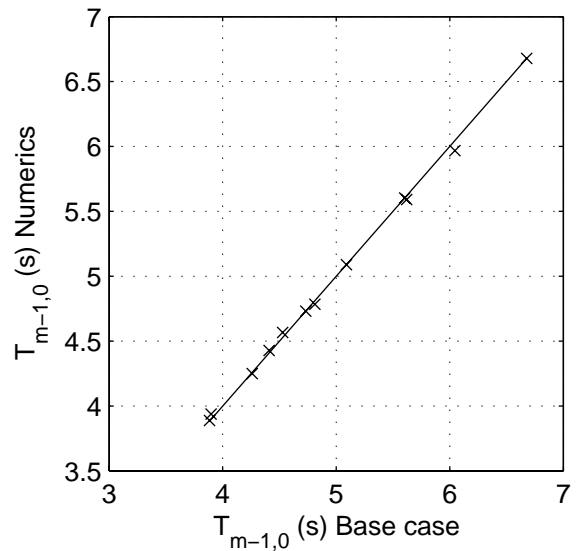
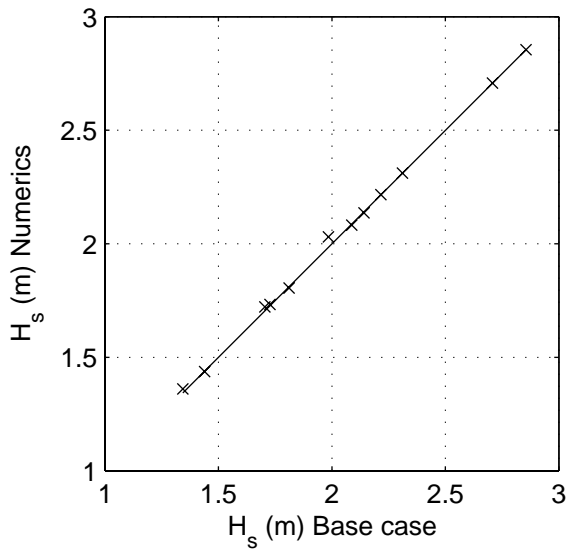
SCAT\_WS\_W01\_N16\_s2p

Calibration SWAN 40.20

A1168

 **Alkyon**

Fig. 4.4.16



Sensitivity of SWAN 40.20 to variation in numerical parameters  
Comparison of base case against:  
Convergence criterion 0.02% & 98%

Area:WS

Grid:W01

N17

Numerics

SCAT\_WS\_W01\_N17\_s2p

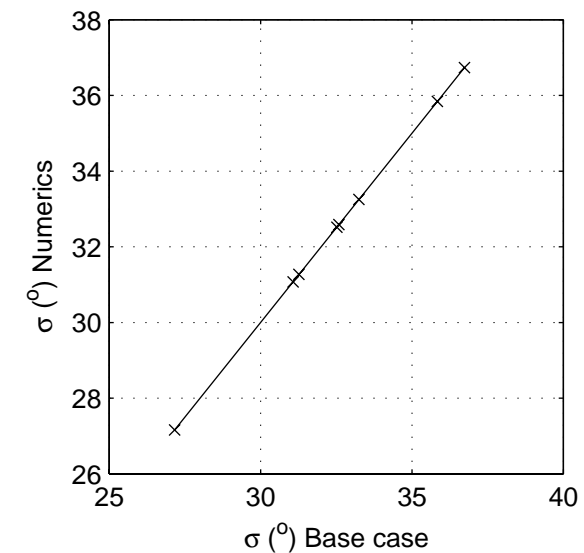
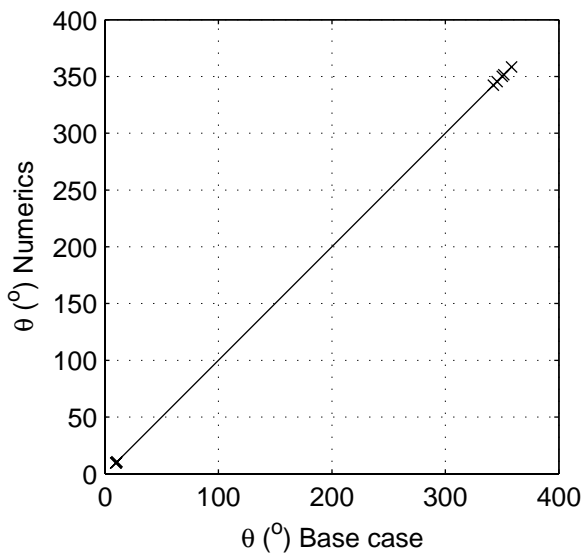
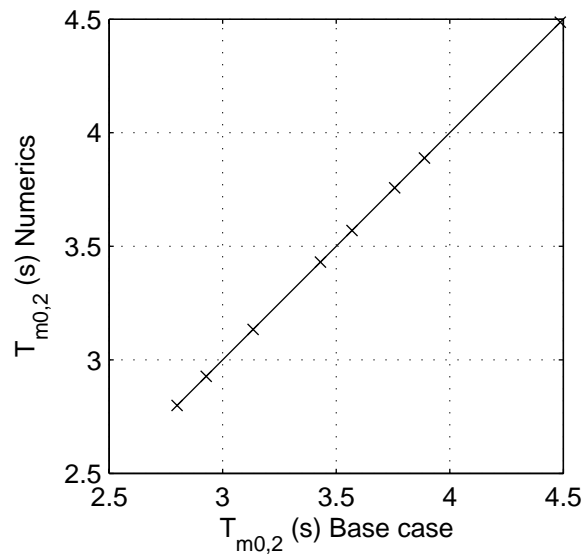
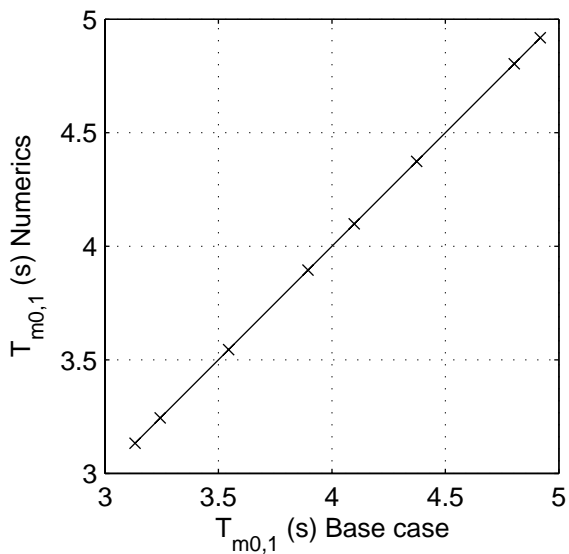
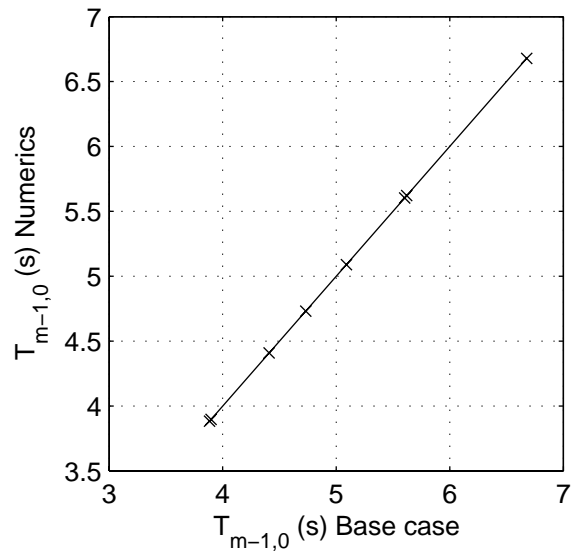
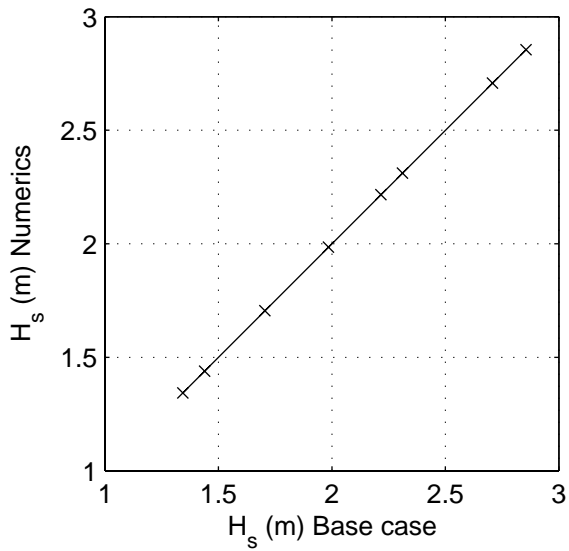
Calibration SWAN 40.20

A1168

 **Alkyon**

Fig. 4.4.17





Sensitivity of SWAN 40.20 to variation in numerical parameters  
Comparison of base case against:  
Convergence criterion 0.01% & 99%

Area:WS

Grid:W01

N18

Numerics

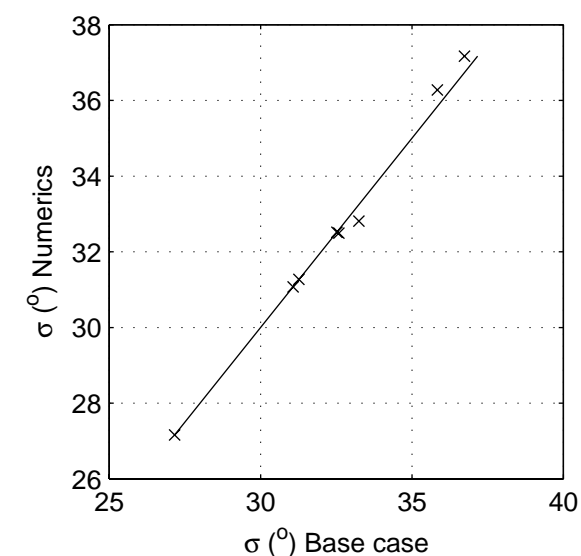
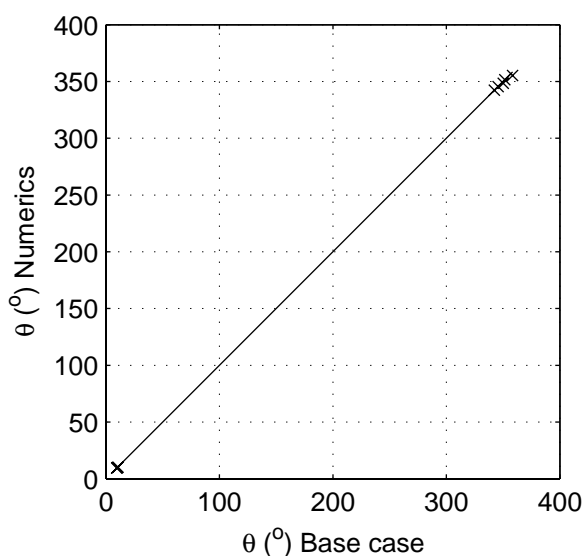
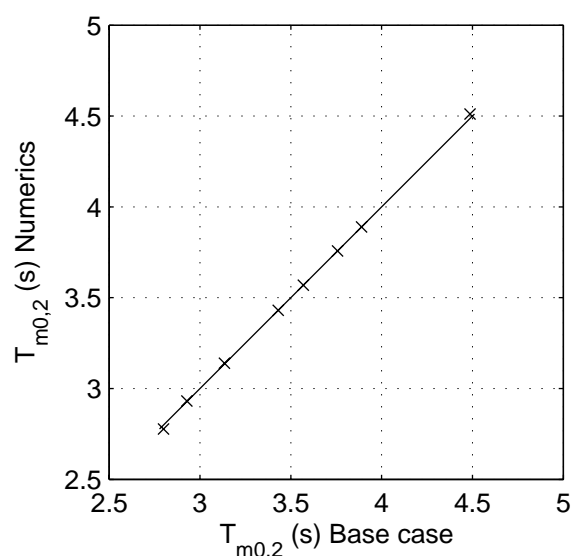
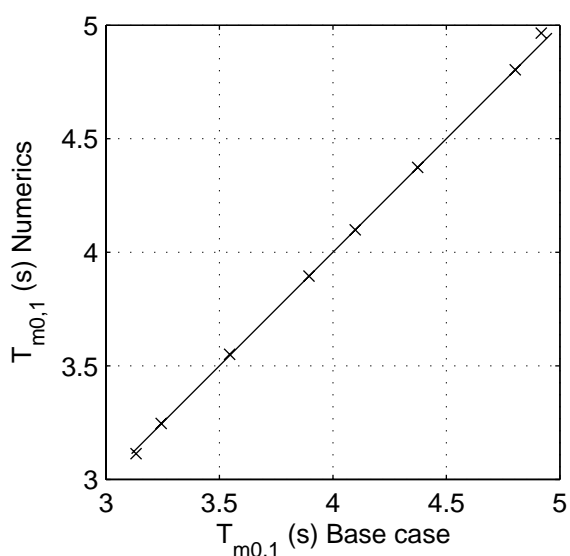
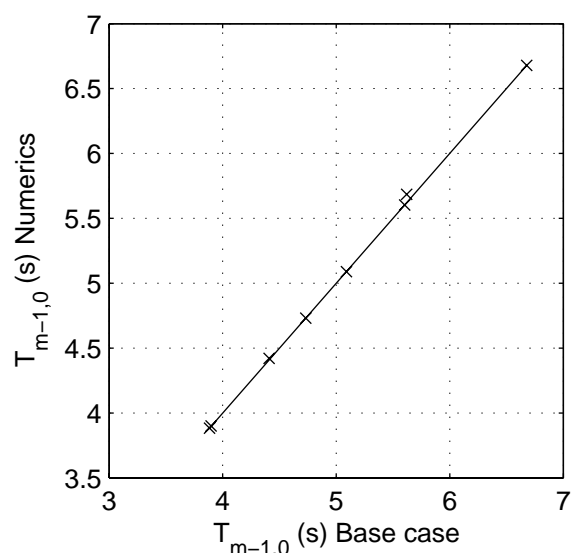
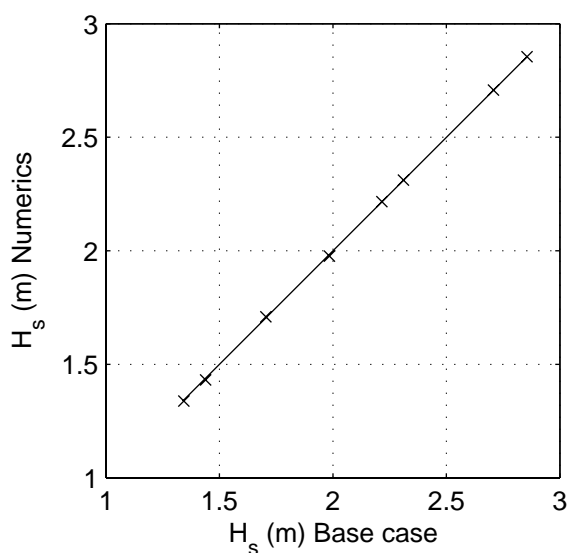
SCAT\_WS\_W01\_N18\_s2p

Calibration SWAN 40.20

A1168

 **Alkyon**

Fig. 4.4.18



Sensitivity of SWAN 40.20 to variation in numerical parameters  
Comparison of base case against:  
Convergence criterion 0.03% & 97%

Area:WS

Grid:W01

N19

Numerics

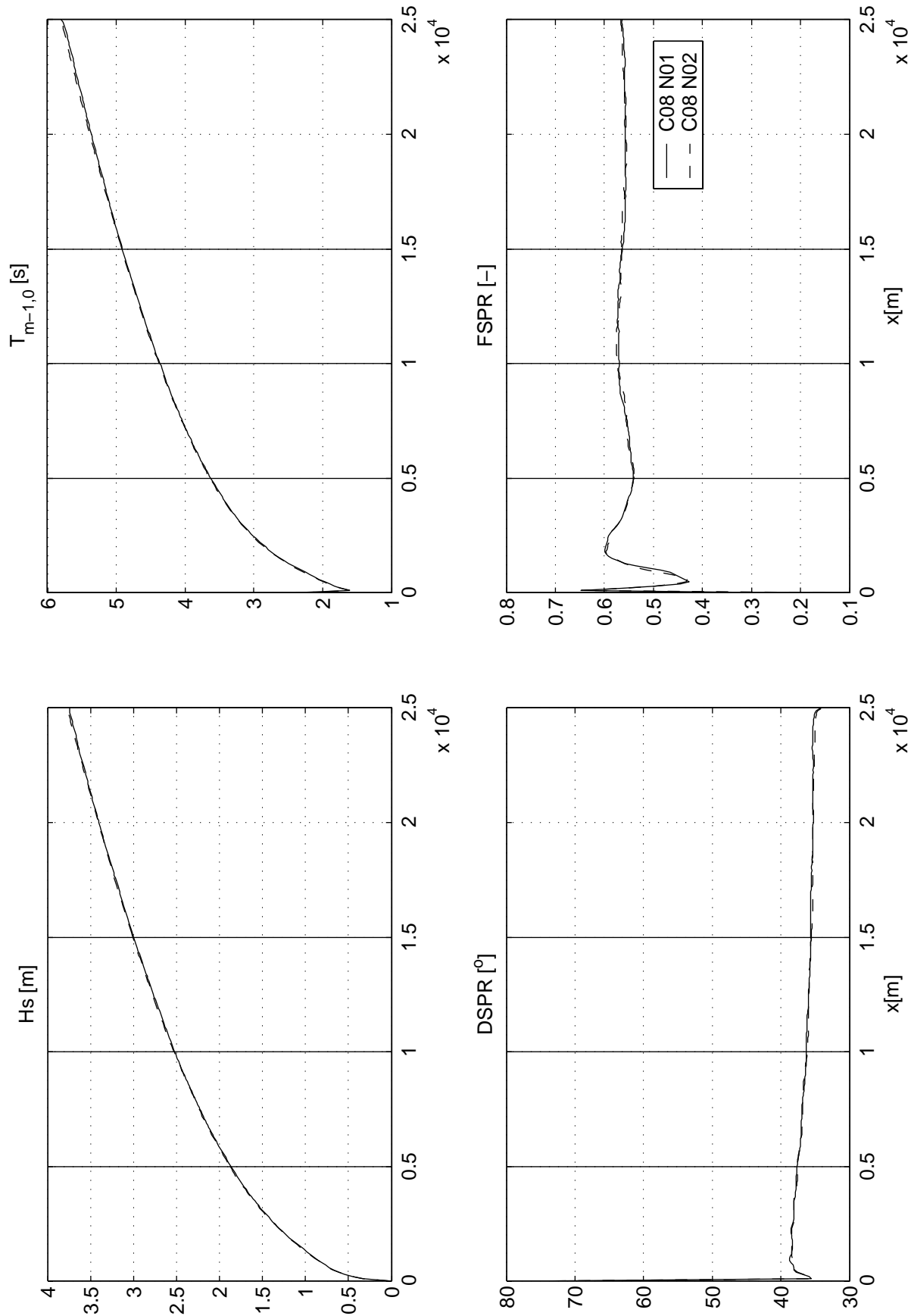
SCAT\_WS\_W01\_N19\_s2p

Calibration SWAN 40.20

A1168

 **Alkyon**

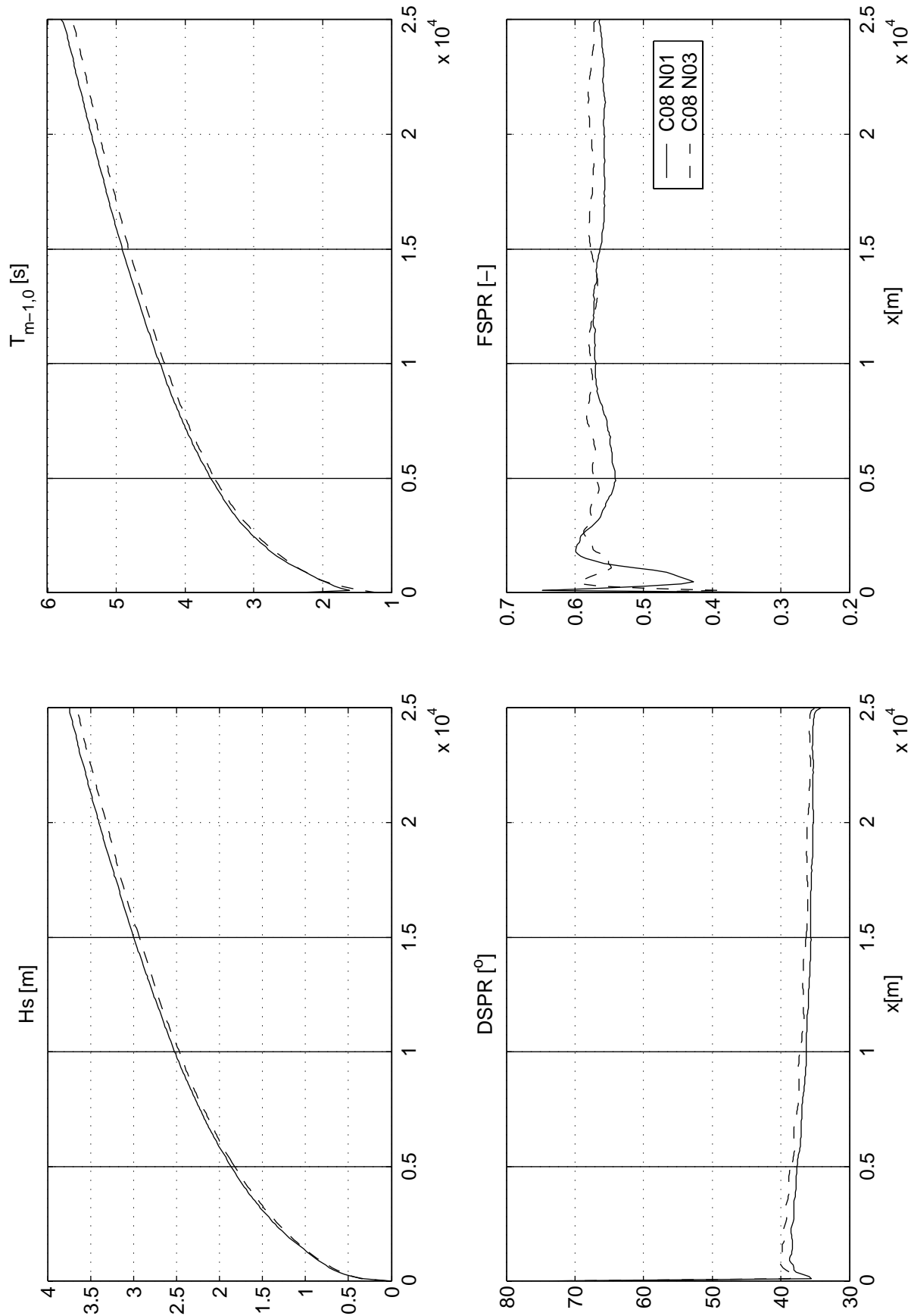
Fig. 4.4.19



Spatial variation of integral wave parameters along fetch  
Fetch limited wave growth.  
Numerical Case:flow; depth=10 m ; u10=30m/s

FL\_C08

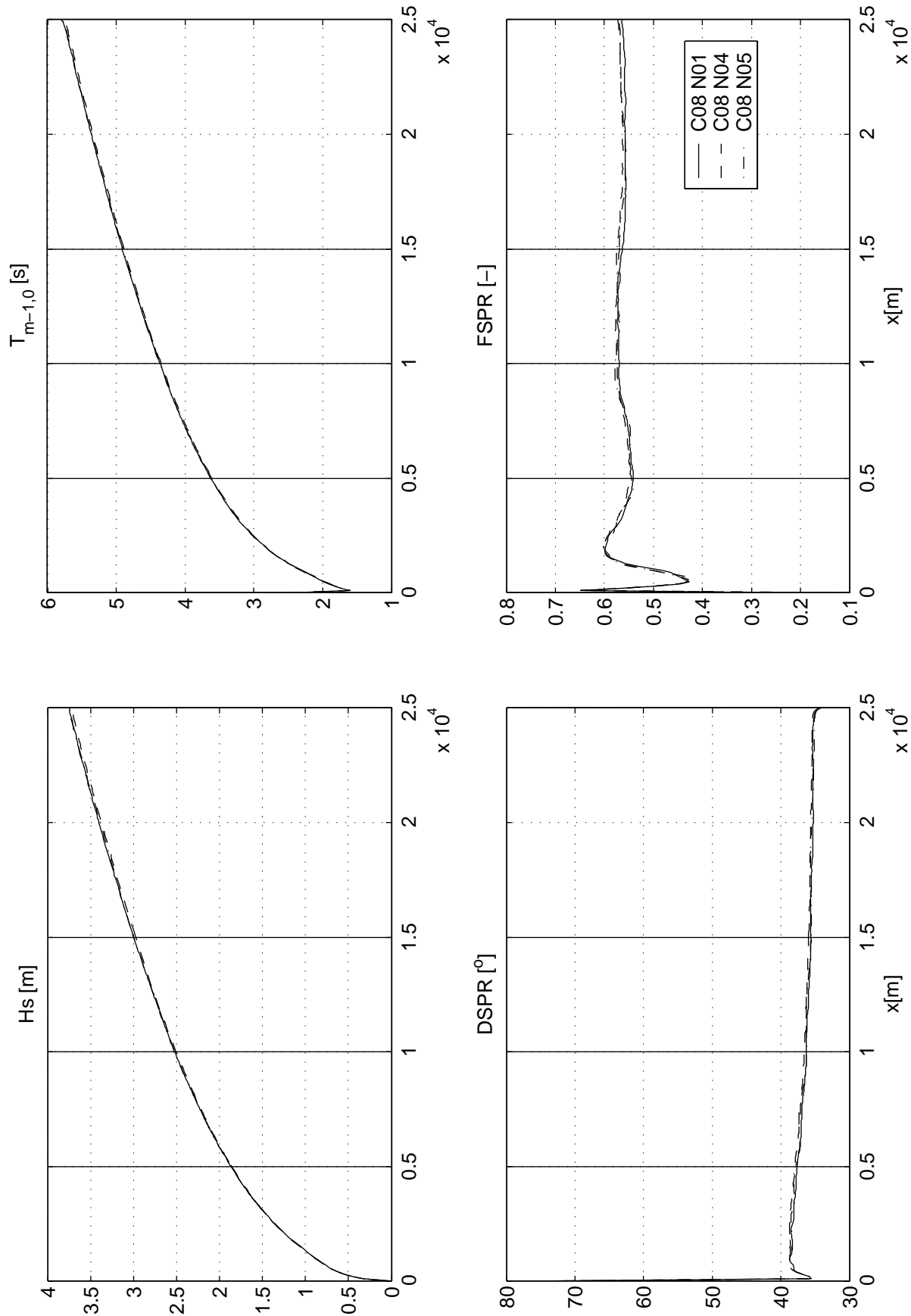
Fetch Limited



Spatial variation of integral wave parameters along fetch  
Fetch limited wave growth.  
Numerical Case:fhigh; depth=10 m ; u10=30m/s

FL\_C08

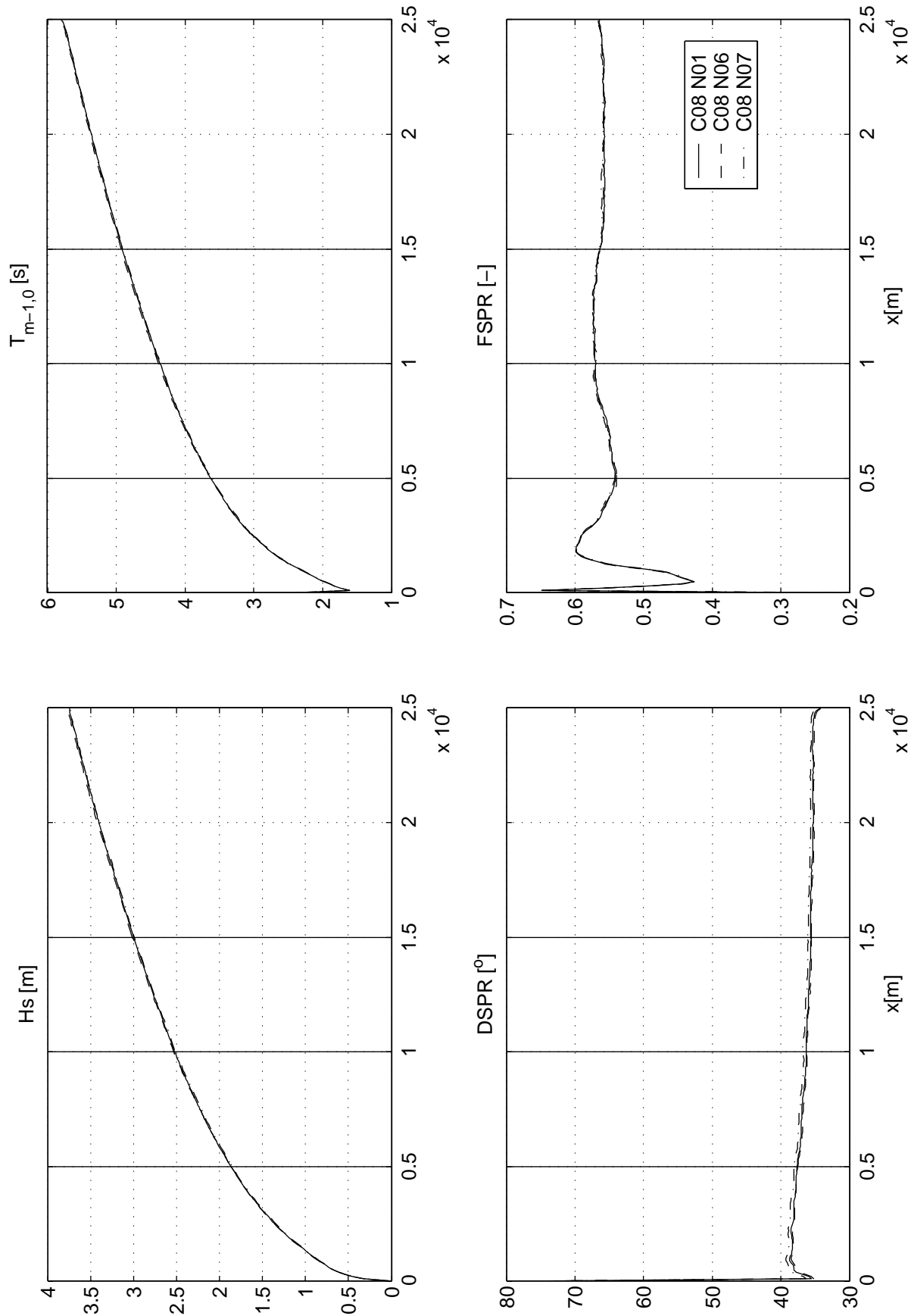
Fetch Limited



Spatial variation of integral wave parameters along fetch  
Fetch limited wave growth.  
Numerical Case:msc; depth=10 m ; u10=30m/s

FL\_C08

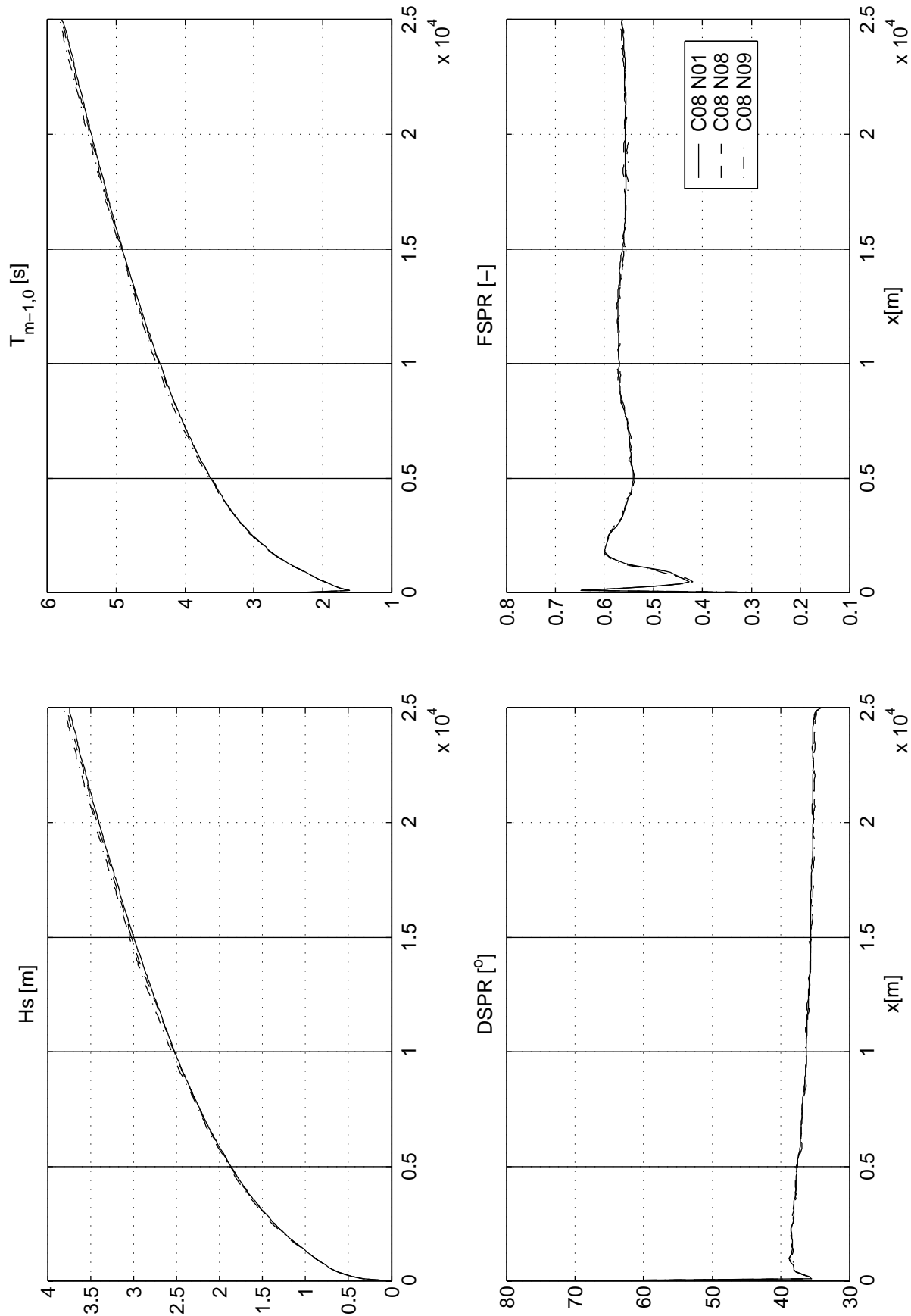
Fetch Limited



Spatial variation of integral wave parameters along fetch  
Fetch limited wave growth.  
Numerical Case:mdc; depth=10 m ; u10=30m/s

FL\_C08

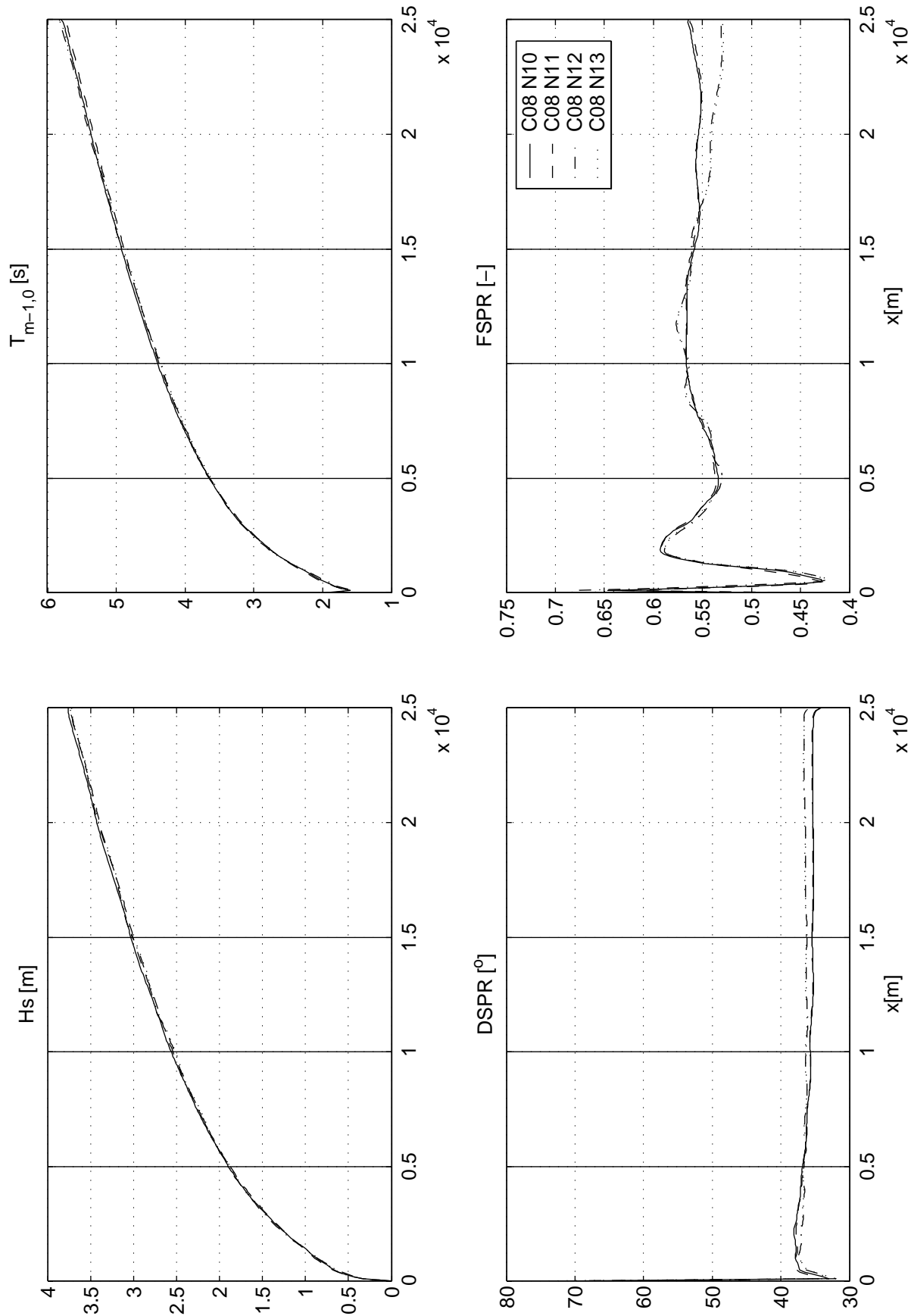
Fetch Limited



Spatial variation of integral wave parameters along fetch  
Fetch limited wave growth.  
Numerical Case:limiter; depth=10 m ; u10=30m/s

FL\_C08

Fetch Limited

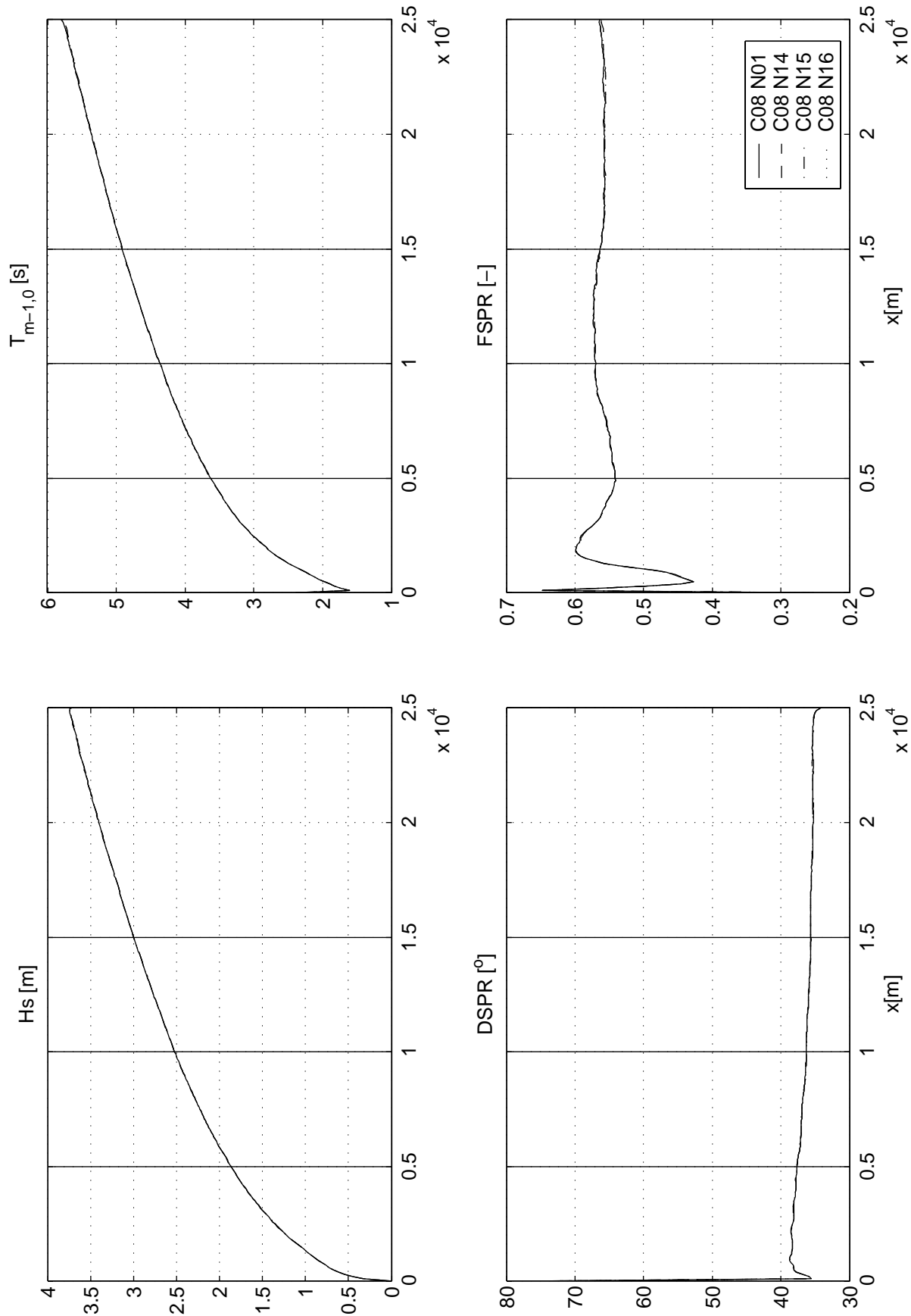


Spatial variation of integral wave parameters along fetch  
Fetch limited wave growth.  
Numerical Case:alfa-limiter; depth=10 m ; u10=30m/s

FL\_C08

Fetch Limited

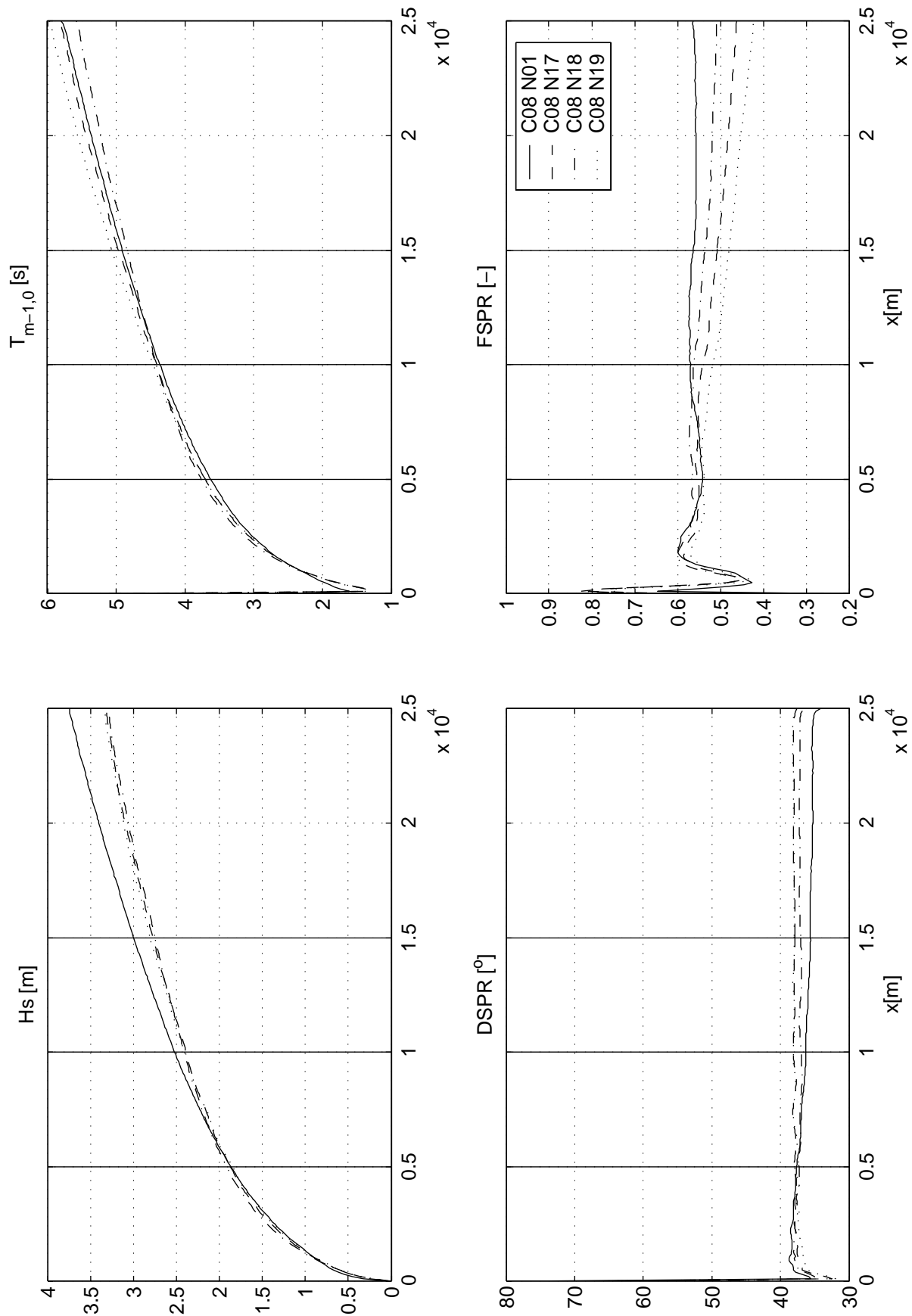




Spatial variation of integral wave parameters along fetch  
Fetch limited wave growth.  
Numerical Case:urslim–ursell–qb; depth=10 m ; u10=30m/s

FL\_C08

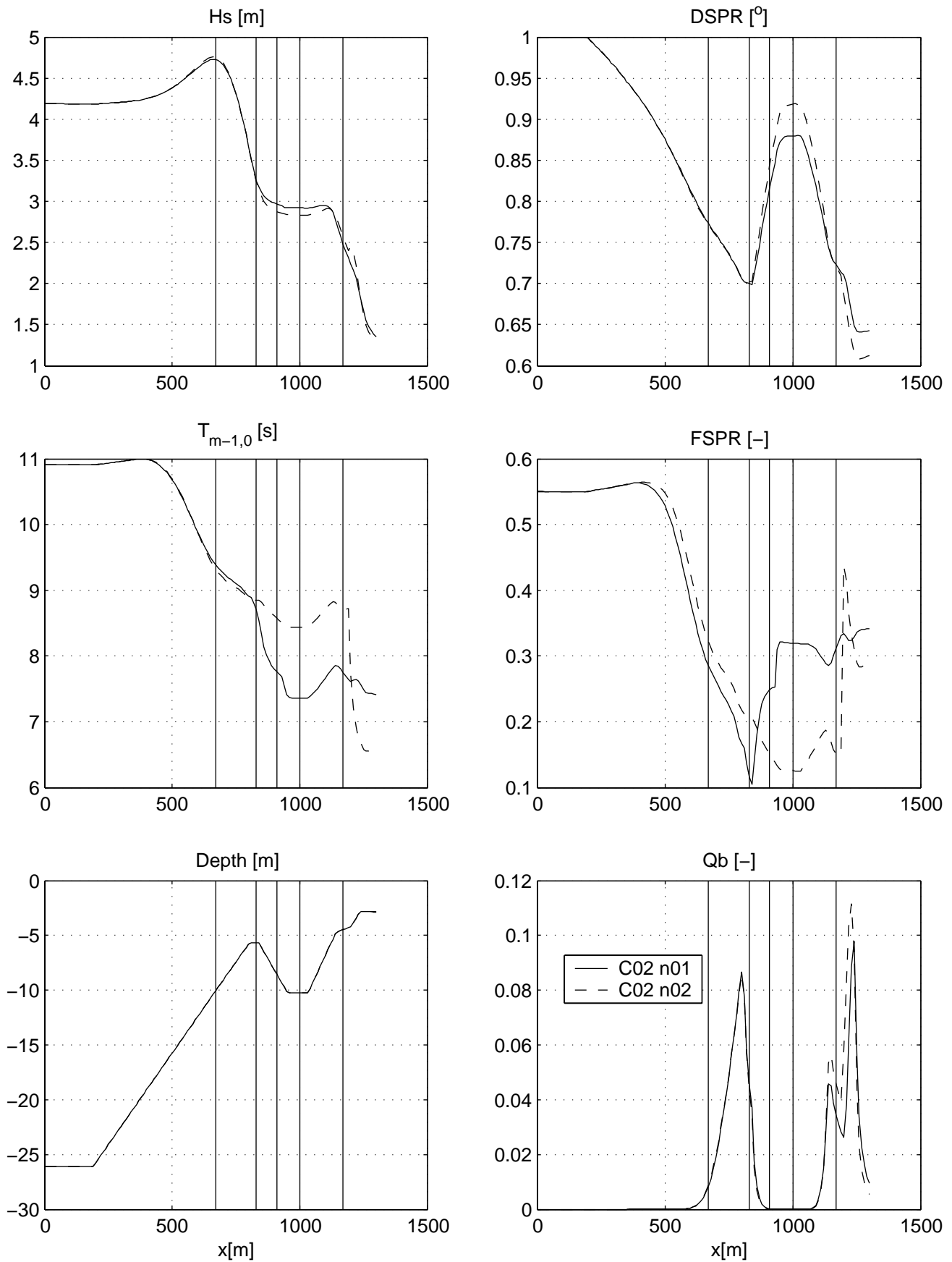
Fetch Limited



Spatial variation of integral wave parameters along fetch  
Fetch limited wave growth.  
Numerical Case:npnts; depth=10 m ; u10=30m/s

FL\_C08

Fetch Limited



Spatial variation of integral wave parameters in Petten wave flume  
Numerical Case:flow

B12

FP\_C02

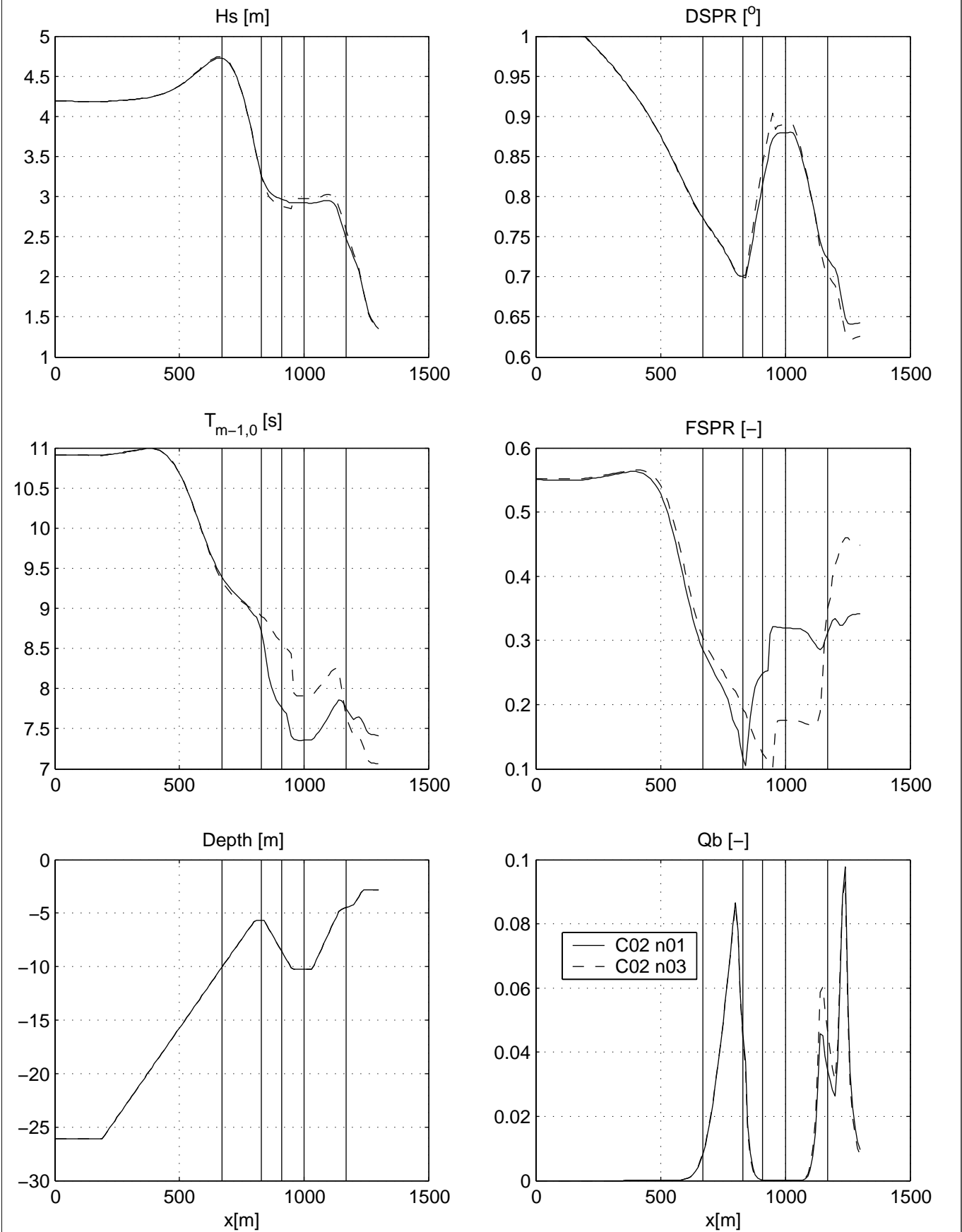
Petten Flume

Calibration SWAN 4020

A1168

 Alkyon

Fig. 4.6.1



Spatial variation of integral wave parameters in Petten wave flume  
Numerical Case:fhigh

B12

FP\_C02

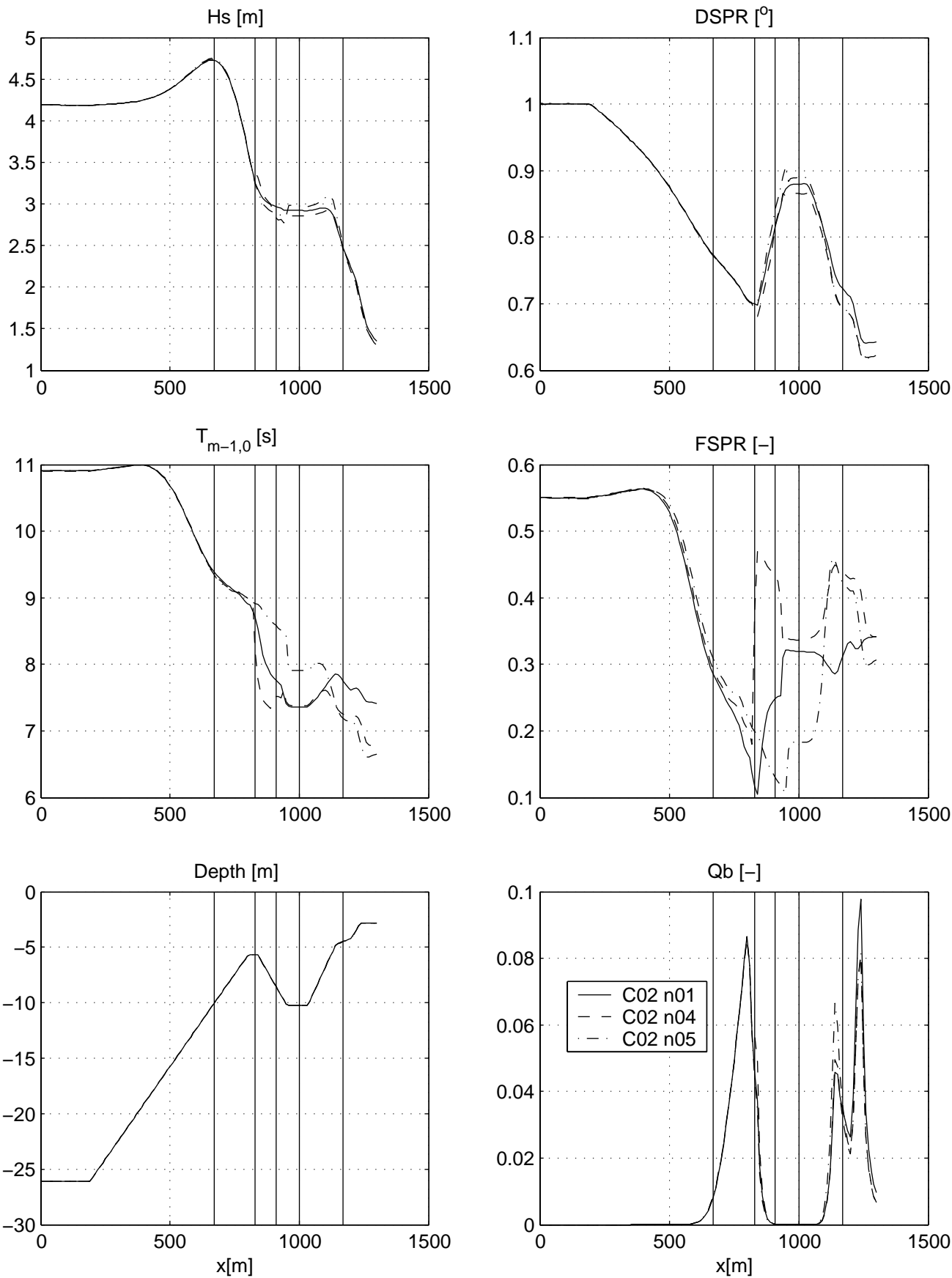
Petten Flume

Calibration SWAN 4020

A1168

Alkyon

Fig. 4.6.2

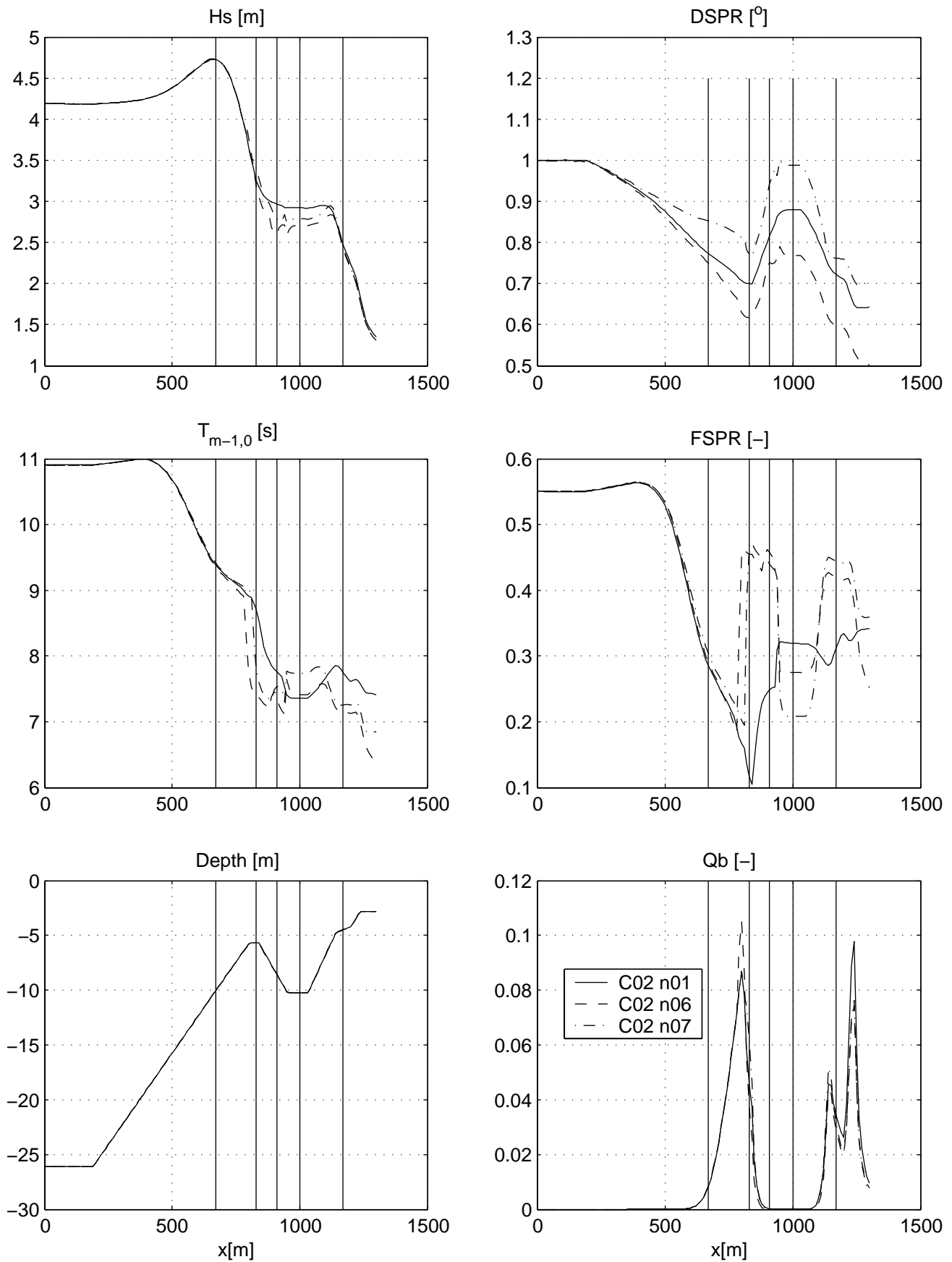


Spatial variation of integral wave parameters in Petten wave flume  
Numerical Case:msc

B12

FP\_C02

Petten Flume



Spatial variation of integral wave parameters in Petten wave flume  
Numerical Case:mdc

B12

FP\_C02

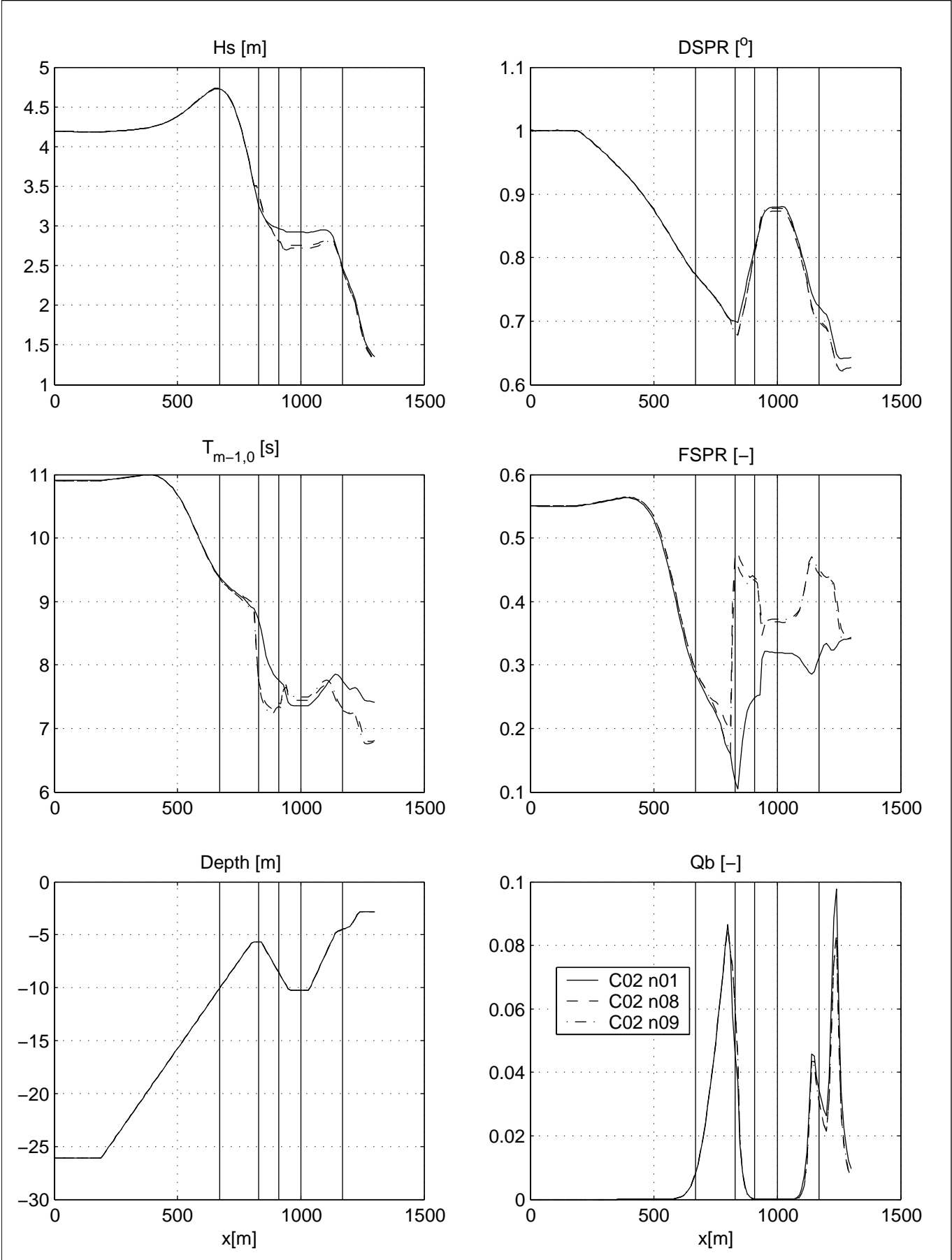
Petten Flume


Calibration SWAN 4020

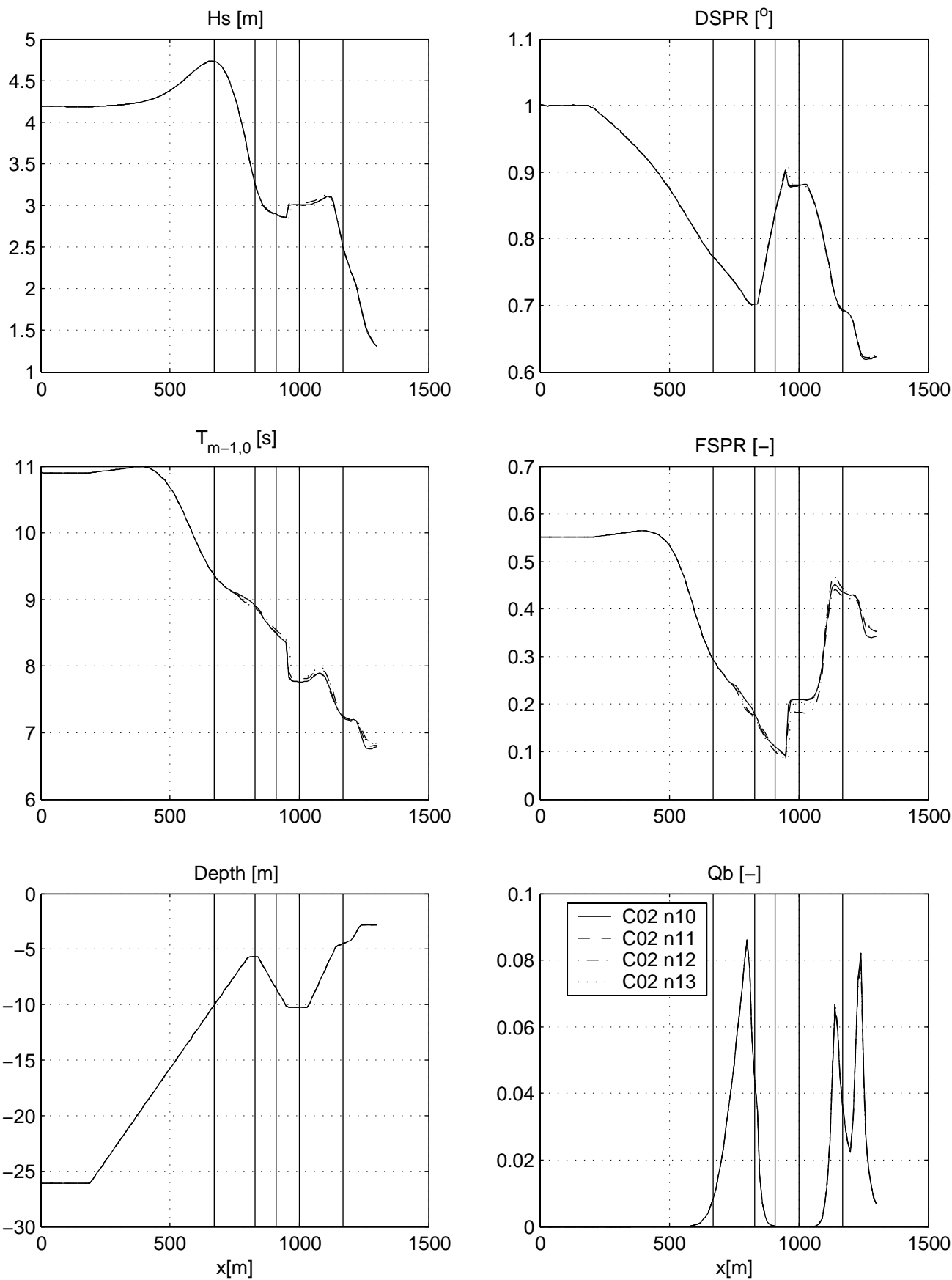
A1168

 Alkyon

Fig. 4.6.4



Spatial variation of integral wave parameters in Petten wave flume Numerical Case:limiter	B12	FP_C02
	Petten Flume	
Calibration SWAN 4020	A1168	 Fig. 4.6.5



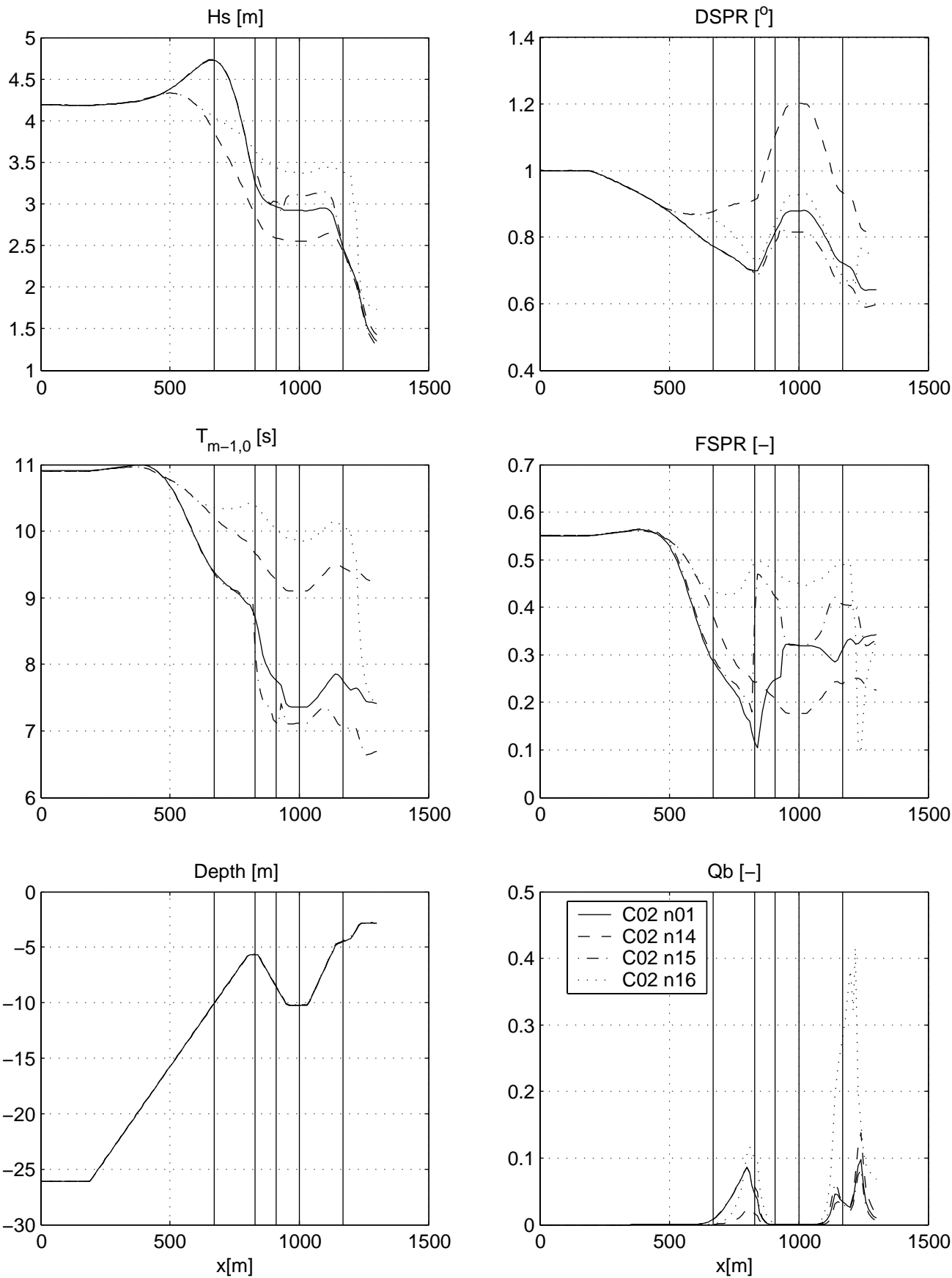
Spatial variation of integral wave parameters in Petten wave flume  
Numerical Case:alfa-limiter

B12

FP\_C02

Petten Flume



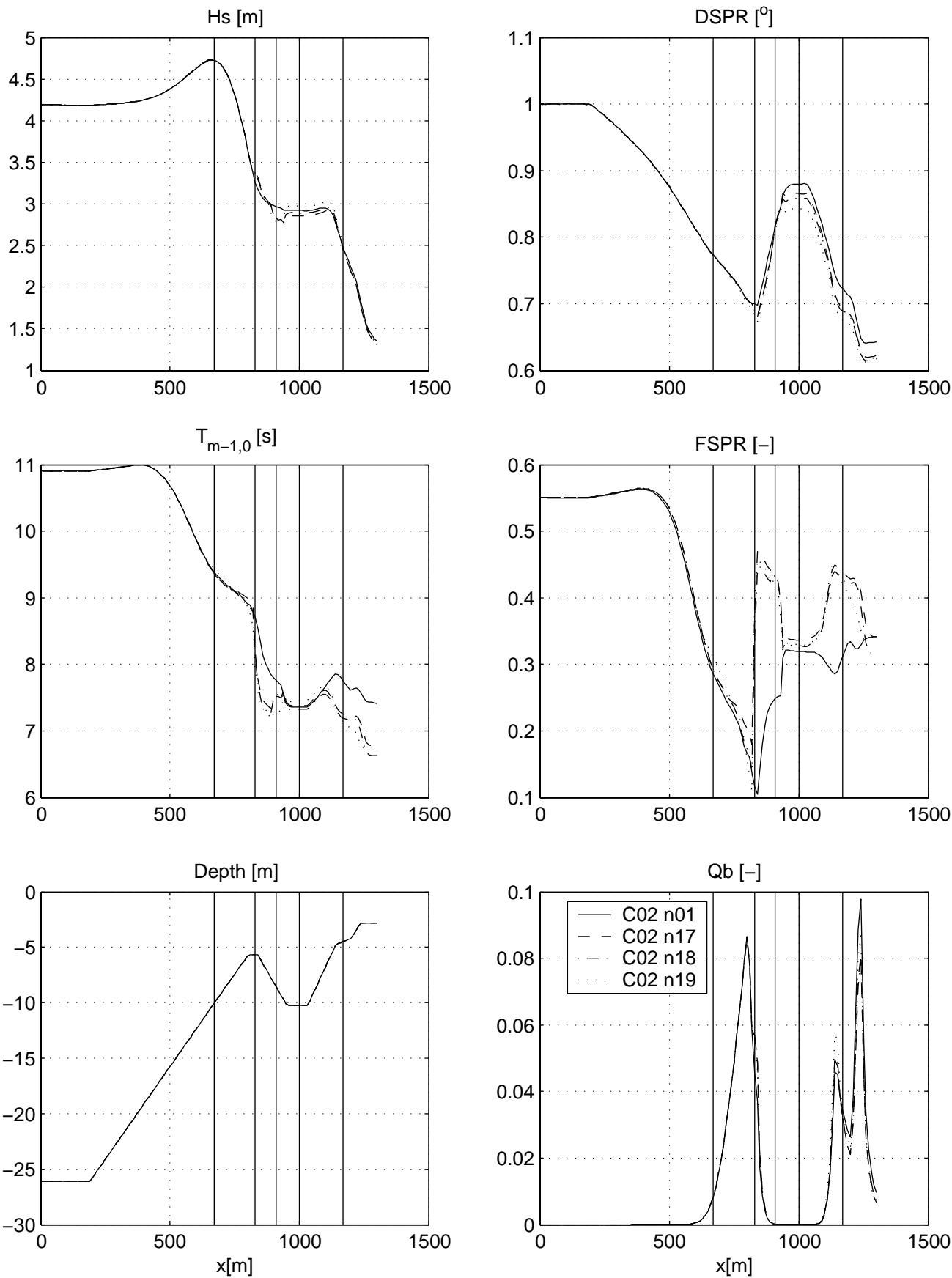


Spatial variation of integral wave parameters in Petten wave flume  
Numerical Case:urslim-ursell-qb

B12

FP\_C02

Petten Flume



Spatial variation of integral wave parameters in Petten wave flume  
Numerical Case:npnts

B12

FP\_C02

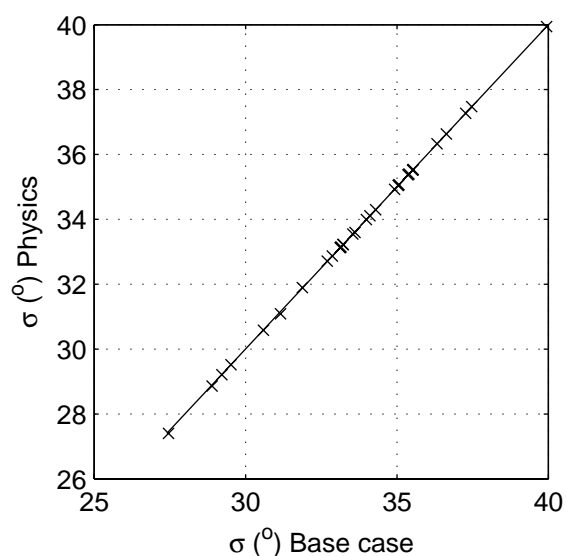
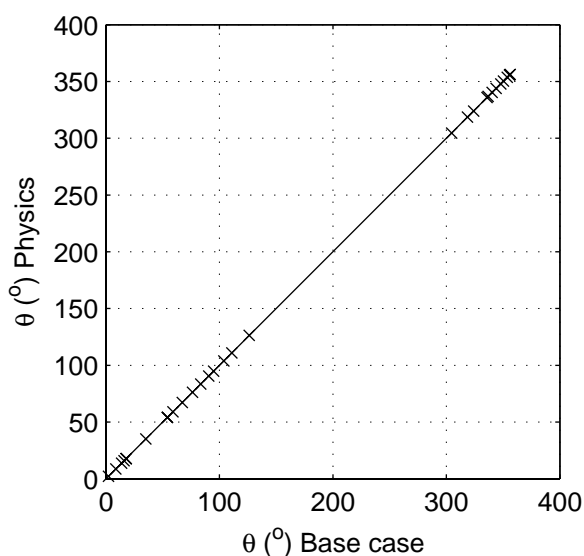
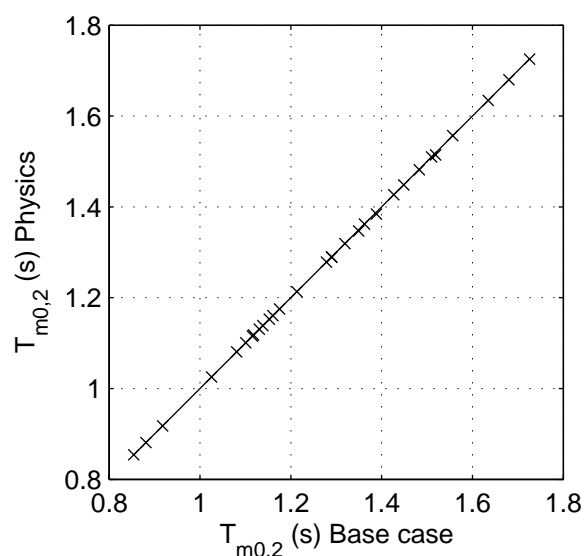
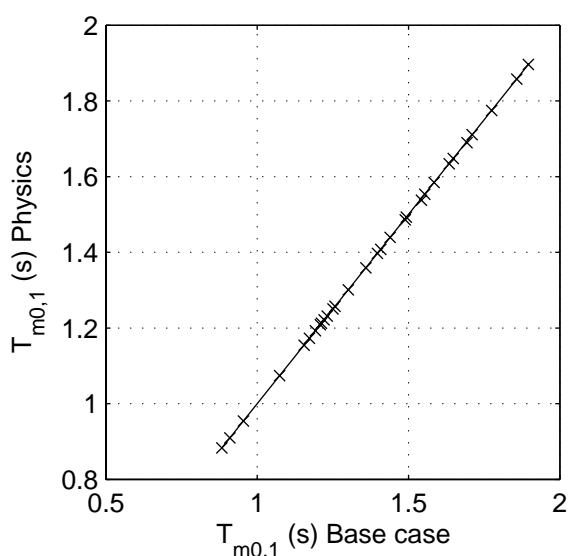
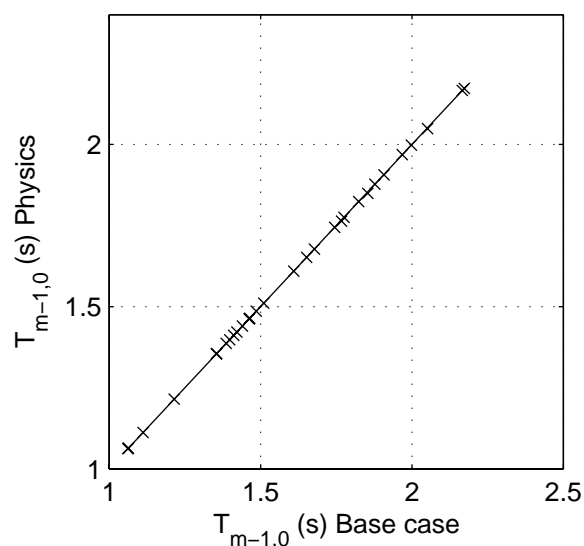
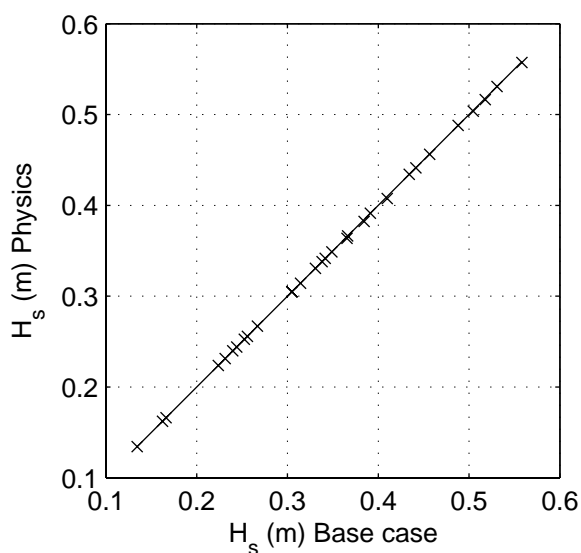
Petten Flume

Calibration SWAN 4020

A1168

Alkyon

Fig. 4.6.8



Sensitivity of SWAN 40.20 to variations in physical parameters  
Comparison of base case against:  
Higher alpha

Area:SL

Grid:SL

P02

Physics

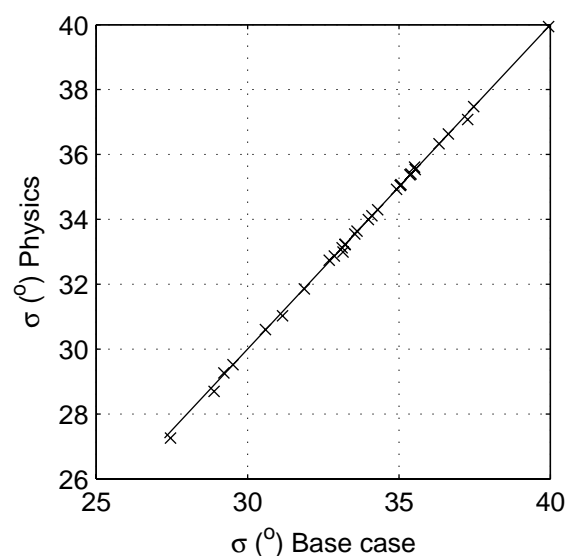
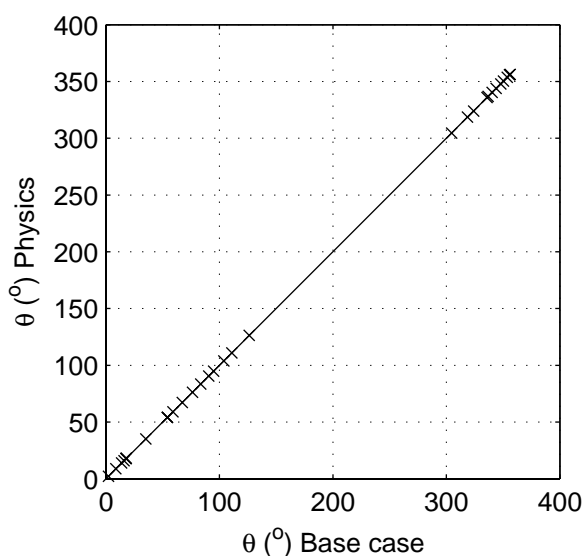
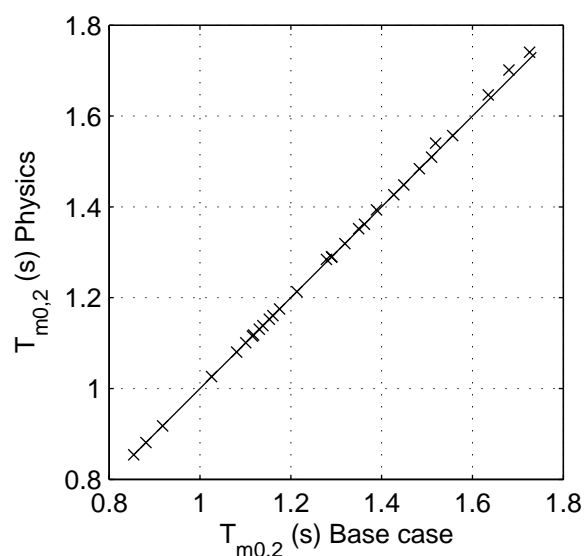
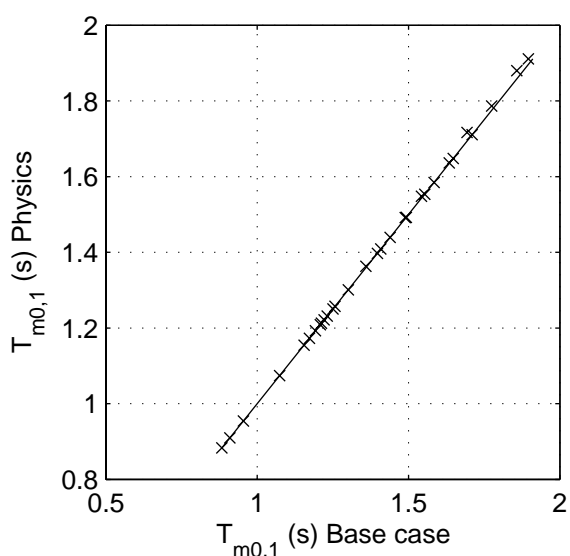
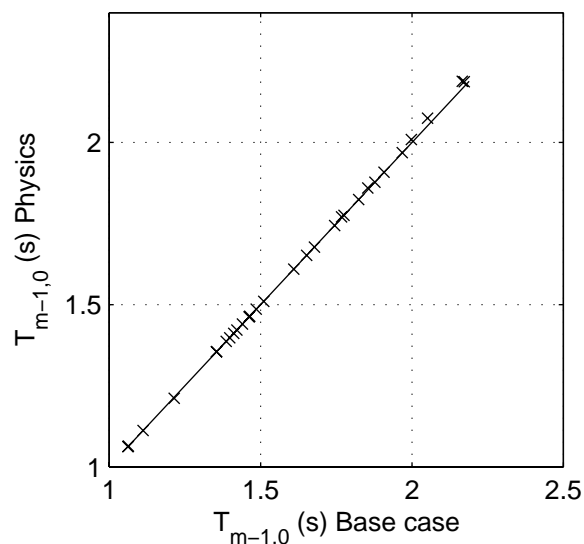
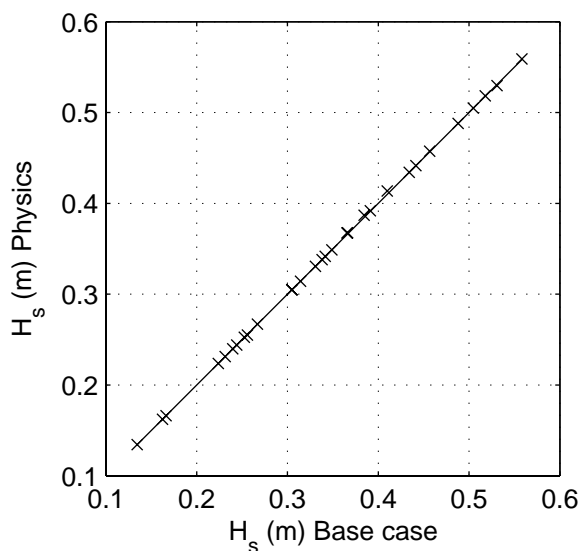
SCAT\_sl\_SL\_P2\_s2p

Calibration SWAN 40.20

A1168

 **Alkyon**

Fig. 5.1.2



Sensitivity of SWAN 40.20 to variations in physical parameters  
Comparison of base case against:  
Lower alpha

Area:SL

Grid:SL

P03

Physics

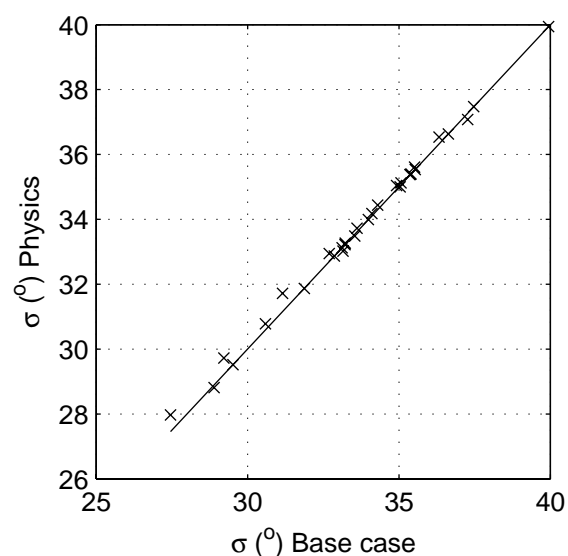
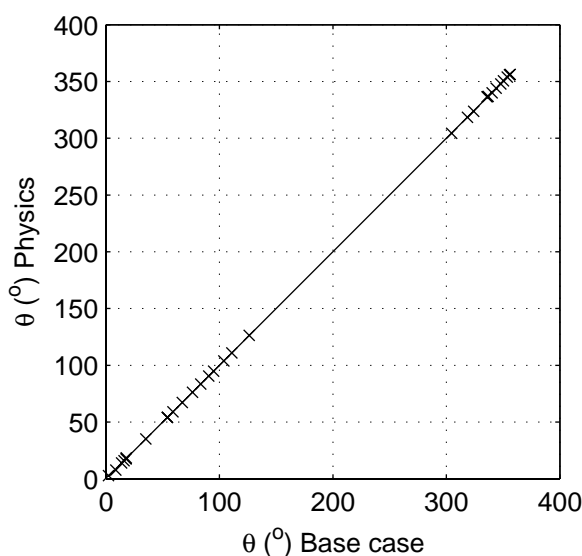
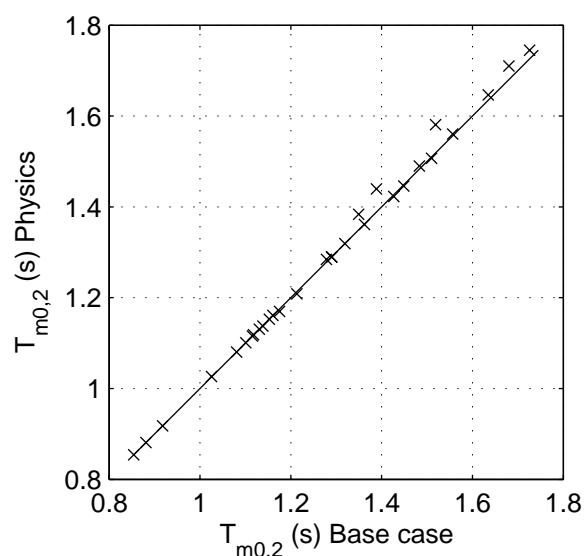
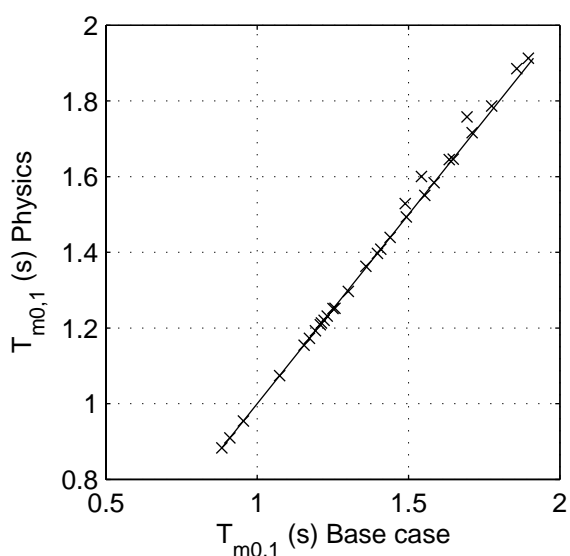
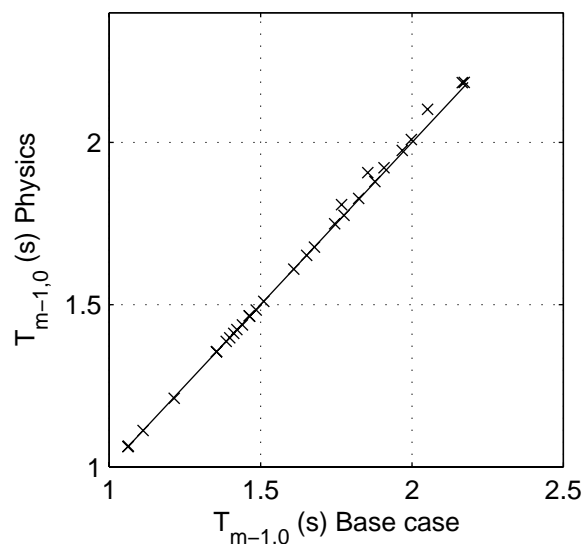
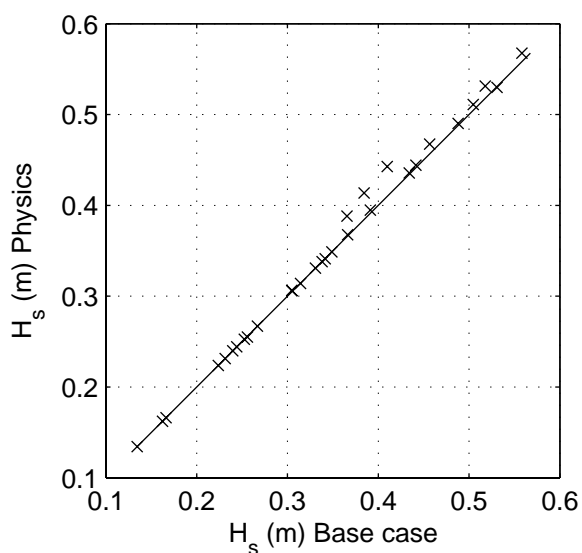
SCAT\_sl\_SL\_P3\_s2p

Calibration SWAN 40.20

A1168

 **Alkyon**

Fig. 5.1.3



Sensitivity of SWAN 40.20 to variations in physical parameters  
Comparison of base case against:  
Higher gamma

Area:SL

Grid:SL

P04

Physics

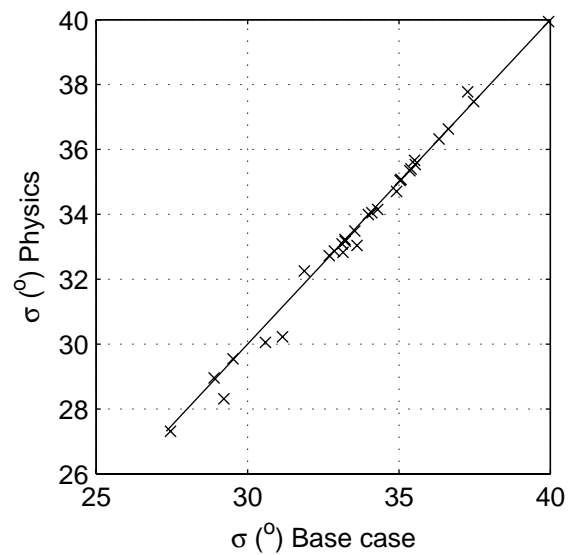
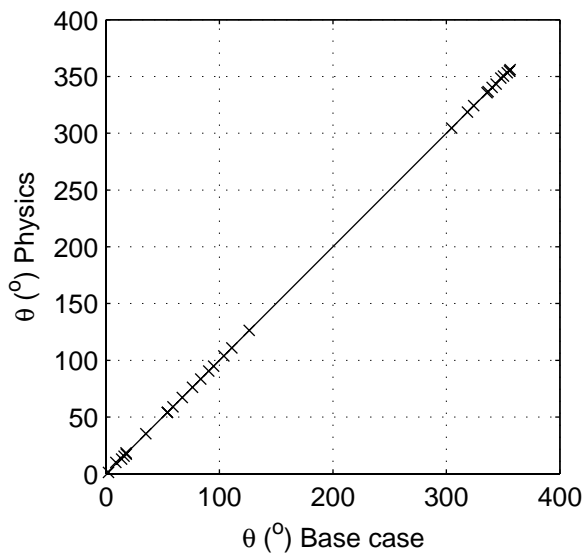
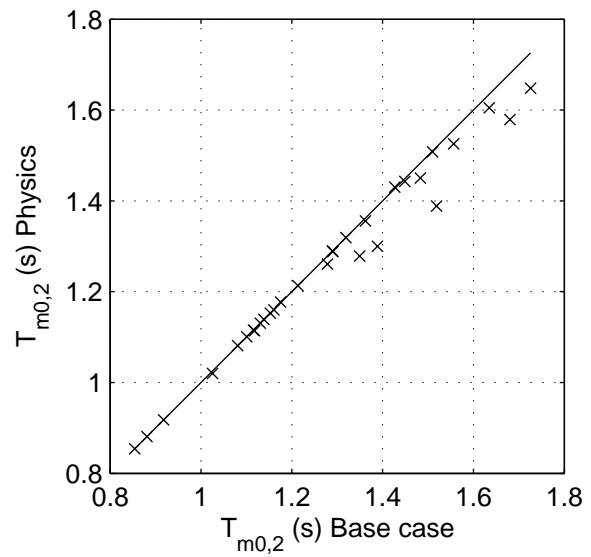
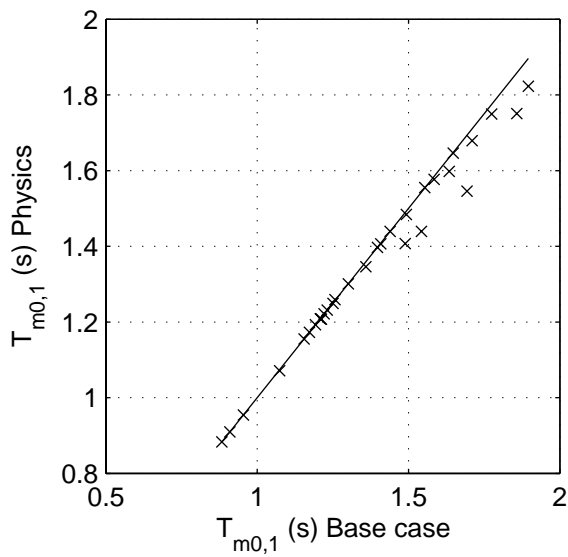
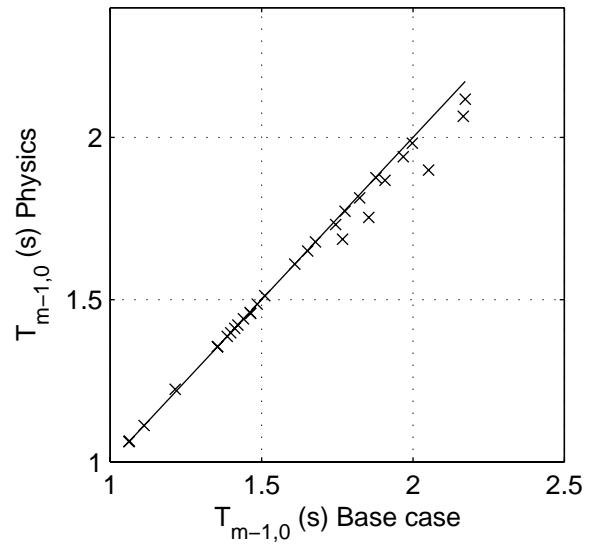
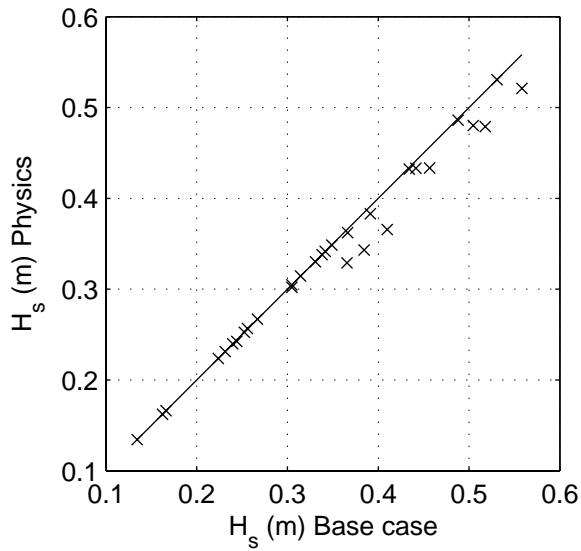
SCAT\_sl\_SL\_P4\_s2p

Calibration SWAN 40.20

A1168

 **Alkyon**

Fig. 5.1.4



Sensitivity of SWAN 40.20 to variations in physical parameters  
Comparison of base case against:  
Lower gamma

Area:SL

Grid:SL

P05

Physics

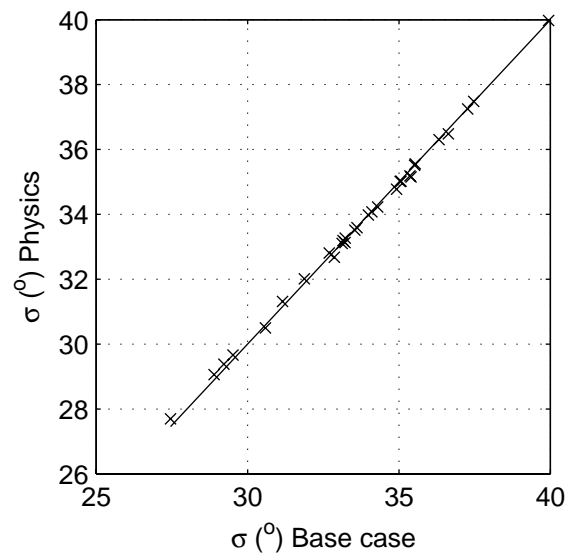
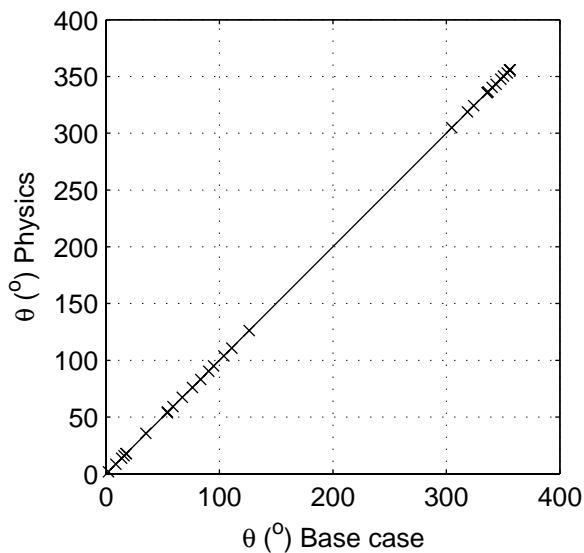
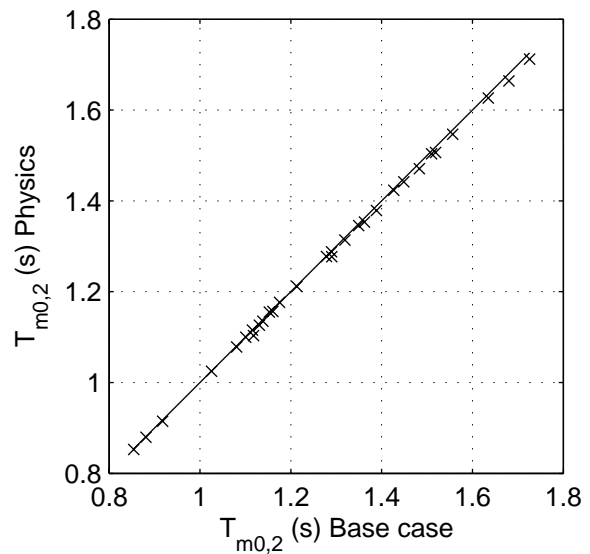
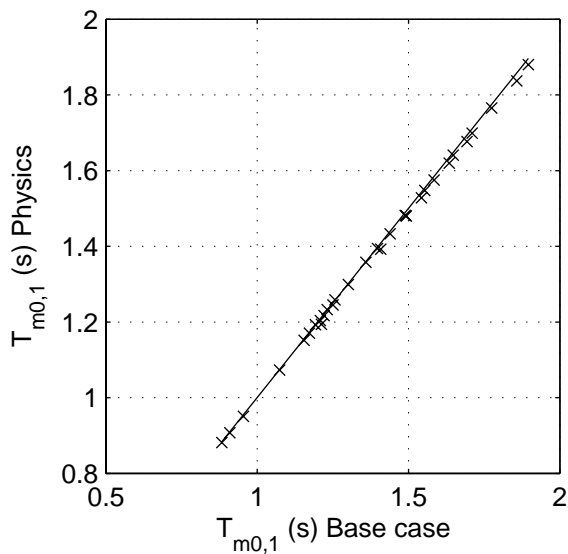
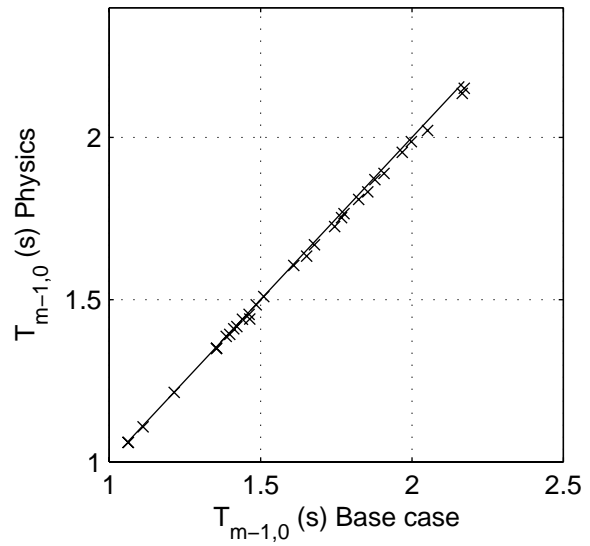
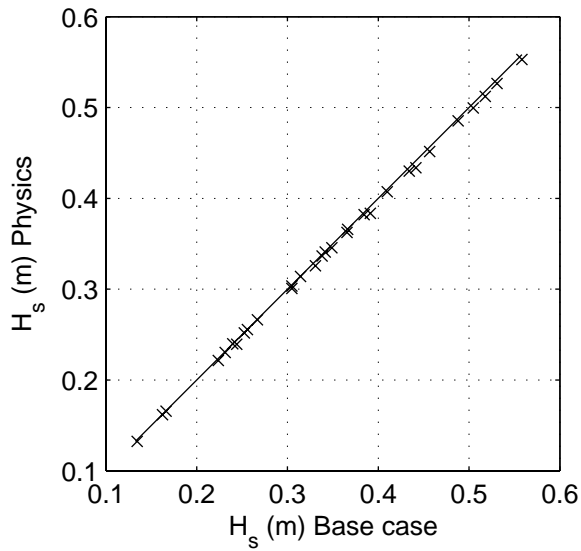
SCAT\_sl\_SL\_P5\_s2p

Calibration SWAN 40.20

A1168

 **Alkyon**

Fig. 5.1.5



Sensitivity of SWAN 40.20 to variations in physical parameters  
Comparison of base case against:  
Stronger Sfric

Area:SL

Grid:SL

P06

Physics

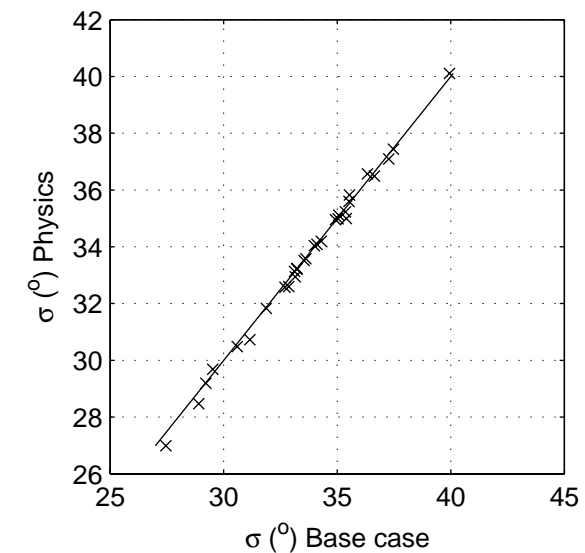
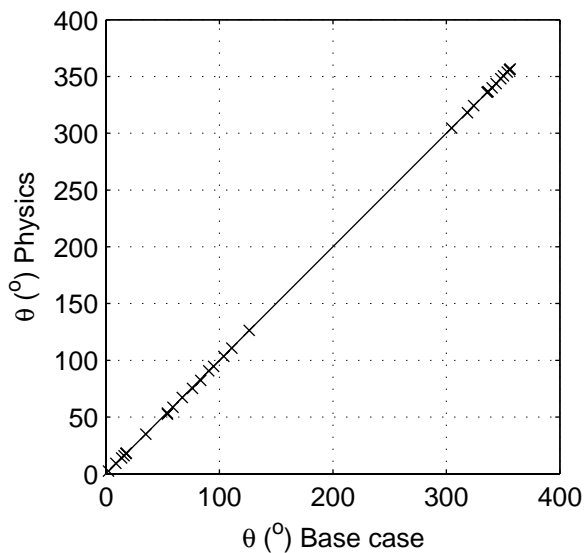
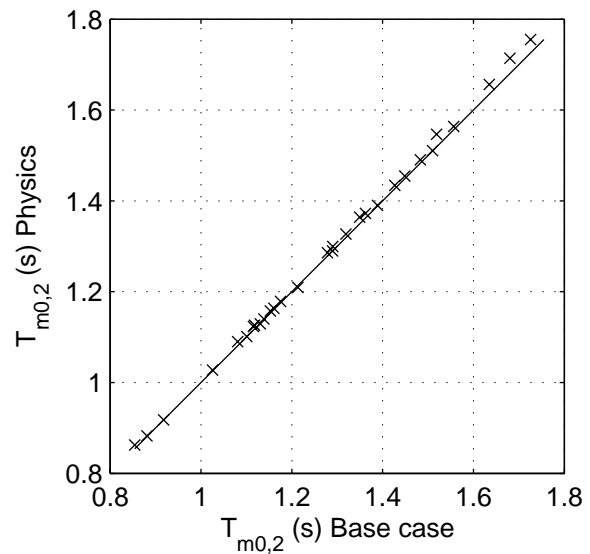
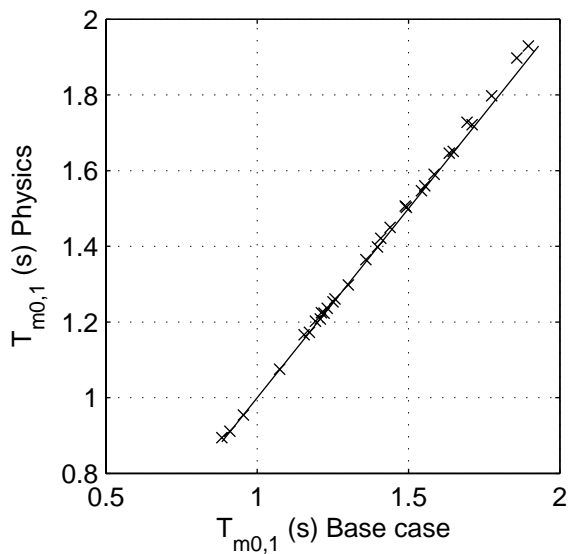
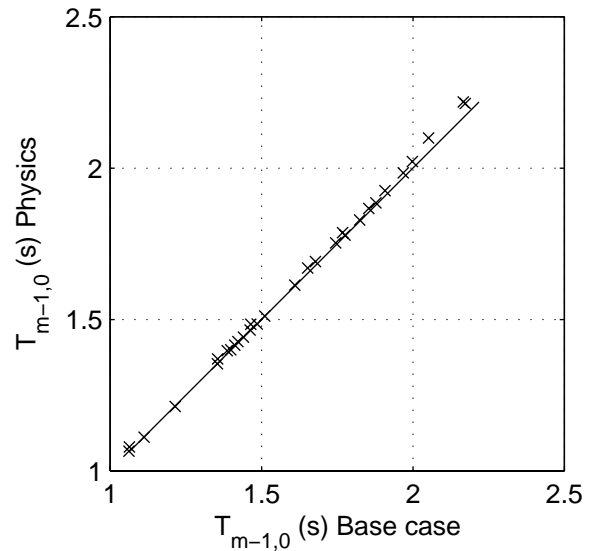
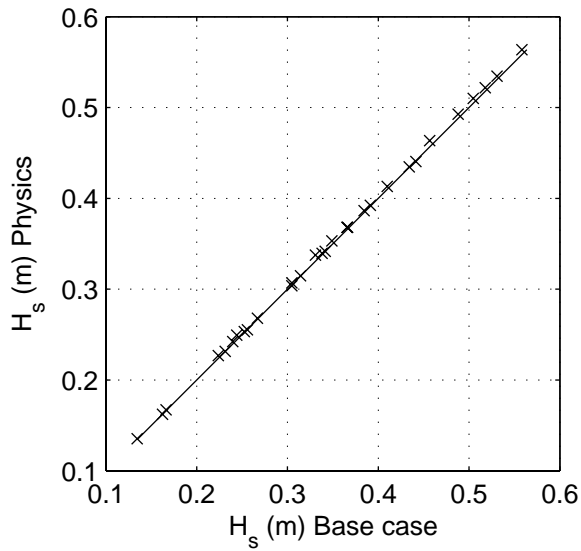
SCAT\_sl\_SL\_P6\_s2p

Calibration SWAN 40.20

A1168

 **Alkyon**

Fig. 5.1.6



Sensitivity of SWAN 40.20 to variations in physical parameters  
Comparison of base case against:  
Weaker Sfric

Area:SL

Grid:SL

P07

Physics

SCAT\_sl\_SL\_P7\_s2p

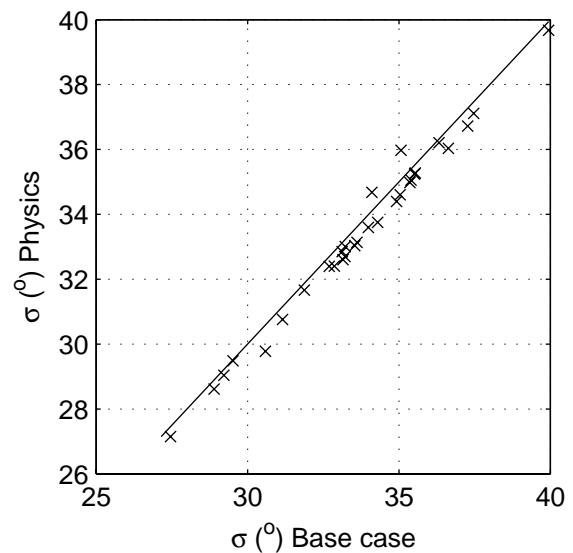
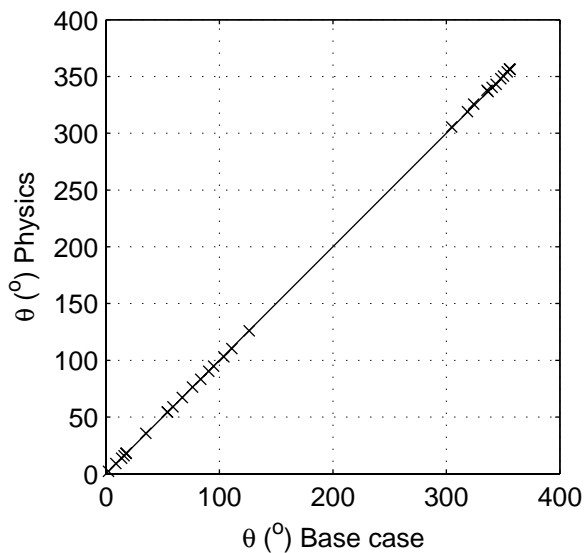
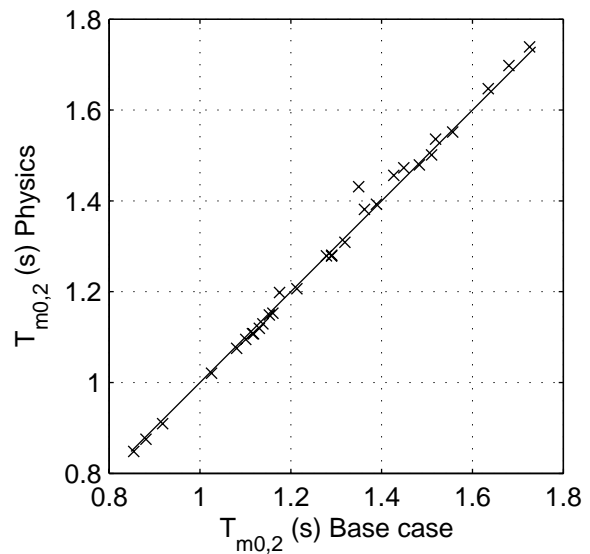
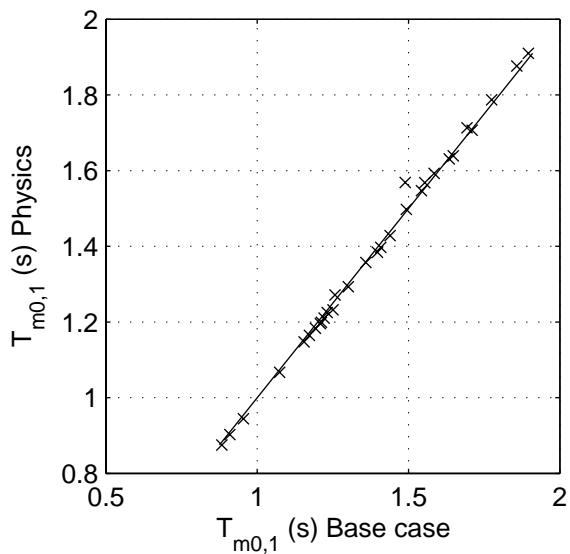
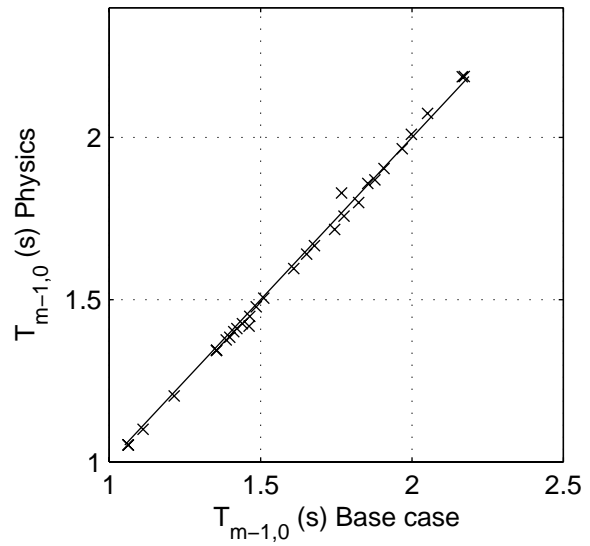
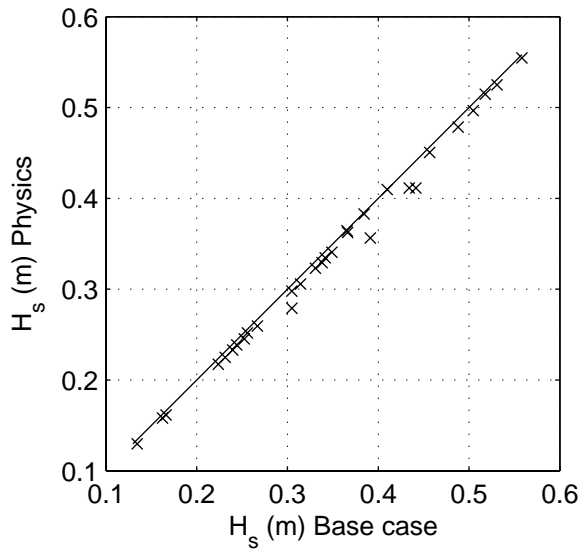
Calibration SWAN 40.20

A1168

 **Alkyon**

Fig. 5.1.7





Sensitivity of SWAN 40.20 to variations in physical parameters  
Comparison of base case against:  
Stronger Swcap

Area:SL

Grid:SL

P08

Physics

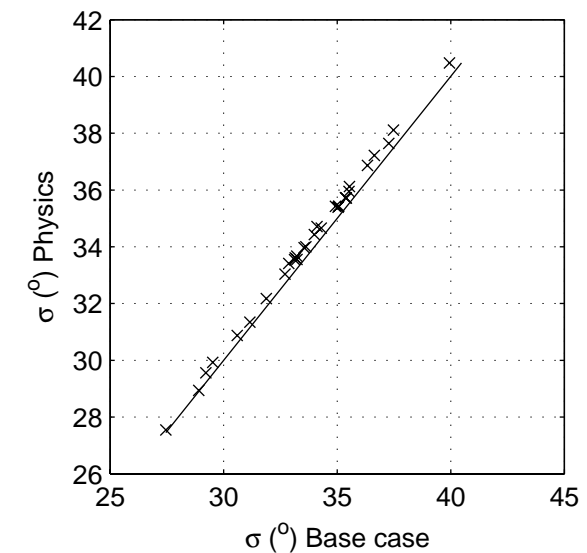
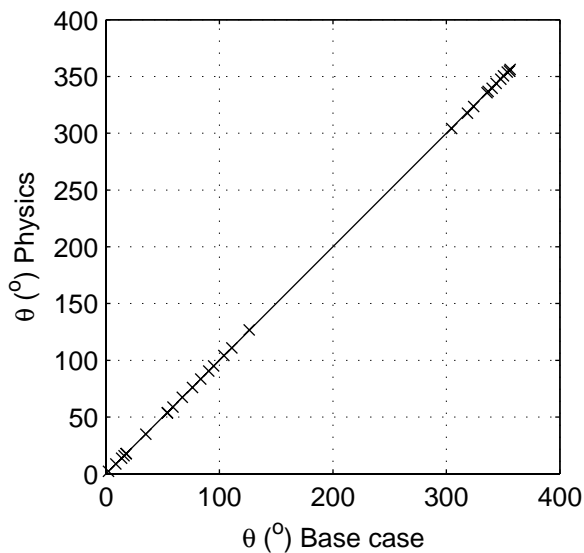
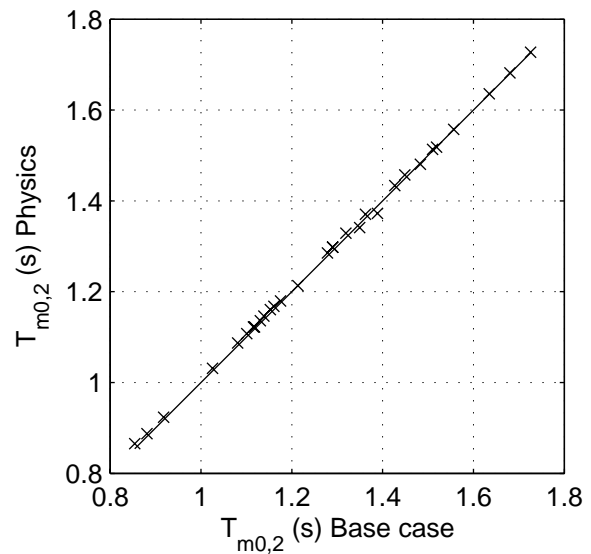
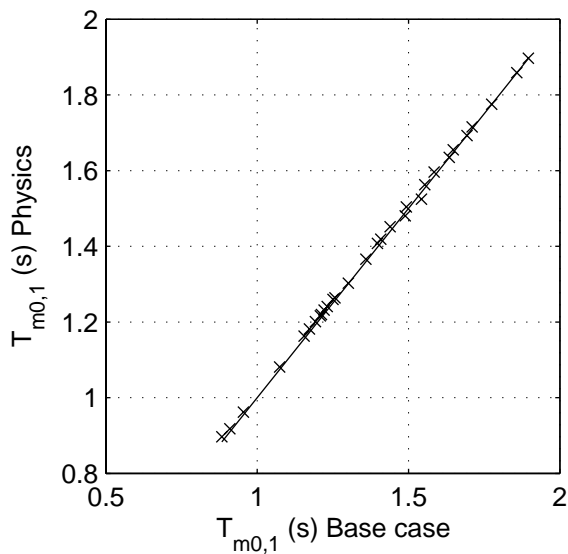
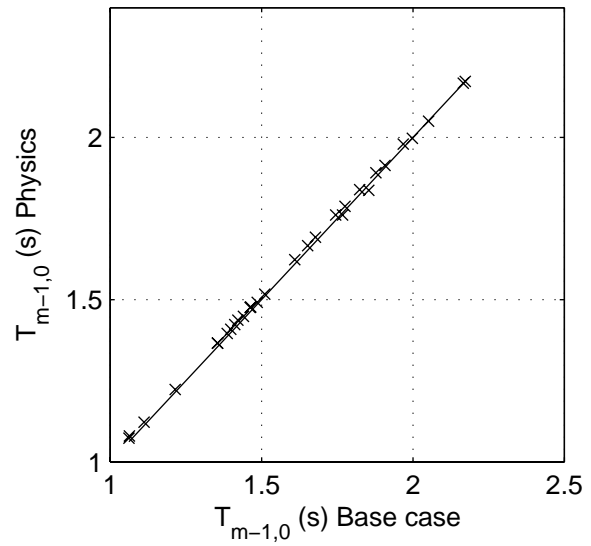
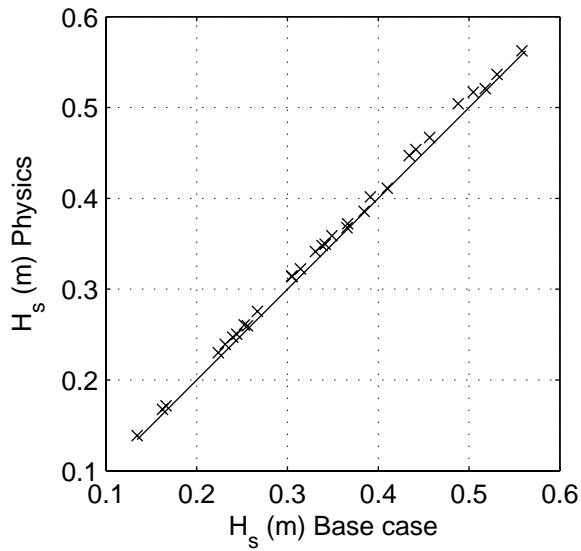
SCAT\_sl\_SL\_P8\_s2p

Calibration SWAN 40.20

A1168

 **Alkyon**

Fig. 5.1.8



Sensitivity of SWAN 40.20 to variations in physical parameters  
Comparison of base case against:  
Weaker Swcap

Area:SL

Grid:SL

P09

Physics

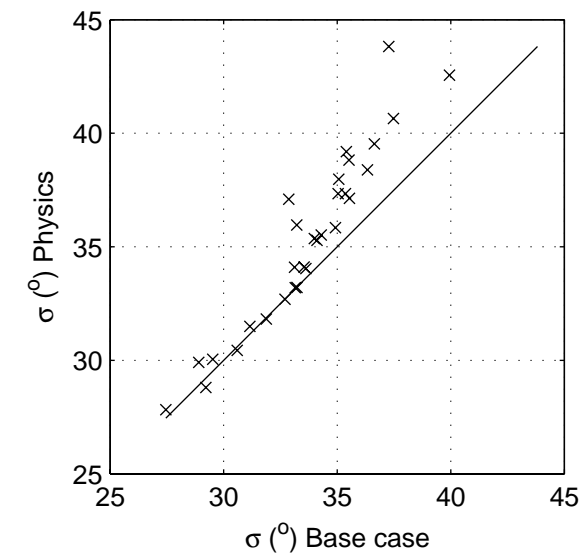
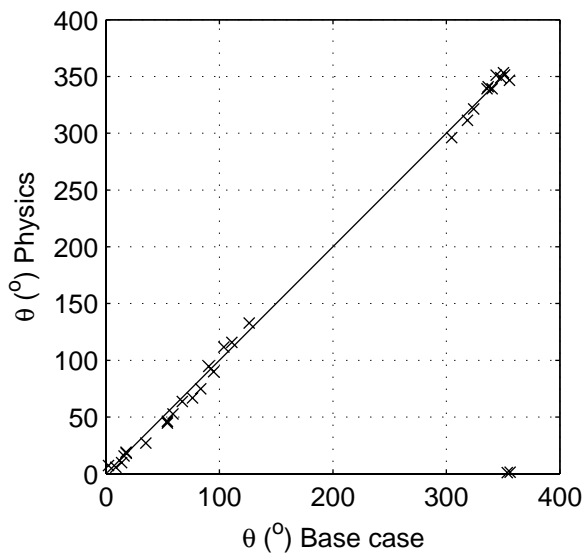
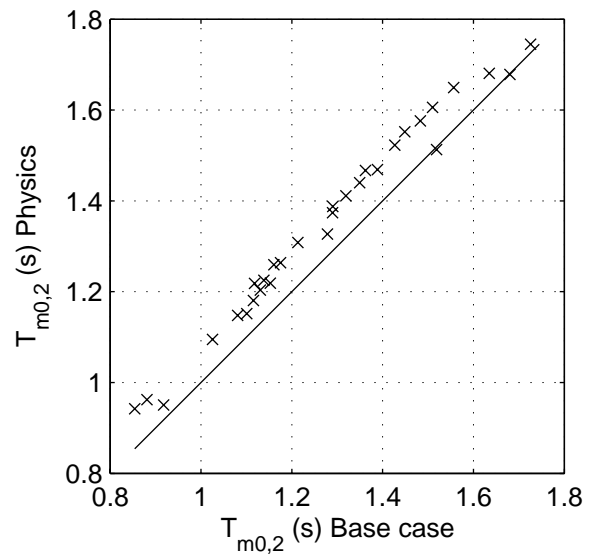
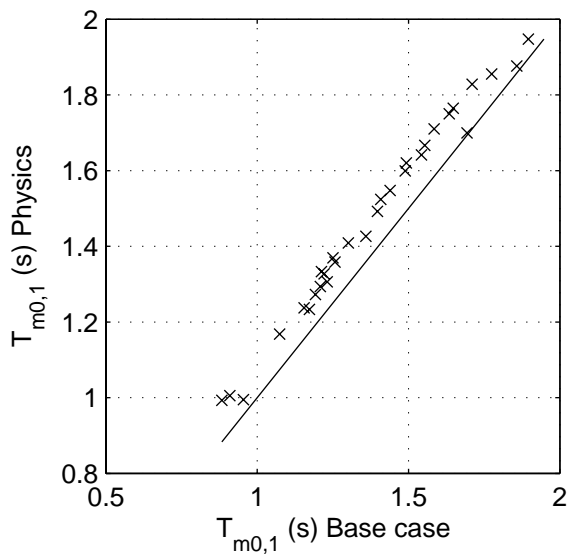
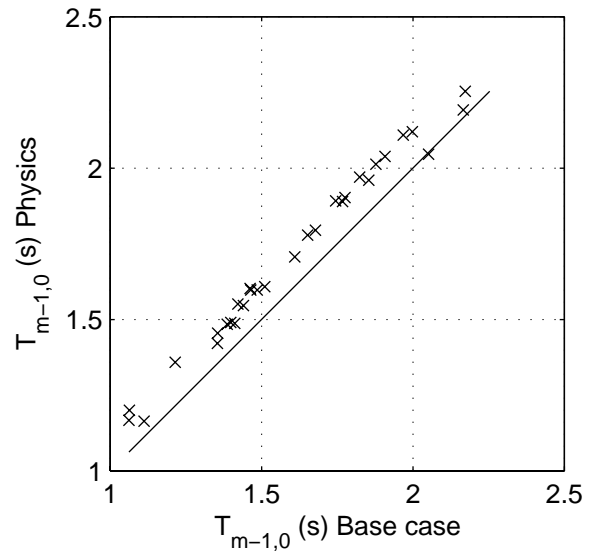
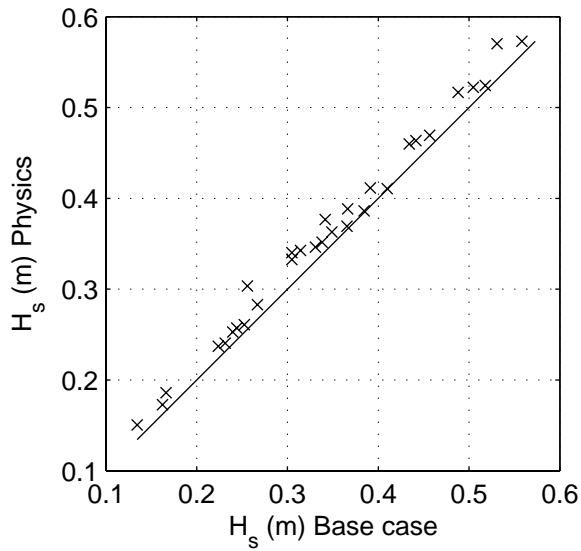
SCAT\_sl\_SL\_P9\_s2p

Calibration SWAN 40.20

A1168

 **Alkyon**

Fig. 5.1.9



Sensitivity of SWAN 40.20 to variations in physical parameters  
Comparison of base case against:  
Higher lambda in SnI4

Area:SL

Grid:SL

P10

Physics

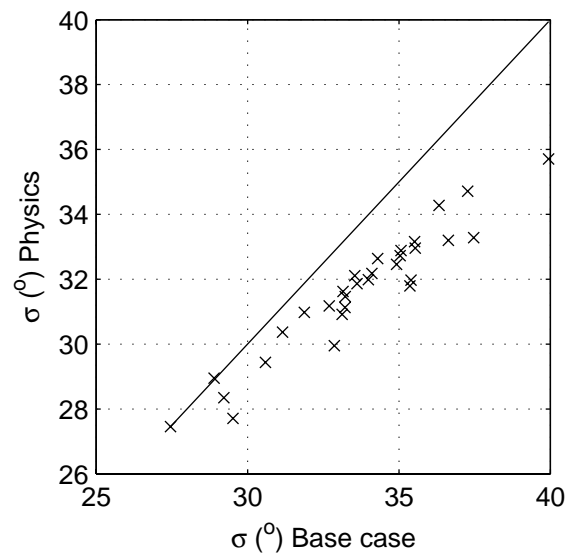
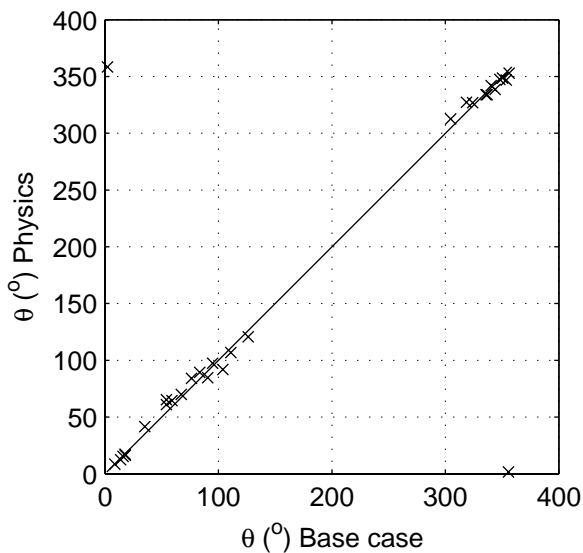
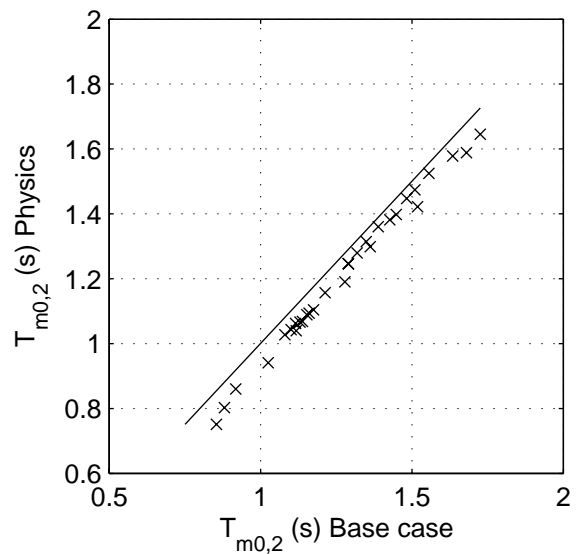
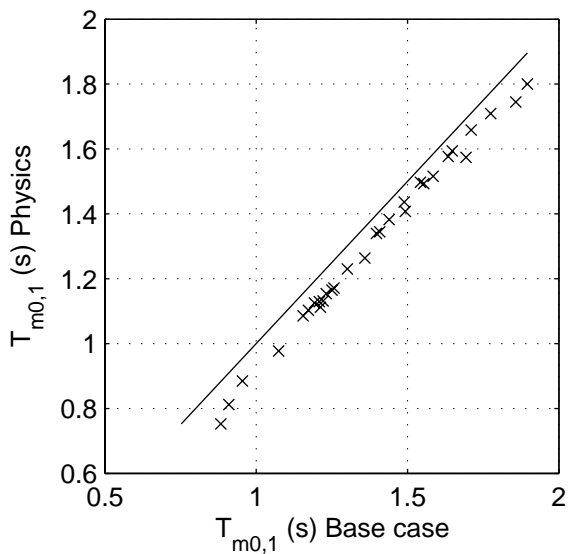
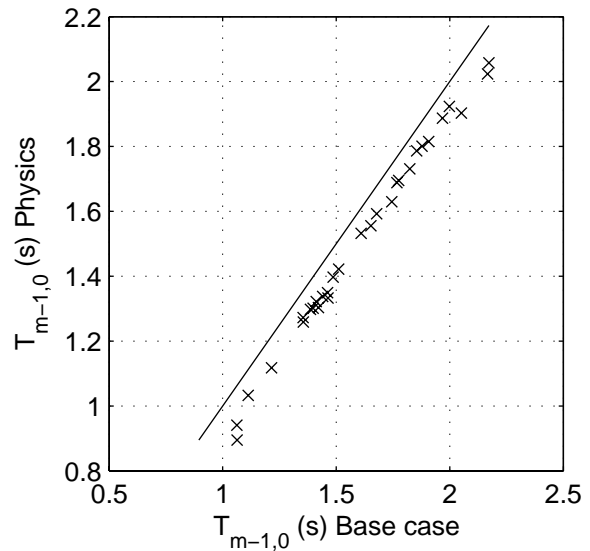
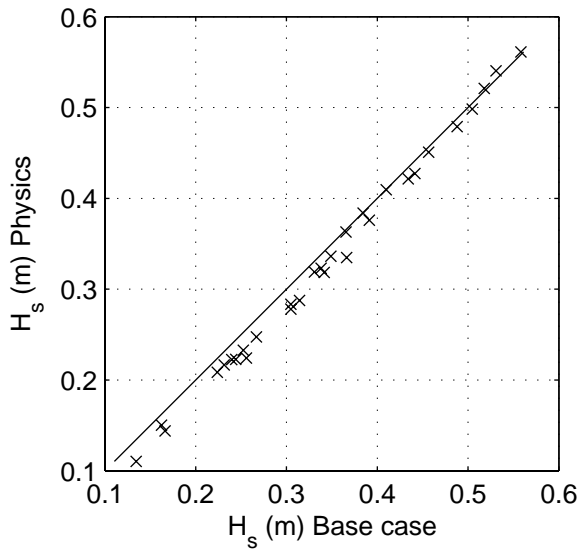
SCAT\_sl\_SL\_P10\_s2p

Calibration SWAN 40.20

A1168

 **Alkyon**

Fig. 5.1.10



Sensitivity of SWAN 40.20 to variations in physical parameters  
Comparison of base case against:  
Lower lambda in SnI4

Area:SL

Grid:SL

P11

Physics

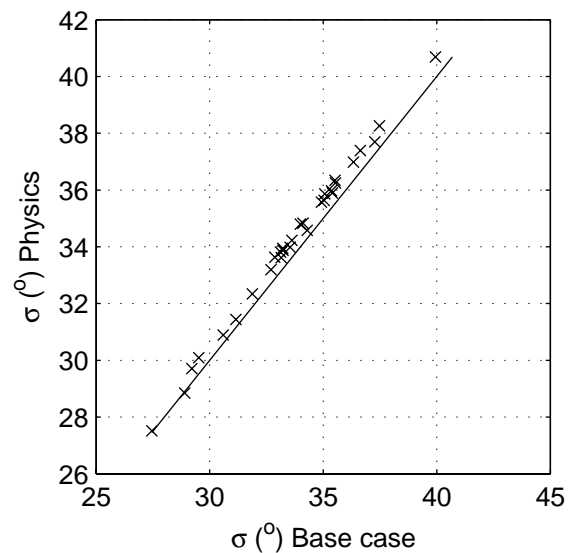
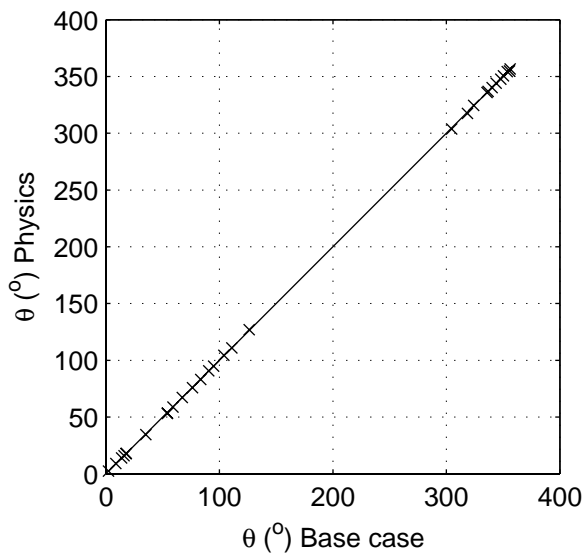
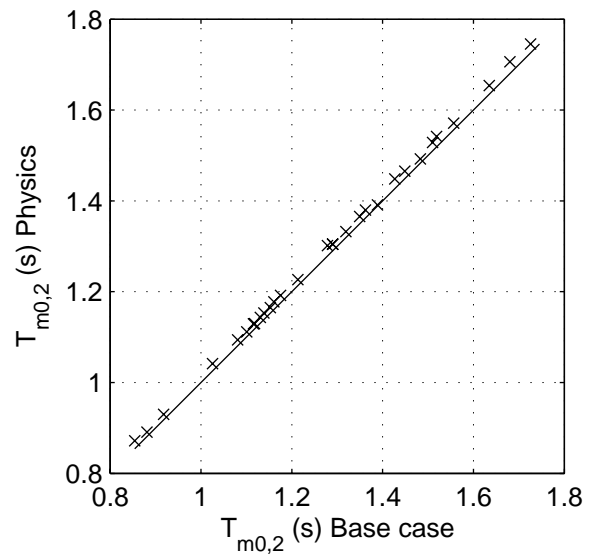
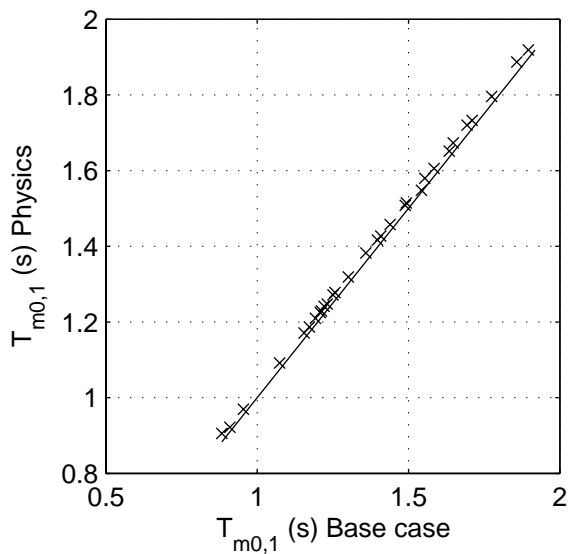
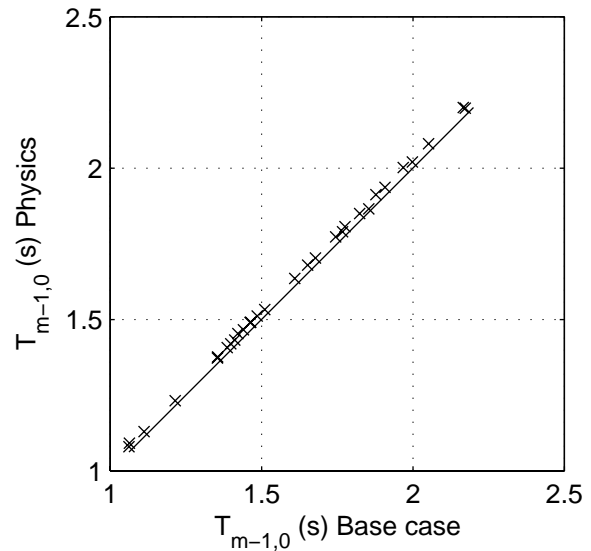
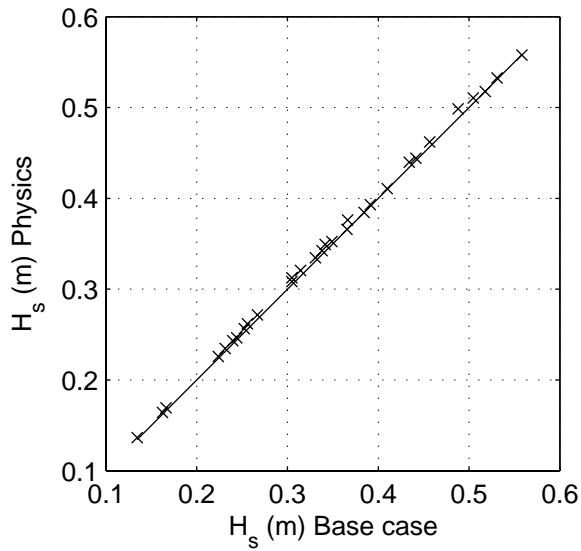
SCAT\_sl\_SL\_P11\_s2p

Calibration SWAN 40.20

A1168

 **Alkyon**

Fig. 5.1.11



Sensitivity of SWAN 40.20 to variations in physical parameters  
Comparison of base case against:  
Stronger SnI4

Area:SL

Grid:SL

P12

Physics

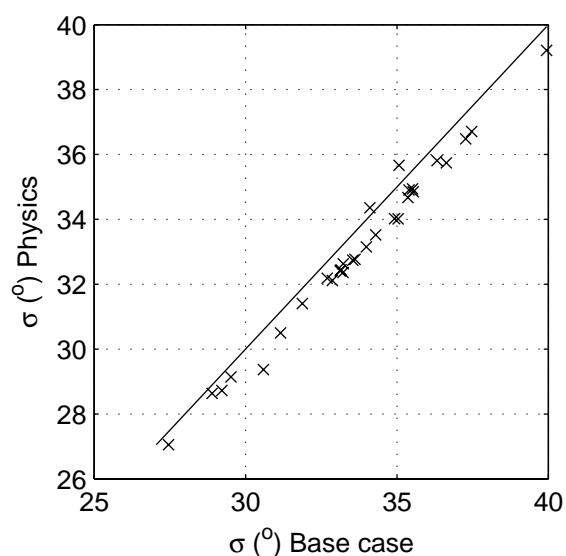
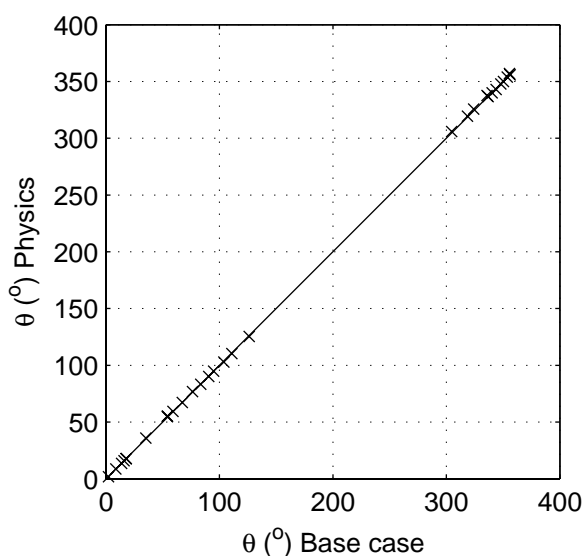
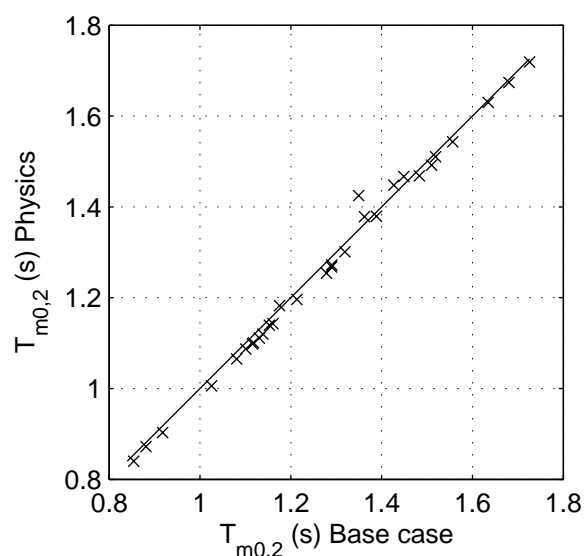
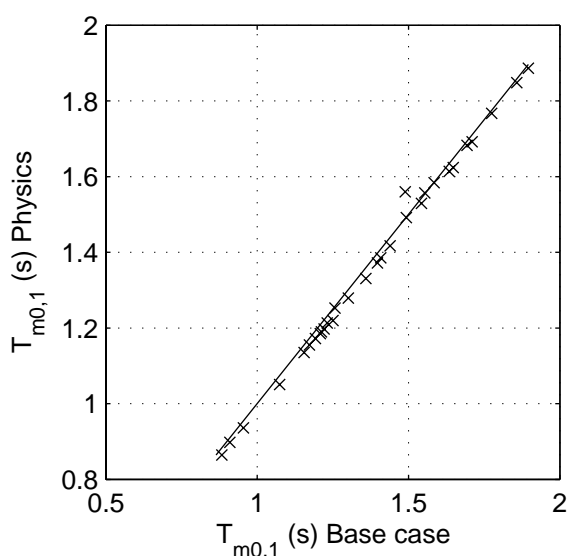
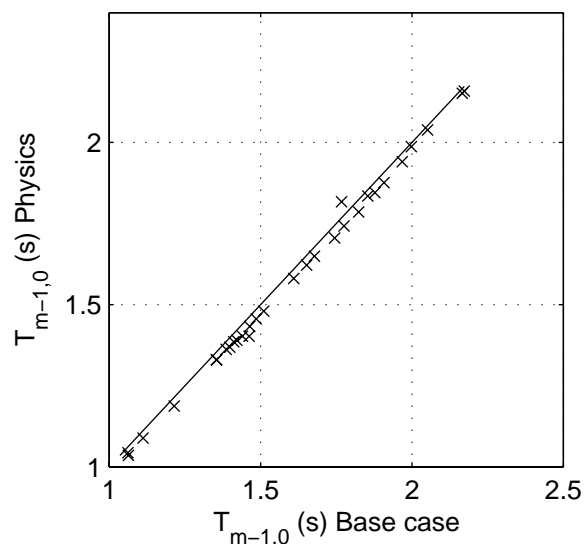
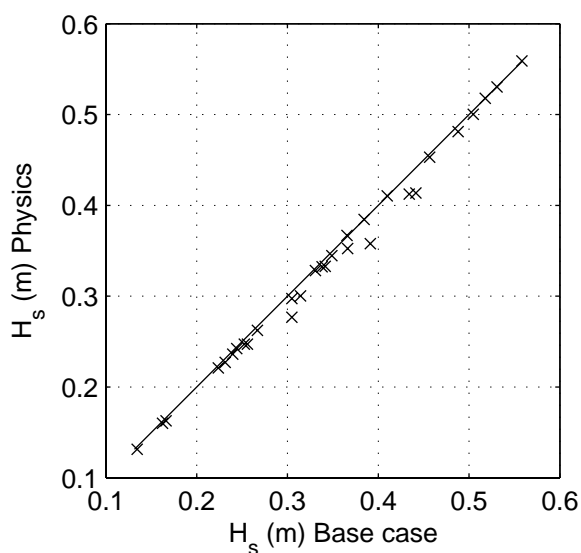
SCAT\_sl\_SL\_P12\_s2p

Calibration SWAN 40.20

A1168

 **Alkyon**

Fig. 5.1.12



Sensitivity of SWAN 40.20 to variations in physical parameters  
Comparison of base case against:  
Weaker SnI4

Area:SL

Grid:SL

P13

Physics

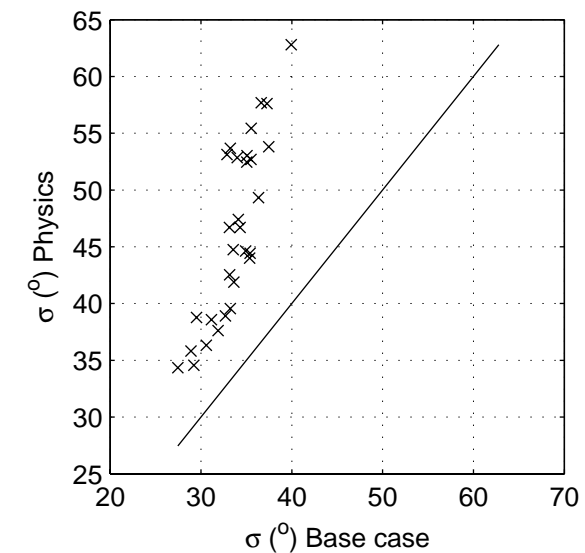
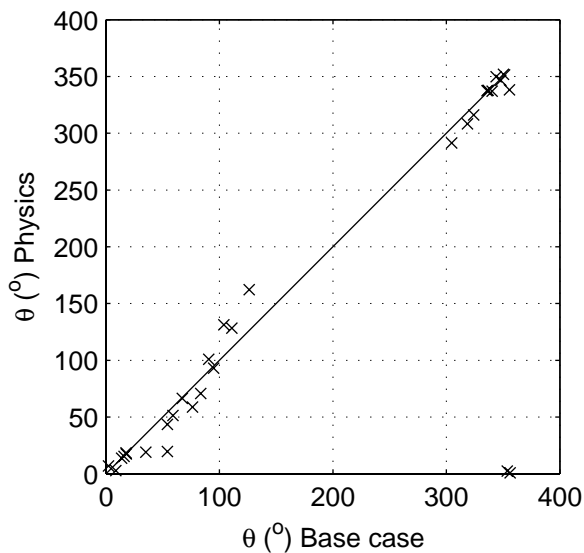
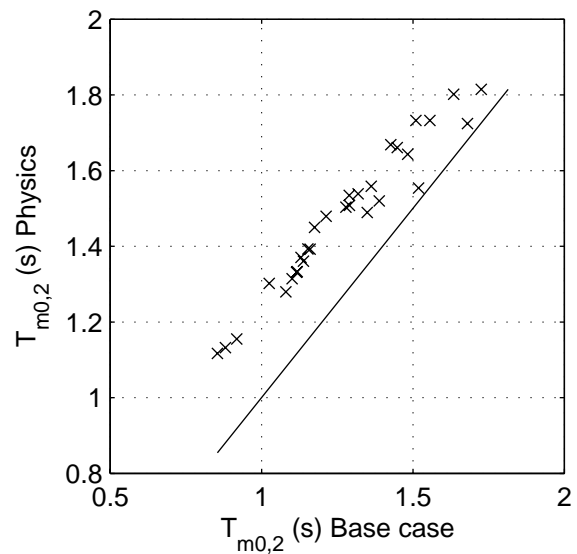
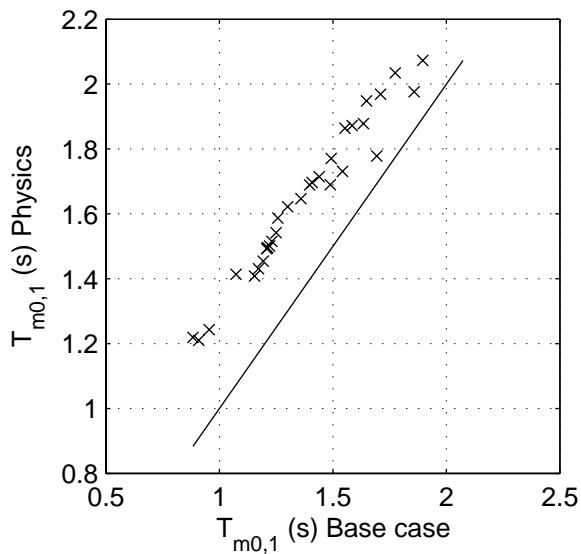
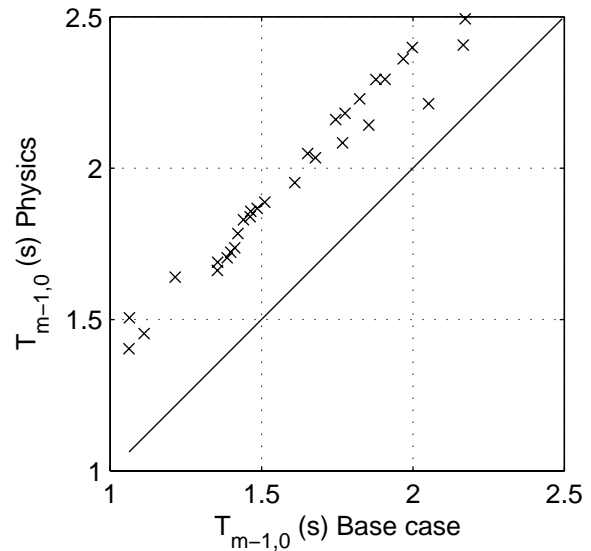
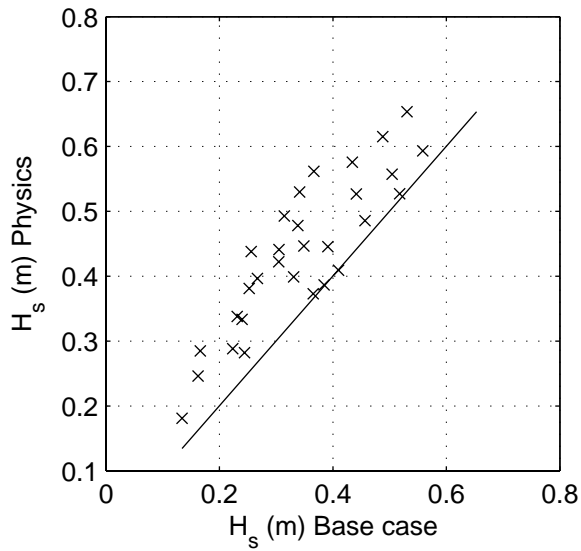
SCAT\_sl\_SL\_P13\_s2p

Calibration SWAN 40.20

A1168

 **Alkyon**

Fig. 5.1.13



Sensitivity of SWAN 40.20 to variations in physical parameters  
Comparison of base case against:  
Cumulative steepness

Area:SL

Grid:SL

P14

Physics

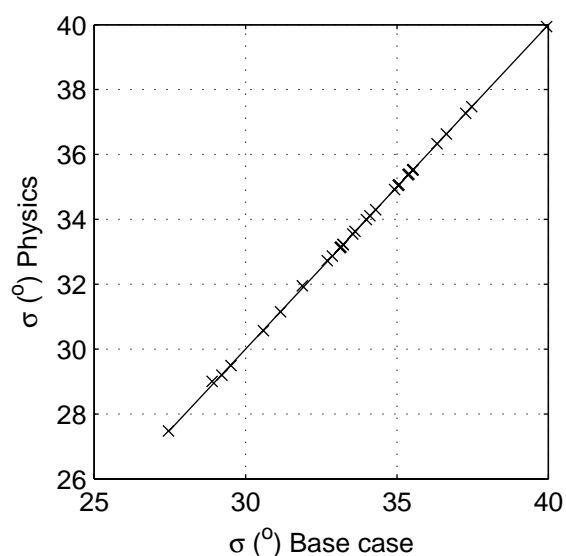
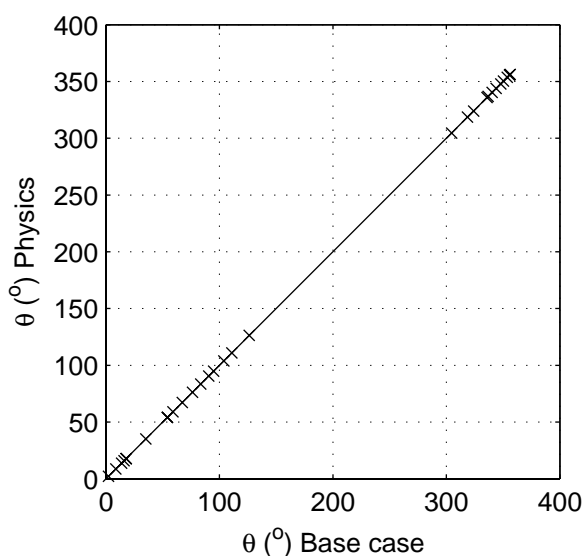
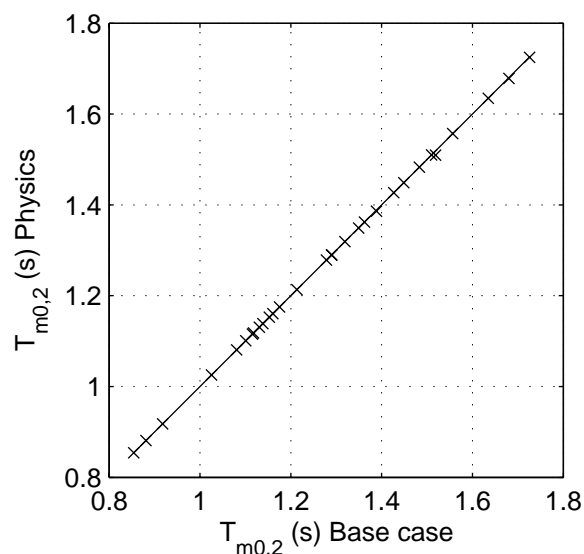
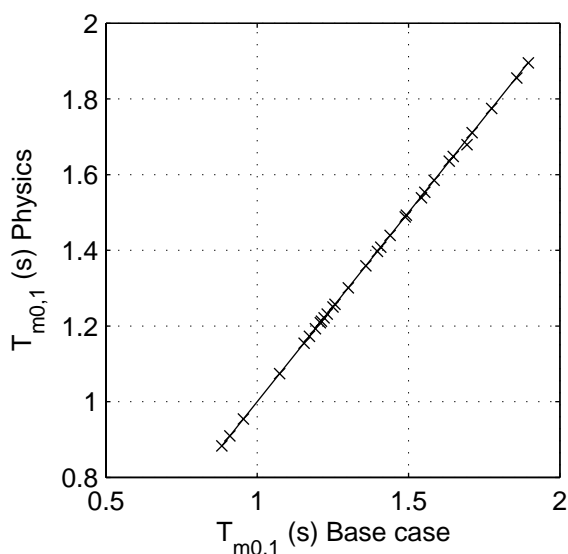
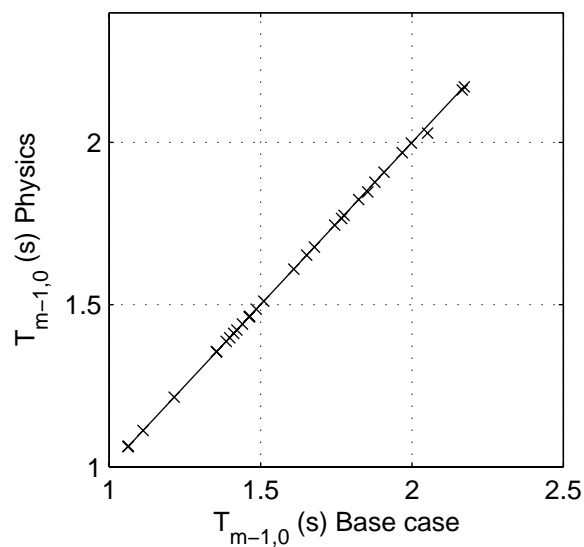
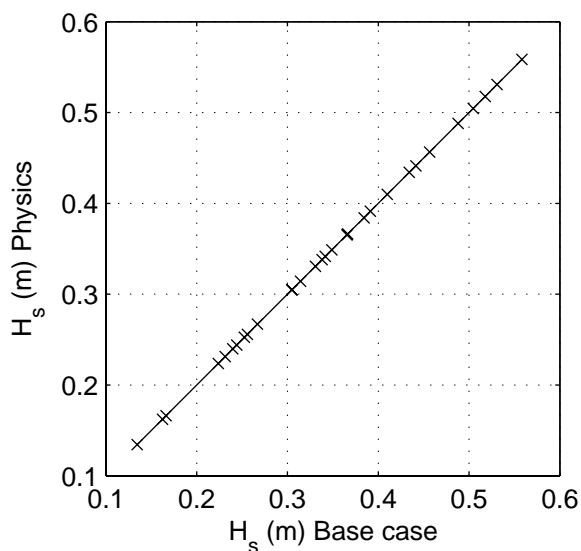
SCAT\_sl\_SL\_P14\_s2p

Calibration SWAN 40.20

A1168

 **Alkyon**

Fig. 5.1.14



Sensitivity of SWAN 40.20 to variations in physical parameters  
Comparison of base case against:  
Stronger triads

Area:SL

Grid:SL

P15

Physics

SCAT\_sl\_SL\_P15\_s2p

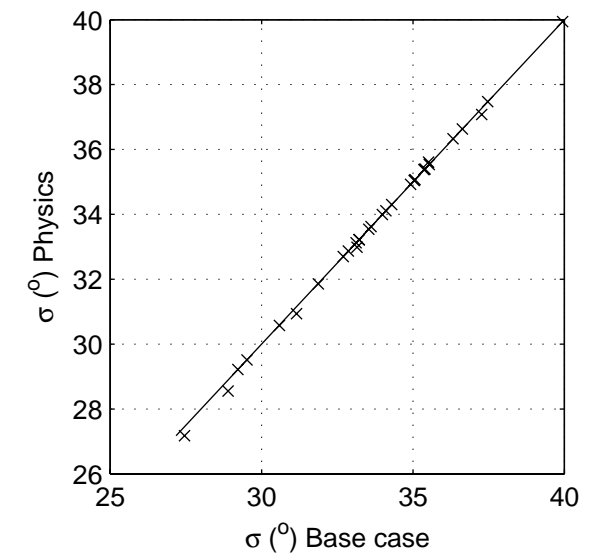
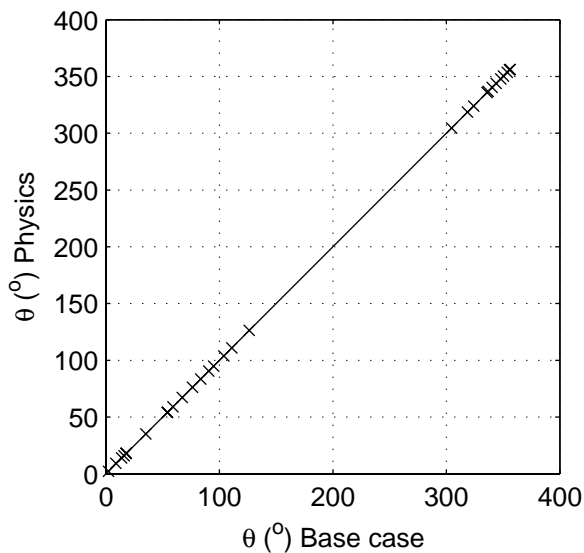
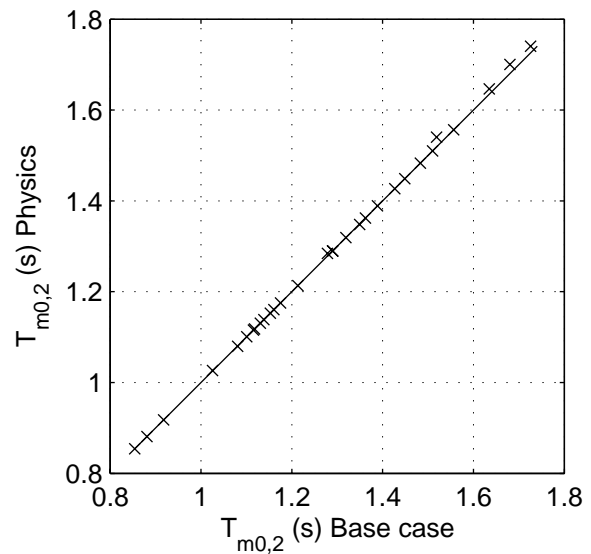
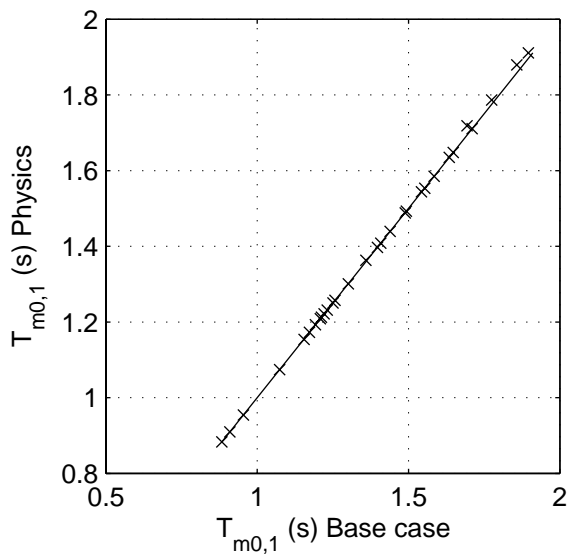
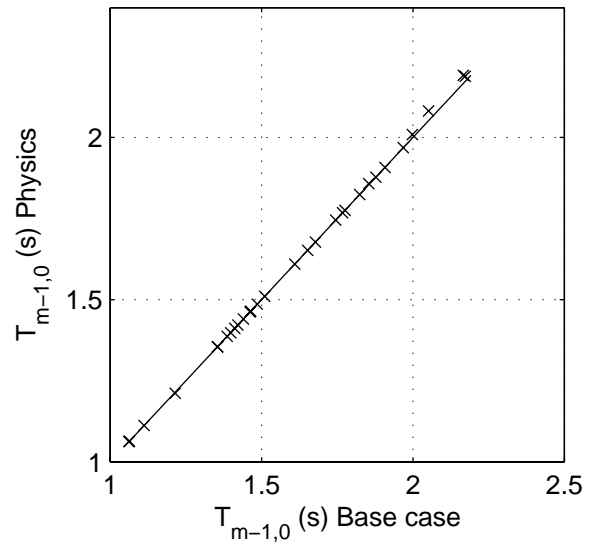
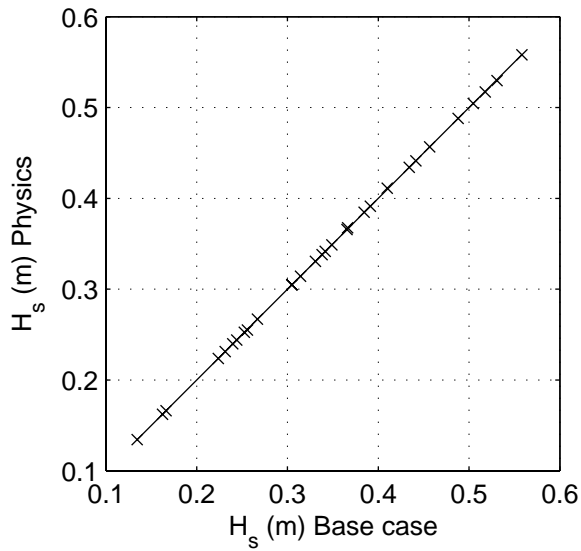
Calibration SWAN 40.20

A1168

 **Alkyon**

Fig. 5.1.15





Sensitivity of SWAN 40.20 to variations in physical parameters  
Comparison of base case against:  
Weaker triads

Area:SL

Grid:SL

P16

Physics

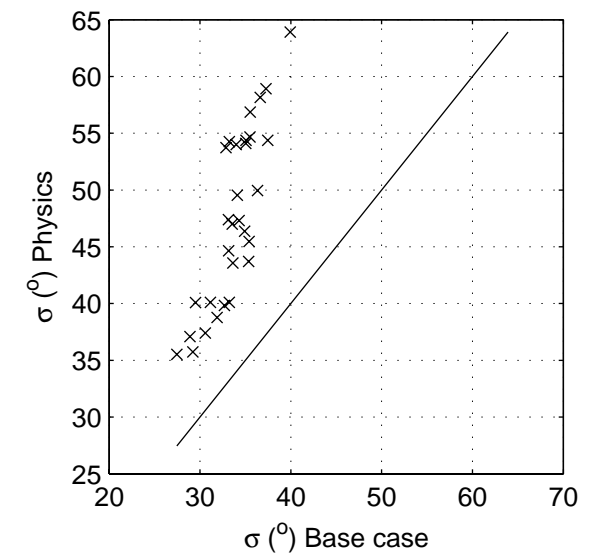
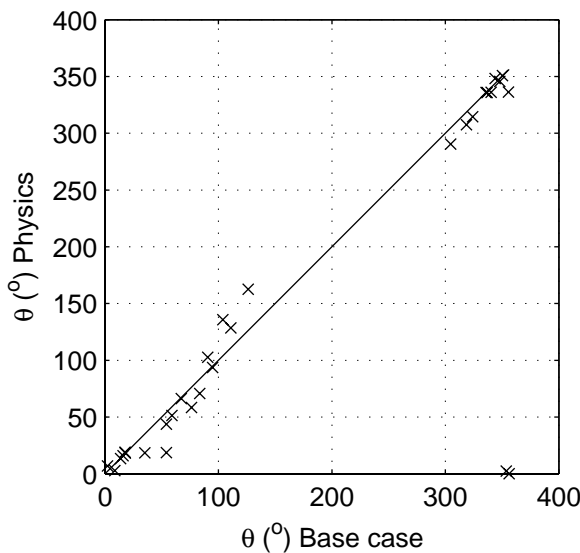
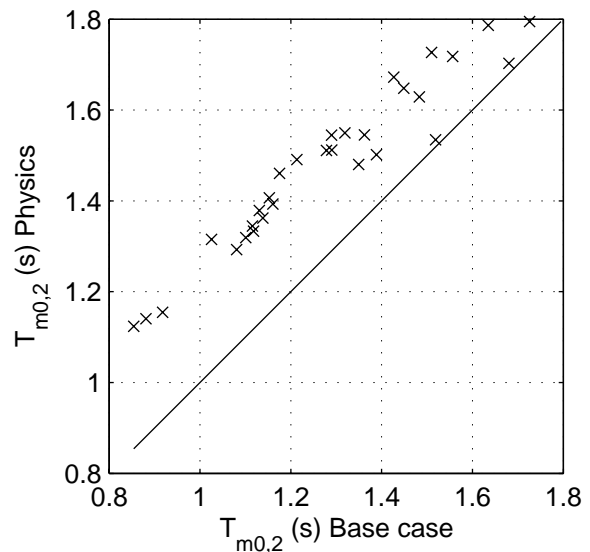
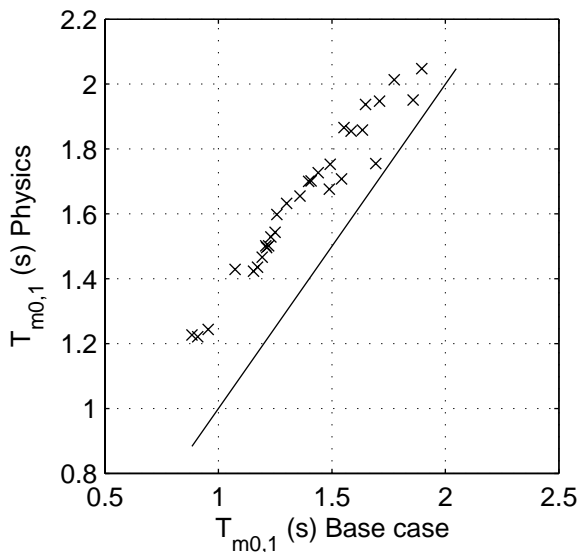
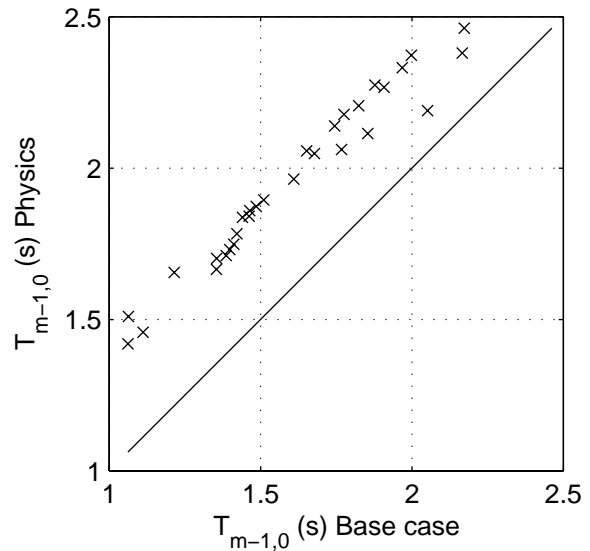
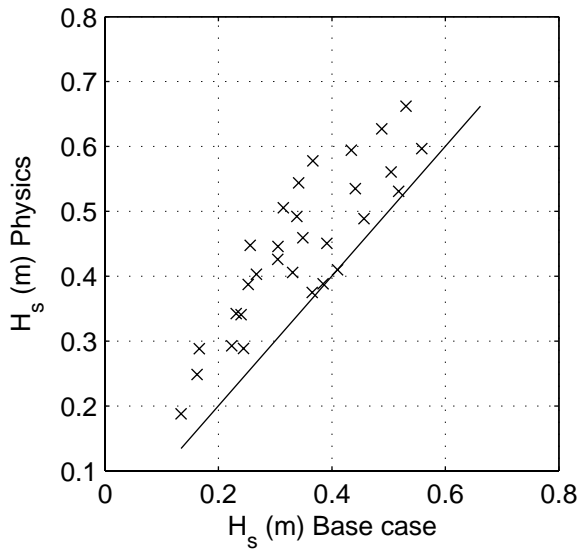
SCAT\_sl\_SL\_P16\_s2p

Calibration SWAN 40.20

A1168

 **Alkyon**

Fig. 5.1.16



Sensitivity of SWAN 40.20 to variations in physical parameters  
Comparison of base case against:  
CSM pow=1

Area:SL

Grid:SL

P17

Physics

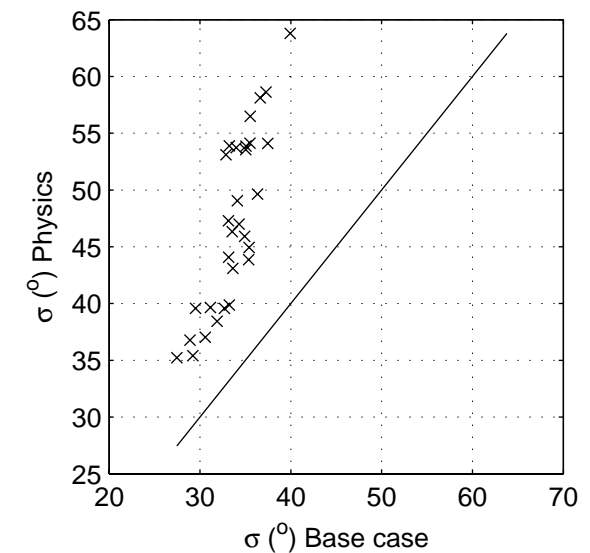
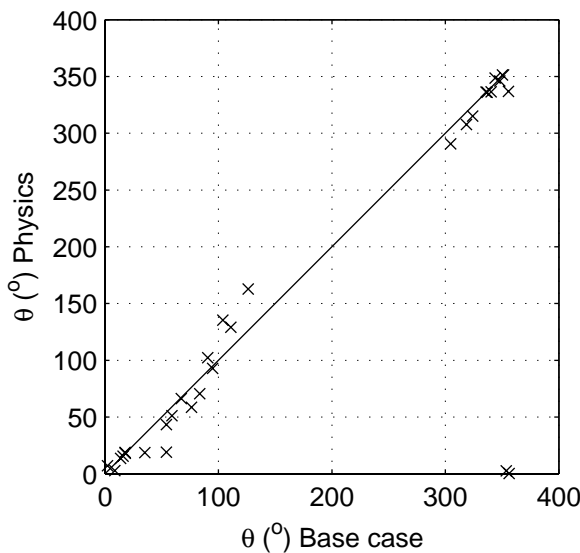
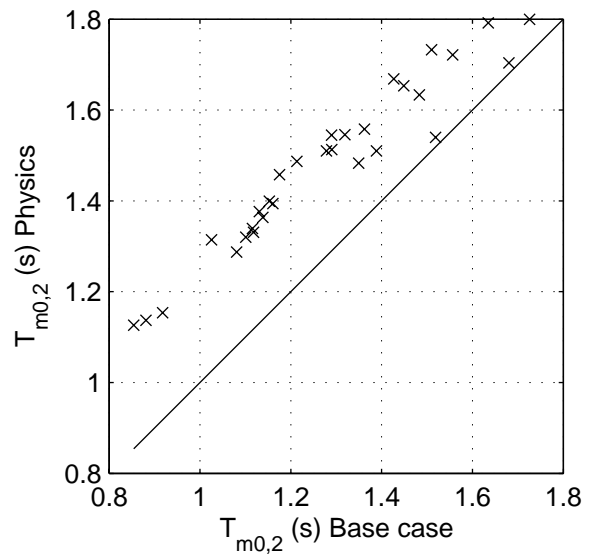
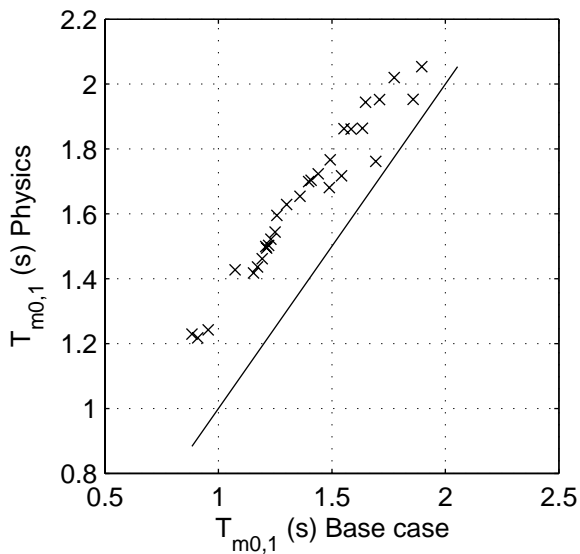
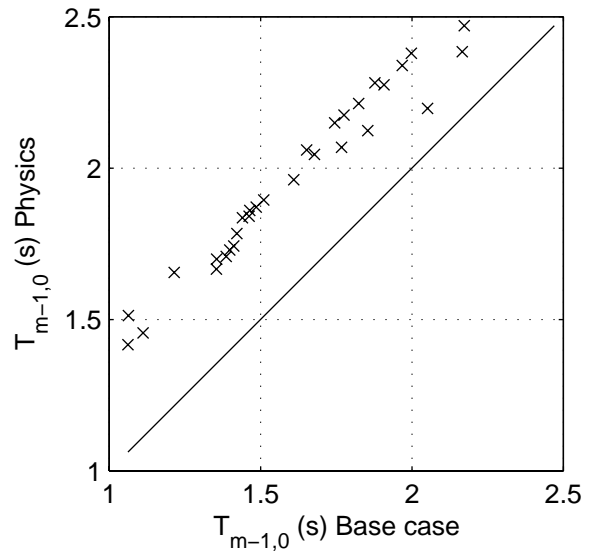
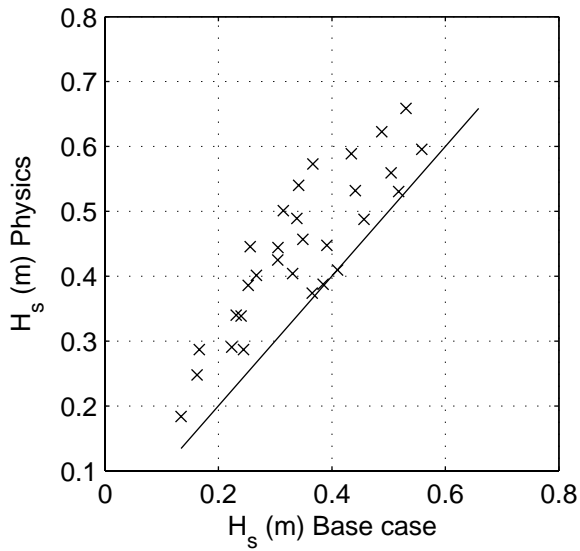
SCAT\_SL\_SL\_P17\_s2p

Calibration SWAN 40.20

A1168

 **Alkyon**

Fig. 5.1.17



Sensitivity of SWAN 40.20 to variations in physical parameters  
Comparison of base case against:  
CSM cst=2.5, pow=0

Area:SL

Grid:SL

P18

Physics

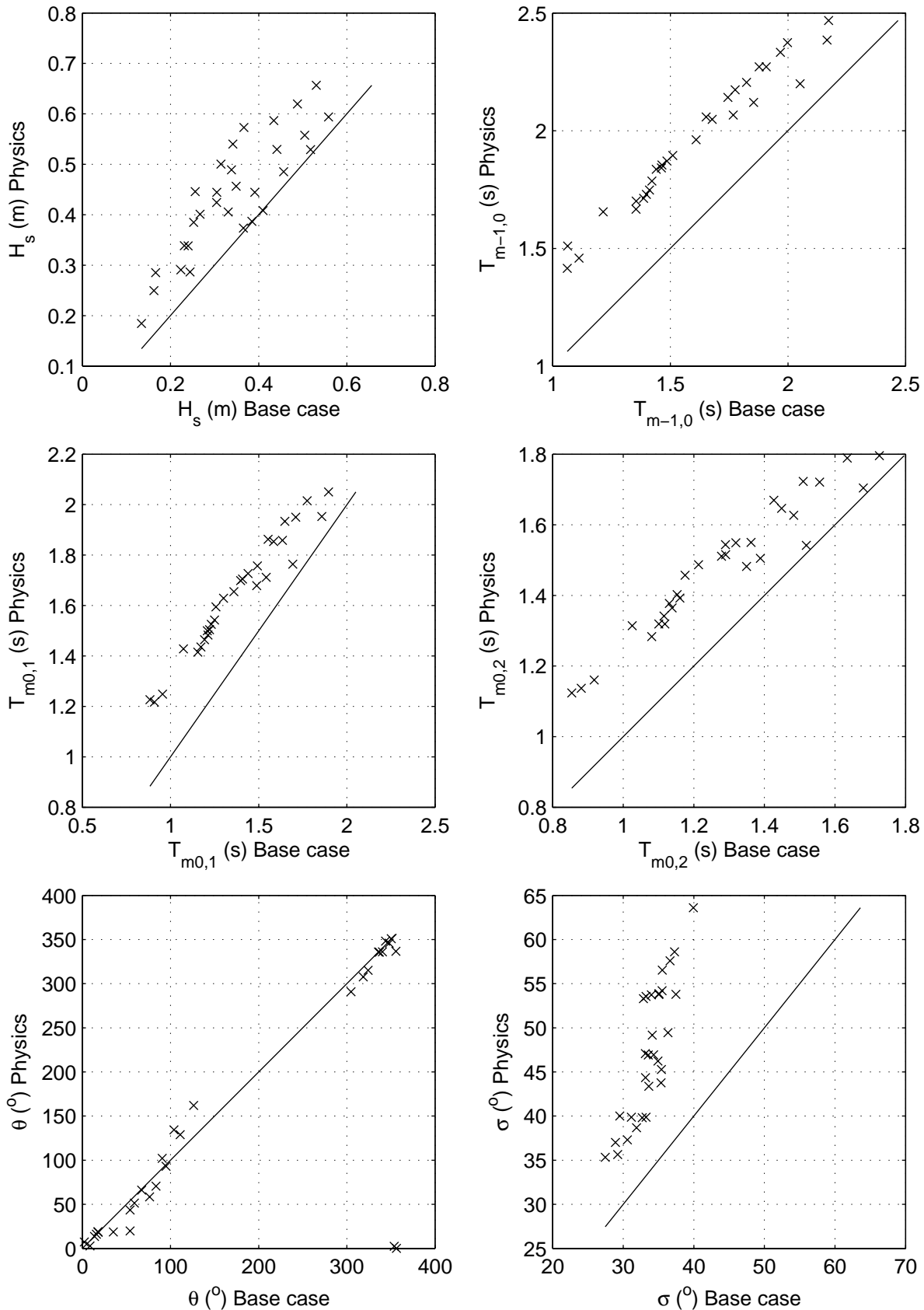
SCAT\_SL\_SL\_P18\_s2p

Calibration SWAN 40.20

A1168

 **Alkyon**

Fig. 5.1.18



Sensitivity of SWAN 40.20 to variations in physical parameters  
Comparison of base case against:  
CSM cst=1.0, pow=0

Area:SL

Grid:SL

P19

Physics

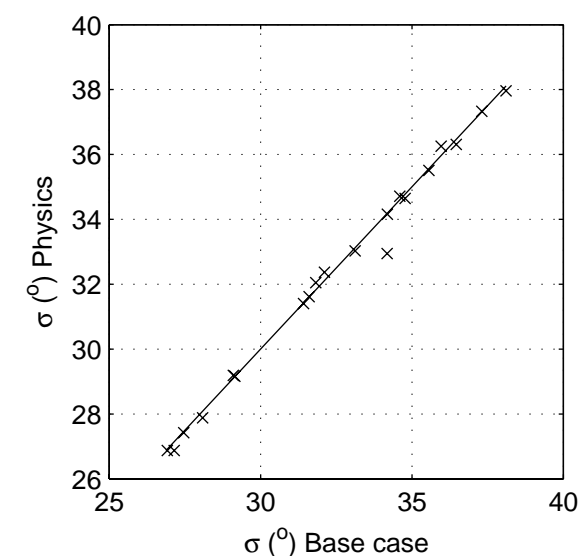
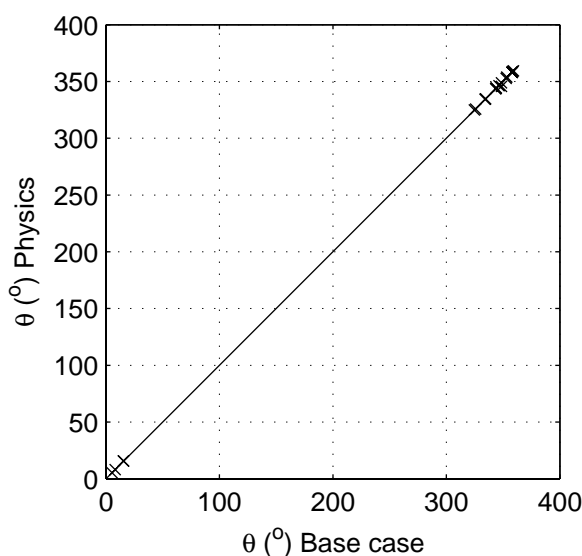
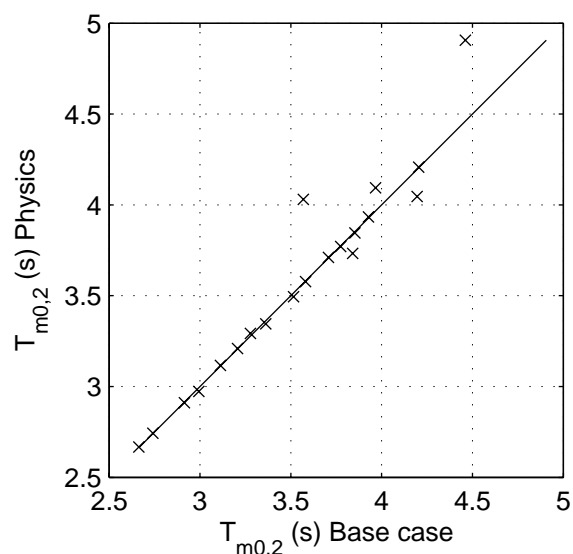
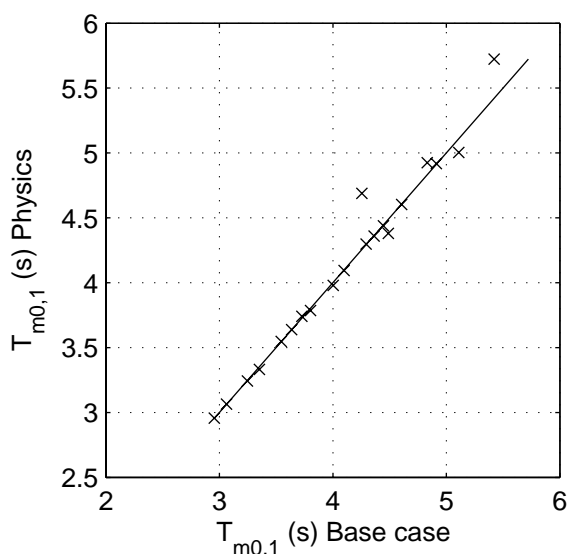
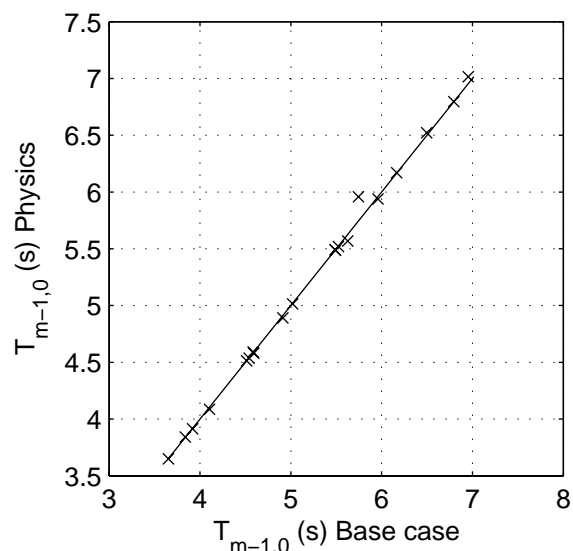
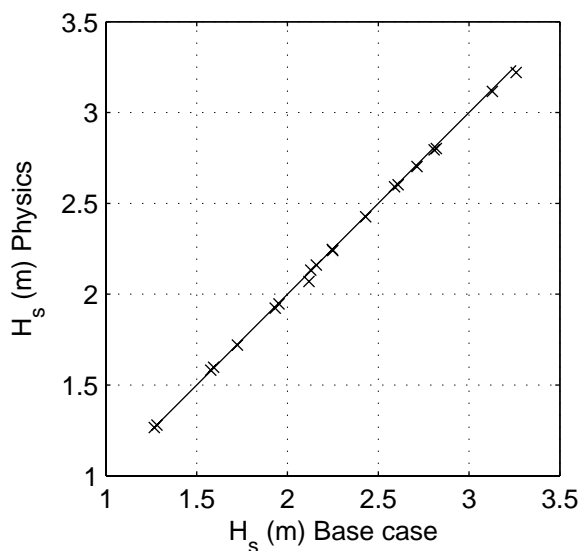
SCAT\_SL\_SL\_P19\_s2p

Calibration SWAN 40.20

A1168

 **Alkyon**

Fig. 5.1.19



Sensitivity of SWAN 40.20 to variations in physical parameters  
Comparison of base case against:  
Higher alpha

Area:WS

Grid:W01

P02

Physics

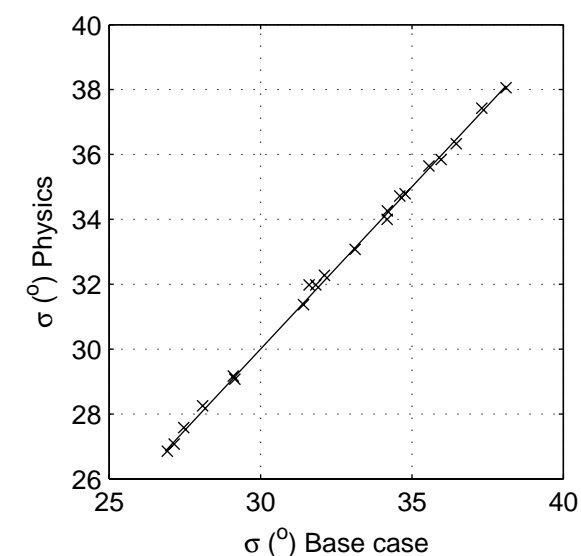
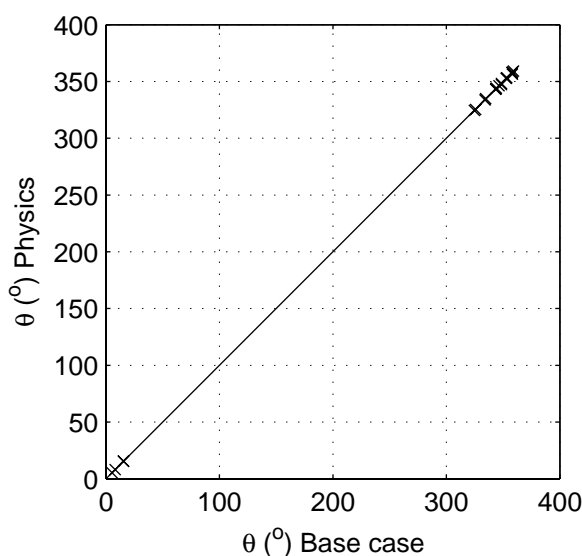
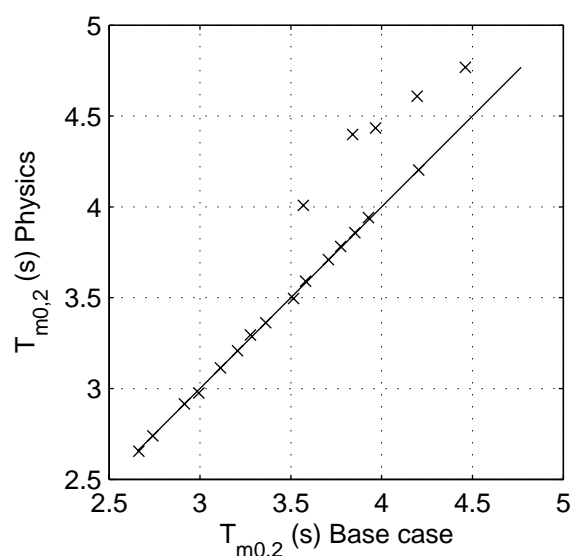
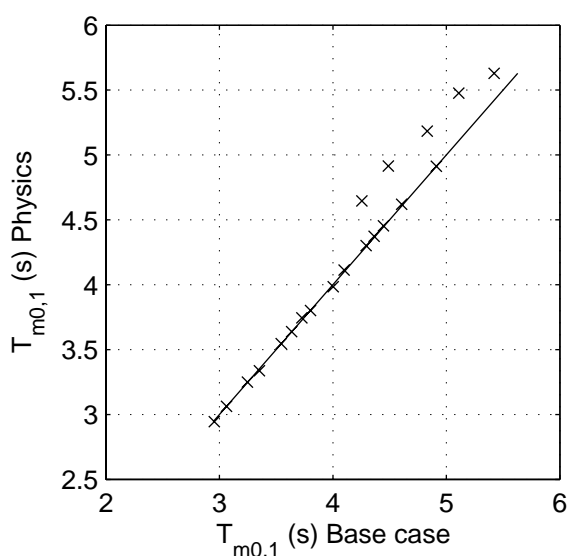
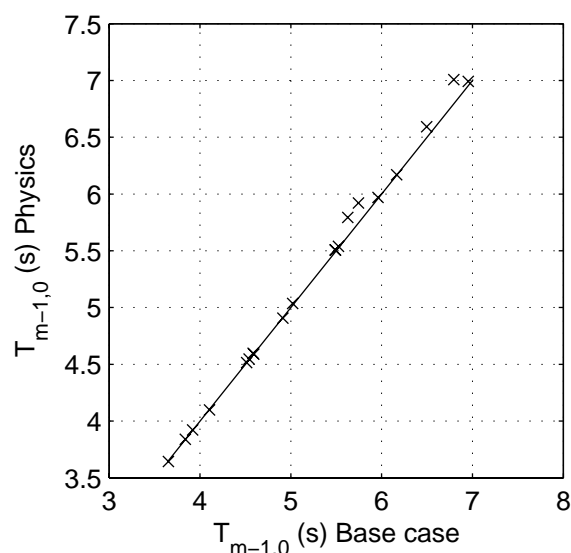
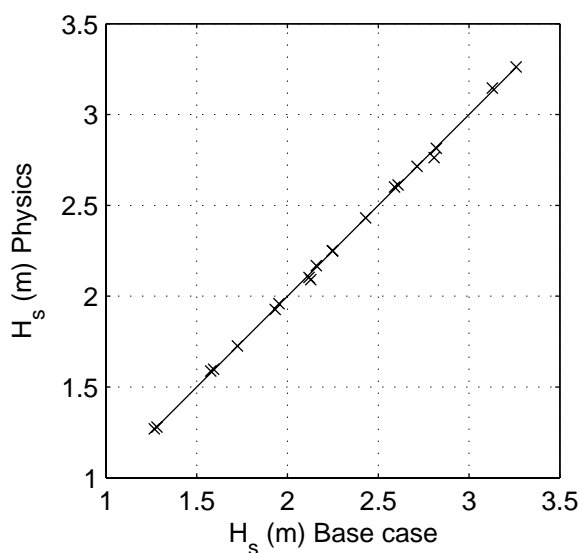
SCAT\_ws\_W01\_P2\_s2p

Calibration SWAN 40.20

A1168

 **Alkyon**

Fig. 5.2.2



Sensitivity of SWAN 40.20 to variations in physical parameters  
Comparison of base case against:  
Lower alpha

Area:WS

Grid:W01

P03

Physics

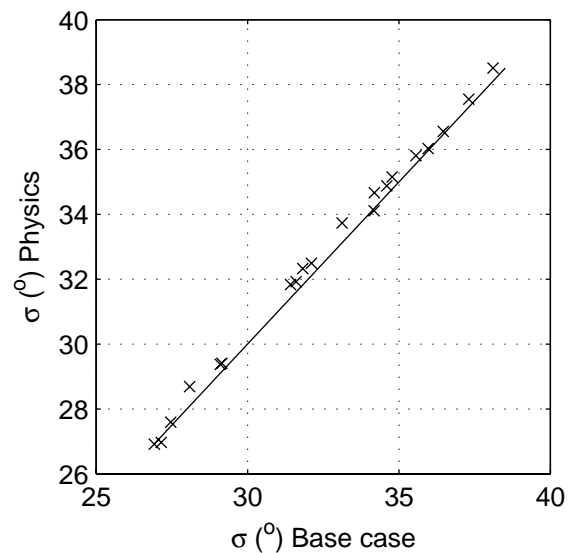
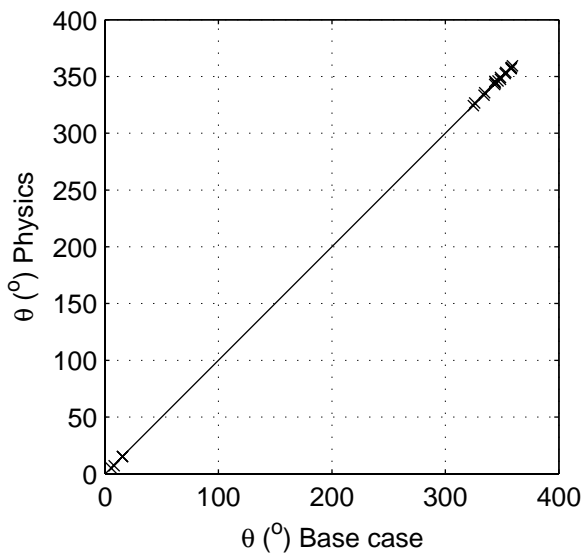
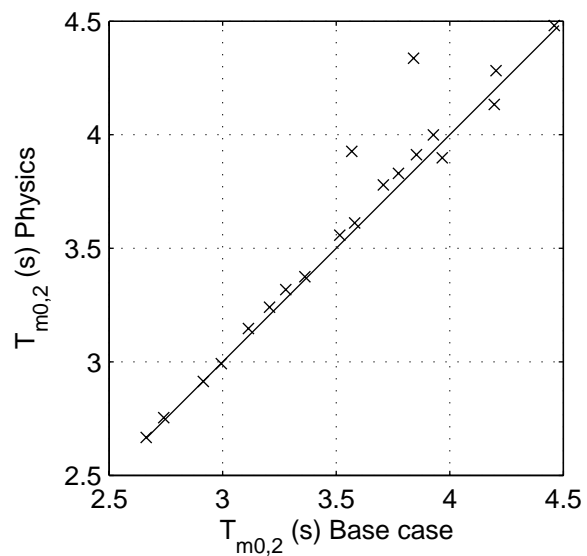
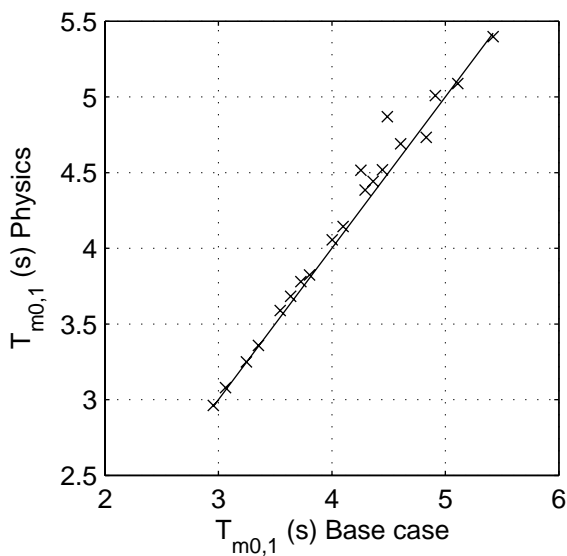
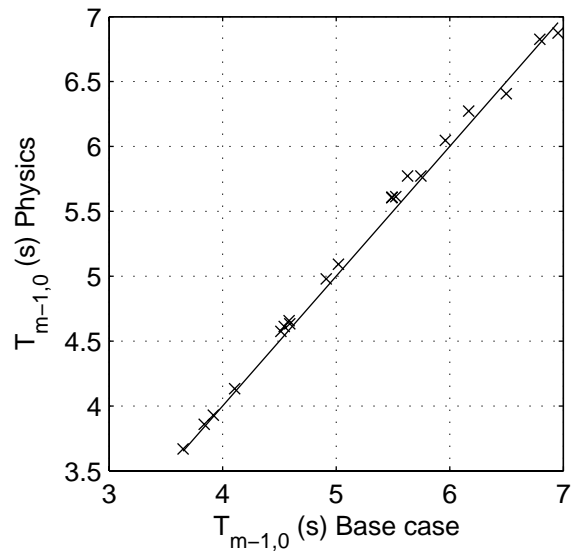
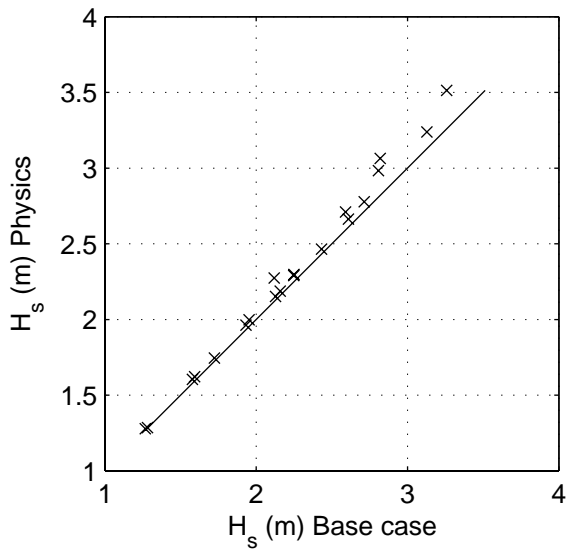
SCAT\_ws\_W01\_P3\_s2p

Calibration SWAN 40.20

A1168

 **Alkyon**

Fig. 5.2.3



Sensitivity of SWAN 40.20 to variations in physical parameters  
Comparison of base case against:  
Higher gamma

Area:WS

Grid:W01

P04

Physics

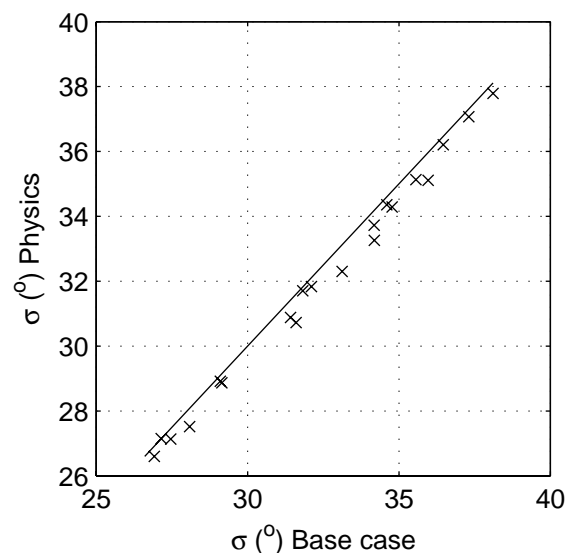
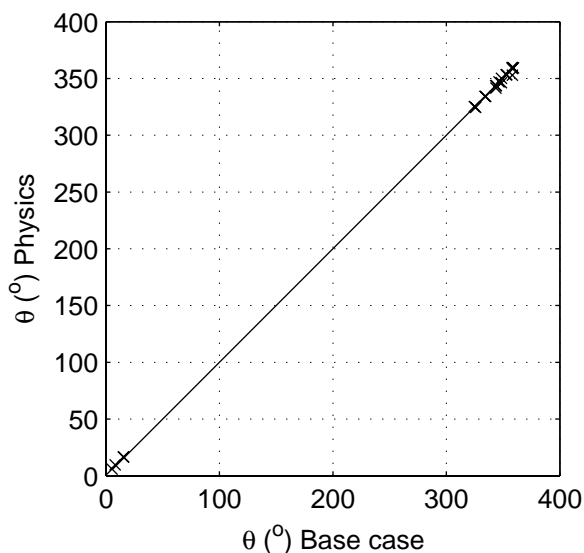
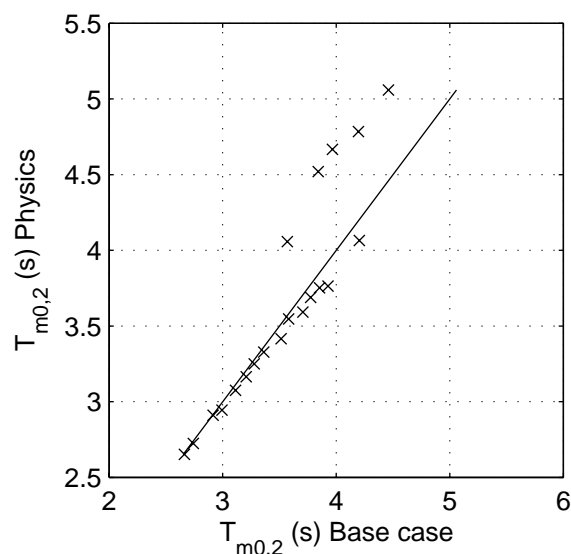
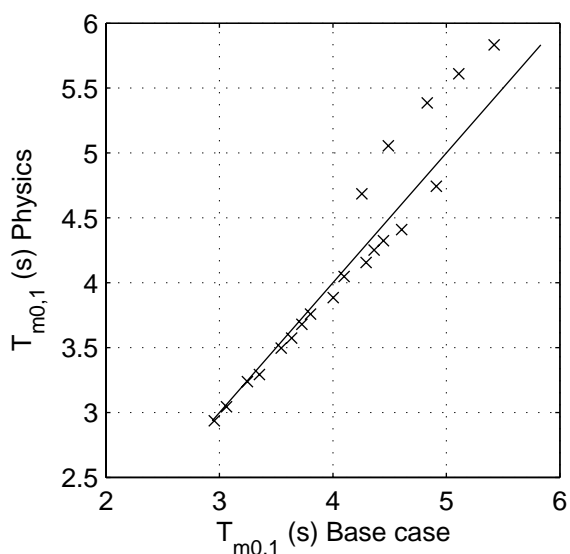
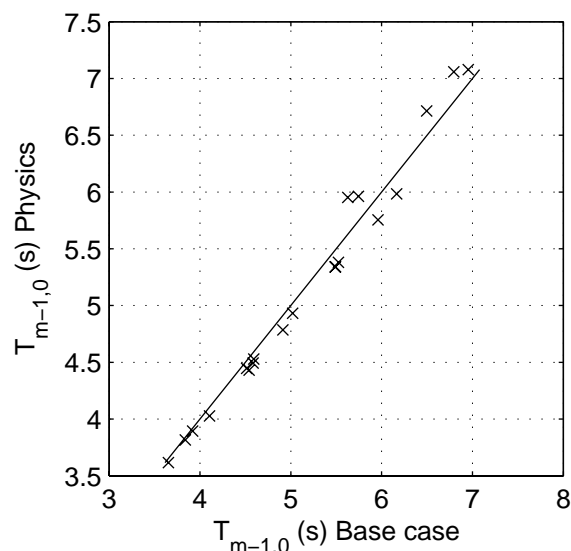
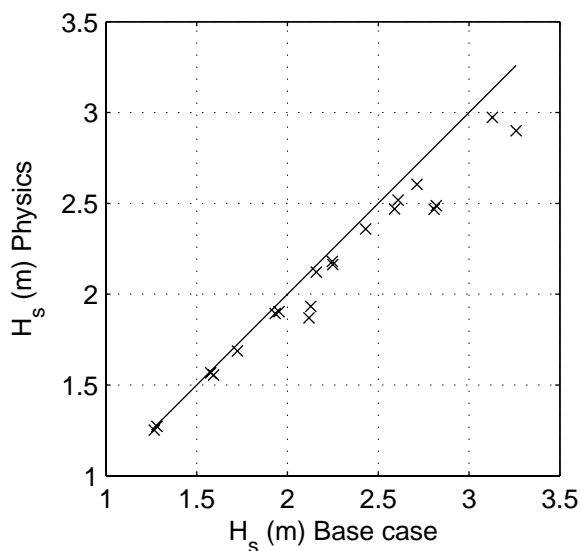
SCAT\_ws\_W01\_P4\_s2p

Calibration SWAN 40.20

A1168

 **Alkyon**

Fig. 5.2.4



Sensitivity of SWAN 40.20 to variations in physical parameters  
Comparison of base case against:  
Lower gamma

Area:WS

Grid:W01

P05

Physics

SCAT\_ws\_W01\_P5\_s2p

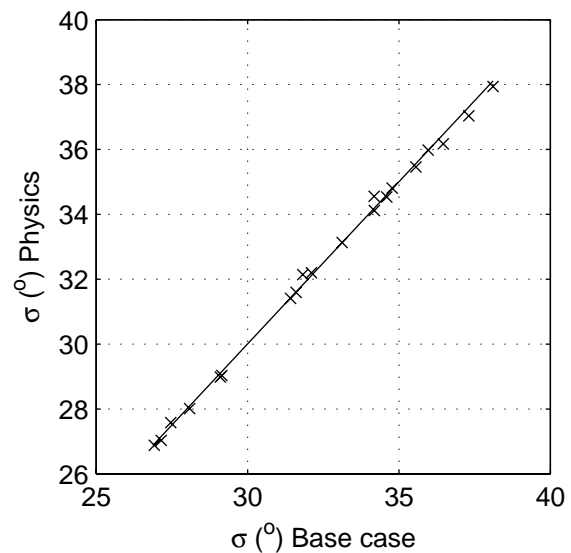
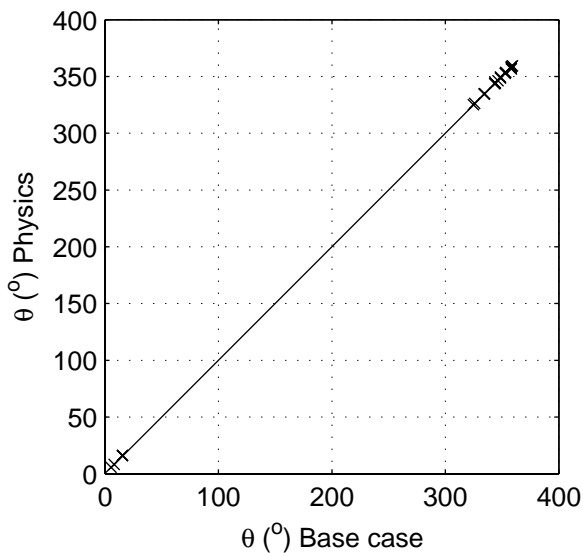
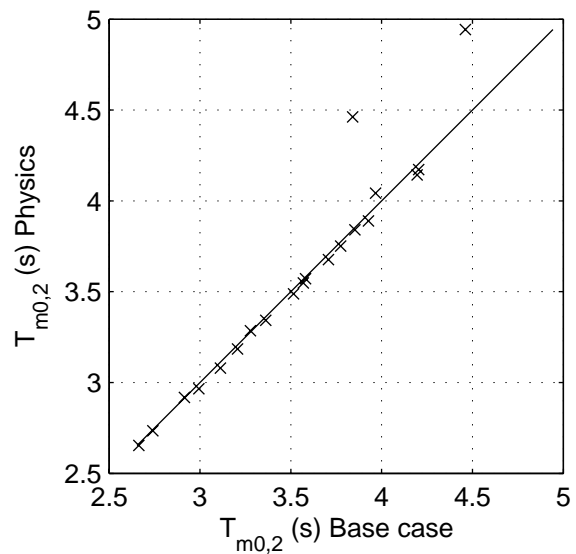
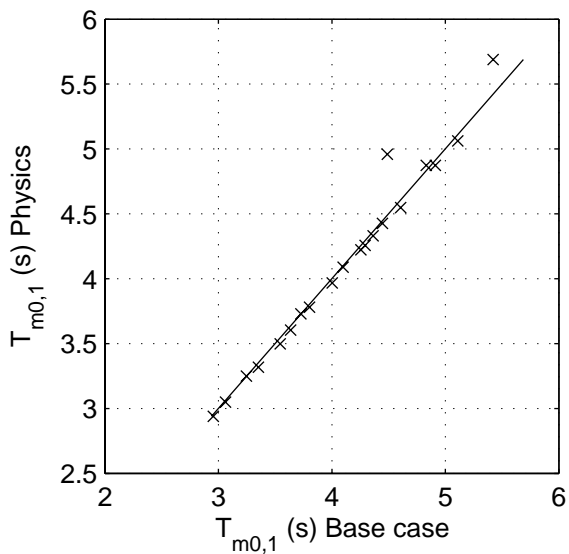
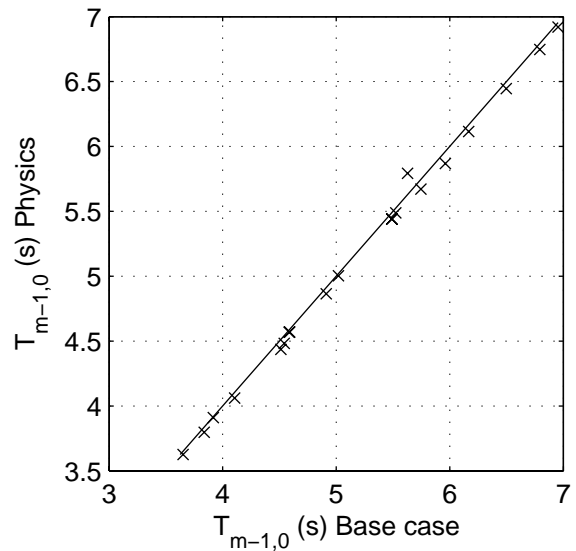
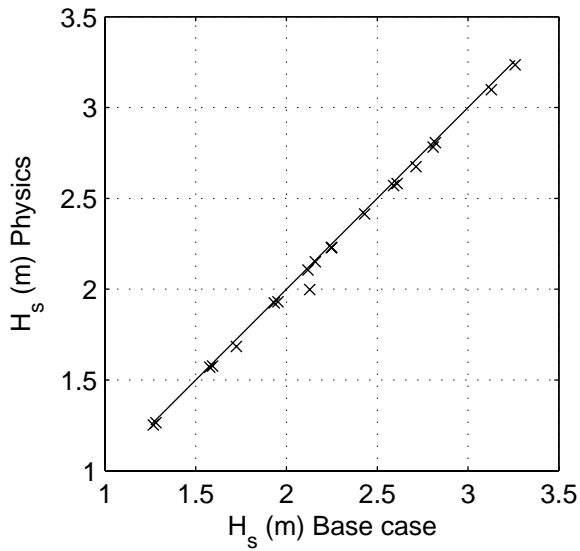
Calibration SWAN 40.20

A1168

 **Alkyon**

Fig. 5.2.5





Sensitivity of SWAN 40.20 to variations in physical parameters  
Comparison of base case against:  
Stronger Sfric

Area:WS

Grid:W01

P06

Physics

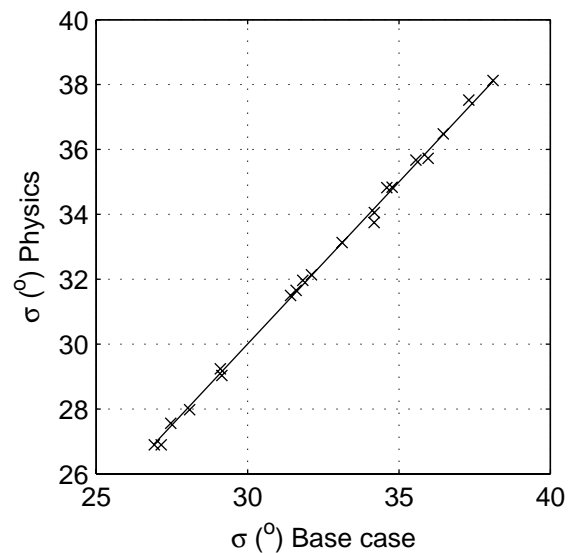
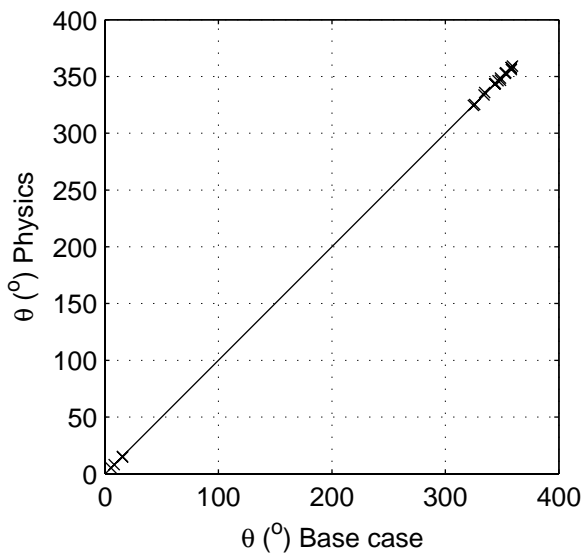
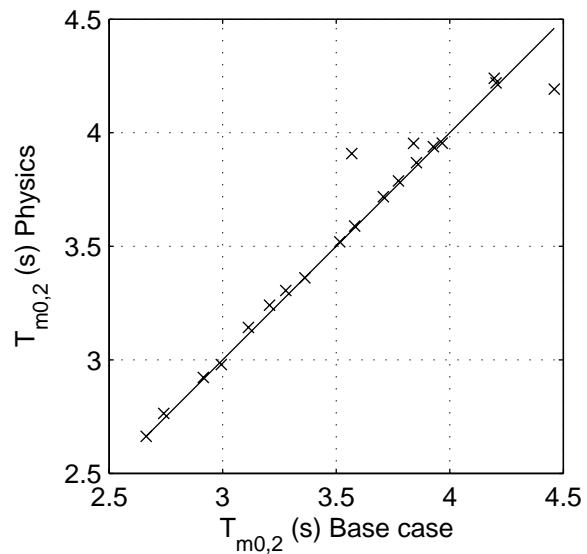
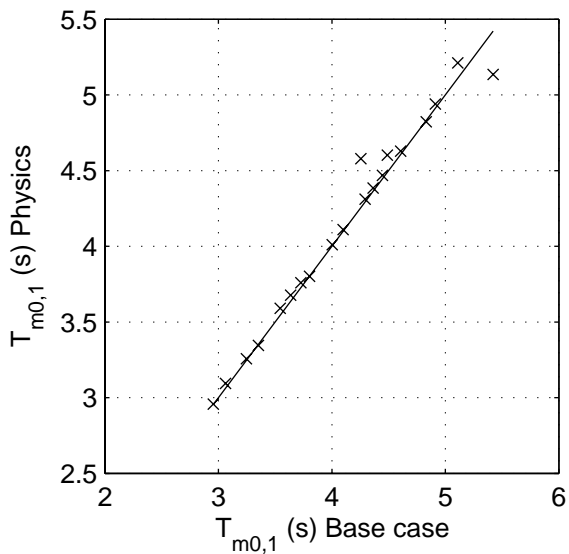
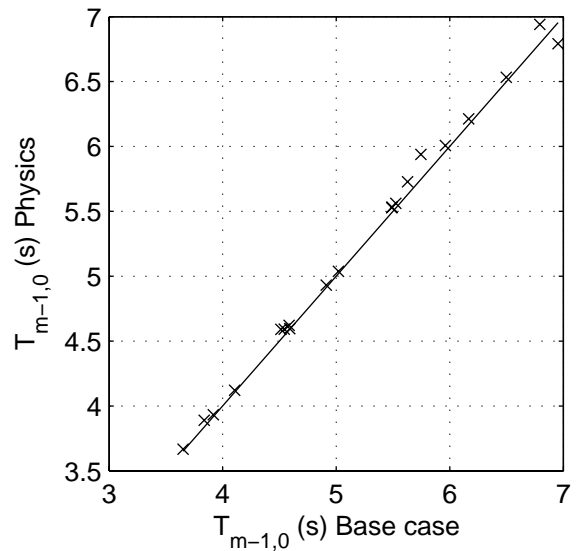
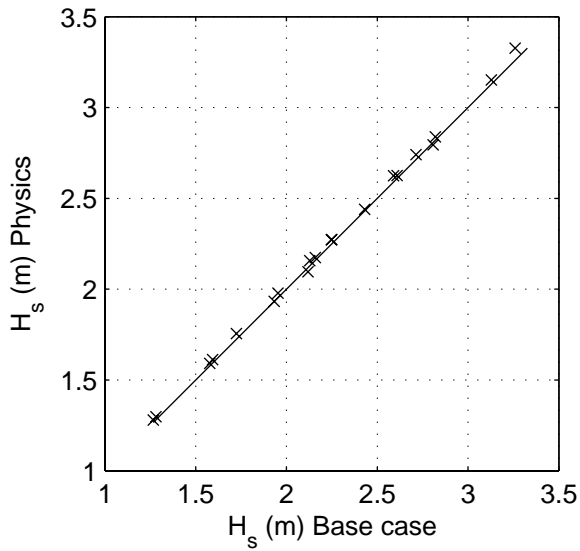
SCAT\_ws\_W01\_P6\_s2p

Calibration SWAN 40.20

A1168

 **Alkyon**

Fig. 5.2.6



Sensitivity of SWAN 40.20 to variations in physical parameters  
Comparison of base case against:  
Weaker Sfric

Area:WS

Grid:W01

P07

Physics

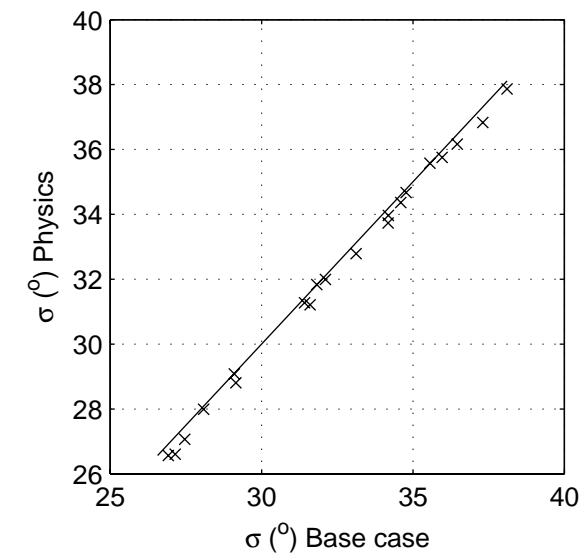
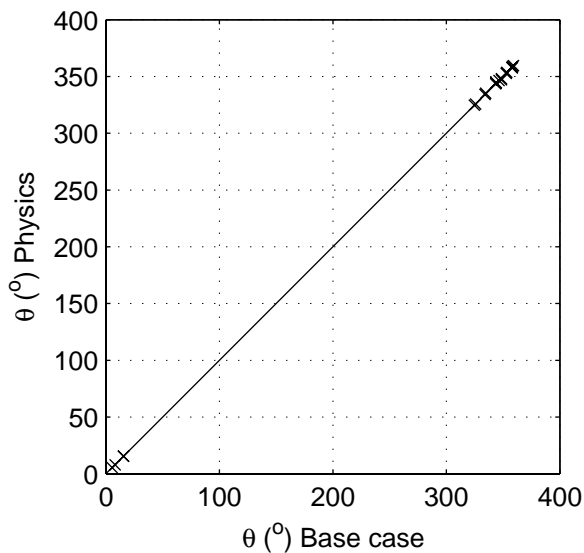
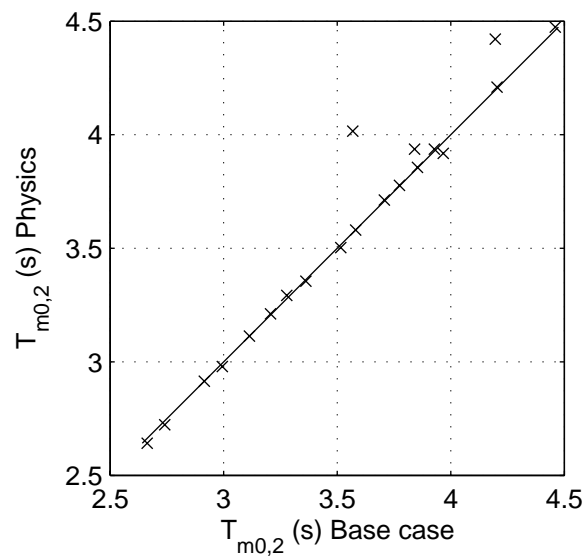
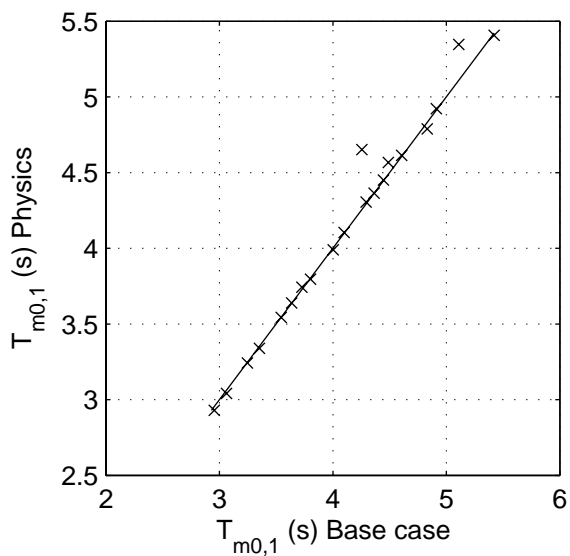
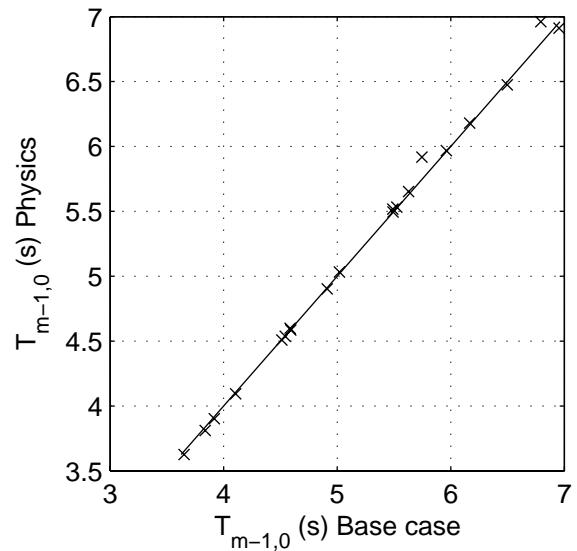
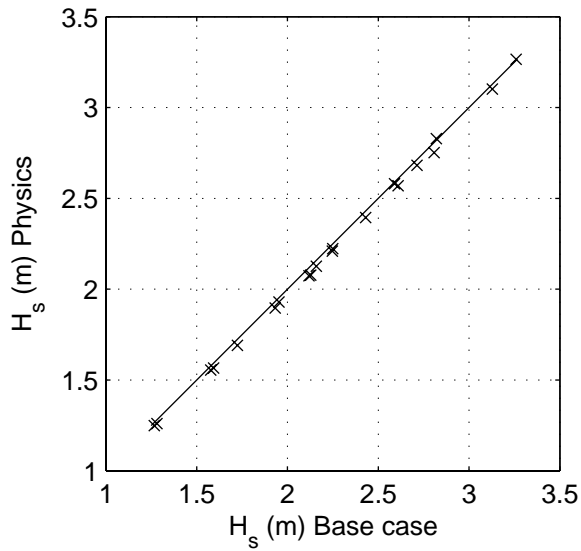
SCAT\_ws\_W01\_P7\_s2p

Calibration SWAN 40.20

A1168

 **Alkyon**

Fig. 5.2.7



Sensitivity of SWAN 40.20 to variations in physical parameters  
Comparison of base case against:  
Stronger Swcap

Area:WS

Grid:W01

P08

Physics

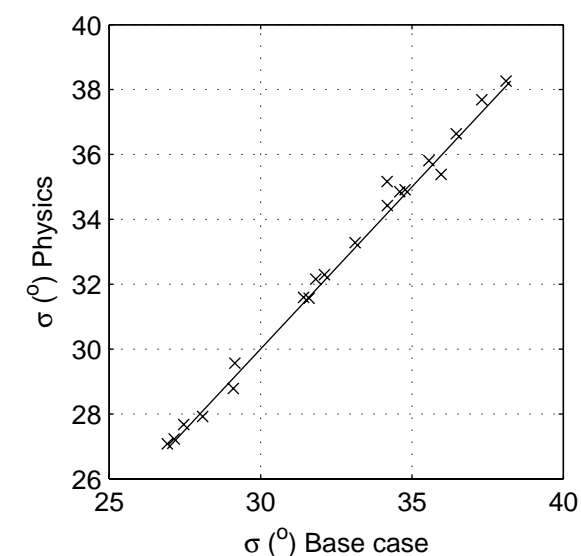
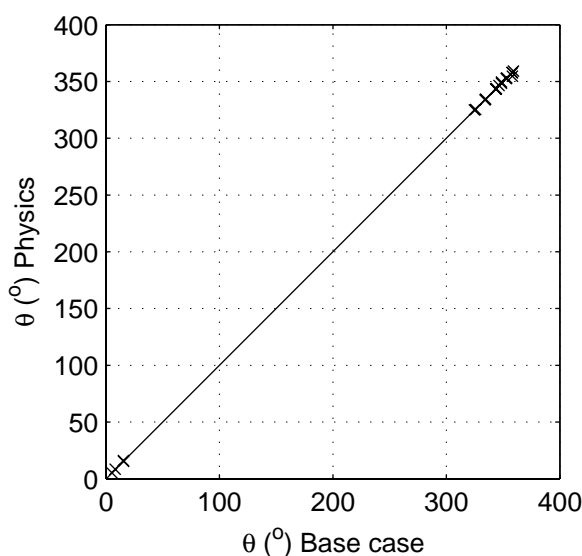
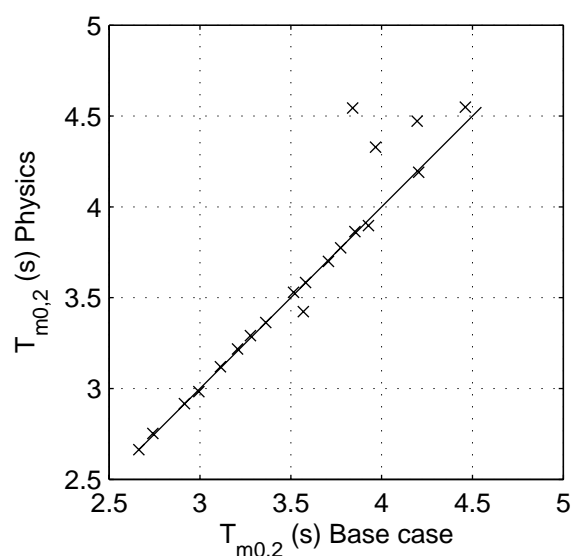
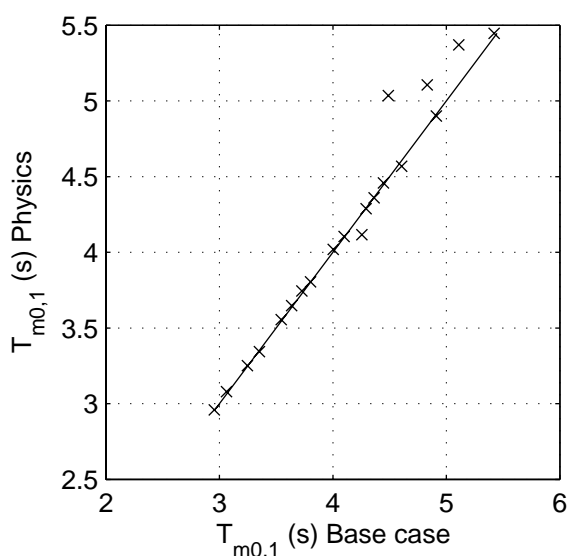
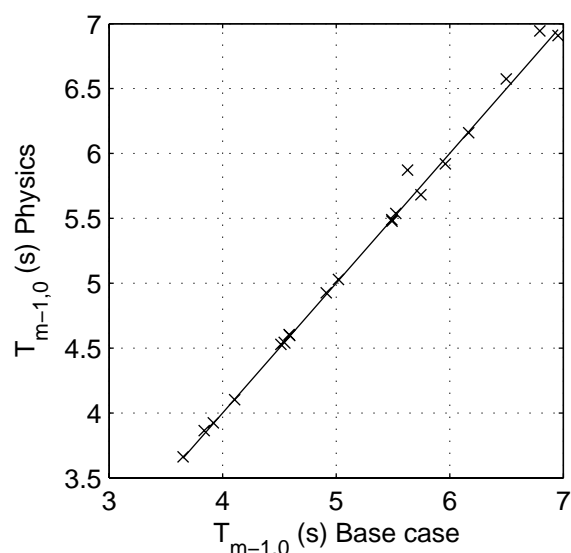
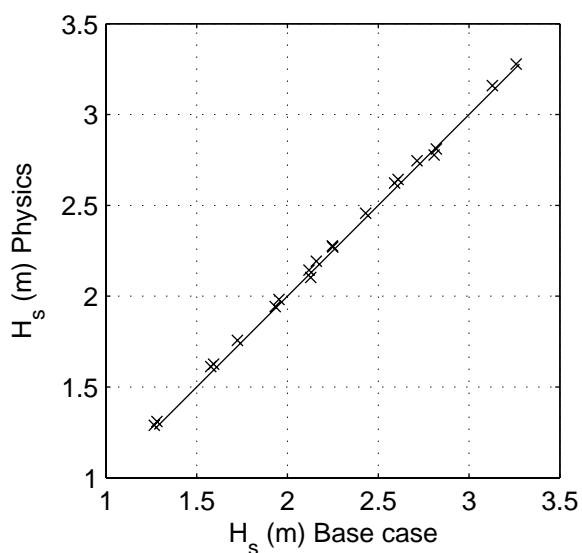
SCAT\_ws\_W01\_P8\_s2p

Calibration SWAN 40.20

A1168

 **Alkyon**

Fig. 5.2.8



Sensitivity of SWAN 40.20 to variations in physical parameters  
Comparison of base case against:  
Weaker Swcap

Area:WS

Grid:W01

P09

Physics

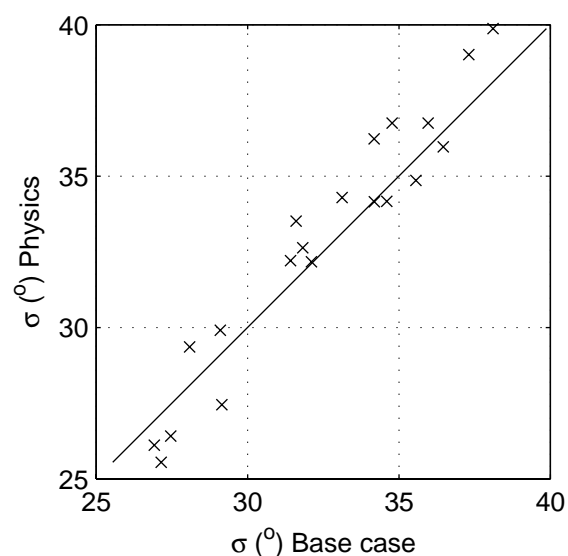
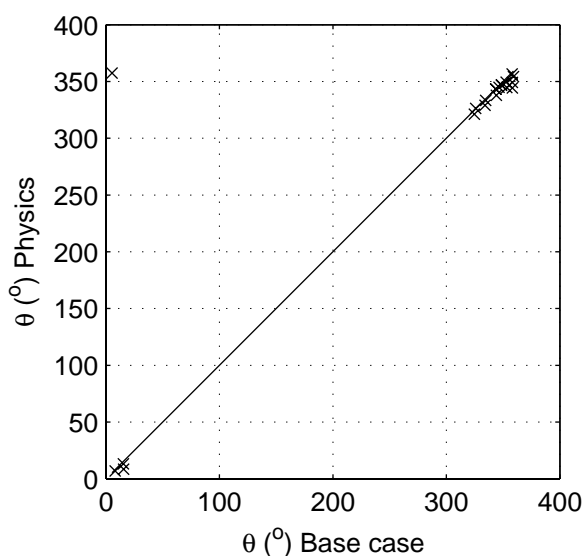
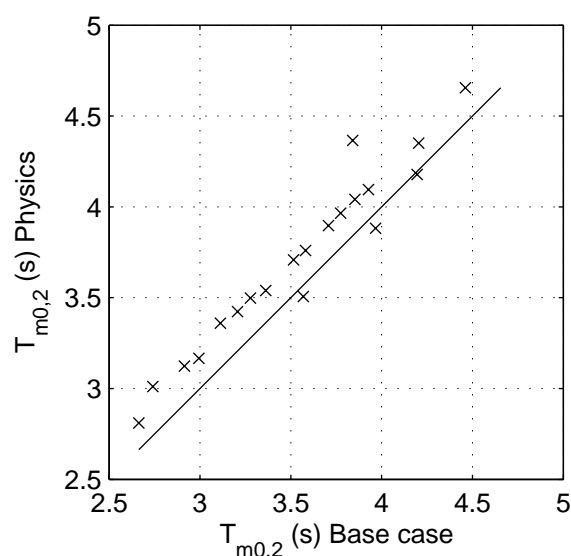
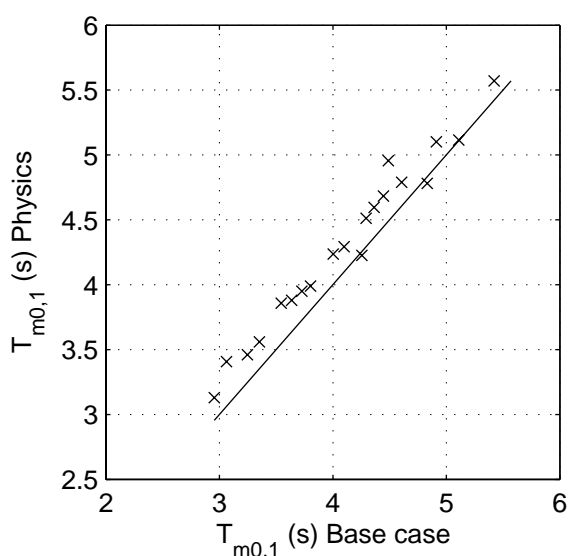
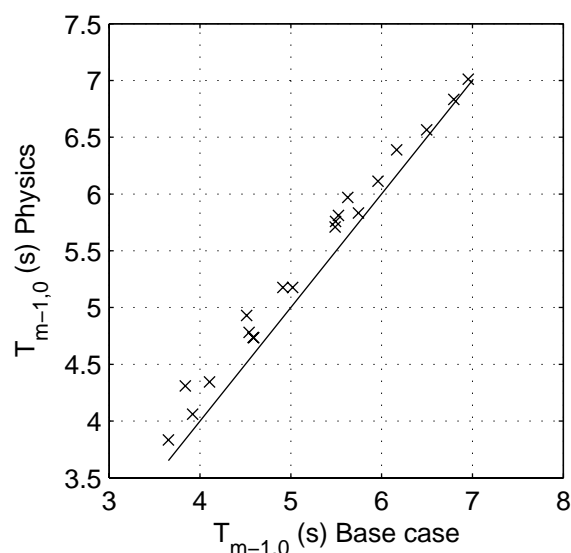
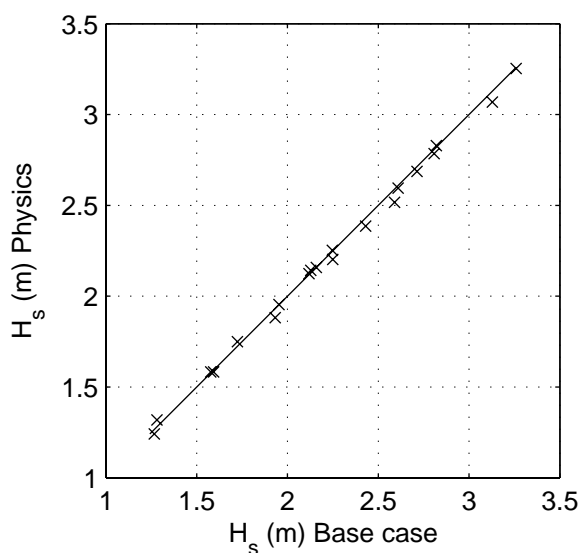
SCAT\_ws\_W01\_P9\_s2p

Calibration SWAN 40.20

A1168

 **Alkyon**

Fig. 5.2.9



Sensitivity of SWAN 40.20 to variations in physical parameters  
Comparison of base case against:  
Higher lambda in SnI4

Area:WS

Grid:W01

P10

Physics

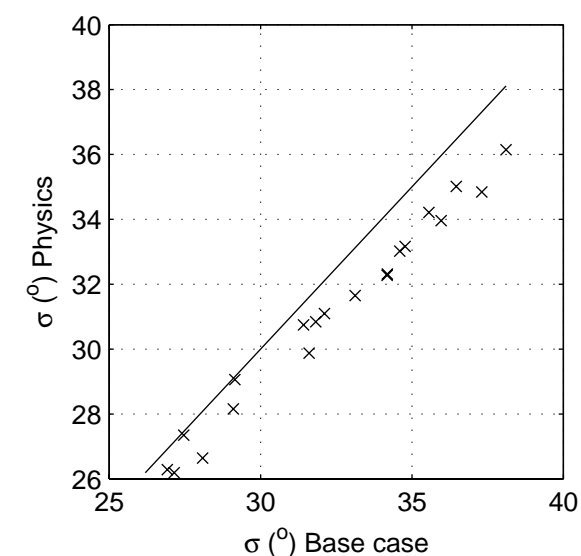
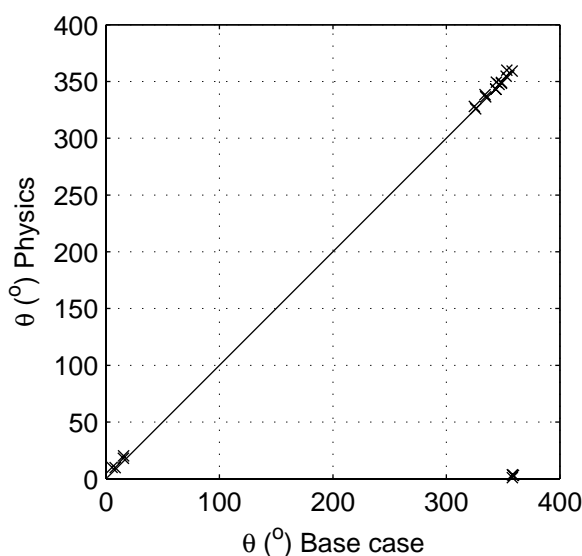
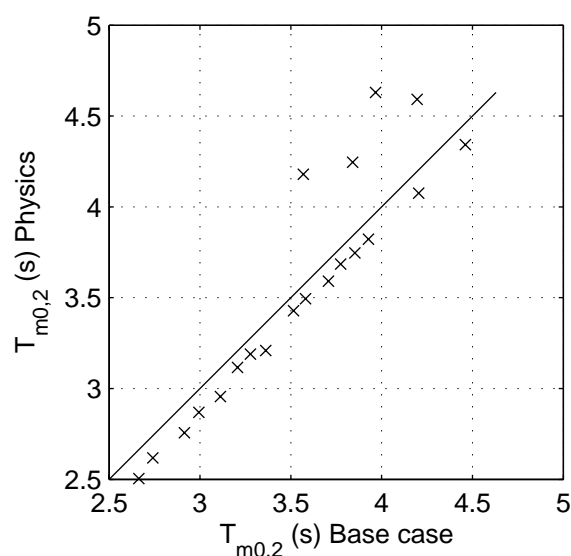
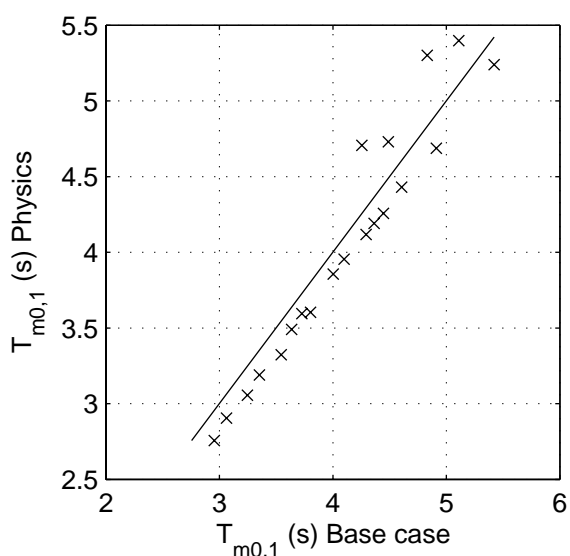
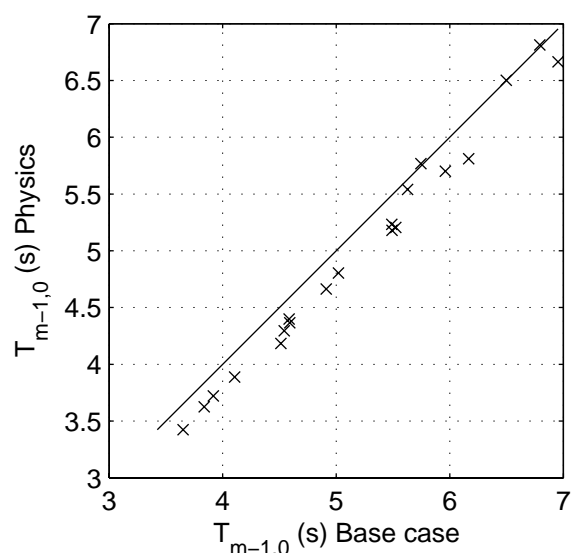
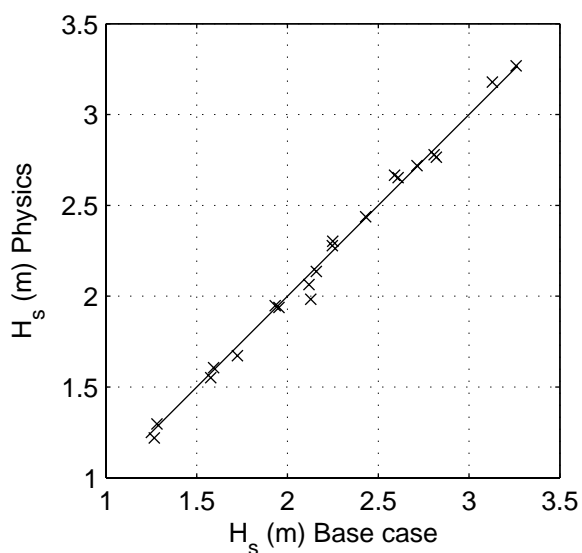
SCAT\_ws\_W01\_P10\_s2p

Calibration SWAN 40.20

A1168

 **Alkyon**

Fig. 5.2.10



Sensitivity of SWAN 40.20 to variations in physical parameters  
Comparison of base case against:  
Lower lambda in SnI4

Area:WS

Grid:W01

P11

Physics

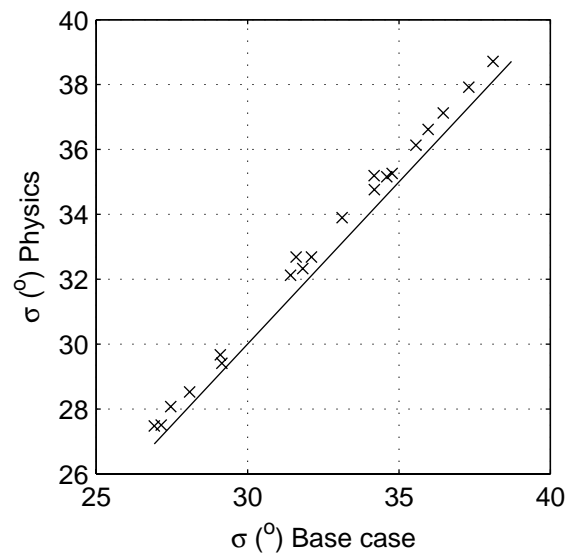
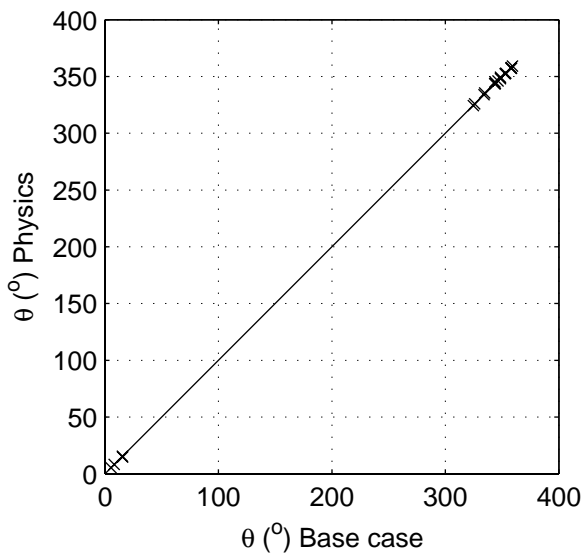
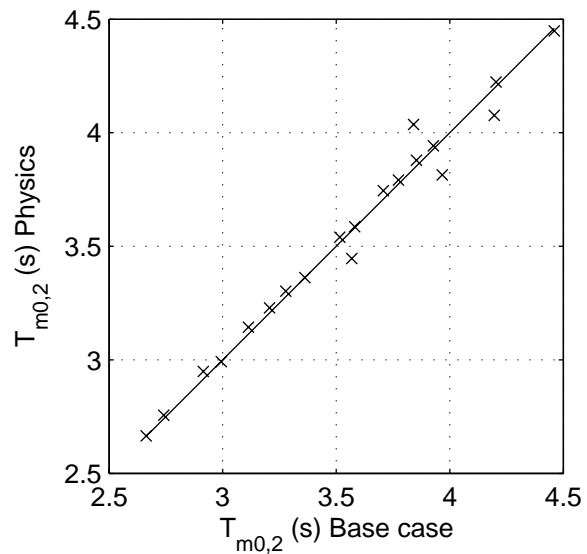
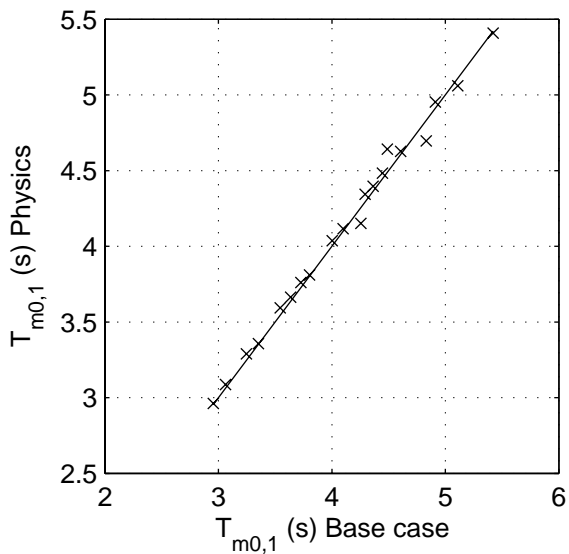
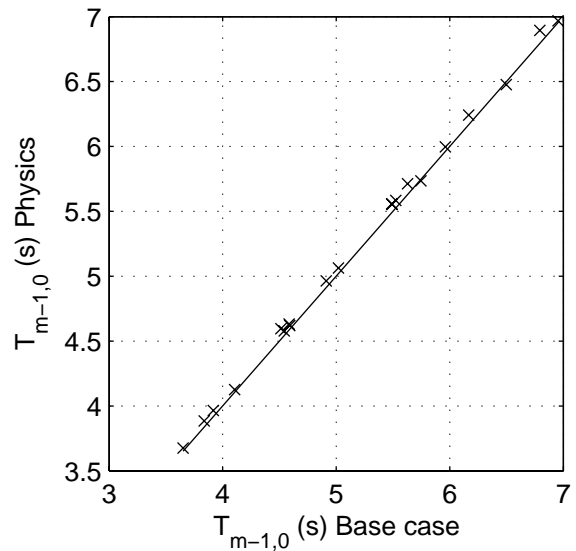
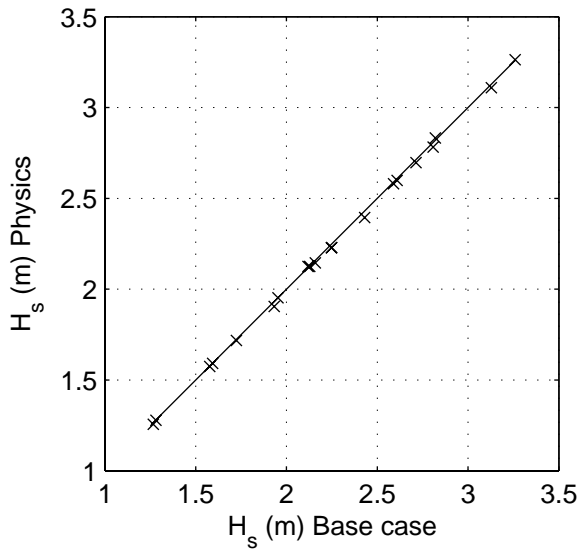
SCAT\_ws\_W01\_P11\_s2p

Calibration SWAN 40.20

A1168

 **Alkyon**

Fig. 5.2.11



Sensitivity of SWAN 40.20 to variations in physical parameters  
Comparison of base case against:  
Stronger Snl4

Area:WS

Grid:W01

P12

Physics

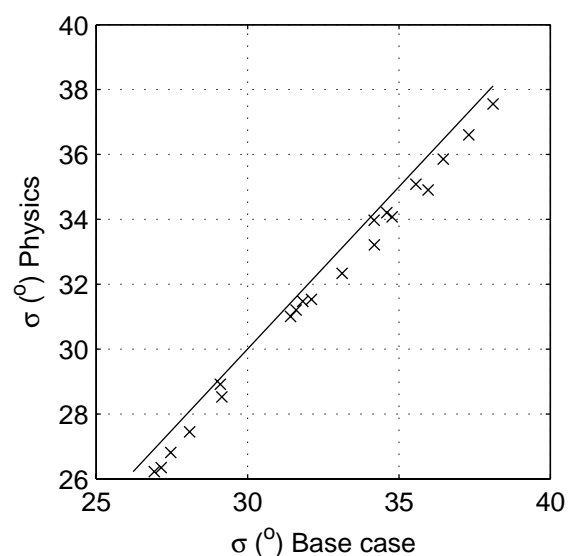
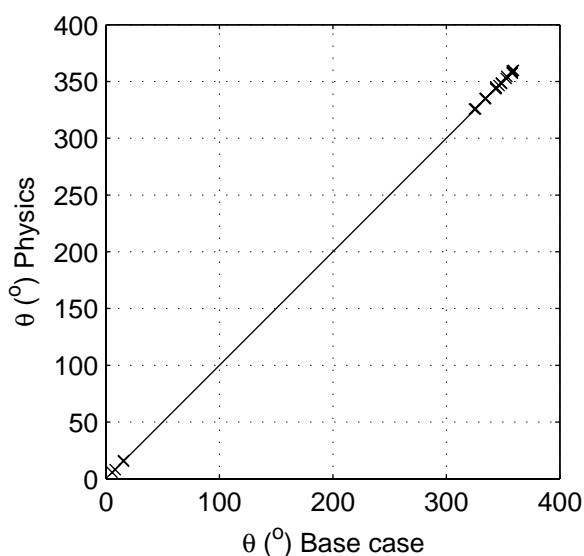
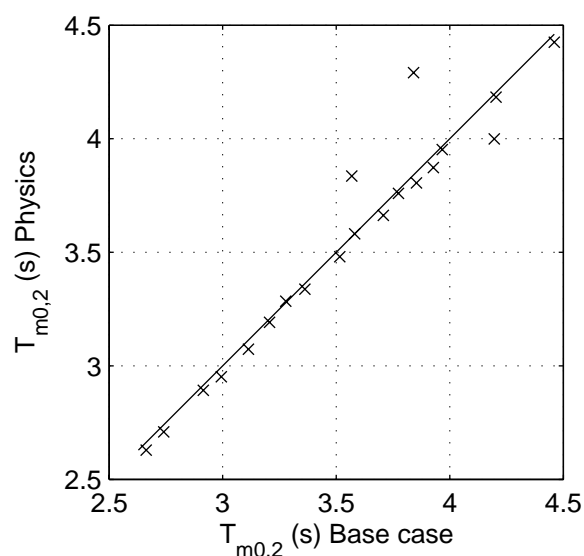
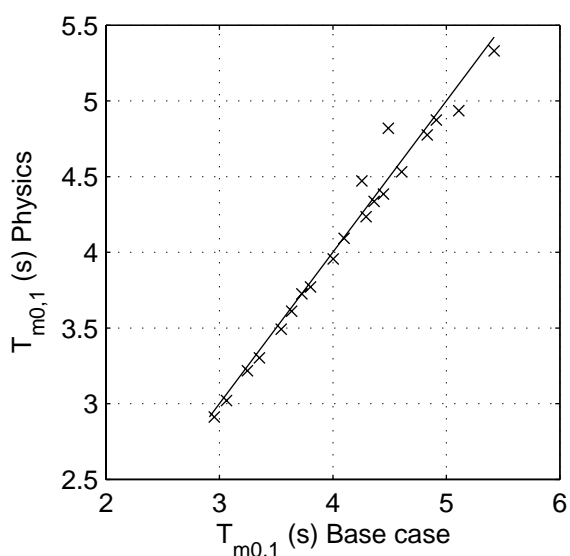
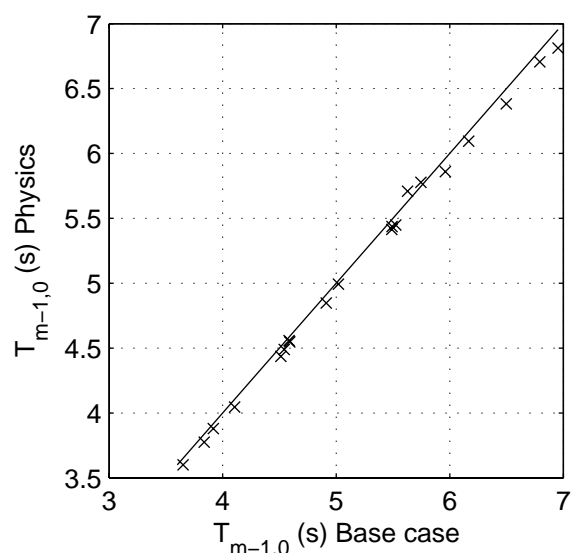
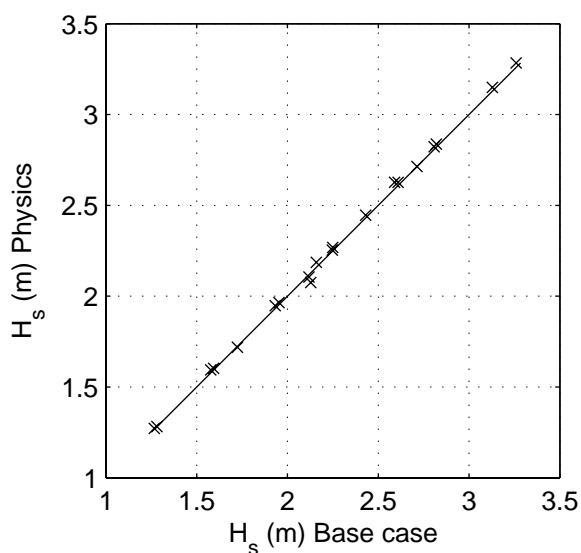
SCAT\_ws\_W01\_P12\_s2p

Calibration SWAN 40.20

A1168

 **Alkyon**

Fig. 5.2.12



Sensitivity of SWAN 40.20 to variations in physical parameters  
Comparison of base case against:  
Weaker Snl4

Area:WS

Grid:W01

P13

Physics

SCAT\_ws\_W01\_P13\_s2p

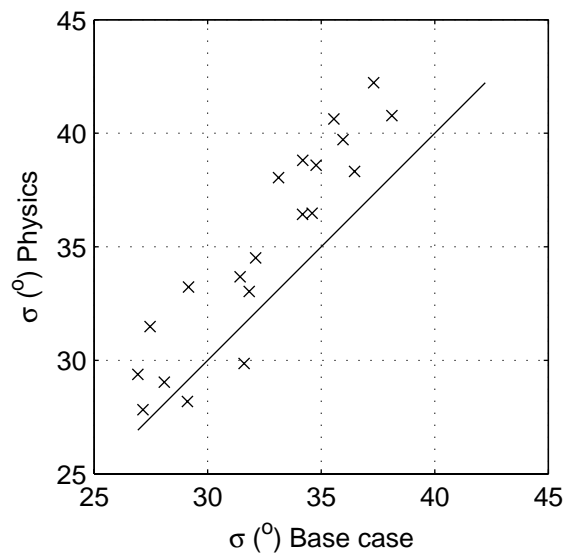
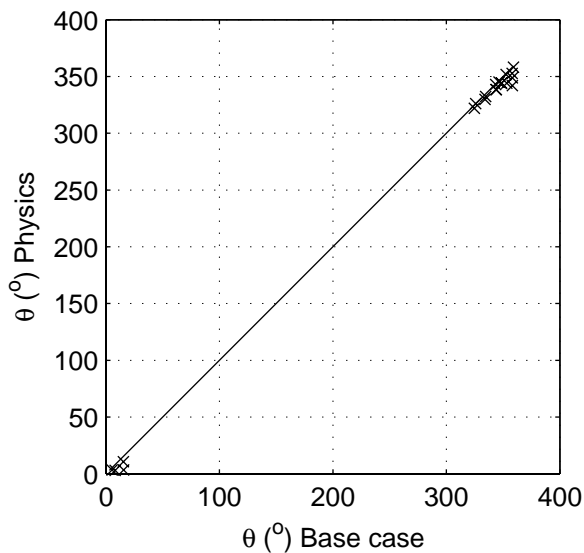
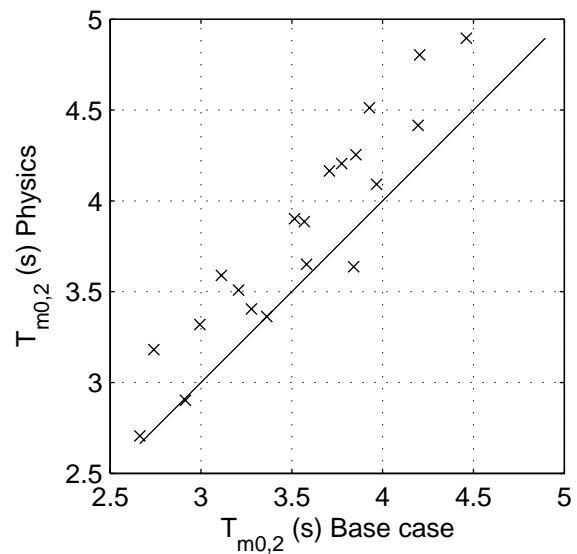
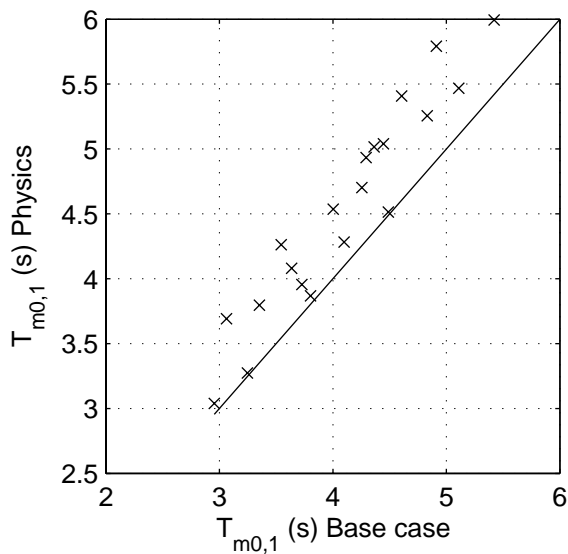
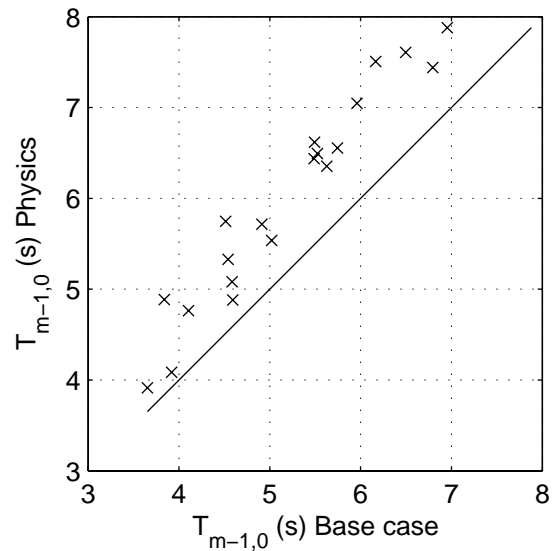
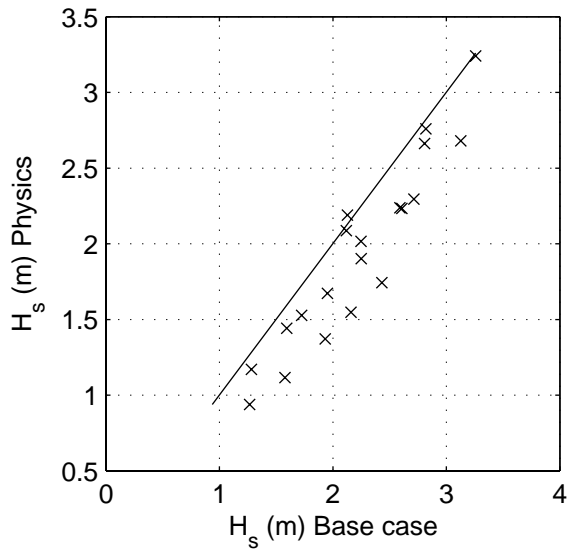
Calibration SWAN 40.20

A1168

 **Alkyon**

Fig. 5.2.13





Sensitivity of SWAN 40.20 to variations in physical parameters  
Comparison of base case against:  
Cumulative steepness

Area:WS

Grid:W01

P14

Physics

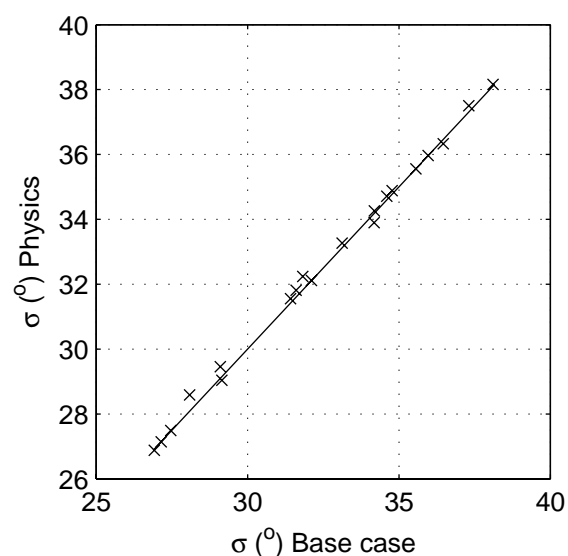
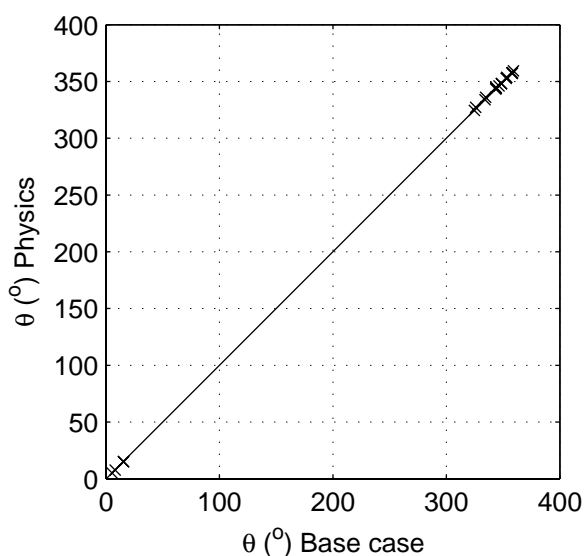
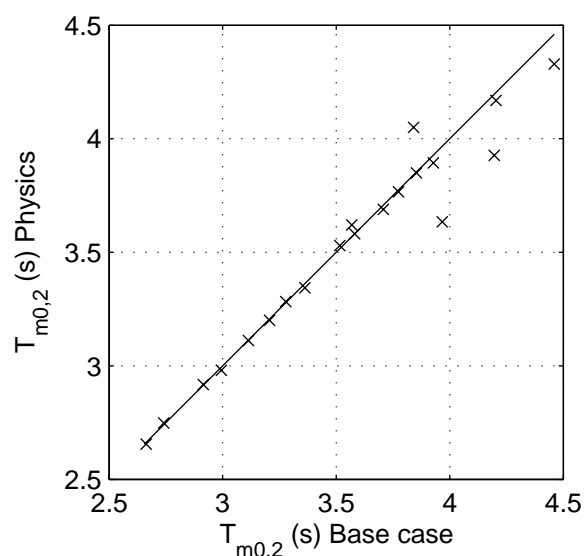
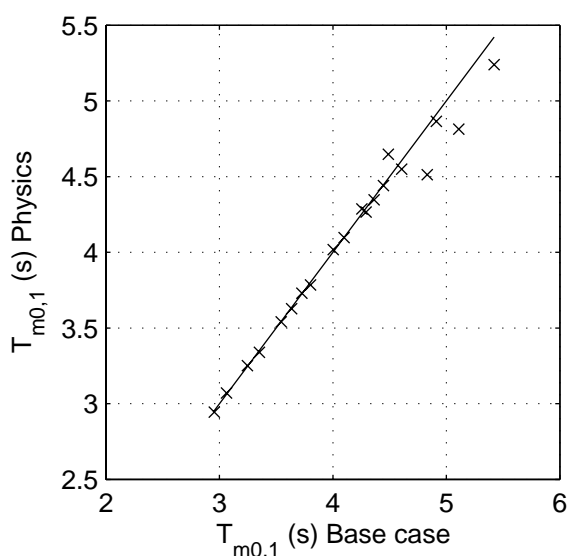
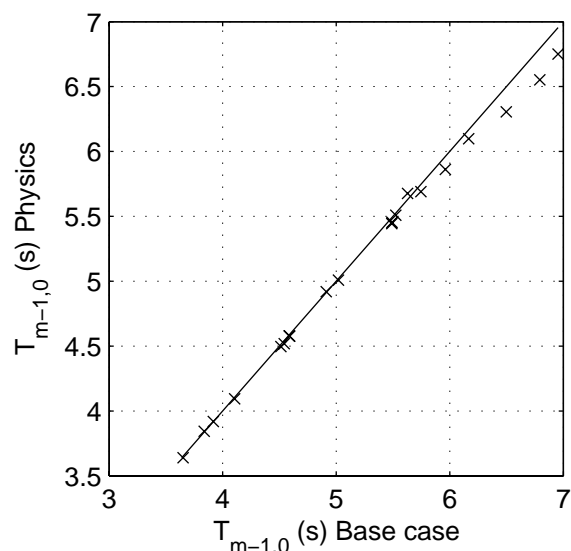
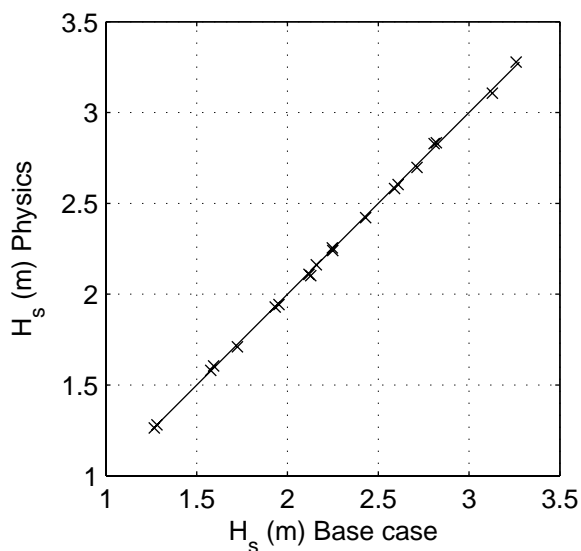
SCAT\_ws\_W01\_P14\_s2p

Calibration SWAN 40.20

A1168

 **Alkyon**

Fig. 5.2.14



Sensitivity of SWAN 40.20 to variations in physical parameters  
Comparison of base case against:  
Stronger triads

Area:WS

Grid:W01

P15

Physics

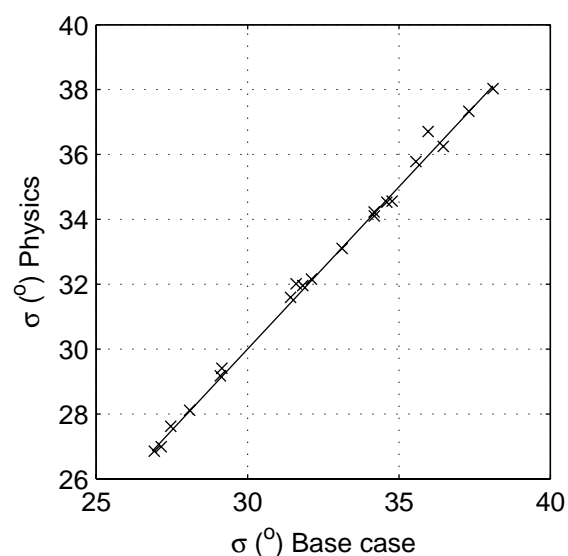
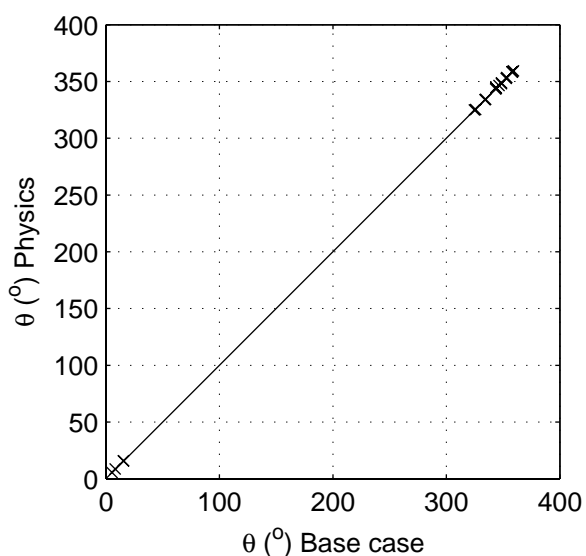
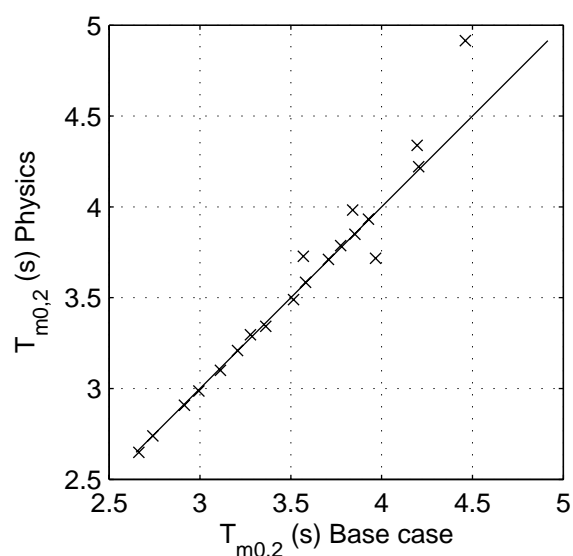
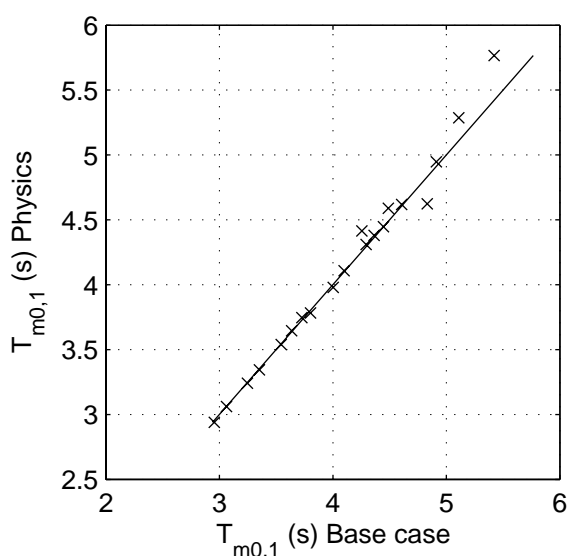
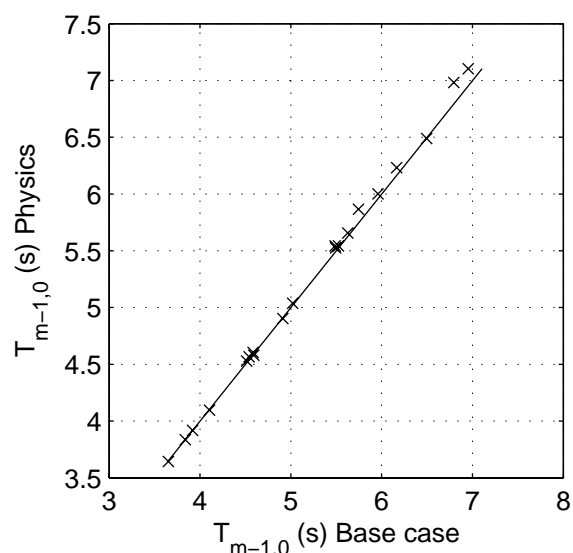
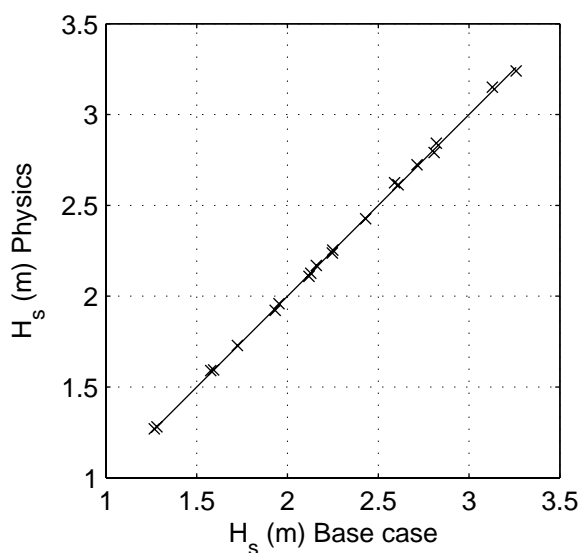
SCAT\_ws\_W01\_P15\_s2p

Calibration SWAN 40.20

A1168

 **Alkyon**

Fig. 5.2.15



Sensitivity of SWAN 40.20 to variations in physical parameters  
Comparison of base case against:  
Weaker triads

Area:WS

Grid:W01

P16

Physics

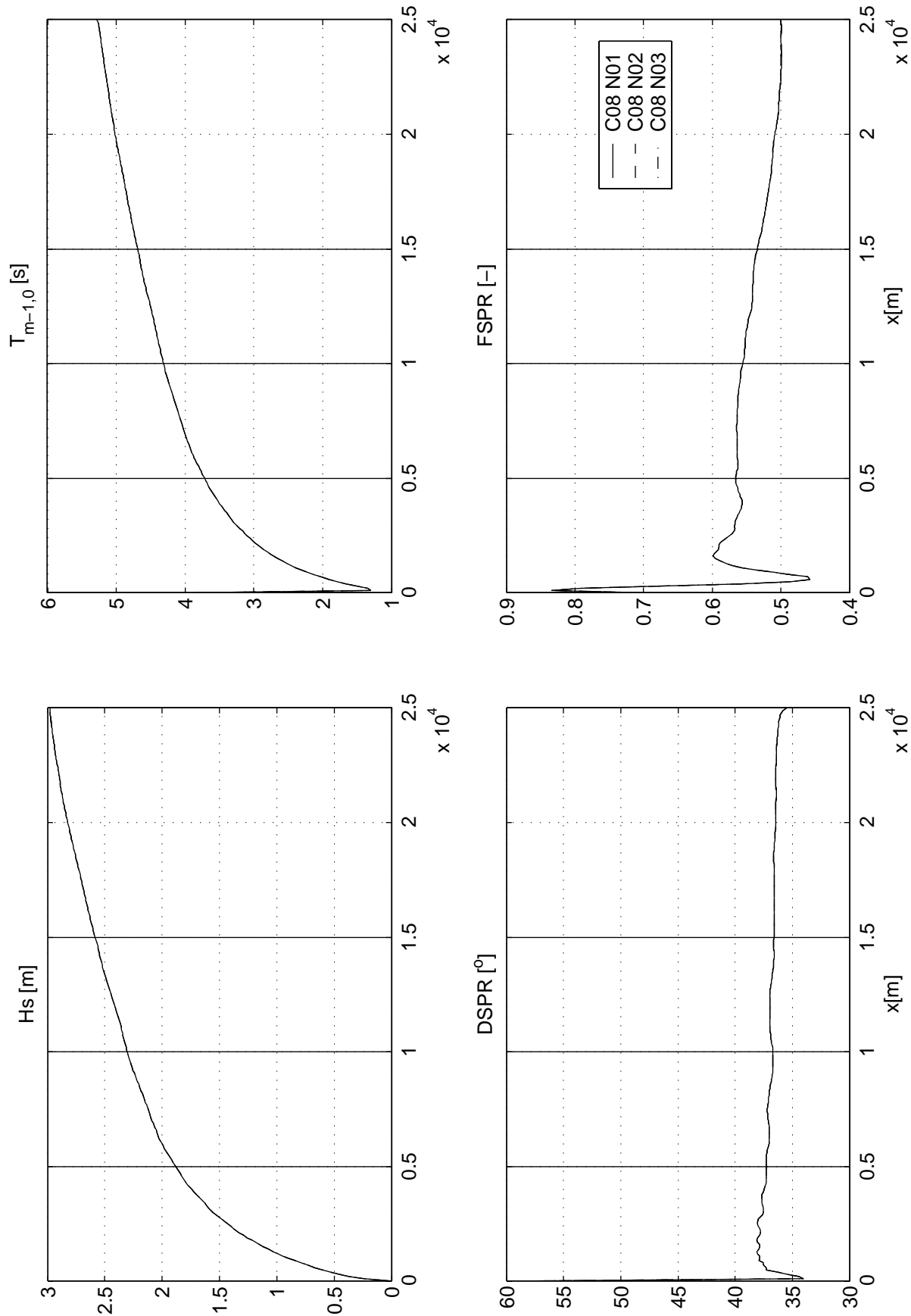
SCAT\_ws\_W01\_P16\_s2p

Calibration SWAN 40.20

A1168

 **Alkyon**

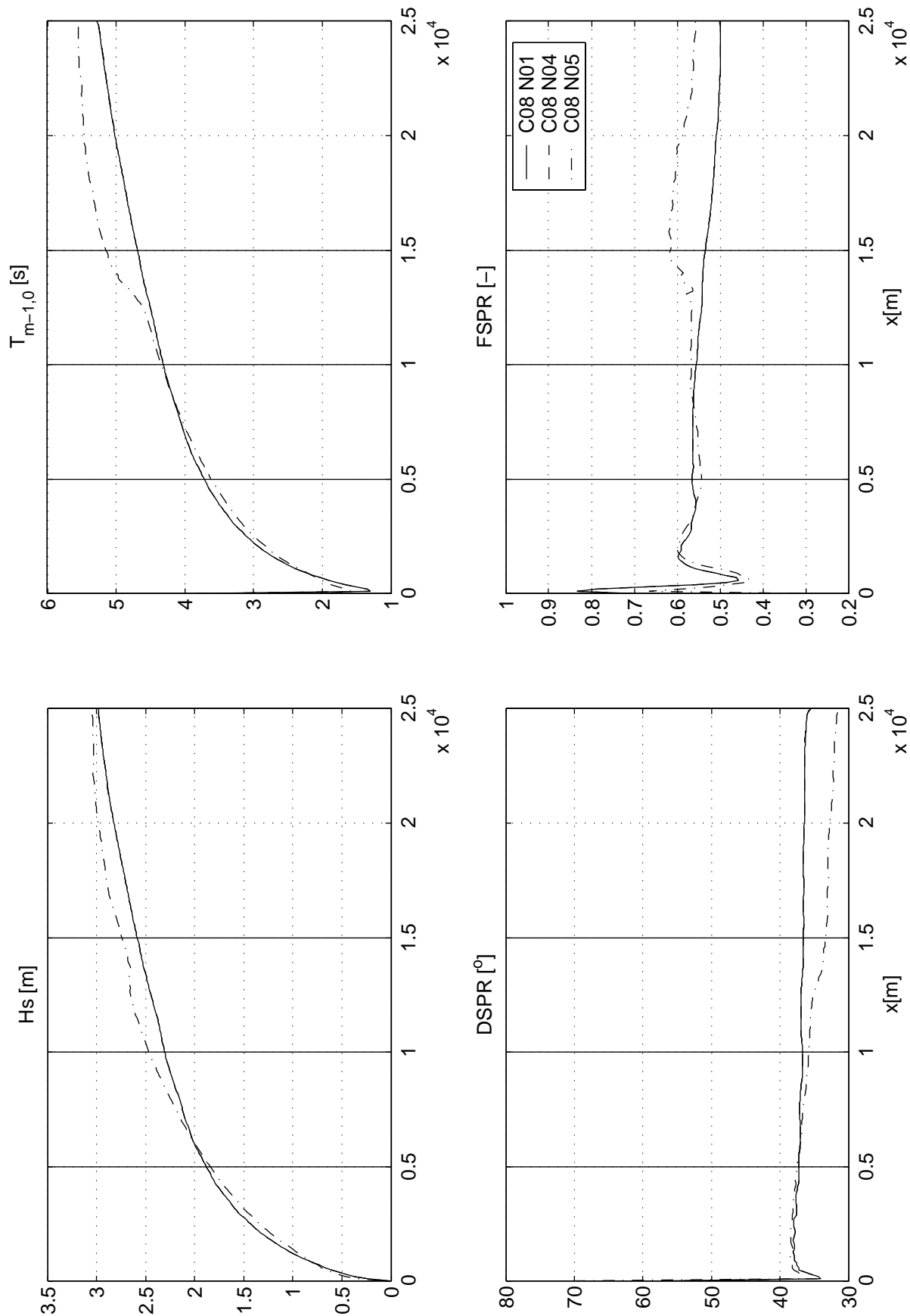
Fig. 5.2.16



Spatial variation of integral wave parameters along fetch  
Fetch limited wave growth.  
Physical Case:surf breaking, alpha; depth=10 m ; u10=30m/s

FL\_C08

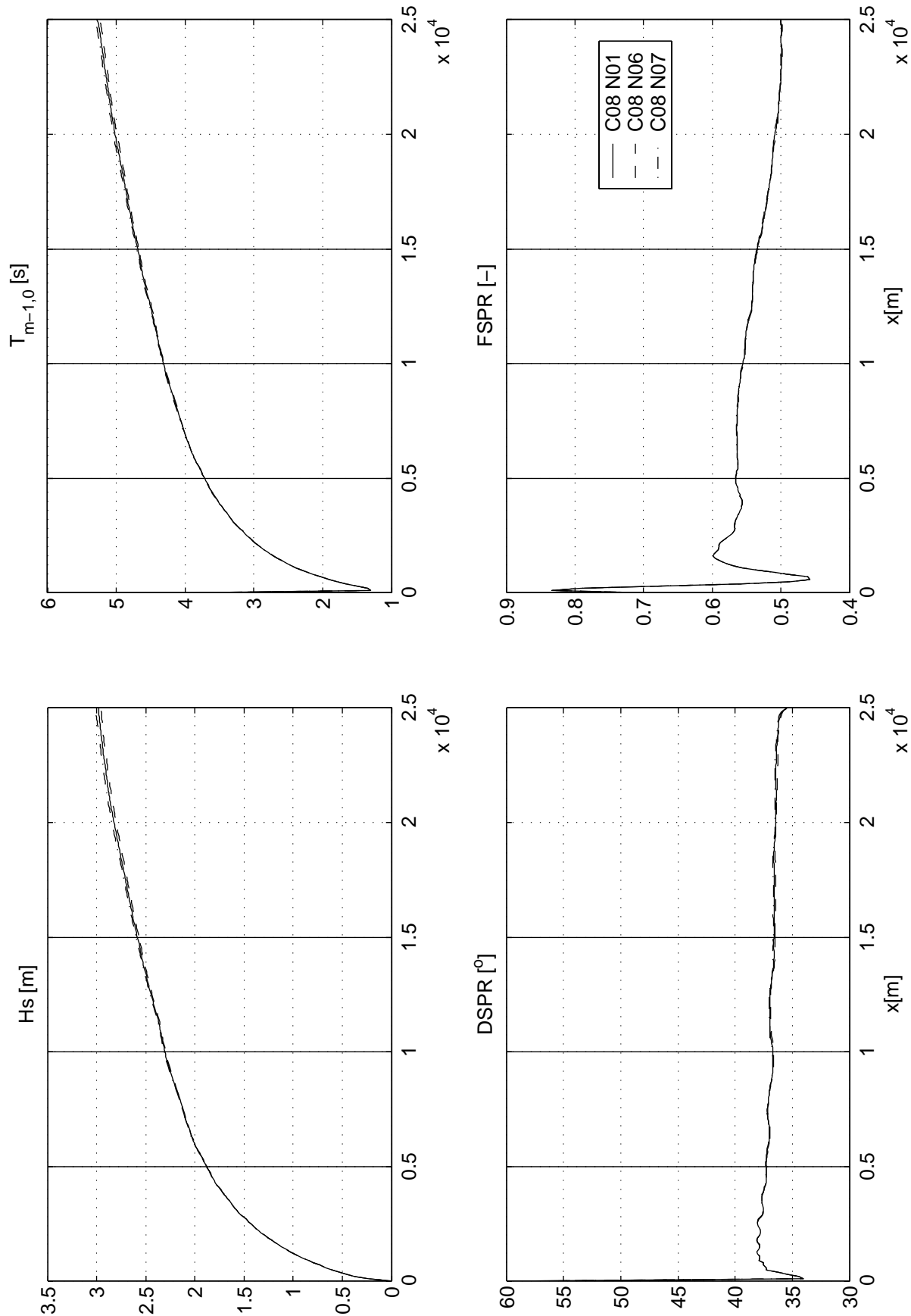
Fetch Limited



Spatial variation of integral wave parameters along fetch  
Fetch limited wave growth.  
Physical Case:surf breaking, gamma; depth=10 m ; u10=30m/s

FL\_C08

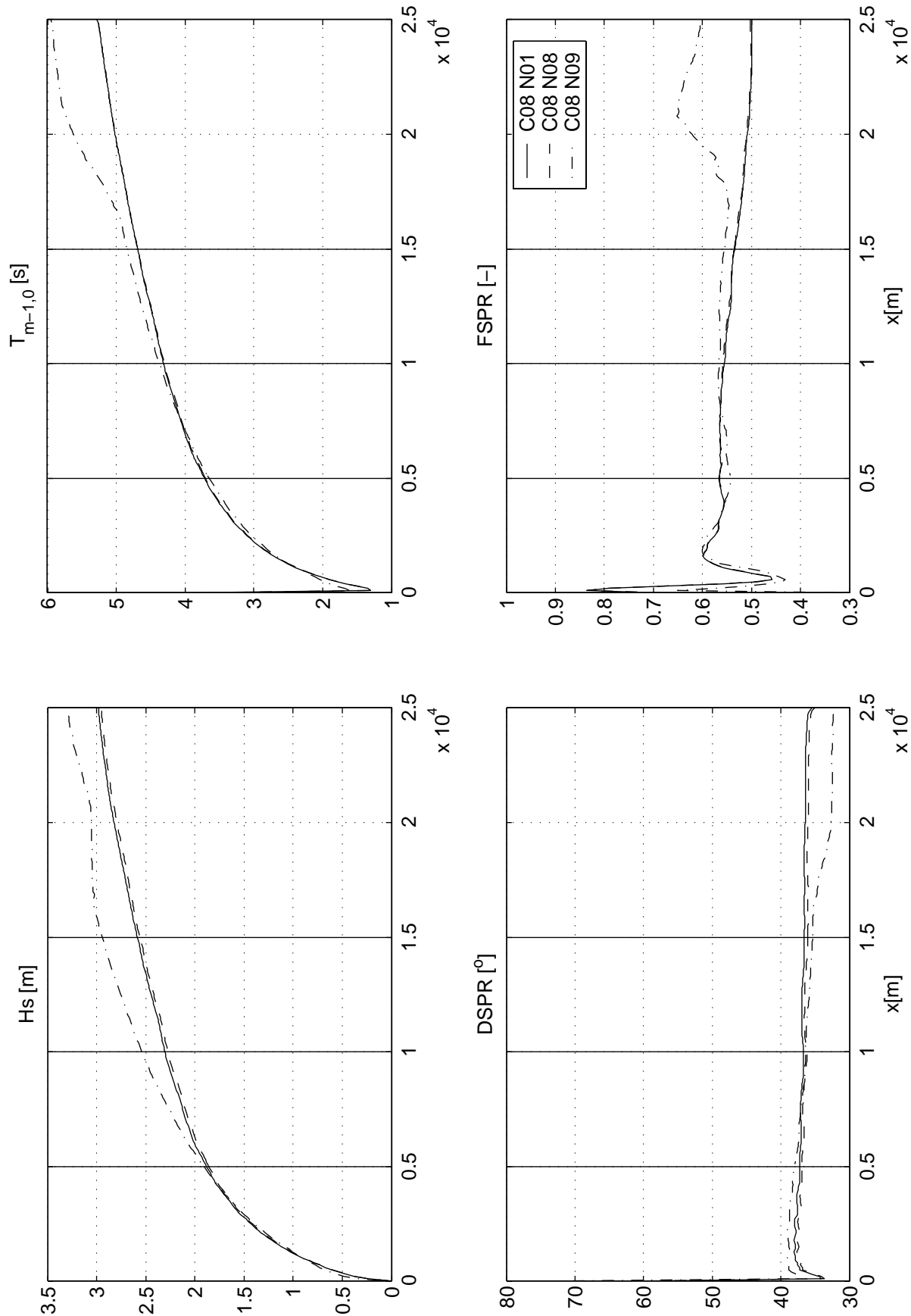
Fetch Limited



Spatial variation of integral wave parameters along fetch  
Fetch limited wave growth.  
Physical Case:bottom friction, cfjon; depth=10 m ; u10=30m/s

FL\_C08

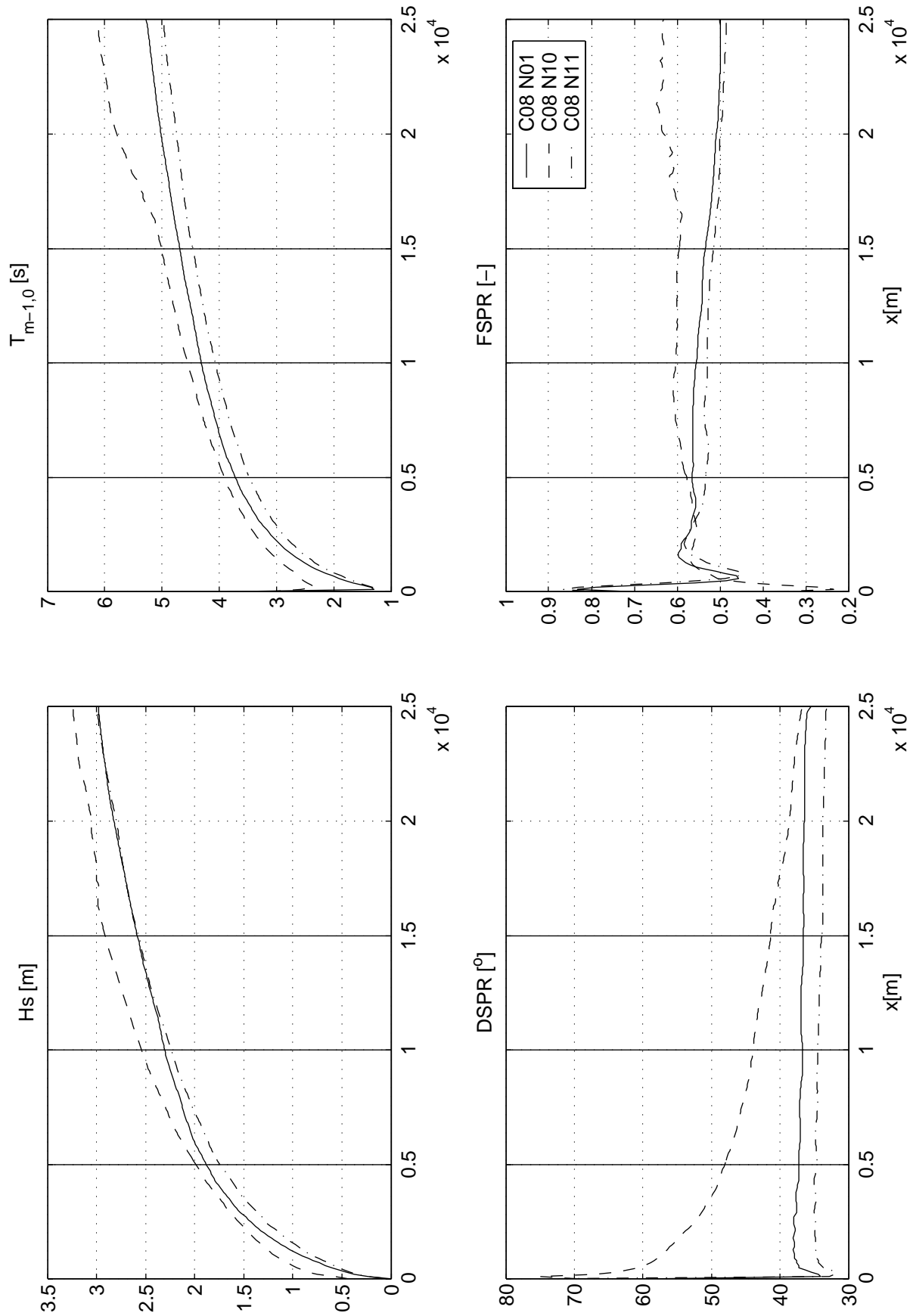
Fetch Limited



Spatial variation of integral wave parameters along fetch  
Fetch limited wave growth.  
Physical Case:whitecapping; depth=10 m ;  $u_{10}=30$ m/s

FL\_C08

Fetch Limited

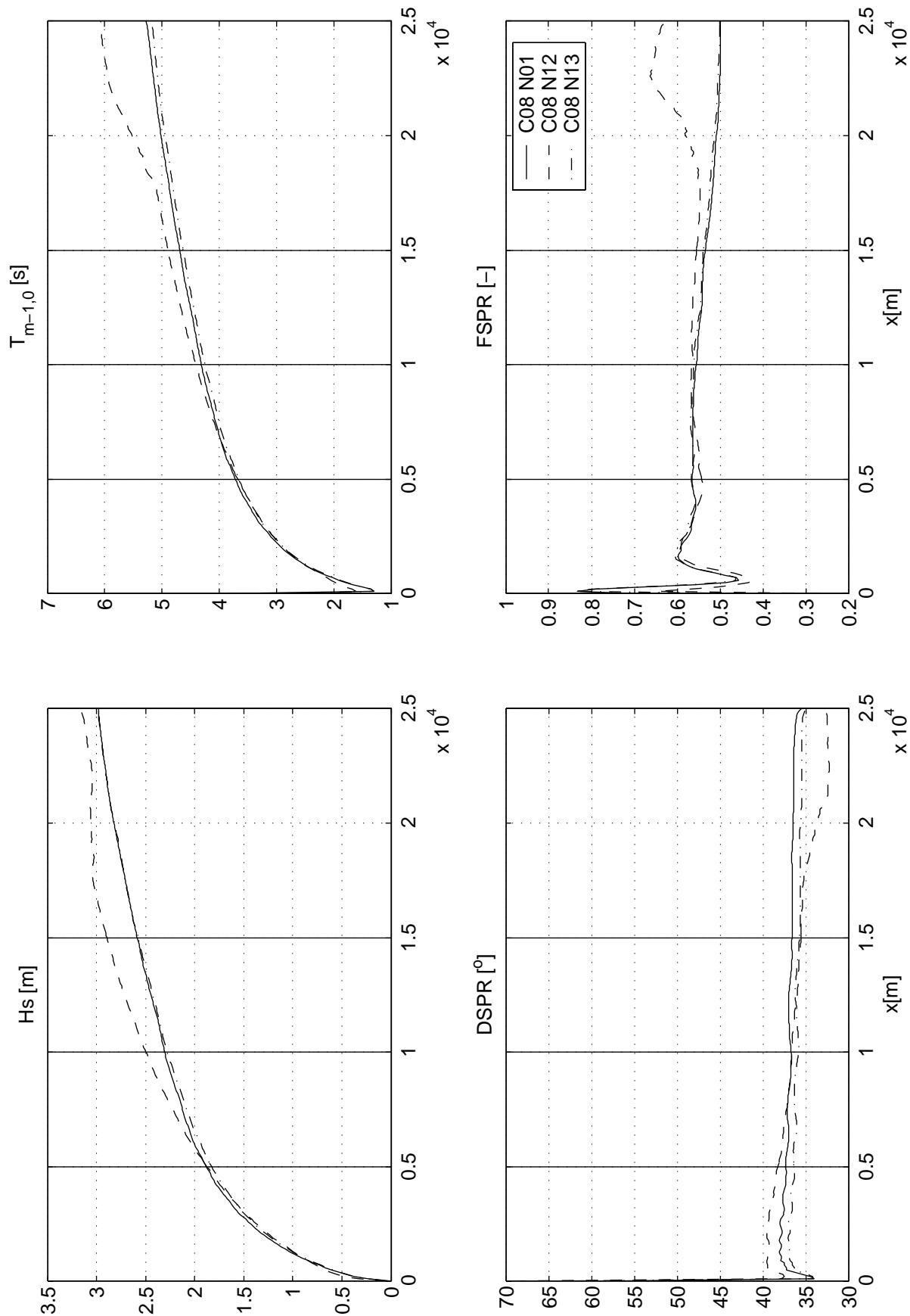


Spatial variation of integral wave parameters along fetch  
Fetch limited wave growth.  
Physical Case:quadruplets lambda; depth=10 m ; u10=30m/s

FL\_C08

Fetch Limited

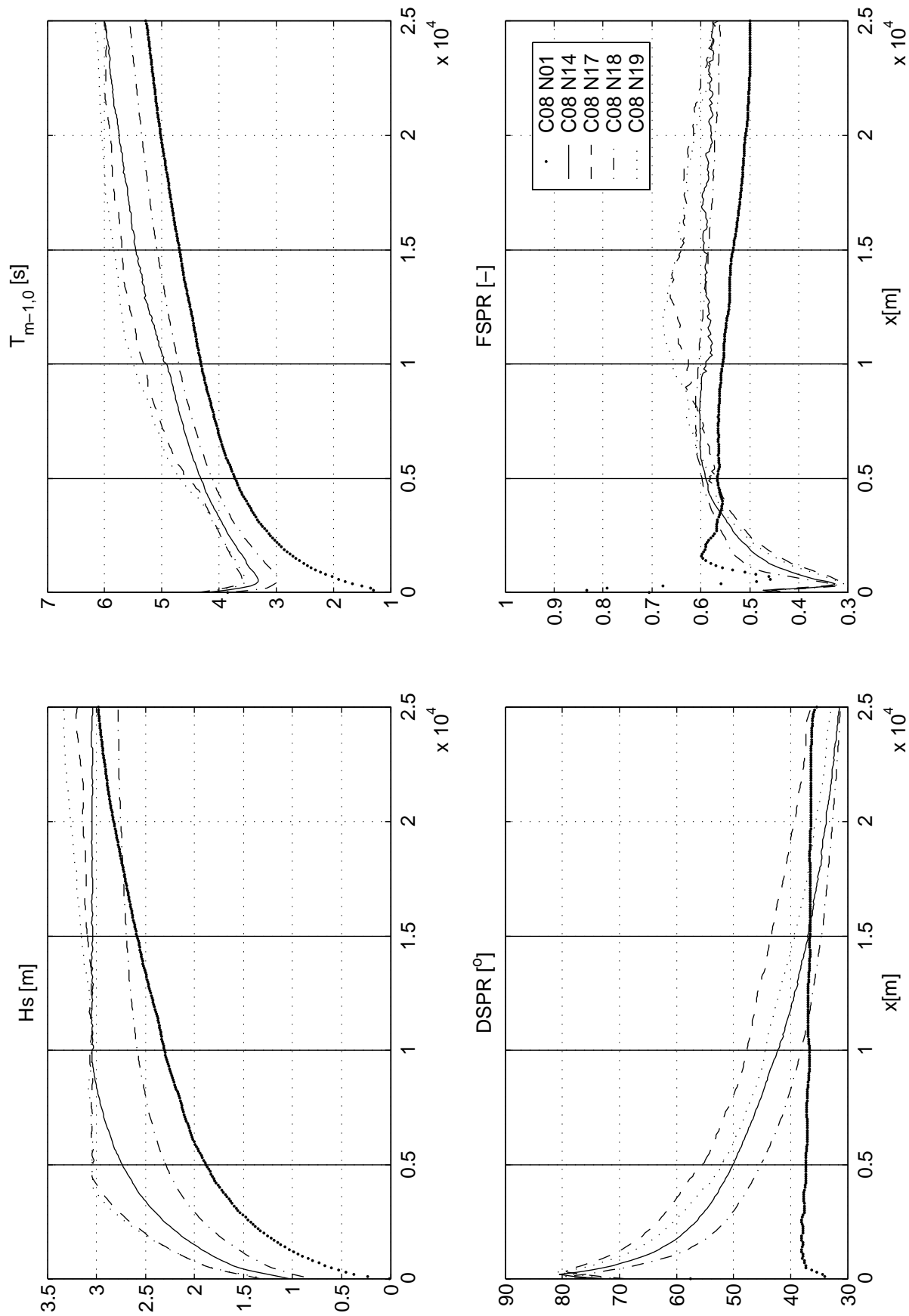




Spatial variation of integral wave parameters along fetch  
Fetch limited wave growth.  
Physical Case:quadruplets Cn14; depth=10 m ; u10=30m/s

FL\_C08

Fetch Limited



Spatial variation of integral wave parameters along fetch

Fetch limited wave growth.

Physical Case:white-capping CSM; depth=10 m ; u10=30m/s

Calibration SWAN 40.20

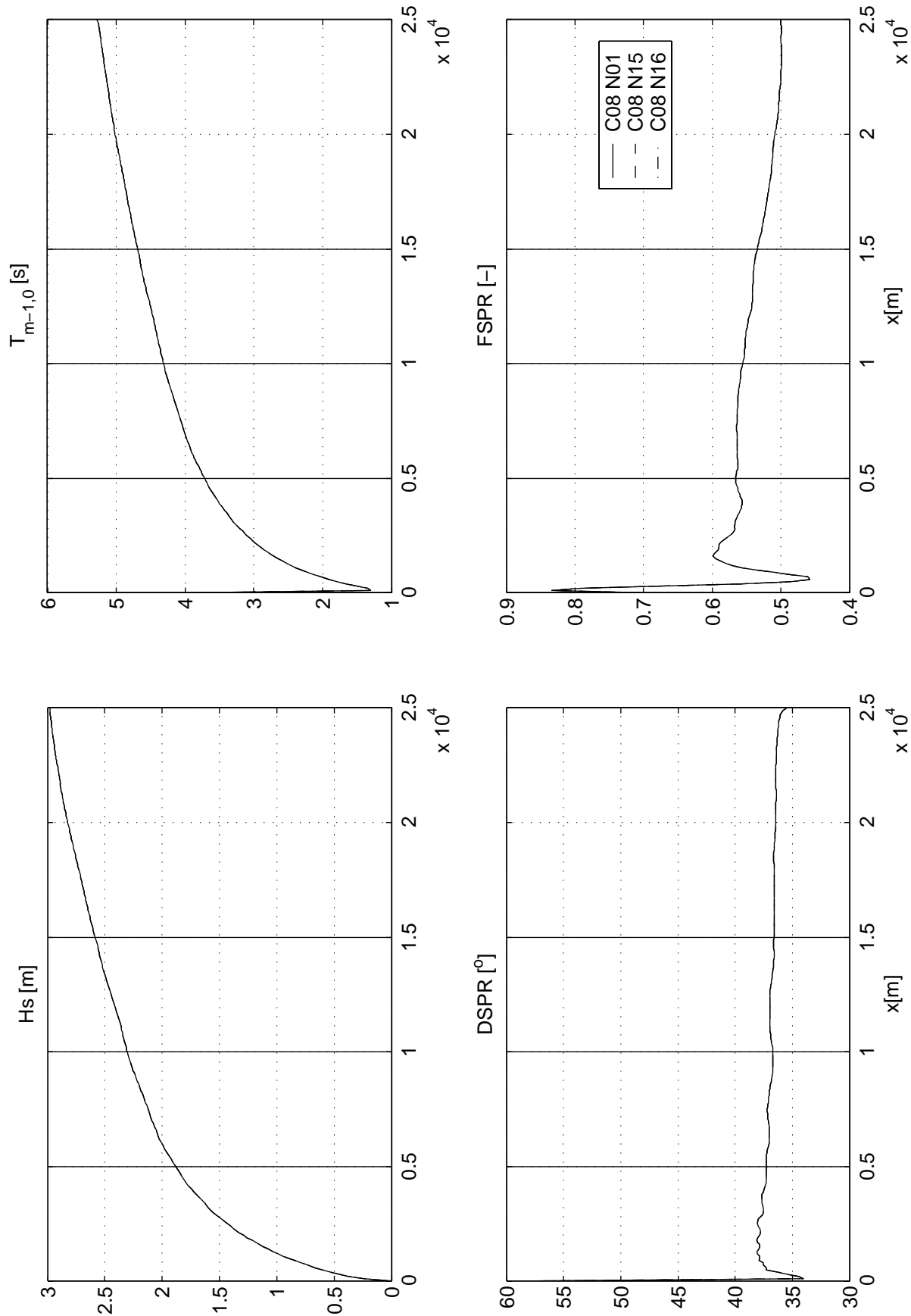
A1168

Alkyon

FL\_C08

Fetch Limited

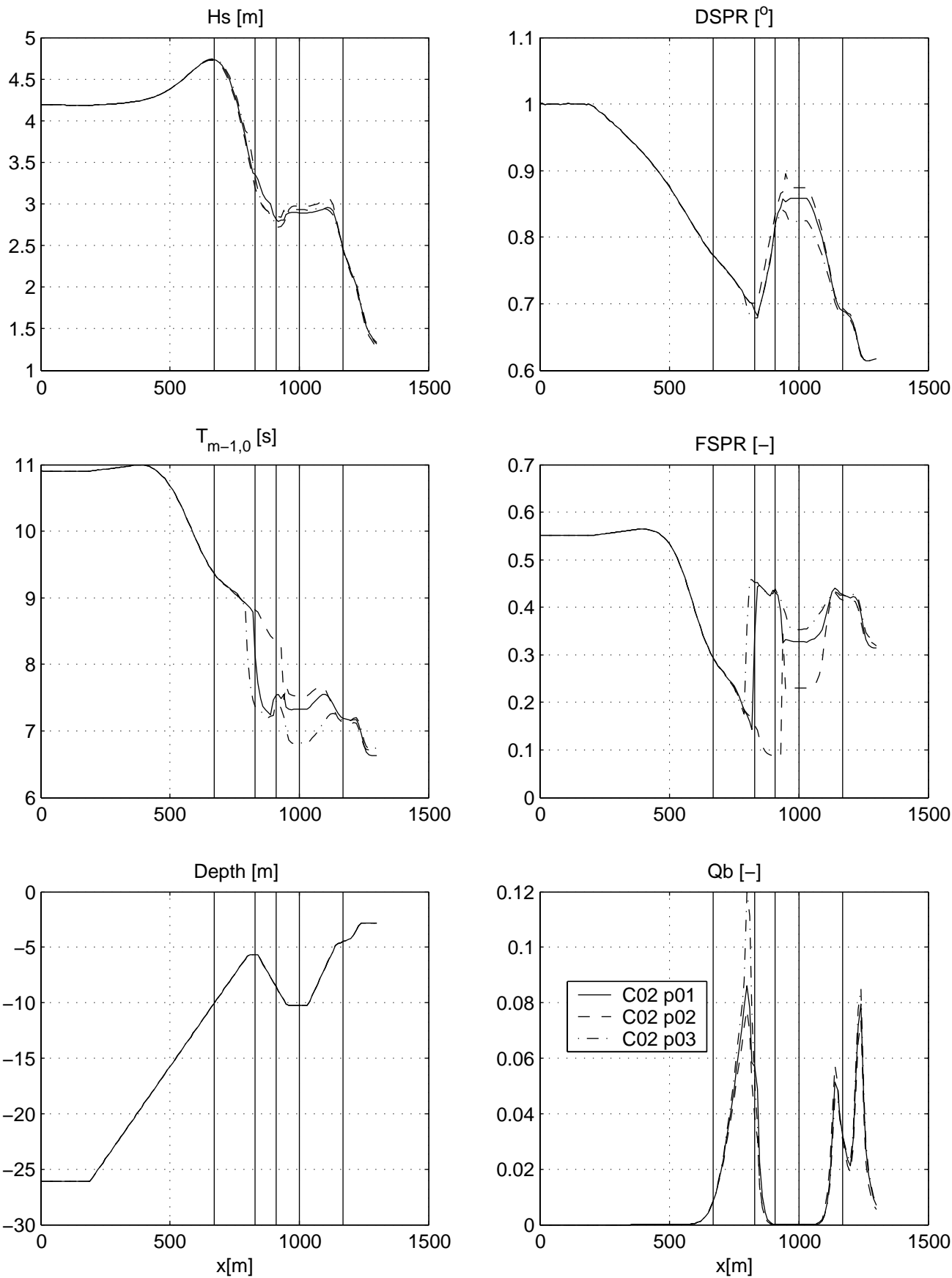
Fig. 5.3.7



Spatial variation of integral wave parameters along fetch  
Fetch limited wave growth.  
Physical Case:triads; depth=10 m ; u10=30m/s

FL\_C08

Fetch Limited



Spatial variation of integral wave parameters in Petten wave flume  
Physical Case:surf breaking, alpha

B12

FP\_C02

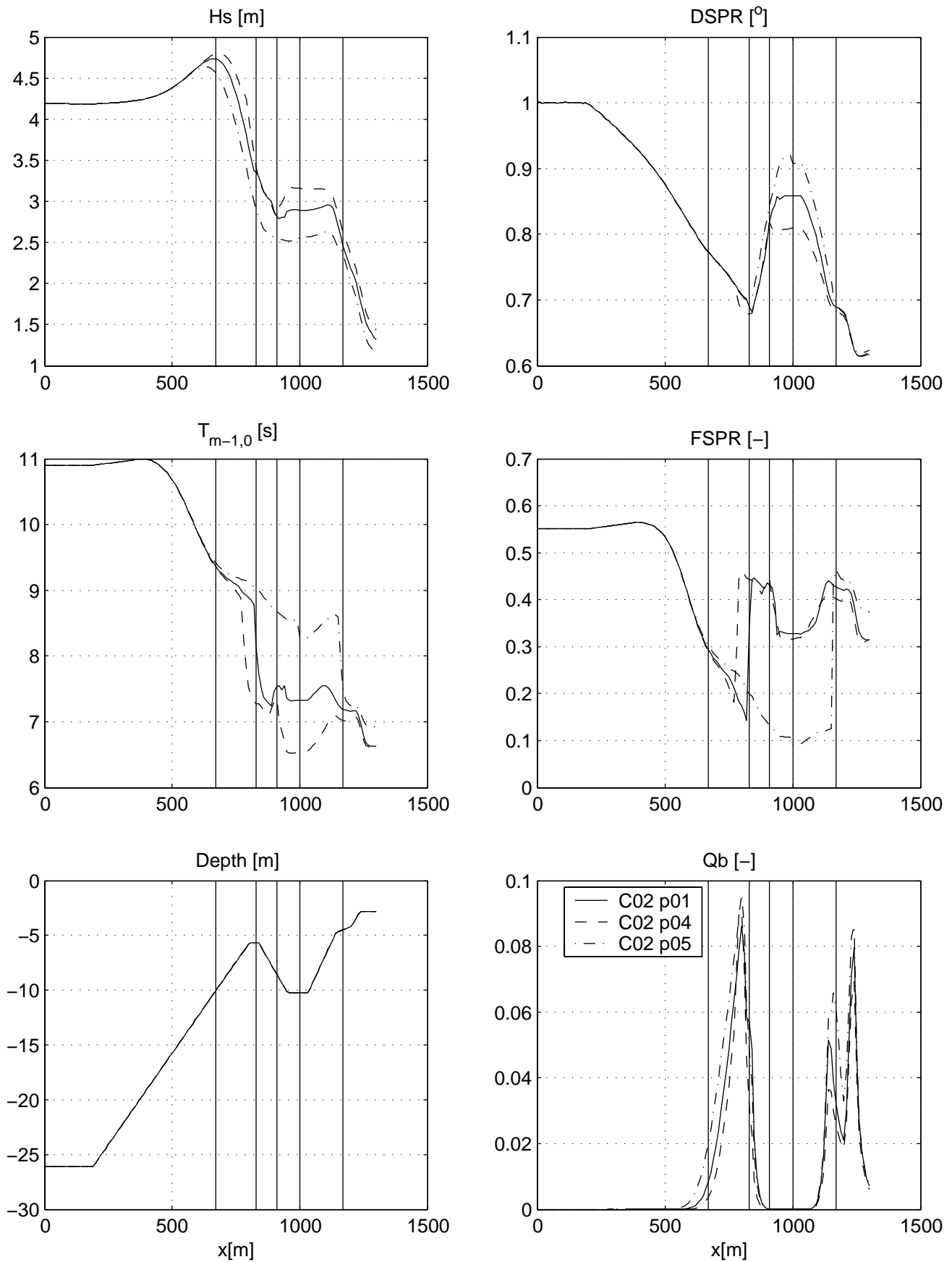
Petten Flume

Calibration SWAN 4020

A1168

Alkyon

Fig. 5.4.1



Spatial variation of integral wave parameters in Petten wave flume  
Physical Case:surf breaking, gamma

B12

FP\_C02

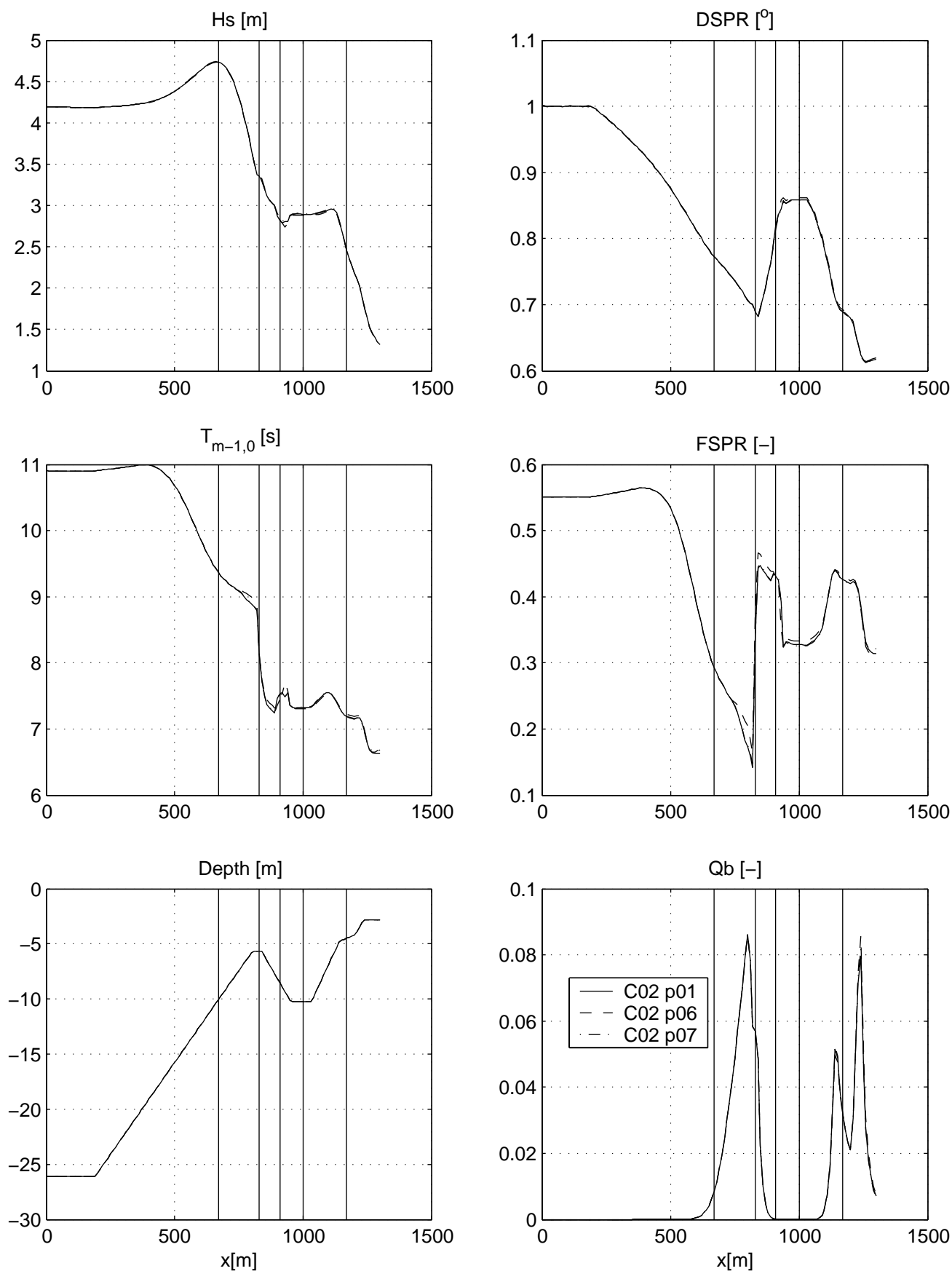
Petten Flume

Calibration SWAN 4020

A1168

 Alkyon

Fig. 5.4.2



Spatial variation of integral wave parameters in Petten wave flume  
Physical Case:bottom friction, cfjon

B12

FP\_C02

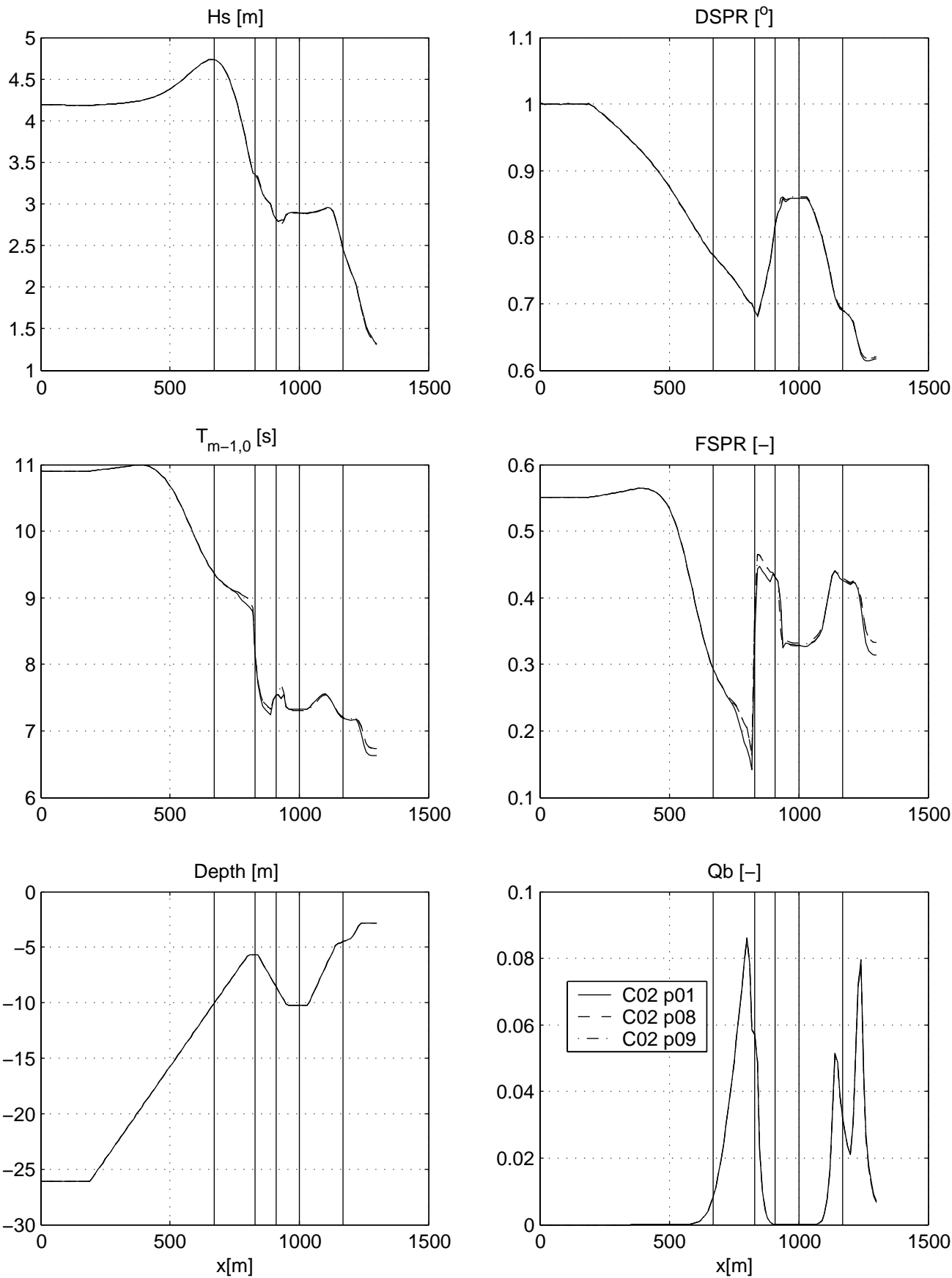
Petten Flume

Calibration SWAN 4020

A1168

Alkyon

Fig. 5.4.3



Spatial variation of integral wave parameters in Petten wave flume  
Physical Case:whitecapping

B12

FP\_C02

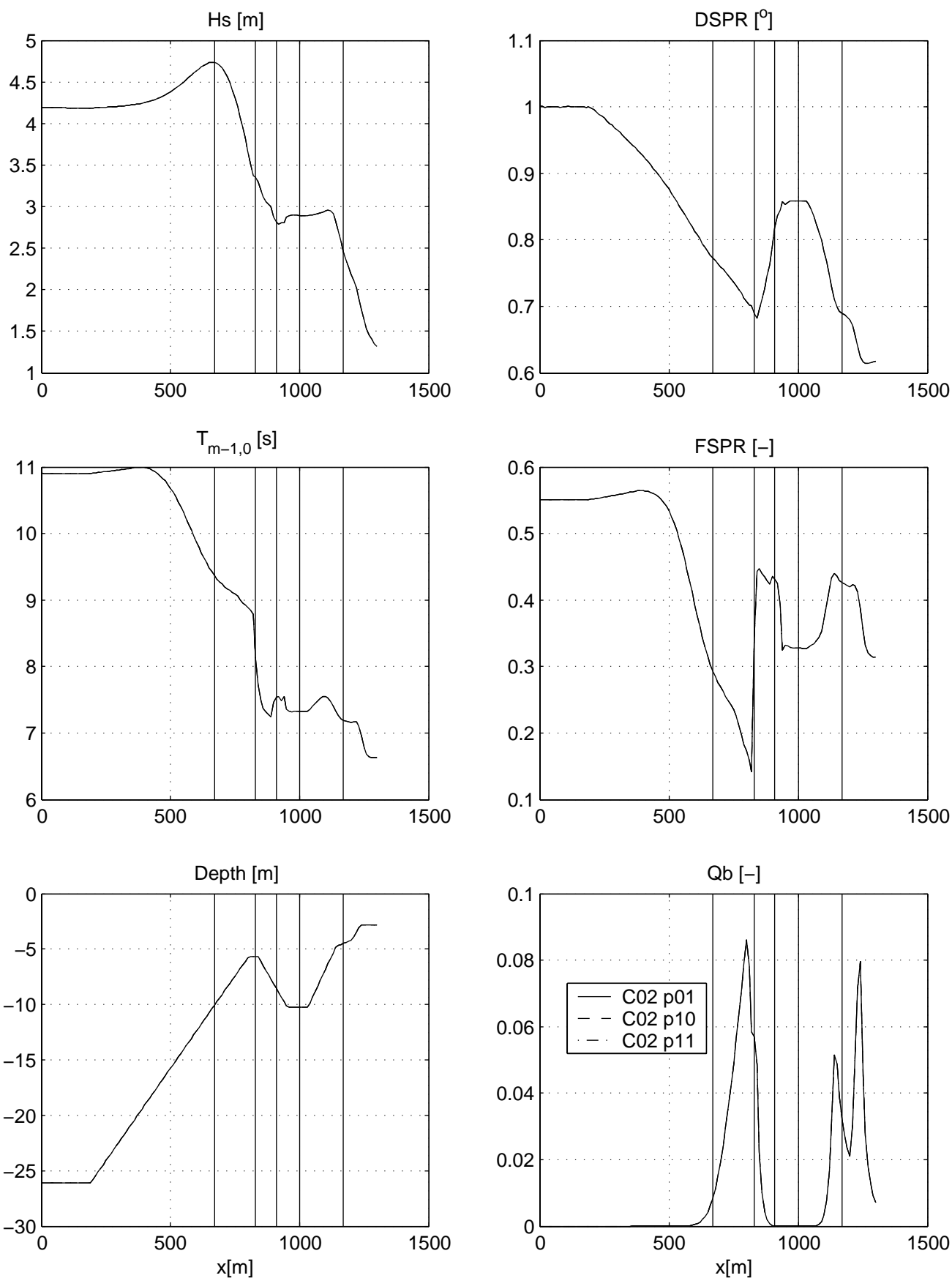
Petten Flume

Calibration SWAN 4020

A1168

Alkyon

Fig. 5.4.4



Spatial variation of integral wave parameters in Petten wave flume  
Physical Case:quadruplets lambda

B12

FP\_C02

Petten Flume

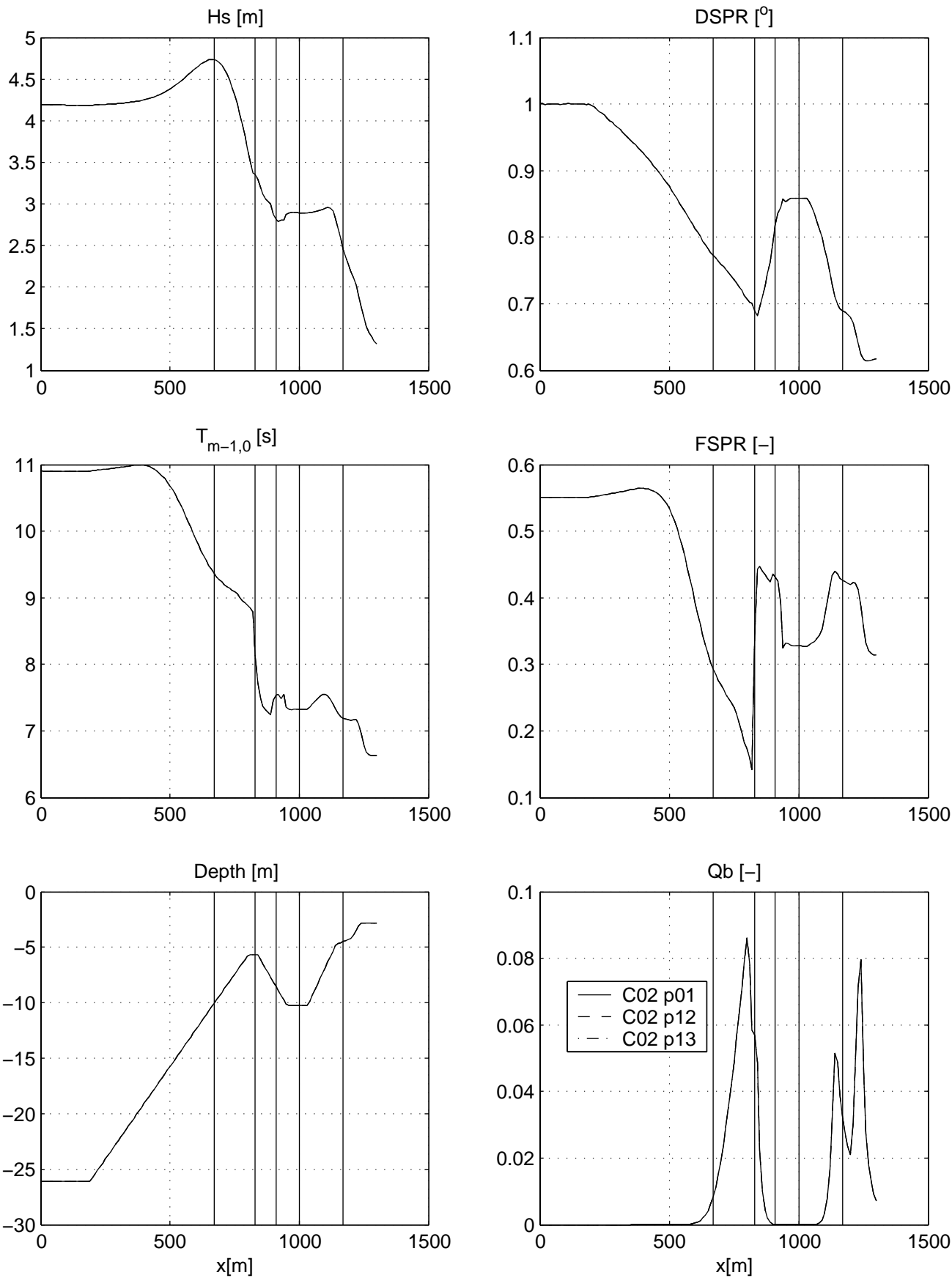
Calibration SWAN 4020

A1168

Alkyon

Fig. 5.4.5





Spatial variation of integral wave parameters in Petten wave flume  
Physical Case:quadruplets Cnl4

B12

FP\_C02

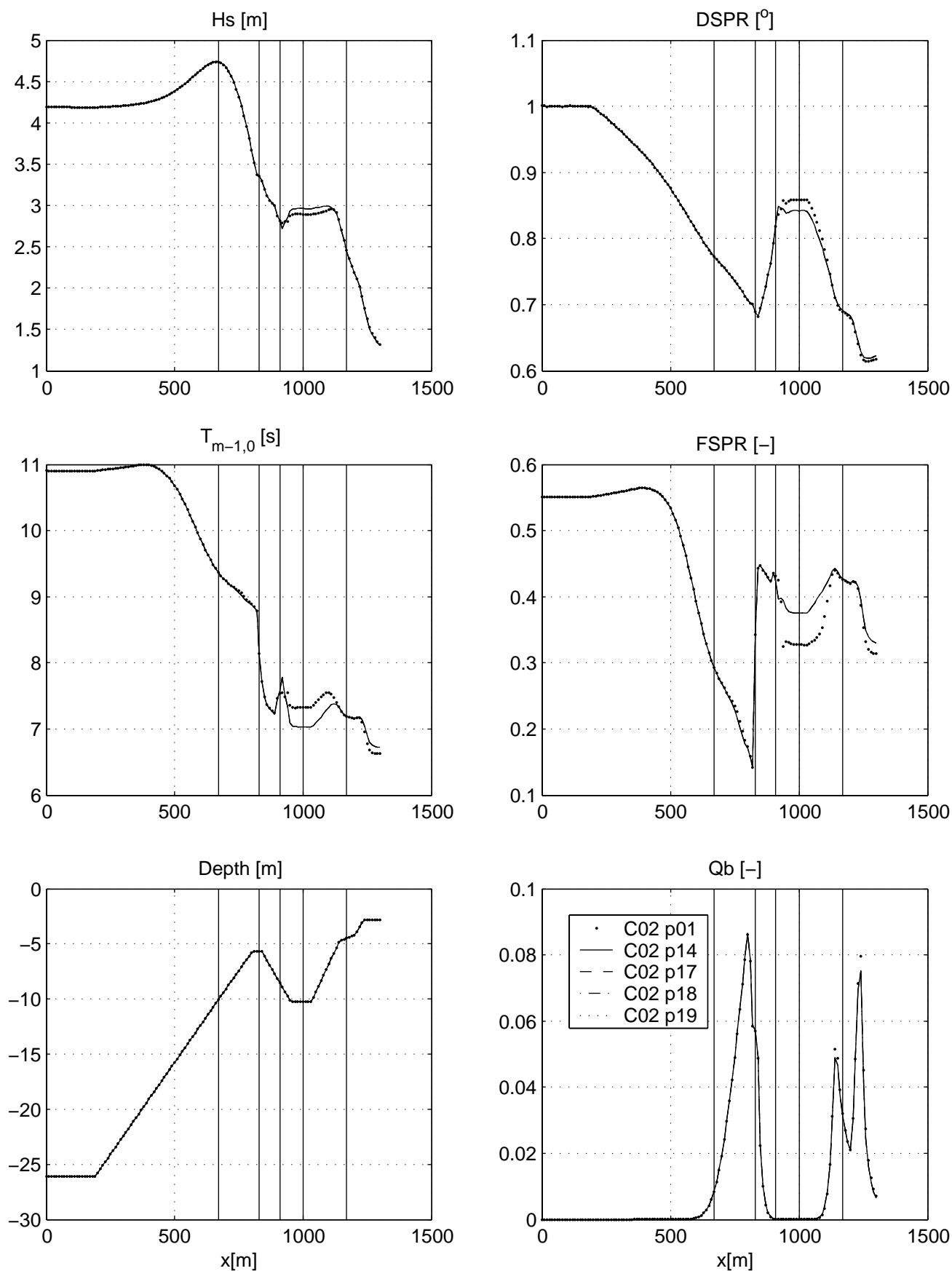
Petten Flume

Calibration SWAN 4020

A1168

Alkyon

Fig. 5.4.6



Spatial variation of integral wave parameters in Petten wave flume  
Physical Case:white-capping CSM

B12

FP\_C02

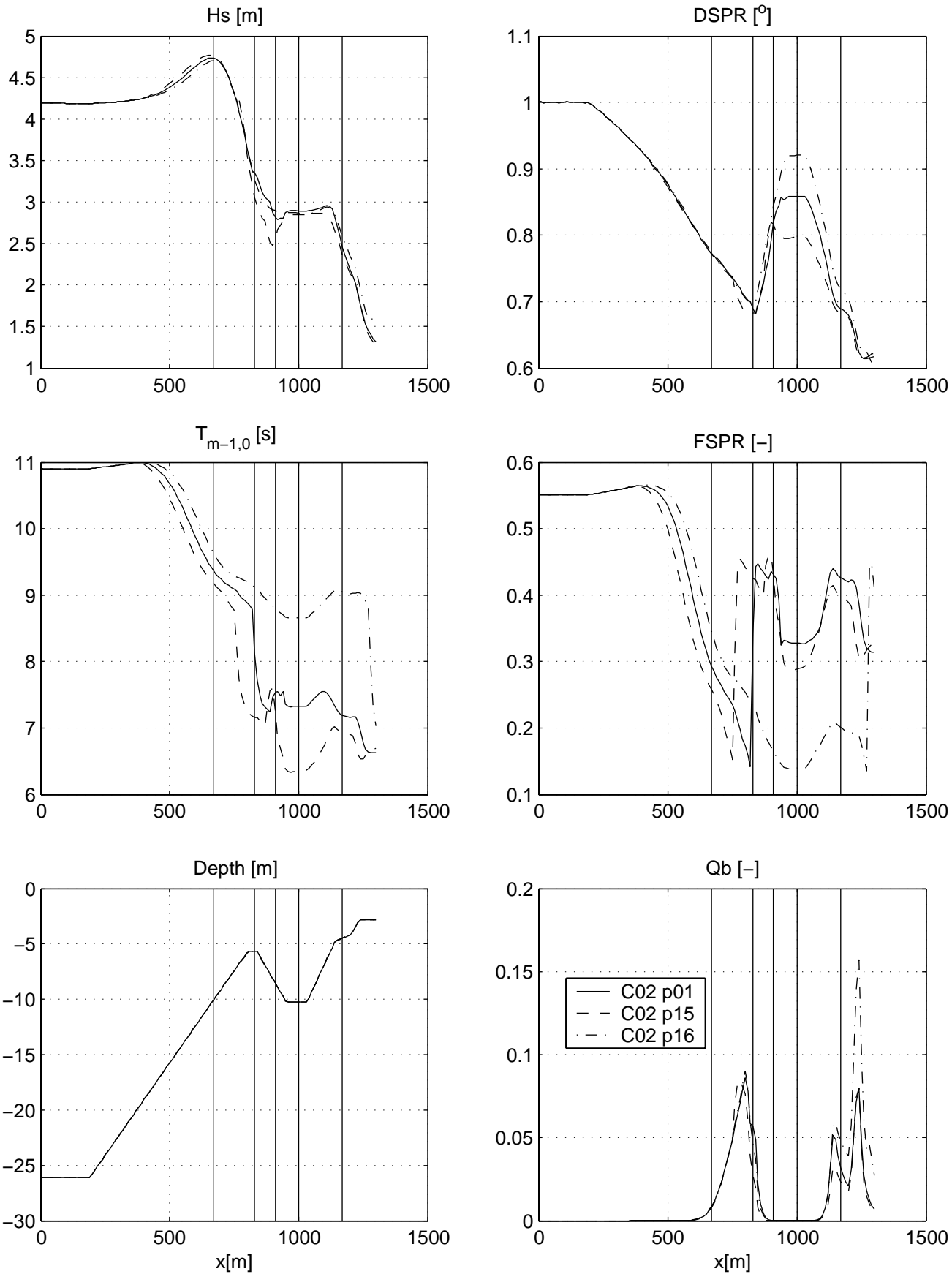
Petten Flume

Calibration SWAN 4020

A1168

 Alkyon

Fig. 5.4.7



Spatial variation of integral wave parameters in Petten wave flume  
Physical Case:triads

B12

FP\_C02

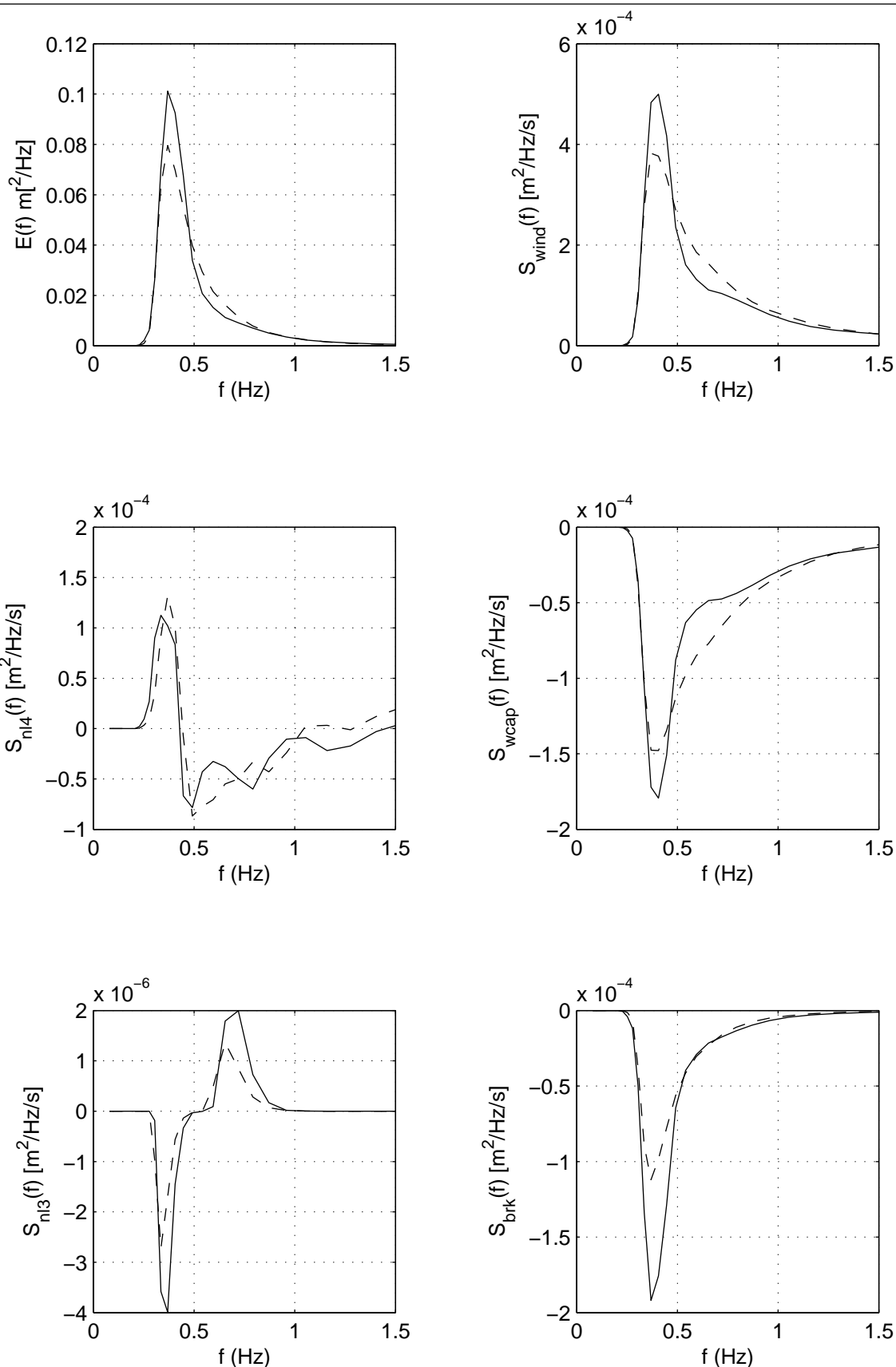
Petten Flume

Calibration SWAN 4020

A1168

Alkyon

Fig. 5.4.8



Two dimensional spectrum and source terms for physical variation

Base case (dashed line)

Higher lambda in Snl4 (solid line)

Area: SL

Grid: SL

Loc: 4

Iteration: 15

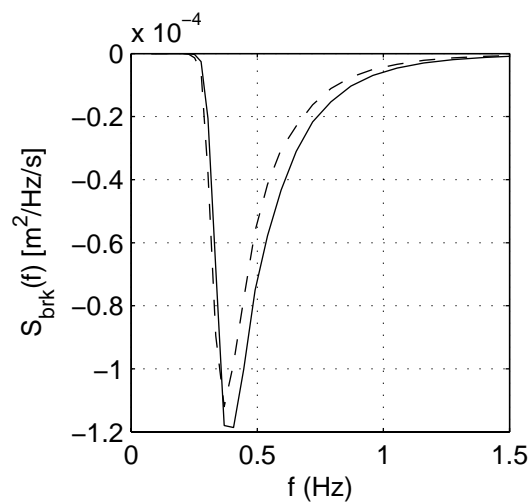
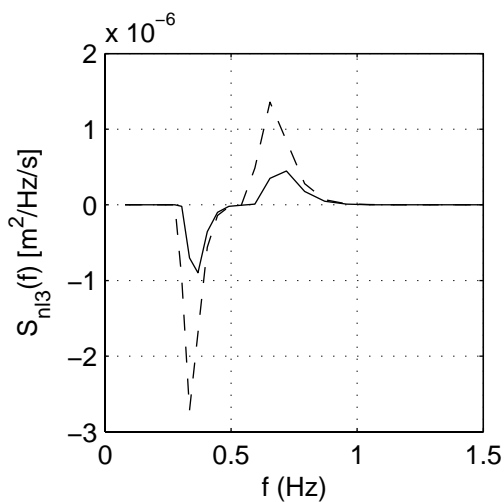
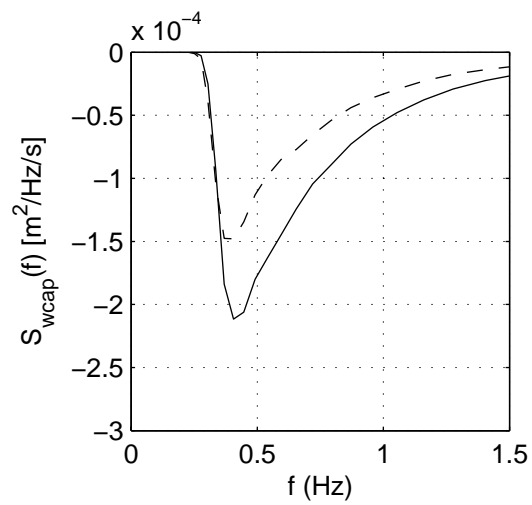
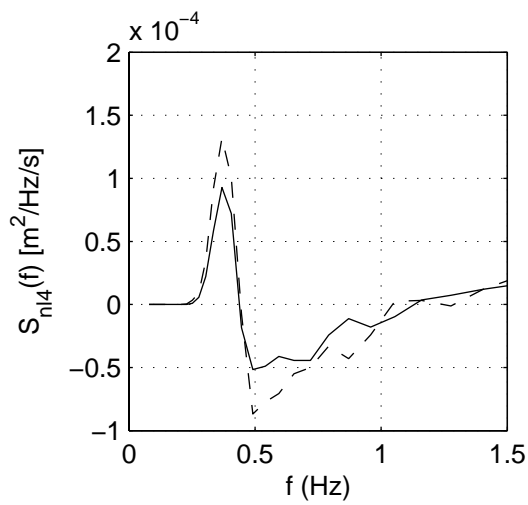
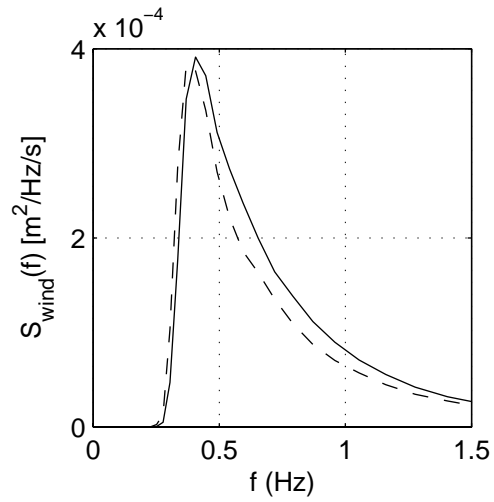
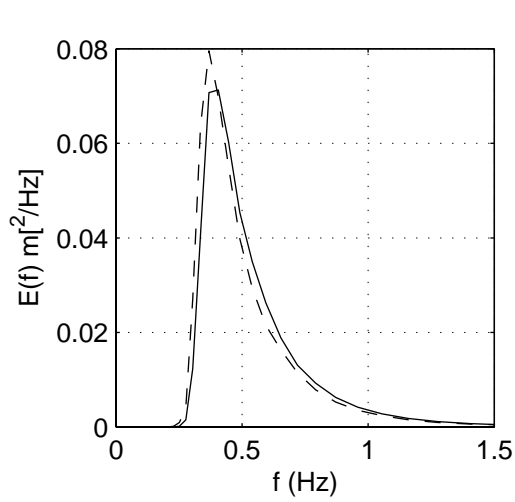
efr\_sl\_sl\_C03\_p10\_L4\_i15

Calibration SWAN 40.20

A1168

 Alkyon

Fig. 5.5.1



Two dimensional spectrum and source terms for physical variation

Base case (dashed line)

Lower lambda in Snl4 (solid line)

Area: SL

Grid: SL

Loc: 4

Iteration: 12

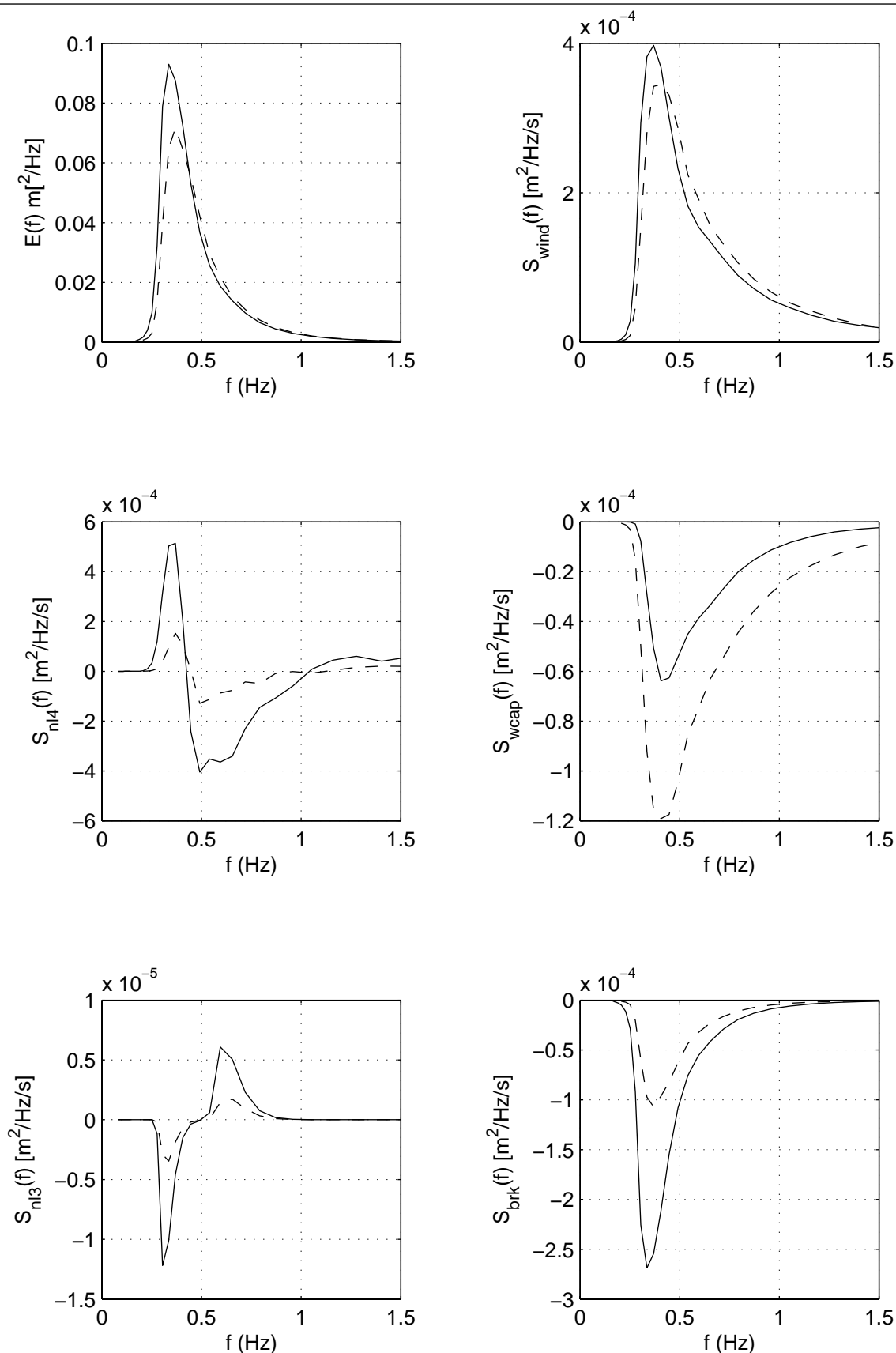
efr\_sl\_sl\_C03\_p11\_L4\_i12

Calibration SWAN 40.20

A1168

 Alkyon

Fig. 5.5.2



Two dimensional spectrum and source terms for physical variation

Base case (dashed line)

Cumulative steepness (solid line)

Area: SL

Grid: SL

Loc: 4

Iteration: 5

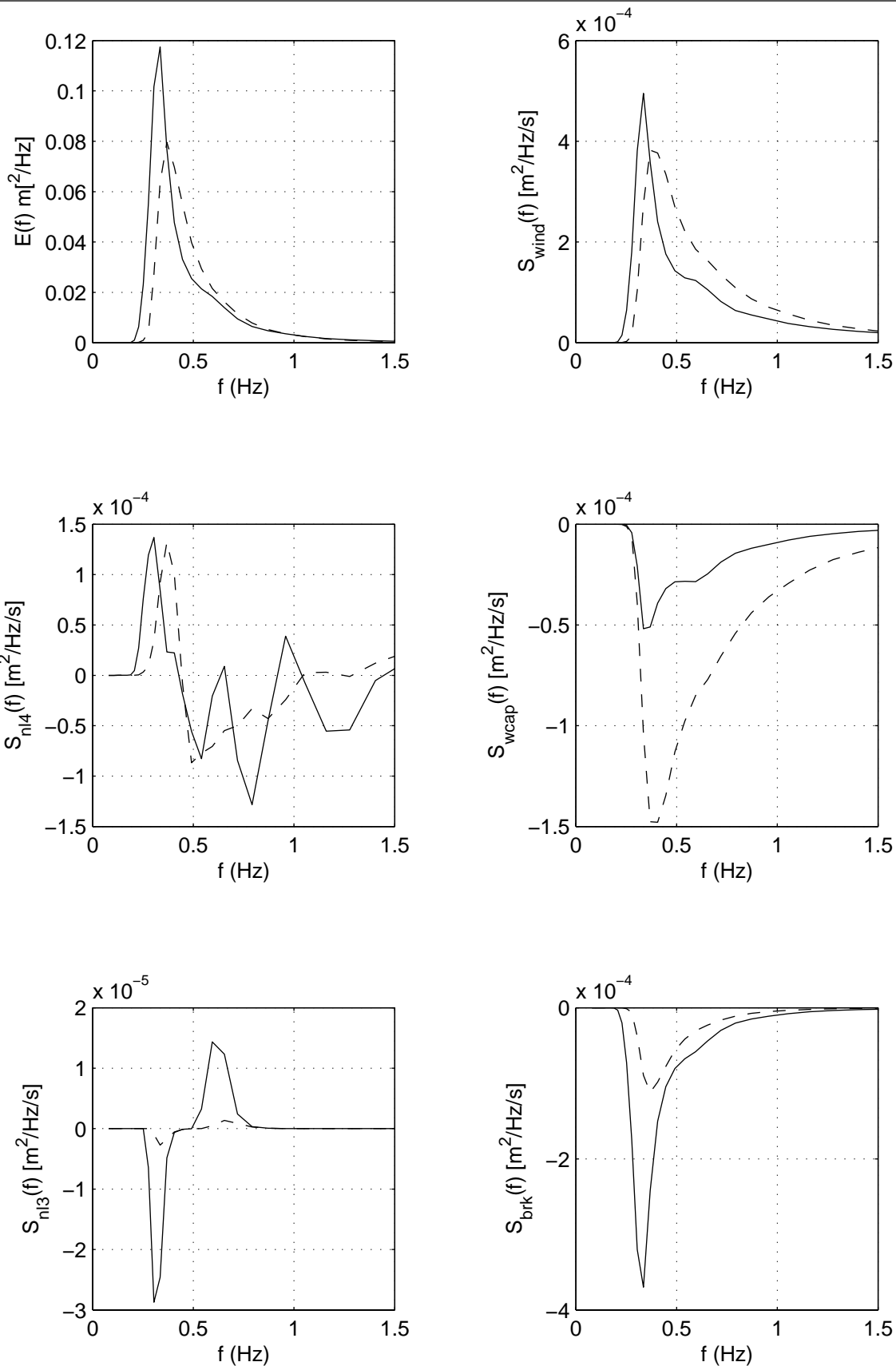
efr\_sl\_sl\_C03\_p14\_L4\_i5

Calibration SWAN 40.20

A1168

 Alkyon

Fig. 5.6.1



Two dimensional spectrum and source terms for physical variation

Base case (dashed line)

Cumulative steepness (solid line)

Area: SL

Grid: SL

Loc: 4

Iteration: 20

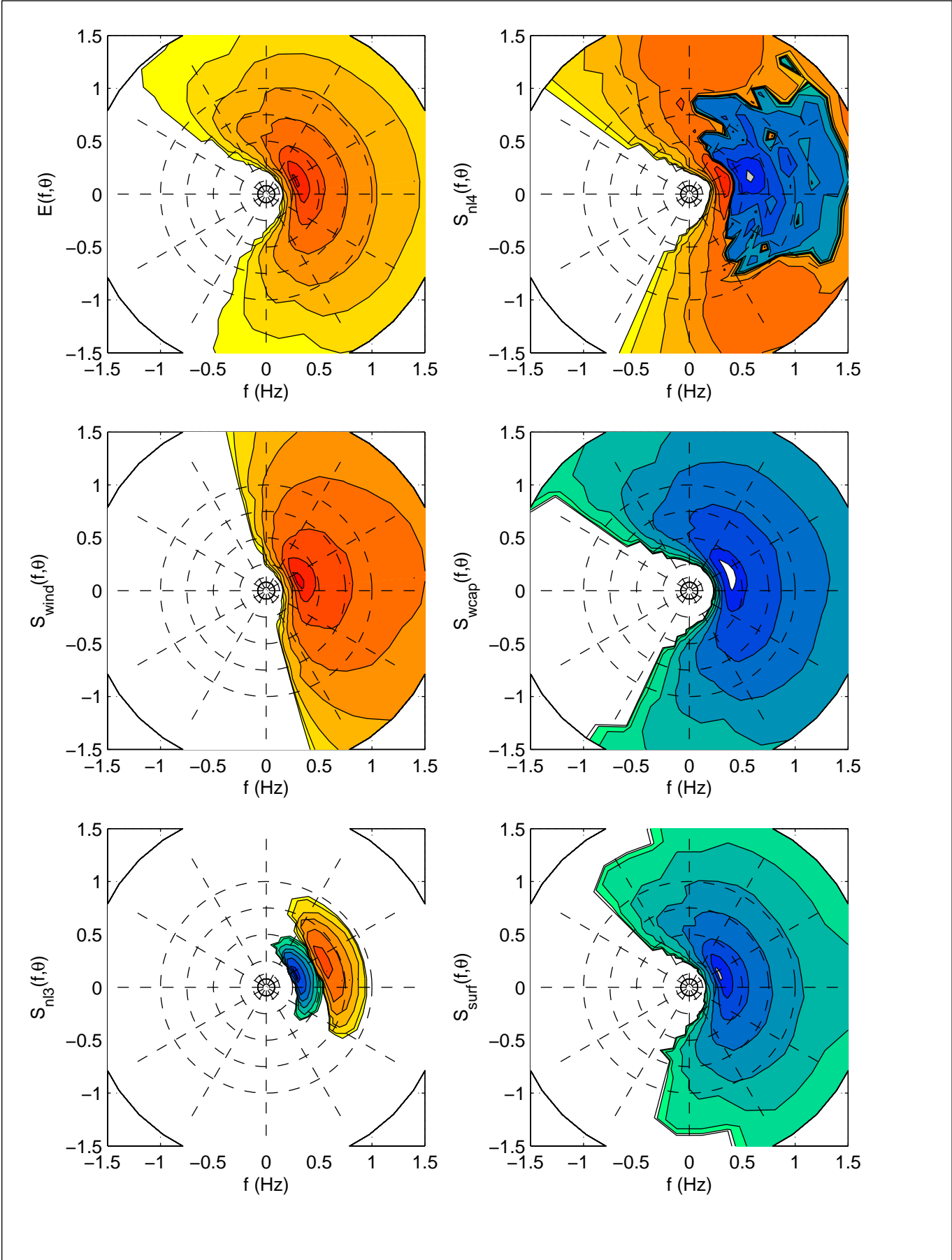
efr\_sl\_sl\_C03\_p14\_L4\_i20

Calibration SWAN 40.20

A1168

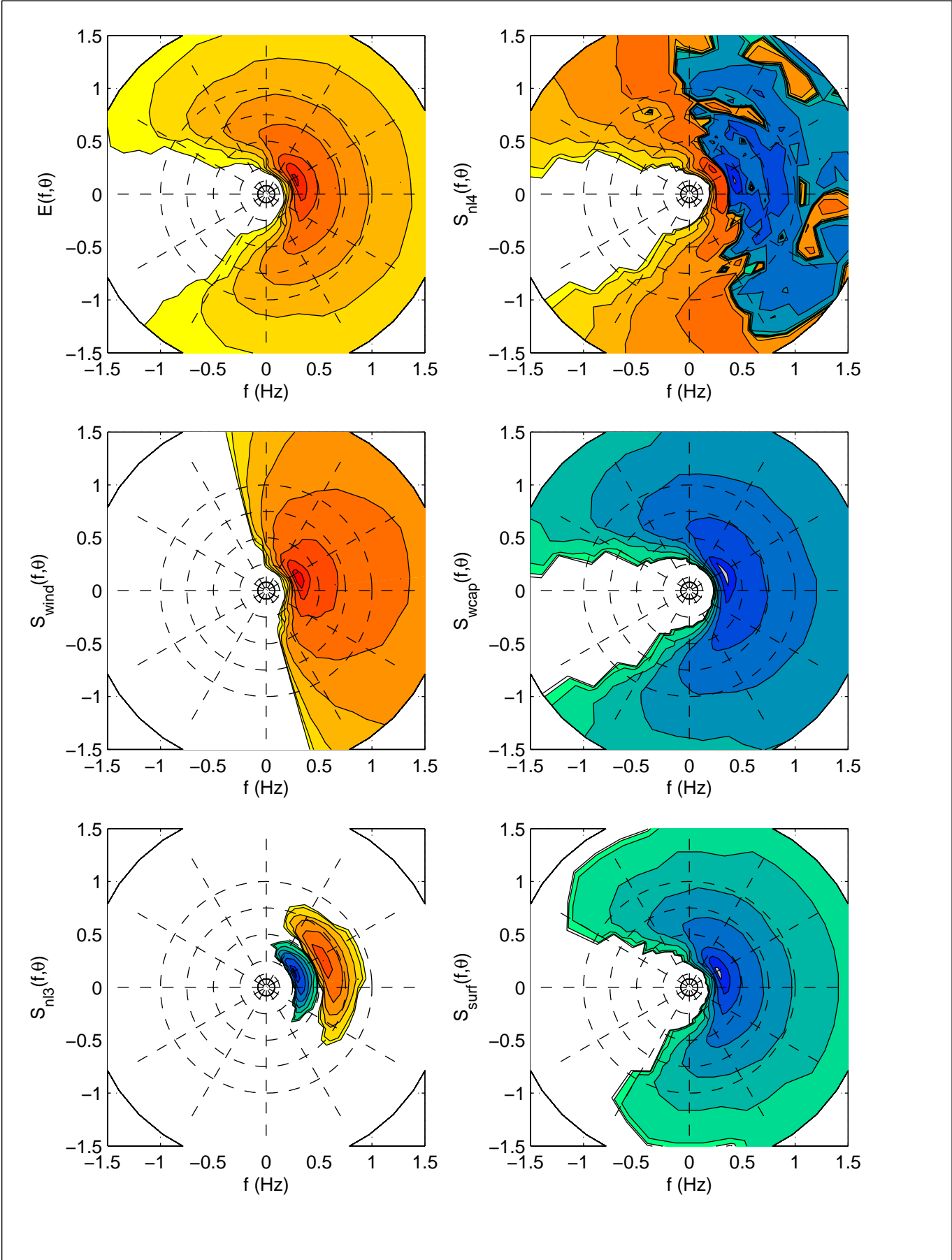


Fig. 5.6.2



Two dimensional spectrum and source terms for physical variation Cumulative steepness	Area: SL	Grid: SL
	Locn: 4	Iteration: 5
	polar_sl_sl_C03_p14_s2d_loc4	
Calibration SWAN 40.20	A1168	Alkyon Fig. 5.7





Two dimensional spectrum and source terms for physical variation  
Cumulative steepness

Area: SL

Grid: SL

Locn: 4

Iteration: 10

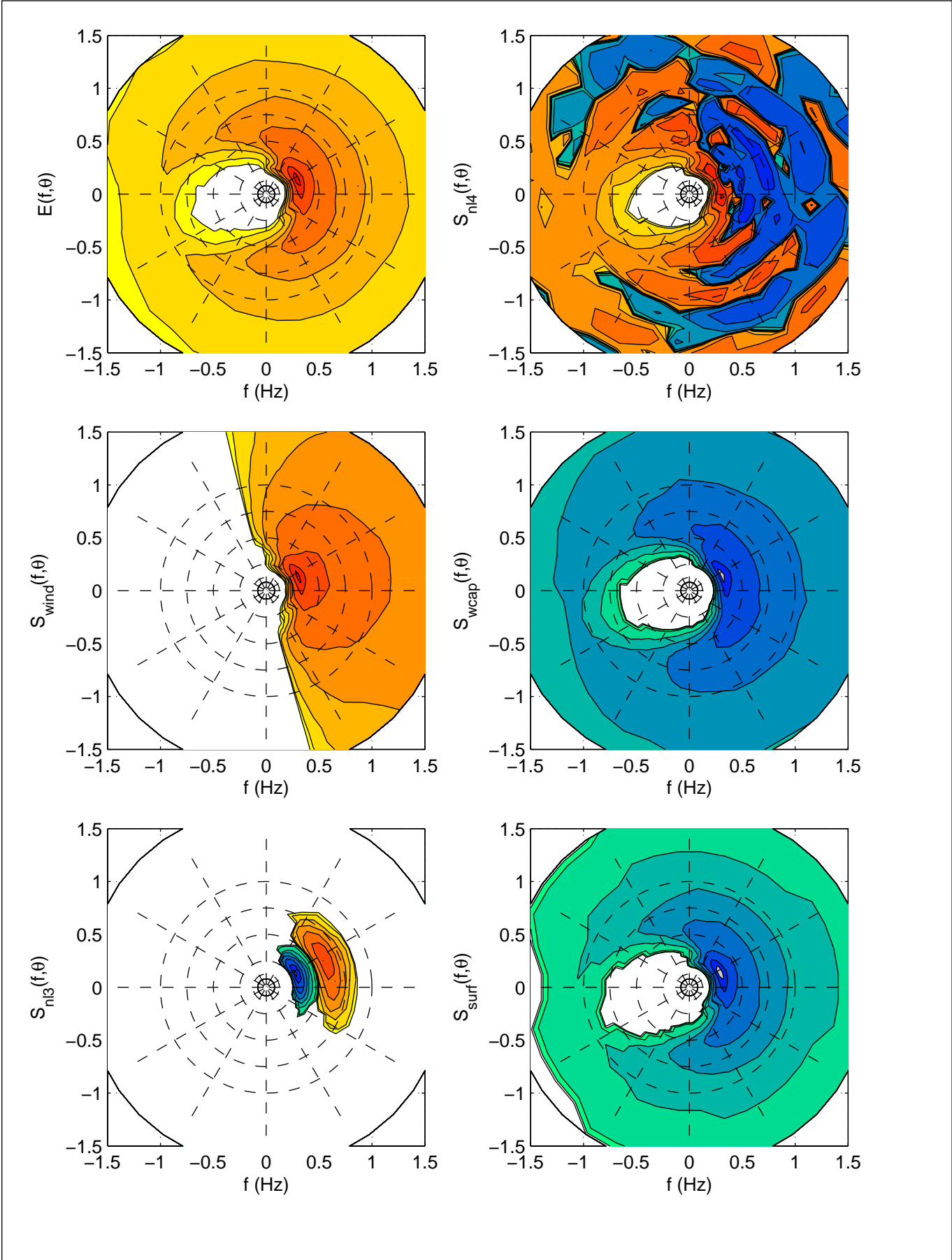
polar\_sl\_sl\_C03\_p14\_s2d\_loc4

Calibration SWAN 40.20

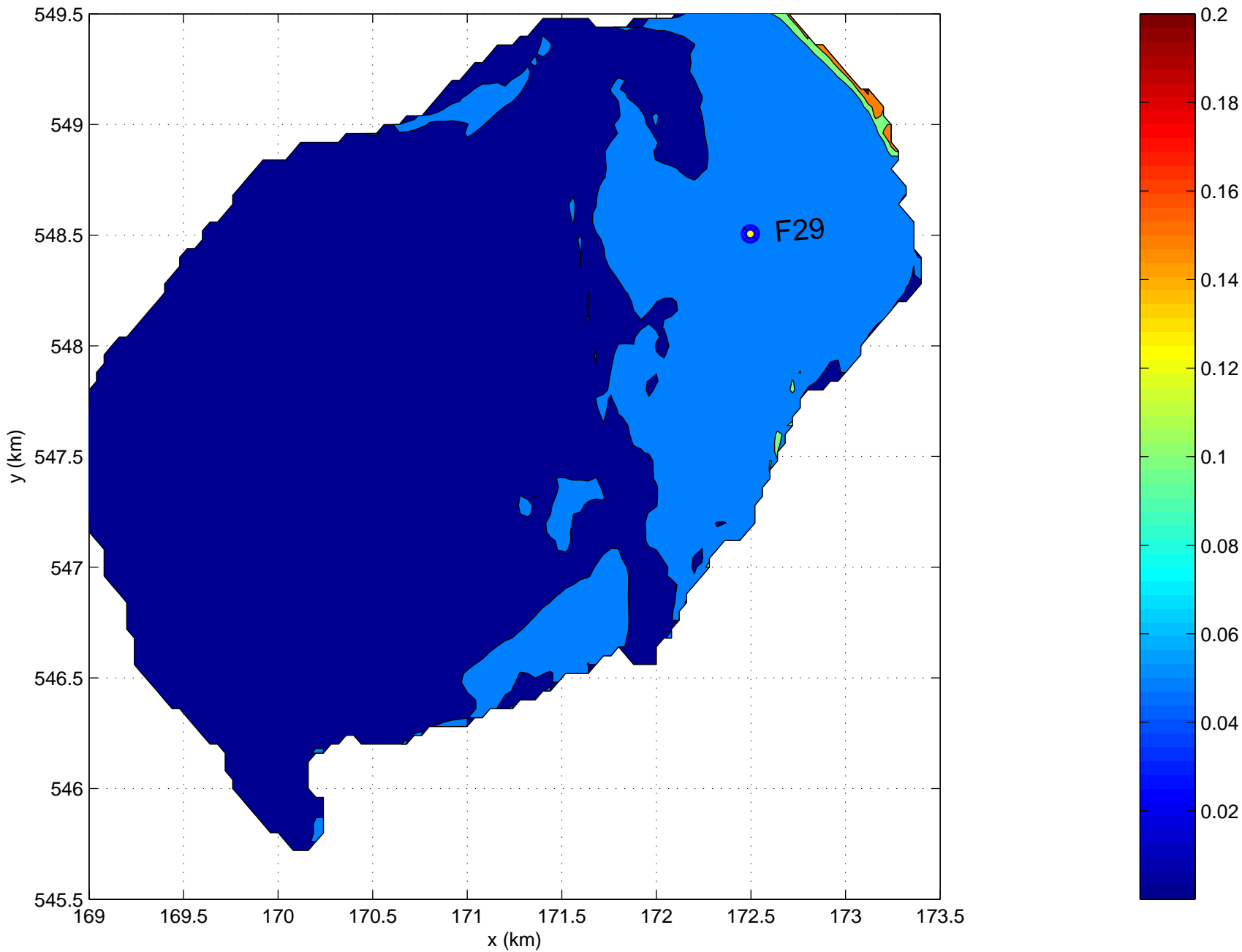
A1168

 Alkyon

Fig. 5.8



Two dimensional spectrum and source terms for physical variation Cumulative steepness	Area: SL	Grid: SL
	Locn: 4	Iteration: 20
	polar_sl_sl_C03_p14_s2d_loc4	
Calibration SWAN 40.20	A1168	Alkyon Fig. 5.9



Spatial variation of SWAN wave parameter Ursell number and location measurement point(s)

Area:SL

Grid:SL

ur

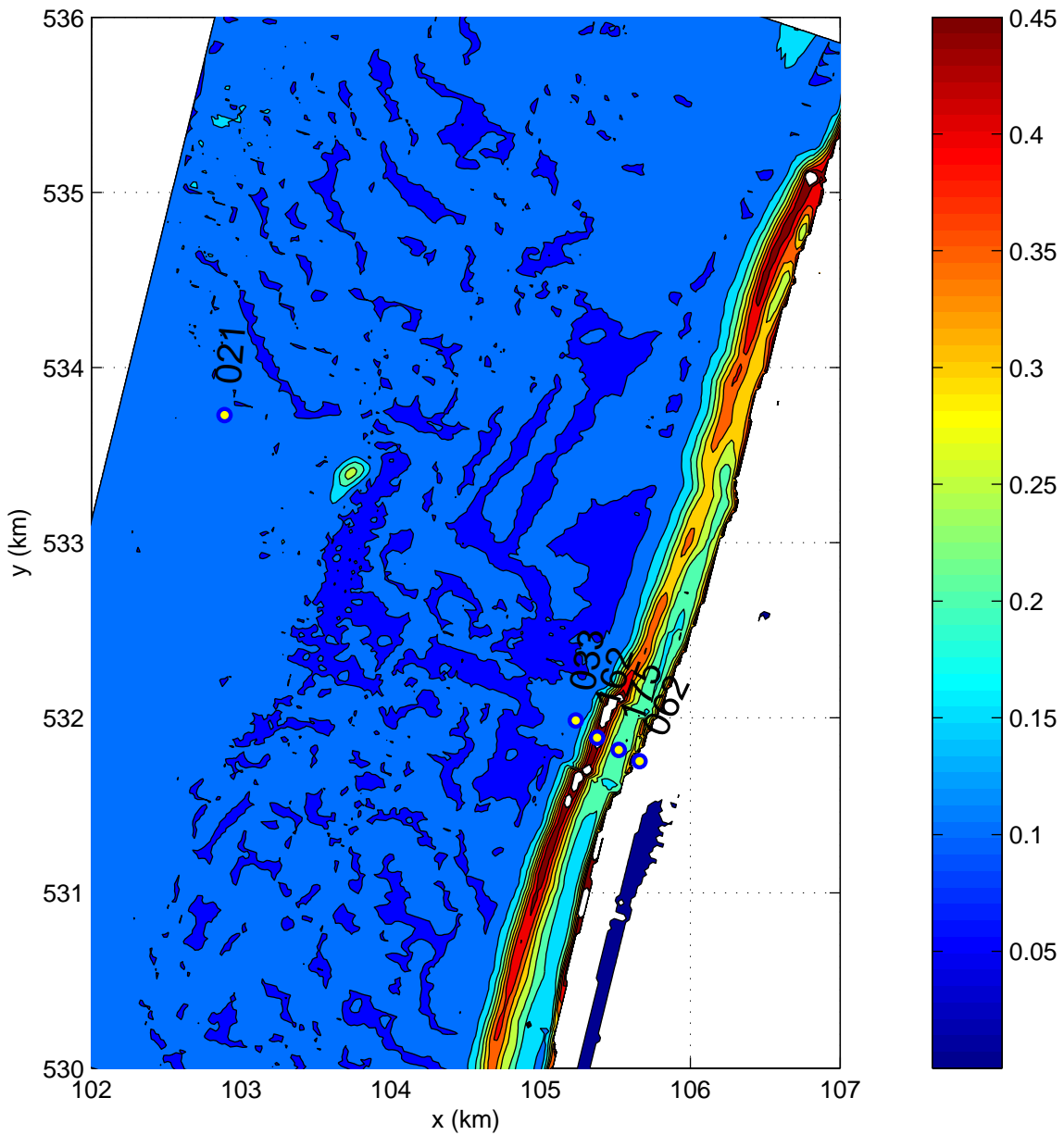
sl\_c03\_n01\_blk\_ur

Calibration SWAN 40.20

A1168

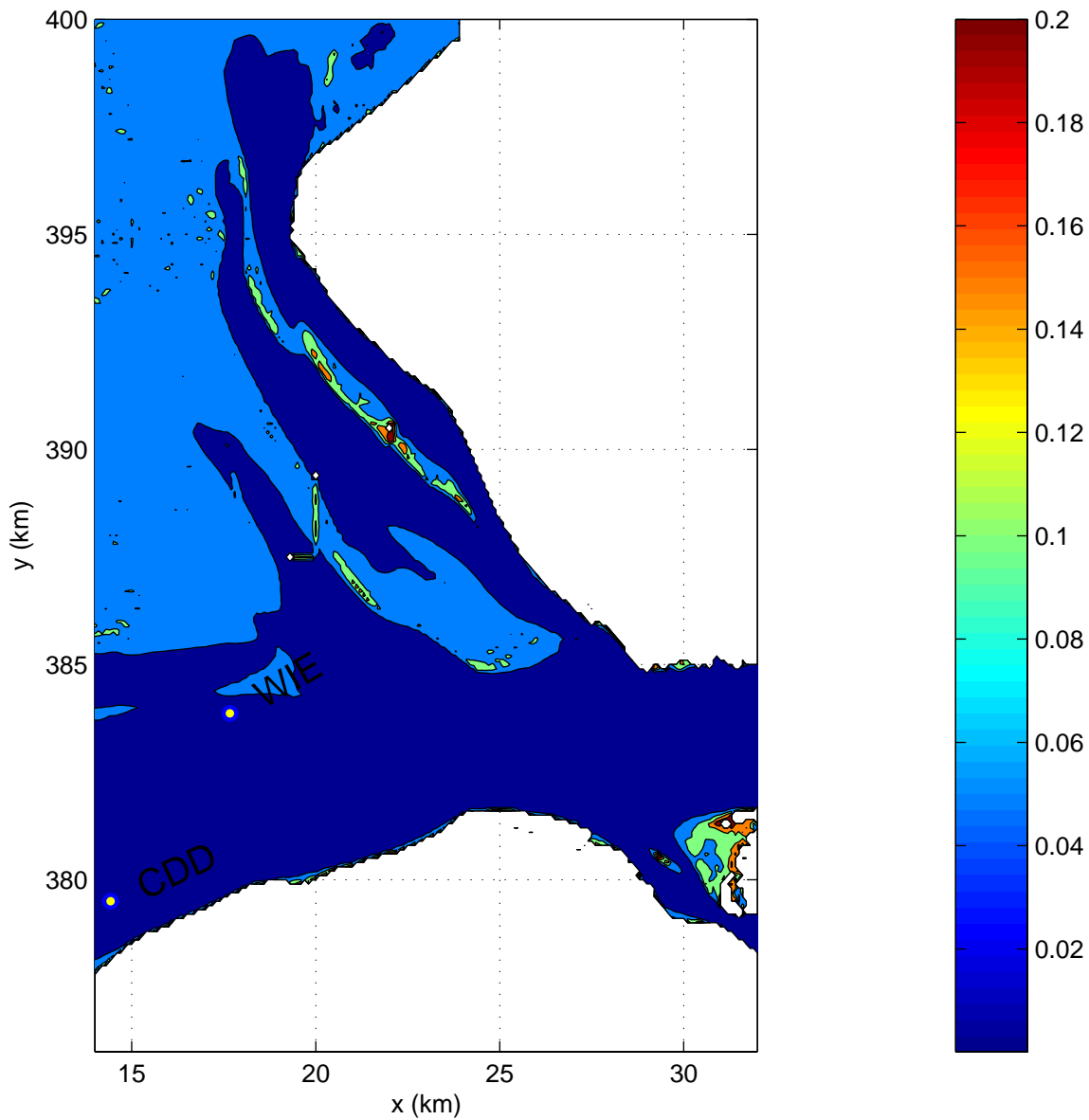


Fig. 5.10



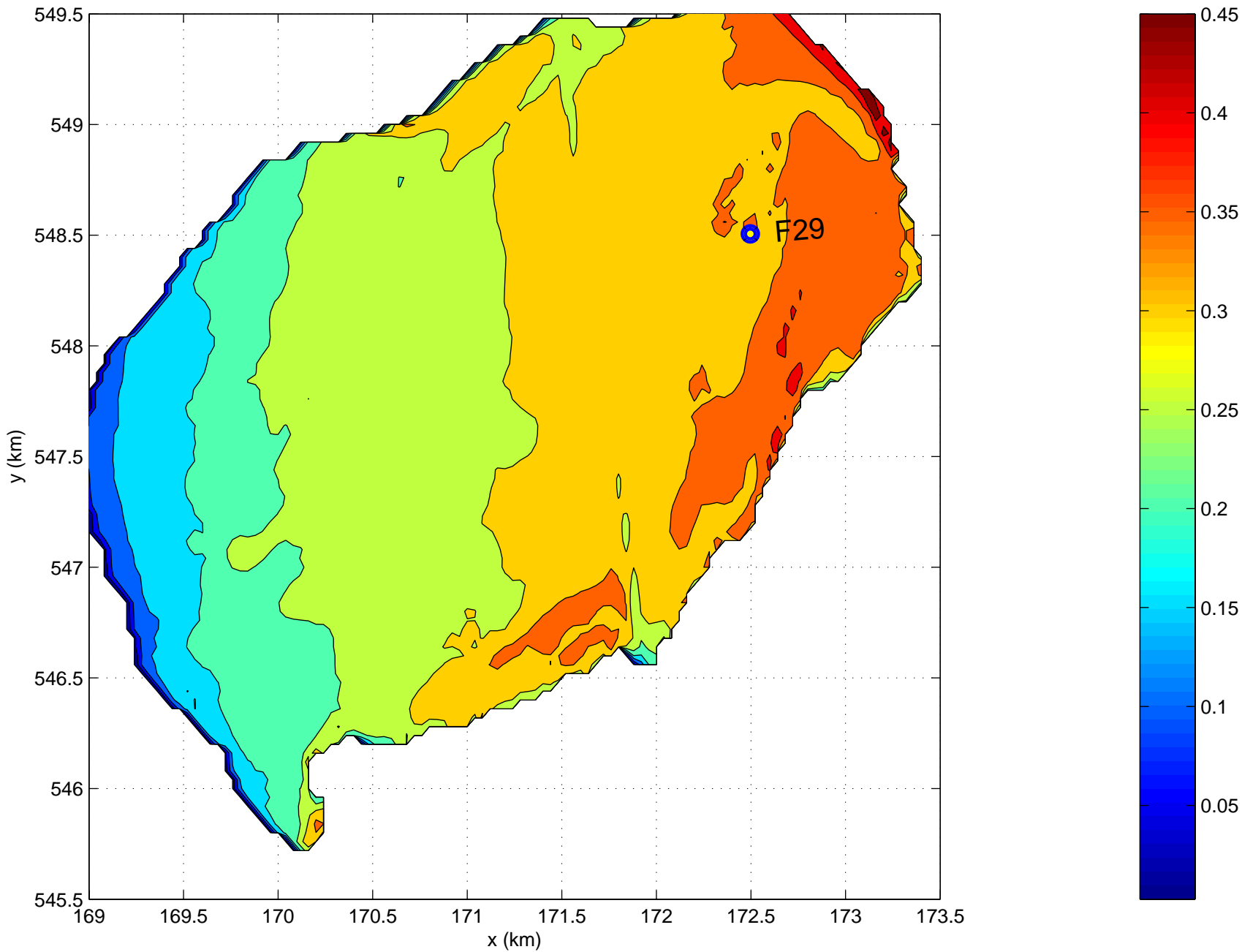
Spatial variation of SWAN wave parameter Ursell number and location measurement point(s)

Calibration SWAN 40.20	A1168		Alkyon	Fig. 5.11
	Area:PT	Grid:E24		
	ur			
	pt_c05_n01_blk_ur			




Spatial variation of SWAN wave parameter Ursell number and location measurement point(s)

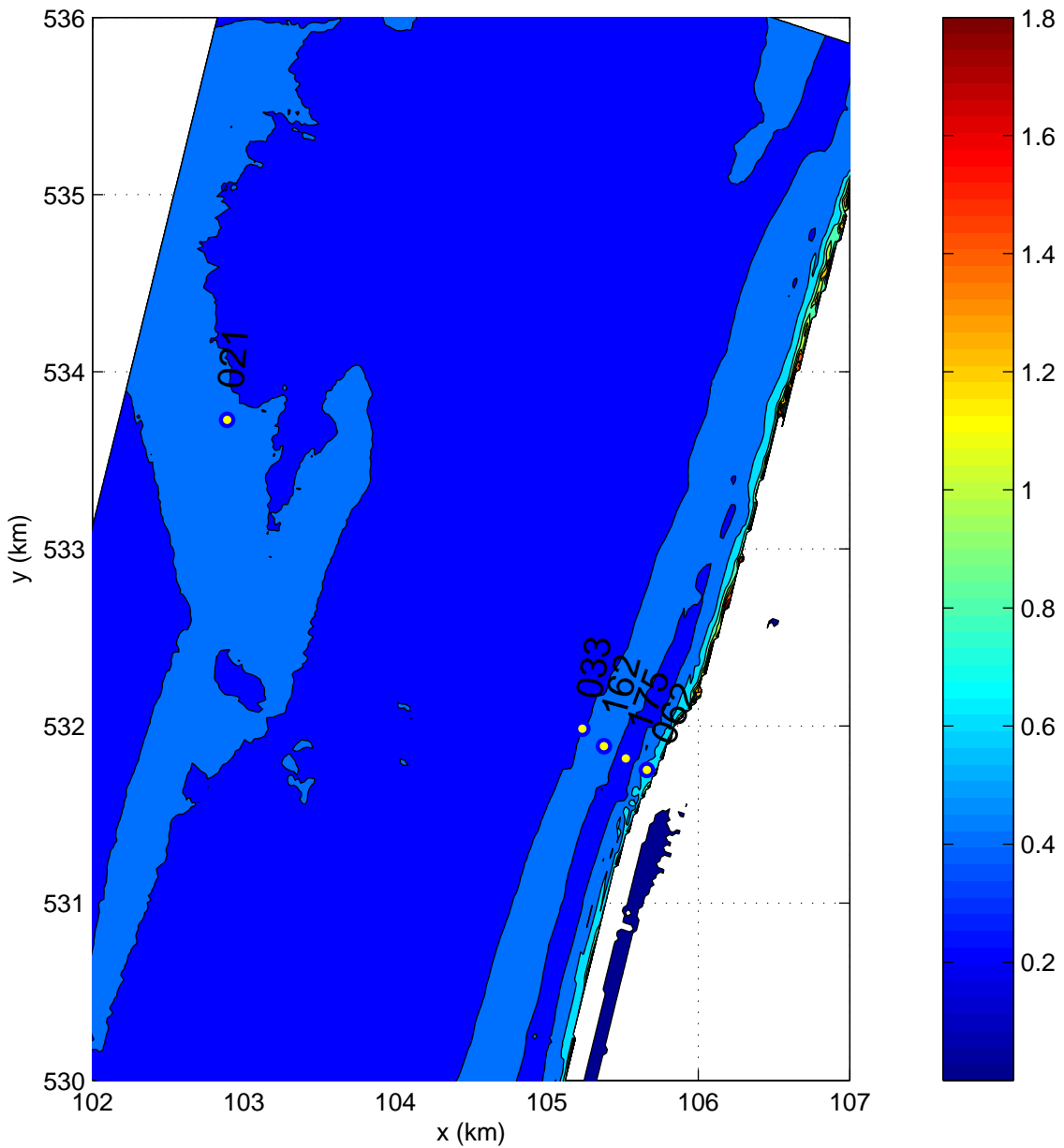
Calibration SWAN 40.20	A1168		Alkyon	Fig. 5.12
	Area:WS	Grid:W01		
	ur			
	ws_c03_n01_blk_ur			



Spatial variation of SWAN wave parameter  $H_s/d$  and location measurement point(s)

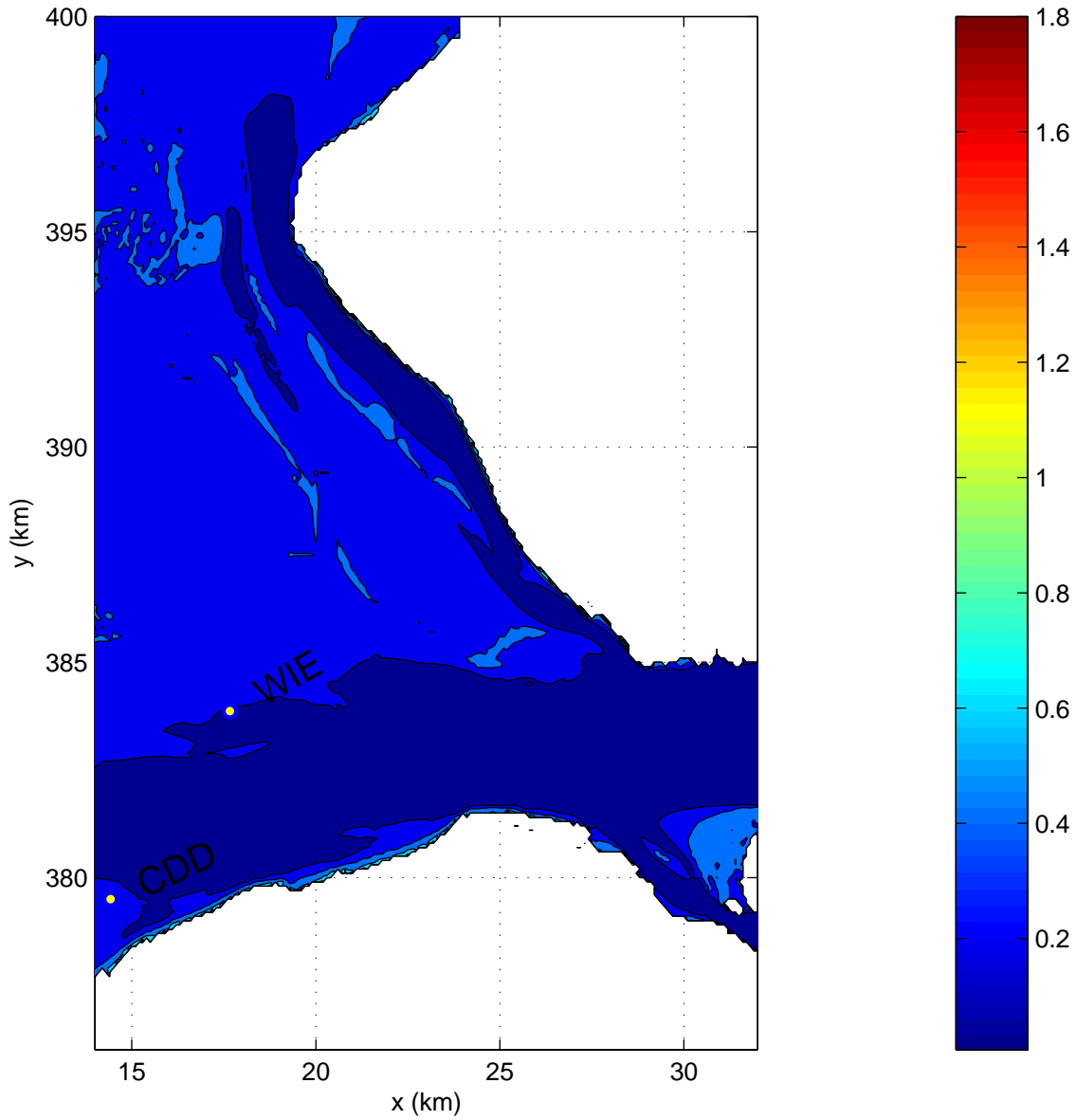
Area:SL		Grid:SL
hd		
sl_c03_n01_blk_hd		

Calibration SWAN 40.20	A1168	 Alkyon	Fig. 5.13
------------------------	-------	--	-----------




Spatial variation of SWAN wave parameter  $H_s/d$  and location measurement point(s)

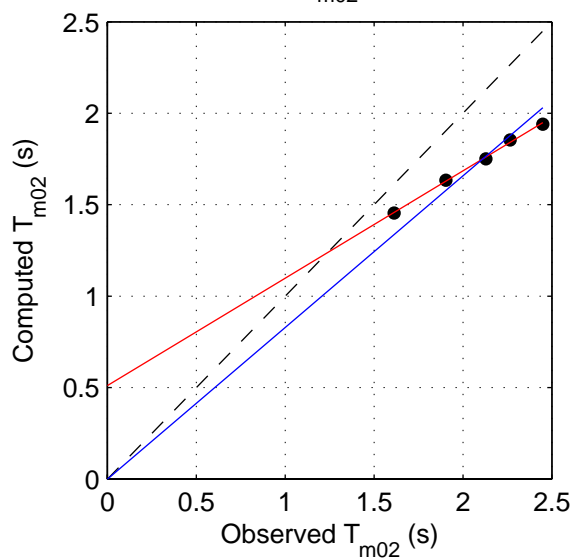
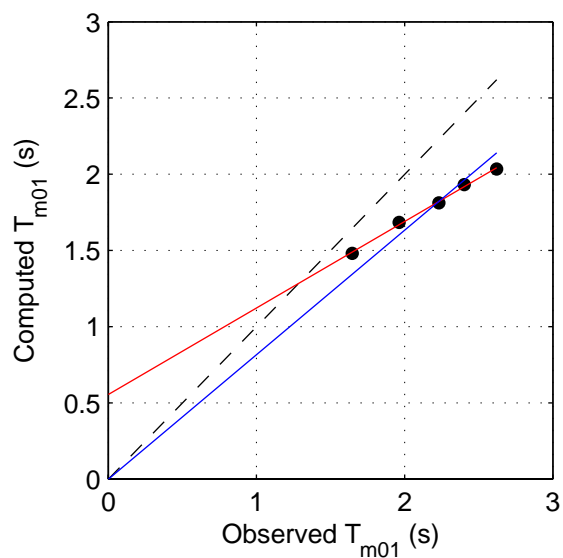
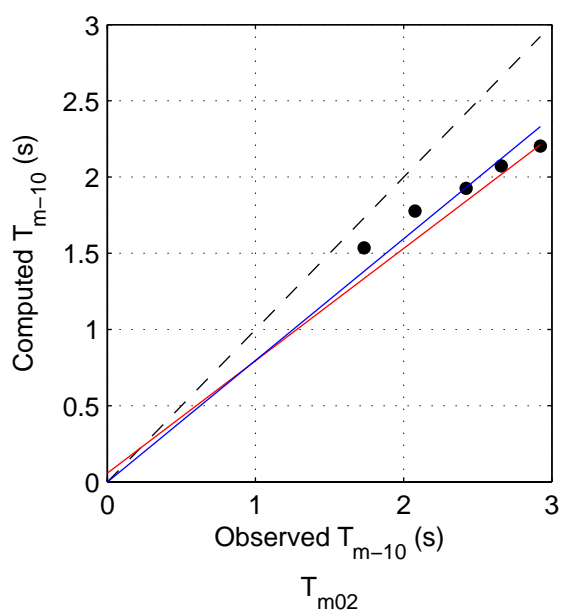
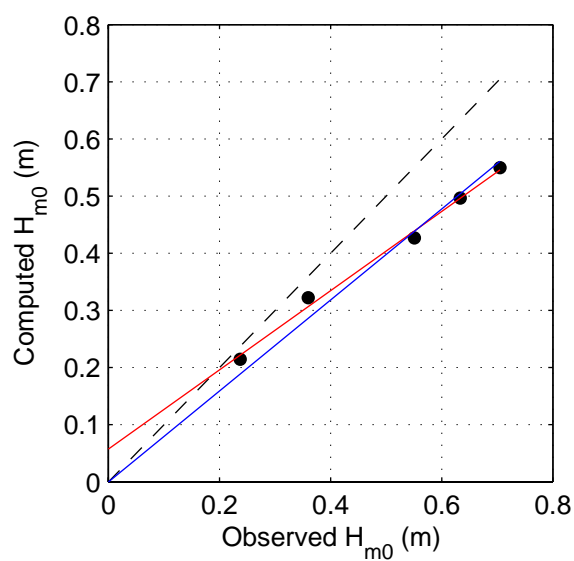
Calibration SWAN 40.20	Area:PT		Grid:E24
	hd		
	pt_c05_n01_blk_hd		
A1168		Alkyon	
		Fig. 5.14	



Spatial variation of SWAN wave parameter  $H_s/d$  and location measurement point(s)

Calibration SWAN 40.20	A1168	
	 Alkyon	Fig. 5.15
	ws_c03_n01_blk_hd	
Area:WS		Grid:W01
hd		





	mean	bias	stdev	rmse	mae	sci	r	a	b	b <sub>0</sub>
H <sub>m0</sub>	0.497	-0.095	0.061	0.110	0.095	0.221	0.997	0.057	0.693	0.796
T <sub>m-10</sub>	2.362	-0.460	0.211	0.497	0.460	0.210	0.997	0.598	0.552	0.798
T <sub>m01</sub>	2.173	-0.384	0.165	0.412	0.384	0.189	0.998	0.555	0.568	0.817
T <sub>m02</sub>	2.072	-0.346	0.135	0.366	0.346	0.177	0.999	0.511	0.587	0.828

Scatter diagrams and statistics of measured and computed  
integral wave parameters in Sloterveer at station F29  
Case N01: Base case, inclusive triads and quadruplets, Qb=1.0

Area: SL

F29

N01

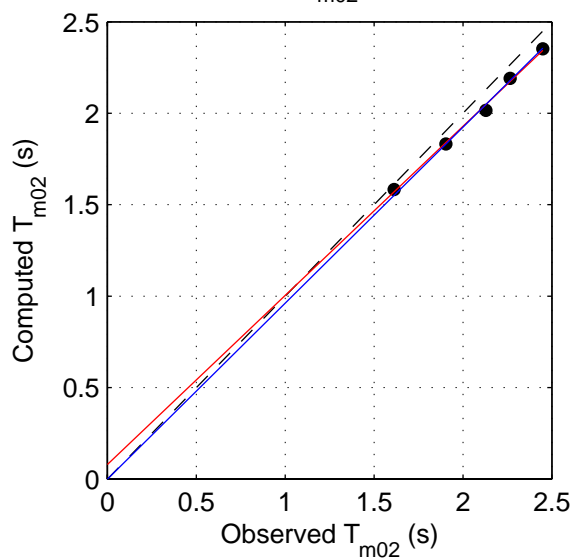
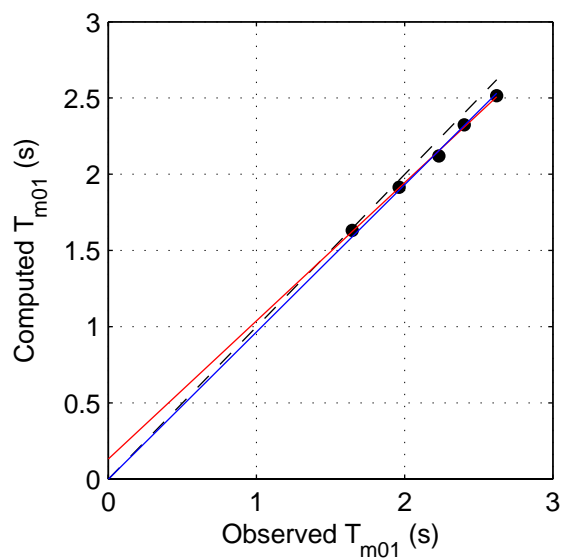
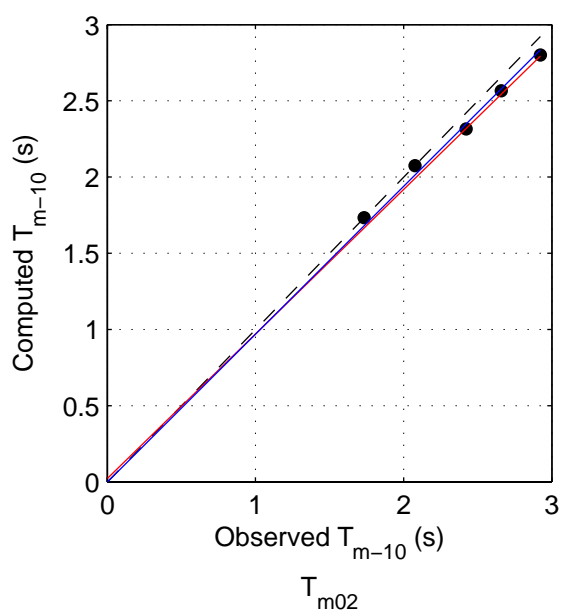
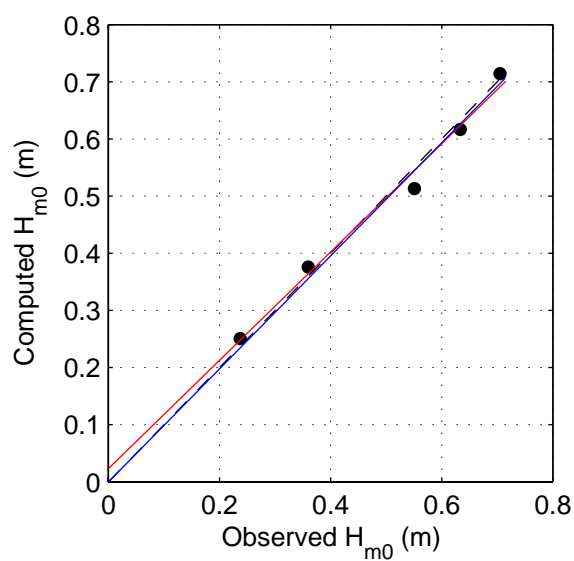
mspec\_SL\_F29\_N01

Calibration SWAN 40.20

A1168

 Alkyon

Fig. 7.2.1



	mean	bias	stdev	rmse	mae	sci	r	a	b	b <sub>0</sub>
H <sub>m0</sub>	0.497	-0.003	0.023	0.021	0.019	0.042	0.994	0.023	0.947	0.989
T <sub>m-10</sub>	2.362	-0.064	0.059	0.083	0.065	0.035	0.998	0.207	0.885	0.970
T <sub>m01</sub>	2.173	-0.071	0.041	0.080	0.071	0.037	0.998	0.133	0.906	0.966
T <sub>m02</sub>	2.072	-0.078	0.032	0.083	0.078	0.040	0.998	0.080	0.924	0.962

Scatter diagrams and statistics of measured and computed  
integral wave parameters in Slotermeer at station F29  
Verification run, set SL

Area: SL

F29

SL

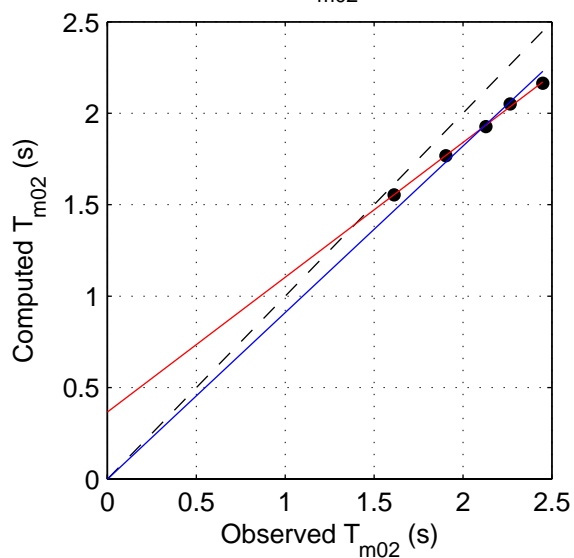
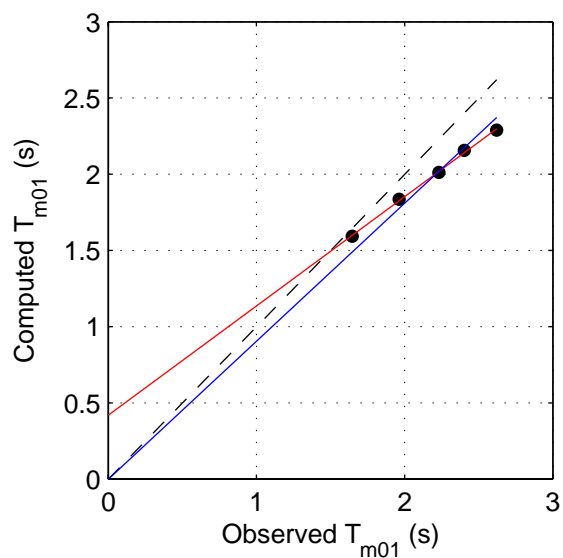
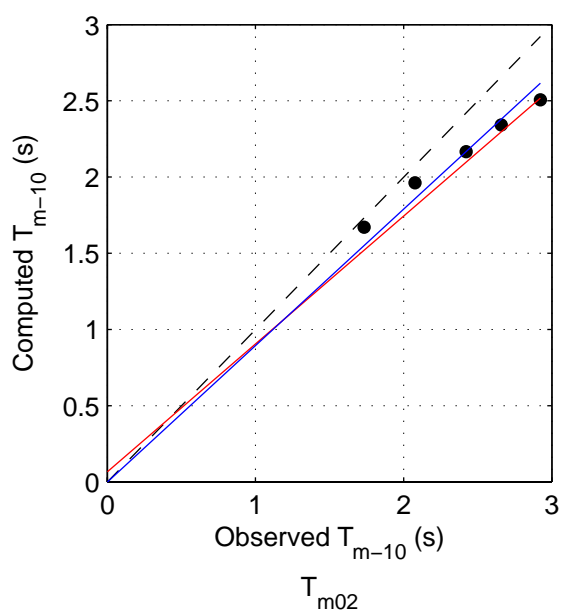
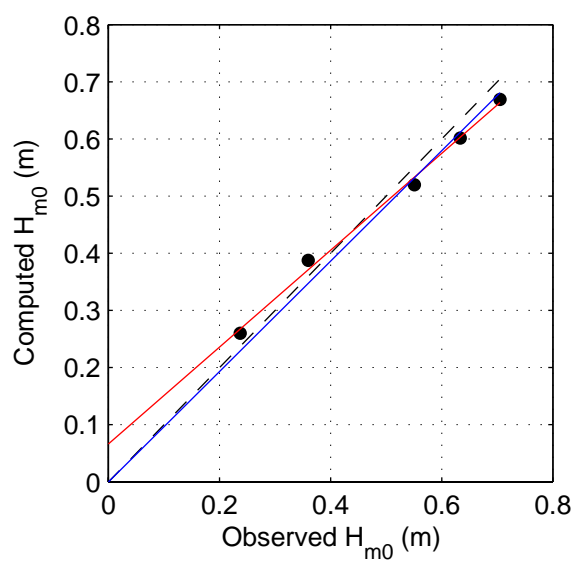
mspec\_SL\_F29\_SL

Calibration SWAN 40.20

A1168

 Alkyon

Fig. 7.2.2



	mean	bias	stdev	rmse	mae	sci	r	a	b	b <sub>0</sub>
$H_{m0}$	0.497	-0.010	0.032	0.030	0.030	0.061	0.998	0.066	0.847	0.966
$T_{m-10}$	2.362	-0.233	0.145	0.267	0.233	0.113	0.998	0.491	0.694	0.895
$T_{m01}$	2.173	-0.195	0.108	0.218	0.195	0.100	0.999	0.419	0.717	0.905
$T_{m02}$	2.072	-0.179	0.086	0.195	0.179	0.094	0.999	0.366	0.737	0.910

Scatter diagrams and statistics of measured and computed  
integral wave parameters in Slotermeer at station F29  
Verification run ALL

Area: SL

F29

ALL

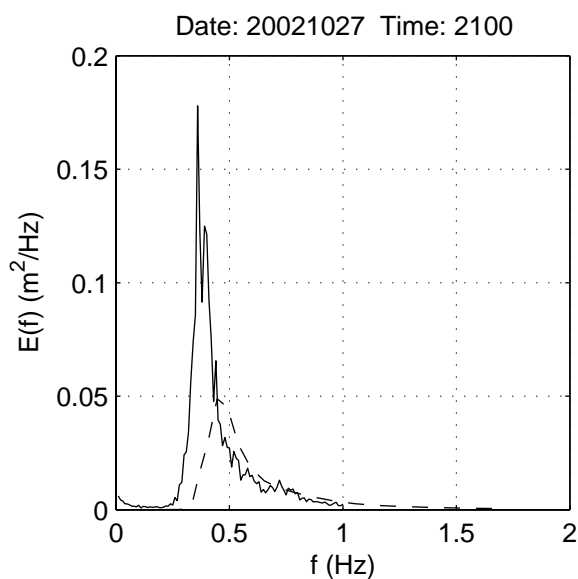
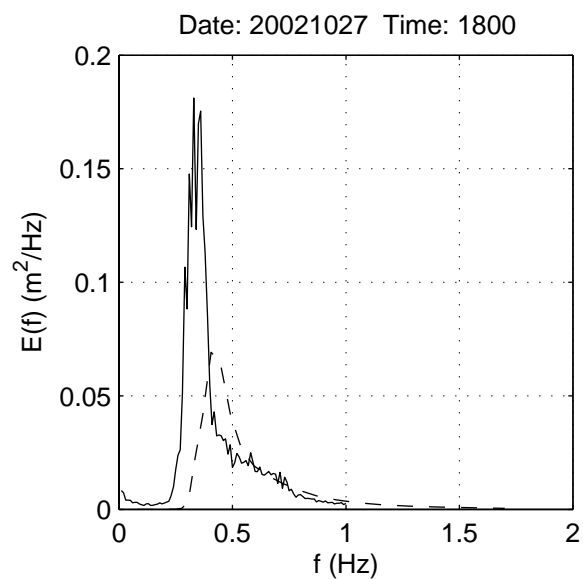
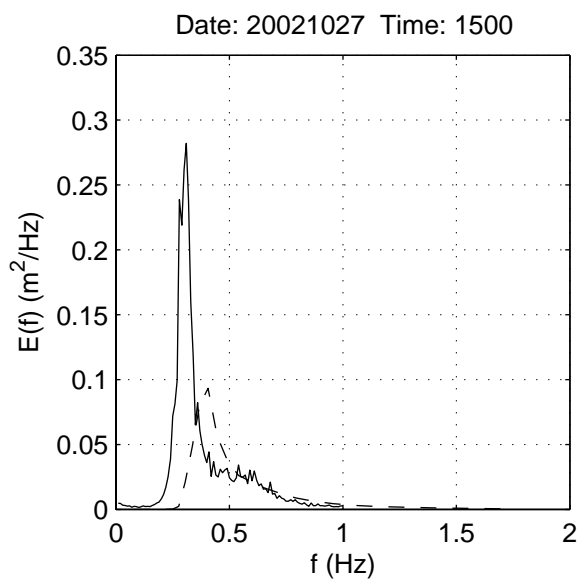
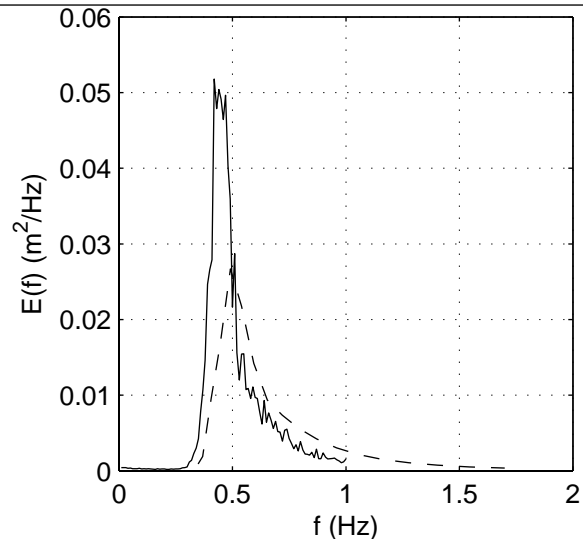
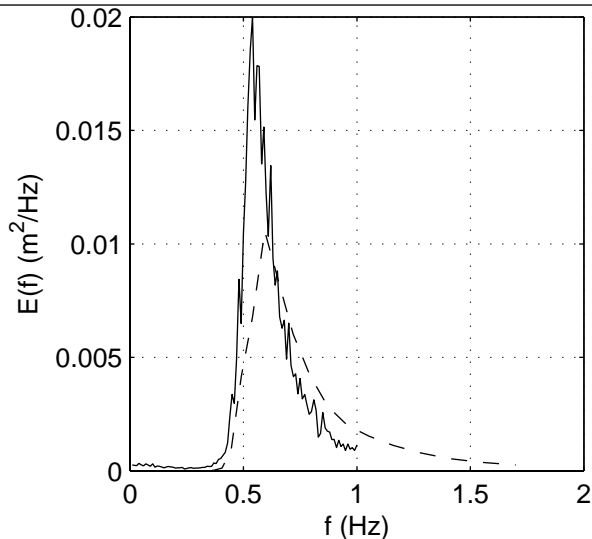
mspec\_SL\_F29\_ALL

Calibration SWAN 40.20

A1168

 Alkyon

Fig. 7.2.3



Comparison of measured (solid line) and computed (dashed line) spectra  
at station in Sloterveer at station F29  
Case N01: Base case, inclusive triads and quadruplets,  $Q_b=1.0$

Area: SL

F29

N01

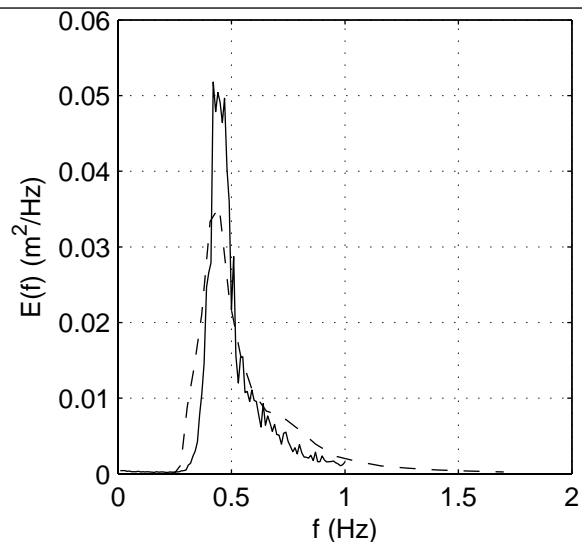
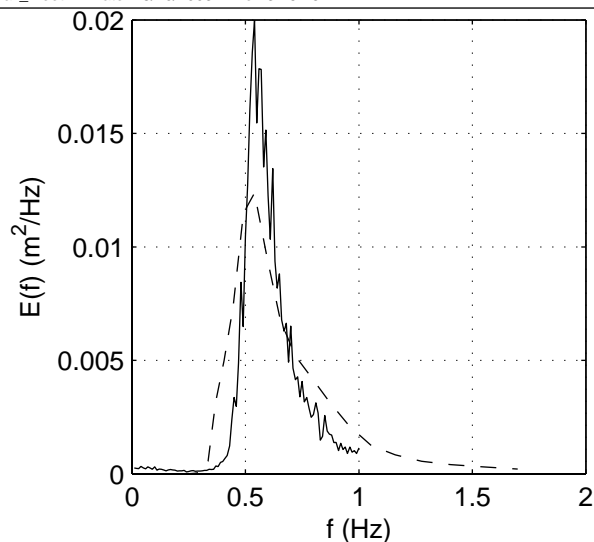
mspec\_SL\_F29\_N01

Calibration SWAN 40.20

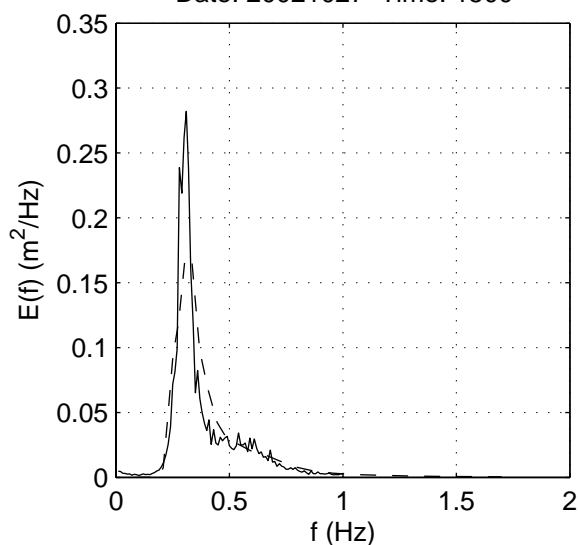
A1168

Alkyon

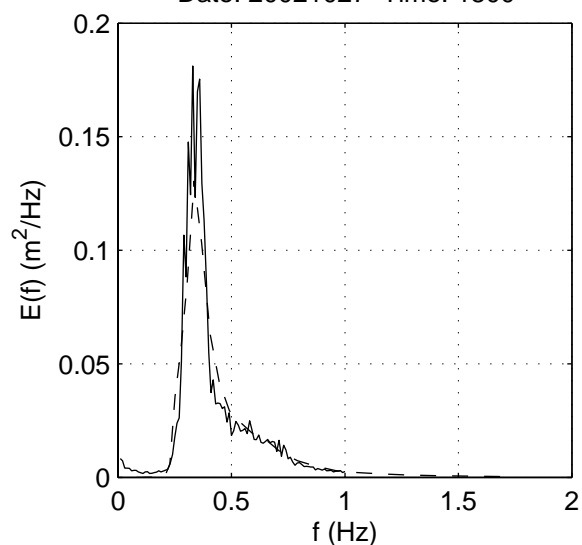
Fig. 7.2.4



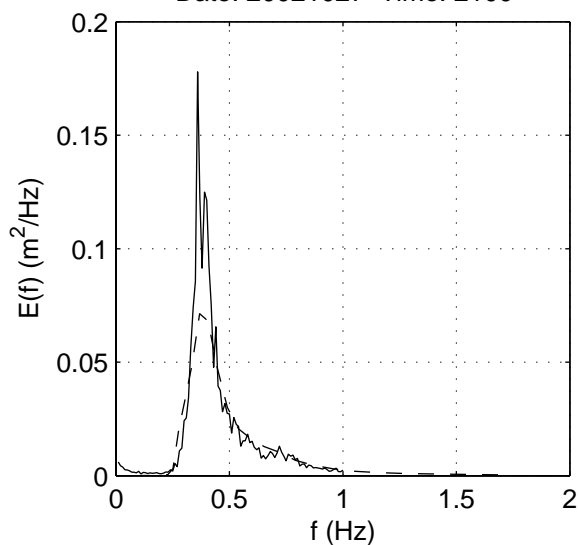
Date: 20021027 Time: 1500



Date: 20021027 Time: 1800



Date: 20021027 Time: 2100



Comparison of measured (solid line) and computed (dashed line) spectra  
at station in Sloterveer at station F29  
Verification run, set SL

Area: SL

F29

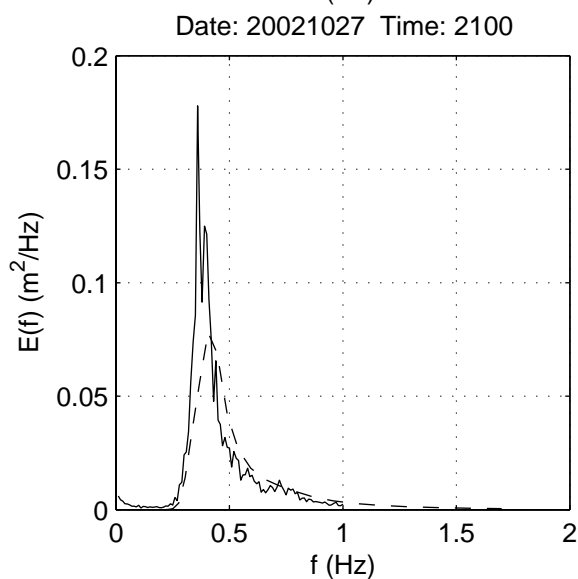
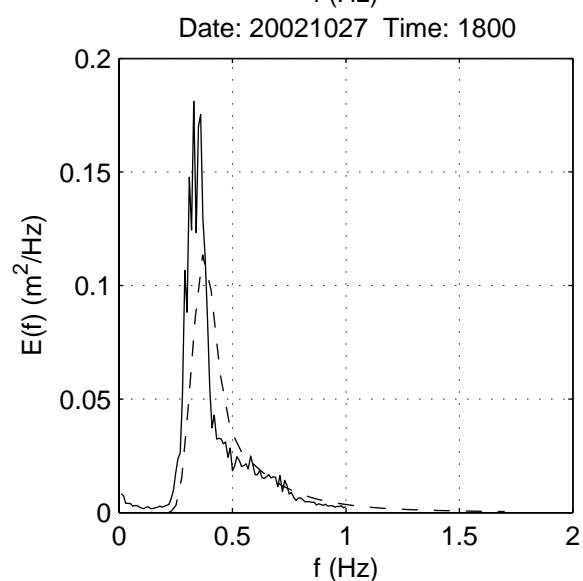
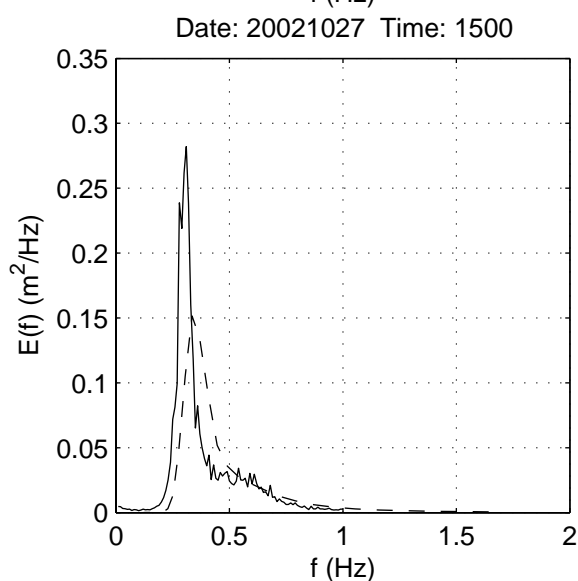
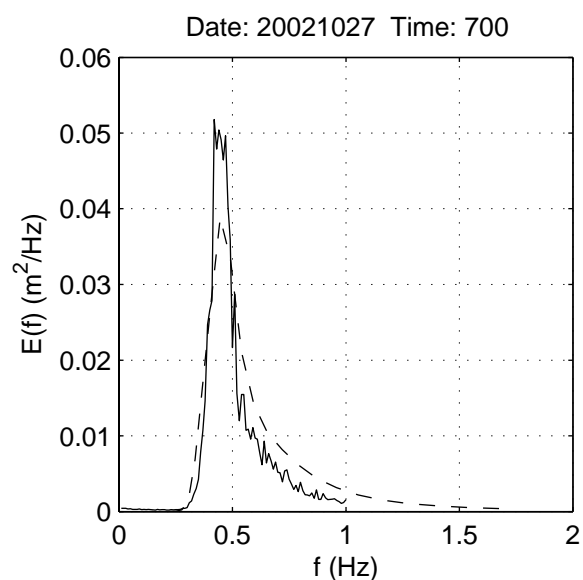
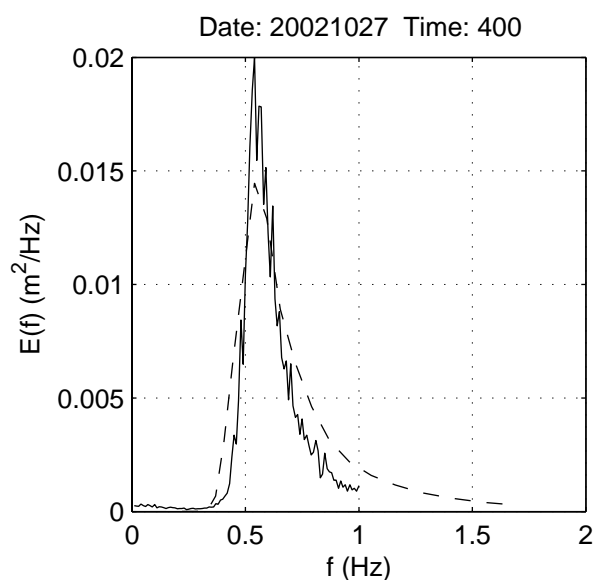
SL

mspec\_SL\_F29\_SL

Calibration SWAN 40.20

A1168

Fig. 7.2.5



Comparison of measured (solid line) and computed (dashed line) spectra  
at station in Slotermeer at station F29  
Verification run, set ALL

Area: SL

F29

ALL

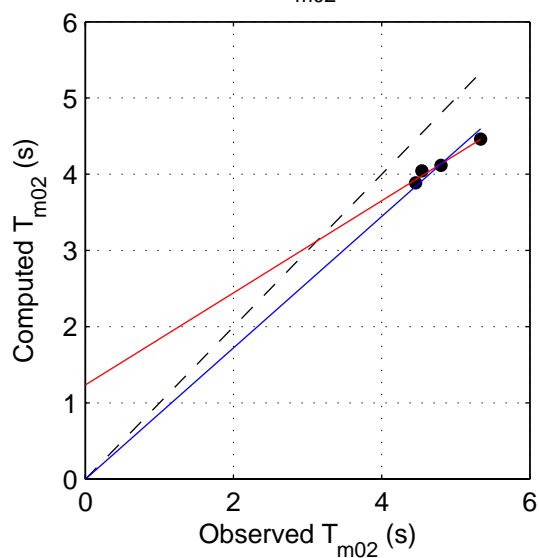
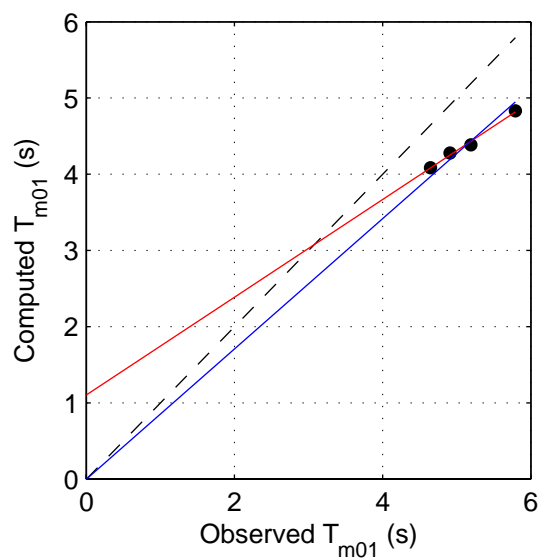
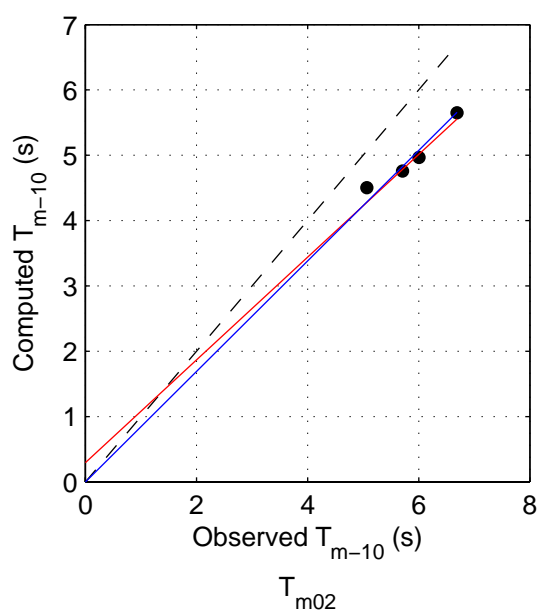
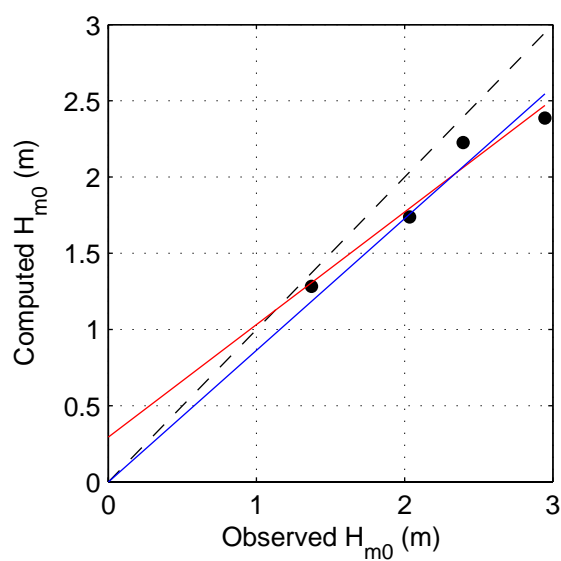
mspec\_SL\_F29\_ALL

Calibration SWAN 40.20

A1168

 **Alkyon**

Fig. 7.2.6



	mean	bias	stdev	rmse	mae	sci	r	a	b	b <sub>0</sub>
H <sub>m0</sub>	2.186	-0.278	0.206	0.331	0.278	0.151	0.974	0.294	0.738	0.864
T <sub>m-10</sub>	5.869	-0.898	0.228	0.920	0.898	0.157	0.972	0.811	0.709	0.846
T <sub>m01</sub>	5.135	-0.739	0.179	0.755	0.739	0.147	0.995	1.103	0.641	0.855
T <sub>m02</sub>	4.785	-0.658	0.162	0.672	0.658	0.141	0.982	1.234	0.605	0.861

Scatter diagrams and statistics of measured and computed  
integral wave parameters in Westerschelde at station CDD  
Case N01: Base case, exclusive triads and quadruplets, Qb=0.00001

Area: WS

CDD

N01

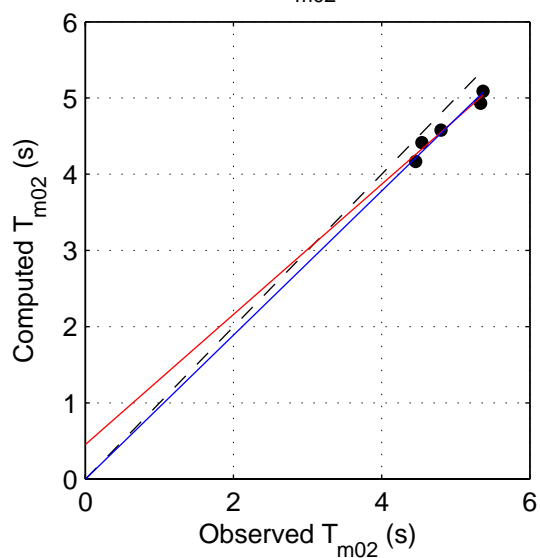
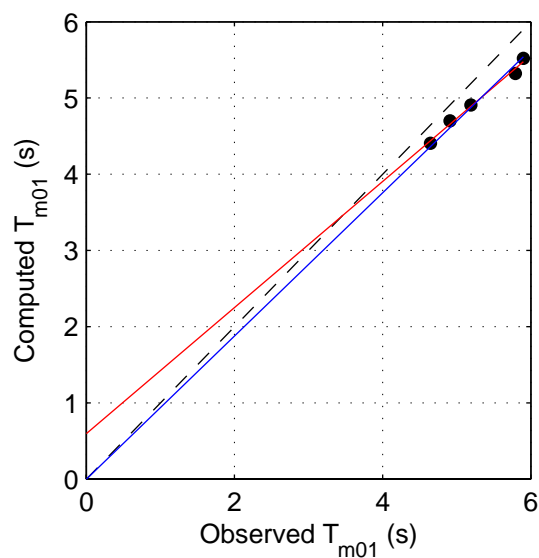
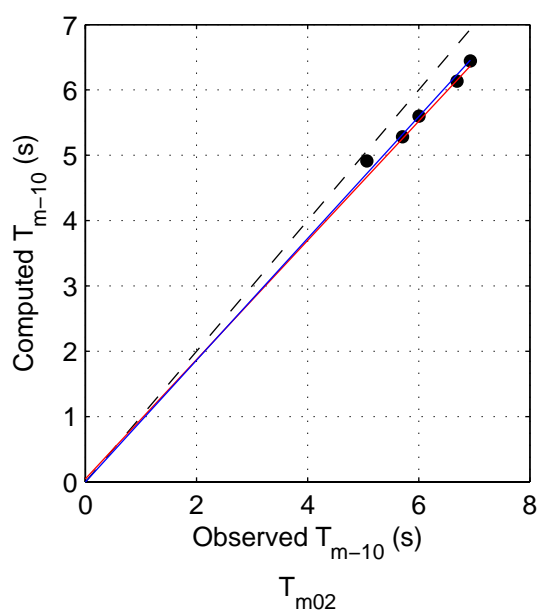
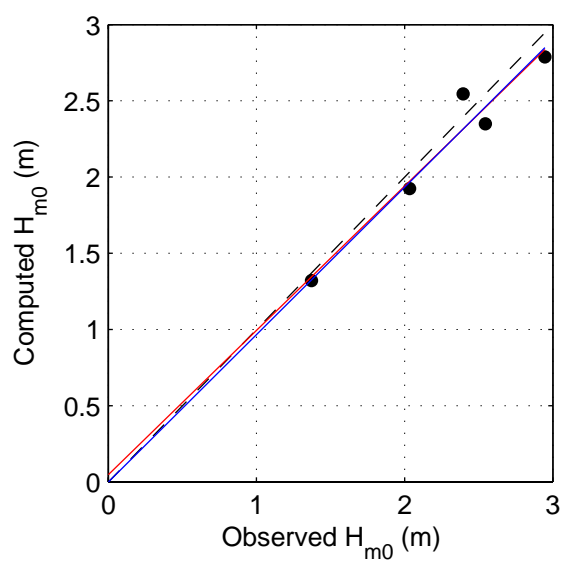
mspec\_WS\_CDD\_n01

Calibration SWAN 40.20

A1168



Fig. 7.3.1



	mean	bias	stdev	rmse	mae	sci	r	a	b	b <sub>0</sub>
$H_{m0}$	2.258	-0.073	0.137	0.142	0.133	0.063	0.973	0.047	0.947	0.967
$T_{m-10}$	6.081	-0.407	0.153	0.429	0.407	0.071	0.994	0.691	0.820	0.932
$T_{m01}$	5.287	-0.316	0.106	0.330	0.316	0.062	0.994	0.598	0.827	0.939
$T_{m02}$	4.902	-0.266	0.101	0.281	0.266	0.057	0.978	0.455	0.853	0.945

Scatter diagrams and statistics of measured and computed  
integral wave parameters in Westerschelde at station CDD  
Verification run, set WS

Area: WS CDD

ALL

mspec\_WS\_CDD\_v01

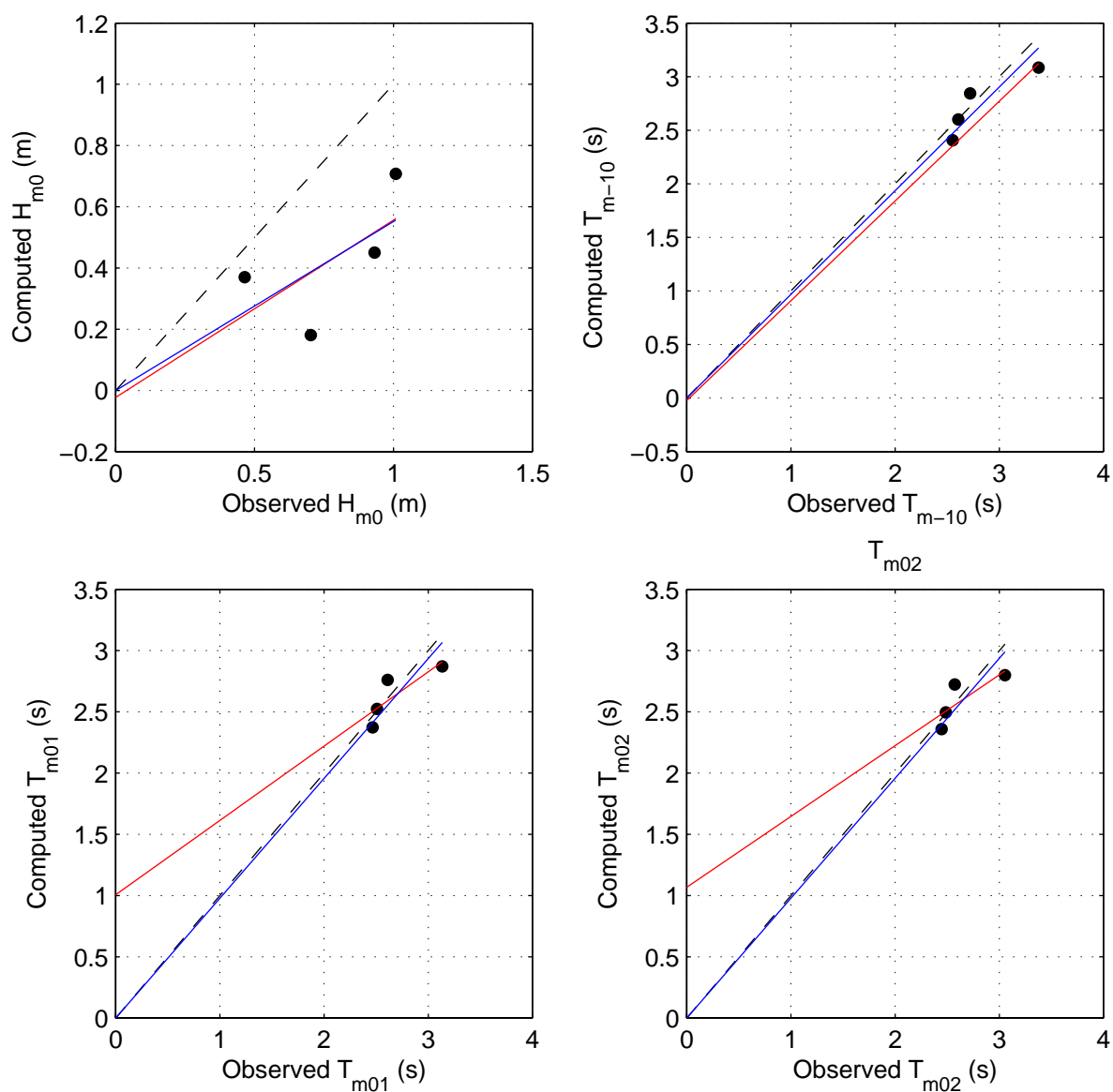
Calibration SWAN 40.20

A1168



Fig. 7.3.2





	mean	bias	stdev	rmse	mae	sci	r	a	b	$b_0$
$H_{m0}$	0.777	-0.349	0.195	0.388	0.349	0.500	0.651	-0.022	0.579	0.552
$T_{m-10}$	2.814	-0.080	0.179	0.175	0.142	0.062	0.891	0.797	0.688	0.968
$T_{m01}$	2.680	-0.048	0.175	0.159	0.131	0.059	0.830	1.007	0.607	0.979
$T_{m02}$	2.640	-0.045	0.170	0.154	0.126	0.058	0.800	1.068	0.578	0.979

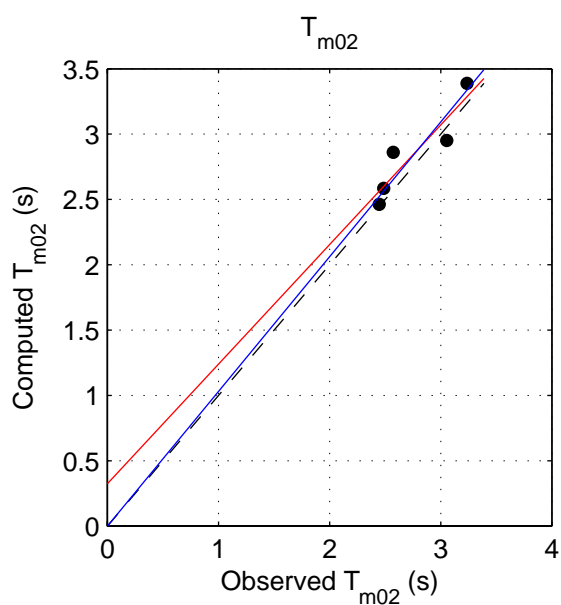
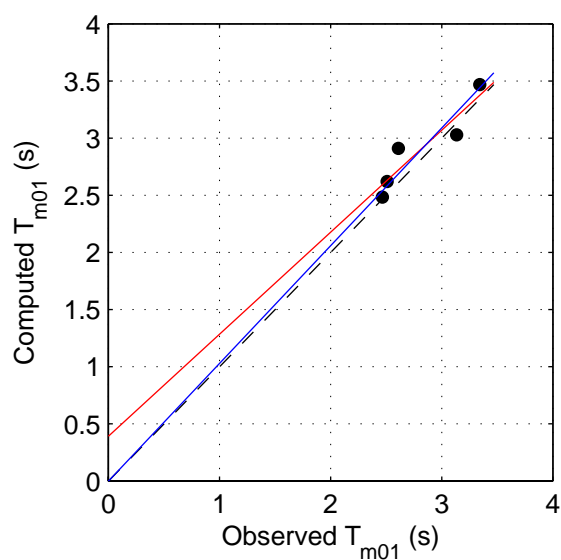
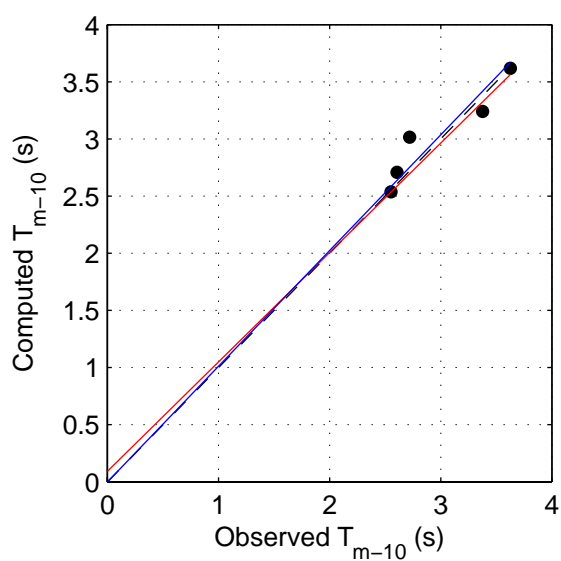
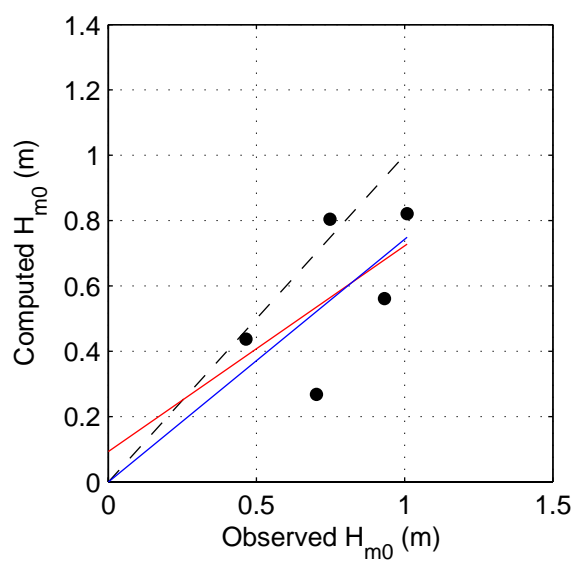
Scatter diagrams and statistics of measured and computed  
integral wave parameters in Westerschelde at station HFP  
Case N01: Base case, exclusive triads and quadruplets,  $Q_b=0.00001$

Area: WS

HFP

N01

mspec\_WS\_HFP\_n01



	mean	bias	stdev	rmse	mae	sci	r	a	b	b <sub>0</sub>
H <sub>m0</sub>	0.771	-0.193	0.212	0.270	0.215	0.351	0.563	0.093	0.629	0.743
T <sub>m-10</sub>	2.977	0.047	0.162	0.152	0.111	0.051	0.947	0.560	0.828	1.012
T <sub>m01</sub>	2.813	0.090	0.150	0.161	0.132	0.057	0.928	0.393	0.892	1.030
T <sub>m02</sub>	2.759	0.091	0.146	0.159	0.131	0.058	0.918	0.324	0.915	1.031

Scatter diagrams and statistics of measured and computed  
integral wave parameters in Westerschelde at station HFP  
Verification run, set WS

Area: WS

HFP

ALL

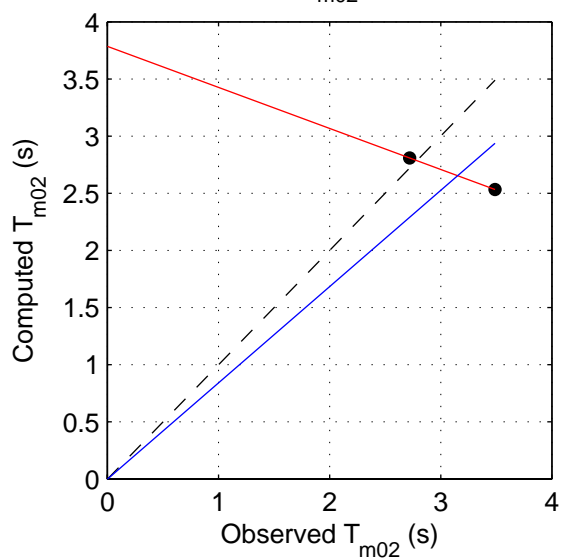
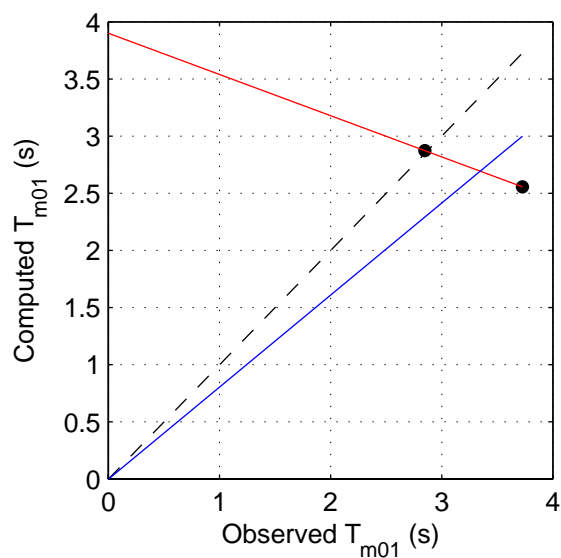
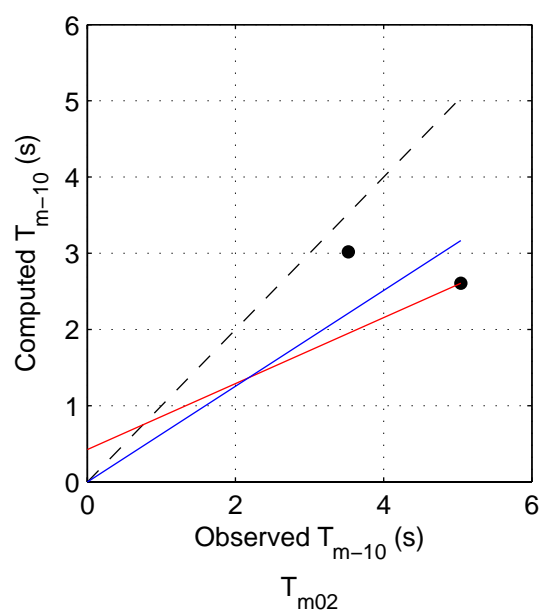
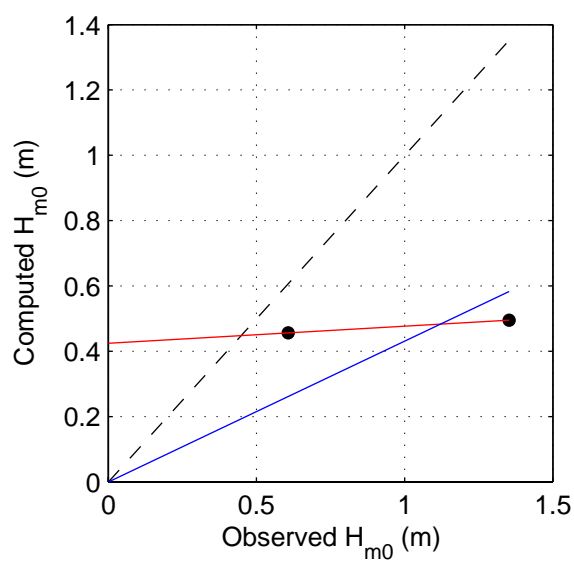
mspec\_WS\_HFP\_v01

Calibration SWAN 40.20

A1168

 Alkyon

Fig. 7.3.4



	mean	bias	stdev	rmse	mae	sci	r	a	b	b <sub>0</sub>
H <sub>m0</sub>	0.980	-0.504	0.499	0.615	0.504	0.628	1.000	0.424	0.053	0.431
T <sub>m-10</sub>	4.283	-1.472	1.365	1.760	1.472	0.411	-1.000	3.974	-0.271	0.628
T <sub>m01</sub>	3.287	-0.573	0.845	0.828	0.597	0.252	-1.000	3.900	-0.361	0.805
T <sub>m02</sub>	3.106	-0.435	0.738	0.679	0.522	0.219	-1.000	3.785	-0.359	0.842

Scatter diagrams and statistics of measured and computed  
integral wave parameters in Westerschelde at station BAT  
Case N01: Base case, exclusive triads and quadruplets, Qb=0.00001

Area: WS

BAT

N01

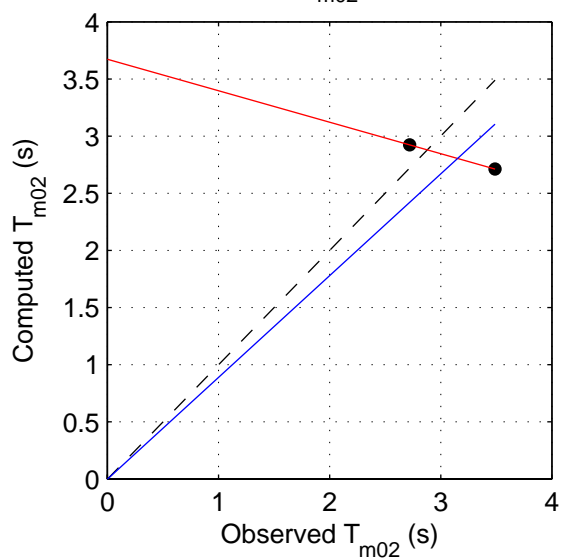
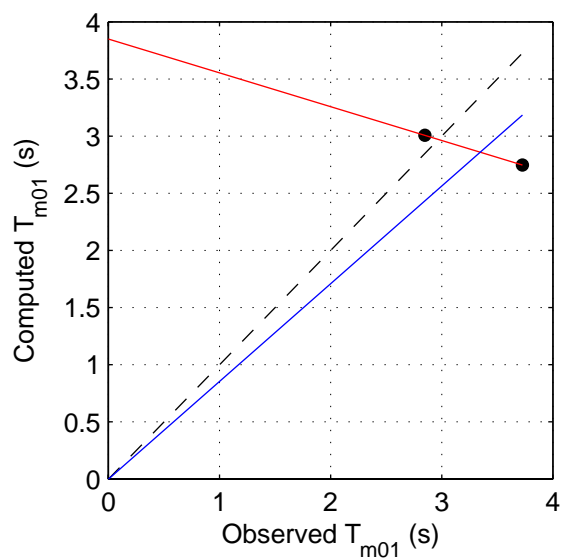
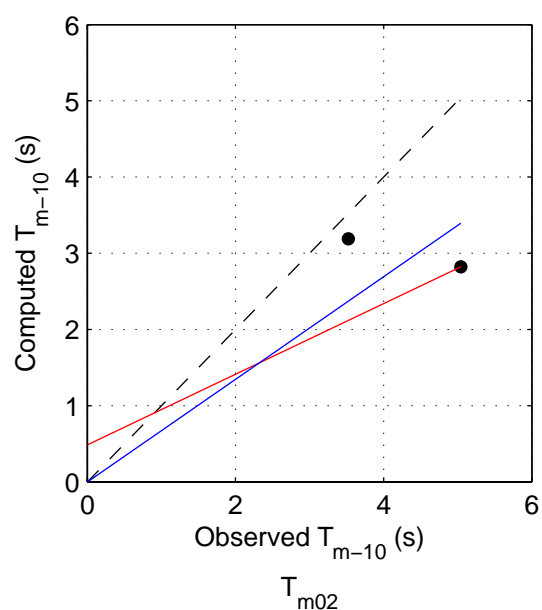
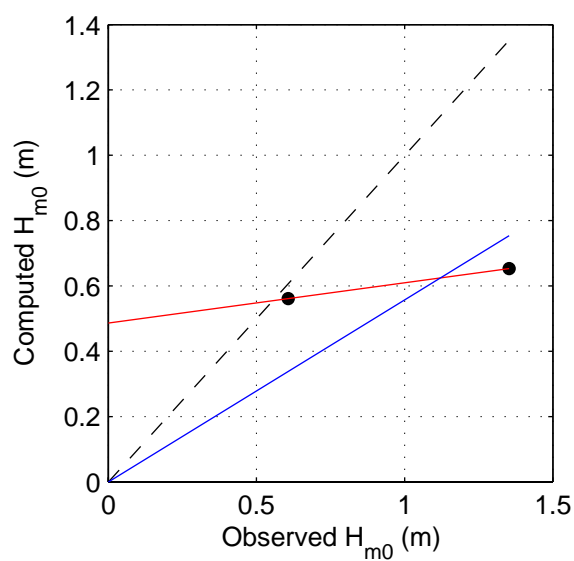
mspec\_WS\_BAT\_n01

Calibration SWAN 40.20

A1168

 Alkyon

Fig. 7.3.5



	mean	bias	stdev	rmse	mae	sci	r	a	b	b <sub>0</sub>
$H_{m0}$	0.980	-0.372	0.462	0.495	0.372	0.506	1.000	0.487	0.123	0.557
$T_{m-10}$	4.283	-1.278	1.335	1.588	1.278	0.371	-1.000	4.048	-0.243	0.673
$T_{m01}$	3.287	-0.411	0.804	0.701	0.569	0.213	-1.000	3.848	-0.296	0.855
$T_{m02}$	3.106	-0.287	0.693	0.568	0.490	0.183	-1.000	3.673	-0.275	0.890

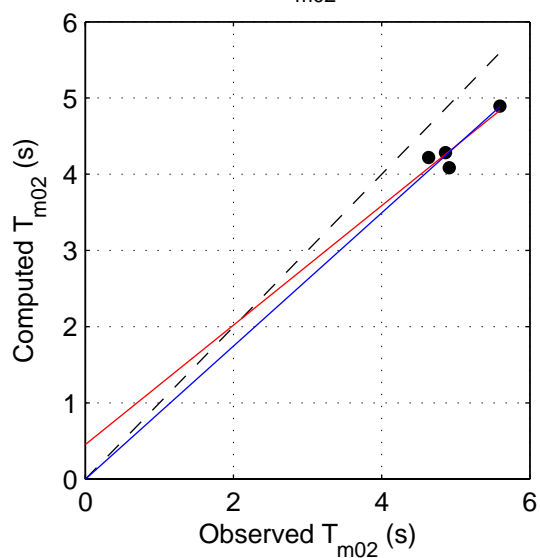
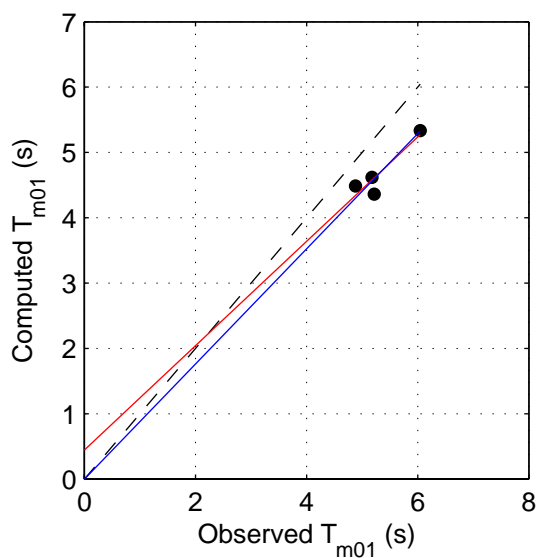
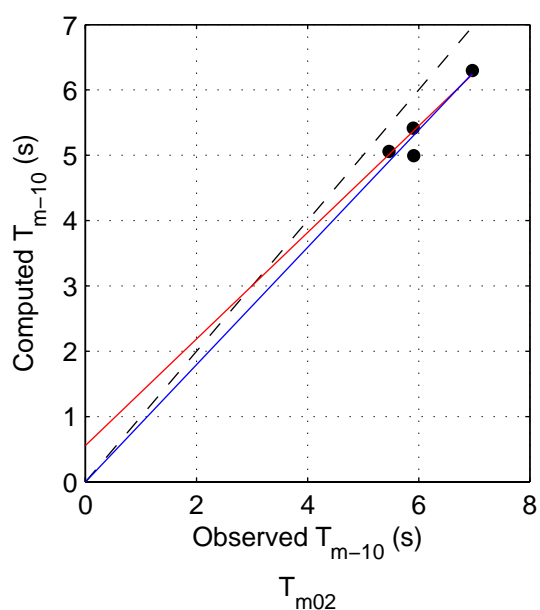
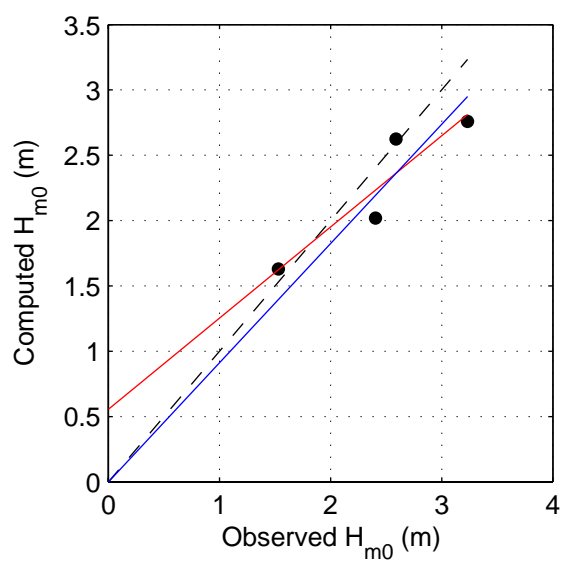
Scatter diagrams and statistics of measured and computed  
integral wave parameters in Westerschelde at station BAT  
Verification run, set WS

Area: WS

BAT

ALL

mspec\_WS\_BAT\_v01



	mean	bias	stdev	rmse	mae	sci	r	a	b	b <sub>0</sub>
H <sub>m0</sub>	2.440	-0.182	0.291	0.310	0.249	0.127	0.927	0.555	0.698	0.912
T <sub>m-10</sub>	6.061	-0.621	0.226	0.651	0.621	0.107	0.935	0.116	0.878	0.897
T <sub>m01</sub>	5.331	-0.630	0.201	0.654	0.630	0.123	0.917	0.443	0.799	0.881
T <sub>m02</sub>	5.000	-0.630	0.176	0.648	0.630	0.130	0.907	0.454	0.783	0.874

Scatter diagrams and statistics of measured and computed  
integral wave parameters in Westerschelde at station WIE  
Case N01: Base case, exclusive triads and quadruplets, Qb=0.00001

Area: WS

WIE

N01

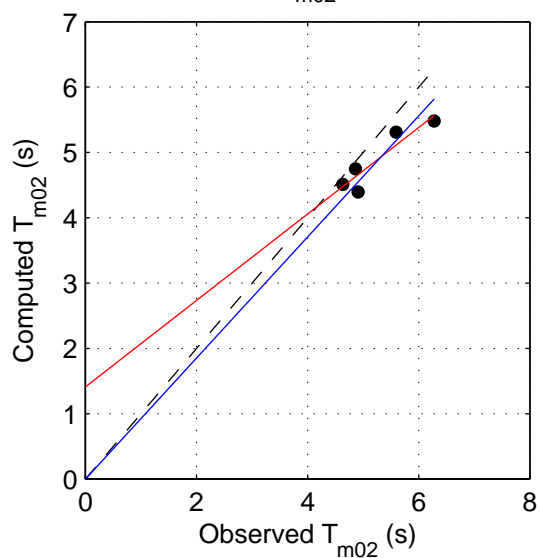
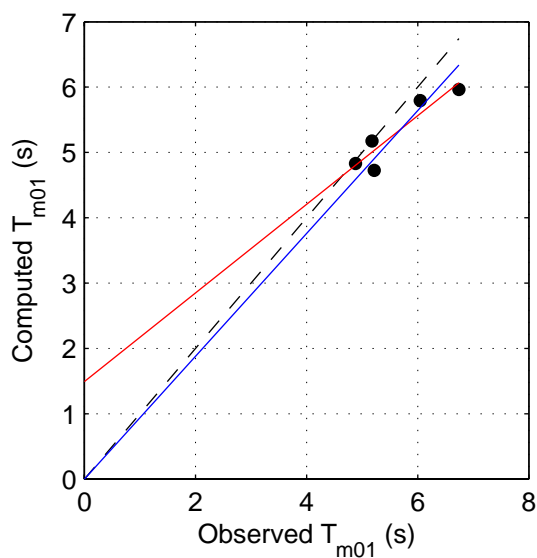
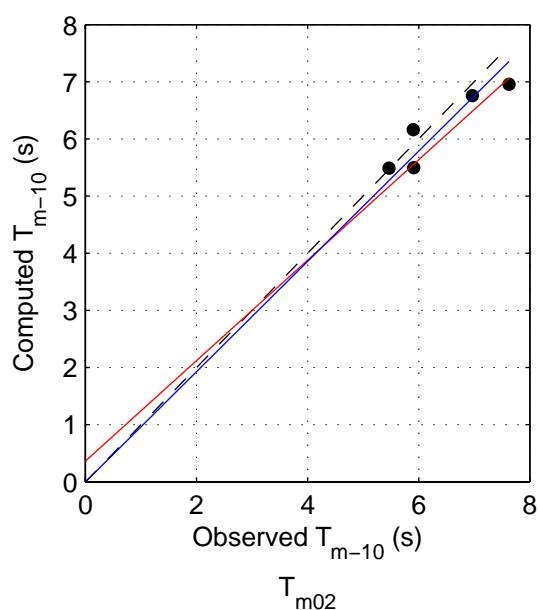
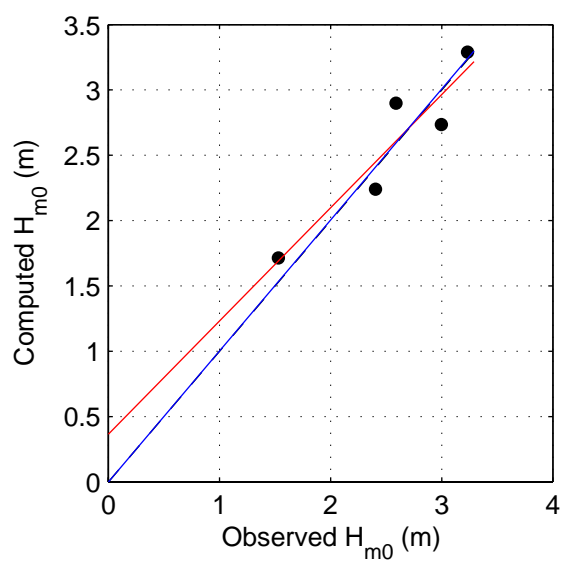
mspec\_WS\_WIE\_n01

Calibration SWAN 40.20

A1168

 Alkyon

Fig. 7.3.7



	mean	bias	stdev	rmse	mae	sci	r	a	b	b <sub>0</sub>
$H_{m0}$	2.551	0.025	0.237	0.214	0.195	0.084	0.933	0.364	0.867	1.002
$T_{m-10}$	6.375	-0.202	0.364	0.383	0.315	0.060	0.927	1.630	0.713	0.964
$T_{m01}$	5.613	-0.315	0.323	0.428	0.315	0.076	0.928	1.491	0.678	0.940
$T_{m02}$	5.256	-0.367	0.292	0.450	0.367	0.086	0.926	1.410	0.662	0.927

Scatter diagrams and statistics of measured and computed  
integral wave parameters in Westerschelde at station WIE  
Verification run, set WS

Area: WS

WIE

ALL

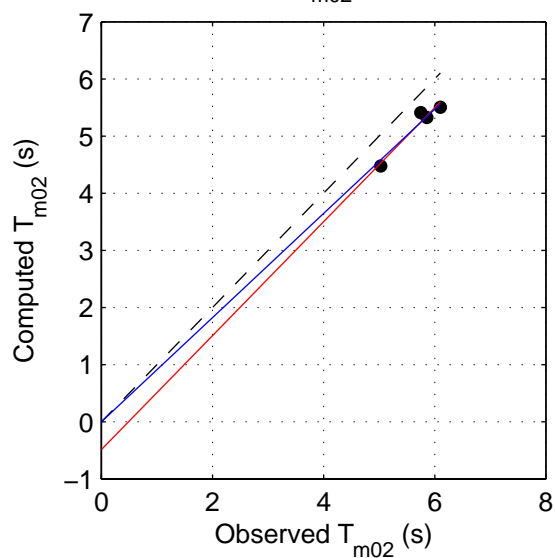
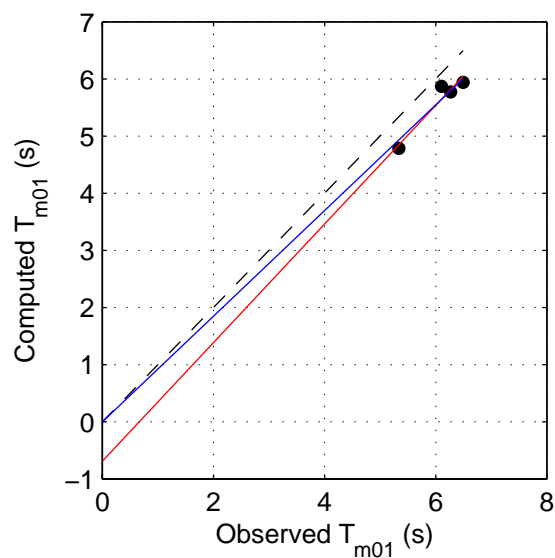
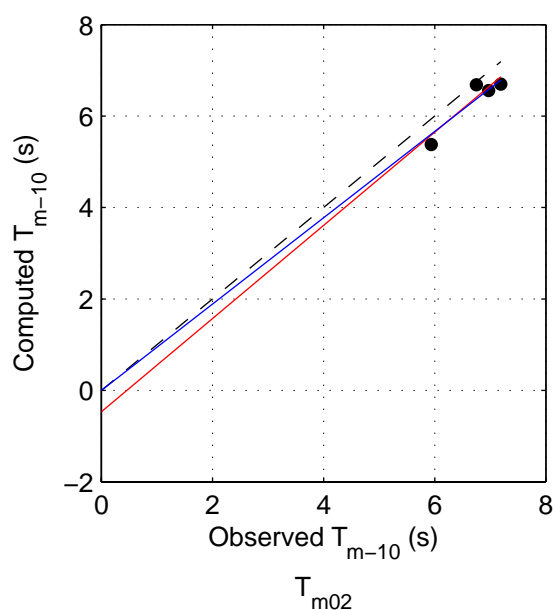
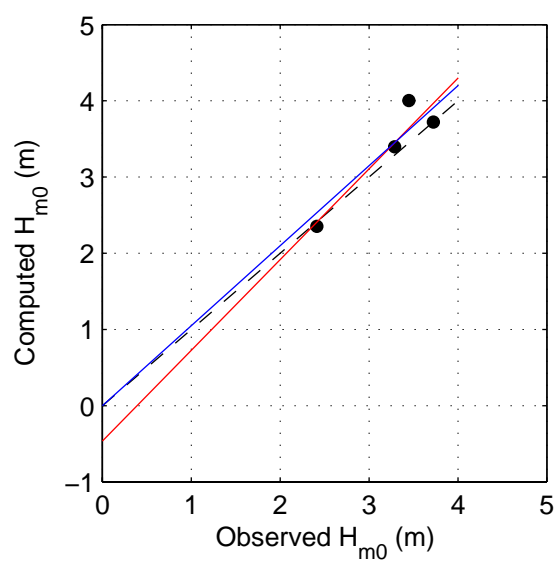
mspec\_WS\_WIE\_v01

Calibration SWAN 40.20

A1168

 Alkyon

Fig. 7.3.8



	mean	bias	stdev	rmse	mae	sci	r	a	b	b <sub>0</sub>
H <sub>m0</sub>	3.219	0.150	0.279	0.284	0.181	0.088	0.934	-0.464	1.191	1.050
T <sub>m-10</sub>	6.711	-0.380	0.219	0.425	0.380	0.063	0.944	-1.069	1.103	0.944
T <sub>m01</sub>	6.052	-0.461	0.151	0.479	0.461	0.079	0.961	-0.685	1.037	0.924
T <sub>m02</sub>	5.686	-0.505	0.114	0.514	0.505	0.090	0.971	-0.485	0.996	0.912

Scatter diagrams and statistics of measured and computed  
integral wave parameters in Westerschelde at station SCW  
Case N01: Base case, exclusive triads and quadruplets, Qb=0.00001

Area: WS

SCW

N01

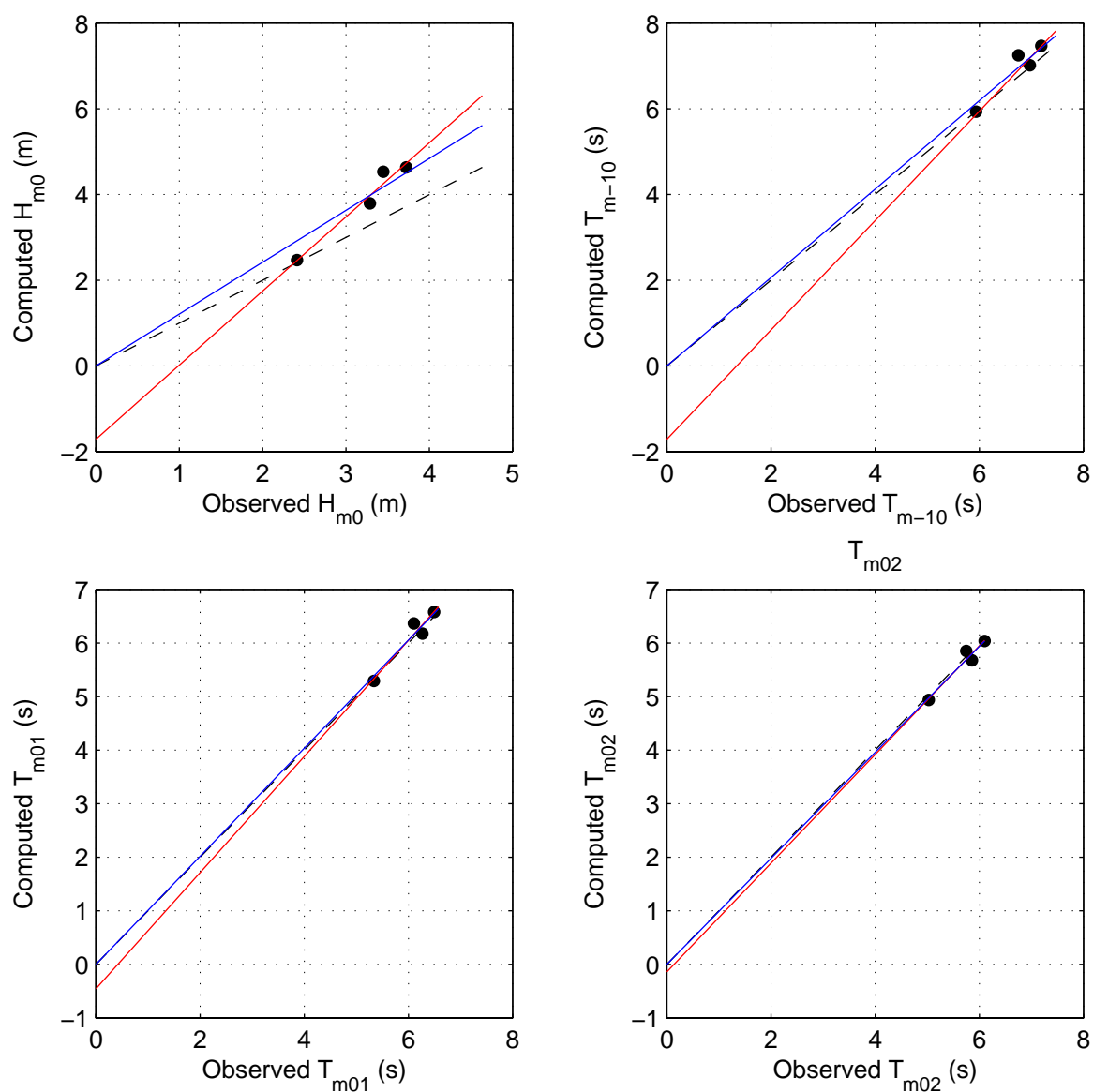
mspec\_WS\_SCW\_n01

Calibration SWAN 40.20

A1168



Fig. 7.3.9



	mean	bias	stdev	rmse	mae	sci	r	a	b	$b_0$
$H_{m0}$	3.219	0.637	0.459	0.751	0.637	0.233	0.979	-1.712	1.730	1.210
$T_{m-10}$	6.711	0.205	0.232	0.287	0.208	0.043	0.952	-1.051	1.187	1.031
$T_{m01}$	6.052	0.050	0.159	0.147	0.122	0.024	0.962	-0.454	1.083	1.009
$T_{m02}$	5.686	-0.061	0.118	0.119	0.110	0.021	0.970	-0.139	1.014	0.989

Scatter diagrams and statistics of measured and computed  
integral wave parameters in Westerschelde at station SCW  
Verification run, set WS

Area: WS

SCW

ALL

mspec\_WS\_SCW\_v01

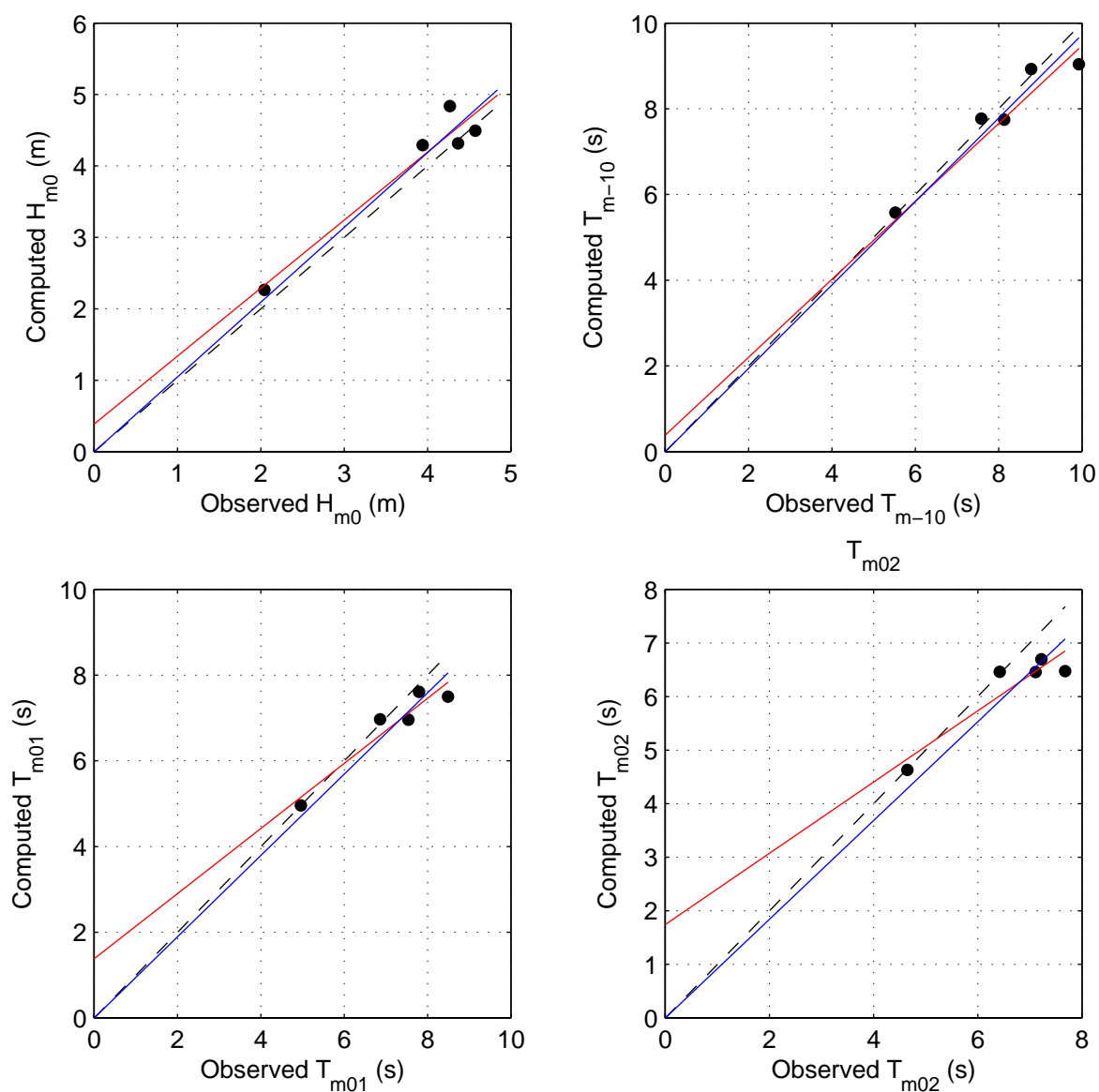
Calibration SWAN 40.20

A1168

 **Alkyon**

Fig. 7.3.10





	mean	bias	stdev	rmse	mae	sci	r	a	b	$b_0$
$H_{m0}$	3.839	0.202	0.274	0.318	0.254	0.083	0.964	0.387	0.952	1.047
$T_{m-10}$	7.990	-0.179	0.458	0.447	0.331	0.056	0.967	1.224	0.824	0.973
$T_{m01}$	7.131	-0.332	0.454	0.524	0.374	0.074	0.955	1.385	0.759	0.948
$T_{m02}$	6.617	-0.473	0.509	0.657	0.488	0.099	0.928	1.743	0.665	0.922

Scatter diagrams and statistics of measured and computed  
integral wave parameters at Petten at station 021  
Case N01: Base case, exclusive triads and quadruplets,  $Q_b=0.00001$

Area: PT

021

N01

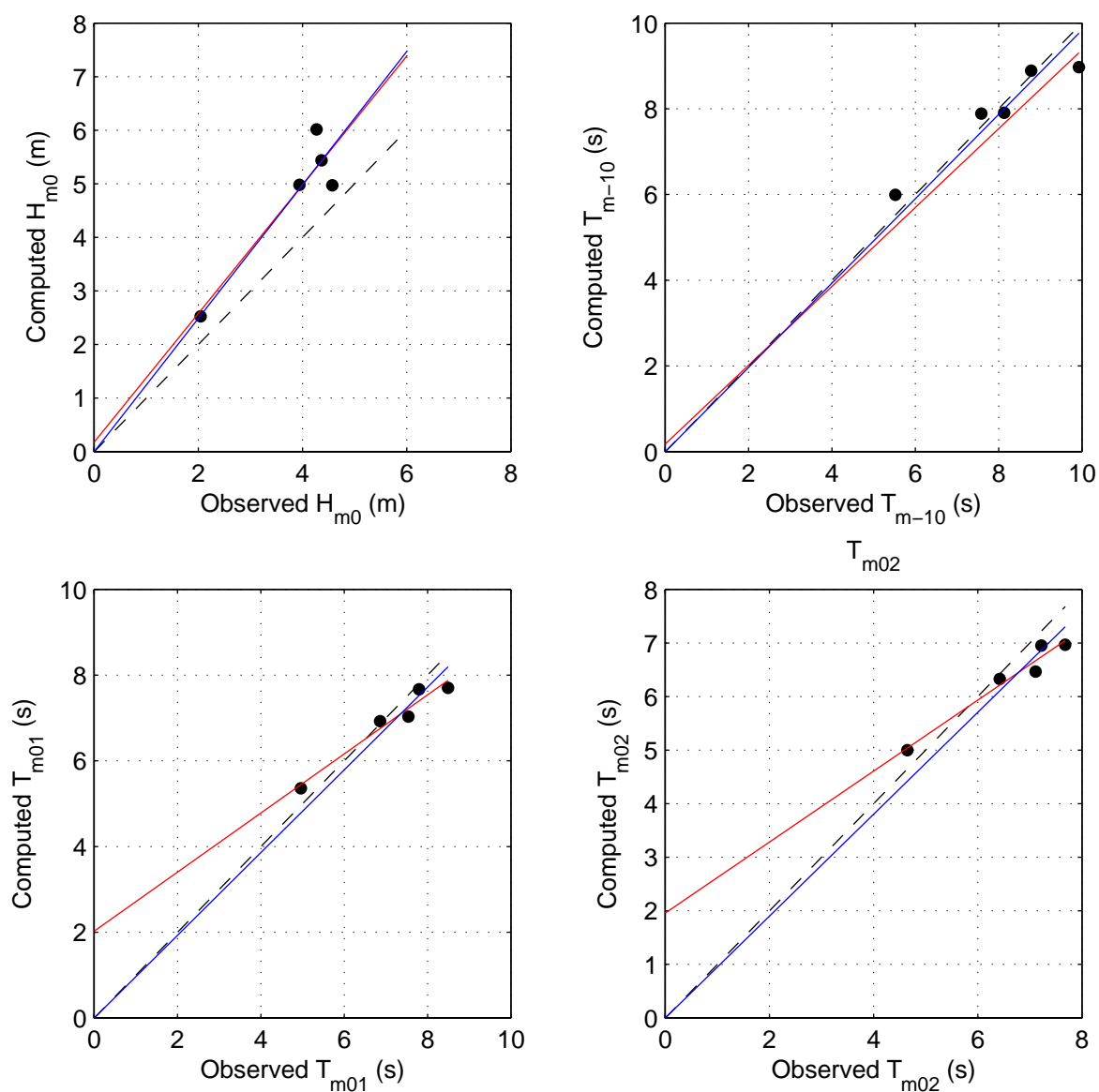
mspec\_PT\_021\_n01

Calibration SWAN 40.20

A1168

 Alkyon

Fig. 7.4.1



	mean	bias	stdev	rmse	mae	sci	r	a	b	$b_0$
$H_{m0}$	3.839	0.948	0.542	1.064	0.948	0.277	0.927	0.178	1.200	1.244
$T_{m-10}$	7.990	-0.061	0.564	0.508	0.411	0.064	0.967	2.253	0.710	0.983
$T_{m01}$	7.131	-0.193	0.469	0.462	0.378	0.065	0.975	2.026	0.689	0.965
$T_{m02}$	6.617	-0.274	0.433	0.474	0.413	0.072	0.979	1.957	0.663	0.951

Scatter diagrams and statistics of measured and computed  
integral wave parameters at Petten at station 021  
Verification run, set ALL

Area: PT

021

Set ALL

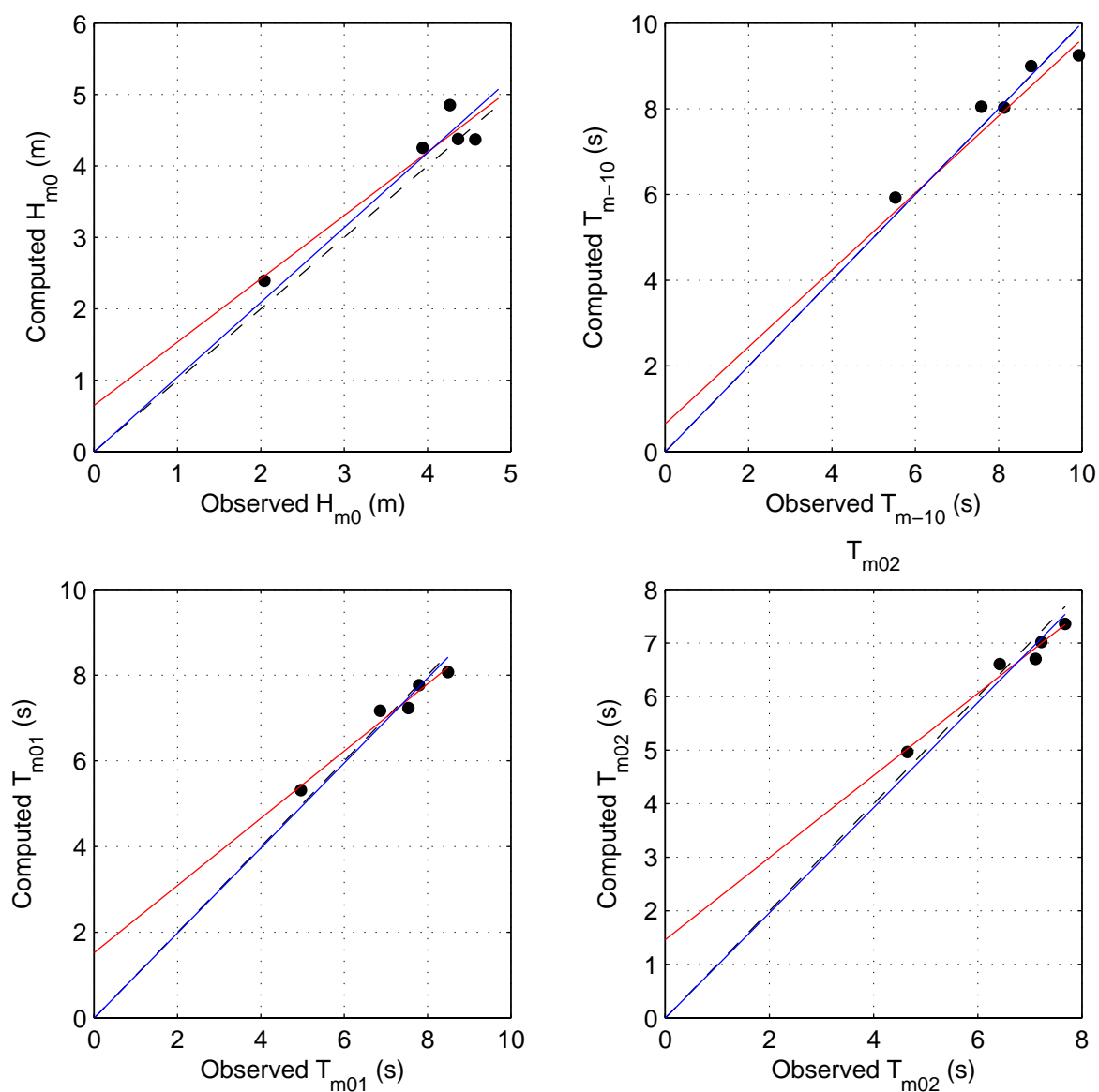
mspec\_PT\_021\_v01

Calibration SWAN 40.20

A1168

 Alkyon

Fig. 7.4.2



	mean	bias	stdev	rmse	mae	sci	r	a	b	$b_0$
$H_{m0}$	3.839	0.210	0.307	0.346	0.291	0.090	0.955	0.650	0.886	1.046
$T_{m-10}$	7.990	0.060	0.468	0.423	0.372	0.053	0.973	1.822	0.780	1.000
$T_{m01}$	7.131	-0.020	0.351	0.315	0.285	0.044	0.983	1.526	0.783	0.991
$T_{m02}$	6.617	-0.087	0.318	0.298	0.286	0.045	0.986	1.461	0.766	0.981

Scatter diagrams and statistics of measured and computed  
integral wave parameters at Petten at station 021  
Verification run, set PT

Area: PT

021

Set PT

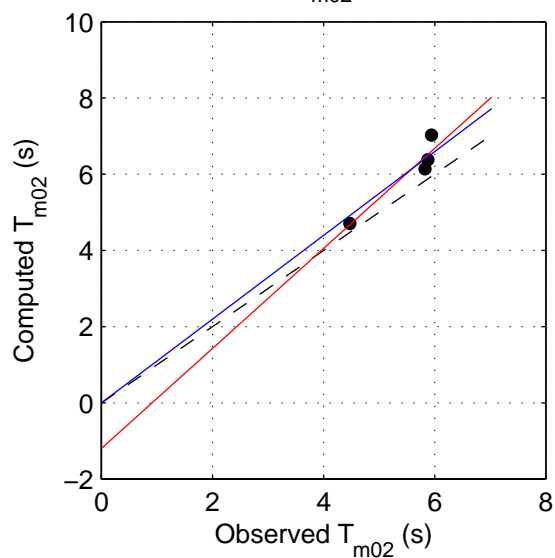
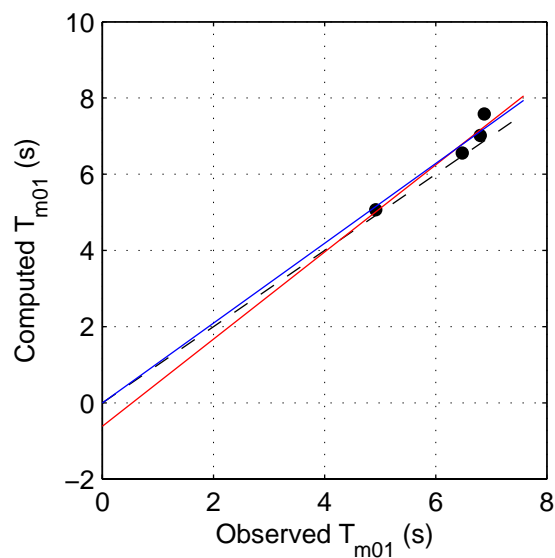
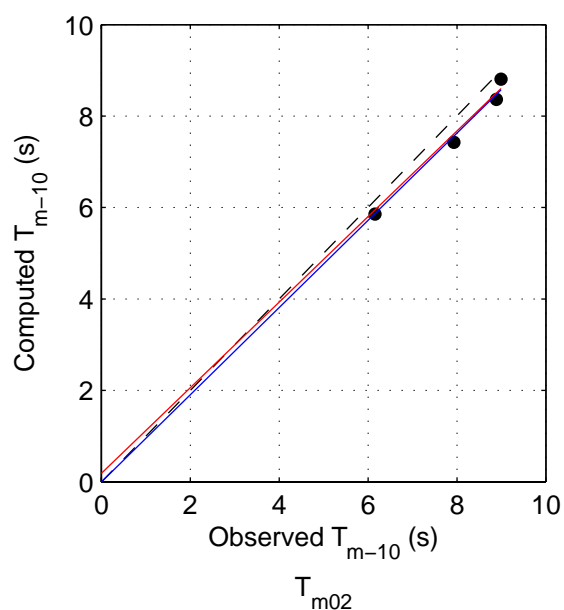
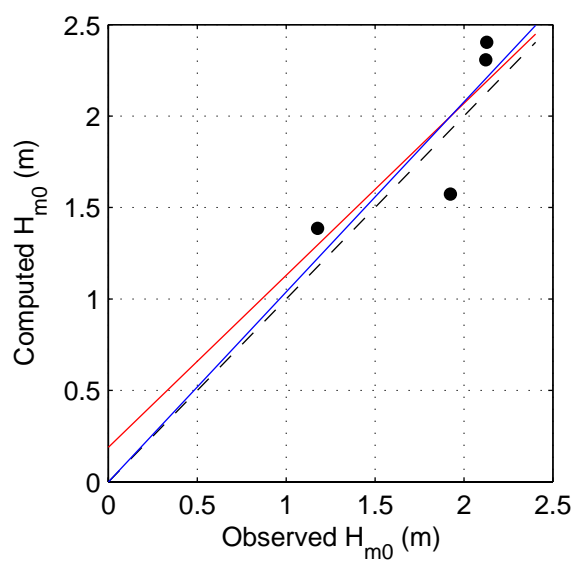
mspec\_PT\_021\_v02

Calibration SWAN 40.20

A1168

 Alkyon

Fig. 7.4.3



	mean	bias	stdev	rmse	mae	sci	r	a	b	b <sub>0</sub>
$H_{m0}$	1.838	0.079	0.289	0.263	0.255	0.143	0.827	0.189	0.940	1.039
$T_{m-10}$	7.992	-0.378	0.163	0.403	0.378	0.050	0.992	-0.258	0.985	0.953
$T_{m01}$	6.269	0.285	0.287	0.378	0.285	0.060	0.971	-0.616	1.144	1.047
$T_{m02}$	5.530	0.533	0.384	0.628	0.533	0.114	0.947	-1.195	1.313	1.099

Scatter diagrams and statistics of measured and computed  
integral wave parameters at Petten at station 062

Case N01: Base case, exclusive triads and quadruplets, Qb=0.00001

Calibration SWAN 40.20

Area: PT

062

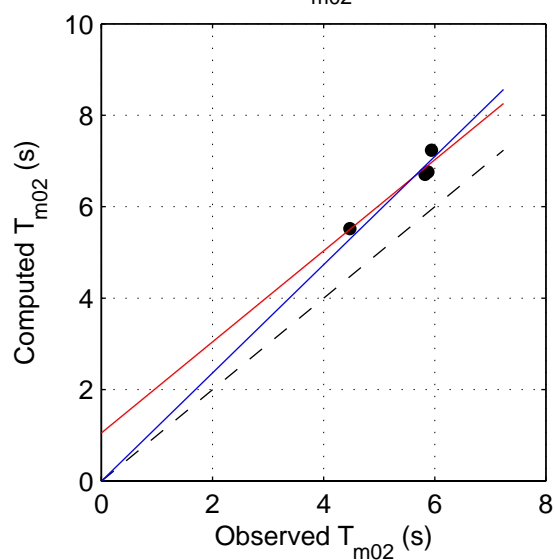
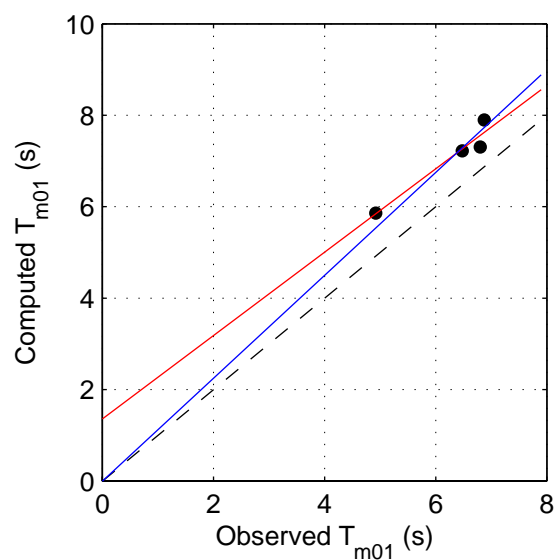
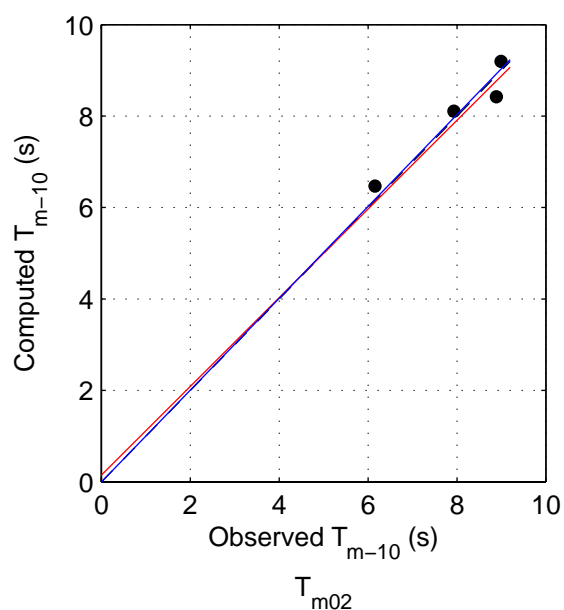
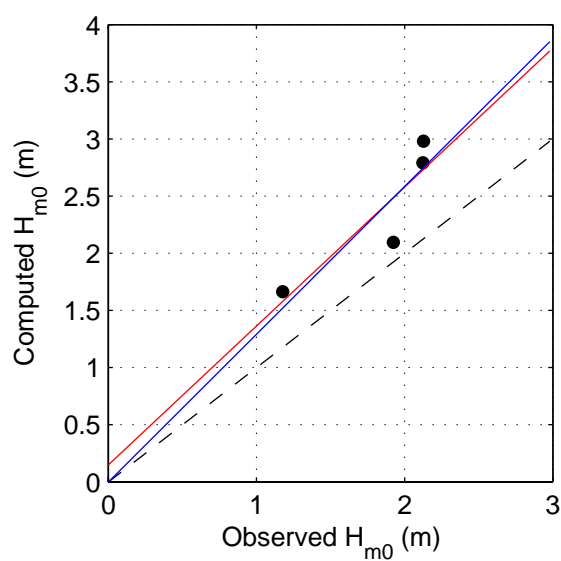
N01

mspec\_PT\_062\_n01

A1168

 Alkyon

Fig. 7.4.4



	mean	bias	stdev	rmse	mae	sci	r	a	b	b <sub>0</sub>
H <sub>m0</sub>	1.838	0.544	0.290	0.600	0.544	0.326	0.895	0.149	1.215	1.293
T <sub>m-10</sub>	7.992	0.057	0.353	0.311	0.289	0.039	0.968	1.289	0.846	1.004
T <sub>m01</sub>	6.269	0.802	0.233	0.827	0.802	0.132	0.967	1.360	0.911	1.125
T <sub>m02</sub>	5.530	1.026	0.197	1.040	1.026	0.188	0.963	1.052	0.995	1.183

Scatter diagrams and statistics of measured and computed  
integral wave parameters at Petten at station 062  
Verification run, set ALL

Area: PT

062

Set ALL

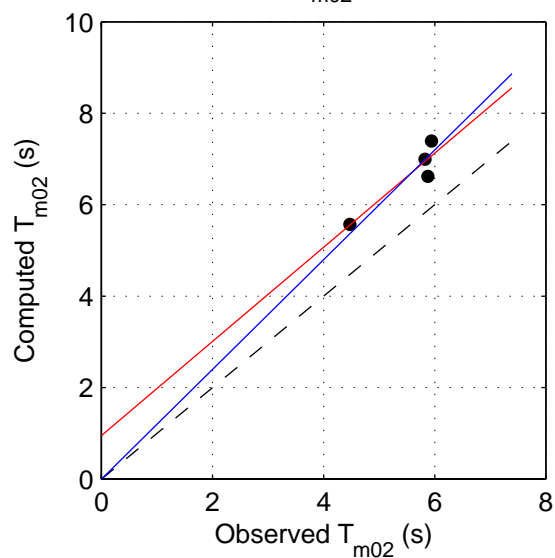
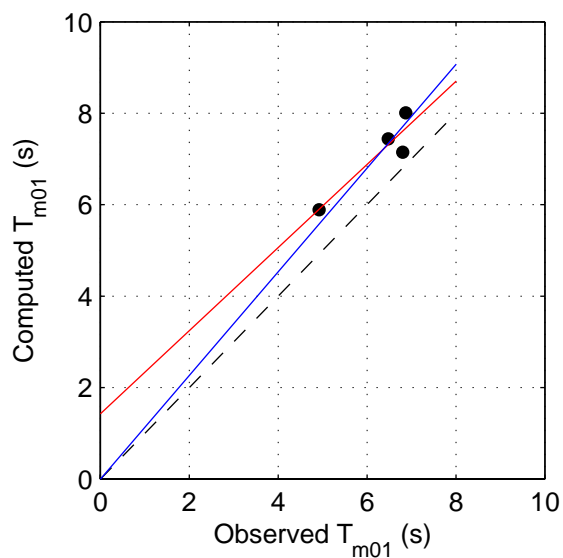
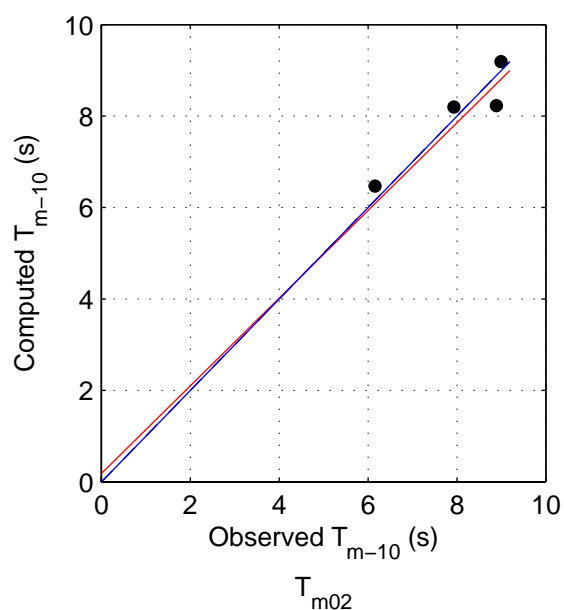
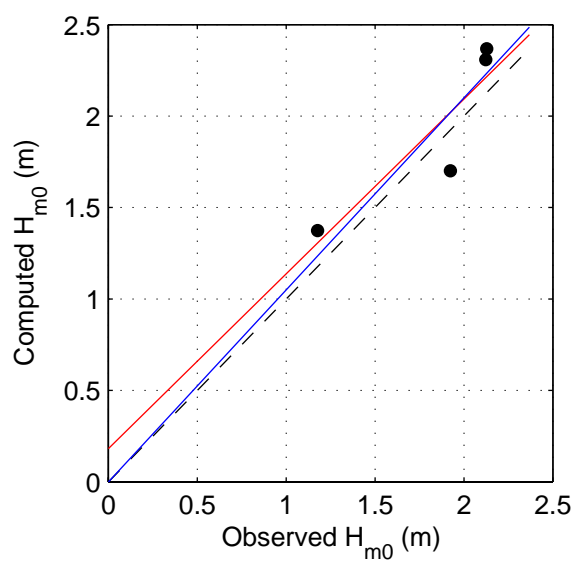
mspec\_PT\_062\_v01

Calibration SWAN 40.20

A1168

 Alkyon

Fig. 7.4.5



	mean	bias	stdev	rmse	mae	sci	r	a	b	b <sub>0</sub>
H <sub>m0</sub>	1.838	0.100	0.217	0.213	0.212	0.116	0.894	0.182	0.955	1.050
T <sub>m-10</sub>	7.992	0.028	0.462	0.401	0.358	0.050	0.939	1.543	0.810	1.000
T <sub>m01</sub>	6.269	0.854	0.346	0.905	0.854	0.144	0.927	1.425	0.909	1.133
T <sub>m02</sub>	5.530	1.113	0.293	1.142	1.113	0.206	0.928	0.952	1.029	1.199

Scatter diagrams and statistics of measured and computed  
integral wave parameters at Petten at station 062  
Verification run, set PT

Area: PT

062

Set PT

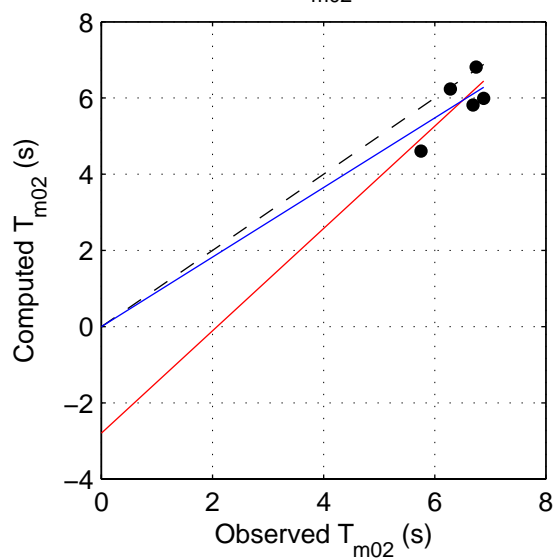
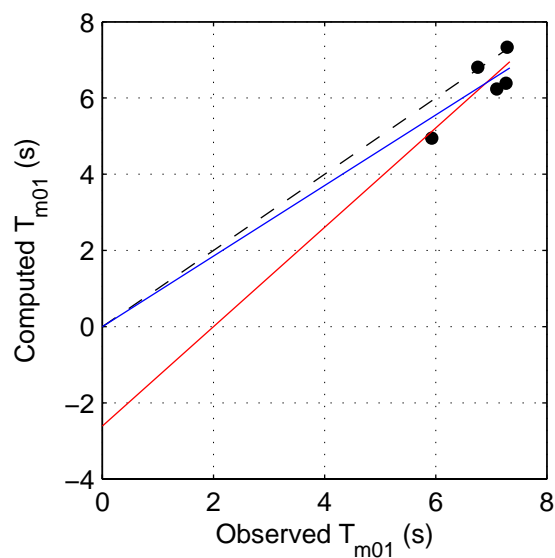
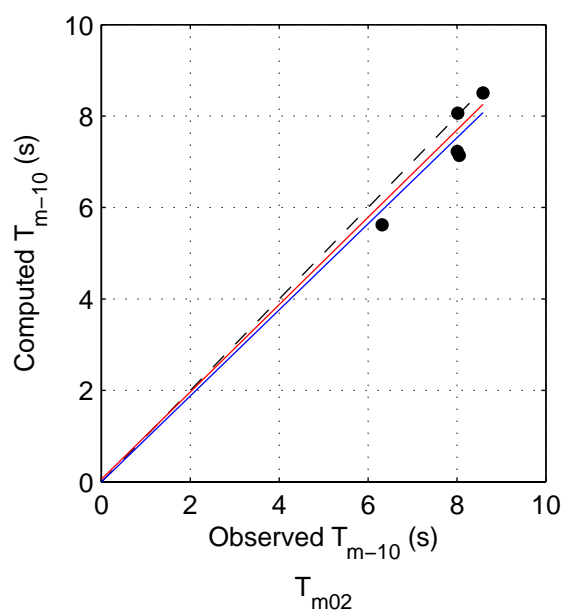
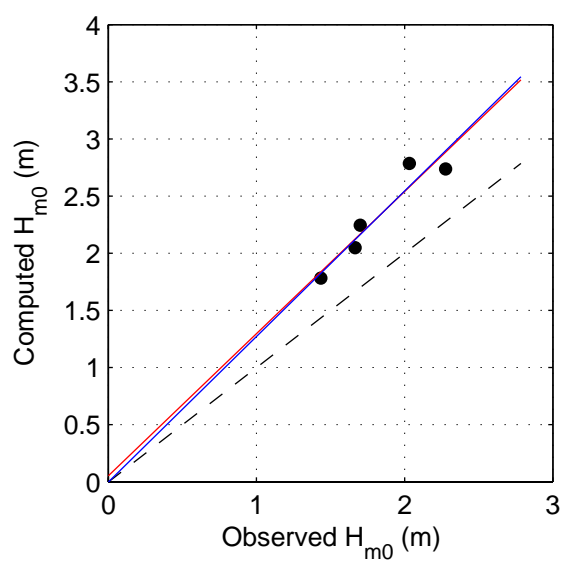
mspec\_PT\_062\_v02

Calibration SWAN 40.20

A1168

 Alkyon

Fig. 7.4.6



	mean	bias	stdev	rmse	mae	sci	r	a	b	b <sub>0</sub>
H <sub>m0</sub>	1.822	0.498	0.162	0.519	0.498	0.285	0.947	0.054	1.244	1.273
T <sub>m-10</sub>	7.797	-0.485	0.437	0.623	0.504	0.080	0.931	-1.992	1.193	0.940
T <sub>m01</sub>	6.868	-0.526	0.528	0.707	0.566	0.103	0.828	-2.609	1.303	0.925
T <sub>m02</sub>	6.471	-0.578	0.549	0.759	0.605	0.117	0.760	-2.796	1.343	0.912

Scatter diagrams and statistics of measured and computed  
integral wave parameters at Petten at station 175

Case N01: Base case, exclusive triads and quadruplets, Qb=0.00001

Area: PT 175

N01

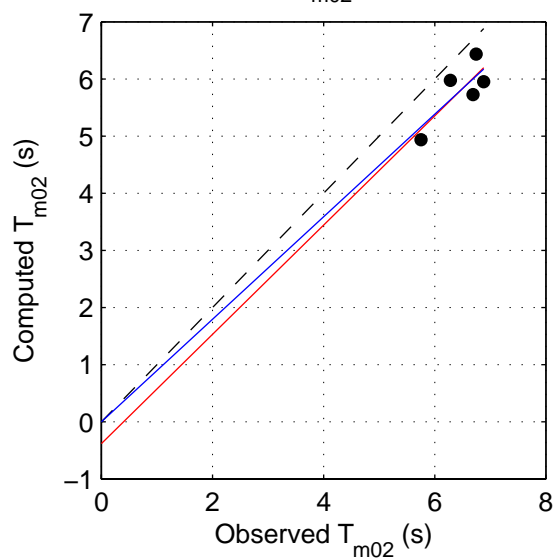
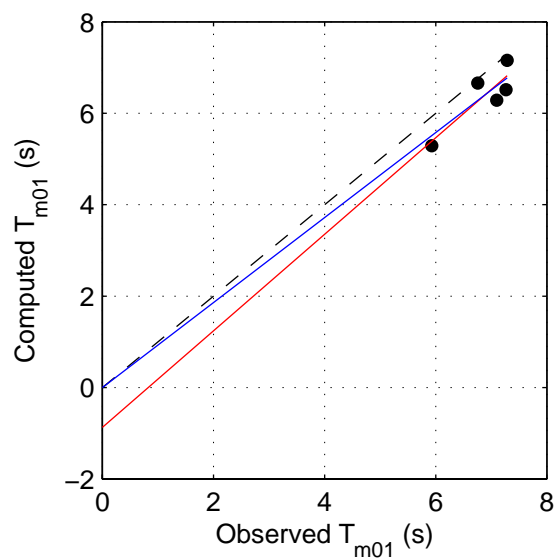
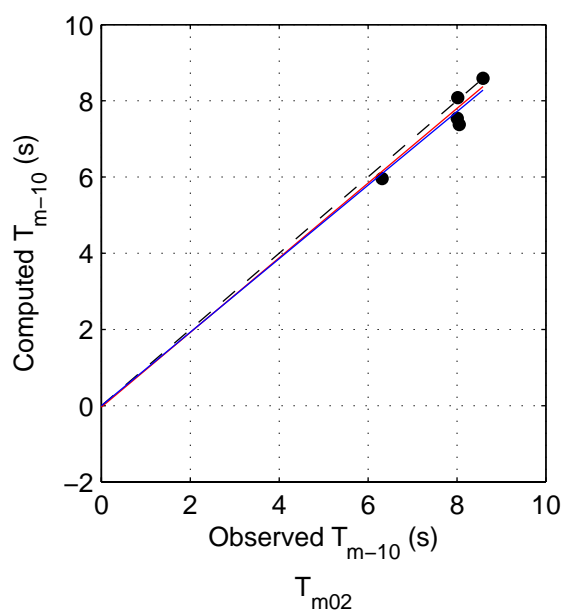
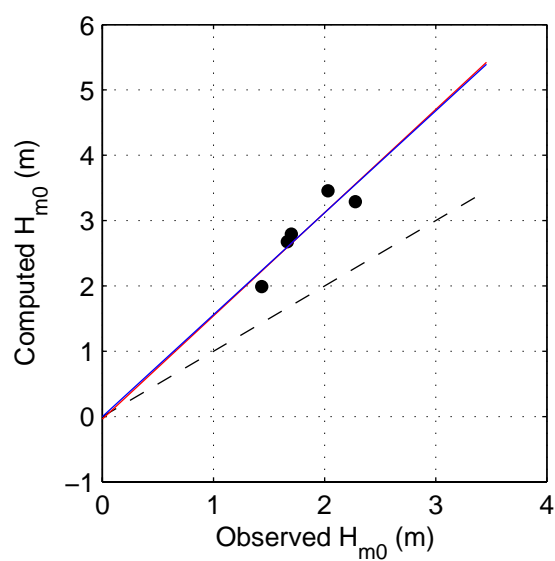
mspec\_PT\_175\_n01

Calibration SWAN 40.20

A1168



Fig. 7.4.7



	mean	bias	stdev	rmse	mae	sci	r	a	b	b <sub>0</sub>
H <sub>m0</sub>	1.822	1.019	0.311	1.056	1.019	0.580	0.906	-0.037	1.580	1.560
T <sub>m-10</sub>	7.797	-0.286	0.313	0.401	0.313	0.051	0.952	-1.009	1.093	0.965
T <sub>m01</sub>	6.868	-0.487	0.346	0.577	0.487	0.084	0.866	-0.869	1.056	0.930
T <sub>m02</sub>	6.471	-0.667	0.332	0.730	0.667	0.113	0.798	-0.380	0.956	0.897

Scatter diagrams and statistics of measured and computed  
integral wave parameters at Petten at station 175  
Verification run, Set ALL

Area: PT 175

Set ALL

mspec\_PT\_175\_v01

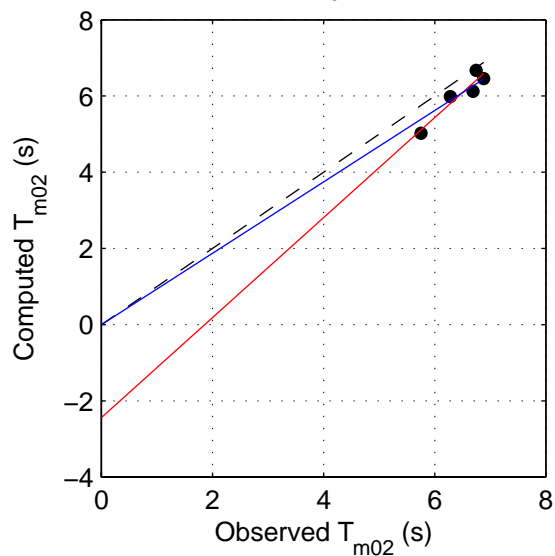
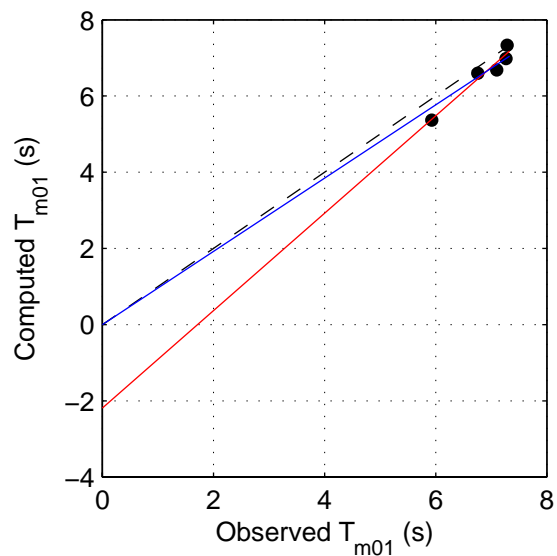
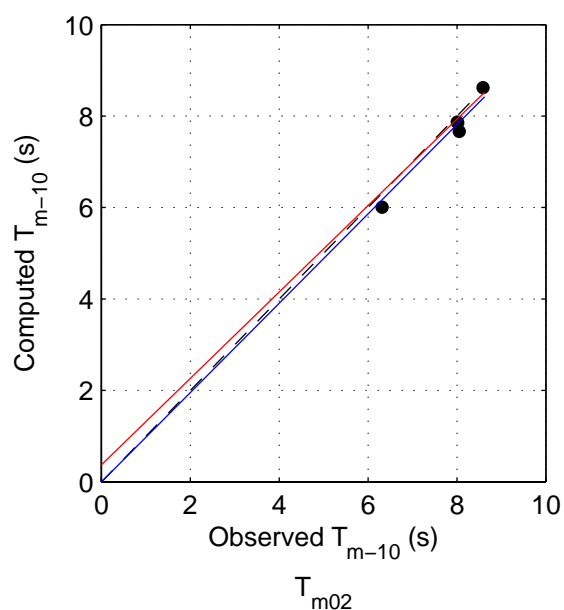
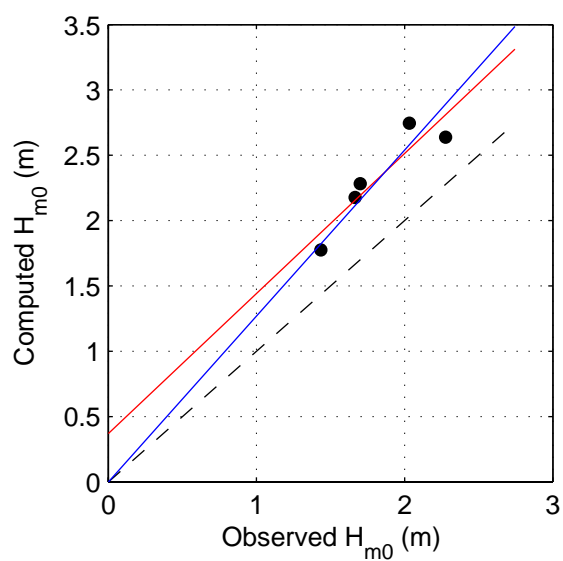
Calibration SWAN 40.20

A1168

 Alkyon

Fig. 7.4.8





	mean	bias	stdev	rmse	mae	sci	r	a	b	b <sub>0</sub>
H <sub>m0</sub>	1.822	0.502	0.156	0.521	0.502	0.286	0.918	0.370	1.072	1.270
T <sub>m-10</sub>	7.797	-0.194	0.165	0.243	0.208	0.031	0.990	-1.041	1.109	0.976
T <sub>m01</sub>	6.868	-0.277	0.234	0.348	0.296	0.051	0.972	-2.189	1.278	0.961
T <sub>m02</sub>	6.471	-0.418	0.254	0.476	0.418	0.074	0.944	-2.438	1.312	0.937

Scatter diagrams and statistics of measured and computed  
integral wave parameters at Petten at station 175  
Verification run, set PT

Area: PT

175

Set PT

mspec\_PT\_175\_v02

Calibration SWAN 40.20

A1168

 Alkyon

Fig. 7.4.9